UNIVERSITY OF COPENHAGEN
FACULTY OF SCIENCE

PhD thesis

Aspects of Quantum Field Theory

Matthias Volk

Charlotte Kristjansen, Jacob L. Bourjaily

August 27, 2021

This thesis has been submitted to the PhD School of The Faculty of Science, University of Copenhagen

Abstract

This PhD thesis consists of two parts:

The topic of the first part is defect conformal field theories that arise as modifications of the well-known AdS_5/CFT_4 correspondence between type IIB superstring theory and $\mathcal{N} = 4$ supersymmetric Yang-Mills theory. We review the supersymmetric D3-D5 probe brane intersection and then study two D3-D7 brane intersections in which supersymmetry is completely broken. We obtain the mass spectrum of the field theories by diagonalizing the quadratic part of the action and derive the propagators, thereby allowing for perturbative computations of correlation functions. The procedure closely follows previous work in the field theory dual of a 1/2-BPS D3-D5 brane intersection. We compute the one-point function of a scalar single-trace operator and the expectation value of a straight Wilson line and compare the results to a computation on the string theory side of the correspondence.

The second part deals with the special functions that arise as integrals over loop momenta in Feynman diagrams in the perturbative computation of scattering amplitudes. Using direct integration techniques we study both integrals that can be computed in terms of multiple polylogarithms as well as others that require new classes of functions. To the latter class of integrals we associate a Calabi-Yau geometry and study its properties. For a class of conformal integrals we are able to obtain this geometry more directly as the leading singularity locus in momentum twistor space. It is generally unknown whether different parameterizations of a given integral lead to different geometries, but we are able to confirm this for the sunrise integrals and the two-loop elliptic double box integral.

Resumé på dansk

Denne doktorafhandling består af to dele:[1]

Emnet for den første del er konforme defektfeltteorier der opstår som modifikationer af den velkendte AdS_5/CFT_4 korrespondance mellem type IIB superstrengteori og $\mathcal{N} = 4$ supersymmetrisk Yang-Mills teori. Vi gennemgår den supersymmetriske D3-D5 sonde/brane-skæring og undersøger derefter to D3-D7 braneskæringer med fuldstændigt brudt supersymmetri. Vi udleder massespektret af feltteorierne ved at diagonalisere den kvadratiske del af virkningen og udleder også propagatorerne, hvilket tillader perturbationsberegninger af korrelationsfunktioner. Fremgangsmåden følger nært tidligere værker i feltteoridualen af en 1/2-BPS D3-D5 braneskæring. Vi udregner et-punkts-funktionen af en skalar enkeltsporsoperator samt forventningsværdien af en lige Wilson-linje og sammenligner resultaterne med en beregning på strengteori-siden af korrespondancen.

Den anden del behandler specialfunktionerne der opstår som integraler over løkkeimpulser i Feynman-diagrammer i perturbationsberegningen af spredningsamplituder. Ved brug af direkte integrationsteknikker undersøger vi både integraler som kan beregnes i form af multiple polylogaritmer samt andre der kræver nye funktionsklasser. Til den sidstnævnte klasse af integraler associerer vi en Calabi-Yau geometri og undersøger dens egenskaber. For en særlig klasse af konforme integraler kan vi udlede denne geometri mere direkte som det førende singularitetslokus i impulstwistorrummet. Det er generelt ukendt om forskellige parametriseringer af et givent integral fører til forskellige geometrier, men vi kan bekræfte dette for solopgangsintegraler og det elliptiske to-løkke-dobbeltboksintegral.

[1] I would like to thank Martin Ravn Christiansen for helping me translate the abstract into Danish.

List of publications

This thesis is based on the following publications:

1. **A. Gimenez Grau, C. Kristjansen, M. Volk, and M. Wilhelm**, "A Quantum Check of Non-Supersymmetric AdS/dCFT," *JHEP* **01** (2019) 007, arXiv:1810.11463 [hep-th].

2. **J. L. Bourjaily, A. J. McLeod, C. Vergu, M. Volk, M. Von Hippel, and M. Wilhelm**, "Embedding Feynman Integral (Calabi-Yau) Geometries in Weighted Projective Space," *JHEP* **01** (2020) 078, arXiv:1910.01534 [hep-th].

3. **J. L. Bourjaily, A. J. McLeod, C. Vergu, M. Volk, M. Von Hippel, and M. Wilhelm**, "Rooting Out Letters: Octagonal Symbol Alphabets and Algebraic Number Theory," *JHEP* **02** (2020) 025, arXiv:1910.14224 [hep-th].

4. **A. Gimenez-Grau, C. Kristjansen, M. Volk, and M. Wilhelm**, "A quantum framework for AdS/dCFT through fuzzy spherical harmonics on S^4," *JHEP* **04** (2020) 132, arXiv:1912.02468 [hep-th].

5. **J. L. Bourjaily, M. Volk, and M. Von Hippel**, "Conformally Regulated Direct Integration of the Two-Loop Heptagon Remainder," *JHEP* **02** (2020) 095, arXiv:1912.05690 [hep-th].

6. **S. Bonansea, K. Idiab, C. Kristjansen, and M. Volk**, "Wilson lines in AdS/dCFT," *Phys. Lett. B* **806** (2020) 135520, arXiv:2004.01693 [hep-th].

7. **C. Vergu and M. Volk**, "Traintrack Calabi-Yaus from Twistor Geometry," *JHEP* **07** (2020) 160, arXiv:2005.08771 [hep-th].

8. **H. Frellesvig, C. Vergu, M. Volk, and M. von Hippel**, "Cuts and Isogenies," *JHEP* **05** (2021) 064, arXiv:2102.02769 [hep-th].

A copy of each paper is included in this file.

Contents

1 Introduction and summary **3**
- 1.1 Defect conformal field theories with holographic duals . . . 3
- 1.2 Aspects of Feynman integrals . . . 4
- 1.3 Acknowledgments . . . 6

2 Defect conformal field theories with holographic duals **7**
- 2.1 Probe branes in type IIB supergravity . . . 7
- 2.2 The D3-D5 system . . . 9
  - 2.2.1 String theory side . . . 10
  - 2.2.2 Field theory side . . . 13
- 2.3 The D3-D7 system . . . 19
  - 2.3.1 String theory side . . . 19
  - 2.3.2 Field theory side . . . 22
- 2.4 Observables . . . 22
  - 2.4.1 One-point functions . . . 23
  - 2.4.2 Wilson lines . . . 27
- 2.5 Summary of own work and outlook . . . 28

3 Aspects of Feynman integrals **31**
- 3.1 Reminder about integration parameters . . . 31
- 3.2 Singularities of Feynman integrals . . . 33
- 3.3 Direct integration . . . 35
  - 3.3.1 Direct integration in terms of multiple polylogarithms . . . 36
  - 3.3.2 Obstructions to direct integration . . . 40
  - 3.3.3 Applications of direct integration to Feynman integrals . . . 43
- 3.4 Non-polylogarithmic Feynman integrals . . . 44
  - 3.4.1 Associating a geometry to a Feynman integral . . . 44
  - 3.4.2 Elliptic and Calabi-Yau geometries . . . 46
- 3.5 Summary of own work and outlook . . . 49

A The AdS/CFT correspondence and $\mathcal{N} = 4$ sYM theory **53**
- A.1 Heuristic derivation of the correspondence . . . 53
- A.2 Dictionaries . . . 55

B Multiple polylogarithms and the symbol **58**
- B.1 Multiple polylogarithms . . . 58
- B.2 The symbol . . . 61

C Momentum twistors **64**

Chapter 1

Introduction and summary

Quantum field theories provide a powerful framework for the computation of physical observables that finds widespread application in many different areas of physics. In particle physics, the Standard Model is formulated as a quantum field theory which has been successful at very precise predictions about scattering amplitudes of elementary particles, as well as other observables such as the magnetic moment of the electron. Quantum field theory methods also find application in many-body systems in condensed matter physics, for example to describe the quantum hall effect. More recently, field-theoretic methods have found application in predicting the wave forms of gravitational waves caused by black hole mergers as well as in cosmology.

This thesis consists of two parts that deal with two different aspects of the general framework that quantum field theories provide: The subject of the first part in chapter 2 is defect conformal field theories with holographic duals. The second part in chapter 3 deals with the special functions that arise as integrals over loop momenta in the computation of Feynman integrals. The two chapters provide the background and additional details for the publications that we have contributed to during the time of this PhD. The publications are part of the thesis and we therefore do not repeat the arguments and calculations given there in the main text. Each paper is referenced and shortly summarized at the end of the chapter where it belongs thematically and a copy is included after the references of the main text. We now give a short introduction to each chapter.

1.1 Defect conformal field theories with holographic duals

Symmetry groups and their representations play a very important role in quantum field theories. The most fundamental example is the notion of a particle, which as Wigner noted in [1] can be described mathematically as an irreducible representation of the isometry group of spacetime. Since symmetries constrain the form of physical observables, one can take it as a rule of thumb that theories with a large amount of symmetries are easier to handle computationally. The isometry group of spacetime is the Poincaré group and according to a famous theorem by Coleman and Mandula (see [2]) this group can only be combined with further internal symmetries in a trivial way, at least if the theory has a mass gap. There are however two well-known ways that circumvent this no-go theorem: By relaxing the assumption on the mass gap and considering a theory with only massless particles, the Poincaré group can be enlarged to the conformal group. Another loophole is to replace the underlying Lie algebra of the Poincaré group by a super Lie algebra which gives rise to supersymmetric theories.

On the one hand, considering theories with conformal symmetry or supersymmetry is very convenient because the enlarged symmetry groups pose constraints on the form of physical

observables such as correlation functions or scattering amplitudes. On the other hand, physical systems often do not possess these symmetries, at least not in an unbroken form. One approach towards more realistic models is therefore to begin with a theory with enlarged symmetry group and then try to break some of its symmetries in a systematic way. The hope is that the more symmetric theory is mathematically and computationally easier to treat and that some of this simplicity survives even when some of the symmetries are broken.

A widely studied quantum field theory that is both conformal and supersymmetric is supersymmetric Yang-Mills (sYM) theory in four dimensions with the maximum number $\mathcal{N} = 4$ of supersymmetries [3, 4]. The exceptional amount of symmetry has made it possible to study this theory and its observables in great detail. Many results in this theory are moreover obtained from the well-known dual description in terms of the low-energy limit of type IIB superstring theory on $AdS_5 \times S^5$ via the AdS/CFT correspondence. Following the approach mentioned above, one can look for deformations that break some of the symmetries of $\mathcal{N} = 4$ sYM and study the resulting theory. Keeping in mind that the original theory has a holographic dual, one can in particular focus on deformations of $\mathcal{N} = 4$ sYM that also have a dual description in the string theory picture. One particular way to achieve this is the subject of the first part of this thesis in chapter 2.

Concretely, we consider the situation where additional Dirichlet branes are added to the well-known picture of N coincident D3 branes in type IIB superstring theory from which the duality between $\mathcal{N} = 4$ sYM and the holographic theory can be motivated and which we remind the reader of in appendix A. On the conformal field theory side, these models give rise to modifications of $\mathcal{N} = 4$ sYM in which conformal symmetry is partially broken by a codimension-one defect and spacetime-dependent vacuum expectation values for some of the fields. We specifically review the so-called D3-D5 and D3-D7 probe brane systems, in which D5 and D7 branes are added to the background of N coincident D3 branes respectively. The D3-D5 system preserves some of the supersymmetry of $\mathcal{N} = 4$ sYM, while the D3-D7 system breaks supersymmetry completely.

Our own contribution to this subject is a framework for perturbative computations in the D3-D7 system on the field theory side beyond leading order in the coupling constant. There are two variants of the D3-D7 system with different symmetry properties and for which the perturbative setups are worked out in [5] and [6]. The perturbative setups are used to test the proposed extension of the AdS/CFT dictionary to conformal field theories with defects. In [5] and [6] this test consists of matching one-point functions of scalar field theory operators between the field and the string theory side. In [7] we add the expectation value of a Wilson line operator as another test. The articles are included at the end of this thesis and a short summary will be given in section 2.5. In many ways, the approach follows the steps that were taken for the D3-D5 system although the details are technically more involved. The one-point functions in the defect versions of $\mathcal{N} = 4$ sYM also have interesting connections to boundary integrability which we comment on at the end.

1.2 Aspects of Feynman integrals

The perturbative expansion of a scattering amplitude in a quantum field theory can be organized into Feynman diagrams. On the one hand, this expansion is very useful, because it provides

a systematic framework for constructing the scattering amplitude for a given process up to a specified order in the expansion. On the other hand, computing higher orders in the expansion with the diagrammatic method in practice quickly becomes impossible for several reasons:[1] The number of diagrams that have to be evaluated scales very badly with the number of external particles and the order of the expansion corresponding to the number of loops in a diagram. This is a combinatorial issue, since the diagrammatic method dictates that for a fixed set of external particles, all diagrams compatible with the external data must be drawn and evaluated. Moreover, the evaluation of a diagram includes a four-dimensional integration over an internal loop momentum for each loop in the diagram. These integrations are in general very difficult to carry out, both numerically and analytically, and for most cases standard analytic functions studied in the mathematics literature are insufficient to express the integrals in closed form.

To address some of these issues, more efficient methods for the construction of an amplitude have been developed, for example (generalized) unitarity [8, 9], recursion relations (for example [10, 11]) or on-shell methods for $\mathcal{N} = 4$ sYM (see for example [12]). While these methods are successful at constructing integrands, they do not bypass the integrations over internal loop momenta that are part of the prescription for going from a set of Feynman diagrams to the scattering amplitude.

Ideally one would like to "solve" these integrations in some way by expressing the integrals over internal momenta in terms of some special functions that are mathematically well-understood. This is the topic of the second part of this thesis in chapter 3. There is a number of reasons for why a rewriting of the integrals in terms of special functions can be useful, for example faster and more reliable numerical evaluations through series expansions, a better understanding of the singularity structure of the amplitude or connections to other fields in mathematics (e.g. number theory) as well as to neighboring areas in physics (e.g. string theory). If one has some knowledge about the class of functions and the singularity structure, then one can moreover combine these two and try to find the amplitude through bootstrap methods which in recent years has successfully been applied to very complicated scattering amplitudes.

It is not known which class of functions is generally best-suited to express Feynman integrals in perturbation theory, but some guidance is provided by very general results due to Landau [13] about the singularities that can occur in the perturbative expansion of scattering amplitudes. In particular, Landau's work not only predicts the location of the singularities of the amplitude, but also its behavior in the neighborhood of such a singularity. This poses constraints on the classes of functions that can be considered. For certain amplitudes the class of multiple polylogarithms defined by Goncharov in [14] has found widespread application, but there are many examples of relatively simple diagrams that cannot be expressed in terms of these functions. More generally, iterated integrals as studied by Chen [15] are a promising candidate that have been shown to work for more complicated integrals that involve elliptic curves.

During this PhD we have on the one hand studied integrals that can be computed algorithmically in terms of multiple polylogarithms using the method of direct integration (see [16]

[1] Besides the practical issues there are also "philosophical" issues with the expansion in terms of Feynman diagrams, for example the fact that in a gauge theory individual diagrams are generally not gauge-invariant, while the full amplitude is. Moreover, it has been observed many times that the result of a laborious computation in terms of Feynman diagrams has a very simple result, suggesting that there should be a better way to obtain the answer.

and [17]). We therefore review the corresponding integration algorithm in some detail. On the other hand, we have been involved in the exploration of the space of functions required beyond multiple polylogarithms. This includes the papers [18, 19, 20] where the focus is in particular on understanding the elliptic and more generally Calabi-Yau geometry that can be associated to non-polylogarithmic Feynman integrals. The corresponding articles are included at the end of this thesis and a short summary will be given in section 2.5.

1.3 Acknowledgments

I would like to thank my supervisors Charlotte Kristjansen and Jacob Bourjaily for their guidance and support throughout the years and for the many doors they have opened up for me. I am particularly grateful for the large amount of freedom that I had when choosing research directions and projects for my PhD and for the trust that they put forward by allowing me this freedom. They were always there when I needed advice and I greatly appreciate the time and effort they invested.

I would like to thank Hjalte Frellesvig, Andrew McLeod, Cristian Vergu, Matt von Hippel, Matthias Wilhelm and Chi Zhang for all the discussions that I had with them either while sharing offices or in the coffee room, as well as during the collaboration on various projects about Feynman integrals and scattering amplitudes. I would similarly like to thank Sara Bonansea, Aleix Gimenez Grau, Dennis Müller and Khalil Idiab for the discussions and collaboration on projects about defect conformal field theories. I benefited greatly from everything that I have learned from them all about physics, mathematics and the real world. I highly appreciate that I was always able to turn to them with my questions and concerns. I am also thankful to all the other people that I have interacted and discussed with at NBI. This includes Emil Bjerrum-Bohr, Kays Haddad, Asger Ipsen, Alexander Kristensson, Lorenzo Menculini, Gerben Oling, Kasper Vardinghus and many others. All of these people have contributed to an environment at NBI that I enjoyed a lot and that I will miss in the future.

I would also like to thank all of my friends that have helped in their own ways during the time of this PhD, in particular Dario, Firat, Franziska, Lorenzo, Manuel, Martin, Matthew, Mattia, Peter, Sorivan, Tish and Wolfgang. I value the time we spent climbing, running, playing, discussing and talking together. I especially want to thank my parents Almuth and Franz, my sisters Antonia and Elisabeth and my brother Paul for their consistent support and understanding. Finally, I thank Sara for her categorical encouragement and non-measurable love.

Chapter 2

Defect conformal field theories with holographic duals

As previously mentioned in the introduction, one of the best-studied quantum field theories is $\mathcal{N} = 4$ sYM theory in four dimensions. Impressive results for physical observables such as correlation functions and scattering amplitudes have been obtained in this theory, often using the exceptional number of symmetries provided by the superconformal group $\mathrm{PSU}(2,2\,|\,4)$. The theory also appears on one side of the best-understood example of a duality between a conformal field theory and a gravitational theory on anti-de Sitter (AdS) space. For the case of $\mathcal{N} = 4$, the counterpart of the correspondence is type IIB supergravity on $\mathrm{AdS}_5 \times S^5$ and the correspondence can be motivated by considering a stack of N coincident D3 branes embedded in ten-dimensional type IIB superstring theory. In this form, the correspondence was originally presented by Maldacena in [21]. We assume some familiarity with the correspondence in this chapter and refer to appendix A for additional details.

By adding additional Dirichlet branes into the background of N coincident D3 branes one can obtain interesting variations of the correspondence. One key motivation for studying such variations is that they allow for a controlled breaking of some of the symmetries that are present in the original setup, in particular some of the conformal symmetry and some or all of the supersymmetries. Another motivation is to introduce fields that transform not in the adjoint, but in the fundamental representation of the gauge group, as well as to describe different flavors of fields. In subsection 2.1 below we discuss some general aspects of embedding probe branes into the background of N coincident D3 branes. Then we study two concrete examples in detail, the supersymmetric D3-D5 and the non-supersymmetric D3-D7 probe brane systems, in subsections 2.2 and 2.3 respectively. In subsection 2.4, we focus on observables such as one-point functions and Wilson line expectation values that can be computed on both sides of the correspondence and therefore constitute a check of the proposed extension of the AdS/CFT correspondence to conformal field theories with defects. In subsection 2.5, we summarize our own contributions to this topic which have published in [5, 6, 7].

2.1 Probe branes in type IIB supergravity

The starting point is the stack of N coincident D3 branes in type IIB superstring theory in ten dimensional Minkowski space as in appendix A.1. Into this background we would like to embed additional Dirichlet p-branes (Dp branes). In general, this means that we should add to the action of type IIB string theory an action for a Dp brane which is of the form (see for

example [22, chapter 13.3])

$$S_{\mathrm{D}p} = -\mu_p \int_{\mathrm{D}p} \mathrm{tr}\left[e^{-\phi}\sqrt{-\det(G+\mathcal{F})}\right] + \mu_p \int_{\mathrm{D}p} \mathrm{tr}\left[e^{\mathcal{F}} \wedge \sum_q C_q\right]. \tag{2.1.1}$$

Here the first term is the usual Dirac-Born-Infeld (DBI) action for a Dp brane with the induced world volume metric G, the dilaton ϕ and the world volume field-strength $\mathcal{F} = 2\pi\alpha' F$.[1] The second term is a Chern-Simons-like term that couples $\mathcal{F}$ to the Ramond-Ramond background fields C_q. The prefactor μ_p is the Dp brane charge and the integrations run over the $(p+1)$-dimensional world volume of the Dp brane. In the following we will always consider a constant dilaton and write $g_s = e^{\phi}$ for the corresponding string coupling.

The Dp brane action changes the equations of motion of IIB supergravity such that $\mathrm{AdS}_5 \times S^5$ is no longer a solution. It turns out, that this so-called *backreaction* of the Dp branes can be neglected if the number of Dp branes is very small compared to the number N of D3 branes (see [23, section 6.1]). In the following, we usually consider the case where only a single Dp brane is added into this background. Neglecting the effects of this brane onto the $\mathrm{AdS}_5 \times S^5$ geometry is called the *probe-brane approximation*.

The geometry of the Dp probe brane follows from the equations of motion derived from the action (2.1.1). In [23, 24] a class of solutions was described that is dual to a defect conformal field theory in four dimensions with a codimension-one interface. The geometry of the Dp brane in this solution is $\mathrm{AdS}_4 \times M^{p-3}$, where M is some manifold that will be specified later. The AdS_4 part of the Dp brane is embedded in the AdS_5 part of the ten-dimensional background as a submanifold; the M^{p-3} part wraps certain cycles of the S^5 part of the background solution. The AdS_4 effectively cuts the four-dimensional boundary of AdS_5 in two halves with a different CFT living on each half. The two halves are glued together by a three-dimensional interface that corresponds to the three-dimensional intersection of the boundary of AdS_4 and the boundary of AdS_5. The embedded AdS_4 preserves a $\mathrm{SO}(2,3) \subset \mathrm{SO}(2,4)$ subgroup of the isometry group of AdS_5. This matches precisely conformal group in three dimensions which is the same as the subgroup of the conformal group in four dimensions that leaves a flat codimension-one defect invariant.

As usual, the Dirichlet branes may be seen as submanifolds on which the open strings of ten-dimensional type IIB superstring theory can end. The setup with N coincident D3 branes and a single Dp branes then gives rise to the following open string excitations:

- **3–3 strings**: There are open strings stretching between the N coincident D3 branes. These degrees of freedom are already present in the original AdS/CFT setup. On the CFT side, they give rise to the degrees of freedom transforming in the adjoint representation of the gauge group $\mathrm{U}(N)$ of $\mathcal{N} = 4$ sYM theory.

- **p–p strings**: The open strings stretching between the probe Dp brane produce new degrees of freedom that are not present in the original AdS/CFT correspondence. It turns out that for $p > 3$ these degrees of freedom decouple. This can be seen by comparing the coupling constants as follows: The Yang-Mills coupling for the 3–3 and the p–p strings is

[1] We assume that there is no Kalb-Ramond B-field.

related to the string coupling g_s by

$$g^2_{\mathrm{D3}} = 2\pi g_s \qquad \text{and} \qquad g^2_{\mathrm{D}p} = (2\pi)^{p-2}\,\alpha'^{(p-3)/2} g_s \tag{2.1.2}$$

respectively. Thus their ratio

$$\frac{g^2_{\mathrm{D3}}}{g^2_{\mathrm{D}p}} = (2\pi)^{p-3}\,\alpha'^{(p-3)/2} \tag{2.1.3}$$

goes to zero in the limit $\alpha' \longrightarrow 0$ if $p > 3$. The p–p string excitations may then be neglected. For $p < 3$ on the other hand, the ratio diverges and the p–p excitations must be taken into account.

- **3–p and p–3 strings**: The open strings between a D3 and the probe Dp brane correspond to new degrees of freedom transforming in the fundamental representation of the U(N) gauge group.

The open strings are restricted by Dirichlet boundary conditions in the directions in which the brane extends and by Neumann boundary conditions in the directions perpendicular to the brane. In particular, the p–3 and 3–p strings have Dirichlet boundary conditions on both ends in the directions that are shared by the D3 and the Dp brane and Neumann boundary conditions on both ends in the directions perpendicular to both type of branes. In the directions perpendicular to one but not to the other Neumann boundary conditions are imposed on one end of the strings and Dirichlet on the other. These directions are called ND or DN directions. It turns out (see [22, chapter 13.4]) that the number ν of ND and DN directions determines the amount of supersymmetry preserved by the probe brane. If $\nu = 0$, the full amount of supersymmetry is preserved; if $\nu = 4$ or $\nu = 8$, half of the supersymmetry of the original setup is preserved.

With this general discussion in mind, we will now consider the following two probe-brane systems and their field theory duals in more detail:

- **D3-D5 system**: Here a probe D5 brane is inserted into the background of N coincident D3 branes. The D5 brane extends in the directions indicated in table 2.1. Note that this setup preserves half of the original amount of supersymmetry, since $\nu = 4$. We review this system in section 2.2.
- **D3-D7 system**: In this system the probe brane is a D7 brane oriented according to table 2.1. Note that here $\nu = 6$, so this setup is *not* supersymmetric. We review this system in section 2.3.

2.2 The D3-D5 system

The D3-D5 probe-brane system was first described by Karch and Randall in [23, 24, 25] as a way to realize conformal field theories with a boundary holographically. In the following we will first review the string theory side of their construction (subsection 2.2.1) and then describe the dual field theory side in subsection 2.2.2.

	0	1	2	3	4	5	6	7	8	9
N coincident D3	✓	✓	✓	✓	×	×	×	×	×	×
Probe D5	✓	✓	✓	×	✓	✓	✓	×	×	×
Probe D7	✓	✓	✓	×	✓	✓	✓	✓	✓	×

Table 2.1: Orientation of the probe branes relative to the N coincident D3 branes in ten dimensions. The symbol ✓ in column i indicates that the world volume of the brane extends in the X^i direction.

2.2.1 String theory side

According to the general discussion in section 2.1, a single D5 probe brane is inserted into the background of N coincident D3 branes. The world volumes of the D3 branes and the D5 brane span the directions marked in table 2.1. The solution discussed in the following first appeared in [23, 24, 25] and can be described either from the point of view of the probe brane or from the point of view of the world volume of the N coincident D3 branes. We begin with the D5 brane point of view, which describes how the probe brane is embedded into the background and from which we will see the geometry of the D5 brane arise.

D5 brane point of view In the near-horizon limit, the background metric of ten-dimensional space time is the metric of $AdS_5 \times S^5$ which we can write in Poincaré coordinates as

$$ds^2_{BG} = \frac{\rho^2}{L^2}\left(-dx_0^2 + dx_1^2 + dx_2^2 + dx_3^2\right) + \frac{L^2}{\rho^2}d\rho^2 + L^2 d\Omega_5^2. \tag{2.2.1}$$

Here ρ is the radial coordinate of the AdS_5 part of the geometry and $d\Omega_5^2$ is the metric on the S^5. The AdS_5 radius of curvature is the same as the radius L of the S^5. The Ramond-Ramond four-form sourced by the D3 branes in this solution is given by

$$C_4 = \frac{\rho^4}{L^4}\, dx_0 \wedge dx_1 \wedge dx_2 \wedge dx_3. \tag{2.2.2}$$

Into this background we embed a single probe D5 brane for which the general action in equation (2.1.1) takes the form

$$S_{D5} = -\mu_5 \int_{D5} \sqrt{-\det(G + \mathcal{F})} + \mu_5 \int_{D5} \mathcal{F} \wedge C_4. \tag{2.2.3}$$

We make the following ansatz for the embedding into the background: The D5 brane world volume extends along the directions (x_0, x_1, x_2, ρ) inside AdS_5 and wraps an S^2 inside the S^5. We take the S^2 to have maximal radius L inside the S^5.[2] Moreover, we assume that the embedding is such that the x_3 direction is given by a function of ρ only, i.e. $x_3 = x_3(\rho)$. Finally, we assume that there are k units of flux through the S^2, sourced by the abelian field-strength living on the brane. This means that we can write the field-strength as

$$\mathcal{F} = 2\pi\alpha' F = \left(\pi\alpha' k\right) \mathrm{vol}(S^2), \qquad k \in \mathbb{N}_0, \tag{2.2.4}$$

[2] One can also allow for an angle ψ so that the S^2 has radius $L\cos(\psi)$ and check that $\psi = 0$ is a solution to the equations of motion for ψ. It also turns out that this is a stable configuration, see [23, section 5] or [26, section 2.1].

where vol(S^2) is the volume-form on the two-sphere S^2. We will comment on the interpretation of this flux momentarily.

With this ansatz, we can proceed to evaluate the action (2.2.3). The induced metric on the world volume of the D5 brane becomes

$$ds^2_{D5} = \frac{\rho^2}{L^2}\left(-dx_0^2 + dx_1^2 + dx_2^2\right) + \left(\frac{\rho^2}{L^2}x_3'(\rho)^2 + \frac{L^2}{\rho^2}\right)d\rho^2 + L^2 d\Omega_2^2. \tag{2.2.5}$$

The field-strength $\mathcal{F}$ was given in equation (2.2.4) and with this information the first term in the action (2.2.3) can be computed. For the second term, we also need the R-R background field C_4 which was given in equation (2.2.2), pulled back to the world volume. After integrating out the S^2 part, the action becomes

$$S_{D5} = -(4\pi)\mu_5 \int_{AdS_4}\left(\sqrt{1+\left(\frac{\pi k}{\sqrt{\lambda}}\right)^2}\rho^2\sqrt{1+\frac{\rho^4}{L^4}x_3'(\rho)^2} + \left(\frac{\pi k}{\sqrt{\lambda}}\right)^2\frac{\rho^4}{L^2}x_3'(\rho)\right). \tag{2.2.6}$$

Varying S_{D5} with respect to x_3 one obtains the following equation of motion for the embedding coordinate $x_3(\rho)$:

$$\frac{\partial}{\partial\rho}\left[\sqrt{1+\left(\frac{\pi k}{\sqrt{\lambda}}\right)^2}\frac{\rho^6 x_3'(\rho)}{\sqrt{1+\frac{\rho^4}{L^4}x_3'(\rho)^2}} + \left(\frac{\pi k}{\sqrt{\lambda}}\right)L^2\rho^4\right] = 0. \tag{2.2.7}$$

This differential equation looks daunting but it turns out to have one particularly simple solution,

$$x_3(\rho) = \left(\frac{\pi k}{\sqrt{\lambda}}\right)\frac{L^2}{\rho}. \tag{2.2.8}$$

Note that in the naive limit $\lambda \longrightarrow \infty$ this solution becomes trivial. In subsection 2.4.1 below, specifically eq. (2.4.9), we will see that a connection with the holographic CFT can be made only in a certain double-scaling limit in which the parameter k^2 is also taken very large. In this region, the solution for $x_3(\rho)$ is non-trivial.

In the x_3-direction the D5 brane sits along the curve $x_3(\rho)$ determined by the solution (2.2.8). Note that as ρ goes to infinity corresponding to the boundary of AdS_5, $x_3(\rho)$ goes to zero. The D5 brane thus separates the boundary into two halves, one with $x_3 > 0$ and one with $x_3 < 0$, as claimed in the general discussion in section 2.1. Inserting the solution (2.2.8) into the induced metric (2.2.5), one indeed finds the metric of $AdS_4 \times S^2$ with AdS_4 radius of curvature $L^2\left(1+\frac{\pi^2k^2}{\lambda}\right)$.

We now come to the interpretation of the flux due to the field strength $\mathcal{F}$ given in equation (2.2.4). The field-strength is excited only in the S^2 directions. We can then consider the second term in the D5 brane action (2.2.3) which becomes

$$\mu_5\int \mathcal{F}\wedge C_4 = \mu_5\left(\pi\alpha' k\right)\int \text{vol}(S^2)\wedge C_4 = k\mu_3\int C_4, \tag{2.2.9}$$

where in the last step we have integrated over the S^2 to produce a factor of 4π and used the relation $\mu_p = \left(4\pi^2\alpha'\right)\mu_{p+2}$ between the Dp brane charges. By integrating out the S^2 we have obtained the effective coupling constant of the D5 brane to the R-R form C_4. Comparing to the last term in the general Dp brane action (2.1.1) we see that the coupling is precisely the same as the coupling of k D3 branes to C_4. The non-zero flux through the S^2 is therefore interpreted as originating from k D3 branes that are "dissolved" in the D5 probe brane.

D3 brane point of view We have now studied the D3-D5 system from the point of view of the D5 brane and seen how it is embedded into the ten-dimensional background. Studying the same system from the point of view of the D3 branes gives a complimentary perspective from which it is easier to make the connection to the defect versions of $\mathcal{N} = 4$ sYM that we will encounter in the next subsection.

The starting point is the world volume theory of N coincident D3 branes, for which the action is the non-abelian generalization of the action shown in (2.1.1) in the case $p = 3$. Expanding this action in α' one obtains[3]

$$S_{\text{D3}} \simeq -\frac{1}{2\pi g_s}\int \mathrm{d}^4x\,\mathrm{tr}\left[\frac{1}{4}F_{\mu\nu}F^{\mu\nu} + \frac{1}{2}\partial_\mu\Phi_i\partial^\mu\Phi_i + \frac{1}{4}\left[\Phi_i,\Phi_j\right]\left[\Phi_i,\Phi_j\right] + \mathcal{O}(\alpha')\right], \tag{2.2.10}$$

where Φ_i for $i = 1,\dots,6$ are $\mathrm{U}(N)$ valued scalar fields and $F_{\mu\nu}$ is the (non-abelian) field-strength, both living on the world volume of the D3 brane. The equations of motions for the scalar fields are

$$\Box\,\Phi_i(x) - \left[\Phi_j(x),\left[\Phi_j(x),\Phi_i(x)\right]\right] = 0, \tag{2.2.11}$$

where $\Box = \partial_\mu\partial^\mu$ is the d'Alembert operator. A particular solution that describes the situation in which k out of the N coincident D3 branes "expand" into a D5 brane are the block matrices

$$\Phi_i(x) = \pm\frac{1}{x_3}\begin{bmatrix}(t_i)_{k\times k} & \mathbf{0}_{k\times(N-k)}\\ \mathbf{0}_{(N-k)\times k} & \mathbf{0}_{(N-k)\times(N-k)}\end{bmatrix} \qquad \text{for} \qquad i\in\{1,2,3\}, \tag{2.2.12}$$

and $\Phi_i = 0$ for $i \in \{4,5,6\}$. The matrices t_i in the upper left block of (2.2.12) form a k-dimensional irreducible[4] representation of the Lie algebra $\mathfrak{su}(2)$, i.e. they satisfy the commutation relations

$$\left[t_i, t_j\right] = i\epsilon_{ijk}t_k. \tag{2.2.13}$$

The solution (2.2.12) is called a *fuzzy funnel*; for each value of $x_3 \neq 0$, the scalars Φ_i, $i \in \{1,2,3\}$, describe a non-commutative two-sphere with radius

$$R^2_{\text{funnel}}(x) = \frac{\left(2\pi\alpha'\right)^2}{k}\sum_{i=1}^{3}\mathrm{tr}\left[\Phi_i(x)\Phi_i(x)\right] = \left(2\pi\alpha'\right)^2\frac{(k-1)(k+1)}{4}\frac{1}{x_3^2}. \tag{2.2.14}$$

As x_3 goes to zero, R_{funnel} diverges which is interpreted as an expansion of k out of the N coincident D3 branes into a D5 brane with k units of flux. In the limit, the brane fills out the space time directions (X^4, X^5, X^6) corresponding to the scalars (Φ_1, Φ_2, Φ_3) and we recover the situation shown in table 2.1.

The two signs in the solution (2.2.12) have the following meaning: If $x_3 > 0$, then choosing the plus sign in Φ_i leads to a negative charge for the D5 brane and thus the D5 brane is in fact an D5 anti-brane. On the other hand, choosing the minus leads to a positive charge and is thus the correct choice for a D5 brane. The sign of the charge can be derived by evaluating the second term in the action (2.1.1) on the solution; this is done in [27, section 3.1].

[3] We are dropping a term proportional to $\int \mathrm{d}^4x\,N$ here.

[4] One can in principle consider reducible representations of $\mathfrak{su}(2)$. This would correspond to several D5 branes emerging from the same k D3 branes [27]

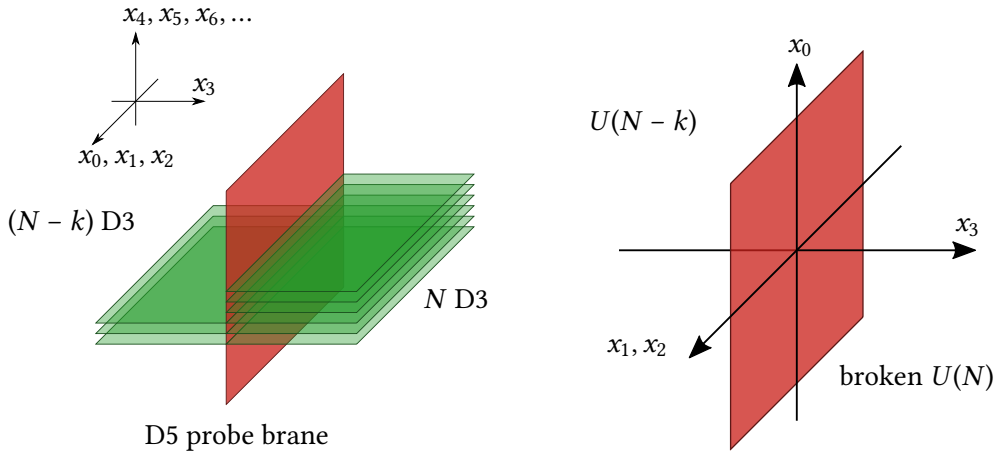

Figure 2.1: Brane configuration in string theory (left) and the dual field theory picture (right) with different gauge groups on each side of the defect at $x_3 = 0$.

Summary The picture that emerges from this section is shown in the left of figure 2.1. Starting with N coincident D3 branes and a single D5 probe brane oriented according to table 2.1, we consider the solution (2.2.12) that corresponds to k out of the N branes dissolving into the probe D5 brane. The D5 brane is embedded into the $AdS_5 \times S^5$ solution to type IIB supergravity and in the probe brane approximation we are neglecting the backreaction of the D5 brane onto the geometry. The geometry of the D5 brane is $AdS_4 \times S^2$ and the parameter k also appears as the flux of a gauge field supported on the D5 world volume through the S^2.

We now analyze the field theory dual to this setup. The 3–3 open strings give rise to the degrees of freedom of a defect version of $\mathcal{N} = 4$ sYM in which some of the scalars acquire a non-zero vacuum expectation value. The 3–5 and 5–3 open strings may correspond to extra degrees of freedom localized on the hyperplane $x_3 = 0$; however, it turns out that they are only present in the case where $k = 0$. The 5–5 strings can be neglected in the near-horizon limit.

2.2.2 Field theory side

As suggested in [23, 24], the field theory dual to the probe-brane system described in the previous subsection should be a four-dimensional defect conformal field theory with a flat codimension-one interface at $x_3 = 0$. A different field theory can live on each of the half-spaces $x_3 > 0$ and $x_3 < 0$ and the two theories may be coupled through a three-dimensional theory living on the interface at $x_3 = 0$. As we will describe in more detail below, this situation can be studied by "folding" the theory for $x_3 < 0$ to $x_3 > 0$ studying a "product theory" on the half-space $x_3 > 0$. Since the string theory side preserves half the amount of supersymmetry, the same should hold for the field theory dual. This is achieved by imposing certain supersymmetry-preserving boundary conditions on the fields at the interface located at $x_3 = 0$.

According to the AdS/CFT correspondence, the field theory dual to type IIB supergravity on $AdS_5 \times S^5$ is $\mathcal{N} = 4$ sYM theory in four dimensions with gauge group U(N). Similarly, the field theory dual to the probe D3-D5 probe-brane system is a defect version of $\mathcal{N} = 4$ sYM in which the rank of the gauge group is U($N - k$) for $x_3 < 0$ and U(N) for $x_3 > 0$. By the folding trick the possible supersymmetric boundary conditions for the fields follow from the boundary

conditions for a version of $\mathcal{N} = 4$ sYM on a half-space with gauge group $\mathrm{U}(N-k) \times \mathrm{U}(N)$. Supersymmetry-preserving boundary conditions for $\mathcal{N} = 4$ on a half-space were considered by Gaiotto and Witten in [28]. Their main results will be reviewed in this section momentarily. Another review of their work was recently given in [29, section 2.1].

The interface at $x_3 = 0$ breaks some of the symmetries of $\mathcal{N} = 4$ sYM theory. Most notably, translations in the x_3-direction (perpendicular to the interface) and rotations that change the plane $x_3 = 0$ are no longer symmetries of the theory. In total, the four-dimensional conformal group $\mathrm{SO}(2,4)$ is reduced to the three-dimensional conformal group $\mathrm{SO}(2,3)$. Note that $\mathrm{SO}(2,3)$ is also the group of isometries of the AdS_4 part of the D5 probe brane. The SO(6) R-symmetry of $\mathcal{N} = 4$ sYM is reduced to $\mathrm{SO}(3) \times \mathrm{SO}(3)$ by the interface. The first SO(3) factor corresponds precisely to the isometries of the S^2 part of the D5 brane geometry.

Half-space with full gauge symmetry The boundary conditions for the four-dimensional defect $\mathcal{N} = 4$ sYM theory are most easily derived by dimensional direction from ten-dimensional $\mathcal{N} = 1$ sYM theory. In ten dimensions, the action of $\mathcal{N} = 1$ sYM is

$$S = \frac{1}{e^2} \int \mathrm{d}^{10}x \, \mathrm{tr} \left[\frac{1}{2} \hat{F}_{IJ} \hat{F}^{IJ} - i\overline{\Psi} \Gamma^I D_I \Psi \right], \tag{2.2.15}$$

where $\hat{F}_{IJ}$ is the field strength of the gauge field $\hat{A}_I$, Ψ is a Majorana-Weyl fermion, and Γ_I are the (16×16)-dimensional matrices satisfying the Clifford algebra $\{\Gamma_I, \Gamma_J\} = 2g_{IJ}$ in ten dimensions. The possible boundary conditions are derived from the requirement that there is no flux of the supercurrent through the boundary. The expression for the supercurrent is

$$J^I = \frac{1}{2} \mathrm{tr} \left[\Gamma^{JK} \hat{F}_{JK} \Gamma^I \Psi \right], \tag{2.2.16}$$

and the condition that the flux vanishes means that the normal component J^3 has to vanish at $x_3 = 0$. This ensures supersymmetry.

As usual in dimensional reduction, the components $\hat{A}_I$ of the gauge field in ten dimensions turn into components A_μ of a four-dimensional gauge field and six real scalars ϕ_i,

$$A_\mu = \hat{A}_\mu, \quad \phi_i = \hat{A}_{i+3}. \tag{2.2.17}$$

In the presence of the boundary the SO(6) R-symmetry of the scalars ϕ_i is broken to the subgroup $\mathrm{SO}(3)_X \times \mathrm{SO}(3)_Y$ where the subscripts X and Y refer to the action on the subsets of scalars

$$(X_1, X_2, X_3) = (\phi_1, \phi_2, \phi_3) \quad \text{and} \quad (Y_1, Y_2, Y_3) = (\phi_4, \phi_5, \phi_6), \tag{2.2.18}$$

respectively. The full bosonic symmetry group of the theory with a boundary is $\mathrm{SO}(2,3) \times \mathrm{SO}(3)_X \times \mathrm{SO}(3)_Y$. As a representation of this group, the **16** of $\mathrm{SO}(1,9)$ in which the fermion Ψ transforms is reducible and the representation space splits into a product $V_8 \otimes V_2$ where the subscript indicates the dimension.

It turns out that one can put Dirichlet boundary conditions on either the first group of scalars (X_1, X_2, X_3) or on the second group (Y_1, Y_2, Y_3), but not on both simultaneously. Putting Dirichlet conditions on (Y_1, Y_2, Y_3), one obtains the following for the bosons at $x_3 = 0$:

$$Y_a \Big|_\partial = 0, \quad \left(D_3 X_a + \frac{u}{2} \epsilon_{abc} [X_b, X_c] \right) \Big|_\partial = 0, \quad \left(\epsilon_{\lambda\mu\nu} F^{3\lambda} + \gamma F_{\mu\nu} \right) \Big|_\partial = 0. \tag{2.2.19}$$

Here and in the following we use the notation $\clubsuit\big|_\partial$ to denote the value of the quantity $\clubsuit$ on the boundary at $x_3 = 0$. For the fermion Ψ the boundary condition is

$$\Gamma_3\Psi\Big|_\partial = \Psi' \otimes v_2, \tag{2.2.20}$$

where v_2 is a fixed vector in V_2. The parameters γ and u in equation (2.2.19) are related by a single parameter a through

$$\gamma = -\frac{2a}{1-a^2}, \quad u = -\frac{2a}{1+a^2}. \tag{2.2.21}$$

Different choices of a yield different boundary conditions that are all compatible with supersymmetry. Important for us are the choices $a = \pm 1$ which gives $u = \pm 1$ and $\gamma = \pm\infty$. These conditions are called *D5-like boundary conditions*. The choices $a = 0$ and $a = \infty$ give $u = \gamma = 0$ and are called *NS5-like boundary conditions*. The family of boundary conditions parameterized by a in this way preserves full gauge symmetry on the boundary.

Reducing the gauge symmetry This procedure can be generalized to allow for boundary conditions that break part of the gauge symmetry. Suppose that we are interested in conditions that only preserve a subgroup $H \subset G$ of the gauge group G. The Lie algebra $\mathfrak{g}$ of G decomposes into the Lie algebra $\mathfrak{h}$ of H and an orthogonal complement,

$$\mathfrak{g} = \mathfrak{h} \oplus \mathfrak{h}^\perp. \tag{2.2.22}$$

With this decomposition we can write every element $\Phi \in \mathfrak{g}$ as $\Phi = \Phi^\checkmark + \Phi^\perp$, where $\Phi^\checkmark \in \mathfrak{h}$ and $\Phi^\perp \in \mathfrak{h}^\perp$. In order to retain supersymmetry on needs that $\mathfrak{h}$ is a Lie algebra (this is trivial) and that $\mathfrak{g}$ has an action on $\mathfrak{h}$, i.e.

$$[\mathfrak{h},\mathfrak{h}] \subseteq \mathfrak{h}, \quad \left[\mathfrak{h},\mathfrak{h}^\perp\right] \subseteq \mathfrak{h}^\perp. \tag{2.2.23}$$

One then imposes NS5-like boundary conditions on the fields $\Phi^\checkmark$ at the boundary:

$$F^\checkmark_{3\mu}\Big|_\partial = 0, \quad X^\checkmark_a\Big|_\partial = 0, \quad D_3 Y^\checkmark_a\Big|_\partial = 0. \tag{2.2.24}$$

The remaining fields $\Phi^\perp$ are restricted by D5-like boundary conditions,

$$F^\perp_{\mu\nu}\Big|_\partial = 0, \quad \left(D_3 X^\perp_a - \frac{1}{2}\epsilon_{abc}\left[X^\perp_b, X^\perp_c\right]^\perp\right)\Big|_\partial = 0, \quad Y^\perp_a\Big|_\partial = 0. \tag{2.2.25}$$

We note that the commutator term is not present in [28] and it vanishes if $\left[\mathfrak{h}^\perp,\mathfrak{h}^\perp\right] \subseteq \mathfrak{h}$.[5] This does not have to be the case however, see also [30, section 2.3] for a similar discussion.

The elements of the subgroup $K \subset G$ that commutes with H become global gauge transformations of the boundary conditions. Away from the boundary the gauge group is G, so the elements of K act as gauge transformations. At $x_3 = 0$ however, the gauge group is H, so the elements of K are not gauge transformations. Instead, they are considered global symmetries.

[5] In this case the quotient G/H is a symmetric space.

Application to the D3-D5 system with an interface The general discussion so far has dealt with $\mathcal{N} = 4$ sYM with a boundary at $x_3 = 0$. The situation in the D3-D5 system is slightly different and consists of an interface at $x_3 = 0$ with a version of $\mathcal{N} = 4$ sYM on each side. The difference between the two sides is the rank of the gauge group. This situation fits into the present framework with the *folding trick*: Instead of discussing two theories, one with gauge group G_+ for $x_3 > 0$ and another one with gauge group G_- for $x_3 < 0$, we flip the theory for negative x_3 by replacing $x_3 \longrightarrow -x_3$ and discuss $\mathcal{N} = 4$ sYM on a half-space with gauge group $G_+ \times G_-$. In order to keep the orientation of the ten-dimensional space, one also has to reverse the sign of an odd number of the scalars ϕ_i. Here one has to reverse the sign of either $(X_1, X_2, X_3)_{G_+}$ or $(X_1, X_2, X_3)_{G_-}$, which are the scalars (X_1, X_2, X_3) with gauge group G_+ and G_- respectively.

For simplicity, we consider the case $k = 1$, i.e. the situation with gauge groups $G_- = \mathrm{U}(N)$ for $x_3 < 0$ and $G_+ = \mathrm{U}(N+1)$ for $x_3 > 0$. The gauge group of the folded theory to which we can apply the general results is $G = \mathrm{U}(N+1) \times \mathrm{U}(N)$. We are looking for boundary conditions that preserve the diagonal subgroup $H = \mathrm{U}(N)_{\mathrm{diag}} \subset G$.

Let us check what the decomposition of the Lie algebra as $\mathfrak{g} = \mathfrak{h} \oplus \mathfrak{h}^\perp$ amounts to in this case. An element Φ of the Lie algebra $\mathfrak{u}(N+1)$ is an $(N+1) \times (N+1)$ matrix. We decompose this as

$$\Phi = \Phi^{\checkmark} + \Phi^{\perp} = \underbrace{\left(\begin{array}{c|ccc} 0 & 0 & \cdots & 0 \\ \hline 0 & & & \\ \vdots & & [\Phi]_{m,n} & \\ 0 & & & \end{array}\right)}_{=\Phi^{\checkmark}} + \underbrace{\left(\begin{array}{c|ccc} [\Phi]_{1,1} & [\Phi]_{2,1} & \cdots & [\Phi]_{N+1,1} \\ \hline [\phi]_{1,2} & & & \\ \vdots & & \mathbf{0} & \\ [\phi]_{1,N+1} & & & \end{array}\right)}_{=\Phi^{\perp}}, \tag{2.2.26}$$

where $\Phi^{\checkmark}$ contains the lower right $N \times N$ block of Φ and $\Phi^{\perp}$ is simply the rest of the matrix. In other words, $\mathfrak{h}$ consists of $(N+1) \times (N+1)$ matrices in which the first row and first column is zero, while $\mathfrak{h}^\perp$ consists of matrices in which the lower right $N \times N$ block is zero. We can check that for any Φ and Ψ,

$$\left[\Phi^{\checkmark}, \Psi^{\checkmark}\right] \in \mathfrak{h}, \quad \left[\Phi^{\checkmark}, \Psi^{\perp}\right] \in \mathfrak{h}^\perp, \quad \mathrm{tr}\left[\Phi^{\checkmark}\Psi^{\perp}\right] = 0, \tag{2.2.27}$$

so this is indeed the correct orthogonal decomposition of $\mathfrak{g}$. On the fields $\Phi^{\checkmark}$ in the $N \times N$ block we now impose the NS5-like boundary condition (2.2.24); on the remaining fields we impose the D5-like conditions (2.2.25). Note that $\left[\Phi^{\perp}, \Psi^{\perp}\right] \notin \mathfrak{h}$ so it we do indeed need the commutator term in the D5-like conditions (2.2.25). Global symmetries are generated by the matrices with a single non-vanishing entry in the $(1,1)$ component since they commute with the elements in $\mathfrak{h}$.

When $k > 1$, the gauge group of the folded theory is similarly $G = \mathrm{U}(N+k) \times \mathrm{U}(N)$. As before, the boundary conditions are supposed to preserve the diagonal subgroup $H = \mathrm{U}(N)_{\mathrm{diag}}$. The decomposition $\Phi = \Phi^{\checkmark} + \Phi^{\perp}$ is as in equation (2.2.26) except that $\Phi^{\perp}$ is non-zero in the first k rows and columns.

Concrete solutions to Nahm equations In equation (2.2.12) we already saw the fuzzy funnel solution for the scalars living on the world volume of N coincident D3 branes that corresponds to a situation where k of the D3 branes expand into a probe D5 brane. By the general AdS/CFT dictionary, this solution carries over to a classical solution for the scalar fields

ϕ_i in four-dimensional $\mathcal{N} = 4$ sYM. Thus, the classical solution in the half-space $x_3 > 0$ is

$$\phi_i^{\mathrm{cl}}(x) = -\frac{1}{x_3}\begin{bmatrix}(t_i)_{k\times k} & \mathbf{0}_{k\times(N-k)}\\ \mathbf{0}_{(N-k)\times k} & \mathbf{0}_{(N-k)\times(N-k)}\end{bmatrix} \quad \text{for} \quad i \in \{1,2,3\} \quad \text{and} \quad x_3 > 0. \tag{2.2.28}$$

All other fields, i.e. the scalars ϕ_i for $i \in \{4,5,6\}$, the gauge field and the fermions, vanish classically. For $x_3 < 0$ all fields are $\mathrm{U}(N-k)$ valued and the classical solution is zero. Recall that the matrices t_i form a k-dimensional representation of the Lie algebra $\mathfrak{su}(2)$, i.e. they satisfy the commutation relations $[t_i, t_j] = i\epsilon_{ijk}t_k$. This is enough to check that the classical solution (2.2.28) satisfies

$$D_3\phi_i^{\mathrm{cl}} - \frac{i}{2}\epsilon_{ijk}\left[\phi_j^{\mathrm{cl}}, \phi_k^{\mathrm{cl}}\right] = 0, \tag{2.2.29}$$

which is the only non-trivial boundary condition coming from equations (2.2.25) and (2.2.24). The set of equations in (2.2.29) are also known as *Nahm equations*.

The classical solution (2.2.28) applies only for $x_3 > 0$, while for $x_3 < 0$ the theory is simply four-dimensional $\mathcal{N} = 4$ sYM with certain boundary conditions on the fields. So far we have not made any statements about the field theory living *on* the defect at $x_3 = 0$. Two cases can be distinguished:

- Case $k = 0$: When $k = 0$, the number of D3 branes is the same on both sides of the D5 brane in figure 2.1. Equivalently, the rank of the gauge group in the defect CFT is the same for $x_3 > 0$ and $x_3 < 0$ and the classical solution (2.2.28) is trivial. In this case, the theory on the interface consists of two complex scalars q^m, $m \in \{1,2\}$, and two Dirac fermions Ψ^i, $i \in \{1,2\}$. Both the scalars and the fermions transform in the fundamental representation of the gauge group and correspond to open string degrees of freedom stretching between the D3 and D5 branes. The string as well as the field theory side of this theory were described in detail in [31]. The new fields on the interface are coupled to the "bulk" fields by restricting the fields of $\mathcal{N} = 4$ sYM to the boundary, taking into account their boundary conditions.

- Case $k \geq 1$: It turns out that the new fields q^m and Ψ^i are not independent degrees of freedom when $k \geq 1$. Instead, they can be expressed in terms of "bulk" fields coming from defect $\mathcal{N} = 4$ sYM restricted to $x_3 = 0$. The argument was originally given in [28, section 3.4.2]; slightly more details may be found in [30, section 3.2.1] and [32, appendix C].

Note that the case $k = 1$ is special: On the one hand, there are no new additional fields on the interface, but on the other hand the classical solution (2.2.28) is still trivial, because the matrices t_i form the one-dimensional representation of $\mathfrak{su}(2)$. This case was studied in detail in [32, 33].

Fluctuations around the classical solution One can now consider fluctuations of the defect CFT fields around the classical solution (2.2.28). Since the classical solution is non-zero only for some of the scalars, but not for any of the other fields, this amounts to expanding the scalars as

$$\phi_i(x) = \phi_i^{\mathrm{cl}}(x) + \tilde{\phi}_i(x), \quad i \in \{1,\dots,6\}, \tag{2.2.30}$$

where $\tilde{\phi}_i(x)$ is the fluctuation.

Inserting this expansion into the action of $\mathcal{N} = 4$ sYM given in equation (A.1.1) one can observe that mass terms for the field fluctuations are generated. Schematically, some of those terms coming from the scalar potential are

$$\mathrm{tr}\left(\left[\phi_i, \phi_j\right]\left[\phi_i, \phi_j\right]\right) \xrightarrow{\phi_i = \phi_i^{\mathrm{cl}} + \tilde{\phi}_i} \mathrm{tr}\left(\left[\phi_i^{\mathrm{cl}}, \tilde{\phi}_j\right]\left[\phi_i^{\mathrm{cl}}, \tilde{\phi}_j\right] + \left[\phi_i^{\mathrm{cl}}, \tilde{\phi}_j\right]\left[\tilde{\phi}_i, \phi_j^{\mathrm{cl}}\right] + \cdots\right). \tag{2.2.31}$$

As can be seen from the second term on the right hand side, the mass terms are not diagonal and mix $\tilde{\phi}_i$ and $\tilde{\phi}_j$ for $i \neq j$. Moreover, for $k > 1$ the classical solution is a non-trivial $N \times N$ matrix and the mass terms therefore also mix up the color structure of different fields. This mixing problem was solved in [34] by expanding the fields in so-called *fuzzy spherical harmonics* which are eigenfunctions of the Laplacian of a fuzzy two-sphere.[6] Each mode on the fuzzy-two sphere corresponds to a scalar with a different mass.[7] Subsequently, position space Feynman rules were obtained allowing for perturbative computations in the defect CFT.

The classical solution (2.2.28) contains a factor x_3^{-1}, so that the mass terms in equation (2.2.31) are proportional to x_3^{-2}. Note that that this is required for scale invariance of the Lagrangian: Under a scaling transformation $x^\mu \longrightarrow \lambda x^\mu$, the scalar fluctuations transform as $\tilde{\phi}_i \longrightarrow \lambda^{-1}\tilde{\phi}_i$. Together with $x_3^{-2} \longrightarrow \lambda^{-2} x_3^{-2}$ this implies that the mass terms (2.2.31) pick up a factor of λ^{-4} which is the correct behavior for a scale-invariant Lagrangian in four dimensions. One can similarly check all the other terms in the expanded Lagrangian given in [34, section 2.2].

The x_3-dependence of the mass terms also means that even after the mixing problem has been solved, the propagators are not simply the flat-space propagators in four dimensions. After the diagonalization each massive mode φ has an action of the form

$$S_{\mathrm{toy}} = -\frac{2}{g_{\mathrm{YM}}^2}\int \mathrm{d}^4x \left[\frac{1}{2}\left(\partial_\mu\varphi\right)\left(\partial^\mu\varphi\right) + \frac{m^2}{x_3^2}\varphi^2\right], \tag{2.2.32}$$

where the "dimensionless mass" m^2 depends on the su(2) representation of the fuzzy spherical harmonic corresponding to φ. Applying the Weyl rescaling

$$\eta_{\mu\nu} \longrightarrow g_{\mu\nu} = x_3^{-2}\eta_{\mu\nu}, \qquad \sqrt{-\eta} \longrightarrow \sqrt{-g} = x_3^{-4}, \qquad \varphi \longrightarrow \overline{\varphi} = x_3\varphi, \tag{2.2.33}$$

this action becomes

$$S_{\mathrm{toy}} \longrightarrow -\frac{2}{g_{\mathrm{YM}}^2}\int \mathrm{d}^4x\,\sqrt{-g}\left[g^{\mu\nu}\left(\partial_\mu\overline{\varphi}\right)\left(\partial_\nu\overline{\varphi}\right) + \left(m^2 - 2\right)\overline{\varphi}^2\right]. \tag{2.2.34}$$

This is the action for a massive scalar $\overline{\varphi}$ of mass $m^2 - 2$ on AdS_4. Consequently, the propagators for the original field φ with x_3-dependent mass is given by (a rescaled version of) the propagator for scalar with mass $m^2 - 2$ in AdS_4. A similar statement holds for the fermions in the theory, c.f. [34, section 4.2].

[6] Fuzzy spherical harmonics first appear in Hoppe's PhD thesis in [35] and were introduced more formally by Madore in [36]. Explicit constructions for fuzzy spherical harmonics in various dimensions in terms of matrices can be found in [37]. We also refer to [34, appendix B] for a review of the S^2 fuzzy spherical harmonics.

[7] This is very similar to an expansion in Kaluza-Klein modes.

2.3 The D3-D7 system

In section 2.2 we reviewed the D3-D5 system and the fuzzy funnel solution (2.2.12) that corresponds to k out of the N D3 branes opening up into a probe D5 brane. The cross-section of the funnel for $x_3 \neq 0$ was a fuzzy two-sphere. A natural generalization is to look for other funnel solutions in which the cross section is a different fuzzy space. The D3-D7 probe brane system provides two such solutions:

- In the first solution, the cross-section of the funnel is a fuzzy four-sphere and the geometry of the D7 brane(s) is $AdS_4 \times S^4$. We will describe the brane construction for this solution in more detail in subsection 2.3.1. The original construction for this model can be found in [26, section 2.2]; a similar D1-D5 brane intersection involving a fuzzy four-sphere was previously treated in [38, sections 3, 4].
- In the second solution, the cross section is a product of two fuzzy spheres and the geometry of the D7 brane is $AdS_4 \times S^2 \times S^2$. We will not describe the brane construction for this solution in detail, because it is very similar to the one for the $AdS_4 \times S^4$ solution as well as for the one for the D3-D5 system. The original reference for this model is [39] and we will mention the most important features at the end of section 2.3.1.

In both cases the probe D7 brane(s) are oriented according to table 2.1. Note that both solutions break supersymmetry completely as the total number of ND and DN directions is six.

2.3.1 String theory side

As in the case of a D5 probe brane there are two complimentary points of views and we begin as before to study the system from the point of view of the probe brane.

D7 brane point of view It turns out that due to the lack of supersymmetry the naive embedding of a single D7 brane with $AdS_4 \times S^4$ geometry is unstable. One way to stabilize the system is to tune the world volume gauge field such that there is a non-zero instanton number on the S^4 part of the geometry. However, this comes at a cost: The world volume gauge field has to be non-abelian and we are forced to consider a number $N_7 > 1$ of coincident D7 branes.

We again write the background metric of $AdS_5 \times S^5$ into which the probe branes are embedded as in (2.2.1). The non-abelian generalization of the action (2.1.1) for D7 branes takes the form

$$S_{D7} = -\mu_7 \int_{D7} \mathrm{str}\left[\sqrt{-\det(G+\mathcal{F})}\right] + \frac{\mu_7}{2}\int_{D7} \mathrm{str}\left[\mathcal{F}\wedge\mathcal{F}\wedge C_4\right], \tag{2.3.1}$$

where str stands for the "symmetrized trace" prescription [40].

Analogously to the D3-D5 system, we make an ansatz for the embedding of the D7 branes into the $AdS_5 \times S^5$ background: The world volume of the D7 extends along the directions (x_0, x_1, x_2, ρ) inside AdS_5 and wraps an S^4 inside the S^5. As before, we take the S^4 to have maximal radius L and we assume that the embedding coordinate x_3 is a function only of ρ. The analogy of the flux in the D5 brane case is the non-vanishing instanton number d_G on the S^4 required for stability,

$$\int_{S^4} \mathrm{tr}\left(\mathcal{F}\wedge\mathcal{F}\right) = 8\pi^2\left(2\pi\alpha'\right)^2 d_G. \tag{2.3.2}$$

In the following we consider a self-dual field strength, so that d_G is positive.

With this ansatz for the embedding, the induced metric on the world volume of the D7 brane becomes

$$\mathrm{d}s^2_{\mathrm{D7}} = \frac{\rho^2}{L^2}\left(-\mathrm{d}x_0^2 + \mathrm{d}x_1^2 + \mathrm{d}x_2^2\right) + \left(\frac{\rho^2}{L^2}x_3'(\rho)^2 + \frac{L^2}{\rho^2}\right)\mathrm{d}\rho^2 + L^2\mathrm{d}\Omega_4^2. \tag{2.3.3}$$

The action (2.3.1) can now be evaluated and after integrating over the S^4 part of the geometry it becomes

$$S_{\mathrm{D7}} = -\mu_7 N_7 \left(\frac{8\pi^2}{3}\right) L^2 \int \mathrm{d}^4x \left((1+Q)\rho^2\sqrt{1+\frac{\rho^4}{L^4}x_3'(\rho)^2} - Q\frac{\rho^4}{L^2}x_3'(\rho)\right). \tag{2.3.4}$$

Note that this is very similar in form to the action for the D5 brane shown in (2.2.6). Consequently the equation of motion for $x_3(\rho)$ is essentially the same as in (2.2.7) and as a solution we find

$$x_3(\rho) = \frac{\Lambda}{\rho}, \quad \Lambda = \frac{Q}{\sqrt{1+2Q}}, \quad Q = \frac{6\pi^2}{\lambda}\frac{d_G}{N_7}. \tag{2.3.5}$$

As before one can verify that the induced metric (2.3.3) evaluated on the solution (2.3.5) becomes the metric of an AdS_4 space with radius of curvature $R^2\left(1+\Lambda^2\right)$.

The second term in the D7 brane action (2.3.1) includes a coupling between the instantons on the S^4 and the R-R four-form C_4. Integrating out the S^4 using (2.3.2) we find that the effective coupling is

$$\frac{\mu_7}{2}\left(8\pi^2\right)\left(2\pi\alpha'\right)^2 d_G = d_G\left(4\pi^2\alpha'\right)^2\mu_7 = d_G\mu_3, \tag{2.3.6}$$

where we again used the relation $\mu_p = \left(4\pi^2\alpha'\right)\mu_{p+2}$. This is precisely the right constant for coupling d_G D3 branes to the four-form. The S^4 instantons are therefore interpreted as d_G D3 branes that are dissolved in the N_7 D7 branes.

The configuration where the D7 brane wraps a maximal S^4 inside the ambient S^5 is unstable. A condition for stability was derived in [26, section 2.2] as follows: For a non-maximal S^4 we have to replace its radius L by $L\cos(\psi)$ where $\psi \in \left[0, \frac{\pi}{2}\right]$. The angle ψ corresponds to a massive field on the world volume of the D7 brane. It turns out that the mass of this field only satisfies the Breitenlohner-Freedman bound for a massive field in AdS_4 if only if

$$Q > \frac{7}{2}. \tag{2.3.7}$$

In particular this bound rules out $d_G = 0$.

D3 brane point of view From the D3 brane point of view we are again looking for a solution to the equations of motion for the scalars Φ_i that were given in (2.2.11). However, this time the solution should describe a number d_G of the D3 branes opening up into a D7 brane. The solution corresponding to the D7 brane with $\mathrm{AdS}_4 \times S^4$ geometry is a fuzzy funnel in which the cross-section is a non-commutative four-sphere,

$$\Phi_i(x) = \pm\frac{1}{2\sqrt{2}x_3}\begin{bmatrix}(G_i)_{d_G\times d_G} & \mathbf{0}_{d_G\times(N-d_G)}\\ \mathbf{0}_{(N-d_G)\times d_G} & \mathbf{0}_{(N-d_G)\times(N-d_G)}\end{bmatrix}, \quad i\in\{1,2,3,4,5\}, \tag{2.3.8}$$

and $\Phi_6 = 0$. The $d_G \times d_G$ matrices G_i can be constructed as an n-fold symmetrized tensor product of γ-matrices and their commutators $G_{ij} = \frac{1}{2}[G_i, G_j]$ are the generators of an irreducible d_G-dimensional representation of $\mathfrak{so}(5)$. The construction as well as many useful properties of the matrices G_i can be found in [41, appendix A]; here we only note that they satisfy

$$d_G = \frac{1}{6}(n+3)(n+2)(n+1) \qquad \text{and} \qquad \sum_{i=1}^{5} G_i G_i = n(n+4)\mathbb{1}_{d_G \times d_G}. \tag{2.3.9}$$

The cross-section of the funnel solution (2.3.8) is a non-commutative four-sphere with radius

$$R_{\text{funnel}}(x) = \frac{\left(2\pi\alpha'\right)^2}{d_G} \sum_{i=1}^{5} \operatorname{tr}\left[\Phi_i(x)\Phi_i(x)\right] = \left(2\pi\alpha'\right)^2 n(n+4)\frac{1}{x_3^2}, \tag{2.3.10}$$

which again diverges at $x_3 = 0$. This is interpreted as the expansion of d_G out of the N coincident D3 branes into the D7 brane located at $x_3 = 0$. As before we recover the brane arrangement shown in table 2.1.

The two signs in the solution (2.3.8) again correspond to D7 branes and anti-branes. It turns out that the sign correlation is reversed compared to the D3-D5 system and one has to choose the plus sign in Φ_i for D7 branes and the minus sign for D7 anti-branes. This is discussed in [38, section 3].

Relation between N_7 and n The number N_7 of probe D7 branes and the integer n are related. Note that in (2.3.9) we have used n to express the dimension d_G of the matrices G_i which equals the number of D3 branes dissolving into the D7 branes. On the other hand, d_G is the instanton number on the S^4, see (2.3.2).

To construct a D7 world volume gauge field satisfying (2.3.2), we have to construct a homogeneous instanton solution on the four-sphere for an SU(N_7) gauge group. The explicit construction may be found in [38, appendix B]. The idea is to start with the BPST instanton for SU(2) gauge theory and replace the generators of the fundamental representation of the SU(2) gauge group by an N_7-dimensional representation of SU(2).

The largest possible S^4 instanton number can be obtained by choosing the irreducible N_7-dimensional representation of SU(2). In this case the instanton number is

$$d_G = \frac{1}{6}N_7(N_7+1)(N_7-1). \tag{2.3.11}$$

Comparing this expression for d_G to the formula given in (2.3.9) we see that we have to identify

$$N_7 = n + 2. \tag{2.3.12}$$

Note that even for $n = 0$, we still have $N_7 > 1$ D7 branes and therefore a non-abelian theory.

The solution with $\mathrm{AdS}_4 \times S^2 \times S^2$ geometry As mentioned in the beginning of section 2.3, there exists another solution where the D7 probe brane has geometry $\mathrm{AdS}_4 \times S^2 \times S^2$ [39]. In this case there are no instantons; instead the world volume gauge field is such that there are k_1 and k_2 units of flux through the first and the second S^2 respectively. Apart from this difference, the construction of the embedding is very similar to the two cases that were discussed in this thesis. Further details may be found in the original paper [39, section 2] or [42, section 3.1].

2.3.2 Field theory side

A lot of the discussion in section 2.2.2 for the field theory dual to the D3-D5 system carries over the D3-D7 system. In particular, we again obtain a defect conformal field theory with gauge groups of different ranks for $x_3 > 0$ and $x_3 < 0$.

The solution (2.3.8) for the scalar fields living on the world volume of the D3 brane translates into a classical solution for five out of the six scalar fields of $\mathcal{N} = 4$ sYM,

$$\phi_i^{\text{cl}}(x) = \frac{1}{2\sqrt{2}x_3} \begin{bmatrix} (G_i)_{d_G \times d_G} & \mathbf{0}_{d_G \times (N-d_G)} \\ \mathbf{0}_{(N-d_G)\times d_G} & \mathbf{0}_{(N-d_G)\times(N-d_G)} \end{bmatrix}, \quad i \in \{1,2,3,4,5\}, \tag{2.3.13}$$

and $\phi_6^{\text{cl}} = 0$. As before the gauge field and the fermions vanish classically. The "size" d_G of the classical solution again translates into the difference of the rank of the gauge groups: for $x_3 > 0$ the gauge group is $\mathrm{U}(N)$, while for $x_3 < 0$ the gauge group is $\mathrm{U}(N - d_G)$. Since the D3-D7 probe brane system is not supersymmetric, the discussion about supersymmetric boundary conditions does not apply. In particular, one can check that the Nahm equations (2.2.29) are not fulfilled for this solution.

In the classical solution corresponding to a D7 probe brane with $\mathrm{AdS}_4 \times S^2 \times S^2$ geometry all six scalar fields acquire a non-zero classical solution,

$$\begin{aligned} \phi_i^{\text{cl}}(x) &= -\frac{1}{x_3} \begin{bmatrix} (t_i)_{k_1\times k_1} \otimes \mathbf{1}_{k_2\times k_2} & \mathbf{0}_{k_1k_2\times(N-k_1k_2)} \\ \mathbf{0}_{(N-k_1k_2)\times k_1k_2} & \mathbf{0}_{(N-k_1k_2)\times(N-k_1k_2)} \end{bmatrix}, \quad i \in \{1,2,3\}, \\ \phi_i^{\text{cl}}(x) &= -\frac{1}{x_3} \begin{bmatrix} \mathbf{1}_{k_1\times k_1} \otimes (t_i)_{k_2\times k_2} & \mathbf{0}_{k_1k_2\times(N-k_1k_2)} \\ \mathbf{0}_{(N-k_1k_2)\times k_1k_2} & \mathbf{0}_{(N-k_1k_2)\times(N-k_1k_2)} \end{bmatrix}, \quad i \in \{4,5,6\}. \end{aligned} \tag{2.3.14}$$

Here the matrices t_i are the same that appeared in the D3-D5 system, i.e. they satisfy the su(2) commutation relations given in (2.2.13). As before, the remaining fields vanish classically. The different gauge groups are $\mathrm{U}(N - k_1k_2)$ for $x_3 < 0$ and $\mathrm{U}(N)$ for $x_3 > 0$.

One important difference compared to the D3-D5 system is that the instanton number d_G and the fluxes k_1 and k_2 cannot be zero, otherwise the solution is unstable. Unlike before we can therefore not consider the case of equal gauge groups on both sides of the interface.

Other than that the discussion about fluctuations around the classical solution on page 17 still applies to the present case. In particular, mass terms of the form shown in (2.2.31) are generated by inserting the expansion $\phi_i = \phi_i^{\text{cl}} + \tilde{\phi}_i$ into the action of $\mathcal{N} = 4$ sYM. The mixing problem for the solution (2.3.13) was solved in [6] and for the solution (2.3.14) in [5]. In both cases, the fields of the defect theory had to be expanded in modes on the respective fuzzy geometry, i.e. in fuzzy spherical harmonics for S^4 and $S^2 \times S^2$ respectively.

2.4 Observables

In the previous sections we have described the D3-D5 and D3-D7 probe brane systems and their field theory duals in some detail. To check and make use of the proposed extension of the usual AdS/CFT duality to these defect conformal field theories, one would like to compare physical observables computed on both sides of the correspondence. It turns out that in particular one-point functions of field theory operators as well as expectation values of field theory Wilson loops can also be computed on the string theory side as we describe in this section.

2.4.1 One-point functions

We focus on computations on the side $x_3 > 0$ of the interface where we have a non-zero classical solution given by either (2.2.28), (2.3.13) or (2.3.14). In this case we are dealing with a defect conformal field theory with a boundary. The reduced conformal symmetry allows for non-trivial one-point functions of conformal operators of the form

$$\langle \mathcal{O}(\hat{x}, x_3) \rangle = \frac{a_{\mathcal{O}}}{x_3^{\Delta}}, \tag{2.4.1}$$

where we are using the notation $\hat{x} = (x_0, x_1, x_2)$ to denote the coordinates on the boundary at $x_3 = 0$. The one-point functions can be computed both in string theory and in the defect CFT. In a certain double-scaling limit they may even be compared allowing for tests of the proposed duality between supergravity on $AdS_5 \times S^5$ with probe branes and defect versions of $\mathcal{N} = 4$ sYM. We will return to this limit below.

The field theory operators that can be matched most easily in the AdS/CFT dictionary are chiral primary operators of conformal dimension Δ. On the AdS side, these operators correspond to supergravity Kaluza-Klein modes with mass $m^2 L^2 = \Delta(\Delta - 4)$. A chiral primary operator in $\mathcal{N} = 4$ sYM is of the form

$$\mathcal{O}_{\Delta,a}(x) = \left(\frac{\left(8\pi^2\right)^{\Delta/2}}{\lambda^{\Delta/2}\sqrt{\Delta}} \right) C_a^{i_1 \cdots i_\Delta} \operatorname{tr}\left[\phi_{i_1}(x) \cdots \phi_{i_\Delta}(x)\right], \tag{2.4.2}$$

where $C_a^{i_1 \cdots i_\Delta}$ is a tensor that is totally symmetric and traceless in the indices $(i_1, \ldots, i_\Delta)$. Each index i_k take values in $\{1, \ldots, 6\}$ and transforms under the action of the SO(6) R-symmetry. Thus $C_a^{i_1 \cdots i_\Delta}$ describes a state labeled by a in the symmetric traceless irreducible representation of SO(6) and a should run from 1 to $\frac{1}{12}(\Delta + 3)(\Delta + 2)^2(\Delta + 1)$.[8]

By construction the chiral primary (2.4.2) has good quantum numbers with respect to the original SO(6) R-symmetry. In the defect CFT however, the R-symmetry is broken to SO(3)×SO(3) in the case of the classical solutions (2.2.28) and (2.3.14) and to SO(5) in the case of the classical solution (2.3.13). It turns out that only those chiral primaries that are symmetric with respect to the residual R-symmetry can have a non-zero one-point function. Moreover, for a given Δ, there is a *unique* linear combination of chiral primaries $\mathcal{O}_{\Delta,a}$ that satisfies this property, both in the case of SO(3) × SO(3) (see [43, appendix A]) and SO(5) (see [42, section 4.1.1]) residual R-symmetry. By abuse of notation we will simply call this linear combination $\mathcal{O}_\Delta$ in the following.

String theory side The GKPW prescription shown in equation (A.2.3) in appendix A.2 gives a general recipe for the computation of field theory correlators from the dual supergravity theory. For a one-point function, the general formula reduces to

$$\langle \mathcal{O}_\Delta(x) \rangle = -\frac{\delta S_{\text{cl}}[s^{(0)}]}{\delta s^{(0)}(x)}. \tag{2.4.3}$$

To use this formula, one first has to identify the supergravity Kaluza-Klein modes on S^5 that are dual to the chiral primaries in (2.4.2). The chiral primaries correspond to an SO(6) representation

[8] The dimension $d(p_1, p_2, p_3)$ of an irreducible SO(6) representation labeled by Dynkin labels $[p_1, p_2, p_3]$ is $d(p_1, p_2, p_3) = \frac{1}{12}(p_1 + 1)(p_2 + 1)(p_3 + 1)(p_1 + p_2 + 2)(p_1 + p_3 + 2)(p_1 + p_2 + p_3 + 3)$. The symmetric traceless representation has Dynkin labels $[\Delta, 0, 0]$.

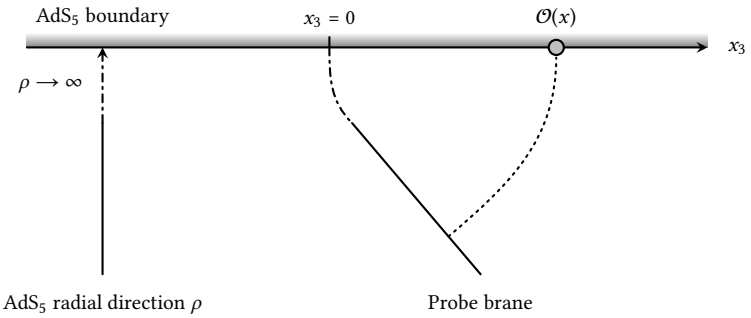

Figure 2.2: Computation of the one-point function in string theory (figure adapted from [42])

with Dynkin labels $[\Delta, 0, 0]$ and the corresponding supergravity modes should transform in the same way. Matching all quantum numbers one finds a particular linear combination $s_{\Delta,a}$ of the fluctuation of the background metric on $AdS_5 \times S^5$ and the five-form field strength on S^5, see [44, section 3.3]. Each mode $s_{\Delta,a}$ is a Kaluza-Klein mode in the expansion of a supergravity field s on $AdS_5 \times S^5$.

The next step is to compute the variation of the classical action S_{cl} with respect to a small change in s. The relevant action here is the action of the probe brane, i.e. the one given in (2.2.3) for the D3-D5 or the one given in (2.3.1) for the $AdS_4 \times S^4$ symmetric solution of the D3-D7 system. The results of this computation may be found in [43, appendix B.2] for the D3-D5 and in [42, section 3.2, section 4.2] for the D3-D7 system.

Finally, one uses that the field theory operator is located at a single point x which corresponds to a source that is simply a δ-function on the AdS_5 boundary,

$$s_\Delta^{(0)}(y) = \delta^{(4)}(x - y). \tag{2.4.4}$$

Effectively, this replaces the supergravity field s with its bulk-to-boundary propagator and the picture that results from this prescription is the following: On the boundary of AdS_5, the field theory operator $\mathcal{O}_\Delta$ sources a supergravity field s_Δ which propagates into the bulk and is integrated over the world volume of the probe brane. This situation is depicted in figure 2.2.

Field theory side On the field theory side, the recipe for computing the one-point functions is rather straightforward. To obtain the classical one-point function of a given scalar single trace operator,

$$\mathcal{O}_\Delta(x) = \mathcal{O}^{i_1 \cdots i_\Delta} \operatorname{tr}\left[\phi_{i_1}(x) \cdots \phi_{i_\Delta}(x)\right], \tag{2.4.5}$$

one simply inserts the classical solution of the scalar fields (c.f. equations (2.2.28), (2.3.14) and (2.3.13)). We denote the classical one-point function as

$$\langle \mathcal{O}_\Delta(x) \rangle^{(0)} = \mathcal{O}^{i_1 \cdots i_\Delta} \operatorname{tr}\left[\phi_{i_1}^{\text{cl}}(x) \cdots \phi_{i_\Delta}^{\text{cl}}(x)\right] = \quad \text{.} \tag{2.4.6}$$

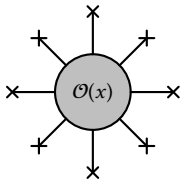

In the diagram on the right hand side, the operator is represented as the blob in the middle and the crosses symbolize the insertion of the classical solution. As mentioned earlier, only the unique chiral primary that respects the residual R-symmetry has a non-vanishing one-point function. If we consider a general single trace operator as in (2.4.5), we may get a non-zero one-point function if it has a non-zero projection onto the unique chiral primary. Note that the insertion of the classical solution leads to an expression that has an x_3-dependence of the form shown in (2.4.1): The classical solutions ϕ_i^{cl} are proportional to x_3^{-1} so that $\langle \mathcal{O}_\Delta(x) \rangle^{(0)}$ is proportional to $x_3^{-\Delta}$.

To go beyond the classical result (2.4.6), one has to take into account fluctuations of the fields around their classical solution as in (2.2.30). Corrections to the classical one-point function can then be computed by a perturbative expansion in the Yang-Mills coupling g_{YM}. This leads to an expansion in position-space Feynman diagrams. To first order in the planar limit $N \to \infty$, the fluctuations contribute two terms, see [34, section 6.1]. The first one is

$$\langle \mathcal{O}_\Delta(x) \rangle^{(1),\text{A}} = \mathcal{O}^{i_1 \cdots i_\Delta} \sum_{m=1}^{\Delta} \text{tr} \left[\phi_{i_1}^{\text{cl}} \cdots \overbrace{\tilde{\phi}_{i_m} \cdots \phi_{i_\Delta}^{\text{cl}}} \right] \int \text{d}^4 y \sum_{V_3} V_3(\Phi_1, \overbrace{\Phi_2, \Phi_3}) =$$

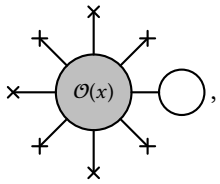

, (2.4.7)

where the sum runs over cubic interaction vertices between the fields and the lines above the equation denote Wick contractions. Similarly to the mass terms that we saw in (2.2.31), such vertices arise when expanding the action of $\mathcal{N} = 4$ sYM around the background classical solution. The second term is

$$\langle \mathcal{O}_\Delta(x) \rangle^{(1),\text{B}} = \sum_{m,n} \mathcal{O}^{i_1 \cdots i_m \cdots i_n \cdots i_\Delta} \text{tr} \left[\phi_{i_1}^{\text{cl}} \cdots \overbrace{\tilde{\phi}_{i_m} \cdots \tilde{\phi}_{i_n}} \cdots \phi_{i_\Delta}^{\text{cl}} \right] =$$

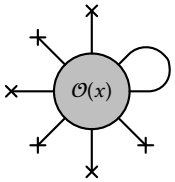

. (2.4.8)

These expressions can be evaluated once a perturbative setup consisting of Feynman rules has been found. For the D3-D5 system this was done in [34], for the two solutions of the D3-D7 system in [5] and [6]. Note that the diagrams in (2.4.7) and (2.4.8) are one-loop diagrams that contain one extra power of $\lambda = N g_{\text{YM}}^2$ compared to the classical result (2.4.6).

For general scalar operators there are further corrections to the one-point function due to renormalization of the operator and corrections to its wave function $\mathcal{O}^{i_1 \cdots i_\Delta}$. This is also described in [34, section 6.1]. However, for 1/2-BPS operators that are often considered in practice these corrections are absent.

Comparing the string and field theory One would like to compare the one-point function computed on the string theory side to the one computed by the perturbative expansion on the field theory side. The supergravity approximation used on the string theory side can be trusted when the radius of curvature L of AdS_5 is much bigger than α'. By the identification of

coupling constants in the AdS/CFT dictionary, this is the case for $\lambda \gg 1$. On the other hand, the perturbative expansion on the field theory side is valid for $\lambda \ll 1$.

The idea to connect the two regions is to make use of the additional parameters that appear as the flux or instanton numbers in the defect CFTs setups. Concretely, in the D3-D5 system with flux parameter k one considers a double-scaling limit first suggested in [45]:

$$\lambda \gg 1, \quad k \gg 1, \quad \frac{\lambda}{\pi^2 k^2} \ll 1. \tag{2.4.9}$$

Since $\lambda \gg 1$, the supergravity approximation is valid. On the other hand, if upon taking $k \gg 1$ the perturbative expansion on the field theory organizes itself in an expansion with effective coupling $\frac{\lambda}{\pi^2 k^2}$, then perturbation theory is justified. Similarly, for the D3-D7 system with $AdS_4 \times S^4$ probe brane geometry one considers the double-scaling limit

$$\lambda \gg 1, \quad n \gg 1, \quad \frac{\lambda}{\pi^2 n^2} \ll 1, \tag{2.4.10}$$

where the integer n is related to the instanton number d_G by the dimension formula (2.3.9).

In a perturbative computation on the field theory side it is easiest not to compute the one-point function of the unique chiral primary with the relevant residual R-symmetry, but to consider the operator

$$\mathcal{O}(x) = \mathrm{tr}\left[\underbrace{Z(x)\cdots Z(x)}_{L}\right] = \mathrm{tr}\left[Z(x)^L\right], \tag{2.4.11}$$

where Z is a complex combination of the scalars in $\mathcal{N} = 4$ sYM, for example $Z = \phi_1 + i\phi_3$.[9] To compare the one-point function of the operator $\mathrm{tr}\left[Z(x)^L\right]$ to the one-point function of the chiral primary $\mathcal{O}_\Delta$ the latter has to be projected onto the former. To this end, $\mathrm{tr}\left[Z(x)^L\right]$ is written as a linear combination of the form

$$\mathrm{tr}\left[Z(x)^L\right] = \sum_a c_a \, \mathcal{O}_{\Delta,a}(x) \tag{2.4.12}$$

for some coefficients c_a. One of the terms in this sum is the unique conformal primary $\mathcal{O}_\Delta$ that is symmetric with respect to the residual R-symmetry and, as remarked earlier, only this operator has a non-vanishing one-point function. In particular this means that in order to compare the first order in the double-scaling parameters, we should compare

$$\frac{\left\langle \mathrm{tr}\left[Z(x)^L\right]\right\rangle^{(1)}}{\left\langle \mathrm{tr}\left[Z(x)^L\right]\right\rangle^{(0)}} \quad \text{and} \quad \frac{\langle \mathcal{O}_\Delta(x)\rangle^{(1)}}{\langle \mathcal{O}_\Delta(x)\rangle^{(0)}}. \tag{2.4.13}$$

This argument was first used in [34, section 7].

Results We briefly summarize the results about one-point functions that were obtained for the D3-D5 and D3-D7 systems respectively. For the D3-D5 system the classical one-point function of the unique chiral primary was computed both in string and field theory in [43] and agreement

[9] It is most convenient to choose $Z = \phi_1 + i\phi_3$ for the D3-D5 system and $Z = \phi_5 + i\phi_6$ for the D3-D7 system with probe brane geometry $AdS_4 \times S^4$. With this choice only one scalar contributes to the classical solution for Z.

between both sides was found in the double-scaling (2.4.9). Feynman rules and propagators for the field theory side were derived in [34] and to first order in the double-scaling parameter agreement was found between the ratios in (2.4.13).

For both classical solutions of the D3-D7 system, one point functions were computed and matched between string and field theory in [42]. Perturbative setups for the two solutions were derived by us in [5] and [6] respectively. In both cases agreement between the one-point function ratios (2.4.13) was found to first order in the double-scaling parameter.

The idea to use a double-scaling limit to compare quantities computed at $\lambda \gg 1$ and $\lambda \ll 1$ is similar to the construction by Berenstein, Maldacena and Nastase (BMN) in [46]. It is well known that the BMN expansion does not work to all orders in the double-scaling parameter due to an order-of-limits problem (see [47, section 4]) and it is conceivable that similar problems arise in the double-scaling limits (2.4.9) and (2.4.10) at higher order.

Connections to integrability As a closing remark, let us mention that the one-point functions of field theory operators discussed in this section have interesting connections to integrability. In particular, the classical one-point functions of certain non-protected scalar operators can be expressed as overlaps between Bethe eigenstates describing the operator and a fixed "boundary state". The overlaps can be expressed in closed form in terms of determinants of Gaudin matrices. For the D3-D5 system, these results are due to [48, 49, 50]; a generalization that takes into account fluctuations and is conjectured by the authors to hold to high orders in λ was found in [51]. For the special case $k = 1$ results for operators involving not only scalars can be found in [33]. By now, all-order in λ results have been bootstrapped using supersymmetric localization [29] and boundary integrability [52, 52]. On the string-theory side the integrability properties of this setup are reflected in certain boundary conditions as recently discussed in [53].

For the D3-D7 system similar results are only known for the solution in which the probe brane has $\mathrm{AdS}_4 \times S^4$ geometry that we described in more detail in section 2.3. Early results were obtained in [54] and a closed overlap formula was presented in [55]. It is known that the D3-D7 system with probe brane geometry $\mathrm{AdS}_4 \times S^2 \times S^2$ is not amenable to the methods used in these references, see [56].

2.4.2 Wilson lines

Observables that can similarly be computed both in string theory and field theory are expectation values of field theory Wilson line operators. We will only sketch the idea in this section and refer to the references at the end of this subsection for more details. For simplicity we consider only a straight Wilson line parallel to the interface at $x_3 = 0$ in this subsection.

A Wilson line operator on the field theory side is given by the trace of a path-ordered exponential,

$$W(\gamma) = \mathrm{tr}\left[\mathrm{Pexp}\left(\int_\gamma \mathcal{A}\right)\right], \tag{2.4.14}$$

where γ is a straight path in the (x_1, x_2)-plane parameterized by $t \mapsto (t, 0, 0, x_3)$, $\mathcal{A}$ is the one-form

$$\mathcal{A} = [iA_0 - \phi_3 \sin(\chi) - \phi_6 \cos(\chi)]\, \mathrm{d}t \tag{2.4.15}$$

and $0 \leq \chi \leq \frac{\pi}{2}$ is an angle. The expectation value $\langle W(\gamma)\rangle$ can be computed classically by inserting the classical solution for the scalar fields into (2.4.15). The first correction to the classical expectation value again consists of two terms similar to the correction terms (2.4.7) and (2.4.8) for the one-point functions. These corrections may be computed using the Feynman rules of the defect CFTs.

The expectation value $\langle W(\gamma)\rangle$ is related to the potential energy $V(x_3)$ between a particle traveling along γ and the interface at $x_3 = 0$ by $\langle W(\gamma)\rangle \simeq \exp(-TV(x_3))$. Here T is the time interval for which the particle is traveling and one has to consider the limit $T \longrightarrow \infty$. The potential energy may also be computed in string theory by solving a minimal surface problem. In the present setting, one computes the action for a classical string that extends from the field theory Wilson line located on the boundary of AdS_5 into the interior. The world-sheet of the string has to be such that it ends perpendicularly on the world volume of the probe brane. As before, the comparison between the string and field theory result is only possible in a double-scaling limit as shown in (2.4.9) and (2.4.10).

Results For the D3-D5 system, the classical expectation value of $W(\gamma)$ was first computed in [45] in the two ways sketched in this section. In the double-scaling limit, agreement was found between the two computations. In [57], this computation was taken to the next order in the double-scaling parameter using the perturbative setup established in [34]. Again, agreement was found between the string and field theory computation. For the D3-D5 system also other Wilson line configurations have been considered, namely circular Wilson loops in [58, 59] and a pair of antiparallel Wilson lines in [60].

For both solutions of the D3-D7 system, we computed $\langle W(\gamma)\rangle$ to leading and next-to-leading order in the double-scaling parameter in [7] using the Feynman rules and propagators found in [5] and [6]. The string and field theory results matched perfectly.

2.5 Summary of own work and outlook

In the previous subsections we have reviewed probe-brane systems in type IIB superstring theory that give rise to defect versions of $\mathcal{N} = 4$ sYM theory under a version of the AdS/CFT correspondence. The different probe brane models considered are summarized in table 2.2. The defect conformal field theories are versions of $\mathcal{N} = 4$ sYM in which some of the scalar fields acquire Lie algebra valued vacuum expectation values in the half space $x_3 > 0$. The symmetry of the vacuum expectation values reflects the geometry of the probe brane on the string theory side. The "size" of the classical solution constitutes a free parameter of the model and corresponds to a flux or non-vanishing instanton number on part of the probe brane geometry. Importantly, the D3-D5 system preserved some amount of supersymmetry, while in the D3-D7 system supersymmetry was completely broken. We also explained how one-point functions of certain scalar field theory operators as well as the expectation values of Wilson lines are observables that can be computed both on the field and on the string theory side of the correspondence. The comparison of quantities is made possible in a double-scaling limit in which the ratio of the 't Hooft coupling λ to the square of the flux or instanton number is held small.

Our own work on this topic during the time of this PhD is related to the D3-D7 system. In subsection 2.3 we have described the classical solutions on the field theory side in some

	D3-D5	D3-D7	D3-D7
Classical solution	t_i (eq. (2.2.28))	G_i (eq. (2.3.13))	$t_i \otimes \mathbb{1}, \mathbb{1} \otimes t_i$ (eq. (2.3.14))
Symmetry of the vevs	$\mathfrak{su}(2)$	$\mathfrak{so}(5)$	$\mathfrak{su}(2) \times \mathfrak{su}(2)$
Probe brane geometry	$AdS_4 \times S^2$	$AdS_4 \times S^4$	$AdS_4 \times S^2 \times S^2$
Supersymmetry	$\frac{1}{2}$-BPS	None	None
Parameter	k	n	k_1, k_2

Table 2.2: Comparison of probe-brane systems described in sections 2.2 and 2.3

detail, but we have not explained how fluctuations around the classical solution are taken into account. In particular, we have not described how the expansion of the $\mathcal{N} = 4$ sYM field in terms of fuzzy spherical harmonics works concretely. This and subsequent calculations that check the proposed extension of the AdS/CFT correspondence to defect CFTs are the subject of the following publications:[10]

1. **A. Gimenez Grau, C. Kristjansen, M. Volk, and M. Wilhelm**, "A Quantum Check of Non-Supersymmetric AdS/dCFT," *JHEP* **01** (2019) 007, arXiv:1810.11463 [hep-th].

   In this paper, we set up the perturbative framework for the defect version of $\mathcal{N} = 4$ sYM theory that is dual to the D3-D7 system in which the D7 brane has geometry $AdS_4 \times S^2 \times S^2$. The classical solution for this case is given in equation (2.3.14). We derive the mass spectrum, the mass eigenstates and the propagators of the theory. We then use those to compute the first correction to the classical solution and to the one-point function of a 1/2-BPS operator due to quantum fluctuations. The result is compared against a string theory computation in a double-scaling limit similar to (2.4.9) and agreement is found.

2. **A. Gimenez-Grau, C. Kristjansen, M. Volk, and M. Wilhelm**, "A quantum framework for AdS/dCFT through fuzzy spherical harmonics on S^4," *JHEP* **04** (2020) 132, arXiv:1912.02468 [hep-th].

   This paper deals with the field theory dual of the D3-D7 system in which the D7 brane has geometry $AdS_4 \times S^4$ and for which the classical solution on the field theory side was given in equation (2.3.13). We proceed in analogy to the previous paper in setting up the perturbative framework and expand the fields of the defect CFT in fuzzy spherical harmonics of S^4. The most complicated part of the paper is the diagonalization of the mass matrix and the derivation of the propagators which requires the coupling of various representations of $\mathfrak{so}(5)$. This step is significantly more involved than in the previous paper due to the representation theory of $\mathfrak{so}(5)$. Once the perturbative setup is found, we compute the first corrections to the classical solution and to the one-point function of a 1/2-BPS operator. As before we find agreement with string theory in the double-scaling limit (2.4.10).

[10] Note that the first two papers include results that were obtained in a MSc thesis written together with A. Gimenez Grau. We include them in the list, because the results were expanded and the papers were published during the time of the PhD.

3. **S. Bonansea, K. Idiab, C. Kristjansen, and M. Volk**, "Wilson lines in AdS/dCFT," *Phys. Lett. B* **806** (2020) 135520, arXiv:2004.01693 [hep-th].

   In this paper, we compute the expectation value of a Wilson line operator inserted in either of the two field theory duals of the D3-D7 system. The computation is made feasible by the propagators and corrections to the classical solutions obtained in the previous two papers. When comparing to a string theory computation as briefly explained in section 2.4.2, we find agreement between the two sides for both defect CFTs.

The propagators for the defect versions of $\mathcal{N} = 4$ sYM theory obtained in these papers have opened the door for further perturbative computations. Such perturbative computations are an important check and input for predictions about physical observables coming from integrability, supersymmetric localization (in the case of the supersymmetric D3-D5 setup, see for example [29]) or as input for the boundary conformal bootstrap program (see for example [61]). Due to the holographic nature of the defect CFTs one may also expect interesting connections to string theory. Naturally, the starting point for further studies is the D3-D5 system which is technically much simpler due to the structure of the classical solution and the additional supersymmetry.

In this setup, we have recently started to compute two-point correlation functions of the stress-energy-momentum tensor. An interesting feature of these correlators is that the operators may either be inserted on the same side of the interface at $x_3 = 0$ or on different sides. While the space-time dependence of the correlators may be fixed using symmetry arguments, the coefficients of the various tensor structures that arise are interesting data that describes the interaction of the bulk theory with the defect. The presence of the interface implies for example that the conservation of the stress-energy-momentum tensor is modified by an operator called the displacement operator that is localized to $x_3 = 0$. Computing correlation functions involving this new operator will allow for tests of various general results about defect CFTs (see for example [62, 63]). With the perturbative framework at hand we can even expect to be able to compute these correlators beyond leading order.

Another exciting application of the perturbative computations of one-point functions in the D3-D7 system is higher-loop integrability. It was first found in the D3-D5 system that the one-point functions of scalar operators may be expressed as overlaps of Bethe eigenstates and a boundary state [48, 49, 50]. Starting from the one-loop correction to the one-point functions computed in [34], the authors of [51] then conjectured and checked a higher-order generalization of these overlap formulas and all-loop versions were subsequently bootstrapped in [29, 52, 64]. Except for the one-loop corrections to the one-point functions, a key input was a closed expression for the overlaps in terms of determinants of Gaudin matrices. Due to [55] such a formula is now available for the $\mathfrak{so}(5)$-symmetric version of the D3-D7 setup. One might hope that it can similarly be generalized beyond the leading order.

Another possible application of the explicitly computed one-point functions is as input for bootstrap methods. In [61] boundary conformal bootstrap as applied for two-point functions in the D3-D5 system and would could imagine a similar program for the D3-D7 setup.

Chapter 3

Aspects of Feynman integrals

The expansion of a scattering amplitude in quantum field theory in terms of a coupling constant can be organized diagrammatically by drawing graphs with a fixed set of external points. In this expansion, the order of the coupling corresponds to the number of closed loops in the graph. Following a set of rules due to Feynman, one can associate a value to each diagram. The value of a diagram is a function on the space of external kinematic data that describes the scattering process, for example the momenta and masses of the particles that are involved.

To obtain the full scattering amplitude for a given process, one is instructed to draw all possible diagrams compatible with the given external data, i.e. the number and species of the involved particles, and compute the value of each diagram. If one is interested in the result up to a fixed order in the coupling constant, all diagrams up to a fixed number of loops have to be considered. It is well known that this leads to an explosion in the number of graphs for processes with a large number of external particles or when going to higher order in the expansion in the coupling. A lot of research has been devoted to bypassing this issue and nowadays there are many methods that construct the scattering amplitude in a more direct or more economical way, for example unitarity methods [8, 9], recursion relations [10] or on-shell methods [12].

However, one problem that remains challenging is the integration over the internal four-momentum that is associated to each loop in a Feynman diagram. These integrations are difficult even numerically and in most cases the usual analytic functions known from the mathematics literature are not enough to express the function that a Feynman diagram defines on the space of external kinematic data.

The integrals and the functions that arise from them are the topic of this chapter. We begin in section 3.1 with a reminder about integration parameters that are often used to transform the momentum-space integrals into a simpler form. We then review the work by Landau on the singularities of integrals in section 3.2. In section 3.3, we review the algorithm that may be used to express certain Feynman integrals in terms of a class of functions known as multiple polylogarithms. There we also encounter obstructions to the integration algorithm and describe how they can sometimes be overcome. In section 3.4, we discuss Feynman integrals that cannot be expressed in terms of multiple polylogarithms due a non-trivial complex geometry that can be associated to them. In section 3.5 we summarize our own work on this topic.

3.1 Reminder about integration parameters

We consider a scalar Feynman diagram G in momentum space with ℓ loops, n internal edges and m external momenta in d dimensions of spacetime. To each loop in the diagram we associate a d-dimensional momentum k_j and to each internal edge a propagator of the form $\left(q_i^2 - m_i^2\right)^{-1}$.

Here, each momentum q_i is a linear combination of the loop and the external momenta p_j, $j \in \{1, \dots, m\}$, with coefficients drawn from the set $\{-1, 0, 1\}$. The value of a diagram is a function of the m external momenta p_j and the internal masses m_i^2, $i \in \{1, \dots, n\}$ defined by the integral

$$I_G = \int \left(\prod_{j=1}^{\ell} \mathrm{d}^d k_j \right) \prod_{i=1}^{n} \frac{1}{q_i^2 - m_i^2}. \tag{3.1.1}$$

Note that due to overall momentum conservation only $m - 1$ of the external momenta are independent. We assume that the integral (3.1.1) is finite, possibly after applying some regularization procedure.

To integrate over the internal momenta one introduces an integration parameter x_i for each edge in the graph and writes

$$\prod_{i=1}^{n} \frac{1}{q_i^2 - m_i^2} = \int_0^\infty \left(\prod_{j=1}^{n} \mathrm{d}x_j \right) \delta\left(1 - \sum_{j=1}^{n} x_j \right) \frac{(n-1)!}{\sum_{i=1}^{n} x_i \left(q_i^2 - m_i^2 \right)} \tag{3.1.2}$$

according to the well-known identity attributed to Feynman [65].[1] The integral (3.1.1) can then be brought into the following form (see for example [67, chapter 1.5]):

$$I_G = \pi^{\ell d/2} \Gamma\left(\nu - \frac{\ell d}{2} \right) \int_0^\infty \left(\prod_{j=1}^{n} \mathrm{d}x_j \right) \delta\left(1 - \sum_{j=1}^{n} x_j \right) \frac{\mathcal{U}^{n-(\ell+1)d/2}}{\mathcal{F}^{n-\ell d/2}}. \tag{3.1.3}$$

Here $\mathcal{U}$ and $\mathcal{F}$ are polynomials[2] in $x_1, \dots, x_n$ with coefficients that are Lorentz-invariant combinations of the external momenta as well as the masses. This expression can also easily be generalized to the case where the propagators in the momentum space integral (3.1.1) are raised to some power. One method to compute the polynomials $\mathcal{U}$ and $\mathcal{F}$ is due to Chisholm [68]: One expresses the sum in on the right-hand side of (3.1.2) as

$$\sum_{i=1}^{n} x_i \left(q_i^2 - m_i^2 \right) = \sum_{i,j=1}^{\ell} A_{ij} \left(k_i \cdot k_j \right) - 2 \sum_{i=1}^{\ell} \sum_{a=1}^{m-1} B_{ia} \left(k_i \cdot p_a \right) + C. \tag{3.1.4}$$

Here A_{ij} are the components of an $\ell \times \ell$ matrix A and similarly B_{ia} are the components of an $\ell \times (m-1)$ matrix. The quantities A, B and C are linear combinations of the integration parameters x_i and the polynomials $\mathcal{U}$ and $\mathcal{F}$ can be computed from them by

$$\mathcal{U} = \det(A), \quad \mathcal{F} = \det(A) \left[C - \sum_{a,b=1}^{m-1} \left(B^{\mathsf{T}} A^{-1} B \right)_{ab} \left(p_a \cdot p_b \right) \right]. \tag{3.1.5}$$

It follows that $\mathcal{U}$ and $\mathcal{F}$ are homogeneous in the integration parameters of degrees $\deg(\mathcal{U}) = \ell$ and $\deg(\mathcal{F}) = \ell + 1$. There exists also a more graph-theoretic way to compute $\mathcal{U}$ and $\mathcal{F}$ from spanning trees and spanning two-forests of a graph. This method may be found in [69, chapter 6.2.3] and is reviewed in [70].

[1] In the paper [65] Feynman writes that the identity was suggested by some work of Schwinger, maybe in [66].

[2] The polynomials $\mathcal{U}$ and $\mathcal{F}$ have various names, for example first and second graph polynomial or first and second Symanzik polynomial.

The main point is that in the form (3.1.3) any Feynman integral is expressed as an integral of a rational function over a relatively simple domain. This makes various tasks such as analyzing its singularities or expressing the integral in terms of known functions easier.[3] The question of singularities is addressed in subsection 3.2 below. With regard to the second point, the integrals in (3.1.3) are amenable to direct integration in terms of a class of functions known as multiple polylogarithms which we will review in subsection 3.3. Subsection 3.4 deals with Feynman integrals that cannot be expressed in terms of multiple polylogarithms.

3.2 Singularities of Feynman integrals

The Feynman integral I_G is a function of Lorentz-invariant combinations of the external momenta and the internal masses. We refer to this data collectively as the kinematic data and from now on denote it simply by $\mathbf{z}$. For special kinematic values $\mathbf{z}_0$ the function I_G has singularities and branch cuts. In this section we review the conditions given by Landau in [13] that determine the locations of the singular points as well as the nature of the singularity. We will not follow the original paper by Landau, but instead use the approach by Polkinghorne and Screaton found in [73, 74].

Landau equations It is convenient to consider the complexification of I_G and to think of the Feynman integral as an integral along some contour in the (higher-dimensional) complex plane. Considering one integration at a time, the integral over one of the Feynman parameters, say x_j, is a contour integral along some contour C_j. The integrand for the integration over x_j can have singularities u_k at various locations in the complex x_j-plane. The external data $\mathbf{z}$ for the x_j-integration consists of the external kinematic data and possibly further integration variables x_i with $i \neq j$. We assume that there is a region Z such that for every $\mathbf{z} \in Z$, the poles $u_k(\mathbf{z})$ do *not* lie on the contour C_j. As the external data $\mathbf{z}$ varies, each singularity $u_k(\mathbf{z})$ moves along a path in the x_j-plane. When $\mathbf{z}$ leaves the region Z, a singularity $u_k(\mathbf{z})$ can cross the contour C_j and the contour has to be deformed in order avoid a singularity. In this way we obtain the analytic continuation of the integral to values $\mathbf{z}$ that are outside the region Z. The value of the integral I_G may depend on the way the contour was deformed which is reflected in the fact that Feynman integrals are in general multi-valued functions.

It is crucial to be able to deform the integration contour, otherwise the integral is divergent. It turns out that there are two situations in which the contour deformation fails:

1. For some value $\mathbf{z}_0$ a singularity u_k passes through an end-point of C_j. Since the end points of C_j are held fixed, the contour cannot be deformed to avoid the singularity. This situation is called an *end-point singularity*.

2. Two singularities u_k and u_l approach C from different sides and coincide for some value $\mathbf{z}_0$. In this case the contour is trapped between u_k and u_l and cannot be deformed to avoid the singularity. This is called a *pinch singularity*.

[3] It also allows one to make contact with the math literature; for example it has been shown in [71] that Feynman integrals are "periods" as defined by Kontsevich and Zagier in [72].

Note that the second case includes the situation where a singularity moves to infinity. The points $\mathbf{z}_0$ where one of those two cases occurs are points where the function $I_G(\mathbf{z})$ has a singular behavior.

This procedure can be iterated to be applicable to the full Feynman integral I_G (see for example [73, section 4]) and it turns out that for a singular behavior one needs that in each integration there is either a pinch or an end-point singularity. From this one can derive a set of equations that (in principle) determine the locations of the points $\mathbf{z}_0$ where I_G has such a behavior. These equations are called *Landau equations* and were first stated by Landau in [13]. Formulated in terms of the polynomial $\mathcal{F}$, the conditions are

$$\mathcal{F} = 0 \tag{3.2.1}$$

as well as

$$\text{either} \quad x_i = 0 \quad \text{or} \quad \frac{\partial \mathcal{F}}{\partial x_i} = 0 \quad \text{for each} \quad i \in \{1, \dots, n\}. \tag{3.2.2}$$

If for some external data $\mathbf{z}_0$, the equations (3.2.1) and (3.2.2) admit a non-trivial solution for the integration parameters x_i, then the integral I_G has a singular behavior at $\mathbf{z}_0$.[4] Note that since $\mathcal{F}$ is homogeneous in the x_i, the second equation (3.2.2) implies the first equation (3.2.1) by Euler's homogeneous function theorem.

Nature of the singularities Landau's paper [13] also derives the asymptotic behavior of the Feynman integral I_G near a singular point $\mathbf{z}_0$. For the derivation, one considers the integral I_G and eliminates one of the integration parameters using the δ-function, say x_n. We denote by $\mathcal{F}'$ the polynomial obtained by $\mathcal{F}$ in this way, i.e.

$$\mathcal{F}'(x_1, \dots, x_{n-1}) = \mathcal{F}(x_1, \dots, x_{n-1}, 1 - x_1 - \cdots - x_{n-1}). \tag{3.2.3}$$

We consider the situation with ν end-point and $n - \nu - 1$ pinch singularities occurring among the remaining $n - 1$ integrations. After relabeling the integration parameters x_i if necessary, the Landau equations (3.2.2) then take the form

$$\begin{aligned} \frac{\partial \mathcal{F}'}{\partial x_i} &= 0 \quad \text{for} \quad i \in \{1, \dots, n - \nu - 1\}, \\ x_i &= 0 \quad \text{for} \quad i \in \{n - \nu, n - \nu + 1, \dots, n - 1\}. \end{aligned} \tag{3.2.4}$$

We denote by $\mathbf{z}_0$ some point in the space of external kinematic data, such that the equations (3.2.4) have a solution and denote the solution by $\overline{x}_i$. To compute an approximation to the integral I_G in the neighborhood of $\mathbf{z}_0$, one can use the method of steepest descent. To this end, one expands the polynomial $\mathcal{F}'$ in a Taylor series in $x_i - \overline{x}_i$ to lowest order, which gives

$$\mathcal{F}' = \mathcal{F}'_0 + \sum_{i=n-\nu}^{n-1} (x_i - \overline{x}_i) \left.\frac{\partial \mathcal{F}'}{\partial x_i}\right|_{x_i = \overline{x}_i} + \frac{1}{2} \sum_{i,j=1}^{n-\nu-1} (x_i - \overline{x}_i)\left(x_j - \overline{x}_j\right) \left.\frac{\partial^2 \mathcal{F}'}{\partial x_i \partial x_j}\right|_{\substack{x_j = \overline{x}_j, \\ x_k = \overline{x}_k}} + \mathcal{O}\left((x_i - \overline{x}_i)^3\right). \tag{3.2.5}$$

[4] To be precise, the condition $\frac{\partial \mathcal{F}}{\partial x_i} = 0$ is a necessary, but not a sufficient condition for a pinch singularity to appear on the physical sheet of the function I_G. It tells us however, that on *some* sheet of I_G that we may access by analytic continuation, a singularity can occur. Note also that in the discussion of the singularities only the denominator of the integral (3.1.3) enters. It is also possible that a singularity does not occur because it is canceled by the numerator in the integral.

Here $\mathcal{F}_0'$ is $\mathcal{F}'$ evaluated at the solution $\overline{x}_i$ and $\mathbf{z}_0$. Roughly speaking the idea is that the biggest contribution to the integral I_G comes from the region where $x_i - \overline{x}_i$ is small, i.e. where the expansion (3.2.5) is a good approximation. Using the method of steepest descend one obtains that near $\mathbf{z}_0$, the integral I_G behaves as

$$I_G \sim \frac{1}{\sqrt{D}} \left(\mathcal{F}_0'\right)^{-\gamma} \left(\prod_{i=n-\nu}^{n-1} \frac{\partial \mathcal{F}'}{\partial x_i} \bigg|_{x_i=\overline{x}_i} \right)^{-1}, \tag{3.2.6}$$

up to numerical factors. In the asymptotic expression (3.2.6), D is the Hessian determinant of the polynomial $\mathcal{F}'$,

$$D = \det \left(\frac{\partial^2 \mathcal{F}'}{\partial x_i \partial x_j} \right) \bigg|_{\substack{x_j=\overline{x}_j, \\ x_k=\overline{x}_k}}, \tag{3.2.7}$$

and the exponent γ is given by

$$\gamma = \frac{1}{2}(n - \nu - d\ell + 1). \tag{3.2.8}$$

Importantly, the asymptotic expansion (3.2.6) is *only* valid if $\gamma > 0$ or if γ is half-integer. If γ is an integer and $\gamma \leq 0$, one can replace $\mathcal{F}'$ by $\mathcal{F}' + t$ and differentiate the integral I_G with respect to t. This increases the exponent of the denominator of the Feynman integral so that the asymptotic expansion (3.2.6) becomes valid. Since the exponent must be at least one, one has to take $|\gamma| + 1$ derivatives and the asymptotic expansion contains a factor $\left(\mathcal{F}_0' + t\right)^{-1}$. The result is then integrated $|\gamma| + 1$ times with respect to t. Thus, for integer $\gamma \leq 0$, the Feynman integral I_G behaves as

$$\mathcal{F}_0^{|\gamma|} \log(\mathcal{F}_0) \tag{3.2.9}$$

near a Landau singularity $\mathbf{z}_0$. For $\gamma > 0$ and half-integer γ the behavior according to (3.2.6) is

$$\mathcal{F}_0^{-\gamma}, \tag{3.2.10}$$

as the derivatives and the Hessian occurring in (3.2.6) are assumed to be non-singular.

The integral (3.1.3) can be a very complicated function of $\mathbf{z}$, yet the behavior near a Landau singularity is remarkably simple. Note in particular that the behavior (3.2.9) only includes a single power of the logarithm and no terms of the form $\log^a(\mathcal{F}_0)$ for some $a > 1$.[5] If we express a Feynman integral as a combination special functions, the location of the Landau singularities should become manifest and the behaviour should be as dictated by equations (3.2.9) and (3.2.10). This poses constraints on the classes of functions that may be considered to express a Feynman integral in closed form.

3.3 Direct integration

In some cases, a Feynman integral I_G can be expressed in terms of special functions. In this section, we review the class of functions known as multiple polylogarithms and in particular

[5] I would like to thank Cristian Vergu for pointing this out to me.

the algorithm that expresses a Feynman integral I_G in terms of these functions. The strategy of starting with a parameterization of the integral such as the one in equation (3.1.3) and transforming the integrand until it matches the definition of some special function is called *direct integration*. This is not the only strategy that one can employ to express Feynman integrals in closed form and another popular method is to find a differential equation that is satisfied by the integral.

3.3.1 Direct integration in terms of multiple polylogarithms

In [14] Goncharov defined multiple polylogarithms (MPLs) by a power series as a generalization of the classical polylogarithms $\mathrm{Li}_n(x)$. The MPLs can also be expressed as an iterated integral, which is more common in the physics literature as it connects more directly to Feynman integrals such as the one shown in equation (3.1.3). As an iterated the integral, MPLs are defined recursively by

$$G(a_1, \dots, a_n; x) = \int_0^x \frac{\mathrm{d}t}{t - a_1} G(a_2, \dots, a_n; t), \quad G(x) = 1, \tag{3.3.1}$$

where $a_1, \dots, a_n \in \mathbb{C}$. In the following we use the notation $\mathbf{a} = (a_1, \dots, a_n)$, i.e. $G(\mathbf{a}; x) \equiv G(a_1, \dots, a_n; x)$ and write $|\mathbf{a}| = n$ for the weight of $G(\mathbf{a}; x)$ which is equal to the number of entries in $\mathbf{a}$. In this section we assume some familiarity with multiple polylogarithms and iterated integrals. Additional details and background may be found in appendix B.

We wish to compute the definite integral

$$I = \int_0^\infty \mathrm{d}x_1 \cdots \mathrm{d}x_n \, f_1(x_1, \dots, x_n), \tag{3.3.2}$$

where $f_1(x_1, \dots, x_n)$ is a rational function of the integration parameters $x_1, \dots, x_n$. The integral will generally again be a function of the external kinematic data $\mathbf{z}$ such as Lorentz-invariant combinations of the momenta or masses. In this section we are mostly interested in the integration algorithm that allows us to express the integral in terms of MPLs defined in (3.3.1). We therefore consider the physical parameters $\mathbf{z}$ to be fixed and generic and hide the dependence of all quantities on them in this section.

Not every rational function f_1 allows the integral (3.3.2) to be computed in terms of MPLs. We will now briefly review an algorithm that can be used for the computation assuming that this is possible and afterwards state a sufficient (but not necessary) criterion for it known as *linear reducibility*. The algorithm is due to Brown and was presented in [75] building on top of earlier work on period integrals on the moduli space of curves of genus zero [76]. The algorithm was improved and implemented by Panzer in [77] in the Maple package `HyperInt`. A description from a slightly different point of view may also be found in [78, appendix D].

Integration algorithm As we will see below, the algorithm depends crucially on being able to find an order of the integration parameters in which the integrand is linearly reducible. We assume that such an order has been found and that after relabeling if necessary the parameters are to be integrated in the order $(x_1, \dots, x_n)$. The idea is to integrate one variable at a time starting with x_1. This produces a sequence of partial integrals given by

$$f_{j+1}(x_{j+1}, \dots, x_n) = \int_0^\infty \mathrm{d}x_j \, f_j(x_j, \dots, x_n), \quad j \in \{1, \dots, n\}. \tag{3.3.3}$$

After n integrations we obtain $I = f_{n+1}$ as the final result. We assume that each step of the integration, the integrand is of the form[6]

$$f_j(x_j, \dots, x_n) = R_j(x_j, \dots, x_n)\, G(\mathbf{a}_j; x_j) G(\mathbf{a}_{j+1}; x_{j+1}) \cdots G(\mathbf{a}_n; x_n), \tag{3.3.4}$$

where each $\mathbf{a}_j$ depends *only* on those integration parameters with index greater than j,

$$\mathbf{a}_j = \mathbf{a}_j(x_{j+1}, \dots, x_n). \tag{3.3.5}$$

The function $R_j(x_j, \dots, x_n)$ in (3.3.4) is a rational function in the remaining integration parameters. The integration over a single parameter x_j consists of three steps:

1. **Construction of a primitive.** As a function of x_j, the rational function R_j has poles at locations that depend on the integration variables $x_{j+1}, \dots, x_n$ with higher index. We denote the set of poles of R_j by Σ_j. By decomposing R_j into partial fractions, it may be written as

$$R_j(x_j, \dots, x_n) = \sum_{a \in \Sigma_j} \sum_{n \geq 0} \frac{Q_{a,n}}{(x_j - a)^n} + \sum_{n \geq 0} Q_n x_j^n, \tag{3.3.6}$$

where $Q_{a,n}$, Q_n and a are independent of x_j. It is important to realize that in order to apply the recursive definition (3.3.1) of the MPLs, the integration variable x_j has to appear *linearly* in the denominators of this decomposition. Once the decomposition (3.3.6) has been computed, a primitive F_j for the integrand (3.3.4) with respect to x_j is found using

$$\int \frac{\mathrm{d}x_j}{x_j - a} G(\mathbf{a}_j; x_j) = G(a, \mathbf{a}_j; x_j), \tag{3.3.7}$$

together with the integration by parts identities

$$\begin{aligned} \int \frac{\mathrm{d}x_j}{(x_j - a)^n} G(\mathbf{a}_j; x_j) &= -\frac{G(\mathbf{a}_j; x_j)}{(n-1)(x_j - a)^{n-1}} + \frac{1}{n-1} \int \frac{\mathrm{d}x_j}{(x_j - a)^{n-1}} \frac{\partial}{\partial x_j} G(\mathbf{a}_j; x_j), \quad n > 1, \\ \int \mathrm{d}x_j\, x_j^n G(\mathbf{a}_j; x_j) &= \frac{x_j^{n+1}}{n+1} G(\mathbf{a}_j; x_j) - \frac{1}{n+1} \int \mathrm{d}x_j\, x_j^{n+1} \frac{\partial}{\partial x_j} G(\mathbf{a}_j; x_j), \quad n \geq 0. \end{aligned} \tag{3.3.8}$$

Note that the derivative of $G(\mathbf{a}_j; x_j)$ appearing on the right-hand side is an MPL of lower weight, so these identities can be applied recursively.

2. **Evaluate the definite integral.** Take the limit of the primitive F_j as $x_j \longrightarrow \infty$ and $x_j \longrightarrow 0$. In this way we obtain a function $\tilde{f}_{j+1}(x_{j+1}, \dots, x_n)$ of the remaining integration parameters,

$$\tilde{f}_{j+1}(x_{j+1}, \dots, x_n) = \operatorname*{Reg}_{x_j \to \infty} F(x_j, \dots, x_n) - \operatorname*{Reg}_{x_j \to 0} F(x_j, \dots, x_n). \tag{3.3.9}$$

The limits are computed using the regularized limits introduced in appendix B in equation (B.1.16).

[6] Note that the integrand in the starting point (3.3.2) is of this form, because the MPLs on the right-hand side can be identically one since $G(x) = 1$.

3. **Ensure the form** (3.3.4)**.** Whenever an MPL of higher weight is created in (3.3.7), the new argument a will generally depend on x_{j+1}. Therefore the function $\tilde{f}_{j+1}$ is not of the form (3.3.4) and cannot serve as the starting point for the next iteration of the integration algorithm.

   Concretely, the problem is that the primitive F_j contains MPLs of the form $G(\tilde{\mathbf{a}}; x_j)$, where $\tilde{\mathbf{a}}$ depends on x_{j+1}. It turns out (see [77, lemma 2.7]) that if the dependence on x_{j+1} is *rational*, one can find a set of other MPLs with arguments $\mathbf{a}$ that are independent of x_{j+1} such that

$$\operatorname*{Reg}_{x_j \to \infty} G(\tilde{\mathbf{a}}; x_j) = \sum_{\mathbf{a}} G(\mathbf{a}; x_{j+1}) \operatorname*{Reg}_{x_{j+1} \to 0} \operatorname*{Reg}_{x_j \to \infty} G(\tilde{\mathbf{b}}_{\mathbf{a}}; x_j). \tag{3.3.10}$$

   Here the arguments $\tilde{\mathbf{b}}_{\mathbf{a}}$ depend on x_{j+1}, but since x_{j+1} is taken to zero on the right-hand side, the end result is a linear combination of MPLs $G(\mathbf{a}; x_{j+1})$ with arguments $\mathbf{a}$ independent of x_{j+1}. We review this procedure in appendix B; here we only note that crucially the transformation requires a factorization of the x_{j+1}-dependent entries of $\tilde{\mathbf{a}}$ into *linear* factors,

$$\tilde{a}_m - \tilde{a}_n = \prod_{\alpha} \left(x_{j+1} - \alpha\right)^{n_\alpha}, \quad 1 \leq n < m \leq |\tilde{\mathbf{a}}|, \quad n_\alpha \in \mathbb{Z}. \tag{3.3.11}$$

   This procedure almost brings the function $\tilde{f}_{j+1}$ into the form in (3.3.4), but recall that the original integrand (3.3.4) had and additional factor $G(\mathbf{a}_{j+1}, x_{j+1})$ that is also an MPL in x_{j+1}. The products of the form $G(\mathbf{a}; x_{j+1})G(\mathbf{a}_{j+1}; x_{j+1})$ may be expanded into a linear combination of G-functions evaluated at x_{j+1} using the shuffle relation (B.1.13). In this way we obtain a function $f_{j+1}(x_{j+1}, \dots, x_n)$ that is of the form (3.3.4) and can serve as the starting point for the integration in the next variable x_{j+1}.

Note that at two steps in the algorithm it is necessary to decompose a polynomial into linear factors: in the partial fraction decomposition (3.3.6) and in the factorization of the integration parameter dependent arguments (3.3.11). This factorization is always possible in an appropriate domain, for example the algebraic closure of the field of rational functions in the remaining variables. However, it may not be possible *rationally*: The roots a in the decomposition (3.3.6) may contain square or higher algebraic roots of the subsequent integration variables. In this case the third step fails. Similarly, the roots α in the factorization (3.3.11) may depend algebraically on the remaining variables. In both cases the integral $\tilde{f}_{j+1}$ can not be brought back into the form (3.3.4) required for the next iteration of the algorithm. We will discuss the obstructions due to algebraic roots in more detail in subsection 3.3.2 below.

Linear reducibility If there exists an order of the integration parameters $x_1, \dots, x_n$ such that at every iteration of the integration algorithm the linear factors can be computed without introducing an algebraic dependence on the remaining integration parameters, then the integrand $f_1(x_1, \dots, x_n)$ in (3.3.2) is called *linearly reducible*. There are polynomial reduction algorithms that can decide in advance if a given integrand is linearly reducible without having to try all permutations of $x_1, \dots, x_n$.

The idea of these reduction algorithms is to keep track of the singularities of the integrands in each iteration of the algorithm, i.e. of the poles of any rational parts as well as arguments of the polylogarithms. To demonstrate the idea, we consider the integration of a single MPL multiplied with a simple rational function,

$$\int \mathrm{d}x \, \frac{1}{(f_0 + f_1 x)(g_0 + g_1 x)} \, G(\mathbf{a}; x) = \left(\frac{1}{f_1 g_0 - f_0 g_1} \right) \int \mathrm{d}x \left(\frac{f_1}{f_0 + f_1 x} - \frac{g_1}{g_0 + g_1 x} \right) G(\mathbf{a}; x). \tag{3.3.12}$$

Here we have decomposed the rational part of the integrand into partial fractions as in (3.3.6). The original integrand has poles at $x = -\frac{f_0}{f_1}$ and $x = -\frac{g_0}{g_1}$. These ratios end up as arguments to a new MPL after integrating over x. If we want to be able to continue with another integration, we must get rid of the dependence on the next integration variable as explained in step three above. The factorization (3.3.11) certainly succeeds rationally if f_0, f_1, g_0 and g_1 are linear in the next variable. Moreover, in the next step we also need the prefactor $(f_1 g_0 - f_0 g_1)^{-1}$ on the right hand side of (3.3.12) to factor linearly.

The simple reduction algorithm presented in [75, section 4.1] formalizes this observation: We begin by defining a set $S = \mathrm{irred}(f_1)$ as all the irreducible factors contained in the integrand f_1. If all polynomials in S are linear in some integration variable x_i, then we write each of them as $f = f_0 + f_1 x_i$. We then define the reduction of S with respect to x_i to be the set

$$S_{(i)} = \mathrm{irred}\left(\{ f_0, f_1 \, : \, f \in S \} \cup \{ f_1 g_0 - f_0 g_1 \, : \, f, g \in S \} \right). \tag{3.3.13}$$

The elements of $S_{(i)}$ are polynomials in the variables that remain, i.e. x_j for $j \neq i$. If there is a variable x_k in which all the polynomials in $S_{(i)}$ are linear, we can iterate this procedure and define $S_{(i,k)}$ as the reduction of S_i with respect to x_k. If we can continue in this way until we have eliminated all variables and found the set $S_{(i_1,\ldots,i_n)}$, then S and the integrand f_1 are called simply linearly reducible.

An improvement of this algorithm is presented in [75, section 4.2] as Fubini reduction based on the following observation: If both $S_{(i,j)}$ and $S_{(j,i)}$ exist, then the integration orders (x_i, x_j) and (x_j, x_i) both lead to an expression in terms of multiple polylogarithms and are therefore admissible. In this case, Fubini's theorem implies that the result of both integrations also has to be the same and an improved upper bound for the set of singularities after integrating over x_i and x_j is the intersection $S_{(i,j)} \cap S_{(j,i)}$. This procedure may again be iterated and if one manages to produce a sequence of polynomial sets such that all variables are eliminated, then the set S is Fubini linearly reducible.

In practice many of the possible singularities computed by either Fubini or simple reduction do not show up. One can give a criterion for when for two polynomials $f, g \in$ one has to to add the resultant $f_1 g_0 - f_0 g_1$ during the reduction step shown in (3.3.13). This was first done in [79, section 6.6] and is elaborated on in [80, section 3.6.4]. A pair (f, g) of polynomials that has to be considered by this criterion is called compatible. The compatibility can be modeled as a graph whose vertices are polynomials and in which two polynomials are connected by an edge if they are compatible. From these considerations one obtains a significantly more powerful reduction algorithm known as compatibility graph reduction that computes a much better approximation to the singularities of the integral.

Linear reducibility is a sufficient criterion for the integration of f_1 to succeed in terms of multiple polylogarithms, but it is not necessary. In particular, even if no order of the integration parameters $x_1, \dots, x_n$ is found in which the integrand f_1 is linearly reducible, a change of variables might bring f_1 into a form in which such an order can be found. For a review of the different reduction algorithms mentioned briefly here we also refer to the thesis [80, sections 3.6.3, 3.6.4] in addition to the original papers [75, 79].

Fibration bases Multiple polylogarithms satisfy many identities, for example shuffle relations which are reviewed in appendix B. In order to simplify or even just compare expressions it is useful to be able to write a combination of polylogarithms in a chosen basis of functions. It turns out that the solution to this problem is essentially again to bring a given polylogarithm into the form (3.3.4), see [75, section 5].

More concretely, let us assume that the integration of the integral I in (3.3.2) succeeded in terms of polylogarithms. If we denote the kinematic variables on which the integral depends by $\mathbf{z} = (z_1, \dots, z_k)$, then after using the shuffle relations if necessary the integral is of the form

$$I(z_1, \dots, z_k) = \lim_{x \to \infty} \sum_{\tilde{\mathbf{a}}} c_{\tilde{\mathbf{a}}} \, G(\tilde{\mathbf{a}}; x). \tag{3.3.14}$$

Here the arguments $\tilde{\mathbf{a}}$ as well as the coefficients $c_{\tilde{\mathbf{a}}}$ depend on $z_1, \dots, z_k$ and we assume that this dependence is rational in both cases. We can then follow the same procedure as in step three of the algorithm above (see also appendix B for more details) and try to rewrite this function in a form as in equation (3.3.4),

$$I(z_1, \dots, z_k) = \sum_{(i_1, \dots, i_k)} c_{(i_1, \dots, i_k)} G(\mathbf{a}_{1,i_1}; z_1) G(\mathbf{a}_{2,i_2}; z_2) \cdots G(\mathbf{a}_{k;i_k}; z_k), \tag{3.3.15}$$

where all the $\mathbf{a}_{1,i_1}$ are independent of z_1, the $\mathbf{a}_{2,i_2}$ are independent of z_1 and z_2 and so on as in (3.3.5). The coefficients $c_{(i_1, \dots, i_k)}$ may be rational functions of $z_1, \dots, z_k$. The decomposition (3.3.15) is unique and depends on the order of the variables $(z_1, \dots, z_k)$. The basis of MPLs associated with a given order $(z_1, \dots, z_k)$ is called a fibration basis. The concept was introduced in [75, section 5]; more details may also be found in [80, section 4.3].

3.3.2 Obstructions to direct integration

As we have seen in subsection 3.3.1, the factorizations into linear factors can introduce an algebraic dependence on subsequent integration parameters. For example, the roots a in the partial fraction decomposition (3.3.6) may be of the form $\sqrt{P(x_{j+1}, \dots, x_n)}$ for some polynomial P that is not a perfect square. In some cases, the algebraic dependence can be removed by a change of variables. In this case we call the root a rationalizable.

Rationalizable roots Note that a root a arising from partial fractioning is algebraic, which means that a and the remaining integration parameters always satisfy a relation of the form $h(a, x_{j+1}, \dots, x_n) = 0$ for some polynomial h. The problem of finding a suitable change of variables amounts to finding a rational parameterization of an affine hypersurface defined by the equation $h(a, x_{j+1}, \dots, x_n) = 0$.

In the following we will abuse language slightly and speak of *the* hypersurface associated to a root a. However one should keep in mind that the Feynman integral depends on kinematic data such as momenta and masses that enter as coefficients in the polynomial h. More correctly, we should therefore speak of a *family* of hypersurfaces for which the kinematic variables play the role of the moduli. This is important, because for special values of the kinematic variables a root can simplify. An easy example is $a = \sqrt{x^2 + kxy + y^2}$ which for $k = 2$ becomes the square root of a perfect square. When we speak of *the* hypersurface we have in mind generic values of the kinematic values for which no such simplification happens.

It is convenient to deal with the parameterization problem projectively by introducing a new variable that makes the polynomial h homogeneous, so that h defines a hypersurface $V(h)$ in an m-dimensional projective space $\mathbb{P}^m$,

$$V(h) = \{[z_0 : \cdots : z_m] \in \mathbb{P}^m \,:\, h(z_0, \ldots, z_m) = 0\} \subset \mathbb{P}^m. \tag{3.3.16}$$

Here we using the notation $[z_0 : \cdots : z_m]$ for the homogeneous coordinates of a point in $\mathbb{P}^m$. A rational parameterization of the $(m-1)$-dimensional hypersurface $V(h)$ is given by a rational map

$$\phi : \mathbb{P}^{m-1} \longrightarrow V(h), \quad t \mapsto [\phi_0(t) : \cdots : \phi_m(t)] \tag{3.3.17}$$

such that

$$h(\phi_0(t), \ldots, \phi_m(t)) = 0 \quad \text{for all} \quad t \in \mathbb{P}^{m-1}. \tag{3.3.18}$$

This map is onto, so a rational parameterization writes the hypersurface $V(h)$ as the image of a projective space with the same dimension as $V(h)$. For most hypersurfaces such a parameterization does not exist. Loosely classifying the hypersurfaces by their dimension, there are the following results about rational parameterizations:

- **Curves.** In the case $m = 2$, the hypersurface $V(h)$ is a plane curve. Clebsch showed in [81] that a plane curve has a rational parameterization if and only if its genus is zero. By the genus-degree formula (see for example [82, chapter 8.3]) a curve of degree d with only ordinary multiple points[7] has genus

$$g = \frac{(d-1)(d-2)}{2} - \sum_{P \in V(h)} \frac{r_P(r_P - 1)}{2}. \tag{3.3.19}$$

  Here r_P is the multiplicity of the point P. If the curve is smooth, all points have multiplicity $r_P = 1$ and the formula reduces to the first term.

  The simplest case is $d = 2$, i.e. a smooth curve of degree two (a smooth conic). A conic may be rationalized by picking a point $P_0 \in V(h)$ and projecting $V(h)$ onto a line that does not contain P_0. For the commonly encountered case where h is of the form

$$h(x, y, z) = y^2 - ax^2 - bxz - cz^2 \tag{3.3.20}$$

[7] A point $P \in V(h)$ is an ordinary point of multiplicity r_P if there are r_P tangents to $V(h)$ at P. For example, the shape "$\propto$" has an ordinary double point, but the shape "$\prec$" does not.

for some coefficients a, b and c, the rationalization map that sends $t = [t_0 : t_1] \in \mathbb{P}^1$ to a point on $V(h)$ is well known:

$$\phi_1(t) = -t_0\left(bt_0 - 2\sqrt{c}t_1\right),\ \phi_2(t) = a\sqrt{c}t_0^2 - t_1\left(bt_0 - \sqrt{c}t_1\right),\ \phi_3(t) = at_0^2 - t_1^2. \tag{3.3.21}$$

One can check that this is a parameterization of the curve, i.e. $h(\phi_1(t), \phi_2(t), \phi_3(t)) = 0$. The corresponding change of variables to rationalize square roots in an otherwise rational integral is known as Euler substitution.

A smooth curve of degree $d \geq 3$ has genus $g \geq 1$ and is therefore not rational. From the genus-degree formula (3.3.19) it follows that a curve of degree d is rational precisely if it has multiple points such that

$$\sum_{P \in V(h)} \frac{r_P(r_P - 1)}{2} = \frac{(d-1)(d-2)}{2}. \tag{3.3.22}$$

Examples are a curve with $\frac{(d-1)(d-2)}{2}$ ordinary double points ($r_P = 2$) or a curve with one point of multiplicity $r_P = d - 1$. For the second case there is an easy algorithm to construct the rationalization map (see for example [83, chapter II.F]). The first case is more complicated, but an algorithm exists and may be found in [84, chapter 4]. An implementation of these algorithms is available for example in the Singular library `paraplanecurves.lib` [85].

- **Surfaces.** For $m = 3$ the hypersurface $V(h)$ is a two-dimensional surface. An old theorem by Castelnuovo states that a surface is rational if and only if certain numerical invariants of the surface that are generalizations of the genus to higher dimensions vanish [86]. An algorithm to compute these invariants and (if possible) a rational parameterization of a general algebraic surface is presented in [87]. If a surface of degree d has a point of multiplicity $d - 1$, then the computation is again significantly simpler and can be handled with the method presented in [88].

- **Higher-dimensional hypersurfaces.** For hypersurfaces of higher dimensions, no general algorithm appears to be known to compute a rational parameterization if possible. As before however, the case where a hypersurface of degree d has a point of multiplicity $d - 1$ is particularly simple. An algorithm for this case was presented in [88] and an implementation is available in [89].

It is important to note that the rationalization procedures usually require that the field in which the coefficients live is extended. Already for the case of a conic this is evident from the appearance of $\sqrt{c}$ in the map (3.3.21). If the coefficients contain further integration parameters, then this may block subsequent integrations; otherwise it may introduce an algebraic dependence on the physical parameters that the integral depends on.

An algebraic dependence on physical parameters may arise even if no rationalization procedure is required to express the integral (3.3.2) in terms of multiple polylogarithms. In particular, this can happen if the integration over the last variable x_n makes it necessary to introduce algebraic roots in order to factor the rational part of the integrand linearly. In either case, an algebraic dependence on physical parameters means that additional work must be done to express the end result in a fibration basis (see page 40): The algebraic roots first have to be expressed rationally by a suitable change of the *kinematic* variables.

Non-rationalizable roots If a hypersurface $V(h)$ associated to a root encountered during the integration process is not rational,[8] there is no hope to express the integral in terms of multiple polylogarithms, at least for generic values of the kinematic parameters. Instead, one can study the hypersurface $V(h)$ itself and attempt to develop a theory of functions and integrals defined on it.

The simplest case of this type is a smooth plane curve of degree three, which by the genus-degree formula (3.3.19) has genus $g = 1$. It is well known that a genus-one curve C together with a choice of a rational point $\mathcal{O} \in C$ determines an elliptic curve.[9] The points on a genus-one curve C cannot be parameterized by a rational map from $\mathbb{P}^1$ to C. Instead Clebsch found in [91] that a new class of functions called elliptic functions are required. The theory of functions on elliptic curves is a classical subject and there are many references for it, for example the books by Lang [92], Silverman [93] or Weil [94]. There also exist generalizations of polylogarithms and multiple polylogarithms to elliptic curves which we will comment more on in subsection 3.4.2 below.

Beyond a hypersurface $V(h)$ that is a curve of genus one, there are curves of higher genus as well as higher-dimensional non-rational hypersurfaces. Examples for curves of genus $g > 1$ associated to Feynman integrals were presented in [95]. In the higher-dimensional cases, it was found that often the d-dimensional hypersurface $V(h)$ is of Calabi-Yau type which means that it has a unique holomorphic d-form that vanishes nowhere on $V(h)$. It is generally hoped that integrals along (relative) homology cycles of differential forms on $V(h)$ will provide a basis of integrals for a given Feynman integral or that the differential equations satisfied by period integrals on such manifolds provide (part of) the differential equation satisfied by the Feynman integral. The Calabi-Yau geometries associated to Feynman integrals will be treated in more detail in subsections 3.4.1 and 3.4.2 below.

3.3.3 Applications of direct integration to Feynman integrals

We now give references to the literature where the method of direct integration in terms of multiple polylogarithms has been applied to Feynman integrals. Note that many of the references given here do not start the integration from a representation of the integral as in (3.1.3) with Mandelstam invariants as their physical parameters. In particular, it is desirable to reduce both the number of physical variables as well as the number of integration parameters before applying the integration algorithm. Regarding the former, one should attempt to express the integral in terms of variables that respect all of its symmetries, for example conformal cross-ratios in the case of conformal integrals. Regarding the latter, one can introduce integration parameters loop-by-loop in a Feynman diagram rather than for all loops at the same time as in (3.1.2). This technique was recently reviewed in [96, section 2.1].

In the context of scattering amplitudes for $\mathcal{N} = 4$ sYM, the authors of [97] demonstrated for planar diagrams that in many cases algebraic roots of physical parameters can be avoided during the integration, if the kinematics are parameterized by momentum twistor variables. This insight

[8] To show that a hypersurface is not rational, one studies so-called birational invariants. Such invariants are numbers (like the genus), groups or rings associated to a given hypersurface. By comparing to data for a projective space of the same dimension one may be able to decide that a hypersurface is not rational, see for example [90, chapter 4].

[9] The rational point $\mathcal{O} \in C$ serves as the origin for the group law on the elliptic curve.

was also used in [98] to compute the two-loop ratio and remainder function for six particles which was previously well known in the literature due to [99, 100, 101]. Crucially however, the authors of [98] computed their result from local, dual-conformally invariant loop integrands using a regulator that preserves dual-conformal symmetry.[10] In [16] we followed a very similar strategy for the two-loop remainder function for seven particles which was previously known due to [103].

In [17] we used direct integration to compute a particular component of the eight-point NMHV amplitude in planar $\mathcal{N} = 4$ sYM theory and analyzed its symbol. A major complication at eight points is the appearance of algebraic letters in the symbol that are not rationalized by the use of momentum twistor variables. For the particular component it turned out that all algebraic letters dropped out of the final result, but their appearance and form has been confirmed using different methods in [104].

Direct integration has also been used to associate a geometry to a given Feynman integral via the occurrence of non-rationalizable roots. In [105], the elliptic curve associated to a two-loop double-box integral was found using direct integration.[11] In [107] and [108] higher-dimensional Calabi-Yau geometries were found by the same method and in [18] we have taken a step towards a more detailed analysis of these geometries. We discuss the idea of associating a geometry with a non-polylogarithmic Feynman integral in more detail in the following section 3.4.

3.4 Non-polylogarithmic Feynman integrals

It is well known that sufficiently complicated Feynman integrals cannot be computed in terms of multiple polylogarithms and that new and more general classes of functions are required. Ideally, one would like to find classes of functions that suffice to express all Feynman integrals occurring in perturbation theory, possibly up to some loop order or number of external legs. At the same time these functions should not be too general, so that an understanding of their analytic properties is still possible. Moreover, the form of their singularities is constraint due to the behavior (3.2.9) and (3.2.10) near a Landau singularity. As a first step towards defining and understanding such functions, one can study a geometry associated to a given integral in more detail.

3.4.1 Associating a geometry to a Feynman integral

We discussed one way to associate a geometry to a Feynman integral in section 3.3.2. In this approach, the geometry is given as the hypersurface associated to a non-rationalizable root encountered in the process of direct integration. We point out again that speaking of "the" hypersurface is imprecise if the Feynman integral depends on kinematic data and that one should instead speak of a family of hypersurfaces whose moduli are (certain combinations of) the kinematic variables. As before, we consider the case of generic kinematic data.

An approach that is similar but not equivalent to direct integration is to analyze the multi-dimensional residues of the integrand: The integrand of a Feynman integral is a rational differential form with poles. In the loop momentum representation (3.1.1) for example there is a

[10] The dual-conformal invariance preserving regulator was first described in [102].

[11] Note that it was previously known due to [106] that the integral in question would involve an elliptic curve.

pole whenever $q_i^2 = m_i^2$, i.e. when an internal particle is on-shell. Similarly, in the representation (3.1.3) there is a pole at $\mathcal{F} = 0$.

The idea of multi-dimensional residues goes back to work by Poincaré in [109] and a standard reference for these so-called Poincaré residues is [90, chapter 5]. Informally, the idea is the following: The Poincaré residue is a map that takes a differential n-form ω with singularities along a hypersurface V and assigns to it a differential $(n-1)$-form denoted $\mathrm{Res}(\omega)$ and called the residue of ω that is well-defined on V. To compute $\mathrm{Res}(\omega)$ one finds local coordinates in which V is given by the vanishing of one coordinate, say $z = 0$, and expresses ω in terms of these coordinates. Then the residue is computed as

$$\mathrm{Res}(\omega) = \mathrm{Res}\left(\alpha \wedge \frac{\mathrm{d}z}{z}\right) = \alpha\big|_V, \tag{3.4.1}$$

where α is an $(n-1)$-form that is non-singular on V so that the restriction to V on the right-hand side makes sense. If $\mathrm{Res}(\omega)$ itself has simple poles along a hypersurface, then the residue map can be applied again. At some point this process stops, either because one has reached a differential zero-form or because the form does not have a pole. A classical example for the latter case is the holomorphic differential $\frac{\mathrm{d}x}{y}$ of an elliptic curve defined by an equation of the form $y^2 = P_3(x)$ for some polynomial $P_3(x)$ of degree three in x with no repeated roots.

The residue of the highest codimension is known as the leading singularity of an integral; in this form it was introduced in [110] (see also [111, section 2.3]) although a similar notion already exists much earlier, see for example [67, section 2.2]. In the more recent version, the idea is exactly what we just described: Starting with the integrand of a Feynman integral, one takes as many residues around the poles in the integrand as possible. From the loop momentum representation (3.1.1) it may seem that the maximum number of residues possible coincides with the number of propagators, but this is false: Jacobian factors can arise when bringing the integrand into a form to which (3.4.1) can be applied and those Jacobians may themselves develop singularities so that further residues can be taken.[12]

If in an application to a Feynman integral the process of taking residues stops with a zero-form, then usually the integral can be computed in terms of multiple polylogarithms. If it is not possible to take enough residues to reach a zero-form, then one is left with a differential form defined on some space whose geometry one can analyze. The latter case was first discussed in [106] where the authors found an elliptic curve in a two-loop integral with ten external particles. This integral is sometimes called the elliptic double box integral.

It is unknown if the direct integration and the leading singularity approach will always associate the same geometry to a given Feynman integral. At least in the case of the elliptic double box agreement was found: In [105] the authors analyzed this integral from the point of view of direct integration and their elliptic curve was found to be the same as the one that we detected by an analysis of its leading singularity in momentum twistor space in [19].

[12] This notion of the leading singularity it closely related to the maximal cut of a Feynman diagram, but not exactly the same. The maximal cut is is related to a discontinuity of the integral due to the work of Cutkosky [112]. The notion of leading singularity as the residue of the highest codimension does not directly have the interpretation as a discontinuity, essentially because the residue procedure requires integration over a contour that is different from the contour of the original Feynman integral. This point is elaborated in [111, section 2.3] and also in [113, section 7.5].

3.4.2 Elliptic and Calabi-Yau geometries

We already mentioned in subsection 3.3.2 that the simplest non-polylogarithmic Feynman integrals involve smooth curves of genus one which can be made into an elliptic curve by choosing an origin for the group law on the curve. Beyond that, both curves of higher genus as well as higher-dimensional geometries occur in Feynman integrals.

The elliptic case The theory of functions on elliptic curves is a well-developed classical subject with a vast literature (see for example the books [92, 93, 94]). It has been known for some time that classical polylogarithms can be generalized to elliptic polylogarithms which are functions on a punctured elliptic curve, see [114, 115, 116]. Recently in [117], Brown and Levin introduced also elliptic multiple polylogarithms as iterated integrals of one-forms that are well-defined on an elliptic curve, analogous to the definition of multiple polylogarithms in equation (3.3.1).

The idea is to iteratively integrate functions that are well-defined on an elliptic curve in the following sense: A complex elliptic curve is isomorphic to a complex torus $\mathbb{C}/\Lambda$, where Λ is a lattice defined by two periods ω_1 and ω_2 (see for example [118, chapter VI]).[13] A well-defined function f from $\mathbb{C}/\Lambda$ to $\mathbb{C}$ should be doubly periodic with respect to the periods ω_1 and ω_2, i.e. $f(\xi) = f(\xi + \omega_1) = f(\xi + \omega_2)$. Since the domain $\mathbb{C}/\Lambda$ of f is compact, the function is bounded[14]; then Liouville's theorem implies that if f is holomorphic everywhere on $\mathbb{C}/\Lambda$ it has to be a constant. Thus, in order to get more interesting functions, one either has to allow for poles, non-holomorphic functions or relax the periodicity constraint to quasi-periodicity. Allowing for poles one obtains meromorphic functions on $\mathbb{C}/\Lambda$ whose simple poles are further constrained by a residue theorem that states that the sum of the residues on $\mathbb{C}/\Lambda$ is equal to zero.

To obtain a function that is well-defined on the torus, one can take any function and sum over the images of translation by the periods. This is how the Weierstrass $\wp$-function is constructed which is a standard example of an elliptic function. It is periodic with respect to shifts by ω_1 and ω_2 and has a double pole at each point in the lattice $\mathbb{C}/\Lambda$. Similarly, the key idea to constructing an elliptic logarithm is to sum over all shifts of the argument of the logarithm according to the double periodicity property. Concretely, one first applies an exponential map so that instead of as $\mathbb{C}/\Lambda$ the elliptic curve is represented as $\mathbb{C}^\star/q^{\mathbb{Z}}$, where $q = e^{2\pi i\tau}$ and $\tau = \frac{\omega_2}{\omega_1}$ and $\mathbb{C}^\star = \mathbb{C} \setminus \{0\}$. The translation by a vector in the lattice Λ then amounts to multiplication by an integer power of q.

As a first step towards elliptic multiple polylogarithms one can then consider the function $\mathrm{Li}_1(z)$ (see [117, section 6]). The naive attempt to sum over all multiplications with q would be a sum of the form $\sum_{n\in\mathbb{Z}} \mathrm{Li}_1(q^n z)$ which does not work, because the series is not convergent. This may be fixed by introducing a damping factor u which leads to the series

$$E_\tau(z;u) = \sum_{n\in\mathbb{Z}} u^n \,\mathrm{Li}_1(q^n z). \tag{3.4.2}$$

[13] If the elliptic curve C is embedded into $\mathbb{P}^2$, then the isomorphism that maps $\mathbb{C}/\Lambda$ to C is given by $\xi \mapsto [\wp(\xi) : \wp'(\xi) : 1]$, where $\wp$ is Weierstrass' elliptic $\wp$-function. The inverse map from C to $\mathbb{C}/\Lambda$ involves elliptic integrals.

[14] We are only interested in continuous functions.

This series converges for $1 < u < |q|^{-1}$. It turns out that the differential of $E_\tau(z;u)$ with respect to z is related to the Kronecker-Eisenstein series $F_\tau(\xi;\alpha)$ by $\mathrm{d}E_\tau(z;u) = F_\tau(\xi;\alpha)\,\mathrm{d}\xi$ with $z = e^{2\pi i\xi}$ and $u = e^{2\pi i\alpha}$ (see [117, lemma 47]). The Kronecker-Eisenstein series is a quasiperiodic function of ξ and may be defined in terms of the Jacobi ϑ-function ϑ_{11} by

$$F_\tau(\xi;\alpha) = \frac{\vartheta_{11}'(0;\tau)\vartheta_{11}(\xi+\alpha;\tau)}{\vartheta_{11}(\xi;\tau)\vartheta_{11}(\alpha;\tau)}. \tag{3.4.3}$$

A reference for this series that appears frequently in the study of elliptic functions is [94].

This "averaging" procedure can be repeated for multiple polylogarithms and one obtains a version of them that is well-defined on the torus. Eventually these functions may be reformulated as integrals of certain one-forms that appear in an expansion of the differential $\mathrm{d}E_\tau(z,u)$ in u. Explicit expressions of these forms can therefore be computed from a slight modification of the Kronecker-Eisenstein series (3.4.3) that makes $F_\tau(\xi;\alpha)$ periodic,

$$\Omega_\tau(\xi;\alpha) = e^{2\pi i\frac{\Im(\xi)}{\Im(\tau)}}F_\tau(\xi;\alpha)\,\mathrm{d}\xi. \tag{3.4.4}$$

The coefficients of α in the expansion of $\Omega_\tau(\xi;\alpha)$ around $\alpha = 0$ gives the desired one forms,

$$\Omega_\tau(\xi;\alpha) = \sum_{n=0}^{\infty}\alpha^{n-1}f_\tau^{(n)}(\xi)\,\mathrm{d}\xi. \tag{3.4.5}$$

In analogy to the multiple polylogarithms $G(a_1,\ldots,a_n;x)$ defined recursively in (3.3.1), a class of elliptic multiple polylogarithms may thus be defined as

$$\Gamma_\tau\left(\begin{smallmatrix}n_1,\ldots,n_r\\ \eta_1,\ldots,\eta_r\end{smallmatrix};\xi\right) = \int_0^\xi \mathrm{d}\zeta\, f_\tau^{(n_1)}(\zeta-\eta_1)\,\Gamma_\tau\left(\begin{smallmatrix}n_2,\ldots,n_r\\ \eta_2,\ldots,\eta_r\end{smallmatrix};t\right), \tag{3.4.6}$$

where we are using the notation and definition given in [119, section 2.2]. In this iterated integral the one-forms are expressed in terms of integration kernels $f_\tau^{(n)}(\xi)$, $n\in\{0,1,2,\ldots\}$ that appear in the expansion (3.4.5). Some explicit examples are given in [119, section 3.3.1]. Crucially, the integration kernels are doubly periodic with respect to the periods 1 and τ,

$$f_\tau^{(n)}(\xi+1), = f_\tau^{(n)}(\xi), \qquad f_\tau^{(n)}(\xi+\tau) = f_\tau^{(n)}(\xi), \tag{3.4.7}$$

which makes them well-defined functions on a torus. With respect to a modular transformation $\gamma\in\mathrm{SL}(2,\mathbb{Z})$, the functions $f^{(n)}$ transform as

$$f_{\gamma\cdot\tau}^{(n)}\left(\frac{\xi}{c\tau+d}\right) = (c\tau+d)^n f_\tau^{(n)}(\xi), \tag{3.4.8}$$

where

$$\gamma = \begin{pmatrix}a & b\\ c & d\end{pmatrix}\in\mathrm{SL}(2,\mathbb{Z}) \quad\text{and}\quad \gamma\cdot\tau = \frac{a\tau+b}{c\tau+d}. \tag{3.4.9}$$

The functions $f^{(n)}$ are *not* meromorphic, but they satisfy the differential equation

$$\frac{\partial}{\partial\bar{\xi}}f_\tau^{(n)}(\xi) = -\frac{\pi}{\Im(\tau)}f_\tau^{(n-1)}(\xi). \tag{3.4.10}$$

It turns out that $f_\tau^{(1)}(\xi)$ has a pole at each lattice point $\xi = m + n\tau$ with $m, n \in \mathbb{Z}$. The other functions $f_\tau^{(n)}$ for $n \geq 2$ are free of poles.

Multiple zeta values are special values of multiple polylogarithms (see (B.1.7) in appendix B) and similarly elliptic multiple zeta values are special values of the functions defined in (3.4.6) when all $\eta_i = 0$ and $\xi = 1$. The functions Γ as well as their special values also appear naturally in scattering amplitudes in string theory, see [120, 121].

For applications to field theory Feynman integrals the elliptic polylogarithms defined in (3.4.6) are not a very natural choice. In particular, recall from section 3.4.1 that the geometry associated to a Feynman integral typically arises as the zero locus of some polynomial which is obtained from the original integrand through algebraic manipulations such as taking residues. Specifically, an elliptic curve would not naturally be given as a complex torus $\mathbb{C}/\Lambda$ but for example as the zero locus of a polynomial of degree three. While it is always possible to describe a complex elliptic curve as a complex torus, passing from the algebraic picture to the complex torus involves non-canonical choices that one might want to avoid. Moreover, if one decides to pass to the torus picture anyways, an explicit dependence on $\bar{\xi}$ will never arise. The integration kernels $f_\tau^{(n)}(\xi)$ on the other hand do have a dependence on $\bar{\xi}$ as can be seen from eq. (3.4.10).

A recursive definition that is more natural from the point of view of a genus-one curve given as the zero-locus of a polynomial of degree three is given in [122, section 3.2]. In [122, section 4.3] the authors moreover define elliptic multiple polylogarithms $\tilde{\Gamma}$ that are very similar to the ones in equation (3.4.6) but using kernels that do not satisfy the periodicity condition (3.4.7). On the other hand, their kernels are meromorphic unlike the kernels $f_\tau^{(n)}(\xi)$ used above. It turns out to be impossible to have kernels that are both meromorphic and doubly periodic *if* one insists on *single* simple poles, see [122, section 4.3]. As explained in [122, section 5] all these different definitions lead to essentially the same class of functions.

A lot of progress has been made on elliptic multiple polylogarithms recently and they have been used to express various non-polylogarithmic Feynman integrals (see for example [123, 124] or [125]). Various tools such as the coaction and the symbol have also been generalized to the elliptic setting [126] and algorithms for numerical evaluation have been released [127].

Calabi-Yau geometries Higher-dimensional geometries associated to Feynman integrals have often been observed to be of Calabi-Yau type. The Calabi-Yau geometry is one direction to consider when looking for generalizations of elliptic curves: A Calabi-Yau manifold of complex dimension n admits a single holomorphic n-form and in the case $n = 1$ one recovers the holomorphic one-form of an elliptic curve.

It is not known what a generalization of (multiple) polylogarithms to a Calabi-Yau manifold with dimension greater than one should be. On the other hand, higher-dimensional analogues of elliptic integrals have indeed been studied and are known as the period integrals of a Calabi-Yau manifold. The period integrals satisfy a system of differential equations known as Picard-Fuchs equations which provides at least part of the system of differential equations that the original Feynman integral satisfies.

There are various ways to derive Picard-Fuchs differential equations, for example the method by Griffiths (see [128]) or the approach by Gel'fand, Kapranov and Zelevinsky (GKZ, see [129]). Both methods have been applied to Feynman integrals, see for example [130, 131, 132] for the former and [133, 134] for the latter approach. The reference [132] also makes connections to

Calabi-Yau mirror symmetry which has been studied extensively in the math and string theory physics literature.

By now there is a long list of Feynman integrals that are known to involve Calabi-Yau geometries in addition to the references already mentioned. The earliest examples can be found in the work by Brown [79, section 12.7]; a K3 surface occurring at high loop order in ϕ^4 theory was diagnosed in [135]. K3 surfaces with relation to virtual QED processes were investigated [136, 137]. Using a residue analysis as explained in subsection 3.4.1 as well as direct integration Calabi-Yau manifolds were identified in large classes of Feynman integrals in [107, 108, 18, 19].

Currently there is no general framework of functions applicable to Feynman integrals that involve Calabi-Yau or potentially even more complicated geometries. It is even an open question whether different parameterizations of a Feynman integral always give rise to the same geometry. Regarding this latter point, we took some steps to answer the question for the elliptic sunrise and double box integrals in [20]; there we made use of the fact that complex elliptic curves can be characterized by a single invariant, the so-called j-invariant. For other Calabi-Yau geometries this is an open problem.

3.5 Summary of own work and outlook

In this chapter we have discussed the integration of Feynman integrals in terms of special functions that depend on the external kinematic data. We have seen that Landau's work determines both where these functions are allowed to have singularities as well as their behavior close to a singularity. In particular, near a singularity a Feynman integral behaves like a logarithm as in equation (3.2.9). We then reviewed the algorithm that expresses a Feynman integral in terms of the class of multiple polylogarithms if possible. We also identified algebraic roots arising from partial fractioning as an obstruction to direct integration that may sometimes be overcome by a rationalizing change of variables. When the obstruction cannot be overcome, we explained how one can associate a geometry to a Feynman integral. This geometry was an elliptic curve in the simplest cases beyond polylogarithms and of Calabi-Yau type in more complicated cases. An important comment was that there are different ways to define such a geometry, for example as a hypersurface associated to a non-rationalizable root encountered during direct integration or as the space on which one cannot take further residues. Sometimes one may even construct the geometry directly in momentum twistor space. Whether the different approaches always lead to the same geometry is a topic for further investigation.

During the time of this PhD we have contributed to the following publications related to the integration and analytic structure of Feynman integrals described in this chapter:

1. **J. L. Bourjaily, M. Volk, and M. Von Hippel**, "Conformally Regulated Direct Integration of the Two-Loop Heptagon Remainder," *JHEP* **02** (2020) 095, arXiv:1912.05690 [hep-th].

   In this paper, we recomputed the two-loop seven-particle remainder function in planar $\mathcal{N} = 4$ sYM theory. The remainder function appears as the logarithm of the two-loop MHV amplitude which can be expressed in terms of dual-conformally invariant double-pentagon integrals (see [111]). These integrals are infrared-divergent and we regulated them using the dual-conformal regulator introduced in [102]. Applying the direct integration method

described in section 3.3.1 together with the rationalization tricks in section 3.3.2, we obtained the same result for the seven-particle remainder function as [103].

2. **J. L. Bourjaily, A. J. McLeod, C. Vergu, M. Volk, M. Von Hippel, and M. Wilhelm**, "Rooting Out Letters: Octagonal Symbol Alphabets and Algebraic Number Theory," *JHEP* **02** (2020) 025, arXiv:1910.14224 [hep-th].

   It had been conjectured for a while that the eight-particle two-loop NMHV amplitudes in $\mathcal{N} = 4$ sYM theory would not be be expressible rationally in terms of momentum-twistor variables. The goal of this paper was to test the conjecture for a simple such amplitude. One particular component of the superamplitude requires only the computation of two eight-point two-loop integrals. We computed these integrals using the methods described in section 3.3.1 at a particular numeric point and analyzed the symbol of the resulting expression. To clean up and simplify the symbol, we had to find identities between algebraic letters for which we used techniques from algebraic number theory. It turned out that in the particular component that we considered all algebraic letters canceled, but their appearance in the eight-particle two-loop NMHV amplitudes has since been confirmed using a different approach (see [104]).

3. **J. L. Bourjaily, A. J. McLeod, C. Vergu, M. Volk, M. Von Hippel, and M. Wilhelm**, "Embedding Feynman Integral (Calabi-Yau) Geometries in Weighted Projective Space," *JHEP* **01** (2020) 078, arXiv:1910.01534 [hep-th].

   This paper shows that many of the Calabi-Yau geometries encountered in Feynman integrals can be realized as a hypersurface in a particular weighted projective space. The hypersurfaces are detected using a residue analysis as described in section 3.4.1. We compute the Hodge numbers of such hypersurfaces using a combinatorial approach due to Batyrev [138]. The main examples of the paper are the three-loop traintrack and three-loop wheel integrals which correspond to a Calabi-Yau two- and three-fold respectively. The analysis is done entirely in Feynman parameters space.

4. **C. Vergu and M. Volk**, "Traintrack Calabi-Yaus from Twistor Geometry," *JHEP* **07** (2020) 160, arXiv:2005.08771 [hep-th].

   It had been conjectured in [107] based on direct integration methods that a certain class of Feynman integrals now known as traintrack integrals contains a Calabi-Yau $(\ell - 1)$-fold at ℓ loops. In this paper, we come to the same conclusion analyzing the leading singularity of these integrals directly in momentum twistor space without the need to introduce integration parameters. For two loops we find the same elliptic curve as [107] as the intersection of two quadrics in $\mathbb{P}^3$. For three loops we construct a K3 surface as a four-fold covering of $\mathbb{P}^1 \times \mathbb{P}^1$ branched over two genus-one curves and describe some of its characteristics such as the dimension of the moduli space and certain automorphisms. We also show how the geometric construction generalizes to higher loops and take some steps towards a supersymmetrization.

5. **H. Frellesvig, C. Vergu, M. Volk, and M. von Hippel**, "Cuts and Isogenies," *JHEP* **05** (2021) 064, arXiv:2102.02769 [hep-th].

In this paper, we address the question of whether different parameterizations of a Feynman integral give rise to the same geometry. We consider first the elliptic sunrise integral in two dimensions for which two different elliptic curves had previously been found in [139, 125] using either Feynman parameterization or a maximal cut in the Baikov representation. The curves were found to be isogenous, but not isomorphic. We explain that this is due to a change of coordinates that is not one-to-one and that when computed more carefully the maximal cut and the Feynman parameter integral give rise to the same elliptic curve. We then perform a similar analysis for the elliptic double box integral in four dimensions and again find that the elliptic curve is the same in different representations.

6. **J. L. Bourjaily, Y.-H. He, A. J. McLeod, M. Spradlin, C. Vergu, M. Volk, M. von Hippel, and M. Wilhelm**, "Direct Integration for Multi-leg Amplitudes: Tips, Tricks, and When They Fail," in *Antidifferentiation and the Calculation of Feynman Amplitudes*. 3, 2021. arXiv:2103.15423 [hep-th].

   This article is a review of the direct integration method, its limits and results obtained in applications to Feynman integrals.

There are many open research question in particular pertaining to Feynman integrals that cannot be expressed in terms of multiple polylogarithms. In particular, the geometries that were described in the articles above must be studied in more details.

An important question to address are the moduli spaces of the Calabi-Yau varieties that have been detected. Just from counting the kinematic parameters that enter in the Feynman integral it is clear that those varieties are not generic, but instead live on some subspace of a generic Calabi-Yau variety of the same dimension. Moreover one can expect that the varieties arising in some Feynman integrals will have special properties such as marked points or a fibration structures that are not present in a generic variety of the same type. For the purpose of expressing a Feynman integral in terms of an iterated integral on some kinematic space, it is necessary to understand the homology and cohomology of the space. An understanding of the moduli spaces and special features associated to the detected varieties will thus be a crucial step towards analytic control over functions associated to non-polylogarithmic (and also non-elliptic) Feynman integrals.

From a detailed study of the varieties and their moduli spaces one can also expect progress on the differential equations that the Feynman integral satisfies. As mentioned previously, there are well-known ways to derive Picard-Fuchs equations for the varieties associated to such integrals, for example the Griffiths-Dwork or the GKZ method. While these methods work for some Feynman integrals as has been demonstrated in the literature, they are very general and do not take into account the special features that can be found in Feynman integral. It is to be expected that a more tailored approach will allow for an extension of these methods to Feynman integrals with a larger number of moduli and larger number of loops.

Eventually one would like to understand the analytic structure of the most complicated Feynman integrals and express them in terms of functions that make analytic properties such as singularities and monodromies manifest. Even in the elliptic case, where elliptic multiple polylogarithms are now available as a tool, these properties are often not very transparent. One might be discouraged by the fact that already the elliptic case is somewhat complicated and that integrals involving more complicated varieties should be expected to be even more involved. On

the other hand, Feynman integrals have many special and striking properties, for example the very simple behavior near Landau singularities that was discussed above and that constrains the analytic structure. Taking into account as many of these properties as possible one can hope to understand even the non-elliptic Feynman integrals reasonably well at some point.

Appendix A

The AdS/CFT correspondence and $\mathcal{N} = 4$ sYM theory

The best-studied instance of the correspondence between a gravitational theory on anti-de Sitter space and a conformal field theory living on its boundary is the duality between type IIB supergravity on $AdS_5 \times S^5$ and $\mathcal{N} = 4$ sYM in four dimensions. This correspondence was established by Maldacena in [21] by considering a stack of N D3 branes in type IIB superstring theory.

A.1 Heuristic derivation of the correspondence

The correspondence between the two theories can be motivated by studying the stack of D3 branes from two different points of view. In the open string perspective, the D3 branes are viewed as the end point for open strings in ten-dimensional Minkowski space. In the closed string perspective, the D3 branes are viewed as a particular solution to the supergravity equations of motion. The equivalence of these two perspectives leads to the AdS/CFT correspondence as we briefly review now.

Open string perspective For the open string perspective, one considers type IIB superstring theory on ten-dimensional Minkowski space $\mathbb{R}^{1,9}$ with a background of N coincident D3 branes. The degrees of freedom in this background are the open strings stretching between the D3 branes as well as closed strings propagating in ten dimensions. In order to stay in the realm of perturbative string theory, the string coupling constant g_s has to be small. In fact, the effective open string coupling in the case of N coincident D3 branes is $g_s N$; for the perturbative picture to be valid one therefore requires $g_s N \ll 1$.

Massive string excitations have a mass of order $\alpha'^{-1/2}$; for energies E much lower than that, i.e. for $E \ll \alpha'^{-1/2}$, these may be neglected and one only considers massless excitations. From the point of view of the world volume theory of the D3 branes, the open string excitations along the world volume directions correspond to a gauge field A_μ and the excitations in the transverse directions to scalars. Together with their fermionic companions, these organize themselves into a four-dimensional $\mathcal{N} = 4$ supermultiplet. Similarly, the massless closed string modes fall into a ten-dimensional $\mathcal{N} = 1$ supermultiplet.

In the limit $\alpha' \longrightarrow 0$, the open and closed string modes decouple. The action for the open

strings becomes the well-known action for $\mathcal{N} = 4$ sYM in four dimensions, which we write as

$$S = \frac{2}{g_{\mathrm{YM}}^2} \int \mathrm{d}^4x \,\mathrm{tr}\Bigg[-\frac{1}{4}F_{\mu\nu}F^{\mu\nu} - \frac{1}{2}\left(D_\mu\phi_i\right)\left(D^\mu\phi_i\right) + \frac{i}{2}\overline{\psi}\gamma^\mu D_\mu\psi \\ + \frac{1}{4}\left[\phi_i,\phi_j\right]\left[\phi_i,\phi_j\right] + \frac{1}{2}\sum_{i=1}^{3}\overline{\psi}_a G^i_{ab}\left[\phi_i,\psi_b\right] + \frac{1}{2}\sum_{i=4}^{6}\overline{\psi}_a G^i_{ab}\left[\phi_i,\psi_b\right]\Bigg]. \tag{A.1.1}$$

Here A_μ is the four-dimensional non-abelian gauge field, each ϕ_i for $i \in \{1,\dots,6\}$ is a real scalar field and each ψ_a for $a \in \{1,\dots,4\}$ is a four Majorana-Weyl fermion. All fields transform in the adjoint representation of the U(N) gauge group and the string coupling g_s has been identified with the coupling of sYM theory by

$$g_{\mathrm{YM}}^2 = 2\pi g_s. \tag{A.1.2}$$

Moreover, in the limit $\alpha' \longrightarrow 0$, the action of the closed string modes simply becomes the action of ten-dimensional supergravity.

Closed string perspective The D3 branes may also be viewed as a special solution to the equations of motion of ten-dimensional type IIB supergravity.[1] These massive, charged branes constitute the background for closed string excitations of type IIB superstring theory. The solution is characterized by a length scale L which can be determined by the requirement that the total charge of N coincident D3 branes should be given by $\mu_3 N$. One finds that L is related to the string theory parameters by

$$\frac{L^4}{\alpha'^2} = 4\pi g_s N. \tag{A.1.3}$$

The background supergravity solution is made up of two regions: If the radial distance r from the D3 branes is very large compared to L, the closed strings essentially do not feel the presence of the branes and the theory reduces to type IIB supergravity on flat, ten-dimensional Minkowski space. On the other hand, in the region $r \ll L$, the background metric becomes the metric of $\mathrm{AdS}_5 \times S^5$ in which both the radius of the sphere and the AdS_5 are given by L. In the low-energy limit $\alpha' \longrightarrow 0$, the two regions decouple from each other.

For the supergravity approximations to be valid, one has to require that the radius of curvature is large compared to α', i.e. $L^4 \gg \alpha'^2$, which due to the identification (A.1.3) means that $g_s N \gg 1$. Note that this is opposite from the open string perspective where we had $g_s N \ll 1$.

Identification of theories Both points of view give rise to two decoupled low-energy systems and in both pictures one of those systems is type IIB supergravity on ten-dimensional Minkowski space $\mathbb{R}^{1,9}$. The two points of view have the same starting point and should describe the same physics which lead Maldacena to conjecture in [21] that the remaining two low-energy systems, namely $\mathcal{N} = 4$ sYM in four dimensions and type IIB supergravity on $\mathrm{AdS}_5 \times S^5$ should also be identified.

We speak of $\mathcal{N} = 4$ sYM as the field theory side of this correspondence and by abuse of language of the $\mathrm{AdS}_5 \times S^5$ side as the string theory side. On the field theory side the parameters

[1] This point of view was established by Polchinski in [140].

are the Yang-Mills coupling g_{YM} and the rank of the gauge group N. On the string theory side, the parameters are the string coupling g_s and the ratio $\frac{L^4}{\alpha'^2}$. As written in (A.1.2) and (A.1.3) they are related by

$$g_{\mathrm{YM}}^2 = 2\pi g_s \qquad \text{and} \qquad 2g_{\mathrm{YM}}^2 N = \frac{L^4}{\alpha'^2}. \tag{A.1.4}$$

Note that in the limit $N \longrightarrow \infty$ which we usually consider, the 't Hooft coupling $\lambda = g_{\mathrm{YM}}^2 N$ is the only parameter and the relation becomes $2\lambda = L^4 \alpha'^{-2}$.

A.2 Dictionaries

To check and make use of the proposed duality, one has to be able to translate objects and physical quantities from one side to the other. This section is a reminder of the most important entries in the dictionary that achieves this translation.

Field-operator map On the field theory side, we are dealing with $\mathcal{N} = 4$ sYM theory which is a superconformal field theory. One class of observables thus consists of correlation functions of gauge invariant operators. These operators are organized in representations of the superconformal algebra $\mathfrak{psu}(2,2|4)$ which has the bosonic subalgebra $\mathfrak{su}(2,2) \times \mathfrak{su}(4)$. The $\mathfrak{su}(2,2) \cong \mathfrak{so}(2,4)$ factor corresponds to the conformal algebra, while the $\mathfrak{su}(4) \cong \mathfrak{so}(6)$ factor represents the R-symmetry. An operator is thus labeled by a conformal dimension Δ, two Lorentz spins (s_1, s_2) for $\mathfrak{so}(1,3) \cong \mathfrak{su}(2) \times \mathfrak{su}(2)$ and three quantum numbers corresponding to the R-symmetry.

On the string theory side, the $\mathfrak{so}(2,4)$ and $\mathfrak{so}(6)$ symmetries correspond to the isometries of the AdS_5 and S^5 factors of the geometry respectively. Under the duality, a field theory operator with a given set of quantum numbers should correspond to a supergravity field with the same quantum numbers. To this end, the supergravity fields are decomposed into Kaluza-Klein modes on the sphere by expanding them in spherical harmonics on S^5 that constitute irreducible representations of $\mathfrak{so}(6)$.

From the AdS_5 point of the view, the Kaluza-Klein modes are massive modes with a certain mass m^2 that is determined by the R-symmetry quantum numbers. Near the boundary of AdS_5, such a massive mode φ has an expansion

$$\varphi(z,x) = \left[\varphi^{(0)}(x) + \mathcal{O}\left(z^2\right)\right] z^{\Delta_-} + \left[\varphi^{(+)}(x) + \mathcal{O}\left(z^2\right)\right] z^{\Delta_+}. \tag{A.2.1}$$

Here z denotes the radial coordinate of AdS_5 in Poincaré coordinates and the four-dimensional boundary with coordinates $x = (x^0, x^1, x^2, x^3)$ is located at $z = 0$. The exponents $\Delta_\pm$ are given by $\Delta_\pm = 2 \pm \sqrt{m^2 + 4}$. Under the correspondence, the boundary value $\varphi^{(0)}$ is identified with the source for a field theory operator $\mathcal{O}_\Delta$ with conformal dimension $\Delta = \Delta_+$. The other boundary value $\phi^{(+)}$ is associated with a vacuum expectation value of $\mathcal{O}_\Delta$.[2]

[2]The association of $\varphi^{(0)}$ with a source and $\varphi^{(+)}$ with a vacuum expectation value can be interchanged if the AdS mass m^2 satisfies $-4 \leq m^2 \leq -3$. For m^2 in this range one can choose to associate $\varphi^{(0)}$ with the vacuum expectation value and $\varphi^{(+)}$ with the source on the field theory side. This leads to two inequivalent theories that differ by a non-zero boundary term in the action. For $-3 < m^2$, the association presented in the main text is the only option. Note that the negative masses are not a stability problem as they lie above the Breitenlohner-Freedman bound $-\frac{d^2}{4} = -4 \leq m^2$.

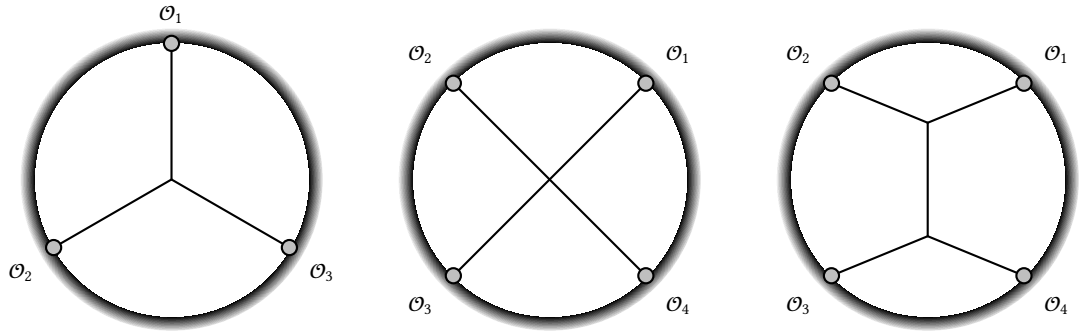

Figure A.1: Witten diagrams for three- and four-point field theory correlators. The circle depicts the boundary of AdS_5 where the operators $\mathcal{O}_i$ are inserted. The solid lines in the interior are AdS_5 bulk-to-boundary and bulk-to-bulk propagators.

Correlation functions of field theory operators are computed by taking functional derivatives of a generating function with respect to sources and subsequently setting the sources to zero. Under the dictionary, the field theory partition function and the supergravity action S_{SG} are identified as

$$\left\langle \exp\left(\int \mathrm{d}^4 x\, \mathcal{O}(x) \varphi^{(0)}(x) \right) \right\rangle_{\text{CFT}} = e^{-S_{\text{SG}}[\varphi]}. \tag{A.2.2}$$

Taking functional derivatives with respect to the source $\phi_i^{(0)}$ for each operator $\mathcal{O}_i$, one can therefore compute field theory correlation functions from the supergravity action by

$$\langle \mathcal{O}_1(x_1) \cdots \mathcal{O}_n(x_n) \rangle = - \frac{\delta S_{\text{cl}}\left[\phi_1^{(0)}, \ldots, \phi_n^{(0)}\right]}{\delta \phi_1^{(0)}(x_1) \cdots \delta \phi_n^{(0)}(x_n)} \bigg|_{\phi_i^{(0)}=0}. \tag{A.2.3}$$

This prescription is due to Gubser, Klebanov and Polyakov [141] as well as Witten [142] and is called GKPW prescription for short. The right-hand side leads to a diagrammatic expansion of field theory correlators in terms of so-called (tree-level) Witten diagrams (see figure A.1).

Other entries in the dictionary The GKPW prescription provides a way to compute the correlation functions of local field theory operators from the dual string theory side. Of course, there are other interesting observables on the field theory side that one would like to compute in this way.

A famous example is the expectation value of a field theory Wilson loop, i.e. the expectation value of a non-local operator of the form

$$W(\gamma) = \operatorname{tr}\left[\operatorname{Pexp}\left(\int_\gamma \mathcal{A} \right) \right], \tag{A.2.4}$$

where $\gamma : t \mapsto (x^0(t), x^1(t), x^2(t), x^3(t))$ is a closed path in four dimensions and $\mathcal{A}$ is a combination of the gauge field A_μ and the scalars ϕ_i of $\mathcal{N} = 4$ sYM,

$$\mathcal{A} = \left(i A_\mu \dot{x}^\mu + |\dot{x}|\, \phi_i n^i \right) \mathrm{d}t \quad \text{with} \quad \delta_{ij} n^i n^j = 1 \quad \text{and} \quad \dot{x}^\mu = \frac{\partial x^\mu}{\partial t}. \tag{A.2.5}$$

The dual description of such a Wilson loop proposed in [143] and [144] is given by a string in $AdS_5 \times S^5$ whose world-sheet ends on the loop γ on the boundary of AdS_5. This string has to minimize the action and the world-sheet then is essentially a surface of minimal area in $AdS_5 \times S^5$ with the prescribed boundary γ.

Another well-known entry is the relation between gluon scattering amplitudes at strong coupling and the minimal area of the worldsheet of a fundamental string on the gravity side. This relation was found in [145]. Since the string has to end on a light-like curve, this establishes a relation between strong coupling gluon amplitudes and light-like Wilson loops. The IR-divergent part of these amplitudes can moreover be compared to an all-loop field-theory conjecture known as the BDS ansatz [146]. One of the relevant quantities that can be compared is the cusp anomalous dimension which was also computed from integrability in [147].

Finally, a connection between the two sides of the correspondence is also established through integrability. On the field theory side, this was first found in [148] by mapping the one-loop dilatation operator of the theory to the Hamiltonian of an integrable spin chain. Generalizations to higher loops and more results are found in [149]. Integrable structures have similarly been found on the string-theory side, in the form of σ-models (see for example [150]).

Appendix B

Multiple polylogarithms and the symbol

B.1 Multiple polylogarithms

Classical polylogarithms and iterated integrals Classical polylogarithms can be defined by the series expansion

$$\mathrm{Li}_n(x) = \sum_{k=1}^{\infty} \frac{x^k}{k^n}, \quad |x| \leq 1, n \in \mathbb{N}. \tag{B.1.1}$$

To analytically continue this function outside the unit disk one expresses $\mathrm{Li}_n(x)$ as an iterated integral. Iterated integrals were studied by Chen in [15] and are defined as follows: Let M be a smooth, complex manifold. Let $\gamma : [0,1] \longrightarrow M$ be a path defined by $t \mapsto (x_1(t), \dots, x_n(t))$ and $\omega_1(x), \dots, \omega_r(x)$ be differential one-forms on M. Then the iterated integral along γ is defined as

$$\int_\gamma \omega_1 \circ \cdots \circ \omega_r = \int_0^1 \gamma^\star \omega_1(t_1) \int_0^{t_1} \gamma^\star \omega_2(t_2) \int_0^{t_2} \cdots \int_0^{t_{r-1}} \gamma^\star \omega_r(t_r), \tag{B.1.2}$$

where $\gamma^\star \omega_i(t_i)$ is the pull-back of ω_i to $[0,1]$. If the one-forms ω_i satisfy a certain integrability criterion, the iterated integral is independent of the path and only depends on the end point $\gamma(0)$ and $\gamma(1)$. In this sense the polylogarithm (B.1.1) can be expressed as an iterated integral as

$$\mathrm{Li}_n(x) = \int_0^x \underbrace{\frac{\mathrm{d}t}{t} \circ \cdots \circ \frac{\mathrm{d}t}{t}}_{n-1} \circ \frac{\mathrm{d}t}{1-t}, \quad n \geq 1. \tag{B.1.3}$$

The notation $\int_0^x$ denotes an integral along a path in the complex plane that begins at zero and ends at x. The iterated integral can also be written recursively as

$$\mathrm{Li}_n(x) = \int_0^x \frac{\mathrm{d}t}{t} \, \mathrm{Li}_{n-1}(t), \quad n \geq 2 \tag{B.1.4}$$

with $\mathrm{Li}_1(x) = -\log(1-x)$.

Multiple polylogarithms Multiple polylogarithms were defined by Goncharov as a generalization of the series (B.1.1) to $d > 1$ variables (see [14]): Let $n_1, \dots, n_d \in \mathbb{N}$ and $x_1, \dots, x_d \in \mathbb{C}$ such that $|x_j| < 1$ for all $m = 1, \dots, d$. Then the multiple polylogarithm of depth d is defined as

$$\mathrm{Li}_{n_1,\dots,n_d}(x_1, \dots, x_d) = \sum_{0<k_1<\cdots<k_d} \frac{x_1^{k_1} \cdots x_d^{k_d}}{k_1^{n_1} \cdots k_d^{n_d}}. \tag{B.1.5}$$

The sum $n = n_1 + \cdots + n_d$ is called the weight. As the classical polylogarithms these functions can be expressed in terms of an iterated integral as

$$\mathrm{Li}_{n_1,\ldots,n_d}(x_1,\ldots,x_d) = (-1)^d \int_0^1 \underbrace{\frac{\mathrm{d}t}{t} \circ \cdots \circ \frac{\mathrm{d}t}{t}}_{n_d-1} \circ \frac{\mathrm{d}t}{t-b_d} \circ \cdots \circ \underbrace{\frac{\mathrm{d}t}{t} \circ \cdots \circ \frac{\mathrm{d}t}{t}}_{n_1-1} \circ \frac{\mathrm{d}t}{t-b_1}, \qquad b_j = \prod_{i=j}^{d} x_i^{-1}. \tag{B.1.6}$$

Note that when the argument(s) are equal to one, the sums in (B.1.1) and (B.1.5) reduce to (multiple) zeta values,

$$\zeta_n = \mathrm{Li}_n(1), \qquad \zeta_{n_1,\ldots,n_d} = \mathrm{Li}_{n_d,\ldots,n_1}(1,\ldots,1). \tag{B.1.7}$$

From the recursive expression (B.1.4), it is also natural to consider the generalization

$$G(a_1,\ldots,a_n;x) = \int_0^x \frac{\mathrm{d}t}{t-a_1} G(a_2,\ldots,a_n;t), \qquad G(x) = 1, \tag{B.1.8}$$

for $a_1,\ldots,a_n \in \mathbb{C}$. If all a_i are zero, one sets $G(0,\ldots,0;x) = \frac{1}{n!}\log^n(x)$. Such integrals were already studied a long time ago, for example by Kummer in [151], Poincaré in [152] or Lappo-Danilevski [153], but as a function of a single variable x. In [154] Goncharov considered them as multivalued analytic functions of $n+1$ variables and this is the perspective that we follow from now on. The functions G are the multiple polylogarithms that are most commonly used in the physics literature nowadays. We sometimes also use the notation $\mathbf{a} = (a_1,\ldots,a_n)$, i.e. $G(\mathbf{a};x) = G(a_1,\ldots,a_n;x)$, and write $|\mathbf{a}| = n$ for the number of entries in $\mathbf{a}$. The relation to the functions $\mathrm{Li}_{n_1,\ldots,n_d}$ defined in (B.1.5) is

$$\mathrm{Li}_{n_1,\ldots,n_d}(x_1,\ldots,x_d) = (-1)^d G(\underbrace{0,\ldots,0}_{n_d-1},b_d,\ldots,\underbrace{0,\ldots,0}_{n_1-1},b_1;1), \qquad b_j = \prod_{i=j}^{d} x_i^{-1}. \tag{B.1.9}$$

In particular this means that in the recursive definition (B.1.8) the weight $n = n_1 + \cdots + n_d = |\mathbf{a}|$ simply corresponds to the number of integrations.

The total differential of the functions G is

$$\begin{aligned}\mathrm{d}G(a_1,\ldots,a_n;x) = {} & G(\hat{a}_1,a_2,\ldots,a_n;x)\,\mathrm{dlog}\left(\frac{x-a_1}{a_2-a_1}\right) + G(a_1,\ldots,a_{n-1},\hat{a}_n;x)\,\mathrm{dlog}\left(\frac{a_{n-1}-a_n}{a_n}\right) \\ & + \sum_{i=2}^{n-1} G(a_1,\ldots,\hat{a}_i,\ldots,a_n;x)\,\mathrm{dlog}\left(\frac{a_{i-1}-a_i}{a_{i+1}-a_i}\right).\end{aligned} \tag{B.1.10}$$

A hat on an argument a_i means that it should omitted, e.g. $G(\hat{a}_1,a_2,\ldots,a_n;x) = G(a_2,\ldots,a_n;x)$.

Chen iterated integrals satisfy shuffle relations [155] which means that the product of two iterated integrals along the same path γ can be expressed as a combination of single integrals along γ,

$$\int_\gamma \omega_1 \circ \cdots \circ \omega_n \cdot \int_\gamma \omega_{n+1} \circ \cdots \circ \omega_{n+m} = \sum_{\sigma\in\Sigma(n,m)} \int_\gamma \omega_{\sigma(1)} \circ \cdots \circ \omega_{\sigma(n+m)}. \tag{B.1.11}$$

Here $\Sigma(n, m)$ is the set of shuffles of $\{1, \dots, n\}$ and $\{n+1, \dots, n+m\}$ which are permutations that preserve the order within each of the two sets,

$$\Sigma(n, m) = \left\{ \sigma \in \Sigma_{n+m} \,:\, \sigma^{-1}(1) < \cdots < \sigma^{-1}(n) \quad \text{and} \quad \sigma^{-1}(n+1) < \cdots < \sigma^{-1}(n+m) \right\}. \tag{B.1.12}$$

In the concrete case this means that the product of two MPLs with weights n and m evaluated at the same point z can be written as a linear combination of MPLs of weight $n+m$ evaluated at z,

$$G(a_1, \dots, a_n; z) G(a_{n+1}, \dots, a_{n+m}; z) = \sum_{\sigma \in \Sigma(n,m)} G(a_{\sigma(1)}, \dots, a_{\sigma(n+m)}; z) \tag{B.1.13}$$

From the series definition (B.1.5) for the functions $\mathrm{Li}_{n_1,\dots,n_d}$ one can derive a similar set of combinatorial relations called stuffle or quasi-shuffle relations. We will not comment further on those and refer to the original paper [156] instead.

Singularities and regularization The integral (B.1.8) diverges for $x \longrightarrow a_1$ and $x \longrightarrow \infty$, and has to be regularized. The limit $x \longrightarrow 0$ is generally finite as long as at least one of the arguments $(a_1, \dots, a_n)$ is non-zero and after applying the regularization procedure that we will describe momentarily,

$$\lim_{x \to 0} G(a_1, \dots, a_n; x) = \begin{cases} 0 & n \geq 1, \\ 1 & n = 0, \end{cases} \qquad \text{if } a_i \neq 0 \text{ for some } i \in \{1, \dots, n\}. \tag{B.1.14}$$

In all cases, the singularities of MPLs are at worst logarithmic, which means that as z approaches a singular point z_0 they have an expansion in powers of logarithms,

$$G(\mathbf{a}; z) = \sum_{k=0}^{N} g^{(k)}_{\mathbf{a},z_0}(z) \begin{cases} \log^k(z - z_0), & z_0 \in \mathbb{C}, \\ \log^k(z), & z_0 = \infty. \end{cases} \tag{B.1.15}$$

The functions $g^{(k)}_{\mathbf{a},z_0}(z)$ are analytic at $z = z_0$ and the regularized limit of a G-function is defined as the lowest term in the expansion (B.1.15),

$$\operatorname*{Reg}_{z \to z_0} G(\mathbf{a}, z) = g^{(0)}_{\mathbf{a},z_0}(z_0) \tag{B.1.16}$$

The limit $\lim_{z \to z_0} G(\mathbf{a}; z)$ coincides with the regularized limit $\operatorname{Reg}_{z \to z_0} G(\mathbf{a}; z)$ whenever the former exists. Thus, the limit of a linear combination,

$$\lim_{z \to z_0} \sum_{\mathbf{a}} c_{\mathbf{a}}(z) G(\mathbf{a}; z) \tag{B.1.17}$$

can be computed term by term with (B.1.16). The function $g^{(k)}_{\mathbf{a};z_0}$ on the right-hand side of (B.1.16) can be obtained explicitly by using the shuffle algebra of the MPLs. This is explained in detail in [80, section 3.3.1]. Importantly, the regularization procedure preserves the shuffle algebra structure.

Removing parameter-dependent arguments In the definition (B.1.8) it is important that the arguments of $G(a_2, \dots, a_n; t)$ in the integrand are independent of the integration parameter t. In the recursive algorithm described in section 3.3.1, this not fulfilled automatically. We briefly review how this dependence can be removed which is the statement of [77, lemma 2.7].

We assume that we have an MPL of weight n of the form $G(a_1(t), \dots, a_n(t); x)$ in which the arguments a_i depend on a parameter t. From the total differential (B.1.10) we find that the derivative with respect to t is

$$\begin{aligned}\partial_t G(a_1, \dots, a_n; x) = {} & G(\hat{a}_1, a_2, \dots, a_n; x)\, \partial_t \log(x - a_1) - G(a_1, \dots, a_{n-1}, \hat{a}_n; x)\, \partial_t \log(a_n) \\ & + \sum_{i=1}^{n-1} \left[G(a_1, \dots, \hat{a}_{i+1}, \dots, a_n; x) - G(a_1, \dots, \hat{a}_i, \dots, a_n; x)\right] \partial_t \log(a_{i+1} - a_i),\end{aligned} \tag{B.1.18}$$

where we have hidden the dependence of $(a_1, \dots, a_n)$ on t in order not to clutter the notation too much. The dependence of the a_i on t is removed recursively in the weight n, i.e. we assume the MPLs occurring in (B.1.18) have already been expressed in the form

$$\sum_{(b_1,\dots,b_{n-1})} c_{(b_1,\dots,b_{n-1})} G(b_1, \dots, b_{n-1}; t), \tag{B.1.19}$$

where the b_i are independent of t.

Now one would like to integrate (B.1.18) over t using the definition (B.1.8). In order to do so, one has to factor the rational prefactors of the MPLs linearly in t. Concretely one factors

$$a_{i+1}(t) - a_i(t) = \prod_\alpha (t - \alpha)^{n_\alpha}, \qquad 1 \le i \le n-1, \quad n_\alpha \in \mathbb{Z}, \tag{B.1.20}$$

after which

$$\partial_t \log(a_{i+1} - a_i) = \sum_\alpha \frac{n_\alpha}{t - \alpha}. \tag{B.1.21}$$

Similarly one factors $x - a_1$ and a_n in the first line of (B.1.18) linearly in t. Note that the roots α may be complicated algebraic expressions, but importantly they are independent of t.

This allows one to apply (B.1.8) and integrate the differential equation (B.1.18). The end result should be a new expression for the original function $G(a_1(t), \dots, a_n(t); x)$, which fixes the integration constant. This constant may be found symbolically as shown in [77, section 2.5]; alternatively one it may be determined numerically as in [78, appendix D].

B.2 The symbol

A very useful quantity to study multiple polylogarithms is the symbol, which was introduced into the physics literature in [157], but appeared already earlier in work by Goncharov [158, section 3]. The idea is to take an iterated integral (B.1.2), where all the one-forms are of the form $\omega_i = \mathrm{dlog}(R_i)$ for some algebraic function R_i, forget the information about the integrations and only keep the information about the forms. Concretely, the symbol $\mathcal{S}$ of an iterated integral of this type is a formal tensor product of all the R_i,

$$\mathcal{S}\left(\int_\gamma \mathrm{dlog}\,(R_1) \circ \cdots \circ \mathrm{dlog}\,(R_n)\right) = R_1 \otimes \cdots \otimes R_n. \tag{B.2.1}$$

This is extended to linear combinations of iterated integrals by linearity, i.e. a general symbol tensor looks like

$$\sum_{(i_1,\ldots,i_n)} c_{(i_1,\ldots,i_n)} R_{i_1} \otimes \cdots \otimes R_{i_n} \tag{B.2.2}$$

for some coefficients $c_{(i_1,\ldots,i_n)}$. In practice, the symbol of a function can often be obtained recursively from its total differential, see [159, section 3.2]. If the total differential of a function $f(x_1,\ldots,x_m)$ of m variables can be written as

$$\mathrm{d}f(x_1,\ldots,x_m) = \sum_i f_i(x_1,\ldots,x_m)\ \mathrm{dlog}\left(R^{(i)}(x_1,\ldots,x_m)\right), \tag{B.2.3}$$

then its symbol $\mathcal{S}$ may be defined recursively by

$$\mathcal{S}(f(x_1,\ldots,x_m)) = \sum_i \mathcal{S}(f_i(x_1,\ldots,x_m)) \otimes R^{(i)}(x_1,\ldots,x_m). \tag{B.2.4}$$

From the total differential in (B.1.10) we can see that this is applicable to the multiple polylogarithms $G(a_1,\ldots,a_n;z)$. Explicitly, the recursive formula then reads

$$\begin{aligned}\mathcal{S}\left(G(a_1,\ldots,a_n;x)\right) = {}& \mathcal{S}\left(G(\hat{a}_1,a_2,\ldots,a_n;x)\right) \otimes \left(\frac{x-a_1}{a_2-a_1}\right) \\ &+ \mathcal{S}\left(G(a_1,\ldots,a_{n-1},\hat{a}_n;x)\right) \otimes \left(\frac{a_{n-1}-a_n}{a_n}\right) \\ &+ \sum_{i=2}^{n-1} \mathcal{S}\left(G(a_1,\ldots,\hat{a}_i,\ldots,a_n;x)\right) \otimes \left(\frac{a_{i-1}-a_i}{a_{i+1}-a_i}\right).\end{aligned} \tag{B.2.5}$$

The identities between symbol tensors are relatively simple, since they are inherited from the functional equations of the logarithm,

$$S \otimes (ab) \otimes T = S \otimes a \otimes T + S \otimes b \otimes T \quad \text{and} \quad S \otimes (\pm 1) \otimes T = 0. \tag{B.2.6}$$

It is often stated (for example in [157]) that the symbol of a constant vanishes which fits with the recursive definition in terms of the total differential of a function. The symbol can however also be obtained as the maximum iteration of a coproduct defined on multiple polylogarithms that turns the algebra of multiple polylogarithms into a Hopf algebra. The coproduct and Hopf algebra were described in [160, section 2] and we will not go into further detail about these structures here. A recent review can be found in [161, section 6]. With this framework, the rule that the symbol of a function vanishes can be refined which is useful for working with symbols over a number field. In this case one can choose the symbol of each element of a sets of multiplicatively independent constants independently. This is discussed in [159, section 3.2] and also in [17, section 2.2], where it was used in practice.

The symbol of the multiple polylogarithms $G(a_1,\ldots,a_n;x)$ is compatible with the shuffle algebra,

$$\mathcal{S}(fg) = \mathcal{S}(f) \,\text{Ш}\, \mathcal{S}(g), \tag{B.2.7}$$

where f and g are multiple polylogarithms. Here Ш denotes the shuffle of symbol tensors,

$$(R_1 \otimes \cdots \otimes R_n) \text{ Ш } (R_{n+1} \otimes \cdots \otimes R_{n+m}) = \sum_{\sigma \in \Sigma(n,m)} R_{\sigma^{-1}(1)} \otimes \cdots \otimes R_{\sigma^{-1}(n+m)}. \tag{B.2.8}$$

This is extended to linear combinations of symbol tensors by linearity.

Not every arbitrary symbol tensor comes from an iterated integral. It was pointed out in [76, section 3.2] that a necessary and sufficient condition for this to be the case is the so-called integrability criterion,

$$\sum_{(i_1,\ldots,i_n)} c_{(i_1,\ldots,i_n)} R_{i_1} \otimes \cdots \otimes R_{i_{p-1}} \otimes R_{i_{p+2}} \otimes \cdots \otimes R_{i_n} \operatorname{dlog}\left(R_{i_p}\right) \wedge \operatorname{dlog}\left(R_{i_{p+1}}\right) = 0, \quad 1 \leq p < n, \tag{B.2.9}$$

which has to hold to all $p \in \{1, \ldots, n-1\}$.

A very general definition of the symbol and an explanation for the connections to and issues with the one given here in terms of the total differential is given in the notes [162, section 9].

Appendix C

Momentum twistors

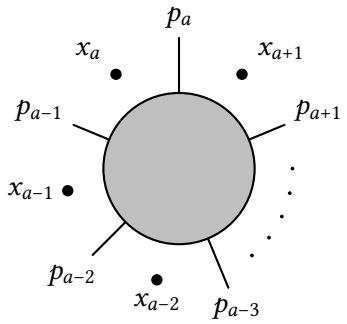

Figure C.1: Dual coordinates

For a planar Feynman diagram (see figure C.1) it is convenient to encode the m external momenta p_i in terms of so-called dual momentum variables x_i,

$$p_i = x_i - x_{i+1}. \tag{C.0.1}$$

In terms of these variables, momentum conservation $\sum_i^m p_i = 0$ simply becomes the condition that the x_i are labeled cyclically, i.e. $x_{m+1} = x_1$. Poincaré-invariant Mandelstam variables are constructed from the dual variables as

$$\left(x_i - x_j\right)^2 = \left(p_i + \cdots + p_{j-1}\right)^2. \tag{C.0.2}$$

In case the Poincaré symmetry is enhanced to conformal symmetry, only cross-ratios of the Mandelstam variables are invariant under the full symmetry. These cross-ratios are defined as

$$(i, j; k, \ell) = \frac{(x_i - x_j)^2 (x_k - x_\ell)^2}{(x_i - x_k)^2 (x_j - x_\ell)^2}. \tag{C.0.3}$$

It is well known that the four-dimensional conformal group $\mathrm{SO}(2,4)$ acts non-linearly on the dual variables x_i. It is known due to Dirac (see [163]) that the action can be linearized: In this so-called embedding formalism, conformally compactified (and complexified) four-dimensional Minkowski space $\mathbb{R}^{1,3}$ is represented as a quadric inside a five-dimensional projective space $\mathbb{P}^5$. If we denote the homogeneous coordinates on $\mathbb{P}^5$ by $[Y_0 : \cdots : Y_5]$, then the hypersurface corresponding to $\mathbb{R}^{1,3}$ is given by the equation

$$Y^2 = Y_0^2 - Y_1^2 + Y_2^2 - Y_3^2 - Y_4^2 - Y_5^2 = 0. \tag{C.0.4}$$

The homogeneous coordinates can be packaged into a 4×4 antisymmetric matrix $X_{\alpha\beta} = -X_{\beta\alpha}$ by

$$X_{01} = \frac{1}{\sqrt{2}}(Y_0 - Y_1), \quad X_{02} = \frac{1}{\sqrt{2}}(iY_3 + Y_4), \quad X_{03} = \frac{1}{\sqrt{2}}(Y_2 - Y_5), \tag{C.0.5}$$

$$X_{12} = -\frac{i}{\sqrt{2}}(Y_2 + Y_5), \quad X_{13} = \frac{1}{\sqrt{2}}(-iY_3 + Y_4), \quad X_{23} = \frac{1}{\sqrt{2}}(Y_0 + Y_1). \tag{C.0.6}$$

The condition for a point to lie on the quadric in equation (C.0.4) and thus belong to Minkowski space then becomes

$$\epsilon^{\alpha\beta\gamma\delta} X_{\alpha\beta} X_{\gamma\delta} = 0. \tag{C.0.7}$$

It turns out that this equation is satisfied if and only if the rank of the matrix $X_{\alpha\beta}$ is two which means that it can be written in the form

$$X_{\alpha\beta} = A_{[\alpha} B_{\beta]} = A_\alpha B_\beta - A_\beta B_\alpha, \quad \alpha, \beta \in \{0, 1, 2, 3\}, \tag{C.0.8}$$

for some twistors A and B which are points in three-dimensional projective space $\mathbb{P}^3$. The two points A and B span a line in $\mathbb{P}^3$ which we denote by (AB). Conversely, given a line $(AB) \subset \mathbb{P}^3$ determined by two points $A, B \in \mathbb{P}^3$, we can construct a matrix $X_{\alpha\beta}$ satisfying (C.0.7) and a point $[Y_0 : \cdots : Y_5]$ that lies on the quadric in equation (C.0.4).

Every dual point x_i in four-dimensional Minkowski space may be represented by such a line $(A_i B_i) \subset \mathbb{P}^3$. The distance $(x_i - x_j)^2$ of two points can be written in terms of the twistors variables as

$$\frac{1}{2}(x_i - x_j)^2 = \frac{\langle A_i B_i A_j B_j \rangle}{\langle A_\infty B_\infty A_i B_i \rangle \langle A_\infty B_\infty A_j B_j \rangle}, \tag{C.0.9}$$

where the four-bracket between the twistors is defined as

$$\langle ABCD \rangle = \epsilon^{\alpha\beta\gamma\delta} A_\alpha B_\beta C_\gamma D_\delta, \tag{C.0.10}$$

The twistors A_∞ and B_∞ represent a line through the point at infinity that breaks conformal to the usual Poincaré symmetry of Minkowski space. One can take for example $A_\infty = [1 : 0 : 0 : 0]$ and $B_\infty = [0 : 1 : 0 : 0]$. Note that if two dual points are light-like separated, i.e. $(x_i - x_j)^2 = 0$, then the four bracket of the twistors vanishes. Geometrically this means that the corresponding lines $(A_i B_i)$ and $(A_j B_j)$ intersect in a point. Note also that the conformal group SO(2, 4) acting non-linearly on the dual points x_i simply becomes the group PGL(4) of coordinate transformations in $\mathbb{P}^3$. A translation between the most important notions in dual space and twistor space may be found in table C.1.

Twistors are originally due to Penrose (see [164]); in the context of scattering amplitudes they were introduced by Hodges in [165] (see also [166]). They have since found a large number of applications in scattering amplitudes, in particular in the context of $\mathcal{N} = 4$ sYM.

Dual momentum space	Momentum twistor space $\mathbb{P}^3$
Point x	Line $L_x = (A_x B_x)$
Distance $(x - y)^2$	Four bracket $\langle A_x B_x A_y B_y \rangle$
Null separation $(x - y)^2 = 0$	Lines L_x and L_y intersect
Conformal transformations SO(2, 4)	PGL(4) transformations

Table C.1: Momentum twistor dictionary

Bibliography

[1] **E. P. Wigner**, *Gruppentheorie und ihre Anwendung auf die Quantenmechanik der Atomspektren*. Vieweg+Teubner Verlag, Wiesbaden, 1931.

[2] **S. R. Coleman and J. Mandula**, "All Possible Symmetries of the S Matrix," *Phys. Rev.* **159** (1967) 1251–1256.

[3] **F. Gliozzi, J. Scherk, and D. I. Olive**, "Supersymmetry, Supergravity Theories and the Dual Spinor Model," *Nucl. Phys. B* **122** (1977) 253–290.

[4] **L. Brink, J. H. Schwarz, and J. Scherk**, "Supersymmetric Yang-Mills Theories," *Nucl. Phys. B* **121** (1977) 77–92.

[5] **A. Gimenez Grau, C. Kristjansen, M. Volk, and M. Wilhelm**, "A Quantum Check of Non-Supersymmetric AdS/dCFT," *JHEP* **01** (2019) 007, arXiv:1810.11463 [hep-th].

[6] **A. Gimenez-Grau, C. Kristjansen, M. Volk, and M. Wilhelm**, "A quantum framework for AdS/dCFT through fuzzy spherical harmonics on S^4," *JHEP* **04** (2020) 132, arXiv:1912.02468 [hep-th].

[7] **S. Bonansea, K. Idiab, C. Kristjansen, and M. Volk**, "Wilson lines in AdS/dCFT," *Phys. Lett. B* **806** (2020) 135520, arXiv:2004.01693 [hep-th].

[8] **Z. Bern, L. J. Dixon, D. C. Dunbar, and D. A. Kosower**, "Fusing gauge theory tree amplitudes into loop amplitudes," *Nucl. Phys. B* **435** (1995) 59–101, arXiv:hep-ph/9409265.

[9] **Z. Bern, L. J. Dixon, D. C. Dunbar, and D. A. Kosower**, "One loop n-point gauge theory amplitudes, unitarity and collinear limits," *Nucl. Phys. B* **425** (1994) 217–260, arXiv:hep-ph/9403226.

[10] **R. Britto, F. Cachazo, B. Feng, and E. Witten**, "Direct proof of tree-level recursion relation in Yang-Mills theory," *Phys. Rev. Lett.* **94** (2005) 181602, arXiv:hep-th/0501052.

[11] **N. Arkani-Hamed, J. L. Bourjaily, F. Cachazo, S. Caron-Huot, and J. Trnka**, "The All-Loop Integrand For Scattering Amplitudes in Planar $\mathcal{N} = 4$ SYM," *JHEP* **01** (2011) 041, arXiv:1008.2958 [hep-th].

[12] **N. Arkani-Hamed, J. L. Bourjaily, F. Cachazo, A. B. Goncharov, A. Postnikov, and J. Trnka**, *Grassmannian Geometry of Scattering Amplitudes*. Cambridge University Press, 4, 2016. arXiv:1212.5605 [hep-th].

[13] **L. D. Landau**, "On analytic properties of vertex parts in quantum field theory," *Nucl. Phys.* **13** (1959) no. 1, 181–192.

[14] **A. B. Goncharov**, "Multiple polylogarithms, cyclotomy and modular complexes," *Math. Res. Lett.* **5** (1998) no. 4, 497–516, arXiv:1105.2076 [math.AG].

[15] **K. T. Chen**, "Iterated path integrals," *Bull. Amer. Math. Soc.* **83** (1977) no. 5, 831–879.

[16] **J. L. Bourjaily, M. Volk, and M. Von Hippel**, "Conformally Regulated Direct Integration of the Two-Loop Heptagon Remainder," *JHEP* **02** (2020) 095, arXiv:1912.05690 [hep-th].

[17] **J. L. Bourjaily, A. J. McLeod, C. Vergu, M. Volk, M. Von Hippel, and M. Wilhelm**, "Rooting Out Letters: Octagonal Symbol Alphabets and Algebraic Number Theory," *JHEP* **02** (2020) 025, arXiv:1910.14224 [hep-th].

[18] **J. L. Bourjaily, A. J. McLeod, C. Vergu, M. Volk, M. Von Hippel, and M. Wilhelm**, "Embedding Feynman Integral (Calabi-Yau) Geometries in Weighted Projective Space," *JHEP* **01** (2020) 078, arXiv:1910.01534 [hep-th].

[19] **C. Vergu and M. Volk**, "Traintrack Calabi-Yaus from Twistor Geometry," *JHEP* **07** (2020) 160, arXiv:2005.08771 [hep-th].

[20] **H. Frellesvig, C. Vergu, M. Volk, and M. von Hippel**, "Cuts and Isogenies," *JHEP* **05** (2021) 064, arXiv:2102.02769 [hep-th].

[21] **J. M. Maldacena**, "The Large-N limit of superconformal field theories and supergravity," *Adv. Theor. Math. Phys.* **2** (1998) 231–252, arXiv:hep-th/9711200.

[22] **J. Polchinski**, *String theory. Vol. 2: Superstring theory and beyond.* Cambridge Monographs on Mathematical Physics. Cambridge University Press, 12, 2007.

[23] **A. Karch and L. Randall**, "Open and closed string interpretation of SUSY CFT's on branes with boundaries," *JHEP* **06** (2001) 063, arXiv:hep-th/0105132.

[24] **A. Karch and L. Randall**, "Locally localized gravity," *JHEP* **05** (2001) 008, arXiv:hep-th/0011156.

[25] **A. Karch and L. Randall**, "Localized gravity in string theory," *Phys. Rev. Lett.* **87** (2001) 061601, arXiv:hep-th/0105108.

[26] **R. C. Myers and M. C. Wapler**, "Transport Properties of Holographic Defects," *JHEP* **12** (2008) 115, arXiv:0811.0480 [hep-th].

[27] **N. R. Constable, R. C. Myers, and O. Tafjord**, "The Noncommutative bion core," *Phys. Rev. D* **61** (2000) 106009, arXiv:hep-th/9911136.

[28] **D. Gaiotto and E. Witten**, "Supersymmetric Boundary Conditions in $\mathcal{N} = 4$ Super Yang-Mills Theory," *J. Statist. Phys.* **135** (2009) 789–855, arXiv:0804.2902 [hep-th].

[29] **S. Komatsu and Y. Wang**, "Non-perturbative defect one-point functions in planar $\mathcal{N} = 4$ super-Yang-Mills," *Nucl. Phys. B* **958** (2020) 115120, arXiv:2004.09514 [hep-th].

[30] **A. Hashimoto, P. Ouyang, and M. Yamazaki**, "Boundaries and defects of $\mathcal{N}$ = 4 SYM with 4 supercharges. Part I: Boundary/junction conditions," *JHEP* **10** (2014) 107, arXiv:1404.5527 [hep-th].

[31] **O. DeWolfe, D. Z. Freedman, and H. Ooguri**, "Holography and defect conformal field theories," *Phys. Rev. D* **66** (2002) 025009, arXiv:hep-th/0111135.

[32] **A. C. Ipsen and K. E. Vardinghus**, "The dilatation operator for defect conformal $\mathcal{N}$ = 4 SYM," arXiv:1909.12181 [hep-th].

[33] **C. Kristjansen, D. Müller, and K. Zarembo**, "Integrable boundary states in D3-D5 dCFT: beyond scalars," *JHEP* **08** (2020) 103, arXiv:2005.01392 [hep-th].

[34] **I. Buhl-Mortensen, M. de Leeuw, A. C. Ipsen, C. Kristjansen, and M. Wilhelm**, "A Quantum Check of AdS/dCFT," *JHEP* **01** (2017) 098, arXiv:1611.04603 [hep-th].

[35] **J. Hoppe**, *Quantum theory of a massless relativistic surface and a two-dimensional bound state problem.* PhD thesis, Massachusetts Institute of Technology, 1982.

[36] **J. Madore**, "The Fuzzy sphere," *Class. Quant. Grav.* **9** (1992) 69–88.

[37] **S. Ramgoolam**, "On spherical harmonics for fuzzy spheres in diverse dimensions," *Nucl. Phys. B* **610** (2001) 461–488, arXiv:hep-th/0105006.

[38] **N. R. Constable, R. C. Myers, and O. Tafjord**, "Non-Abelian brane intersections," *JHEP* **06** (2001) 023, arXiv:hep-th/0102080.

[39] **O. Bergman, N. Jokela, G. Lifschytz, and M. Lippert**, "Quantum Hall Effect in a Holographic Model," *JHEP* **10** (2010) 063, arXiv:1003.4965 [hep-th].

[40] **A. A. Tseytlin**, "On non-abelian generalization of Born-Infeld action in string theory," *Nucl. Phys. B* **501** (1997) 41–52, arXiv:hep-th/9701125.

[41] **J. Castelino, S. Lee, and W. Taylor**, "Longitudinal five-branes as four spheres in matrix theory," *Nucl. Phys. B* **526** (1998) 334–350, arXiv:hep-th/9712105.

[42] **C. Kristjansen, G. W. Semenoff, and D. Young**, "Chiral primary one-point functions in the D3-D7 defect conformal field theory," *JHEP* **01** (2013) 117, arXiv:1210.7015 [hep-th].

[43] **K. Nagasaki and S. Yamaguchi**, "Expectation values of chiral primary operators in holographic interface CFT," *Phys. Rev. D* **86** (2012) 086004, arXiv:1205.1674 [hep-th].

[44] **S. Lee, S. Minwalla, M. Rangamani, and N. Seiberg**, "Three point functions of chiral operators in D = 4, $\mathcal{N}$ = 4 SYM at large N," *Adv. Theor. Math. Phys.* **2** (1998) 697–718, arXiv:hep-th/9806074.

[45] **K. Nagasaki, H. Tanida, and S. Yamaguchi**, "Holographic Interface-Particle Potential," *JHEP* **01** (2012) 139, arXiv:1109.1927 [hep-th].

[46] **D. E. Berenstein, J. M. Maldacena, and H. S. Nastase**, "Strings in flat space and pp waves from $\mathcal{N}$ = 4 superYang-Mills," *JHEP* **04** (2002) 013, arXiv:hep-th/0202021.

[47] **N. Beisert, V. Dippel, and M. Staudacher**, "A Novel long range spin chain and planar N=4 super Yang-Mills," *JHEP* **07** (2004) 075, arXiv:hep-th/0405001.

[48] **M. de Leeuw, C. Kristjansen, and K. Zarembo**, "One-point Functions in Defect CFT and Integrability," *JHEP* **08** (2015) 098, arXiv:1506.06958 [hep-th].

[49] **I. Buhl-Mortensen, M. de Leeuw, C. Kristjansen, and K. Zarembo**, "One-point Functions in AdS/dCFT from Matrix Product States," *JHEP* **02** (2016) 052, arXiv:1512.02532 [hep-th].

[50] **M. De Leeuw, C. Kristjansen, and G. Linardopoulos**, "Scalar one-point functions and matrix product states of AdS/dCFT," *Phys. Lett. B* **781** (2018) 238–243, arXiv:1802.01598 [hep-th].

[51] **I. Buhl-Mortensen, M. de Leeuw, A. C. Ipsen, C. Kristjansen, and M. Wilhelm**, "Asymptotic One-Point Functions in Gauge-String Duality with Defects," *Phys. Rev. Lett.* **119** (2017) no. 26, 261604, arXiv:1704.07386 [hep-th].

[52] **T. Gombor and Z. Bajnok**, "Boundary states, overlaps, nesting and bootstrapping AdS/dCFT," *JHEP* **10** (2020) 123, arXiv:2004.11329 [hep-th].

[53] **G. Linardopoulos and K. Zarembo**, "String integrability of defect CFT and dynamical reflection matrices," *JHEP* **05** (2021) 203, arXiv:2102.12381 [hep-th].

[54] **M. de Leeuw, C. Kristjansen, and G. Linardopoulos**, "One-point functions of non-protected operators in the SO(5) symmetric D3–D7 dCFT," *J. Phys. A* **50** (2017) no. 25, 254001, arXiv:1612.06236 [hep-th].

[55] **M. De Leeuw, T. Gombor, C. Kristjansen, G. Linardopoulos, and B. Pozsgay**, "Spin Chain Overlaps and the Twisted Yangian," *JHEP* **01** (2020) 176, arXiv:1912.09338 [hep-th].

[56] **M. de Leeuw, C. Kristjansen, and K. E. Vardinghus**, "A non-integrable quench from AdS/dCFT," *Phys. Lett. B* **798** (2019) 134940, arXiv:1906.10714 [hep-th].

[57] **M. de Leeuw, A. C. Ipsen, C. Kristjansen, and M. Wilhelm**, "One-loop Wilson loops and the particle-interface potential in AdS/dCFT," *Phys. Lett. B* **768** (2017) 192–197, arXiv:1608.04754 [hep-th].

[58] **J. Aguilera-Damia, D. H. Correa, and V. I. Giraldo-Rivera**, "Circular Wilson loops in defect Conformal Field Theory," *JHEP* **03** (2017) 023, arXiv:1612.07991 [hep-th].

[59] **S. Bonansea, S. Davoli, L. Griguolo, and D. Seminara**, "Circular Wilson loops in defect $\mathcal{N}$ = 4 SYM: phase transitions, double-scaling limits and OPE expansions," *JHEP* **03** (2020) 084, arXiv:1911.07792 [hep-th].

[60] **M. Preti, D. Trancanelli, and E. Vescovi**, "Quark-antiquark potential in defect conformal field theory," *JHEP* **10** (2017) 079, arXiv:1708.04884 [hep-th].

[61] **M. de Leeuw, A. C. Ipsen, C. Kristjansen, K. E. Vardinghus, and M. Wilhelm**, "Two-point functions in AdS/dCFT and the boundary conformal bootstrap equations," *JHEP* **08** (2017) 020, arXiv:1705.03898 [hep-th].

[62] **L. Bianchi, M. Lemos, and M. Meineri**, "Line Defects and Radiation in $\mathcal{N} = 2$ Conformal Theories," *Phys. Rev. Lett.* **121** (2018) no. 14, 141601, arXiv:1805.04111 [hep-th].

[63] **L. Bianchi and M. Lemos**, "Superconformal surfaces in four dimensions," *JHEP* **06** (2020) 056, arXiv:1911.05082 [hep-th].

[64] **T. Gombor and Z. Bajnok**, "Boundary state bootstrap and asymptotic overlaps in AdS/dCFT," *JHEP* **03** (2021) 222, arXiv:2006.16151 [hep-th].

[65] **R. P. Feynman**, "Space-time approach to quantum electrodynamics," *Phys. Rev.* **76** (1949) 769–789.

[66] **J. S. Schwinger**, "Quantum electrodynamics. 2. Vacuum polarization and selfenergy," *Phys. Rev.* **75** (1948) 651.

[67] **R. Eden, P. Landshoff, D. Olive, and J. Polkinghorne**, *The Analytic S-Matrix*. Cambridge University Press, 2002.

[68] **J. S. R. Chisholm**, "Calculation of S-matrix elements," *Mathematical Proceedings of the Cambridge Philosophical Society* **48** (1952) no. 2, 300–315.

[69] **C. Itzykson and J. B. Zuber**, *Quantum Field Theory*. International Series In Pure and Applied Physics. McGraw-Hill, New York, 1980.

[70] **C. Bogner and S. Weinzierl**, "Feynman graph polynomials," *Int. J. Mod. Phys. A* **25** (2010) 2585–2618, arXiv:1002.3458 [hep-ph].

[71] **C. Bogner and S. Weinzierl**, "Periods and Feynman integrals," *J. Math. Phys.* **50** (2009) 042302, arXiv:0711.4863 [hep-th].

[72] **M. Kontsevich and D. Zagier**, "Periods," in *Mathematics unlimited—2001 and beyond*, pp. 771–808. Springer, Berlin, 2001.

[73] **J. C. Polkinghorne and G. R. Screaton**, "The analytic properties of perturbation theory. I," *Nuovo Cimento (10)* **15** (1960) 289–300.

[74] **J. C. Polkinghorne and G. R. Screaton**, "The analytic properties of perturbation theory. II," *Nuovo Cimento (10)* **15** (1960) 925–931.

[75] **F. Brown**, "The massless higher-loop two-point function," *Comm. Math. Phys.* **287** (2009) no. 3, 925–958, arXiv:0804.1660 [math.AG].

[76] **F. C. S. Brown**, "Multiple zeta values and periods of moduli spaces $\overline{\mathfrak{M}}_{0,n}$," *Ann. Sci. Éc. Norm. Supér. (4)* **42** (2009) no. 3, 371–489, arXiv:0606419 [math.AG].

[77] **E. Panzer**, "Algorithms for the symbolic integration of hyperlogarithms with applications to Feynman integrals," *Comput. Phys. Commun.* **188** (2015) 148–166, arXiv:1403.3385 [hep-th].

[78] **C. Anastasiou, C. Duhr, F. Dulat, and B. Mistlberger**, "Soft triple-real radiation for Higgs production at N3LO," *JHEP* **07** (2013) 003, arXiv:1302.4379 [hep-ph].

[79] **F. C. S. Brown**, "On the periods of some Feynman integrals," arXiv:0910.0114 [math.AG].

[80] **E. Panzer**, *Feynman integrals and hyperlogarithms*. PhD thesis, Humboldt U., 2015. arXiv:1506.07243 [math-ph].

[81] **A. Clebsch**, "Ueber diejenigen ebenen Curven, deren Coordinaten rationale Functionen eines Parameters sind," *J. Reine Angew. Math.* **64** (1865) 43–65.

[82] **W. Fulton**, *Algebraic curves. An introduction to algebraic geometry*. W. A. Benjamin, Inc., New York-Amsterdam, 1969. Notes written with the collaboration of Richard Weiss, Mathematics Lecture Notes Series.

[83] **P. Samuel**, *Géométrie projective*. Mathématiques. Presses Universitaires de France, Paris, 1986.

[84] **J. R. Sendra, F. Winkler, and S. Pérez-Díaz**, *Rational algebraic curves*, vol. 22 of *Algorithms and Computation in Mathematics*. Springer, Berlin, 2008. A computer algebra approach.

[85] **J. Böhm, W. Decker, S. Laplagne, and F. Seelisch**, "`paraplanecurves.lib` — A singular library for the parametrization of rational curves." `https://www.singular.uni-kl.de`, 2013.

[86] **G. Castelnuovo**, "Sulle superficie di genere O," *Memorie della Società Italiana delle Scienze* **3** (1896) 103–123.

[87] **J. Schicho**, "Rational parametrization of surfaces," *J. Symbolic Comput.* **26** (1998) no. 1, 1–29.

[88] **M. Besier, D. Van Straten, and S. Weinzierl**, "Rationalizing roots: an algorithmic approach," *Commun. Num. Theor. Phys.* **13** (2019) 253–297, arXiv:1809.10983 [hep-th].

[89] **M. Besier, P. Wasser, and S. Weinzierl**, "RationalizeRoots: Software Package for the Rationalization of Square Roots," *Comput. Phys. Commun.* **253** (2020) 107197, arXiv:1910.13251 [cs.MS].

[90] **P. Griffiths and J. Harris**, *Principles of algebraic geometry*. Wiley Classics Library. John Wiley & Sons, Inc., New York, 1994. Reprint of the 1978 original.

[91] **A. Clebsch**, "Ueber diejenigen Curven, deren Coordinaten sich als elliptische Functionen eines Parameters darstellen lassen," *J. Reine Angew. Math.* **64** (1865) 210–270.

[92] **S. Lang**, *Elliptic functions*, vol. 112 of *Graduate Texts in Mathematics*. Springer-Verlag, New York, second ed., 1987. With an appendix by J. Tate.

[93] **J. H. Silverman**, *Advanced topics in the arithmetic of elliptic curves*, vol. 151 of *Graduate Texts in Mathematics*. Springer-Verlag, New York, 1994.

[94] **A. Weil**, *Elliptic functions according to Eisenstein and Kronecker*. Ergebnisse der Mathematik und ihrer Grenzgebiete, Band 88. Springer-Verlag, Berlin-New York, 1976.

[95] **R. Huang and Y. Zhang**, "On Genera of Curves from High-loop Generalized Unitarity Cuts," *JHEP* **04** (2013) 080, arXiv:1302.1023 [hep-ph].

[96] **J. L. Bourjaily, Y.-H. He, A. J. McLeod, M. Spradlin, C. Vergu, M. Volk, M. von Hippel, and M. Wilhelm**, "Direct Integration for Multi-leg Amplitudes: Tips, Tricks, and When They Fail," in *Antidifferentiation and the Calculation of Feynman Amplitudes*. 3, 2021. arXiv:2103.15423 [hep-th].

[97] **J. L. Bourjaily, A. J. McLeod, M. von Hippel, and M. Wilhelm**, "Rationalizing Loop Integration," *JHEP* **08** (2018) 184, arXiv:1805.10281 [hep-th].

[98] **J. L. Bourjaily, F. Dulat, and E. Panzer**, "Manifestly Dual-Conformal Loop Integration," *Nucl. Phys. B* **942** (2019) 251–302, arXiv:1901.02887 [hep-th].

[99] **V. Del Duca, C. Duhr, and V. A. Smirnov**, "An Analytic Result for the Two-Loop Hexagon Wilson Loop in $\mathcal{N}$ = 4 SYM," *JHEP* **03** (2010) 099, arXiv:0911.5332 [hep-ph].

[100] **V. Del Duca, C. Duhr, and V. A. Smirnov**, "The Two-Loop Hexagon Wilson Loop in N = 4 SYM," *JHEP* **05** (2010) 084, arXiv:1003.1702 [hep-th].

[101] **J. Golden, A. B. Goncharov, M. Spradlin, C. Vergu, and A. Volovich**, "Motivic Amplitudes and Cluster Coordinates," *JHEP* **01** (2014) 091, arXiv:1305.1617 [hep-th].

[102] **J. L. Bourjaily, S. Caron-Huot, and J. Trnka**, "Dual-Conformal Regularization of Infrared Loop Divergences and the Chiral Box Expansion," *JHEP* **01** (2015) 001, arXiv:1303.4734 [hep-th].

[103] **J. Golden and M. Spradlin**, "An analytic result for the two-loop seven-point MHV amplitude in $\mathcal{N}$ = 4 SYM," *JHEP* **08** (2014) 154, arXiv:1406.2055 [hep-th].

[104] **S. He, Z. Li, and C. Zhang**, "Two-loop Octagons, Algebraic Letters and $\bar{Q}$ Equations," *Phys. Rev. D* **101** (2020) no. 6, 061701, arXiv:1911.01290 [hep-th].

[105] **J. L. Bourjaily, A. J. McLeod, M. Spradlin, M. von Hippel, and M. Wilhelm**, "Elliptic Double-Box Integrals: Massless Scattering Amplitudes beyond Polylogarithms," *Phys. Rev. Lett.* **120** (2018) no. 12, 121603, arXiv:1712.02785 [hep-th].

[106] **S. Caron-Huot and K. J. Larsen**, "Uniqueness of two-loop master contours," *JHEP* **10** (2012) 026, arXiv:1205.0801 [hep-ph].

[107] **J. L. Bourjaily, Y.-H. He, A. J. Mcleod, M. Von Hippel, and M. Wilhelm**, "Traintracks through Calabi-Yau Manifolds: Scattering Amplitudes beyond Elliptic Polylogarithms," *Phys. Rev. Lett.* **121** (2018) no. 7, 071603, arXiv:1805.09326 [hep-th].

[108] **J. L. Bourjaily, A. J. McLeod, M. von Hippel, and M. Wilhelm**, "Bounded Collection of Feynman Integral Calabi-Yau Geometries," *Phys. Rev. Lett.* **122** (2019) no. 3, 031601, arXiv:1810.07689 [hep-th].

[109] **H. Poincaré**, "Sur les résidus des intégrales doubles," *Acta Math.* **9** (1887) no. 1, 321–380.

[110] **F. Cachazo**, "Sharpening The Leading Singularity," arXiv:0803.1988 [hep-th].

[111] **N. Arkani-Hamed, J. L. Bourjaily, F. Cachazo, and J. Trnka**, "Local Integrals for Planar Scattering Amplitudes," *JHEP* **06** (2012) 125, arXiv:1012.6032 [hep-th].

[112] **R. E. Cutkosky**, "Singularities and discontinuities of Feynman amplitudes," *J. Math. Phys.* **1** (1960) 429–433.

[113] **S. Abreu, R. Britto, C. Duhr, and E. Gardi**, "Cuts from residues: the one-loop case," *JHEP* **06** (2017) 114, arXiv:1702.03163 [hep-th].

[114] **D. Zagier**, "The Bloch-Wigner-Ramakrishnan polylogarithm function," *Math. Ann.* **286** (1990) no. 1-3, 613–624.

[115] **A. Beĭlinson and A. Levin**, "The elliptic polylogarithm," in *Motives (Seattle, WA, 1991)*, vol. 55 of *Proc. Sympos. Pure Math.*, pp. 123–190. Amer. Math. Soc., Providence, RI, 1994.

[116] **A. Levin**, "Elliptic polylogarithms: an analytic theory," *Compositio Math.* **106** (1997) no. 3, 267–282.

[117] **F. C. S. Brown and A. Levin**, "Multiple elliptic polylogarithms," arXiv:1110.6917 [math.NT].

[118] **J. H. Silverman**, *The arithmetic of elliptic curves*, vol. 106 of *Graduate Texts in Mathematics*. Springer, Dordrecht, second ed., 2009.

[119] **J. Broedel, C. R. Mafra, N. Matthes, and O. Schlotterer**, "Elliptic multiple zeta values and one-loop superstring amplitudes," *JHEP* **07** (2015) 112, arXiv:1412.5535 [hep-th].

[120] **J. Broedel, N. Matthes, and O. Schlotterer**, "Relations between elliptic multiple zeta values and a special derivation algebra," *J. Phys. A* **49** (2016) no. 15, 155203, arXiv:1507.02254 [hep-th].

[121] **J. Broedel, N. Matthes, G. Richter, and O. Schlotterer**, "Twisted elliptic multiple zeta values and non-planar one-loop open-string amplitudes," *J. Phys. A* **51** (2018) no. 28, 285401, arXiv:1704.03449 [hep-th].

[122] **J. Broedel, C. Duhr, F. Dulat, and L. Tancredi**, "Elliptic polylogarithms and iterated integrals on elliptic curves. Part I: general formalism," *JHEP* **05** (2018) 093, arXiv:1712.07089 [hep-th].

[123] **J. Broedel, C. Duhr, F. Dulat, and L. Tancredi**, "Elliptic polylogarithms and iterated integrals on elliptic curves II: an application to the sunrise integral," *Phys. Rev. D* **97** (2018) no. 11, 116009, arXiv:1712.07095 [hep-ph].

[124] **J. Broedel, C. Duhr, F. Dulat, B. Penante, and L. Tancredi**, "Elliptic polylogarithms and Feynman parameter integrals," *JHEP* **05** (2019) 120, arXiv:1902.09971 [hep-ph].

[125] **C. Bogner, S. Müller-Stach, and S. Weinzierl**, "The unequal mass sunrise integral expressed through iterated integrals on $\overline{\mathcal{M}}_{1,3}$," *Nucl. Phys. B* **954** (2020) 114991, arXiv:1907.01251 [hep-th].

[126] **J. Broedel, C. Duhr, F. Dulat, B. Penante, and L. Tancredi**, "Elliptic symbol calculus: from elliptic polylogarithms to iterated integrals of Eisenstein series," *JHEP* **08** (2018) 014, arXiv:1803.10256 [hep-th].

[127] **M. Walden and S. Weinzierl**, "Numerical evaluation of iterated integrals related to elliptic Feynman integrals," *Comput. Phys. Commun.* **265** (2021) 108020, arXiv:2010.05271 [hep-ph].

[128] **P. A. Griffiths**, "On the periods of certain rational integrals. I, II," *Ann. of Math. (2) 90 (1969), 460-495; ibid. (2)* **90** (1969) 496–541.

[129] **I. M. Gel'fand, M. M. Kapranov, and A. V. Zelevinsky**, "Generalized Euler integrals and A-hypergeometric functions," *Adv. Math.* **84** (1990) no. 2, 255–271.

[130] **S. Müller-Stach, S. Weinzierl, and R. Zayadeh**, "Picard-Fuchs equations for Feynman integrals," *Commun. Math. Phys.* **326** (2014) 237–249, arXiv:1212.4389 [hep-ph].

[131] **S. Bloch, M. Kerr, and P. Vanhove**, "A Feynman integral via higher normal functions," *Compos. Math.* **151** (2015) no. 12, 2329–2375, arXiv:1406.2664 [hep-th].

[132] **S. Bloch, M. Kerr, and P. Vanhove**, "Local mirror symmetry and the sunset Feynman integral," *Adv. Theor. Math. Phys.* **21** (2017) 1373–1453, arXiv:1601.08181 [hep-th].

[133] **K. Bönisch, F. Fischbach, A. Klemm, C. Nega, and R. Safari**, "Analytic structure of all loop banana integrals," *JHEP* **05** (2021) 066, arXiv:2008.10574 [hep-th].

[134] **A. Klemm, C. Nega, and R. Safari**, "The l-loop Banana Amplitude from GKZ Systems and relative Calabi-Yau Periods," *JHEP* **04** (2020) 088, arXiv:1912.06201 [hep-th].

[135] **F. Brown and O. Schnetz**, "A K3 in ϕ^4," *Duke Math. J.* **161** (2012) no. 10, 1817–1862, arXiv:1006.4064 [math.AG].

[136] **D. Festi and D. van Straten**, "Bhabha scattering and a special pencil of K3 surfaces," *Commun. Number Theory Phys.* **13** (2019) no. 2, 463–485, arXiv:1809.04970 [math.AG].

[137] **M. Besier, D. Festi, M. Harrison, and B. Naskręcki**, "Arithmetic and geometry of a K3 surface emerging from virtual corrections to Drell–Yan scattering," *Commun. Num. Theor. Phys.* **14** (2020) no. 4, 863–911, arXiv:1908.01079 [math.AG].

[138] **V. V. Batyrev**, "Dual polyhedra and mirror symmetry for Calabi-Yau hypersurfaces in toric varieties," *J. Algebraic Geom.* **3** (1994) no. 3, 493–535.

[139] **L. Adams and S. Weinzierl**, "Feynman integrals and iterated integrals of modular forms," *Commun. Num. Theor. Phys.* **12** (2018) 193–251, arXiv:1704.08895 [hep-ph].

[140] **J. Polchinski**, "Dirichlet Branes and Ramond-Ramond charges," *Phys. Rev. Lett.* **75** (1995) 4724–4727, arXiv:hep-th/9510017.

[141] **S. S. Gubser, I. R. Klebanov, and A. M. Polyakov**, "Gauge theory correlators from noncritical string theory," *Phys. Lett. B* **428** (1998) 105–114, arXiv:hep-th/9802109.

[142] **E. Witten**, "Anti-de Sitter space and holography," *Adv. Theor. Math. Phys.* **2** (1998) 253–291, arXiv:hep-th/9802150.

[143] **J. M. Maldacena**, "Wilson loops in large N field theories," *Phys. Rev. Lett.* **80** (1998) 4859–4862, arXiv:hep-th/9803002.

[144] **S.-J. Rey, S. Theisen, and J.-T. Yee**, "Wilson-Polyakov loop at finite temperature in large N gauge theory and anti-de Sitter supergravity," *Nucl. Phys. B* **527** (1998) 171–186, arXiv:hep-th/9803135.

[145] **L. F. Alday and J. M. Maldacena**, "Gluon scattering amplitudes at strong coupling," *JHEP* **06** (2007) 064, arXiv:0705.0303 [hep-th].

[146] **Z. Bern, L. J. Dixon, and V. A. Smirnov**, "Iteration of planar amplitudes in maximally supersymmetric Yang-Mills theory at three loops and beyond," *Phys. Rev. D* **72** (2005) 085001, arXiv:hep-th/0505205.

[147] **N. Beisert, B. Eden, and M. Staudacher**, "Transcendentality and Crossing," *J. Stat. Mech.* **0701** (2007) P01021, arXiv:hep-th/0610251.

[148] **J. A. Minahan and K. Zarembo**, "The Bethe ansatz for N=4 superYang-Mills," *JHEP* **03** (2003) 013, arXiv:hep-th/0212208.

[149] **N. Beisert, C. Kristjansen, and M. Staudacher**, "The Dilatation operator of conformal N=4 superYang-Mills theory," *Nucl. Phys. B* **664** (2003) 131–184, arXiv:hep-th/0303060.

[150] **I. Bena, J. Polchinski, and R. Roiban**, "Hidden symmetries of the AdS(5) x S**5 superstring," *Phys. Rev. D* **69** (2004) 046002, arXiv:hep-th/0305116.

[151] **E. E. Kummer**, "Ueber die Transcendenten, welche aus wiederholten Integrationen rationaler Formeln entstehen," *J. Reine Angew. Math.* **21** (1840) 74–90.

[152] **H. Poincaré**, "Sur les groupes des équations linéaires," *Acta Math.* **4** (1884) no. 1, 201–312.

[153] **J. A. Lappo-Danilevski**, "Théorie algorithmique des corps de Riemann," *Mat. Sb.* **34** (1927) 113.

[154] **A. B. Goncharov**, "Multiple polylogarithms and mixed Tate motives," arXiv:math/0103059.

[155] **R. Ree**, "Lie elements and an algebra associated with shuffles," *Ann. of Math. (2)* **68** (1958) 210–220.

[156] **M. E. Hoffman**, "Quasi-shuffle products," *J. Algebraic Combin.* **11** (2000) no. 1, 49–68.

[157] **A. B. Goncharov, M. Spradlin, C. Vergu, and A. Volovich**, "Classical Polylogarithms for Amplitudes and Wilson Loops," *Phys. Rev. Lett.* **105** (2010) 151605, arXiv:1006.5703 [hep-th].

[158] **A. B. Goncharov**, "A simple construction of Grassmannian polylogarithms," *Adv. Math.* **241** (2013) 79–102, arXiv:0908.2238 [math.AG].

[159] **C. Duhr, H. Gangl, and J. R. Rhodes**, "From polygons and symbols to polylogarithmic functions," *JHEP* **10** (2012) 075, arXiv:1110.0458 [math-ph].

[160] **A. B. Goncharov**, "Galois symmetries of fundamental groupoids and noncommutative geometry," *Duke Math. J.* **128** (2005) no. 2, 209–284, arXiv:0208144 [math.AG].

[161] **C. Duhr and F. Dulat**, "PolyLogTools — polylogs for the masses," *JHEP* **08** (2019) 135, arXiv:1904.07279 [hep-th].

[162] **F. Brown**, "Notes on motivic periods," arXiv:1512.06410 [math.NT].

[163] **P. A. M. Dirac**, "Wave equations in conformal space," *Annals Math.* **37** (1936) 429–442.

[164] **R. Penrose**, "Twistor algebra," *J. Math. Phys.* **8** (1967) 345.

[165] **A. Hodges**, "Eliminating spurious poles from gauge-theoretic amplitudes," *JHEP* **05** (2013) 135, arXiv:0905.1473 [hep-th].

[166] **L. J. Mason and D. Skinner**, "Dual Superconformal Invariance, Momentum Twistors and Grassmannians," *JHEP* **11** (2009) 045, arXiv:0909.0250 [hep-th].

JHEP

Published for SISSA by Springer

Received: November 15, 2018
Accepted: December 11, 2018
Published: January 2, 2019

A quantum check of non-supersymmetric AdS/dCFT

Aleix Gimenez Grau, Charlotte Kristjansen, Matthias Volk and Matthias Wilhelm

Niels Bohr Institute, Copenhagen University,
Blegdamsvej 17, 2100 Copenhagen Ø, Denmark

E-mail: aleix.gimenez@desy.de, kristjan@nbi.ku.dk, mvolk@nbi.ku.dk, matthias.wilhelm@nbi.ku.dk

Abstract: Via a challenging field-theory computation, we confirm a supergravity prediction for the non-supersymmetric D3-D7 probe-brane system with probe geometry $AdS_4 \times S^2 \times S^2$, stabilized by fluxes. Supergravity predicts, in a certain double-scaling limit, the value of the one-point functions of chiral primaries of the dual defect version of $\mathcal{N} = 4$ SYM theory, where the fluxes translate into $\mathrm{SO}(3) \times \mathrm{SO}(3)$-symmetric, Lie-algebra-valued vacuum expectation values for all six scalar fields. Using a generalization of the technique based on fuzzy spherical harmonics developed for the related D3-D5 probe-brane system, we diagonalize the resulting mass matrix of the field theory. Subsequently, we calculate the planar one-loop correction to the vacuum expectation values of the scalars in dimensional reduction and find that it is UV finite and non-vanishing. We then proceed to calculating the one-loop correction to the planar one-point function of any single-trace scalar operator and explicitly evaluate this correction for a 1/2-BPS operator of length L at two leading orders in the double-scaling limit, finding exact agreement with the supergravity prediction.

Keywords: 1/N Expansion, AdS-CFT Correspondence, Supersymmetric Gauge Theory

ArXiv ePrint: 1810.11463

https://doi.org/10.1007/JHEP01(2019)007

JHEP01(2019)007

Contents

1 Introduction and summary **2**

2 Mass matrix **4**
- 2.1 Expansion of the action 4
- 2.2 Boson mass matrix 6
  - 2.2.1 Decomposition of the color matrices and easy fields 8
  - 2.2.2 Complicated fields 10
- 2.3 Fermion mass matrix 17
- 2.4 Summary of the spectrum 19

3 Propagators **20**
- 3.1 Scalar propagators 20
- 3.2 Fermionic propagators 21
- 3.3 Color and flavor part of the propagators 22

4 One-loop corrections to the classical solution **25**

5 One-loop corrections to single-trace operators **27**
- 5.1 General single-trace operators 28
- 5.2 One-loop one-point function of $\mathrm{tr}\, Z^L$ 29

6 Outlook **31**

A Conventions **32**
- A.1 Field-theory conventions 32
- A.2 Lie algebra $\mathfrak{su}(2)$ and fuzzy spherical harmonics 33

B Color and flavor part of the propagators **34**

C One-loop correction to the scalar vacuum expectation values **37**
- C.1 Calculation of the effective vertex 37
- C.2 Contraction of the stick 41
- C.3 Spacetime integral 42

D Color traces **42**

JHEP01(2019)007

1 Introduction and summary

Introducing defects such as boundaries or interfaces in conformal field theories (CFTs) does not only make these theories more adapt to experimental situations in condensed matter systems but also constitutes a natural step in exploring the limits of applicability of modern approaches to quantum field theory such as duality, integrability and the conformal bootstrap program, see e.g. [1]. From the latter perspective, various defect versions of the four-dimensional maximally supersymmetric Yang-Mills ($\mathcal{N}=4$ SYM) theory constitute particularly interesting arenas for investigation.

An example of such a defect CFT is the field theory dual to the D3-D5 probe-brane setup with k units of background gauge-field flux [2, 3], see [4] for a review. The presence of the flux translates into the rank of the gauge group of the defect field theory being different on the two sides of a codimension-one defect placed at $x_3=0$ and three of the scalar fields of $\mathcal{N}=4$ SYM theory carrying vacuum expectation values (vevs) given by the generators of a k-dimensional irreducible representation of $\mathfrak{su}(2)$ for $x_3>0$. This setup partly breaks conformal symmetry as well as supersymmetry. Conformal symmetry is reduced from $\mathrm{SO}(4,2)$ to $\mathrm{SO}(3,2)$ and the supersymmetry is reduced to three-dimensional $\mathcal{N}=4$ [5, 6]. The presence of the defect implies that operators can acquire non-vanishing one-point functions of the form [7]

$$\langle \mathcal{O}_\Delta \rangle(x) = \frac{C}{x_3^\Delta}, \tag{1.1}$$

with Δ denoting the conformal dimension, and due to the vevs this can happen already at tree level for certain scalar operators. Using the language of integrability, it was possible to express in one compact formula the tree-level one-point functions of all bulk single-trace scalar operators of the defect CFT [8–11]. Furthermore, by a rather demanding field-theory calculation involving the diagonalization of the highly non-trivial mass matrix using fuzzy spherical harmonics, it was possible to extend the compact formula for one-point functions to one-loop order in the SU(2) sector of the theory [12–14]. What is more, the one-loop computation allowed for a comparison with a prediction originating from supergravity [15] and despite the partial breaking of both conformal and supersymmetry a perfect match was found [12, 13]. More precisely, the supergravity computation involved taking the double-scaling limit [16][1]

$$\lambda \to \infty, \qquad k \to \infty, \qquad \frac{\lambda}{k^2} \quad \text{fixed}, \tag{1.2}$$

where λ is the 't Hooft coupling, and performing a perturbative expansion in λ/k^2. From the result of this computation, a prediction for the ratio of the one-loop and the tree-level value of the one-point function of the chiral primary $\mathrm{tr}\, Z^L$ in the double-scaling limit could be inferred [12].

[1] This double-scaling limit is reminiscent of the Berenstein-Maldacena-Nastase limit [17], which breaks down at four-loop order [18–20]. While the present double-scaling limit breaks down for non-protected operators already at one-loop order, it holds for protected operators such as $\mathrm{tr}\, Z^L$ to at least $(L-1)$-loop order [14].

JHEP01(2019)007

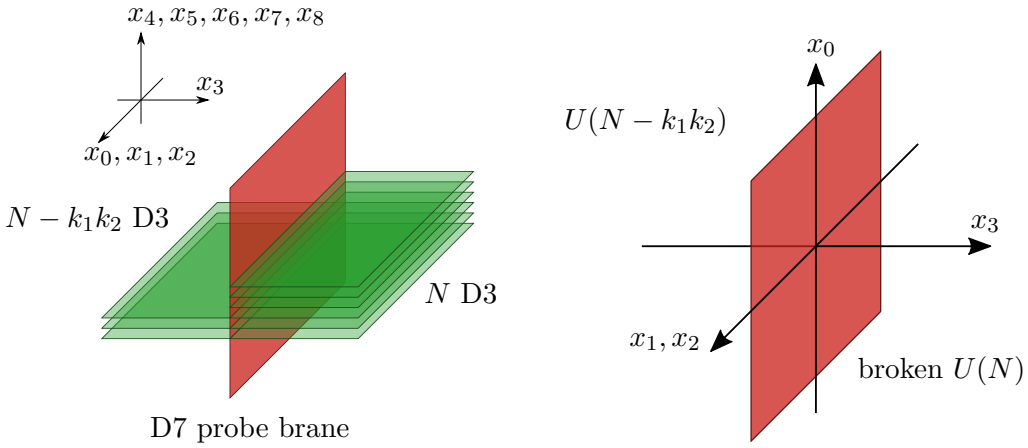

Figure 1. Brane configuration in string theory (left) and the dual field-theory picture (right) with different gauge groups on each side of the defect at $x_3 = 0$.

A similar prediction can be extracted from a supergravity computation performed in a closely related but completely non-supersymmetric setup, namely that of a D3-D7 probe-brane system [21]. The D3-D7 probe-brane system has two configurations which are of relevance for us, namely one where the geometry of the D7 brane is $AdS_4 \times S^2 \times S^2$ and one where the geometry is $AdS_4 \times S^4$. In both cases, the configuration has to be stabilized by adding either fluxes k_1 and k_2 on the two S^2's [22] or a non-trivial instanton bundle on the S^4 [23]. These flux-stabilized configurations have interesting applications from the condensed matter perspective giving rise to strongly coupled Dirac fermions in 2+1 dimensions, see e.g. [22–29]. The former configuration has a dual defect CFT where all six scalar fields of $\mathcal{N} = 4$ SYM theory are assigned vevs in the form of generators of the $(k_1 \times k_2)$-dimensional irreducible representation of $\mathfrak{su}(2) \times \mathfrak{su}(2)$ on one side of the defect; see figure 1. In the latter case, only five out of the scalar fields are assigned vevs and these transform in an irreducible SO(5) representation. For both cases, it is possible to introduce a double-scaling parameter and to evaluate the one-point function as an expansion in this parameter [21]. Furthermore, in both cases the system is stable if the double-scaling parameter is sufficiently small. Reference [21] gives the leading order result of this evaluation and the higher orders can be extracted by a straightforward extension of this work. For the $AdS_4 \times S^2 \times S^2$ symmetric configuration, the double-scaling limit is introduced as follows [21]:

$$\lambda \to \infty, \qquad k_1, k_2 \to \infty, \qquad \frac{\lambda}{(k_1^2 + k_2^2)} \qquad \text{fixed.} \tag{1.3}$$

Keeping also the ratio k_1/k_2 finite and assuming $(k_1 - k_2)$ to be of the same order as k_1 and k_2, the supergravity prediction for the one-point function of the unique SO(3) × SO(3)-symmetric chiral primary of (even) length L reads

$$\begin{aligned}\frac{\langle \mathcal{O}_L \rangle}{\langle \mathcal{O}_L \rangle_{\text{tree}}} = 1 + \frac{\lambda}{4\pi^2(k_1^2 + k_2^2)} \frac{1}{(L-1)(k_1^2 + k_2^2)^2} \Big(& 4(k_1k_2)^2 + (L^3 + 3L - 2)(k_1^4 + k_2^4) \\ & + 2(L-1)(L+2)k_1k_2(k_1^2 - k_2^2)\cot[(L+2)\psi_0] \Big) + \mathcal{O}\left(\frac{\lambda^2}{(k_1^2 + k_2^2)^2}\right),\end{aligned} \tag{1.4}$$

JHEP01(2019)007

where $\psi_0 = \arctan(k_1/k_2)$. Notice that the prediction carries over to any other chiral primary with a non-trivial projection on an SO(3) × SO(3)-symmetric one, such as e.g. $\mathrm{tr}\, Z^L$. For the $AdS_4 \times S^4$ configuration, supergravity also gives a prediction for the one-point function, however, with less structure as only one parameter is involved. In the remainder of this paper, we shall demonstrate how the rather intricate prediction (1.4) can be reproduced via a solid field-theory calculation. The major challenge of the computation is the diagonalization of the mass matrix of the theory, which requires a significant further development of the technique based on fuzzy spherical harmonics introduced in [12, 13]. The challenge is even bigger in the case of the SO(5)-symmetric vevs. Our refined method works for that case as well but with considerably more effort. We plan to return to this case in a future publication [30]. With the present work, we do not only provide a detailed positive test of AdS/dCFT in a situation where supersymmetry is completely broken; we also set up a perturbative framework which makes possible the evaluation of numerous other quantities in the defect CFT in question.

Our paper is structured as follows. In section 2, we diagonalize the highly non-trivial mass matrix that arises due to the vevs. In section 3, we determine the resulting propagators of the mass eigenstates, which take the form of AdS_4 propagators, and subsequently the propagators of the fields occurring in the action. Having thus set up the framework for calculating quantum corrections in this defect CFT, we calculate the first quantum correction to the classical solution in section 4, which we find to be non-vanishing. We proceed to calculate the one-loop correction to the one-point function of general single-trace operators, and in particular to $\mathrm{tr}\, Z^L$, in section 5. In section 6, we conclude with an outlook on possible future directions and interesting problems our perturbative framework can be applied to. Several appendices contain our conventions (appendix A) as well as details on technical parts of the calculations (appendices B–D).

2 Mass matrix

In this section, we diagonalize the mass matrix that arises due to the scalar vevs. Following the strategy of [12, 13], we begin by expanding the action around the classical solution in section 2.1. We then proceed to diagonalize the mass matrices for the bosons and fermions in sections 2.2 and 2.3, respectively. We summarize the result in section 2.4.

2.1 Expansion of the action

The defect CFT we study contains two types of fields: the ones of $\mathcal{N} = 4$ SYM theory transforming in the adjoint of the gauge group and the fundamental fields living on the three-dimensional defect. However, the fields living on the defect will not contribute to the one-loop one-point functions of bulk[2] operators as explained in [13], and we accordingly neglect the corresponding part of the action. The action for the bulk fields is the one of

[2]Note that 'bulk' refers to four-dimensional Minkowski space without the defect; it should not be confused with the bulk of the dual AdS_5.

JHEP01(2019)007

standard $\mathcal{N}=4$ SYM theory in four dimensions,

$$S_{\mathcal{N}=4} = \frac{2}{g_{\rm YM}^2}\int \mathrm{d}^4x\ \mathrm{tr}\Big(-\frac{1}{4}F_{\mu\nu}F^{\mu\nu} - \frac{1}{2}D_\mu\phi_i D^\mu\phi_i + \frac{i}{2}\bar\psi\gamma^\mu D_\mu\psi \\ + \frac{1}{4}[\phi_i,\phi_j][\phi_i,\phi_j] + \frac{1}{2}\sum_{i=1}^{3}\bar\psi G^i[\phi_i,\psi] + \frac{1}{2}\sum_{i=4}^{6}\bar\psi G^i[\phi_i,\gamma_5\psi]\Big). \tag{2.1}$$

We describe in appendix A our field-theory conventions, which follow the ones of [13]. In particular, we explicitly give the matrices G^i $(i=1,\ldots,6)$, which arise in the reduction from ten- to four-dimensional SYM theory. The ψ_i for $i=1,\ldots,4$ are four-dimensional Majorana fermions, and all these fields transform in the adjoint of U(N),

$$D_\mu\phi_i = \partial_\mu\phi_i - i[A_\mu,\phi_i], \quad D_\mu\psi_i = \partial_\mu\psi_i - i[A_\mu,\psi_i]. \tag{2.2}$$

The classical equations of motion of (2.1) are

$$\nabla^2\phi_i^{\rm cl} = \left[\phi_j^{\rm cl},\left[\phi_j^{\rm cl},\phi_i^{\rm cl}\right]\right], \quad i=1,\ldots,6, \tag{2.3}$$

where we are setting the fermions and gauge fields to zero classically, and are looking for time-independent solutions for the scalars. A solution to the equations of motion for the six scalar fields with SO(3) $\times$ SO(3) symmetry is [21][3]

$$\begin{aligned}\phi_i^{\rm cl}(x) &= -\frac{1}{x_3}\left(t_i^{k_1}\otimes\mathbb{1}_{k_2}\right)\oplus 0_{N-k_1k_2} \qquad \text{for} \quad i=1,2,3,\\ \phi_i^{\rm cl}(x) &= -\frac{1}{x_3}\left(\mathbb{1}_{k_1}\otimes t_{i-3}^{k_2}\right)\oplus 0_{N-k_1k_2} \qquad \text{for} \quad i=4,5,6.\end{aligned} \tag{2.4}$$

Here the matrices $t_i^{k_a}$ constitute the k_a-dimensional irreducible representation of $\mathfrak{su}(2)$; thus, the solution has $\mathfrak{su}(2)\times\mathfrak{su}(2)$ symmetry. In the case $k_1=1$ or $k_2=1$, the vevs (2.4) reduce to the ones in the supersymmetric D3-D5 setup [13]; hence, we will always assume $k_1,k_2\geq 2$. The classical solution (2.4) applies for $x_3>0$ and is responsible for breaking the gauge group from U(N) to U($N-k_1k_2$) for $x_3>0$. All other fields vanish classically in this region. For $x_3<0$, all fields have gauge group U($N-k_1k_2$) and the vevs for these fields vanish.

We expand the action around the classical solution as

$$\phi_i(x) = \phi_i^{\rm cl}(x) + \tilde\phi_i(x). \tag{2.5}$$

The gauge fixing is implemented by introducing fermionic ghost fields c and $\bar c$ transforming as Lorentz scalars, following [13, 32]. The terms in the expanded action that are linear in

[3]The prefactor $\frac{1}{x_3}$ ensures scale invariance of the defect field theory and is important for the dual probe-brane interpretation. A set-up where the classical fields were similar but not carrying the $\frac{1}{x_3}$ prefactor was studied in [31], where in order to stabilize the system extra mass and interaction terms were added to the $\mathcal{N}=4$ SYM action.

JHEP01(2019)007

$\tilde{\phi}_i$ vanish by the classical equations of motion. All fields have a canonically normalized (quadratic) kinetic term,

$$S_{\text{kin}} = \frac{2}{g_{\text{YM}}^2} \int \mathrm{d}^4x \ \mathrm{tr} \left(\frac{1}{2} A_\mu \partial_\nu \partial^\mu A^\nu + \frac{1}{2} \tilde{\phi}_i \partial_\nu \partial^\nu \tilde{\phi}_i + \frac{i}{2} \bar{\psi} \gamma^\mu \partial_\mu \psi + \bar{c} \partial_\mu \partial^\mu c \right). \tag{2.6}$$

The mass term for the bosons becomes

$$\begin{aligned} S_{\text{m,b}} = \frac{2}{g_{\text{YM}}^2} \int \mathrm{d}^4x \ \mathrm{tr} \Bigg(& -\frac{1}{2} \tilde{\phi}_j [\phi_i^{\text{cl}}, [\phi_i^{\text{cl}}, \tilde{\phi}_j]] - \tilde{\phi}_i [[\phi_i^{\text{cl}}, \phi_j^{\text{cl}}], \tilde{\phi}_j] \\ & - \frac{1}{2} A_\mu [\phi_i^{\text{cl}}, [\phi_i^{\text{cl}}, A^\mu]] + 2i [A^\mu, \tilde{\phi}_i] \partial_\mu \phi_i^{\text{cl}} \Bigg), \end{aligned} \tag{2.7}$$

while the mass term for the four Majorana fermions ψ_i and the ghosts c and $\bar{c}$ is

$$S_{\text{m,f}} = \frac{2}{g_{\text{YM}}^2} \int \mathrm{d}^4x \ \mathrm{tr} \left(\frac{1}{2} \sum_{i=1}^{3} \bar{\psi} G^i [\phi_i^{\text{cl}}, \psi] + \frac{1}{2} \sum_{i=4}^{6} \bar{\psi} G^i [\phi_i^{\text{cl}}, \gamma_5 \psi] - \sum_{i=1}^{6} \bar{c} [\phi_i^{\text{cl}}, [\phi_i^{\text{cl}}, c]] \right). \tag{2.8}$$

The expanded action also contains cubic and quartic interaction vertices between the different fields. The cubic interactions are given by

$$\begin{aligned} S_{\text{cubic}} = \frac{2}{g_{\text{YM}}^2} \int \mathrm{d}^4x \ \mathrm{tr} \Bigg(& i [A^\mu, A^\nu] \partial_\mu A_\nu + [\phi_i^{\text{cl}}, \tilde{\phi}_j] [\tilde{\phi}_i, \tilde{\phi}_j] + i [A^\mu, \tilde{\phi}_i] \partial_\mu \tilde{\phi}_i + [A_\mu, \phi_i^{\text{cl}}] [A^\mu, \tilde{\phi}_i] \\ & + \frac{1}{2} \bar{\psi} \gamma^\mu [A_\mu, \psi] + \frac{1}{2} \sum_{i=1}^{3} \bar{\psi} G^i [\tilde{\phi}_i, \psi] + \frac{1}{2} \sum_{i=4}^{6} \bar{\psi} G^i [\tilde{\phi}_i, \gamma_5 \psi] + i (\partial_\mu \bar{c}) [A_\mu, c] - \bar{c} [\phi_i^{\text{cl}}, [\tilde{\phi}_i, c]] \Bigg). \end{aligned} \tag{2.9}$$

The quartic interaction vertices are identical to the quartic vertices present in the action (2.1). They do not play a role for the one-loop correction to the one-point functions of bulk operators, starting to contribute only at two-loop order [13].

The mass terms (2.7) and (2.8) are not diagonal, neither in flavor nor in color, and have to be diagonalized in order to obtain the mass spectrum of the theory and thus the propagators. Moreover, note that unlike actual mass terms, the terms (2.7) and (2.8) depend on the inverse distance to the defect via the vevs (2.4). This dependence can be understood in terms of an effective AdS_4 space, as was found in [13, 16] and is discussed in detail in section 3.

In the remainder of the paper, we will use Euclidean signature.

2.2 Boson mass matrix

In this section, we will treat the mass term for the bosons, while the mass term for the fermions will be treated in section 2.3.

JHEP01(2019)007

Inserting the classical solution (2.4) into the mass term (2.7) for the bosons, the latter can be written as

$$\begin{aligned} S_{\mathrm{m,b}} = \frac{2}{g_{\mathrm{YM}}^2}\int \mathrm{d}^4x \frac{1}{x_3^2}\,\mathrm{tr}\Bigg(&-\frac{1}{2}\sum_{j=1}^{6}\tilde{\phi}_j\left[(L^{(1)})^2+(L^{(2)})^2\right]\tilde{\phi}_j - \frac{1}{2}A_\mu\left[(L^{(1)})^2+(L^{(2)})^2\right]A^\mu \\ &+ i\sum_{i,j,k=1}^{3}\epsilon_{ijk}\tilde{\phi}_i L_j^{(1)}\tilde{\phi}_k + i\sum_{i,j,k=1}^{3}\epsilon_{ijk}\tilde{\phi}_{i+3}L_j^{(2)}\tilde{\phi}_{k+3} \\ &+ i\sum_{i=1}^{3}\left[\tilde{\phi}_i L_i^{(1)}A_3 - A_3 L_i^{(1)}\tilde{\phi}_i\right] + i\sum_{i=1}^{3}\left[\tilde{\phi}_{i+3}L_i^{(2)}A_3 - A_3 L_i^{(2)}\tilde{\phi}_{i+3}\right]\Bigg). \end{aligned} \tag{2.10}$$

The operators $L_i^{(1)}$ and $L_i^{(2)}$ for $i=1,2,3$ are defined as the adjoint of the classical solution,

$$L_i^{(1)} \equiv \mathrm{ad}\left[\left(t_i^{k_1}\otimes \mathbb{1}_{k_2}\right)\oplus 0_{N-k_1k_2}\right], \quad L_i^{(2)} \equiv \mathrm{ad}\left[\left(\mathbb{1}_{k_1}\otimes t_i^{k_2}\right)\oplus 0_{N-k_1k_2}\right], \tag{2.11}$$

where as usual $(\mathrm{ad}A)\,B \equiv [A,B]$. They satisfy the commutation relations of $\mathfrak{su}(2)\times\mathfrak{su}(2)$,

$$\left[L_i^{(1)},L_j^{(1)}\right] = i\epsilon_{ijk}L_k^{(1)}, \quad \left[L_i^{(2)},L_j^{(2)}\right] = i\epsilon_{ijk}L_k^{(2)}, \quad \left[L_i^{(1)},L_j^{(2)}\right] = 0. \tag{2.12}$$

Furthermore, we write $(L^{(a)})^2 \equiv \sum_i (L_i^{(a)})^2$ for the quadratic Casimirs corresponding to the two sectors with $a=1,2$. We will use their eigenvalues $\ell_1(\ell_1+1)$ and $\ell_2(\ell_2+1)$ to label irreducible representations of $\mathfrak{su}(2)\times\mathfrak{su}(2)$ by (ℓ_1,ℓ_2). As in [13], we find that we can distinguish two types of bosons: if their mass term is already diagonal in flavor the fields are called "easy" bosons, while the ones for which flavor and color mix are called "complicated".

We rewrite (2.10) as

$$\begin{aligned} S_{\mathrm{m,b}} = \frac{2}{g_{\mathrm{YM}}^2}\int \mathrm{d}^4x \left(\frac{-1}{2\,x_3^2}\right)\mathrm{tr}\Bigg(&E^\dagger\left[(L^{(1)})^2+(L^{(2)})^2\right]E \\ &+ \tilde{C}^\dagger\left[(L^{(1)})^2+(L^{(2)})^2 - 2\tilde{S}_i^{(1)}L_i^{(1)} - 2\tilde{S}_i^{(2)}L_i^{(2)}\right]\tilde{C}\Bigg), \end{aligned} \tag{2.13}$$

where we have grouped the fields into vectors of easy and complicated fields E and $\tilde{C}$ respectively,

$$E = \begin{pmatrix} A_0 \\ A_1 \\ A_2 \end{pmatrix}, \quad \tilde{C} = \begin{pmatrix} \tilde{\phi}_1 \\ \vdots \\ \tilde{\phi}_6 \\ A_3 \end{pmatrix}. \tag{2.14}$$

The seven-dimensional matrices $\tilde{S}_i^{(1)}$ and $\tilde{S}_i^{(2)}$ act on the flavor index while the operators $L_i^{(1)}$ and $L_i^{(2)}$ act on the color part of the quantum fields. We see from (2.13) that for the easy fields we only need to diagonalize the operator $(L^{(1)})^2+(L^{(2)})^2$ in color space. The

JHEP01(2019)007

mass term for the complicated fields mixes different flavors by means of the matrices $\tilde{S}_i^{(1)}$ and $\tilde{S}_i^{(2)}$ and we will have to diagonalize the color and flavor part simultaneously. Note that compared to the solution where only three scalar fields get non-trivial SO(3)-symmetric vevs studied in [13], all scalars $\tilde{\phi}_i$ are now complicated bosons and only the three components of the gauge fields A_0, A_1, A_2 and the ghost field remain easy. We will denote the eigenvalues of the matrices inside the trace in (2.13) by m^2.

2.2.1 Decomposition of the color matrices and easy fields

In order to proceed with the diagonalization, we decompose the color part of a generic field Φ in blocks:

$$\Phi = [\Phi]_{n,n'} E^n{}_{n'} + [\Phi]_{n,a} E^n{}_a + [\Phi]_{a,n} E^a{}_n + [\Phi]_{a,a'} E^a{}_{a'}, \tag{2.15}$$

with $n, n' = 1, \ldots, k_1 k_2$ and $a, a' = k_1 k_2 + 1, \ldots, N$. Here $E^n{}_{n'}$ are $N \times N$ matrices with a single non-vanishing entry, namely a 1 at position (n, n'). The fields $[\Phi]_{n,a}$ and $[\Phi]_{a,n}$ will often be referred to as fields in the off-diagonal block.

The fields $[\Phi]_{a,a'}$ in the $(N - k_1 k_2) \times (N - k_1 k_2)$ block are massless since

$$L_i^{(1)}\, E^a{}_{a'} = \left[\left(t_i^{k_1} \otimes \mathbb{1}_{k_2} \right) \oplus 0_{N-k_1 k_2}, E^a{}_{a'} \right] = 0, \tag{2.16}$$

and similarly for $L_i^{(2)}$. One can think of this result as the statement that the indices a and a' are singlets under $\mathfrak{su}(2) \times \mathfrak{su}(2)$.

The matrices $E^n{}_a$ and $E^a{}_n$ transform in the $(k_1 \times k_2)$-dimensional irreducible representation of $\mathfrak{su}(2) \times \mathfrak{su}(2)$,

$$\begin{aligned} L_i^{(1)}\, E^n{}_a &= E^{n'}{}_a [t_i^{k_1} \otimes \mathbb{1}_{k_2}]_{n',n}, \quad & L_i^{(1)}\, E^a{}_n &= -[t_i^{k_1} \otimes \mathbb{1}_{k_2}]_{n,n'} E^a{}_{n'}, \\ L_i^{(2)}\, E^n{}_a &= E^{n'}{}_a [\mathbb{1}_{k_1} \otimes t_i^{k_2}]_{n',n}, \quad & L_i^{(2)}\, E^a{}_n &= -[\mathbb{1}_{k_1} \otimes t_i^{k_2}]_{n,n'} E^a{}_{n'}. \end{aligned} \tag{2.17}$$

Equivalently, each index n transforms in the same representation as t_i, namely the one with spins $\ell_1 = \frac{k_1 - 1}{2}$ and $\ell_2 = \frac{k_2 - 1}{2}$. It follows that the matrices $E^n{}_a$ and $E^a{}_n$ already diagonalize the quadratic Casimir operators,

$$(L^{(1)})^2\, E^n{}_a = \frac{k_1^2 - 1}{4} E^n{}_a, \qquad (L^{(1)})^2\, E^a{}_n = \frac{k_1^2 - 1}{4} E^a{}_n, \tag{2.18}$$

and analogously for $(L^{(2)})^2$. The matrices $E^n{}_a$ and $E^a{}_n$ transform into each other under Hermitian conjugation, and this behavior carries over to the fields $[\Phi]_{n,a}$ and $[\Phi]_{a,n}$ in the off-diagonal block:

$$(E^n{}_a)^\dagger = E^a{}_n, \quad [\Phi]_{n,a}^\dagger \equiv \left([\Phi]_{n,a} \right)^\dagger = [\Phi]_{a,n}\,. \tag{2.19}$$

Moreover, they are orthogonal and normalized in the sense that

$$\begin{aligned} \mathrm{tr} \left[(E^n{}_a)^\dagger\, E^{n'}{}_{a'} \right] &= \delta^{nn'} \delta_{aa'}, \quad & \mathrm{tr} \left[(E^a{}_n)^\dagger\, E^{n'}{}_{a'} \right] &= 0, \\ \mathrm{tr} \left[(E^a{}_n)^\dagger\, E^{a'}{}_{n'} \right] &= \delta^{aa'} \delta_{nn'}, \quad & \mathrm{tr} \left[(E^n{}_a)^\dagger\, E^{a'}{}_{n'} \right] &= 0. \end{aligned} \tag{2.20}$$

JHEP01(2019)007

For easy fields $[\Phi]_{n,a}$ and $[\Phi]_{a,n}$, for which $(L^{(1)})^2 + (L^{(2)})^2$ is the complete mass term, we thus find the masses

$$m^2_{\text{easy}} \equiv \frac{k_1^2 - 1}{4} + \frac{k_2^2 - 1}{4}, \tag{2.21}$$

which have multiplicity $2k_1k_2(N - k_1k_2)$.

Finally, the matrices $E^n{}_{n'}$ contain two n indices, and therefore they transform as the product of two $(k_1 \times k_2)$-dimensional irreducible representations of $\mathfrak{su}(2) \times \mathfrak{su}(2)$. This product is reducible and decomposes as

$$\left(\frac{k_1 - 1}{2}, \frac{k_2 - 1}{2}\right) \otimes \left(\frac{k_1 - 1}{2}, \frac{k_2 - 1}{2}\right) = \bigoplus_{\ell_1=0}^{k_1-1} \bigoplus_{\ell_2=0}^{k_2-1} (\ell_1, \ell_2), \tag{2.22}$$

where (ℓ_1, ℓ_2) is the $\mathfrak{su}(2) \times \mathfrak{su}(2)$ representation with spins ℓ_1 and ℓ_2 and dimension $(2\ell_1 + 1) \times (2\ell_2 + 1)$. Note that the fields $[\Phi]_{n,a}$ and $[\Phi]_{a,n}$ in the off-diagonal block have spins $\ell_1 = \frac{k_1-1}{2}$ and $\ell_2 = \frac{k_2-1}{2}$, which appears as one of the terms in the decomposition (2.22). Thus, any results for the masses in the off-diagonal blocks can be obtained from the result in the $k_1k_2 \times k_1k_2$ block by the simple replacement rule

$$\ell_1 \to \frac{k_1 - 1}{2} \quad \text{and} \quad \ell_2 \to \frac{k_2 - 1}{2}. \tag{2.23}$$

This justifies that in the following we will mostly focus on the $k_1k_2 \times k_1k_2$ block.

In the case of the field theory where only three scalar fields get non-trivial SO(3)-symmetric vevs, dual to the D3-D5 probe-brane setup, the mass term for the easy bosons is L^2. In [13], it was found that the diagonalization in the corresponding $k \times k$ block could be solved by expressing the fields in a basis of fuzzy spherical harmonics $\hat{Y}^m_\ell$ constituting an irreducible spin-ℓ representation of $\mathfrak{su}(2)$. In the present case, the mass term for the easy bosons contains the operator $(L^{(1)})^2 + (L^{(2)})^2$, and since $(L^{(1)})^2$ and $(L^{(2)})^2$ commute with each other, we can diagonalize them simultaneously. The eigenstates of $(L^{(1)})^2 + (L^{(2)})^2$ are therefore the tensor products $\hat{Y}^{m_1}_{\ell_1} \otimes \hat{Y}^{m_2}_{\ell_2}$ of two fuzzy spherical harmonics. We use this basis to express the fields in the $k_1k_2 \times k_1k_2$ block as

$$\sum_{n,n'=1}^{k_1k_2} [\Phi]_{n,n'} E^n{}_{n'} = \sum_{\ell_1=0}^{k_1-1} \sum_{\ell_2=0}^{k_2-1} \sum_{m_1=-\ell_1}^{\ell_1} \sum_{m_2=-\ell_2}^{\ell_2} \Phi_{\ell_1,m_1;\ell_2,m_2} \hat{Y}^{m_1}_{\ell_1} \otimes \hat{Y}^{m_2}_{\ell_2}. \tag{2.24}$$

The properties of the basis states $\hat{Y}^{m_1}_{\ell_1} \otimes \hat{Y}^{m_2}_{\ell_2}$ follow from the properties of the fuzzy spherical harmonics $\hat{Y}^m_\ell$, which are reviewed in appendix A.2. An important property is the behavior under Hermitian conjugation, which carries over to the field components $\Phi_{\ell_1,m_1;\ell_2,m_2}$:

$$\begin{aligned} \left(\hat{Y}^{m_1}_{\ell_1} \otimes \hat{Y}^{m_2}_{\ell_2}\right)^\dagger &= (-1)^{m_1}(-1)^{m_2} \hat{Y}^{-m_1}_{\ell_1} \otimes \hat{Y}^{-m_2}_{\ell_2}, \\ (\Phi_{\ell_1,m_1;\ell_2,m_2})^\dagger &= (-1)^{m_1}(-1)^{m_2} \Phi_{\ell_1,-m_1;\ell_2,-m_2}. \end{aligned} \tag{2.25}$$

JHEP01(2019)007

m^2	Multiplicity
$\ell_1(\ell_1+1)+\ell_2(\ell_2+1)$	$(2\ell_1+1)(2\ell_2+1)$
$(k_1^2-1)/4+(k_2^2-1)/4$	$2k_1k_2(N-k_1k_2)$
0	$(N-k_1k_2)(N-k_1k_2)$

Table 1. Masses for the easy bosons A_0, A_1 and A_2 (as well as the ghosts c), including the $k_1k_2 \times k_1k_2$, the $k_1k_2 \times (N-k_1k_2)$ and the $(N-k_1k_2) \times (N-k_1k_2)$ blocks. Here $\ell_1 = 0, \ldots, k_1-1$ and $\ell_2 = 0, \ldots, k_2-1$.

The operators $L_i^{(1)}$ and $L_i^{(2)}$ act on the basis states as

$$\begin{aligned}
(L^{(1)})^2\ \hat{Y}^{m_1}_{\ell_1} \otimes \hat{Y}^{m_2}_{\ell_2} &= \ell_1(\ell_1+1)\ \hat{Y}^{m_1}_{\ell_1} \otimes \hat{Y}^{m_2}_{\ell_2}, \\
L_3^{(1)}\ \hat{Y}^{m_1}_{\ell_1} \otimes \hat{Y}^{m_2}_{\ell_2} &= \sqrt{\ell_1(\ell_1+1)}\langle \ell_1, m_1; 1, 0 | \ell_1, m_1\rangle\ \hat{Y}^{m_1}_{\ell_1} \otimes \hat{Y}^{m_2}_{\ell_2}, \\
L_\pm^{(1)}\ \hat{Y}^{m_1}_{\ell_1} \otimes \hat{Y}^{m_2}_{\ell_2} &= \mp\sqrt{2\ell_1(\ell_1+1)}\langle \ell_1, m_1; 1, \pm 1 | \ell_1, m_1 \pm 1\rangle\ \hat{Y}^{m_1\pm 1}_{\ell_1} \otimes \hat{Y}^{m_2}_{\ell_2},
\end{aligned} \tag{2.26}$$

with the ladder operators $L_\pm^{(1)} = L_1^{(1)} \pm iL_2^{(1)}$ and analogous expressions for $(L^{(2)})^2$, $L_3^{(2)}$ and $L_\pm^{(2)}$. Here and in the following, $\langle \ell, m_\ell; s, m_s | j, m_j\rangle$ denotes the $\mathfrak{su}(2)$ Clebsch-Gordan coefficient for coupling the two angular momenta ℓ and s to the total angular momentum j. For the case $s = 1$ and $j = \ell$ in (2.26), they are

$$\langle \ell, m; 1, \pm 1 | \ell, m \pm 1\rangle = \mp\frac{\sqrt{\ell(\ell+1) - m(m\pm 1)}}{\sqrt{2\ell(\ell+1)}},\ \langle \ell, m; 1, 0 | \ell, m\rangle = \frac{m}{\sqrt{\ell(\ell+1)}}. \tag{2.27}$$

Furthermore, the basis states are orthogonal and normalized such that

$$\mathrm{tr}\left[\left(\hat{Y}^{m_1'}_{\ell_1'} \otimes \hat{Y}^{m_2'}_{\ell_2'}\right)^\dagger \hat{Y}^{m_1}_{\ell_1} \otimes \hat{Y}^{m_2}_{\ell_2}\right] = \delta_{\ell_1',\ell_1}\ \delta_{\ell_2',\ell_2}\ \delta_{m_1,m_1'}\ \delta_{m_2,m_2'}. \tag{2.28}$$

Using this basis, we see that the mass eigenvalues of the fields $\Phi_{\ell_1,m_1;\ell_2,m_2}$ are

$$m^2_{\text{easy}} \equiv \ell_1(\ell_1+1) + \ell_2(\ell_2+1), \tag{2.29}$$

where we must take all combinations of $\ell_1 = 0, \ldots, k_1-1$ and $\ell_2 = 0, \ldots, k_2-1$. The multiplicity is the dimension of the corresponding $\mathfrak{su}(2) \times \mathfrak{su}(2)$ representation, i.e. $(2\ell_1+1)(2\ell_2+1)$. As discussed before, the masses of the fields in the $(N-k_1k_2) \times (N-k_1k_2)$ block are zero. Finally, the masses (2.21) in the $k_1k_2 \times (N-k_1k_2)$ and the $(N-k_1k_2) \times k_1k_2$ blocks are indeed obtained from (2.29) by the replacement rule (2.23). We summarize the masses of the easy fields in table 1.

2.2.2 Complicated fields

For the complicated fields the decomposition in terms of $\mathfrak{su}(2) \times \mathfrak{su}(2)$ representations is not sufficient, because we also need to solve the problem of flavor mixing. Since $(L^{(1)})^2 + (L^{(2)})^2$ commutes with $\tilde{S} \cdot L \equiv \tilde{S}_i^{(1)} L_i^{(1)} + \tilde{S}_i^{(2)} L_i^{(2)}$ we can diagonalize the two terms in (2.13) simultaneously. Thus the masses will have the form $\ell_1(\ell_1+1) + \ell_2(\ell_2+1) - 2\lambda$, where λ are the eigenvalues of the mixing matrix $\tilde{S} \cdot L$.

JHEP01(2019)007

Rewriting the matrices $\tilde{S}_i$. The seven-dimensional matrices $\tilde{S}_i$ are given in block form by

$$\tilde{S}_i \equiv \tilde{S}_i^{(1)} = \begin{pmatrix} \tilde{T}_i & 0 & \tilde{R}_i \\ 0 & 0 & 0 \\ \tilde{R}_i^\dagger & 0 & 0 \end{pmatrix}, \quad \tilde{S}_{i+3} \equiv \tilde{S}_i^{(2)} = \begin{pmatrix} 0 & 0 & 0 \\ 0 & \tilde{T}_i & \tilde{R}_i \\ 0 & \tilde{R}_i^\dagger & 0 \end{pmatrix}, \quad i = 1, 2, 3. \tag{2.30}$$

In the previous equation, $\tilde{R}_j$ is a 3×1 matrix that has an i in the j-th component and zeros everywhere else, namely $(\tilde{R}_j)_k = i\,\delta_{jk}$. On the other hand, the three-dimensional matrices $\tilde{T}_i$ are given by

$$\tilde{T}_1 = \begin{pmatrix} 0 & 0 & 0 \\ 0 & 0 & -i \\ 0 & i & 0 \end{pmatrix}, \quad \tilde{T}_2 = \begin{pmatrix} 0 & 0 & i \\ 0 & 0 & 0 \\ -i & 0 & 0 \end{pmatrix}, \quad \tilde{T}_3 = \begin{pmatrix} 0 & -i & 0 \\ i & 0 & 0 \\ 0 & 0 & 0 \end{pmatrix}. \tag{2.31}$$

These matrices form an irreducible representation of the $\mathfrak{su}(2)$ Lie algebra, so they can be brought into the usual form for the spin-one representation

$$T_1 = \frac{1}{\sqrt{2}} \begin{pmatrix} 0 & 1 & 0 \\ 1 & 0 & 1 \\ 0 & 1 & 0 \end{pmatrix}, \quad T_2 = \frac{1}{\sqrt{2}} \begin{pmatrix} 0 & -i & 0 \\ i & 0 & -i \\ 0 & i & 0 \end{pmatrix}, \quad T_3 = \begin{pmatrix} 1 & 0 & 0 \\ 0 & 0 & 0 \\ 0 & 0 & -1 \end{pmatrix}, \tag{2.32}$$

using the unitary transformation

$$U = \frac{1}{\sqrt{2}} \begin{pmatrix} -1 & 0 & 1 \\ -i & 0 & -i \\ 0 & \sqrt{2} & 0 \end{pmatrix}. \tag{2.33}$$

Hence, the matrices $\tilde{S}_i$ can be rewritten as

$$S_i^{(1)} + S_j^{(2)} = V^\dagger \left(\tilde{S}_i^{(1)} + \tilde{S}_j^{(2)} \right) V = \begin{pmatrix} T_i & 0 & R_i \\ 0 & T_j & R_j \\ R_i^\dagger & R_j^\dagger & 0 \end{pmatrix}, \tag{2.34}$$

with

$$T_i = U^\dagger \tilde{T}_i U, \quad R_i = U^\dagger \tilde{R}_i, \quad V = \begin{pmatrix} U & 0 & 0 \\ 0 & U & 0 \\ 0 & 0 & 1 \end{pmatrix}. \tag{2.35}$$

The vector of complicated fields has to be transformed accordingly:

$$C = V^\dagger \tilde{C} = \begin{pmatrix} C^{(1)} \\ C^{(2)} \\ A_3 \end{pmatrix}, \tag{2.36}$$

where the three-dimensional vectors $C^{(1)}$ and $C^{(2)}$ are defined by

$$C^{(1)} \equiv \begin{pmatrix} C_+^{(1)} \\ C_0^{(1)} \\ C_-^{(1)} \end{pmatrix} \equiv \begin{pmatrix} \frac{1}{\sqrt{2}}(-\tilde{\phi}_1 + i\tilde{\phi}_2) \\ \tilde{\phi}_3 \\ \frac{1}{\sqrt{2}}(+\tilde{\phi}_1 + i\tilde{\phi}_2) \end{pmatrix}, \quad C^{(2)} \equiv \begin{pmatrix} C_+^{(2)} \\ C_0^{(2)} \\ C_-^{(2)} \end{pmatrix} \equiv \begin{pmatrix} \frac{1}{\sqrt{2}}(-\tilde{\phi}_4 + i\tilde{\phi}_5) \\ \tilde{\phi}_6 \\ \frac{1}{\sqrt{2}}(+\tilde{\phi}_4 + i\tilde{\phi}_5) \end{pmatrix}. \tag{2.37}$$

JHEP01(2019)007

The subscripts $+, -, 0$ denote the eigenvalues with respect to T_3. One can also check that

$$R_i^\dagger L_i^{(1)} = i\left(\frac{L_+^{(1)}}{\sqrt{2}}, -L_3^{(1)}, -\frac{L_-^{(1)}}{\sqrt{2}}\right), \quad R_i^\dagger L_i^{(2)} = i\left(\frac{L_+^{(2)}}{\sqrt{2}}, -L_3^{(2)}, -\frac{L_-^{(2)}}{\sqrt{2}}\right). \tag{2.38}$$

After the flavor transformation (2.33), the seven-dimensional matrix that mixes the flavors in the mass term for the complicated bosons is

$$S \cdot L = S_i^{(1)} L_i^{(1)} + S_i^{(2)} L_i^{(2)} = \begin{pmatrix} T_i L_i^{(1)} & 0 & R_i L_i^{(1)} \\ 0 & T_i L_i^{(2)} & R_i L_i^{(2)} \\ R_i^\dagger L_i^{(1)} & R_i^\dagger L_i^{(2)} & 0 \end{pmatrix}. \tag{2.39}$$

In the diagonalization of (2.39), we have to distinguish the cases where one ℓ_a is 0 and where both ℓ_a are bigger than 0.[4] For simplicity, we begin with the easier case where one ℓ_a is 0. Note that this formally reduces the diagonalization problem to the one where only three of the scalar fields get non-trivial SO(3)-symmetric vevs that was solved in [12, 13]. We will now present a different solution to this diagonalization problem that has a straightforward generalization to the classical solution with SO(3) × SO(3) symmetry considered in this paper. In the following, we also drop all references to a.

Diagonalization of $T_i L_i$. After the flavor transformation in the previous section, the four-dimensional matrix $S \cdot L \equiv S_i L_i$ has the form

$$S_i L_i = \begin{pmatrix} T_i L_i & R_i L_i \\ R_i^\dagger L_i & 0 \end{pmatrix}. \tag{2.40}$$

It is important to realize that if we find an eigenvector of $T_i L_i$ that is annihilated by $R_i^\dagger L_i$ we can obtain an eigenvector of $S \cdot L$ by padding it with a zero to make it four-dimensional. We will thus first look for states Φ such that

$$T_i L_i \, \Phi = \lambda_\Phi \, \Phi \quad \text{and} \quad R_i^\dagger L_i \, \Phi = 0. \tag{2.41}$$

This does not yield all eigenstates of $S \cdot L$, but we will see that the remaining ones are obtained by diagonalizing a simple 2×2 matrix.

If we define a total "angular momentum" operator $J_i = L_i + T_i$, then

$$T_i L_i = \frac{1}{2}\left(J^2 - L^2 - T^2\right) = \frac{1}{2}\left(J^2 - L^2 - 2\right). \tag{2.42}$$

Hence, the diagonalization of the term $T_i L_i$ reduces to the problem of finding a set of common eigenstates for J^2, J_3 and L^2. This is the well-known problem of addition of angular momentum, which can be solved using Clebsch-Gordan coefficients. The matrices T_i form the three-dimensional (spin-one) representation of $\mathfrak{su}(2)$ and the matrices L_i form the spin-ℓ representation. Thus, the fields $(C_{m_s})_{\ell m}$ in (2.37) have well-defined quantum numbers ℓ, m and m_s for L^2, L_3 and T_3 respectively. The fields with total angular momentum j, magnetic

[4] The case where $\ell_1 = \ell_2 = 0$ is trivial as the corresponding fields are massless.

JHEP01(2019)007

quantum number m_j and angular momentum ℓ are found in terms of Clebsch-Gordan coefficients $\langle \ell, m; s, m_s | j, m_j \rangle$ by

$$B_{j,m_j;\ell} = \sum_{m_s=-1}^{+1} \sum_{m=-\ell}^{\ell} \delta_{m+m_s,m_j} \langle \ell, m; 1, m_s | j, m_j \rangle \, (C_{m_s})_{\ell m}. \tag{2.43}$$

Here the total angular momentum can in general take the three values $j = \ell, \ell \pm 1$. For the case $\ell = 0$, however, there is only one total angular momentum $j = 1$; this necessitates the aforementioned distinction between $\ell_a = 0$ and $\ell_a \neq 0$. The dependence on ℓ will generally be dropped, and we will use the notation $(B_\alpha)_{j,m_j} \equiv B_{j,m_j;\ell=j-\alpha}$. For example, the state B_+ has total angular momentum $j = \ell + 1$ and $m_j = -\ell - 1, \ldots, \ell + 1$. Using this notation and summing explicitly over m, (2.43) becomes

$$(B_\alpha)_{j,m_j} = \sum_{m_s=-1}^{+1} \langle \ell - \alpha, m_j - m_s; 1, m_s | j, m_j \rangle \, (C_{m_s})_{\ell-\alpha, m_j - m_s}. \tag{2.44}$$

We can write out the basis states corresponding to (2.43) in vector form. Since the 3×3 matrices T_i are the standard spin-one representation of $\mathfrak{su}(2)$, cf. (2.32), we have

$$T_3 \, \hat{e}_{m_s} = m_s \, \hat{e}_{m_s} \quad \text{with} \quad \hat{e}_{+1} = \begin{pmatrix} 1 \\ 0 \\ 0 \end{pmatrix}, \quad \hat{e}_0 = \begin{pmatrix} 0 \\ 1 \\ 0 \end{pmatrix}, \quad \hat{e}_{-1} = \begin{pmatrix} 0 \\ 0 \\ 1 \end{pmatrix}. \tag{2.45}$$

The basis states that are eigenstates of J^2, J_3 and L^2 can thus be written as

$$\begin{aligned} \hat{Y}_{j,m_j;\ell} &\equiv \sum_{m_s=-1}^{+1} \langle \ell, m_j - m_s; 1, m_s | j, m_j \rangle \, \hat{Y}_\ell^{m_j - m_s} \otimes \hat{e}_{m_s} \\ &= \begin{pmatrix} \langle \ell, m_j - 1; 1, +1 | j, m_j \rangle \, \hat{Y}_\ell^{m_j - 1} \\ \langle \ell, m_j; 1, 0 | j, m_j \rangle \, \hat{Y}_\ell^{m_j} \\ \langle \ell, m_j + 1; 1, -1 | j, m_j \rangle \, \hat{Y}_\ell^{m_j + 1} \end{pmatrix}. \end{aligned} \tag{2.46}$$

The Clebsch-Gordan coefficients for the case $j = \ell$ were given in (2.27). For $j = \ell \pm 1$, we have

$$\begin{aligned} \langle \ell, m; 1, \pm 1 | \ell + 1, m \pm 1 \rangle &= \frac{\sqrt{(\ell + 1 \pm m)(\ell + 2 \pm m)}}{\sqrt{2(\ell + 1)(2\ell + 1)}}, \\ \langle \ell, m; 1, 0 | \ell + 1, m \rangle &= \frac{\sqrt{(\ell + 1 - m)(\ell + 1 + m)}}{\sqrt{(\ell + 1)(2\ell + 1)}}, \\ \langle \ell, m; 1, \pm 1 | \ell - 1, m \pm 1 \rangle &= \frac{\sqrt{(\ell - 1 \mp m)(\ell \mp m)}}{\sqrt{2\ell(2\ell + 1)}}, \\ \langle \ell, m; 1, 0 | \ell - 1, m \rangle &= \frac{\sqrt{(\ell - m)(\ell + m)}}{\sqrt{\ell(2\ell + 1)}}. \end{aligned} \tag{2.47}$$

JHEP01(2019)007

We find three sets of eigenstates for $j = \ell \pm 1$ and $j = \ell$ with eigenvalues

$$\begin{aligned} T_i L_i \, \hat{Y}_{j=\ell+1,m_j;\ell} &= \ell \, \hat{Y}_{j=\ell+1,m_j;\ell}, \\ T_i L_i \, \hat{Y}_{j=\ell,m_j;\ell} &= -\hat{Y}_{j=\ell,m_j;\ell}, \\ T_i L_i \, \hat{Y}_{j=\ell-1,m_j;\ell} &= (-\ell-1) \, \hat{Y}_{j=\ell-1,m_j;\ell}. \end{aligned} \tag{2.48}$$

We will show below that the first and the last states satisfy the second condition in (2.41), namely

$$R_i^\dagger L_i \, \hat{Y}_{j,m_j;\, j\pm1} = 0. \tag{2.49}$$

The fields $B_\pm$ can thus be made into eigenstates of $S \cdot L$ by padding with zeros. The multiplicity of the corresponding eigenvalue is the dimension of the $\mathfrak{su}(2)$ representation, i.e. $2j+1 = 2(\ell \pm 1) + 1$.

Diagonalization of the remaining 2×2 matrix. We can expand the complicated scalars in the basis of total angular momentum eigenstates and A_3 in the basis of fuzzy spherical harmonics $\hat{Y}_{\ell,m}$, so that the four-dimensional vector of complicated fields is

$$C = \begin{pmatrix} \sum_{j,m_j,\ell} B_{j,m_j;\,\ell} \hat{Y}_{j,m_j;\ell} \\ \sum_{\ell,m} (A_3)_{\ell,m} \hat{Y}_\ell^m \end{pmatrix}. \tag{2.50}$$

We know how $T_i L_i$ acts on the basis states $\hat{Y}_{j,m_j;\ell}$ obtained from the Clebsch-Gordan procedure from (2.48). Now we will calculate how $R_i^\dagger L_i$, i.e. the last row in $S \cdot L$ as given in (2.40), acts on $Y_{j,m_j;\ell}$. Using that the ladder operators act as given in (2.26) together with (2.38) and the completeness relation of the Clebsch-Gordan coefficients, one obtains

$$\begin{aligned} R_i^\dagger L_i \, \hat{Y}_{j,m_j;\ell} &= -i\sqrt{\ell(\ell+1)} \sum_{m_s} \langle \ell, m_j - m_s; 1, m_s | j, m_j \rangle \langle \ell, m_j - m_s; 1, m_s | \ell, m_j \rangle \, \hat{Y}_\ell^{m_j} \\ &= -i \, \delta_{j,\ell} \sqrt{\ell(\ell+1)} \, \hat{Y}_\ell^{m_j}. \end{aligned} \tag{2.51}$$

This vanishes unless $j = \ell$. The states $\hat{Y}_{j,m_j;\ell}$ with $j = \ell \pm 1$ are thus annihilated by $R_i^\dagger L_i$ and can simply be padded with a zero block to give eigenstates of $S \cdot L$ as we have claimed before. Using (2.48) and (2.51), we can find the matrix elements of both $T_i L_i$ and $R_i L_i$:

$$\begin{aligned} \mathrm{tr}\left(\hat{Y}^\dagger_{j',m';\ell'} \, T_i L_i \, \hat{Y}_{j,m;\ell} \right) &= \mu_{j,\ell} \, \delta_{m,m'} \delta_{\ell,\ell'} \delta_{j,j'}, \\ \mathrm{tr}\left((\hat{Y}^{m'}_{\ell'})^\dagger \, R_i^\dagger L_i \, \hat{Y}_{j,m;\ell} \right) &= -i \, \delta_{m,m'} \, \delta_{\ell,\ell'} \, \delta_{j,\ell'} \sqrt{\ell(\ell+1)}, \\ \mathrm{tr}\left(\hat{Y}^\dagger_{j',m';\ell'} \, R_i L_i \, \hat{Y}^m_\ell \right) &= +i \, \delta_{m,m'} \, \delta_{\ell,\ell'} \, \delta_{\ell,j'} \sqrt{\ell(\ell+1)}. \end{aligned} \tag{2.52}$$

The matrix elements $\mu_{j,\ell}$ in the first line are $\mu_{\ell+1,\ell} = \ell$, $\mu_{\ell,\ell} = -1$ and $\mu_{\ell-1,\ell} = -\ell - 1$, cf. (2.48). The third line follows naturally from complex conjugation of the second line and $L_i^\dagger = L_i$.

JHEP01(2019)007

Mass eigenstate	Mass m^2	Multiplicity
B_+	$\ell_1(\ell_1-1)$	$2\ell_1+3$
B_-	$(\ell_1+1)(\ell_1+2)$	$2\ell_1-1$
D_+	$\ell_1(\ell_1-1)$	$2\ell_1+1$
D_-	$(\ell_1+1)(\ell_1+2)$	$2\ell_1+1$

Table 2. Masses and eigenstates of the complicated bosons in the $k_1k_2 \times k_1k_2$ block for the case $\ell_2 = 0$ and $\ell_1 = 1, \ldots, k_1 - 1$. The case $\ell_1 = 0$ and $\ell_2 = 1, \ldots, k_1 - 1$ is obtained by relabeling. In the case $\ell_1 = \ell_2 = 0$, the masses vanish, while the case $\ell_1 \neq 0$ and $\ell_2 \neq 0$ is shown in table 3.

We now insert the vector of complicated fields C given in (2.50) into the flavor mixing term in the action, obtaining

$$\begin{aligned}\mathrm{tr}\left[C^\dagger S_i L_i\, C\right] = \sum_{\ell=1}^{k-1}\Bigg[\ell \sum_{m=-\ell-1}^{\ell+1}(B_+)^\dagger_{\ell+1,m}(B_+)_{\ell+1,m} - (\ell+1)\sum_{m=-\ell+1}^{\ell-1}(B_-)^\dagger_{\ell-1,m}(B_-)_{\ell-1,m} \\ + \sum_{m=-\ell}^{\ell}\begin{pmatrix}(B_0)^\dagger_{\ell,m} & (A_3)^\dagger_{\ell,m}\end{pmatrix}\begin{pmatrix}-1 & -i\sqrt{\ell(\ell+1)} \\ +i\sqrt{\ell(\ell+1)} & 0\end{pmatrix}\begin{pmatrix}(B_0)_{\ell,m} \\ (A_3)_{\ell,m}\end{pmatrix}\Bigg].\end{aligned} \tag{2.53}$$

The fields $B_\pm$ diagonalize the full 4×4 matrix as we discussed before. What remains to be diagonalized is the 2×2 matrix in the last line of the previous equation. Note in particular that this matrix does not depend on the magnetic quantum number. The fields that achieve the diagonalization are

$$\begin{aligned}D_+ &= \frac{1}{\sqrt{2\ell+1}}\left(-i\sqrt{\ell}B_0 + \sqrt{\ell+1}A_3\right), \\ D_- &= \frac{1}{\sqrt{2\ell+1}}\left(i\sqrt{\ell+1}B_0 + \sqrt{\ell}A_3\right),\end{aligned} \tag{2.54}$$

with eigenvalues $\lambda_+ = \ell$ and $\lambda_- = -\ell - 1$. Notice from this result that the masses are integer numbers, even though from (2.53) we could have expected square roots in the spectrum. This is actually an indication that the spectrum can be obtained in a simpler way, namely only using Clebsch-Gordan coefficients as in [13].

This concludes the diagonalization of the 4×4 sub-block of the seven-dimensional flavor mixing matrix, which is relevant for the case where one ℓ_a is 0. We summarize the result in table 2. We have effectively rederived the spectrum of the bosons for the classical solution considered in [13] where only three of the scalar fields get non-trivial SO(3)-symmetric vevs. Our method is however different and can be extended to the present classical solution with $\mathrm{SO}(3) \times \mathrm{SO}(3)$ symmetry. In particular, we will find a natural generalization of the 2×2 matrix in (2.53).

Full mixing matrix. Let us now diagonalize the full seven-dimensional matrix (2.39) in the case where $\ell_1 \neq 0$ and $\ell_2 \neq 0$. Following the steps discussed for the 4×4 sub-block relevant for the case where one $\ell_a = 0$, we define fields $B^{(1)}$ and $B^{(2)}$ with total

JHEP01(2019)007

Mass eigenstate	Mass m^2	Multiplicity
$B^{(1)}_+$	$m^2_{(1),+} = \ell_1(\ell_1-1)+\ell_2(\ell_2+1)$	$(2\ell_1+3)(2\ell_2+1)$
$B^{(1)}_-$	$m^2_{(1),-} = (\ell_1+1)(\ell_1+2)+\ell_2(\ell_2+1)$	$(2\ell_1-1)(2\ell_2+1)$
$B^{(2)}_+$	$m^2_{(2),+} = \ell_1(\ell_1+1)+\ell_2(\ell_2-1)$	$(2\ell_1+1)(2\ell_2+3)$
$B^{(2)}_-$	$m^2_{(2),-} = \ell_1(\ell_1+1)+(\ell_2+1)(\ell_2+2)$	$(2\ell_1+1)(2\ell_2-1)$
D_0	$m^2_0 = \ell_1(\ell_1+1)+\ell_2(\ell_2+1)+2$	$(2\ell_1+1)(2\ell_2+1)$
D_+	$m^2_+ = \ell_1(\ell_1+1)+\ell_2(\ell_2+1)-2\lambda_+$	$(2\ell_1+1)(2\ell_2+1)$
D_-	$m^2_- = \ell_1(\ell_1+1)+\ell_2(\ell_2+1)-2\lambda_-$	$(2\ell_1+1)(2\ell_2+1)$

Table 3. Masses and eigenstates of the complicated bosons in the $k_1k_2 \times k_1k_2$ block in the SO(3) × SO(3)-symmetric case. One must consider all combinations of $\ell_1 = 1,\dots,k_1-1$ and $\ell_2 = 1,\dots,k_2-1$. The masses for the fields in the off-diagonal blocks are obtained by the replacements $\ell_1 \to \frac{k_1-1}{2}$ and $\ell_2 \to \frac{k_2-1}{2}$, while the corresponding multiplicities are obtained by the same replacement followed by a multiplication with $2(N-k_1k_2)$.

angular momentum in each sector. As before, they are given in terms of Clebsch-Gordan coefficients by

$$(B^{(1)})_{j_1,m_1,\ell_1;\ell_2,m_2} = \sum_{m_s=-1}^{+1} \langle \ell_1, m_1-m_s; 1, m_s | j_1, m_1\rangle \, (C^{(1)}_{m_s})_{\ell_1,m_1;\ell_2,m_2}, \tag{2.55}$$

$$(B^{(2)})_{\ell_1,m_1;j_2,m_2,\ell_2} = \sum_{m_s=-1}^{+1} \langle \ell_2, m_2-m_s; 1, m_s | j_2, m_2\rangle \, (C^{(2)}_{m_s})_{\ell_1,m_1;\ell_2,m_2}. \tag{2.56}$$

We can also write out the corresponding basis states explicitly:

$$(\hat{Y}^{(1)})_{j_1,m_1,\ell_1;\ell_2,m_2} \equiv \hat{Y}_{j_1,m_1;\ell_1} \otimes \hat{Y}^{m_2}_{\ell_2}, \quad (\hat{Y}^{(2)})_{\ell_1,m_1;j_2,m_2,\ell_2} \equiv \hat{Y}^{m_1}_{\ell_1} \otimes \hat{Y}_{j_2,m_2;\ell_2}. \tag{2.57}$$

Now using the natural generalization of the matrix elements in (2.52), one can see that the four fields $B^{(1)}_\pm$ and $B^{(2)}_\pm$ diagonalize the full 7×7 matrix (2.39). It remains to diagonalize a 3×3 matrix, which is a simple generalization of (2.53):

$$\Big((B^{(1)}_0)^\dagger \; (B^{(2)}_0)^\dagger \; (A_3)^\dagger\Big) \begin{pmatrix} -1 & 0 & -i\sqrt{\ell_1(\ell_1+1)} \\ 0 & -1 & -i\sqrt{\ell_2(\ell_2+1)} \\ +i\sqrt{\ell_1(\ell_1+1)} & +i\sqrt{\ell_2(\ell_2+1)} & 0 \end{pmatrix} \begin{pmatrix} B^{(1)}_0 \\ B^{(2)}_0 \\ A_3 \end{pmatrix}. \tag{2.58}$$

Here we have dropped the quantum numbers from the fields to unclutter the notation. This matrix has eigenvalues

$$\lambda_0 = -1, \quad \lambda_\pm = -\frac{1}{2} \pm \sqrt{\ell_1(\ell_1+1)+\ell_2(\ell_2+1)+\tfrac{1}{4}}, \tag{2.59}$$

and the corresponding diagonal fields are

$$\begin{aligned} D_0 &= \frac{1}{\sqrt{N_0}}\Big(-\sqrt{\ell_2(\ell_2+1)}B^{(1)}_0 + \sqrt{\ell_1(\ell_1+1)}B^{(2)}_0\Big), \\ D_\pm &= \frac{1}{\sqrt{N_\pm}}\Big(i\sqrt{\ell_1(\ell_1+1)}B^{(1)}_0 + i\sqrt{\ell_2(\ell_2+1)}B^{(2)}_0 + \lambda_\mp A_3\Big), \end{aligned} \tag{2.60}$$

JHEP01(2019)007

with

$$\begin{aligned} N_\pm &= \lambda_\mp(\lambda_\mp - \lambda_\pm) \\ &= \frac{1}{2}\left(1 + 4\ell_1(\ell_1+1) + 4\ell_2(\ell_2+1) \pm \sqrt{1 + 4\ell_1(\ell_1+1) + 4\ell_2(\ell_2+1)}\right), \\ N_0 &= -\lambda_+\lambda_- = \ell_1(\ell_1+1) + \ell_2(\ell_2+1). \end{aligned} \tag{2.61}$$

Since $\lambda_\pm$ contains a square root, it is clear that it is impossible to obtain the spectrum of masses using only a Clebsch-Gordan decomposition, but a more general procedure like the one we have presented is required.

2.3 Fermion mass matrix

Inserting the classical solution (2.4) into the mass term for the Majorana fermions (2.8), we find

$$S_{\mathrm{m,f}} = \frac{2}{g_{\mathrm{YM}}^2}\int \mathrm{d}^4x \left(\frac{-1}{2\,x_3}\right) \mathrm{tr}\left(\sum_{i=1}^{3} \bar\psi_j (G_i^{(1)})_{jk} L_i^{(1)} \psi_k + \sum_{i=1}^{3} \bar\psi_j (G_i^{(2)})_{jk} L_i^{(2)} (\gamma_5 \psi_k)\right), \tag{2.62}$$

where $G_i^{(1)} \equiv G_i$ and $G_i^{(2)} \equiv G_{i+3}$ for $i = 1, 2, 3$. Since $[G_i^{(1)}, G_j^{(2)}] = 0$ and $[L_i^{(1)}, L_j^{(2)}] = 0$, we can diagonalize both terms in (2.62) simultaneously. We give the form of the matrices $G_i^{(1)}$ and $G_i^{(2)}$ in appendix A using the same conventions as [13]. From [13], we also know that the matrices $G_i^{(1)}$ can be transformed into block-diagonal form with

$$U = \frac{1}{\sqrt{2}}\begin{pmatrix} 0 & -i & -1 & 0 \\ 0 & 1 & i & 0 \\ -1 & 0 & 0 & i \\ i & 0 & 0 & -1 \end{pmatrix} \quad \Rightarrow \quad U^\dagger G_i^{(1)} U = -\begin{pmatrix} \sigma_i & 0 \\ 0 & \sigma_i \end{pmatrix} = -\mathbb{1}_2 \otimes \sigma_i. \tag{2.63}$$

Here σ_i are the usual Pauli matrices. Acting with U on the remaining matrices $G_i^{(2)}$ gives

$$U^\dagger G_i^{(2)} U = i\,\sigma_i \otimes \mathbb{1}_2. \tag{2.64}$$

The extra factor of i is consistent with the fact that the matrices $G_i^{(2)}$ are anti-Hermitian and it is also required to make the term with γ_5 in (2.62) Hermitian. On the fermions, the transformation U yields

$$U^\dagger \begin{pmatrix} \psi_1 \\ \psi_2 \\ \psi_3 \\ \psi_4 \end{pmatrix} = \frac{1}{\sqrt{2}}\begin{pmatrix} -\psi_3 - i\psi_4 \\ i\psi_1 + \psi_2 \\ -\psi_1 - i\psi_2 \\ -i\psi_3 - \psi_4 \end{pmatrix} = \begin{pmatrix} C_{++} \\ C_{-+} \\ C_{+-} \\ C_{--} \end{pmatrix} \equiv C_F. \tag{2.65}$$

Here the subscripts on $C_{m_{s_1}, m_{s_2}}$ indicate that the field has spin $\frac{1}{2}$ and magnetic quantum number m_{s_1} with respect to $\frac{1}{2}\mathbb{1}_2 \otimes \sigma_3$, and spin $\frac{1}{2}$ and magnetic quantum number m_{s_2} with respect to $\frac{1}{2}\sigma_3 \otimes \mathbb{1}_2$. The fields also have orbital angular momentum ℓ_a and magnetic quantum number m_a with respect to $L^{(a)}$ for $a = 1, 2$. This problem is closely related to

JHEP01(2019)007

the one studied in [13], with the difference that here we have two copies of the spin-orbit coupling problem.

To diagonalize the mass matrix, we define the total angular momentum operators

$$J_i^{(1)} = L_i^{(1)} + \frac{1}{2}\mathbb{1}_2 \otimes \sigma_i, \quad J_i^{(2)} = L_i^{(2)} + \frac{1}{2}\sigma_i \otimes \mathbb{1}_2, \tag{2.66}$$

so the terms inside the trace in (2.62) take the form

$$-\bar{C}_F \left[(J^{(1)})^2 - (L^{(1)})^2 - \frac{1}{2}\left(\frac{1}{2}+1\right)\right] C_F + \bar{C}_F \left[(J^{(2)})^2 - (L^{(2)})^2 - \frac{1}{2}\left(\frac{1}{2}+1\right)\right] (i\gamma_5)\, C_F. \tag{2.67}$$

The notation $\bar{C}_F$ means the following: transpose the four-dimensional vector of fermions C_F as given in (2.65) and take the Dirac conjugate $\bar{\psi} \equiv \psi^\dagger \gamma^0$ of each fermion inside of it. The explicit formula for the diagonal fields in terms of the Clebsch-Gordan coefficients is given by

$$B^{j_1 j_2}_{\ell_1, m_{j_1}; \ell_2, m_{j_2}} = \sum_{\substack{m_{s_1}, m_1 \\ m_{s_2}, m_2}} \langle \ell_1, m_1; \tfrac{1}{2}, m_{s_1} | j_1, m_{j_1}\rangle \langle \ell_2, m_2; \tfrac{1}{2}, m_{s_2} | j_2, m_{j_2}\rangle (C_{m_{s_1}, m_{s_2}})_{\ell_1, m_1; \ell_2, m_2}, \tag{2.68}$$

where the total angular momentum is $j_a = \ell_a \pm \frac{1}{2}$. In total, there are four combinations from combining $j_1 = \ell_1 \pm \frac{1}{2}$ with $j_2 = \ell_2 \pm \frac{1}{2}$ in all possible ways, each with a multiplicity of $(2j_1+1)(2j_2+1)$. The eigenvalues of each term in (2.62) are

$$j(j+1) - \ell(\ell+1) - \frac{1}{2}\left(\frac{1}{2}+1\right) = \begin{cases} \ell & \text{for} \quad j = \ell + \frac{1}{2}, \\ -\ell - 1 & \text{for} \quad j = \ell - \frac{1}{2}. \end{cases} \tag{2.69}$$

After the diagonalization, the quadratic part of the action for the fermions takes the schematic form

$$S = \frac{2}{g_{\rm YM}^2} \int \mathrm{d}^4 x \sum_\alpha \mathrm{tr} \left[\frac{i}{2} \bar{B}_\alpha \gamma^\mu \partial_\mu B_\alpha - \frac{1}{2x_3} \bar{B}_\alpha \left(c_\alpha + i\, d_\alpha \gamma_5\right) B_\alpha \right]. \tag{2.70}$$

Here the index α is running over all the diagonal fields B. We will now use a chiral rotation to rewrite this action in a form where the mass term is positive and does not contain the $i\gamma_5$ part. Following the procedure described in [33], one finds that the required transformation is

$$B_\alpha = \cos\left(\tfrac{\theta}{2}\right) B'_\alpha - i \sin\left(\tfrac{\theta}{2}\right) \gamma_5 B'_\alpha, \qquad \theta \equiv \arg(c + id). \tag{2.71}$$

Notice that this transformation preserves the Majorana property, namely the fields B'_α are also Majorana fermions. Using this transformation, one can check that the resulting action has the form

$$S = \frac{2}{g_{\rm YM}^2} \int \mathrm{d}^4 x \sum_\alpha \mathrm{tr} \left[\frac{i}{2} \bar{B}'_\alpha \gamma^\mu \partial_\mu B'_\alpha - \frac{m_\alpha}{2x_3} \bar{B}'_\alpha B'_\alpha \right], \tag{2.72}$$

with $m_\alpha = |c_\alpha + i d_\alpha| = \sqrt{c_\alpha^2 + d_\alpha^2}$. We list the values of c_α, d_α and m_α along with their multiplicities in table 4.

JHEP01(2019)007

Mass eigenstate	c	d	Mass $m = \lvert c + id \rvert$	Multiplicity
$B^{\ell_1+\frac{1}{2},\ell_2+\frac{1}{2}}$	$-\ell_1$	ℓ_2	$m_{++} = \sqrt{\ell_1^2 + \ell_2^2}$	$(\ell_1+1)(\ell_2+1)$
$B^{\ell_1+\frac{1}{2},\ell_2-\frac{1}{2}}$	$-\ell_1$	$-\ell_2-1$	$m_{+-} = \sqrt{\ell_1^2 + (\ell_2+1)^2}$	$(\ell_1+1)\ell_2$
$B^{\ell_1-\frac{1}{2},\ell_2+\frac{1}{2}}$	ℓ_1+1	ℓ_2	$m_{-+} = \sqrt{(\ell_1+1)^2 + \ell_2^2}$	$\ell_1(\ell_2+1)$
$B^{\ell_1-\frac{1}{2},\ell_2-\frac{1}{2}}$	ℓ_1+1	$-\ell_2-1$	$m_{--} = \sqrt{(\ell_1+1)^2 + (\ell_2+1)^2}$	$\ell_1\ell_2$

Table 4. Eigenvalues and eigenstates of the fermions in the SO(3) × SO(3)-symmetric case in the $k_1k_2 \times k_1k_2$ block. One must consider all combinations of $\ell_1 = 0, \ldots, k_1-1$ and $\ell_2 = 0, \ldots, k_2-1$. For the definition of c and d, see (2.70). The values for c, d and m for the fields in the off-diagonal blocks are obtained by the replacements $\ell_1 \to \frac{k_1-1}{2}$ and $\ell_2 \to \frac{k_2-1}{2}$, while the corresponding multiplicities are obtained by the same replacement followed by a multiplication with $2(N - k_1k_2)$.

2.4 Summary of the spectrum

We have now derived the spectrum for the defect CFT with SO(3) × SO(3)-symmetric vevs. For the easy bosons (and the ghosts), we had to diagonalize the operator $(L^{(1)})^2 + (L^{(2)})^2$ which was achieved by expanding the fields in the $k_1k_2 \times k_1k_2$ block in fuzzy spherical harmonics. The fields in the off-diagonal blocks were already eigenstates of this operator. We list the masses and multiplicities of the easy bosons in table 1.

For the complicated bosons, the mass term reads

$$(L^{(1)})^2 + (L^{(2)})^2 - 2S \cdot L, \tag{2.73}$$

where the term $S \cdot L$ is responsible for mixing fields of different flavor. Knowing that $(L^{(1)})^2 + (L^{(2)})^2$ is diagonalized by an expansion in fuzzy spherical harmonics, we have subsequently obtained the eigenstates of $S \cdot L$ in two steps. Since we were coupling the spin-ℓ with the spin-one representation of $\mathfrak{su}(2)$, we had to distinguish between the case where either ℓ_1 or ℓ_2 were zero and the case where both ℓ_a were non-zero. The case $\ell_a = 0$ formally reduced the diagonalization problem to the one solved in [13], which we solved using a slightly different approach that was also applicable to the second case where both $\ell_1 \neq 0$ and $\ell_2 \neq 0$. For this case, we first diagonalized the 3×3 blocks $T_iL_i^{(1)}$ and $T_iL_i^{(2)}$ using angular momentum coupling. The eigenstates with $j_1 = \ell_1 \pm 1$ and $j_2 = \ell_2 \pm 1$ could trivially be padded with zeros to give eigenstates of the full matrix and their eigenvalues are given in (2.48). For the remaining eigenstates, we had to diagonalize the 3×3 matrix in (2.58) and found $D_\pm$ and D_0 in (2.60) with eigenvalues $\lambda_\pm$ and λ_0 in (2.59). Adding the contribution from $(L^{(1)})^2 + (L^{(2)})^2$, we obtain the masses shown in table 2 for the case where one of the ℓ_a is zero and in table 3 for the general case where $\ell_1 \neq 0$ and $\ell_2 \neq 0$. Note that we are only listing the masses and multiplicities for the fields $[\Phi]_{n,n'}$ in the $k_1k_2 \times k_1k_2$ block here. To obtain the masses and multiplicities of the fields in the off-diagonal block, we use the replacement rule (2.23). The multiplicity also receives an extra factor of $2(N - k_1k_2)$ from the size of the two blocks. Additionally there are $(N - k_1k_2) \times (N - k_1k_2)$ massless fields $[\Phi]_{a,a'}$.

JHEP01(2019)007

Finally, we found that the spectrum of the fermions could be obtained by simply employing the angular momentum techniques from [13] for each sector. The only additional step was the chiral rotation which allowed us to trade the term with $i\gamma_5$ in the action for a standard mass term. The fermion spectrum is shown in table 4.

Let us compare the spectrum for the defect CFT with SO(3) × SO(3)-symmetric vevs dual to the D3-D7 brane system derived here to the one for the defect CFT dual to the D3-D5 probe-brane system, where only three scalar fields get non-trivial SO(3)-symmetric vevs, derived in [13]. In the D3-D5 system, the spectrum can be derived using Clebsch-Gordan coefficients only, i.e. it is not necessary to employ the two-step process that we used to rederive it here. In the D3-D7 system however, Clebsch-Gordan coefficients are not sufficient as can be seen from the appearance of square roots in the mass eigenvalues. Furthermore, in the D3-D5 system, supersymmetry was visible in the spectrum. Defining $\nu = \sqrt{m^2 + \frac{1}{4}}$ for the bosons and comparing it with the mass $|m_f|$ of the fermions, one could see that the steps between these parameters were half-integers. This could be attributed to supersymmetry in AdS_4, where the conformal dimensions are given by $\Delta = \frac{3}{2} + \nu$ for the bosons and $\Delta = \frac{3}{2} + |m_f|$ for the fermions. The conformal dimensions within one supermultiplet however differ by $\frac{1}{2}$ which implies the observed relation between ν and $|m_f|$. In the present case, we can only relate three of the masses that appear in the spectrum of the bosons; namely, we find the relation

$$\nu_- = \sqrt{m_-^2 + \tfrac{1}{4}} = \nu_{\text{easy}} + 1, \quad \nu_+ = \sqrt{m_+^2 + \tfrac{1}{4}} = \nu_{\text{easy}} - 1. \tag{2.74}$$

This is consistent with the fact that supersymmetry is broken in the D3-D7 system.

3 Propagators

In this section, we take into account the effect that the x_3-dependence of the 'masses' has on the propagators of the scalars (subsection 3.1) and the fermions (subsection 3.2), following [13]. We then derive the propagators of the flavor eigenstates that occur in the action in terms of the propagators of the mass eigenstates. Thus, this section provides the framework for doing perturbative calculations in this defect CFT.

3.1 Scalar propagators

The propagator for a generic scalar field with mass term $\frac{m^2}{x_3^2}$ is the solution to

$$\left(-\partial_\mu \partial^\mu + \frac{m^2}{x_3^2}\right) K^{m^2}(x,y) = \frac{g_{\text{YM}}^2}{2}\,\delta(x-y). \tag{3.1}$$

As noted in [16], the propagator of a scalar with mass $\frac{m^2}{x_3^2}$ in $(d+1)$-dimensional Minkowski space is related to the propagator of a scalar with constant mass $\tilde{m}^2$ in AdS_{d+1}. The relation is explicitly given by

$$K^{m^2}(x,y) = \frac{g_{\text{YM}}^2}{2}(x_3 y_3)^{-\frac{d-1}{2}} K^{\tilde{m}^2}_{\text{AdS}}(x,y), \quad \tilde{m}^2 = m^2 - \frac{d^2-1}{4}. \tag{3.2}$$

JHEP01(2019)007

In our case, d is the dimension of the defect, i.e. $d = 3$. Using that $\tilde{m}^2 = \Delta(\Delta - d)$ in AdS_{d+1}, we find that the scaling dimension Δ is

$$\Delta = \frac{d}{2} + \nu, \quad \nu \equiv \sqrt{m^2 + \tfrac{1}{4}}. \tag{3.3}$$

A closed expression for the scalar propagator in AdS_{d+1} using Euclidean signature can be found e.g. in [34]:

$$K^{\Delta}_{\text{AdS}}(x,y) = \frac{\Gamma(\Delta)\,\xi(x,y)^{\Delta}}{2^{\Delta}(2\Delta - d)\pi^{d/2}\Gamma(\Delta - \frac{d}{2})}\, {}_2F_1\left(\tfrac{\Delta}{2}, \tfrac{\Delta+1}{2}; \Delta - \tfrac{d}{2} + 1; \xi^2(x,y)\right) \tag{3.4}$$

with

$$\xi(x,y) = \frac{2x_3 y_3}{x_3^2 + y_3^2 + (x_0 - y_0)^2 + (x_1 - y_1)^2 + (x_2 - y_2)^2}. \tag{3.5}$$

For the Feynman-diagram calculation, we will require the propagator evaluated at $x = y$. In this case, the propagator diverges (in the UV) and needs to be regularized. Our regularization of choice is dimensional regularization (or rather dimensional reduction, as we discuss below). Moreover, we want to keep the codimension of the defect at 1, such that its dimension becomes $d = 3 - 2\epsilon$. The expression (3.4) cannot be used in this case. Instead,

$$K^{\nu}(x,x) = \frac{g_{\text{YM}}^2}{2}\frac{1}{16\pi^2 x_3^2}\left[m^2\left(-\frac{1}{\epsilon} - \log(4\pi) + \gamma_{\text{E}} - 2\log(x_3) + 2\Psi(\nu + \tfrac{1}{2}) - 1\right) - 1\right], \tag{3.6}$$

which is derived from an integral representation of (3.4), see [13]. Above, γ_{E} denotes the Euler-Mascheroni constant and Ψ denotes the digamma function.

3.2 Fermionic propagators

After the chiral rotation, the action for the Majorana fermions takes the form

$$S = \frac{2}{g_{\text{YM}}^2}\int \mathrm{d}^4x\ \mathrm{tr}\left[\frac{i}{2}\bar{\psi}'\gamma^{\mu}\partial_{\mu}\psi' - \frac{m}{2x_3}\bar{\psi}'\psi'\right], \tag{3.7}$$

where the mass $m > 0$, cf. (2.72). The fermionic propagator is the solution to

$$\left(-i\gamma^{\mu}\partial_{\mu} + \frac{m}{x_3}\right) K_F^m(x,y) = \frac{g_{\text{YM}}^2}{2}\delta(x-y). \tag{3.8}$$

These propagators were derived in [13, 35],

$$K_F^m(x,y) = \left[i\gamma^{\mu}\partial_{\mu} + \frac{m}{x_3}\right]\left[K^{\nu=m-\frac{1}{2}}(x,y)\mathcal{P}_- + K^{\nu=m+\frac{1}{2}}(x,y)\mathcal{P}_+\right], \tag{3.9}$$

with $\mathcal{P}_{\pm} = \frac{1}{2}(1 \pm i\gamma^3)$ and $K^{\nu}(x,y)$ being the bosonic propagator.

The fermionic propagator will later be required in the calculation of the one-loop correction to the classical solution (section 4), where fermions can circulate in a loop. As

JHEP01(2019)007

all spinor indices have to be contracted in this case, we will be interested in the spinor trace of the propagator. Using (3.6), one can show that the trace of the fermionic propagator, regularized for $x = y$, is [13]

$$\operatorname{tr} K_F^m(x,x) = \frac{g_{\mathrm{YM}}^2}{8\pi^2 x_3^3}\Big[m^3 + m^2 - 3m - 1 + m(m^2-1)\left(-\frac{1}{\epsilon} - \log(4\pi) + \gamma_{\mathrm{E}} - 2\log(x_3) + 2\Psi(m) - 2\right)\Big]. \tag{3.10}$$

It will later be convenient to have an expression for the propagators between the fermion fields before the chiral rotation. Before the chiral rotation, the action takes the form (2.70),

$$S = \frac{2}{g_{\mathrm{YM}}^2}\int \mathrm{d}^4x\ \operatorname{tr}\left[\frac{i}{2}\bar\psi\gamma^\mu\partial_\mu\psi - \frac{1}{2x_3}\bar\psi(c+id\gamma_5)\psi\right]. \tag{3.11}$$

Here ψ could be any of the fields B_α, either in the $k_1k_2 \times k_1k_2$, the $(N-k_1k_2)\times k_1k_2$ or the $k_1k_2\times(N-k_1k_2)$ block. Since the mass m is related to the parameters c and d by $m = |c+id|$, the propagators between the original fields ψ and chirally rotated fields ψ' are

$$\langle\psi(x)\bar\psi(y)\rangle = \tilde K_F^{c,d}(x,y), \qquad \langle\psi'(x)\bar\psi'(y)\rangle = K_F^{m=|c+id|}(x,y). \tag{3.12}$$

Using the transformation (2.71), one can see that the relation between them is

$$\tilde K_F^{c,d} = \cos^2\left(\tfrac{\theta}{2}\right)K_F^{|c+id|} - \sin^2\left(\tfrac{\theta}{2}\right)\gamma_5 K_F^{|c+id|}\gamma_5 - \sin\left(\tfrac{\theta}{2}\right)\cos\left(\tfrac{\theta}{2}\right)\{\gamma_5, K_F^{|c+id|}\}, \tag{3.13}$$

where $\theta \equiv \arg(c+id)$. We will always be interested in the trace of this propagator, possibly multiplied by $i\gamma_5$. Using the explicit form of the fermionic propagator (3.9) and trigonometric identities, we find

$$\operatorname{tr}\tilde K_F^{c,d} = \frac{c}{|m|}\operatorname{tr}K_F^{m=|c+id|}, \qquad \operatorname{tr}\left(i\gamma_5\tilde K_F^{c,d}\right) = \frac{d}{|m|}\operatorname{tr}K_F^{m=|c+id|}. \tag{3.14}$$

3.3 Color and flavor part of the propagators

In sections 2.2 and 2.3 we have found the mass eigenstates of the theory, and the propagators between them can be obtained as described in sections 3.1 and 3.2. However, it will prove convenient to also derive the propagators between the fields that originally appeared in the action of $\mathcal{N}=4$ SYM theory, namely the six scalars, the gauge field, the Majorana fermions and the ghosts. The reason is that it would be extremely cumbersome to rewrite the interaction vertices (2.9) in terms of the diagonal fields. Note that we are still giving the propagators for the color components $[\Phi]_{n,a}$ and $[\Phi]_{a,n}$ defined in (2.15) as well as $\Phi_{\ell_1,m_1;\ell_2,m_2}$ defined in (2.24), which partially diagonalize the color part of the mixing problem.[5]

[5]Recall that the massless fields $[\Phi]_{a,a'}$ have ordinary propagators. The massless fields from the $k_1k_2\times k_1k_2$ block can only propagate for $x_3 > 0$ and appropriate boundary conditions have to be imposed at the defect for these fields. In the D3-D5 case, supersymmetry puts constraints on the possible choices of boundary conditions, cf. [36, 37], but in the present case we have no such guidelines. The choice of boundary conditions for these fields, however, will not affect the results in the large-N limit.

JHEP01(2019)007

To find these propagators, we express the original fields in terms of the diagonal fields. For example, for the bosons we have to undo the three steps of the diagonalization: the flavor transformation (2.36), the Clebsch-Gordan procedure (2.55) and the diagonalization of the final 3×3 matrix (2.60). The details of this calculation are shown in appendix B.

The mass term of the complicated bosons is diagonalized in terms of the fields $B_\pm^{(1)}$, $B_\pm^{(2)}$, D_0 and $D_\pm$. Thus the propagators between these fields are simply the scalar propagators $K^{m^2}(x,y)$ from section 3.1 with the corresponding mass eigenvalue from table 3. The eigenvalues $\lambda_\pm$ and normalization constants $N_\pm$ and N_0 were given in (2.59) and (2.61), but we repeat them here for convenience:

$$\lambda_\pm = -\frac{1}{2} \pm \sqrt{\ell_1(\ell_1+1) + \ell_2(\ell_2+1) + \tfrac{1}{4}},\ N_\pm = \lambda_\mp\left(\lambda_\mp - \lambda_\pm\right),\ N_0 = -\lambda_+\lambda_-. \tag{3.15}$$

For the matrix elements of the $\mathfrak{su}(2)$ generators t_i, we use the shorthand notation

$$[t_i^{(\ell_1)}]_{m_1,m_1'} \equiv [t_i^{2\ell_1+1}]_{\ell_1-m_1+1,\ell_1-m_1'+1}, \quad [t_i^{(\ell_2)}]_{m_2,m_2'} \equiv [t_i^{2\ell_2+1}]_{\ell_2-m_2+1,\ell_2-m_2'+1}. \tag{3.16}$$

Explicit expressions for the generators t_i are given in appendix A.2. The propagators involving easy fields are diagonal in flavor, and we find

$$\langle (A_0)_{\ell_1 m_1;\ell_2 m_2} (A_0)^\dagger_{\ell_1' m_1';\ell_2' m_2'} \rangle = \delta_{\ell_1\ell_1'}\delta_{\ell_2\ell_2'}\delta_{m_1,m_1'}\delta_{m_2,m_2'} \underbrace{K^{m^2=\ell_1(\ell_1+1)+\ell_2(\ell_2+1)}}_{\equiv K^{\text{easy}}}, \tag{3.17}$$

where one could replace A_0 with any of the other easy fields A_1, A_2 or c. For the propagators involving A_3 and scalars of different sectors, we find

$$\langle (\tilde\phi_i^{(1)})_{\ell_1 m_1;\ell_2 m_2} (\tilde\phi_j^{(2)})^\dagger_{\ell_1' m_1';\ell_2' m_2'} \rangle = \delta_{\ell_1\ell_1'}\delta_{\ell_2\ell_2'}[t_i^{(\ell_1)}]_{m_1,m_1'}[t_j^{(\ell_2)}]_{m_2,m_2'} \underbrace{\left(\frac{K^{m_-^2}}{N_-} + \frac{K^{m_+^2}}{N_+} - \frac{K^{m_0^2}}{N_0}\right)}_{\equiv K^\phi_{\text{opp}}}, \tag{3.18}$$

$$\begin{aligned}\langle (\tilde\phi_i^{(1)})_{\ell_1 m_1;\ell_2 m_2} (A_3)^\dagger_{\ell_1' m_1';\ell_2' m_2'} \rangle &= -\langle (A_3)_{\ell_1 m_1;\ell_2 m_2} (\tilde\phi_i^{(1)})^\dagger_{\ell_1' m_1';\ell_2' m_2'} \rangle \\ &= -i\delta_{\ell_1\ell_1'}\delta_{\ell_2\ell_2'}[t_i^{(\ell_1)}]_{m_1 m_1'}\delta_{m_2 m_2'} \underbrace{\left(\frac{\lambda_+}{N_-}K^{m_-^2} + \frac{\lambda_-}{N_+}K^{m_+^2}\right)}_{\equiv K^{\phi,A}},\end{aligned} \tag{3.19}$$

$$\langle (A_3)_{\ell_1 m_1;\ell_2 m_2} (A_3)^\dagger_{\ell_1' m_1';\ell_2' m_2'} \rangle = \delta_{\ell_1\ell_1'}\delta_{\ell_2\ell_2'}\delta_{m_1 m_1'}\delta_{m_2 m_2'} \underbrace{\left(\frac{\lambda_+^2}{N_-}K^{m_-^2} + \frac{\lambda_-^2}{N_+}K^{m_+^2}\right)}_{\equiv K^{A,A}}, \tag{3.20}$$

with $\tilde\phi_i^{(1)} \equiv \tilde\phi_i$ and $\tilde\phi_i^{(2)} \equiv \tilde\phi_{i+3}$. For the propagator between scalars from the same sector, we find

$$\begin{aligned}&\langle (\tilde\phi_i^{(1)})_{\ell_1 m_1;\ell_2 m_2} (\tilde\phi_j^{(1)})^\dagger_{\ell_1' m_1';\ell_2' m_2'} \rangle = \delta_{\ell_1\ell_1'}\delta_{\ell_2\ell_2'}\delta_{m_2 m_2'} \\ &\Bigg[\delta_{ij}\delta_{m_1 m_1'} \underbrace{\left(\frac{\ell_1+1}{2\ell_1+1}K^{m^2_{(1),+}} + \frac{\ell_1}{2\ell_1+1}K^{m^2_{(1),-}}\right)}_{\equiv K^{\phi,(1)}_{\text{sing}}} - i\epsilon_{ijk}[t_k^{(\ell_1)}]_{m_1,m_1'} \underbrace{\left(\frac{K^{m^2_{(1),+}}}{2\ell_1+1} - \frac{K^{m^2_{(1),-}}}{2\ell_1+1}\right)}_{\equiv K^{\phi,(1)}_{\text{anti}}} \\ &- [t_i^{(\ell_1)}t_j^{(\ell_1)}]_{m_1,m_1'} \underbrace{\left(\frac{K^{m^2_{(1),+}}}{(2\ell_1+1)(\ell_1+1)} + \frac{K^{m^2_{(1),-}}}{(2\ell_1+1)\ell_1} - \frac{\ell_2(\ell_2+1)}{\ell_1(\ell_1+1)}\frac{K^{m_0^2}}{N_0} - \frac{K^{m_-^2}}{N_-} - \frac{K^{m_+^2}}{N_+}\right)}_{\equiv K^{\phi,(1)}_{\text{sym}}}\Bigg].\end{aligned} \tag{3.21}$$

From (3.19) and (3.21), the propagators for the other sector are obtained by a simple relabeling, e.g.

$$\langle(\tilde{\phi}_i^{(2)})_{\ell_1 m_1;\ell_2 m_2}(\tilde{\phi}_j^{(2)})^\dagger_{\ell_1' m_1';\ell_2' m_2'}\rangle = \langle(\tilde{\phi}_i^{(1)})_{\ell_2 m_2;\ell_1 m_1}(\tilde{\phi}_j^{(1)})^\dagger_{\ell_2' m_2';\ell_1' m_1'}\rangle, \tag{3.22}$$

where the (implicit) dependence of the masses on ℓ_1 and ℓ_2 must be taken into account as well. In the following, we will often use the combination of spacetime propagators K^{easy}, K^{ϕ}_{opp}, $K^{\phi,A}$, $K^{A,A}$, $K^{\phi,(a)}_{\text{sing}}$, $K^{\phi,(a)}_{\text{anti}}$ and $K^{\phi,(a)}_{\text{sym}}$ defined in (3.17)–(3.21).[6]

Before the chiral rotation, the quadratic part of the action for the fermions is diagonalized by the fields $B^{\ell_1+\frac{1}{2},\ell_2+\frac{1}{2}}$, $B^{\ell_1+\frac{1}{2},\ell_2-\frac{1}{2}}$, $B^{\ell_1-\frac{1}{2},\ell_2+\frac{1}{2}}$ and $B^{\ell_1-\frac{1}{2},\ell_2-\frac{1}{2}}$. Written in terms of these fields, the action still contains γ_5. Therefore, the propagators between them are of the form $\tilde{K}_F^{c,d}$ in (3.13), where the eigenvalues c and d are given in table 4. In the calculations in this paper, the propagators always appear inside a spinor trace, possibly multiplied by γ_5, and they can be transformed to the propagators K_F^m by means of (3.14) which relates them to the propagators after the chiral rotation. Undoing the diagonalization of the fermion mass matrix, we find

$$\begin{aligned}
&\langle(\psi_i)_{\ell_1 m_1;\ell_2 m_2}(\overline{\psi_j})_{\ell_1' m_1';\ell_2' m_2'}\rangle = \frac{\delta_{\ell_1\ell_1'}\delta_{\ell_2\ell_2'}}{(2\ell_1+1)(2\ell_2+1)} \\
&\Big\{ + \delta_{ij}\delta_{m_1 m_1'}\delta_{m_2 m_2'}\Big[\ell_1\ell_2\ \tilde{K}_F^{\ell_1+1,-\ell_2-1} + \ell_1(\ell_2+1)\ \tilde{K}_F^{\ell_1+1,\ell_2} \\
&\quad + (\ell_1+1)\ell_2\ \tilde{K}_F^{-\ell_1,-\ell_2-1} + (\ell_1+1)(\ell_2+1)\ \tilde{K}_F^{-\ell_1,\ell_2}\Big] \\
&\quad - [G_n^{(1)}]_{ij}[t_n^{(\ell_1)}]_{m_1 m_1'}\delta_{m_2 m_2'}\Big[(\ell_2+1)\left(\tilde{K}_F^{-\ell_1,\ell_2} - \tilde{K}_F^{\ell_1+1,\ell_2}\right) \\
&\quad + \ell_2\left(\tilde{K}_F^{-\ell_1,-\ell_2-1} - \tilde{K}_F^{\ell_1+1,-\ell_2-1}\right)\Big] \\
&\quad - i[G_n^{(2)}]_{ij}[t_n^{(\ell_2)}]_{m_2 m_2'}\delta_{m_1 m_1'}\Big[(\ell_1+1)\left(\tilde{K}_F^{-\ell_1,\ell_2} - \tilde{K}_F^{-\ell_1,-\ell_2-1}\right) \\
&\quad + \ell_1\left(\tilde{K}_F^{\ell_1+1,\ell_2} - \tilde{K}_F^{\ell_1+1,-\ell_2-1}\right)\Big] \\
&\quad + i[G_{n_1}^{(1)}G_{n_2}^{(2)}]_{ij}[t_{n_1}^{(\ell_1)}]_{m_1 m_1'}[t_{n_2}^{(\ell_2)}]_{m_2 m_2'}\Big[\tilde{K}_F^{\ell_1+1,-\ell_2-1} - \tilde{K}_F^{\ell_1+1,\ell_2} - \tilde{K}_F^{-\ell_1,-\ell_2-1} + \tilde{K}_F^{-\ell_1,\ell_2}\Big]\Big\}.
\end{aligned} \tag{3.23}$$

The propagators given so far are valid for fields in the $k_1k_2 \times k_1k_2$ block, not the fields in the $(N-k_1k_2)\times k_1k_2$ and $k_1k_2\times(N-k_1k_2)$ blocks. As we argued in section 2.2.1, we can simply replace

$$\ell_1 \to \frac{k_1-1}{2} \quad \text{and} \quad \ell_2 \to \frac{k_2-1}{2} \tag{3.24}$$

everywhere to obtain the masses for the fields in the off-diagonal blocks. For the fields themselves, we replace $(\Phi)_{\ell_1 m_1;\ell_2 m_2} \to [\Phi]_{n,a}$. To obtain the corresponding mass eigenstates,

[6] The cases where either $\ell_1 = 0$ or $\ell_2 = 0$ required special treatment in the diagonalization of the boson mass matrix, see the discussion in section 2.2.2. In these cases, the spectrum reduces to the one in table 2, which was originally found in [13]. While the boson masses in table 3 do not have the correct limit for $\ell_1 = 0$ or $\ell_2 = 0$, the propagators presented in this section indeed reduce to the ones found in [13].

JHEP01(2019)007

we have to replace the matrices $\hat{Y}^{m_1}_{\ell_1} \otimes \hat{Y}^{m_2}_{\ell_2}$ by $E^n{}_a$, resulting in a replacements of the orthonormality condition (2.28) with (2.20) and similar changes in the non-diagonal matrix part. We find for the propagators between the easy fields,

$$\langle [A_0]_{n,a} [A_0]^\dagger_{n',a'} \rangle = \delta_{a,a'} \delta_{n,n'} K^{\text{easy}}, \tag{3.25}$$

where as above A_0 could be any of the easy fields A_0, A_1, A_2 and c. For the remaining propagators, we find

$$\langle [\tilde{\phi}^{(1)}_i]_{n,a} [\tilde{\phi}^{(2)}_j]^\dagger_{n',a'} \rangle = \delta_{a,a'} [t^{k_1}_i \otimes t^{k_2}_j]_{n,n'} K^{\phi}_{\text{opp}}, \tag{3.26}$$

$$\langle [\tilde{\phi}^{(1)}_i]_{n,a} [A_3]^\dagger_{n',a'} \rangle = -\langle [A_3]_{n,a} [\tilde{\phi}^{(1)}_i]^\dagger_{n',a'} \rangle = -i\delta_{a,a'} [t^{k_1}_i \otimes \mathbb{1}_{k_2}]_{n,n'} K^{\phi,A}, \tag{3.27}$$

$$\langle [A_3]_{n,a} [A_3]^\dagger_{n',a'} \rangle = \delta_{a,a'} \delta_{n,n'} K^{A,A} \tag{3.28}$$

and

$$\begin{aligned} \langle [\tilde{\phi}^{(1)}_i]_{n,a} [\tilde{\phi}^{(1)}_j]^\dagger_{n',a'} \rangle = \delta_{a,a'} \Big[& \delta_{ij} \delta_{n,n'} K^{\phi,(1)}_{\text{sing}} - i\epsilon_{ijk} [t^{k_1}_k \otimes \mathbb{1}_{k_2}]_{n,n'} K^{\phi,(1)}_{\text{anti}} \\ & - [t^{k_1}_i t^{k_1}_j \otimes \mathbb{1}_{k_2}]_{n,n'} K^{\phi,(1)}_{\text{sym}} \Big]. \end{aligned} \tag{3.29}$$

As above, we can simply obtain the expressions for the scalars from the other sectors from (3.27) and (3.29), e.g.

$$\langle [\tilde{\phi}^{(2)}_i]_{n,a} [A_3]^\dagger_{n',a'} \rangle = -i\delta_{a,a'} [\mathbb{1}_{k_1} \otimes t^{k_2}_i]_{n,n'} K^{\phi,A}. \tag{3.30}$$

Note that it is understood that the replacement rule (3.24) is applied everywhere, in particular also in K^{easy}, K^{ϕ}_{opp}, $K^{\phi,A}$, $K^{A,A}$, $K^{\phi,(1)}_{\text{sing}}$, $K^{\phi,(1)}_{\text{anti}}$, and $K^{\phi,(1)}_{\text{sym}}$ defined in (3.17)–(3.21). No new complications arise for the fermions in the off-diagonal block and it is straightforward to obtain the propagators between them from (3.23).

4 One-loop corrections to the classical solution

With the propagators at hand, we are now able to study many different quantities perturbatively. In this section, we start by calculating the first quantum correction to the classical solution, i.e. to the vevs of the scalars. While it is not observable itself, it occurs as a part of the calculation of many observables, including the one-loop corrections to one-point functions of scalar single-trace operators considered in the subsequent section. We find that the first quantum correction to the scalar vevs is non-vanishing, unlike in the D3-D5 system, where the vevs of the scalars were not corrected at one-loop order [13].

The one-loop vacuum expectation value of the scalars is [13]

$$\langle \phi_i \rangle_{\text{1-loop}}(x) = \overbrace{\tilde{\phi}_i(x) \int \mathrm{d}^4 y \sum_{\Phi_1,\Phi_2,\Phi_3} V_3(\Phi_1(y), \overbrace{\Phi_2(y), \Phi_3(y)}}^{}). \tag{4.1}$$

Here, the sum of all the contractions of cubic interactions occurs where one of the fields, which we call Φ_1, remains uncontracted. The field Φ_1 is then contracted with $\tilde{\phi}_i$ and the position of the interaction is integrated over to obtain $\langle \phi_i \rangle_{\text{1-loop}}$.[7]

[7] The only conceivable contribution of the defect fields at one-loop order is through a cubic defect vertex V_3. However, the defect fields Φ_2 and Φ_3 are massless in this case, resulting in a massless tadpole integral that vanishes due to conformal symmetry.

JHEP01(2019)007

The calculation of (4.1) requires the evaluation of propagators at the same spacetime points, i.e. $K^{\nu}(y,y)$ and $\operatorname{tr} K_F^m(y,y)$. This introduces divergences which we regularize using dimensional regularization, cf. (3.6) and (3.10). Dimensional regularization in $4-2\epsilon$ dimensions changes the number of components of the gauge field to $n_A = 4-2\epsilon$ while keeping the number of scalars and fermions fixed. This breaks supersymmetry and is therefore not a convenient regularization scheme for standard $\mathcal{N}=4$ theory; for instance, non-renormalization theorems due to supersymmetry are only applicable if supersymmetry is preserved by the regulator. Usually, supersymmetry can be restored in dimensional reduction by introducing additional 2ϵ scalars in the action [38, 39], which has been successfully applied in $\mathcal{N}=4$ theory (see e.g. [40, 41] and references therein).[8] In the defect theory, the regularization procedure must be chosen in a way that is compatible with the theory without the defect, i.e. with $\mathcal{N}=4$ SYM theory. The reason is that the entire UV behavior of the theory with defect is governed by the theory without the defect. One can see this by considering the scalar propagator (3.2) in the limit $x \to y$, where it reduces to the propagator for a scalar in $\mathcal{N}=4$ SYM theory in four dimensions. In the following, we will therefore work in a version of dimensional reduction where we introduce 2ϵ scalars behaving as the easy components of the gauge fields. We also note that dimensional reduction has been applied successfully in [13] for the D3-D5 system, where it was crucial for the one-loop correction to the vevs to vanish.

We will work in the planar limit, where $N \to \infty$ and $g_{\text{YM}} \to 0$, such that the 't Hooft coupling $\lambda = N g_{\text{YM}}^2$ remains fixed. The computation of $\langle \phi_i \rangle_{\text{1-loop}}$ is technically involved, so we present it in detail in appendix C, while here we will focus on the results. We find that the one-loop correction to the scalar vevs is

$$\begin{aligned}\langle \phi_i^{(a)} \rangle(x) &= \langle \phi_i^{(a)} \rangle_{\text{tree}}(x) + \langle \phi_i^{(a)} \rangle_{\text{1-loop}}(x) + \mathcal{O}(\lambda^2) \\ &= \left(1 + \frac{\lambda}{16\pi^2} W^{(a)}(k_1,k_2) + \mathcal{O}(\lambda^2)\right) \langle \phi_i^{(a)} \rangle_{\text{tree}}(x),\end{aligned} \tag{4.2}$$

for $a = 1, 2$. This result is valid for arbitrary $k_1, k_2 \geq 2$, and the functions $W^{(1)}(k_1,k_2)$ and $W^{(2)}(k_1,k_2)$ are

$$\begin{aligned}W^{(1)}(k_1,k_2) = &-\frac{1}{2}\left(3m_{\text{easy}}^2 - 4 + \frac{16}{k_1^2+k_2^2-2}\right)\Psi\left(\nu_{\text{easy}}+\tfrac{1}{2}\right) \\ &- \frac{(k_1-2)(k_1+3)}{2k_1(k_1-1)} m_{(1),-}^2 \Psi\left(\nu_{(1),-}+\tfrac{1}{2}\right) - \frac{(k_2-2)}{2k_2} m_{(2),-}^2 \Psi\left(\nu_{(2),-}+\tfrac{1}{2}\right) \\ &- \frac{(k_1+2)(k_1-3)}{2k_1(k_1+1)} m_{(1),+}^2 \Psi\left(\nu_{(1),+}+\tfrac{1}{2}\right) - \frac{(k_2+2)}{2k_2} m_{(2),+}^2 \Psi\left(\nu_{(2),+}+\tfrac{1}{2}\right) \\ &- \left(\frac{1}{2} + \frac{4}{k_1^2+k_2^2-2}\frac{(k_2^2-1)}{(k_1^2-1)}\right) m_0^2 \Psi\left(\nu_0+\tfrac{1}{2}\right) + \frac{1}{2} - \frac{8}{k_1^2+k_2^2-2} \\ &+ \frac{(k_1+1)(k_2-1)}{k_1 k_2}(m_{--}^2-1)\left(\Psi(m_{--}) + \frac{1}{2m_{--}}\right)\end{aligned}$$

[8] For sufficiently high loop orders, dimensional reduction is known to become inconsistent though [42–45].

JHEP01(2019)007

$$
\begin{aligned}
&+\frac{(k_1+1)(k_2+1)}{k_1k_2}(m_{-+}^2-1)\left(\Psi(m_{-+})+\frac{1}{2m_{-+}}\right)\\
&+\frac{(k_1-1)(k_2-1)}{k_1k_2}(m_{+-}^2-1)\left(\Psi(m_{+-})+\frac{1}{2m_{+-}}\right)\\
&+\frac{(k_1-1)(k_2+1)}{k_1k_2}(m_{++}^2-1)\left(\Psi(m_{++})+\frac{1}{2m_{++}}\right)
\end{aligned}
\tag{4.3}
$$

and

$$
W^{(2)}(k_1,k_2)=W^{(1)}(k_2,k_1). \tag{4.4}
$$

The masses and $\nu=\sqrt{m^2+\frac{1}{4}}$ are functions of k_1 and k_2 that are explicitly given in tables 1, 3 and 4, where in the latter two the replacement $\ell_a\to\frac{k_a-1}{2}$ is understood. While we have suppressed this dependence in (4.3), it is understood to be taken into account in (4.4). Note that we have used (2.74) to write $\Psi\left(\nu_-+\frac{1}{2}\right)$ and $\Psi\left(\nu_++\frac{1}{2}\right)$ in terms of $\Psi\left(\nu_{\text{easy}}+\frac{1}{2}\right)$.

On top of the planar limit, we can employ the double-scaling limit introduced in (1.3). We find

$$
\begin{aligned}
\left\langle\phi_i^{(1)}\right\rangle_{1-\text{loop}}(x)&\simeq-\frac{\lambda}{4\pi^2(k_1^2+k_2^2)}\frac{2k_2^4}{(k_1^2+k_2^2)^2}\left\langle\phi_i^{(1)}\right\rangle_{\text{tree}},\\
\left\langle\phi_i^{(2)}\right\rangle_{1-\text{loop}}(x)&\simeq-\frac{\lambda}{4\pi^2(k_1^2+k_2^2)}\frac{2k_1^4}{(k_1^2+k_2^2)^2}\left\langle\phi_i^{(2)}\right\rangle_{\text{tree}},
\end{aligned}
\tag{4.5}
$$

where $\simeq$ signifies that we are only keeping the leading powers in k_1 and k_2. Notice that the expansion yields a result that has the desired expansion in the double-scaling parameter $\frac{\lambda}{(k_1^2+k_2^2)}$.

Finally, let us note that the one-loop corrections to the vevs of all other fields are vanishing.

5 One-loop corrections to single-trace operators

In this section, we consider planar one-point functions of gauge-invariant bulk operators of the defect CFT. We start with general single-trace operators (subsection 5.1) following [13] and then specialize to the 1/2-BPS operator $\operatorname{tr} Z^L$ (subsection 5.2). In particular, we consider operators with well-defined scaling dimensions Δ, normalized such that in the theory without the defect the two-point functions are[9]

$$
\langle\mathcal{O}_a(x)\mathcal{O}_b(y)\rangle=\frac{\delta_{ab}}{|x-y|^{2\Delta_a}}. \tag{5.1}
$$

[9]The latter requirement is necessary for the one-point functions to be observable. In general, only $\langle\mathcal{O}\rangle/||\mathcal{O}||$ is observable, where the norm $||\mathcal{O}||$ is given by the two-point function far away from the defect.

JHEP01(2019)007

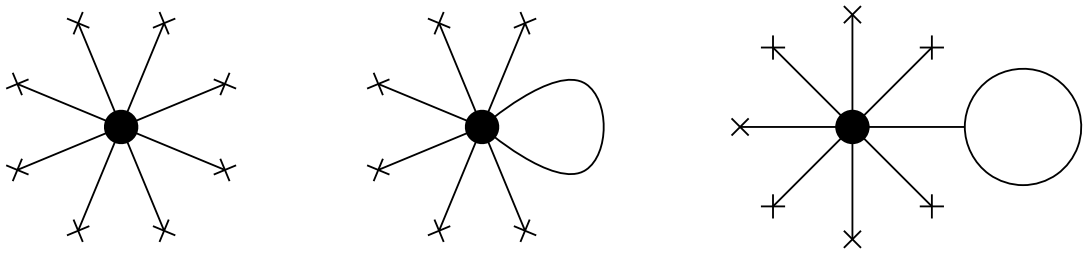

(a) Tree level (b) Tadpole (c) Lollipop

Figure 2. Diagrams that contribute at tree level (a) and one-loop order (b)-(c) to a single-trace operator such as $\langle \mathrm{tr}\, Z^L \rangle_{L=8}$ (in the planar limit). The black dot denotes the operator and the crosses signify the insertion of the classical solution.

On the grounds of conformal symmetry, we know that the one-loop one-point function of these operator in the defect CFT will be of the form

$$\langle \mathcal{O}_{\Delta(\lambda)}(x) \rangle = \frac{c}{x_3^{\Delta_0+\gamma}} = \frac{c}{x_3^{\Delta_0}} \Big(1 + \gamma \log x_3 + \dots \Big), \tag{5.2}$$

where Δ_0 is the bare and γ the anomalous conformal dimension of the operator.

5.1 General single-trace operators

We will consider a general single-trace operator built out of the scalars,

$$\mathcal{O}(x) = \mathcal{O}^{i_1 i_2 \dots i_L}\, \mathrm{tr}(\phi_{i_1} \phi_{i_2} \dots \phi_{i_L})(x), \tag{5.3}$$

which is required to have a well-defined scaling dimension. At leading order, this requires the operator $\mathcal{O}$ to be an eigenstate of the one-loop dilatation operator and hence the wave function $\mathcal{O}^{i_1 i_2 \dots i_L}$ to be a solution of the one-loop Bethe ansatz [46].

We can evaluate the one-point function of this operator at tree level by inserting the classical solution (2.4) for the fields ϕ_i:

$$\langle \mathcal{O} \rangle_{\mathrm{tree}}(x) = \mathcal{O}^{i_1 i_2 \dots i_L}\, \mathrm{tr}(\phi^{\mathrm{cl}}_{i_1} \phi^{\mathrm{cl}}_{i_2} \dots \phi^{\mathrm{cl}}_{i_L})(x). \tag{5.4}$$

At one-loop level, there are two diagrams that contribute to the one-point function, see figure 2. Following [12, 13], we will call them lollipop and tadpole diagram.

The lollipop diagram is one-particle reducible and describes the one-loop correction to the classical solution. Its contribution is obtained by considering all fields ϕ_i at their classical value ϕ_i^{cl}, except for the one at position i_j, which is replaced by its one-loop correction. We then sum for all possible values of $j = 1, \dots L$,

$$\langle \mathcal{O} \rangle_{\mathrm{lol}}(x) = \mathcal{O}^{i_1 i_2 \dots i_L} \sum_{j=1}^{L} \mathrm{tr}(\phi^{\mathrm{cl}}_{i_1} \dots \langle \phi_{i_j} \rangle_{\text{1-loop}} \dots \phi^{\mathrm{cl}}_{i_L})(x). \tag{5.5}$$

JHEP01(2019)007

For a particular $\mathcal{O}$, this diagram can be evaluated using the correction to the vevs (4.2) which we have calculated in the previous section.

The tadpole diagram is obtained by expanding the fields around the classical solution as $\phi_i = \phi_i^{\text{cl}} + \tilde{\phi}_i$, and keeping only the quadratic terms in the quantum part $\tilde{\phi}_i$. The two quantum fields in a particular term of this sum must be Wick contracted, and one obtains

$$\begin{aligned}\langle \mathcal{O} \rangle_{\text{tad}}(x) &= \sum_{j_1,j_2=1}^{L} \mathcal{O}^{i_1 \dots i_{j_1} \dots i_{j_2} \dots i_L} \operatorname{tr}(\phi_{i_1}^{\text{cl}} \dots \overbrace{\tilde{\phi}_{i_{j_1}} \dots \tilde{\phi}_{i_{j_2}}} \dots \phi_{i_L}^{\text{cl}})(x) \\ &= \sum_{j=1}^{L} \mathcal{O}^{i_1 \dots i_j i_{j+1} \dots i_L} \operatorname{tr}(\phi_{i_1}^{\text{cl}} \dots E^n{}_a E^a{}_{n'} \dots \phi_{i_L}^{\text{cl}}) \langle [\tilde{\phi}_{i_j}]_{n,a} [\tilde{\phi}_{i_{j+1}}]_{a,n'} \rangle .\end{aligned} \tag{5.6}$$

In the second line, we have used that in the large-N limit only contractions from neighboring fields contribute. Moreover, propagators between fields in the off-diagonal block scale like $N - k_1 k_2 \simeq N$, whereas propagators from the $k_1 k_2 \times k_1 k_2$ block would scale like $k_1 k_2 \ll N$, so we are only keeping the former. One can a priori calculate this diagram for any particular operator $\mathcal{O}$ by using the propagators in (3.26) and (3.29).

The one-point function of a general operator $\mathcal{O}$ can receive two additional corrections at one-loop order. If the contribution from the tadpole diagram in (5.6) is UV-divergent, the divergence has to be canceled by the renormalization constant $\mathcal{Z} = 1 + \mathcal{Z}_{\text{1-loop}} + \mathcal{O}(\lambda^2)$. At one-loop order, the corresponding correction to $\langle \mathcal{O} \rangle$ is

$$\langle \mathcal{O} \rangle_{\text{1-loop},\mathcal{Z}}(x) = \langle \mathcal{Z}_{\text{1-loop}} \mathcal{O} \rangle_{\text{tree}}(x). \tag{5.7}$$

The second additional correction to $\langle \mathcal{O} \rangle$ arises from the first quantum correction to the wave function $\mathcal{O}^{i_1 i_2 \dots i_L}$ of the operator. Since we are considering operators with well-defined conformal dimension at one-loop level, $\mathcal{O}^{i_1 i_2 \dots i_L}$ is already a one-loop eigenstate found by diagonalizing the one-loop dilatation operator. The first quantum correction therefore comes from the two-loop eigenstate $\mathcal{O}^{i_1 i_2 \dots i_L}_{\text{2-loop}}$,

$$\langle \mathcal{O} \rangle_{\text{1-loop},\mathcal{O}}(x) = \mathcal{O}^{i_1 i_2 \dots i_L}_{\text{2-loop}} \operatorname{tr}(\phi_{i_1}^{\text{cl}} \phi_{i_2}^{\text{cl}} \cdots \phi_{i_L}^{\text{cl}})(x). \tag{5.8}$$

Thus, the one-loop one-point function of a generic single-trace operator is

$$\langle \mathcal{O} \rangle_{\text{1-loop}}(x) = \langle \mathcal{O} \rangle_{\text{lol}}(x) + \langle \mathcal{O} \rangle_{\text{tad}}(x) + \langle \mathcal{O} \rangle_{\text{1-loop},\mathcal{Z}}(x) + \langle \mathcal{O} \rangle_{\text{1-loop},\mathcal{O}}(x). \tag{5.9}$$

Finally, we note that the planar one-point function of a multi-trace operator is given by the product of the one-point functions of its single-trace factors.

5.2 One-loop one-point function of $\operatorname{tr} Z^L$

We will now particularize the results from the previous subsection for the 1/2-BPS operator $\mathcal{O} = \operatorname{tr} Z^L$, where $Z = \phi_3 + i\phi_6$. The tree-level one-point function of $\operatorname{tr} Z^L$ is obtained by replacing all fields by their classical value:

$$\langle \operatorname{tr} Z^L \rangle_{\text{tree}} = \operatorname{tr}\left[(Z^{\text{cl}})^L \right] \simeq \frac{(-i)^L (k_1^2 + k_2^2)^{\frac{L}{2}+1} \sin\left[(L+2)\psi_0\right]}{2^L x_3^L (L+1)(L+2)}. \tag{5.10}$$

JHEP01(2019)007

This and other color traces have been collected in appendix D. In the above equation, we have defined the angle $\psi_0 = \arctan(k_1/k_2)$. Moreover, the symbol $\simeq$ is used here and in what follows to indicate that we are only keeping the leading-order term in the limit where k_1 and k_2 are large. The result vanishes unless L is even, so this will be implicitly assumed in the following discussion.

Now we proceed to study the one-point function of $\operatorname{tr} Z^L$ beyond tree level. Since the operator $\operatorname{tr} Z^L$ is 1/2-BPS, in the theory without the defect it is protected from quantum corrections; therefore, $\langle \mathcal{O} \rangle_{\text{1-loop},\mathcal{Z}}(x) = 0$ and $\langle \mathcal{O} \rangle_{\text{1-loop},\mathcal{O}}(x) = 0$. However, for the latter statement to be true, we must use a renormalization scheme that preserves the supersymmetry of the theory without the defect, and therefore it is required that we use dimensional reduction in our calculation. We conclude that if we use dimensional reduction, only the lollipop and tadpole diagrams contribute at one-loop order,

$$\langle \operatorname{tr} Z^L \rangle_{\text{lol}} = L \operatorname{tr}\left[(Z^{\text{cl}})^{L-1}\langle Z\rangle_{\text{1-loop}}\right], \quad \langle \operatorname{tr} Z^L \rangle_{\text{tad}} = L \operatorname{tr}\left[(Z^{\text{cl}})^{L-2}\overbrace{Z\,Z}\right]. \tag{5.11}$$

In the remainder of this section, we will evaluate these two diagrams.

To calculate the lollipop diagram, we use (5.11) and the one-loop correction to the vevs (4.5):

$$\begin{aligned}\langle \operatorname{tr} Z^L \rangle_{\text{lol}} &\simeq \frac{\lambda L}{2\pi^2 x_3 (k_1^2+k_2^2)^3}\Big(k_2^4 \operatorname{tr}\left[(Z^{\text{cl}})^{L-1}\, t_3^{k_1}\otimes \mathbb{1}_{k_2}\right] + i\, k_1^4 \operatorname{tr}\left[(Z^{\text{cl}})^{L-1}\,\mathbb{1}_{k_1}\otimes t_3^{k_2}\right]\Big) \\ &\simeq \frac{\lambda (-i)^L (k_1^2+k_2^2)^{\frac{L}{2}-3}}{2^{L+1}\pi^2 (L+1)(L+2) x_3^L}\Big(\left(k_2^2-k_1^2\right)\left(k_1^4+k_2^4+(k_1k_2)^2(L+2)\right)\sin(L\psi_0) \\ &\quad - k_1k_2(k_1^4+k_2^4) L\cos(L\psi_0)\Big).\end{aligned} \tag{5.12}$$

In the second line, we have used (D.7) in appendix D to compute the color traces.

Finally, the contribution from the tadpole diagram (5.11) is

$$\begin{aligned}\langle \operatorname{tr} Z^L \rangle_{\text{tad}} = NL\Bigg(&\operatorname{tr}\left[(Z^{\text{cl}})^{L-2}\mathbb{1}_{k_1}\otimes\left(t_3^{k_2}\right)^2\right] K_{\text{sym}}^{\phi,(2)} - \operatorname{tr}\left[(Z^{\text{cl}})^{L-2}\left(t_3^{k_1}\right)^2\otimes\mathbb{1}_{k_2}\right] K_{\text{sym}}^{\phi,(1)} \\ &+ \operatorname{tr}\left[(Z^{\text{cl}})^{L-2}\right]\left(K_{\text{sing}}^{\phi,(1)} - K_{\text{sing}}^{\phi,(2)}\right) + 2i \operatorname{tr}\left[(Z^{\text{cl}})^{L-2} t_3^{k_1}\otimes t_3^{k_2}\right] K_{\text{opp}}^{\phi}\Bigg),\end{aligned} \tag{5.13}$$

where we have used the propagators (3.18) and (3.21). We can expand this expression in the limit where k_1 and k_2 are large, which combined with the color traces in appendix D gives

$$\langle \operatorname{tr} Z^L \rangle_{\text{tad}} \simeq \frac{\lambda L (-i)^L (k_1^2+k_2^2)^{\frac{L}{2}-1}}{2^{L+2}\pi^2 (L-1)(L+2) x_3^L}\Big[2k_1k_2\cos(L\psi_0) - \left(k_1^2-k_2^2\right)\sin(L\psi_0)\Big]. \tag{5.14}$$

Notice that the tadpole diagram does not depend on the regulator ϵ from dimensional regularization. In fact, even though (5.14) is applicable only in the double-scaling limit, the regulator drops from the tadpole diagram even for finite k_1 and k_2. This is an important consistency check; since $\operatorname{tr} Z^L$ is a 1/2-BPS operator, it should not be renormalized, so we should not find any UV-divergences and the terms proportional to $\frac{1}{\epsilon}$ should cancel.

JHEP01(2019)007

We can combine the tree-level result (5.10), the lollipop diagram (5.12) and the tadpole diagram (5.14) to obtain

$$\frac{\langle \operatorname{tr} Z^L \rangle}{\langle \operatorname{tr} Z^L \rangle_{\text{tree}}} = 1 + \frac{\lambda}{4\pi^2 (L-1)\left(k_1^2+k_2^2\right)^3}\Bigg(4(k_1 k_2)^2 + (L^2+3L-2)\left(k_1^4+k_2^4\right) \\ + 2(L-1)(L+2)k_1 k_2 \left(k_1^2-k_2^2\right)\cot[(L+2)\psi_0]\Bigg) + \mathcal{O}\left(\frac{\lambda^2}{(k_1^2+k_2^2)^2}\right). \tag{5.15}$$

Note that the result has indeed an expansion in the parameter $\frac{\lambda}{(k_1^2+k_2^2)}$ as suggested by the string-theory dual of the defect CFT. Moreover, the result (5.15) precisely agrees with the supergravity prediction (1.4) quoted in the introduction![10]

6 Outlook

While the main result of the present paper is a highly non-trivial positive test of AdS/dCFT for a configuration where supersymmetry is completely broken, an important accompanying achievement is the establishment of a perturbative framework for the SO(3) × SO(3)-symmetric defect CFT involved. A crucial step of this achievement was of course the determination of the exact mass spectrum of the theory using fuzzy spherical harmonics, but an equally essential step was the rewriting of the resulting propagators of the theory in terms of generators of $\mathfrak{su}(2) \times \mathfrak{su}(2)$. Worth stressing is also the recognition that dimensional reduction constitutes an appropriate regularization scheme being compatible with the supersymmetry of the underlying bulk CFT which governs the UV behavior of the defect CFT. We have used our perturbative framework to calculate the one-loop correction to the classical solution in the planar limit and obtained an explicit result for the one-point function of $\operatorname{tr} Z^L$ in the double-scaling limit; in the future, it would be interesting to go to finite N (following [13, 47]), to obtain explicit results at finite k_1 and k_2 for $\operatorname{tr} Z^L$ and to go to higher loop orders. With the perturbative framework in place, the scene is also set for the calculation of quantum corrections to other quantities of interest in the defect CFT, such as other types of correlation functions or Wilson loops. In the case of the simpler D3-D5 probe-brane setup, the calculation of a simple Wilson line to one-loop order [48] confirmed the prediction of a classical string-theory calculation [16] consisting of evaluating the area of a minimal surface in the double-scaling limit (1.2). The circular Wilson loop of the D3-D5 defect CFT was analyzed in [49] and the case of two anti-parallel Wilson lines was considered in a search for a Gross-Ooguri transition in [50]. Finally, the calculation of two-point functions of the defect CFT allowed for data mining in $\mathcal{N} = 4$ SYM theory by means of the boundary conformal bootstrap equations [37]. A special class of two-point functions was considered in [51].

In the case of the defect CFT based on the D3-D5 probe-brane setup, where only three scalar fields get non-trivial SO(3) symmetric vevs, the one-point function problem showed

[10] To be precise, the supergravity prediction is for the unique SO(3) × SO(3)-symmetric chiral primary operator built from L scalar fields [21]; while this operator is not equal to $\operatorname{tr} Z^L$, $\operatorname{tr} Z^L$ has a non-vanishing projection on it (induced by the norm from the two-point function far away from the defect), such that the ratio of the one-point function and the tree-level one-point function of both operators coincide.

JHEP01(2019)007

very strong signs of integrability. Hence, it was possible to express the tree-level one-point function of any scalar operator in a closed formula valid for any value of the representation label k [11]. The formula could be extended to one-loop order in the SU(2) sub-sector and a conjecture for an all-loop asymptotic formula for this sub-sector was put forward as well [14], which extends the match with the supergravity prediction [15] for $\langle \mathrm{tr}\, Z^L \rangle$ in the double-scaling limit to all loop-orders smaller than L. The calculation of a tree-level one-point function can be formulated as the evaluation of the overlap between a Bethe state describing the operator in question and a so-called matrix product state [8], and the apparent integrability of the one-point function problem in the D3-D5 probe-brane set-up was suggested to be a consequence of the matrix product state being annihilated by all the odd charges of the integrable spin chain underlying the spectrum of $\mathcal{N} = 4$ SYM theory [52]. One can explicitly check that the matrix product state of relevance for the computation of one-point functions of the $\mathrm{SO}(3) \times \mathrm{SO}(3)$-symmetric defect CFT is *not* annihilated by the odd charges of the $\mathcal{N} = 4$ SYM spin chain [53]. In accordance with this, it has only been possible to derive results for tree-level one-point functions of non-protected operators on a case by case basis [53].

On the other hand, one can prove that the matrix product state of relevance for the computation of the one-point functions of the earlier mentioned SO(5)-symmetric defect CFT based on the non-supersymmetric D3-D7 probe-brane system with probe geometry $AdS_4 \times S^4$ is indeed annihilated by the odd charges of the $\mathcal{N} = 4$ SYM spin chain [11]. Although only a few exact tree-level results and in particular no closed formula exist so far [54], this observation indicates that setting up the perturbative program for the SO(5)-symmetric defect CFT could potentially be very rewarding. We have already taken the first step in this direction by explicitly determining the mass spectrum of the theory via a further generalization of the method of fuzzy spherical harmonics [30], and we hope to be able to report on the completion of the program in the near future.

Acknowledgments

We thank M. de Leeuw, A. C. Ipsen, G. Semenoff, K. E. Vardinghus and K. Zarembo for useful discussions. C.K. and M.W. were supported in part by FNU through grant number DFF-4002-00037. M.W. in addition was supported in part by an ERC Starting Grant (No. 757978) and a grant from the Villum Fonden.

A Conventions

In this appendix, we summarize our conventions for field-theory calculations (appendix A.1) and fuzzy spherical harmonics (appendix A.2).

A.1 Field-theory conventions

Throughout the paper, we choose the metric of Minkowski space to have mostly positive signature, i.e. $\eta^{\mu\nu} = \mathrm{diag}(-1, +1, \ldots, +1)$. We will work in (3+1) dimensions, and we will denote by $d = 3$ the dimension of the codimension-one defect. For the fermionic fields, we

JHEP01(2019)007

take the four-dimensional γ-matrices to be

$$\gamma^\mu = \begin{pmatrix} 0 & \sigma^\mu \\ \bar{\sigma}^\mu & 0 \end{pmatrix}, \quad \gamma^5 = i\gamma^0\gamma^1\gamma^2\gamma^3 = \begin{pmatrix} -\mathbb{1}_2 & 0 \\ 0 & \mathbb{1}_2 \end{pmatrix}, \tag{A.1}$$

with $\sigma^\mu = (\mathbb{1}_2, \sigma^i)$, $\bar{\sigma}^\mu = (\mathbb{1}_2, -\sigma^i)$ and $\{\gamma^\mu, \gamma^\nu\} = -2\eta^{\mu\nu}$.

For the four-dimensional matrices G^i that appear in the reduction of the spinors in ten dimensions to four dimensions, we use the same conventions as in [13]:

$$\begin{aligned} &G^1 \equiv G^{(1)}_1 = i\begin{pmatrix} 0 & -\sigma_3 \\ \sigma_3 & 0 \end{pmatrix}, \quad G^2 \equiv G^{(1)}_2 = i\begin{pmatrix} 0 & \sigma_1 \\ -\sigma_1 & 0 \end{pmatrix}, G^3 \equiv G^{(1)}_3 = \begin{pmatrix} \sigma_2 & 0 \\ 0 & \sigma_2 \end{pmatrix}, \\ &G^4 \equiv G^{(2)}_1 = i\begin{pmatrix} 0 & -\sigma_2 \\ -\sigma_2 & 0 \end{pmatrix}, G^5 \equiv G^{(2)}_2 = \begin{pmatrix} 0 & -\mathbb{1}_2 \\ \mathbb{1}_2 & 0 \end{pmatrix}, \quad G^6 \equiv G^{(2)}_3 = i\begin{pmatrix} \sigma_2 & 0 \\ 0 & -\sigma_2 \end{pmatrix}. \end{aligned} \tag{A.2}$$

The matrices in the first line are Hermitian, $(G^{(1)}_i)^\dagger = G^{(1)}_i$, while those in the second line are anti-Hermitian, $(G^{(2)}_i)^\dagger = -G^{(2)}_i$. Their (anti-)commutation relations are

$$\begin{aligned} \left\{G^{(1)}_i, G^{(1)}_j\right\} &= +2\delta_{ij}, & \left[G^{(1)}_i, G^{(1)}_j\right] &= -2i\epsilon_{ijk}G^{(1)}_k, \\ \left\{G^{(2)}_i, G^{(2)}_j\right\} &= -2\delta_{ij}, & \left[G^{(2)}_i, G^{(2)}_j\right] &= -2\epsilon_{ijk}G^{(2)}_k. \end{aligned} \tag{A.3}$$

The two sets commute, $\left[G^{(1)}_i, G^{(2)}_j\right] = 0$.

A.2 Lie algebra $\mathfrak{su}(2)$ and fuzzy spherical harmonics

For the vevs with SO(3) × SO(3) symmetry, we will need explicit expressions for the generators t_i of the corresponding Lie algebra as well as for the fuzzy spherical harmonics $\hat{Y}^m_\ell$ that serve as a basis for the fields in color space. Those are given here using the same conventions as [13].

The basis matrices $E^i{}_j$ are defined to have a 1 at position (i, j), i.e. $[E^i{}_j]_{m,n} = \delta_{i,m}\delta_{j,n}$. We use the same form of the k-dimensional matrices t_i of $\mathfrak{su}(2)$ that was used in [8], namely

$$t_+ = \sum_{n=1}^{k-1} c_{k,n} E^n{}_{n+1}, \quad t_- = \sum_{n=1}^{k-1} c_{k,n} E^{n+1}{}_n, \quad t_3 = \sum_{n=1}^{k} d_{k,n} E^n{}_n, \tag{A.4}$$

with the coefficients

$$c_{k,n} = \sqrt{n(k-n)}, \quad d_{k,n} = \frac{1}{2}(k - 2n + 1). \tag{A.5}$$

Defining also $t_1 = \frac{1}{2}(t_+ + t_-)$ and $t_2 = \frac{1}{2i}(t_+ - t_-)$, these matrices satisfy the commutation relations of $\mathfrak{su}(2)$,

$$[t_i, t_j] = i\epsilon_{ijk}t_k. \tag{A.6}$$

JHEP01(2019)007

The k-dimensional matrices t_i can be used to construct $\mathfrak{su}(2)$ representations $\hat{Y}_\ell^m$ of spin ℓ, for $\ell = 0, 1, \ldots, k-1$, cf. [55, 56]. The $k \times k$ matrices $\hat{Y}_\ell^m$ are essentially given by a symmetric and traceless polynomial of degree ℓ in the generators t_i,

$$\hat{Y}_\ell^m = 2^\ell \sqrt{\frac{(k-\ell-1)!}{(k+\ell)!}} \left(\frac{k^2-1}{4}\right)^{\ell/2} \sum_{i_1,\ldots,i_\ell} f^{\ell m}_{i_1,\ldots,i_\ell} \hat{x}_{i_1} \cdots \hat{x}_{i_\ell}, \quad \ell = 1, \ldots, k-1, \tag{A.7}$$

where the $\mathfrak{su}(2)$ generators have been rescaled to

$$\hat{x}_i = \sqrt{\frac{4}{k^2-1}} t_i \quad \Rightarrow \quad \sum_i \hat{x}_i \hat{x}_i = \mathbb{1}_k, \tag{A.8}$$

and the coefficients $f^{\ell m}_{i_1,\ldots,i_\ell}$ implement the symmetry and tracelessness conditions. Note that the last equation defines the fuzzy two-sphere with coordinates $\hat{x}_i$ and that the construction (A.7) stems from the observation that on a normal two-sphere a basis of functions can be constructed as a homogeneous polynomial in the Cartesian coordinates x_i, $i = 1, 2, 3$. These functions are the well-known spherical harmonics Y_ℓ^m.

We now give some properties of $\hat{Y}_\ell^m$ that are important for our purposes. With the normalization as above, they satisfy

$$\left(\hat{Y}_\ell^m\right)^\dagger = (-1)^m \hat{Y}_\ell^{-m} \quad \text{and} \quad \operatorname{tr}\left[\left(\hat{Y}_\ell^m\right)^\dagger \hat{Y}_{\ell'}^{m'}\right] = \delta_{\ell\ell'}\delta_{mm'}. \tag{A.9}$$

We also make use of the relation between the generators t_i and $\hat{Y}_\ell^m$ for $\ell = 1$, namely

$$t_1 = c\left(\hat{Y}_1^{-1} - \hat{Y}_1^1\right), \quad t_2 = ic\left(\hat{Y}_1^{-1} + \hat{Y}_1^1\right), \quad t_3 = c\sqrt{2}\hat{Y}_1^0 \tag{A.10}$$

with

$$c = \frac{(-1)^{k+1}}{2}\sqrt{\frac{k(k^2-1)}{6}}. \tag{A.11}$$

B Color and flavor part of the propagators

In this appendix, we derive the propagators between the fields that originally appeared in the action of $\mathcal{N} = 4$ SYM theory. We focus on the propagators involving the six scalars and the gauge field; the propagators involving the Majorana fermions can be obtained in a similar way. To obtain the propagators, we will express the original fields in terms of the fields in which the mass term of the action becomes diagonal. For example, for the complicated bosons with $\ell_1, \ell_2 \neq 0$, we have to undo the three steps of the diagonalization: the flavor transformation (2.36), the Clebsch-Gordan procedure (2.55) and the diagonalization of the final 3×3 matrix (2.60).

After the flavor transformation, $S \cdot L$ is in the form (2.39) and the transformed vector of complicated fields is

$$V^\dagger C = \begin{pmatrix} C^{(1)} \\ C^{(2)} \\ A_3 \end{pmatrix}, \tag{B.1}$$

JHEP01(2019)007

where $C^{(1)}$ and $C^{(2)}$ were given in (2.37). In the 3×3 blocks $T_iL_i^{(1)}$ and $T_iL_i^{(2)}$, we diagonalize using Clebsch-Gordan coefficients and obtain the eigenstates $(B^{(1)})_{j_1,m_1,\ell_1;\ell_2,m_2}$ and $(B^{(2)})_{\ell_1,m_1;j_2,m_2,\ell_2}$. The relation to the fields $C_\pm^{(a)}$ and $C_0^{(a)}$ with $a=1,2$ is

$$(C_\pm^{(a)})_{\ell m}=\sum_j\langle \ell,m;1,\pm1|j,m\pm1\rangle(B^{(a)})_{j,m\pm1;\ell},\ (C_0^{(a)})_{\ell m}=\sum_j\langle \ell,m;1,0|j,m\rangle(B^{(a)})_{j,m;\ell}. \tag{B.2}$$

For $j_1=\ell_1\pm1$ and $j_2=\ell_2\pm1$, these fields diagonalize $S\cdot L$ and it only remains to diagonalize the 3×3 matrix in (2.58). The fields $D_\pm$ and D_0 in which the mass term is diagonal were given in (2.60). Inverting this relation, we find

$$\begin{aligned}
B_0^{(1)}&=-\sqrt{\ell_2(\ell_2+1)}\,\frac{D_0}{\sqrt{N_0}}-i\sqrt{\ell_1(\ell_1+1)}\left(\frac{D_+}{\sqrt{N_+}}+\frac{D_-}{\sqrt{N_-}}\right),\\
B_0^{(2)}&=+\sqrt{\ell_1(\ell_1+1)}\,\frac{D_0}{\sqrt{N_0}}-i\sqrt{\ell_2(\ell_2+1)}\left(\frac{D_+}{\sqrt{N_+}}+\frac{D_-}{\sqrt{N_-}}\right),\\
A_3&=\frac{\lambda_-}{\sqrt{N_+}}D_++\frac{\lambda_+}{\sqrt{N_-}}D_-.
\end{aligned} \tag{B.3}$$

We begin with the propagators between scalars from different sectors and those involving A_3 using the notation described in section 3.3. They contain at most one $\mathfrak{su}(2)$ Clebsch-Gordan coefficient from each sector, which we can express as the matrix element of an $\mathfrak{su}(2)$ generator t_i. In particular, we do not yet encounter products of $\mathfrak{su}(2)$ generators unlike in the propagators for scalars from the same sector. For convenience, we define

$$[r_s^\ell]_{m,m'}\equiv\sqrt{\ell(\ell+1)}\langle\ell,m;1,s|\ell,m+s\rangle\delta_{m',m+s}, \tag{B.4}$$

for $s=-1,0,1$. One can check that $r_\pm=\mp t_\mp/\sqrt{2}$, $r_0=t_3$, $r_s^\dagger=r_{-s}$ and finally

$$[(r_s^\ell)^\dagger]_{m,m'}=\sqrt{\ell(\ell+1)}\langle\ell,m-s;1,s|\ell,m\rangle\delta_{m',m-s}. \tag{B.5}$$

Using this notation, it will be easier to keep track of factors $\pm1/\sqrt{2}$. The propagators involving A_3 are

$$\begin{aligned}
\langle(C_s^{(1)})_{\ell_1m_1;\ell_2m_2}(A_3)^\dagger_{\ell_1'm_1';\ell_2'm_2'}\rangle&=-i\delta_{\ell_1\ell_1'}\delta_{\ell_2\ell_2'}\delta_{m_2m_2'}[r_s^{\ell_1}]_{m_1,m_1'}\left(\frac{\lambda_+}{N_-}K^{m_-^2}+\frac{\lambda_-}{N_+}K^{m_+^2}\right),\\
\langle(A_3)_{\ell_1m_1;\ell_2m_2}(C_s^{(1)})^\dagger_{\ell_1'm_1';\ell_2'm_2'}\rangle&=i\delta_{\ell_1\ell_1'}\delta_{\ell_2\ell_2'}\delta_{m_2m_2'}[(r_s^{\ell_1})^\dagger]_{m_1,m_1'}\left(\frac{\lambda_+}{N_-}K^{m_-^2}+\frac{\lambda_-}{N_+}K^{m_+^2}\right),\\
\langle(A_3)_{\ell_1m_1;\ell_2m_2}(A_3)^\dagger_{\ell_1'm_1';\ell_2'm_2'}\rangle&=\delta_{\ell_1\ell_1'}\delta_{\ell_2\ell_2'}\delta_{m_1m_1'}\delta_{m_2m_2'}\left(\frac{\lambda_+^2}{N_-}K^{m_-^2}+\frac{\lambda_-^2}{N_+}K^{m_+^2}\right).
\end{aligned} \tag{B.6}$$

To obtain the same propagators for $C_s^{(2)}$, we simply relabel as in (3.22). For the propagators that mix the two blocks, we need

$$\begin{aligned}
\langle(B_0^{(1)})_{\ell_1m_1;\ell_2m_2}(B_0^{(2)})^\dagger_{\ell_1'm_1';\ell_2'm_2'}\rangle&=\delta_{\ell_1\ell_1'}\delta_{\ell_2\ell_2'}\delta_{m_1m_1'}\delta_{m_2m_2'}\\
&\quad\times\sqrt{\ell_1(\ell_1+1)}\sqrt{\ell_2(\ell_2+1)}\left(\frac{K^{m_-^2}}{N_-}+\frac{K^{m_+^2}}{N_+}-\frac{K^{m_0^2}}{N_0}\right),
\end{aligned} \tag{B.7}$$

JHEP01(2019)007

and we obtain

$$\langle (C_s^{(1)})_{\ell_1 m_1;\ell_2 m_2} (C_{s'}^{(2)})^\dagger_{\ell_1' m_1';\ell_2' m_2'} \rangle = \delta_{\ell_1 \ell_1'} \delta_{\ell_2 \ell_2'} [r_s^{\ell_1}]_{m_1,m_1'} [(r_{s'}^{\ell_2})^\dagger]_{m_2,m_2'} \times \left(\frac{K^{m_-^2}}{N_-} + \frac{K^{m_+^2}}{N_+} - \frac{K^{m_0^2}}{N_0} \right). \tag{B.8}$$

Converting to the fields ϕ_i is a matter of undoing the flavor transformation,

$$\langle (\tilde{\phi}_i^{(1)})_{\ell_1 m_1;\ell_2 m_2} (\tilde{\phi}_j^{(2)})^\dagger_{\ell_1' m_1';\ell_2' m_2'} \rangle = \delta_{\ell_1 \ell_1'} \delta_{\ell_2 \ell_2'} [t_i^{(\ell_1)}]_{m_1,m_1'} [t_j^{(\ell_2)}]_{m_2,m_2'} \left(\frac{K^{m_-^2}}{N_-} + \frac{K^{m_+^2}}{N_+} - \frac{K^{m_0^2}}{N_0} \right), \tag{B.9}$$

$$\begin{aligned} \langle (\tilde{\phi}_i^{(1)})_{\ell_1 m_1;\ell_2 m_2} (A_3)^\dagger_{\ell_1' m_1';\ell_2' m_2'} \rangle &= -\langle (A_3)_{\ell_1 m_1;\ell_2 m_2} (\tilde{\phi}_i^{(1)})^\dagger_{\ell_1' m_1';\ell_2' m_2'} \rangle \\ &= -i \delta_{\ell_1 \ell_1'} \delta_{\ell_2 \ell_2'} [t_i^{(\ell_1)}]_{m_1 m_1'} \delta_{m_2 m_2'} \left(\frac{\lambda_+}{N_-} K^{m_-^2} + \frac{\lambda_-}{N_+} K^{m_+^2} \right), \end{aligned} \tag{B.10}$$

with $\tilde{\phi}_i^{(1)} \equiv \tilde{\phi}_i$ and $\tilde{\phi}_i^{(2)} \equiv \tilde{\phi}_{i+3}$. We obtain the analogue of the last equation for the second sector by relabeling as in (3.22).

As anticipated, the propagators between scalars from the same sector contain products of Clebsch-Gordan coefficients and are therefore more involved. For simplicity let us focus on one sector, say the first one for concreteness. We define the combination $K^0_{(1)}$ as

$$\langle (B_0^{(1)})_{\ell_1 m_1;\ell_2 m_2} (B_0^{(1)})^\dagger_{\ell_1' m_1';\ell_2' m_2'} \rangle = \delta_{\ell_1 \ell_1'} \delta_{\ell_2 \ell_2'} \delta_{m_1 m_1'} \delta_{m_2 m_2'} \times \underbrace{\left[\frac{\ell_2(\ell_2+1)}{N_0} K^{m_0^2} + \ell_1(\ell_1+1) \left(\frac{K^{m_-^2}}{N_-} + \frac{K^{m_+^2}}{N_+} \right) \right]}_{\equiv K^0_{(1)}}. \tag{B.11}$$

The propagators with $C_0^{(1)}$ are

$$\begin{aligned} &\langle (C_\pm^{(1)})_{\ell_1 m_1;\ell_2 m_2} (C_0^{(1)})^\dagger_{\ell_1' m_1';\ell_2' m_2'} \rangle = \delta_{\ell_1 \ell_1'} \delta_{\ell_2 \ell_2'} \frac{[t_\mp^{(\ell_1)}]_{m_1,m_1'}}{\sqrt{2}} \delta_{m_2 m_2'} \\ &\times \left(- \frac{\ell_1 \mp m_1 - 1}{(2\ell_1+1)\ell_1} K^{m^2_{(1),-}} + \frac{\ell_1 \pm m_1 + 2}{(2\ell_1+1)(\ell_1+1)} K^{m^2_{(1),+}} + \frac{\mp m_1 - 1}{\ell_1(\ell_1+1)} K^0_{(1)} \right), \\ &\langle (C_0^{(1)})_{\ell_1 m_1;\ell_2 m_2} (C_0^{(1)})^\dagger_{\ell_1' m_1';\ell_2' m_2'} \rangle = \delta_{\ell_1 \ell_1'} \delta_{\ell_2 \ell_2'} \delta_{m_1 m_1'} \delta_{m_2 m_2'} \\ &\times \left(\frac{(\ell_1 - m_1 + 1)(\ell_1 + m_1 + 1)}{(2\ell_1+1)(\ell_1+1)} K^{m^2_{(1),+}} + \frac{(\ell_1 - m_1)(\ell_1 + m_1)}{(2\ell_1+1)\ell_1} K^{m^2_{(1),-}} + \frac{m_1^2}{\ell_1(\ell_1+1)} K^0_{(1)} \right). \end{aligned} \tag{B.12}$$

JHEP01(2019)007

The propagators between $C_{\pm}^{(1)}$ are

$$\begin{aligned}
\langle (C_{\pm}^{(1)})_{\ell_1 m_1;\ell_2 m_2} (C_{\pm}^{(1)})_{\ell_1' m_1';\ell_2' m_2'} \rangle &= \frac{1}{2}\delta_{\ell_1\ell_1'}\delta_{\ell_2\ell_2'}\delta_{m_2 m_2'}\left[\frac{[t_{\mp}^{(\ell_1)} t_{\pm}^{(\ell_1)}]_{m_1,m_1'}}{\ell_1(\ell_1+1)} K^0_{(1)}\right. \\
&\left. + \delta_{m_1 m_1'}\left(\frac{(\ell_1 \mp m_1)(\ell_1 \mp m_1 - 1)}{(2\ell_1+1)\ell_1} K^{m^2_{(1),-}} + \frac{(\ell_1 \pm m_1 + 1)(\ell_1 \pm m_1 + 2)}{(2\ell_1+1)(\ell_1+1)} K^{m^2_{(1),+}}\right)\right], \\
\langle (C_{\pm}^{(1)})_{\ell_1 m_1;\ell_2 m_2} (C_{\mp}^{(1)})_{\ell_1' m_1';\ell_2' m_2'} \rangle &= \frac{1}{2}\delta_{\ell_1\ell_1'}\delta_{\ell_2\ell_2'}[t_{\mp}^{(\ell_1)} t_{\mp}^{(\ell_1)}]_{m_1,m_1'}\delta_{m_2 m_2'} \\
&\times \left(\frac{K^{m^2_{(1),-}}}{(2\ell_1+1)\ell_1} - \frac{K^{m^2_{(1),0}}}{\ell_1(\ell_1+1)} + \frac{K^{m^2_{(1),+}}}{(2\ell_1+1)(\ell_1+1)}\right).
\end{aligned} \tag{B.13}$$

Undoing the flavor transformation and inserting $K^0_{(1)}$ from (B.11), we find that the propagator between two scalars from the same sector is

$$\begin{aligned}
&\langle (\tilde{\phi}_i^{(1)})_{\ell_1 m_1;\ell_2 m_2} (\tilde{\phi}_j^{(1)})^{\dagger}_{\ell_1' m_1';\ell_2' m_2'} \rangle = \delta_{\ell_1\ell_1'}\delta_{\ell_2\ell_2'}\delta_{m_2 m_2'} \\
&\left[\delta_{ij}\delta_{m_1 m_1'}\left(\frac{\ell_1+1}{2\ell_1+1} K^{m^2_{(1),+}} + \frac{\ell_1}{2\ell_1+1} K^{m^2_{(1),-}}\right) - i\epsilon_{ijk}[t_k^{(\ell_1)}]_{m_1,m_1'}\left(\frac{K^{m^2_{(1),+}}}{2\ell_1+1} - \frac{K^{m^2_{(1),-}}}{2\ell_1+1}\right)\right. \\
&\left. - [t_i^{(\ell_1)} t_j^{(\ell_1)}]_{m_1,m_1'}\left(\frac{K^{m^2_{(1),+}}}{(2\ell_1+1)(\ell_1+1)} + \frac{K^{m^2_{(1),-}}}{(2\ell_1+1)\ell_1} - \frac{\ell_2(\ell_2+1)}{\ell_1(\ell_1+1)}\frac{K^{m_0^2}}{N_0} - \frac{K^{m_-^2}}{N_-} - \frac{K^{m_+^2}}{N_+}\right)\right],
\end{aligned} \tag{B.14}$$

with an analogous expression for the other sector obtained by relabeling as in (3.22). We note that the terms with δ_{ij} and ϵ_{ijk} are the same as in [13] and that the last one would vanish in the setup of that reference.

C One-loop correction to the scalar vacuum expectation values

In this appendix, we present in detail the calculation of the correction to the scalar vevs summarized in section 4. We split the calculation in three parts: we obtain the effective vertex V_{eff} in section C.1, the contraction of the vertex with the external field is computed in section C.2 and finally the remaining spacetime integral is performed in section C.3.

C.1 Calculation of the effective vertex

To compute the one-loop correction to the vevs of the scalars, we will need to know the effective one-particle vertex defined by

$$V_{\text{eff}}(y) \equiv \sum_{\Phi_1,\Phi_2,\Phi_3} V_3(\Phi_1(y), \overbrace{\Phi_2(y), \Phi_3(y)}), \tag{C.1}$$

where the sum is carried over all inequivalent contractions of cubic vertices in (2.9). We will start by calculating all the contractions assuming the limit $N \to \infty$, but keeping k_1 and k_2 finite. We will continue to use equal signs in equations where the large-N limit has been used. Then we will collect all contributions, and show that the regulator ϵ drops out.

JHEP01(2019)007

The calculation of the contractions proceeds identically to [13], but the propagators are different in the two setups. In this section, capital Latin indices I, J, K will run from 1 to 6, whereas lowercase Latin indices i, j, k will run from 1 to 3. We will perform dimensional reduction at the end of the calculation, so in the intermediate results we will explicitly keep the dependence on the number of fields of each species. All contractions come with a factor $\frac{2}{g_{\rm YM}^2}$, which we will include at the end when we add all the contributions.

Since we are working in the large-N limit, all propagators will involve only fields in the off-diagonal block. When we write a general propagator $K^{\cdots}$, it will be the one defined in section 3.3, but with the replacement $\ell_i \to (k_i - 1)/2$ implicitly understood.

Simple contractions. All the contractions in this paragraph can be immediately obtained from [13] by adapting the notation. The ghost contractions are

$$V_{\rm G} \equiv -\operatorname{tr}\left(\overbrace{\bar{c}[\phi_I^{\rm cl}, [\tilde{\phi}_I, c]}]\right) = -n_c \frac{2N}{y_3} K^{\rm easy} \operatorname{tr}\left(\tilde{\phi}_I t_I\right), \tag{C.2}$$

$$\operatorname{tr}\left(i(\partial_\mu \overbrace{\bar{c}})[A^\mu, c]]\right) = 0. \tag{C.3}$$

All the contributions from the vertex that couples three gauge fields vanish due to the symmetry of the propagator,

$$\operatorname{tr}\left(i[A^\mu, \overbrace{A^\nu]\partial_\mu A_\nu}\right) = \operatorname{tr}\left(i[\overbrace{A^\mu, A^\nu]\partial_\mu A_\nu}\right) = \operatorname{tr}\left(i[\overbrace{A^\mu, A^\nu]\partial_\mu A_\nu}\right) = 0. \tag{C.4}$$

Finally, we consider the vertex $\operatorname{tr}\left(i[A^\mu, \tilde{\phi}_I]\partial_\mu \tilde{\phi}_I\right)$. The first two contractions give

$$\operatorname{tr}\left(i[A^\mu, \overbrace{\tilde{\phi}_I]\partial_\mu \tilde{\phi}_I}\right) = 0, \tag{C.5}$$

and

$$V_1 \equiv \operatorname{tr}\left(i[\overbrace{A^\mu, \tilde{\phi}_I]\partial_\mu \tilde{\phi}_I}\right) = +2N \left(\partial_3 K^{A,\phi}\right) \operatorname{tr}\left(\tilde{\phi}_I\, t_I\right). \tag{C.6}$$

Note that in the last equation we have carried out an integration by parts to move the derivative from the field to the propagator. This is allowed because the effective vertex will always be contracted with a scalar $\tilde{\phi}_i$ and then integrated, as in (4.1). For the last contraction, note that we can use (D.21) from [13], because as in that case, we have $K^{\phi,A} \propto K^{\nu-1} - K^{\nu+1}$. Thus, we find

$$V_2 \equiv \operatorname{tr}\left(i[\overbrace{A^\mu, \tilde{\phi}_I]\partial_\mu \tilde{\phi}_I}\right) = +N \left(\partial_3 K^{\phi,A}\right) \operatorname{tr}\left(\tilde{\phi}_I t_I\right). \tag{C.7}$$

Interaction of three scalars. We can rewrite the interaction vertex involving three scalars as

$$\operatorname{tr}\left([\phi_I^{\rm cl}, \tilde{\phi}_J][\tilde{\phi}_I, \tilde{\phi}_J]\right) = \operatorname{tr}\left(\tilde{\phi}_I[\tilde{\phi}_J, [\phi_I^{\rm cl}, \tilde{\phi}_J]]\right). \tag{C.8}$$

JHEP01(2019)007

There are three inequivalent contractions:

$$V_3 \equiv \mathrm{tr}\left(\tilde{\phi}_I[\overbrace{\tilde{\phi}_J,[\phi_I^{\mathrm{cl}},\tilde{\phi}_J}]]\right) = \frac{2N}{y_3}\left(n_{\phi,(1)}K^{\phi,(1)}_{\mathrm{sing}} - \frac{k_1^2-1}{4}K^{\phi,(1)}_{\mathrm{sym}}\right)\mathrm{tr}\left(\tilde{\phi}_I t_I\right) + (1\leftrightarrow 2), \tag{C.9}$$

$$\begin{aligned} V_4 \equiv \mathrm{tr}\left(\tilde{\phi}_I[\overbrace{\tilde{\phi}_J,[\phi_I^{\mathrm{cl}},\tilde{\phi}_J}]]\right) = \frac{2N}{y_3}\Bigg[&- K^{\phi,(1)}_{\mathrm{sing}} - \frac{n_{\phi,(1)}-1}{2}\left(K^{\phi,(1)}_{\mathrm{anti}} + K^{\phi,(1)}_{\mathrm{sym}}\right) \\ &+ \frac{k_1^2-1}{4}K^{\phi,(1)}_{\mathrm{sym}} - \frac{k_2^2-1}{4}K^{\phi}_{\mathrm{opp}}\Bigg]\mathrm{tr}\left(\tilde{\phi}_i^{(1)}t_i^{(1)}\right) + (1\leftrightarrow 2), \end{aligned} \tag{C.10}$$

and

$$V_5 \equiv \mathrm{tr}\left(\tilde{\phi}_I[\overbrace{\tilde{\phi}_J,[\phi_I^{\mathrm{cl}},\tilde{\phi}_J}]]\right) = -\frac{N}{y_3}(n_{\phi,(1)}-1)\left(2K^{\phi,(1)}_{\mathrm{anti}} + K^{\phi,(1)}_{\mathrm{sym}}\right)\mathrm{tr}\left(\tilde{\phi}_i^{(1)}t_i^{(1)}\right) + (1\leftrightarrow 2). \tag{C.11}$$

Interaction of one scalar with two gauge fields. Next we rewrite the interaction between one scalar and two gauge fields as

$$\mathrm{tr}\left([A^\mu,\phi_I^{\mathrm{cl}}][A_\mu,\tilde{\phi}_I]\right) = \mathrm{tr}\left(\tilde{\phi}_I[A^\mu,[\phi_I^{\mathrm{cl}},A_\mu]]\right). \tag{C.12}$$

For $\mu = 0,1,2 \equiv i$, there is only one possible contraction:

$$V_6 \equiv \mathrm{tr}\left(\tilde{\phi}_I[\overbrace{A^i,[\phi_I^{\mathrm{cl}},A_i}]]\right) = n_{A,\mathrm{easy}}\frac{2N}{y_3}K^{\mathrm{easy}}\,\mathrm{tr}\left(\tilde{\phi}_I t_I\right). \tag{C.13}$$

In this contraction the chosen regularization procedure becomes relevant, because in $d = 3-2\epsilon$ space dimensions $n_{\mathrm{A,easy}} = 3-2\epsilon$. We are working in dimensional reduction [38, 39] and should therefore add 2ϵ scalars to the action that behave exactly as the easy components of the gauge field. Thus, we should also consider the contraction

$$V_7 \equiv \mathrm{tr}\left(\tilde{\phi}_I[\overbrace{A^{2\epsilon},[\phi_I^{\mathrm{cl}},A_{2\epsilon}}]]\right) = 2\epsilon\frac{2N}{y_3}K^{\mathrm{easy}}\,\mathrm{tr}\left(\tilde{\phi}_I t_I\right). \tag{C.14}$$

Adding the previous two equations, we find $n_{\mathrm{A,easy}} + 2\epsilon = 3$ as a prefactor. Since $n_{\mathrm{A,easy}}$ only appears in this vertex, we can effectively say that in dimensional reduction $n_{\mathrm{A,easy}} = 3$ exactly.

For $\mu = 3$, there are three possible contractions. The first one gives

$$V_8 \equiv \mathrm{tr}\left(\tilde{\phi}_I[\overbrace{A^3,[\phi_I^{\mathrm{cl}},A_3}]]\right) = \frac{2N}{y_3}K^{A,A}\,\mathrm{tr}\left(\tilde{\phi}_I t_I\right), \tag{C.15}$$

while the other two do not contribute to the effective vertex:

$$\mathrm{tr}\left(\overbrace{\tilde{\phi}_I[A^3,[\phi_I^{\mathrm{cl}},A_3}]]\right) = \mathrm{tr}\left(\tilde{\phi}_I[\overbrace{A^3,[\phi_I^{\mathrm{cl}},A_3}]]\right) = 0. \tag{C.16}$$

JHEP01(2019)007

Fermions in the loop. The action contains three cubic vertices including fermions. The first one is

$$V_{\mathrm{F},1} = \frac{1}{2}\sum_{i=1}^{3} \mathrm{tr}\left(\overbrace{\bar{\psi}_j G^i_{jk}[\tilde{\phi}_i, \psi_k]}\right) = N n_\psi \,\mathrm{tr}\left(t_i^{(1)}\tilde{\phi}_i^{(1)}\right)\mathrm{tr}\,\tilde{K}_F^{(1)}, \tag{C.17}$$

the second vertex gives a similar result,

$$V_{\mathrm{F},2} = \frac{1}{2}\sum_{i=4}^{6} \mathrm{tr}\left(\overbrace{\bar{\psi}_j G^i_{jk}[\tilde{\phi}_i, \gamma_5\psi_k]}\right) = -N n_\psi \,\mathrm{tr}\left(t_i^{(2)}\tilde{\phi}_i^{(2)}\right)\mathrm{tr}\left(i\gamma_5\tilde{K}_F^{(2)}\right), \tag{C.18}$$

and the last contraction vanishes,

$$\frac{1}{2}\,\mathrm{tr}\left(\overbrace{\bar{\psi}_j\gamma^\mu[A_\mu, \psi_j]}\right) = 0. \tag{C.19}$$

It is important to remember that when the fermion propagators are being regulated one has to use (3.14) and (3.10). The combinations of propagators (C.17) and (C.18) are

$$\begin{aligned}
\tilde{K}_F^{(1)} &= \frac{1}{(2\ell_1+1)(2\ell_2+1)}\left[(\ell_2+1)\left(\tilde{K}_F^{-\ell_1,\ell_2} - \tilde{K}_F^{\ell_1+1,\ell_2}\right) + \ell_2\left(\tilde{K}_F^{-\ell_1,-\ell_2-1} - \tilde{K}_F^{\ell_1+1,-\ell_2-1}\right)\right],\\
\tilde{K}_F^{(2)} &= \frac{1}{(2\ell_1+1)(2\ell_2+1)}\left[(\ell_1+1)\left(\tilde{K}_F^{-\ell_1,\ell_2} - \tilde{K}_F^{-\ell_1,-\ell_2-1}\right) + \ell_1\left(\tilde{K}_F^{\ell_1+1,\ell_2} - \tilde{K}_F^{\ell_1+1,-\ell_2-1}\right)\right],
\end{aligned} \tag{C.20}$$

and the replacement (2.23) is understood.

Summing up all vertices. The full effective vertex is the sum of all the contractions calculated in the previous subsection. We also have to remember to restore the overall prefactor of $\frac{2}{g^2_{\mathrm{YM}}}$ of the action, i.e.

$$V_{\mathrm{eff}} = \frac{2}{g^2_{\mathrm{YM}}}\left(V_{\mathrm{G}} + V_1 + V_2 + V_3 + V_4 + V_5 + V_6 + V_7 + V_8 + V_{\mathrm{F},1} + V_{\mathrm{F},2}\right). \tag{C.21}$$

Inserting the expressions from the previous paragraphs, we see that the vertex contains a part that depends on the regulator terms $f_\epsilon(y) = -\frac{1}{\epsilon} - \log(4\pi) + \gamma_{\mathrm{E}} - 2\log(y_3) - 1$ and a part that is finite as $\epsilon \to 0$,

$$V_{\mathrm{eff}} = V_{\mathrm{eff},\epsilon} + V_{\mathrm{eff,fin}}. \tag{C.22}$$

The ϵ-dependent part is

$$\begin{aligned}
V_{\mathrm{eff},\epsilon}(y; k_1, k_2) = \frac{-N}{32\pi^2 y_3^3} f_\epsilon(y)\Big[&(k_1^2+k_2^2)(n_{\mathrm{c}} + 2n_\psi - n_{\phi,(1)} - n_{\phi,(2)} - n_{\mathrm{A,easy}})\\
&- 2(n_{\mathrm{c}} + 2n_\psi + 5n_{\phi,(1)} - n_{\phi,(2)} - n_{\mathrm{A,easy}} - 18)\Big]\,\mathrm{tr}\left(\tilde{\phi}_i^{(1)} t_i^{(1)}\right) + (1 \leftrightarrow 2).
\end{aligned} \tag{C.23}$$

This is zero for $n_{\mathrm{A,easy}} = 3, n_{\mathrm{c}} = 1, n_\psi = 4$ and $n_{\phi,(1)} = n_{\phi,(2)} = 3$. Note that here we are using that we can keep $n_{\mathrm{A,easy}} = 3$ in dimensional reduction, cf. the discussion after (C.13). The finite part is

$$V_{\mathrm{eff,fin}}(y; k_1, k_2) = \frac{-N}{2\pi^2 y_3^3}\left(W^{(1)}(k_1,k_2)\,\mathrm{tr}\left(\tilde{\phi}_i^{(1)} t_i^{(1)}\right) + W^{(2)}(k_1,k_2)\,\mathrm{tr}\left(\tilde{\phi}_i^{(2)} t_i^{(2)}\right)\right), \tag{C.24}$$

where the functions $W^{(1)}(k_1,k_2)$ and $W^{(2)}(k_1,k_2)$ are given in (4.3) and (4.4) in the main text. This result is exact, i.e. we have not expanded for large k_1 and k_2.

JHEP01(2019)007

C.2 Contraction of the stick

Now we proceed to contract the external field with the effective vertex. The traces $\mathrm{tr}(\tilde{\phi}_j^{(b)} t_j^{(b)})$ with $b = 1, 2$ coming from the effective vertex will be contracted with an external field $\tilde{\phi}_i^{(a)}$. For simplicity, let us consider the case where we are contracting fields from the first sector, i.e. the case $a = b = 1$. Notice that $t_j^{(1)}$ is a matrix in the $k_1 k_2 \times k_1 k_2$ block padded with zeros. Thus, when we multiply it with $\tilde{\phi}_j^{(1)}$ only the $k_1 k_2 \times k_1 k_2$ block survives when taking the trace. Expanding $\tilde{\phi}_i^{(1)}$ and $\tilde{\phi}_j^{(1)}$ in this block in terms of fuzzy spherical harmonics and their Hermitian conjugates, we obtain

$$\begin{aligned} \overbrace{\tilde{\phi}_i^{(1)} \,\mathrm{tr}(\tilde{\phi}_j^{(1)} t_j^{(1)})} = \Big\langle (\tilde{\phi}_i^{(1)})_{\ell_1,m_1;\ell_2,m_2} (\tilde{\phi}_j^{(1)})^\dagger_{\ell_1',m_1';\ell_2',m_2'} \Big\rangle \\ \hat{Y}^{m_1}_{\ell_1} \otimes \hat{Y}^{m_2}_{\ell_2} \,\mathrm{tr}\left[\left(\hat{Y}^{m_1'}_{\ell_1'} \otimes \hat{Y}^{m_2'}_{\ell_2'} \right)^\dagger \left(t_j^{k_1} \otimes \mathbb{1}_{k_2} \right) \right]. \end{aligned} \tag{C.25}$$

In the previous expression, the trace can be simplified further. We start by expanding the matrices t_i and $\mathbb{1}$ in terms of the fuzzy spherical harmonics $\hat{Y}_\ell^m$ as

$$t_i^{k_1} = \sum_{m_1=\pm 1,0} (c_i)_{m_1} \hat{Y}^{m_1}_{\ell_1=1}, \quad \mathbb{1}_{k_2} = (-1)^{k_2+1} \sqrt{k_2}\, \hat{Y}^{m_2=0}_{\ell_2=0}. \tag{C.26}$$

The explicit coefficients $(c_i)_{m_1}$ can be obtained from (A.10) and (A.11) in appendix A.2. Using that the $\hat{Y}_\ell^m$ are traceless for $\ell > 0$ and proportional to the identity for $\ell = 0$, we obtain

$$\begin{aligned} \mathrm{tr}\left[\left(\hat{Y}^{m_1'}_{\ell_1'} \otimes \hat{Y}^{m_2'}_{\ell_2'} \right)^\dagger (t_j^{k_1} \otimes \mathbb{1}_{k_2}) \right] &= \mathrm{tr}\left[\left(\hat{Y}^{m_1'}_{\ell_1'} \right)^\dagger t_j^{k_1} \right] \mathrm{tr}\left[\left(\hat{Y}^{m_2'}_{\ell_2'} \right)^\dagger \right] \\ &= (-1)^{k_2+1} \sqrt{k_2}\, \delta_{\ell_1',1}\, \delta_{\ell_2',0}\, \delta_{m_2',0}\, (c_j)_{m_1'}. \end{aligned} \tag{C.27}$$

Inserting this into (C.25), we find that the propagator between the scalars has to be evaluated for $\ell_2 = \ell_2' = m_2 = m_2' = 0$ and $\ell_1 = \ell_1' = 1$. The explicit form of the propagator is

$$\begin{aligned} \langle (\tilde{\phi}_i)_{1,m_1} (\tilde{\phi}_j)^\dagger_{1,m_1'} \rangle = \delta_{ij} \delta_{m_1,m_1'} \left(\tfrac{2}{3} K^{m^2=0} + \tfrac{1}{3} K^{m^2=6} \right) \\ - \tfrac{i}{3} \epsilon_{ijk} [t_k^{k_1=3}]_{2-m_1,2-m_1'} \left(K^{m^2=0} - K^{m^2=6} \right). \end{aligned} \tag{C.28}$$

Combining this propagator with the explicit form of c_j^m and the 3×3 matrices $t_i^{k_1=3}$, we obtain

$$\overbrace{\tilde{\phi}_i^{(1)} \,\mathrm{tr}(\tilde{\phi}_j^{(1)} t_j^{(1)})} = (t_i^{k_1} \otimes \mathbb{1}_{k_2}) K^{m^2=6}, \quad \overbrace{\tilde{\phi}_i^{(2)} \,\mathrm{tr}(\tilde{\phi}_j^{(2)} t_j^{(2)})} = (\mathbb{1}_{k_1} \otimes t_i^{k_2}) K^{m^2=6}. \tag{C.29}$$

The contractions where the external field and the one inside the trace are from different sectors vanish,

$$\overbrace{\tilde{\phi}_i^{(1)} \,\mathrm{tr}(\tilde{\phi}_j^{(2)} t_j^{(2)})} = \overbrace{\tilde{\phi}_i^{(2)} \,\mathrm{tr}(\tilde{\phi}_j^{(1)} t_j^{(1)})} = 0. \tag{C.30}$$

The contraction of the easy components A_0, A_1 and A_2 of the gauge field with the vertex vanishes because the propagator between them and the scalars is zero. Furthermore, we find

$$\overbrace{A_3 \,\mathrm{tr}(\tilde{\phi}_j^{(1)} t_j^{(1)})} = \overbrace{A_3 \,\mathrm{tr}(\tilde{\phi}_j^{(2)} t_j^{(2)})} = 0. \tag{C.31}$$

This shows that only the vevs of the scalars receive one-loop corrections.

JHEP01(2019)007

C.3 Spacetime integral

In order to evaluate the correction to the scalar vevs (4.1), we are only missing the calculation of the integral over y. The propagator in the integral has mass $m^2 = 6$, or equivalently $\nu = \frac{5}{2}$, and it can be expressed in terms of elementary functions,

$$\begin{aligned} K^{\nu=\frac{5}{2}}(x,y) &= \frac{g_{\rm YM}^2}{2}\frac{\xi(x,y)^4}{10\pi^2 x_3 y_3}\,{}_2F_1\left(2,\tfrac{5}{2};\tfrac{7}{2};\xi(x,y)^2\right) \\ &= \frac{g_{\rm YM}^2}{2}\frac{1}{4\pi^2 x_3 y_3}\left(\frac{2\xi^2-3}{\xi^2-1} - \frac{3\,\mathrm{arctanh}(\xi)}{\xi}\right). \end{aligned} \tag{C.32}$$

In the second equality, we have dropped the explicit dependence of ξ on x and y to simplify the notation. In the integral, this propagator will be multiplied by a factor of $1/(y_3)^3$ that comes from the effective vertex. Thus, the integral is

$$\begin{aligned} \int \mathrm{d}^4 y \frac{1}{y_3^3} K^{\nu=\frac{5}{2}}(x,y) &= \frac{g_{\rm YM}^2}{2}\frac{1}{4\pi^2}\int_0^\infty \mathrm{d}y_3 \int_0^\infty \mathrm{d}r \int \mathrm{d}\Omega\, \frac{r^2}{x_3 y_3^4}\left(\frac{2\xi^2-3}{\xi^2-1} - \frac{3\,\mathrm{arctanh}(\xi)}{\xi}\right) \\ &= \frac{g_{\rm YM}^2}{2}\frac{1}{5}\int_0^\infty \mathrm{d}y_3 \begin{cases} (x_3)^{-2} & \text{for } 0 \le y_3 < x_3 \\ (x_3)^3 (y_3)^{-5} & \text{for } 0 \le x_3 < y_3 \end{cases} = \frac{g_{\rm YM}^2}{2}\frac{1}{4x_3}, \end{aligned} \tag{C.33}$$

where we have used spherical coordinates defined by $r^2 = (x_0-y_0)^2 + (x_1-y_1)^2 + (x_2-y_2)^2$ and we are working in Euclidean signature as anticipated when we discussed the spacetime part of the scalar propagator.

One can combine the effective vertex (C.24), the contractions (C.29) and the spacetime integral (C.33) to obtain the correction to the vevs given in (4.2) of the main text.

D Color traces

For the calculation of $\langle \mathrm{tr}\, Z^L \rangle$ to one-loop order in section 5.2, we need expressions for the color traces. More precisely, we need to calculate traces where $(Z^{\rm cl})^L$ is multiplied with a number of $\mathfrak{su}(2)$ generators t_i from each sector.

It was shown in [13] that

$$\mathrm{tr}\left[(t_3^k)^L\right] = (-1)^{L+1}\frac{2}{L+1}B_{L+1}\left(\tfrac{1-k}{2}\right) = \frac{k^{L+1}}{2^L(L+1)} + \mathcal{O}(k^L), \tag{D.1}$$

for L even while $\mathrm{tr}\left[(t_3^k)^L\right] = 0$ for L odd. Here $B_{L+1}(k)$ denotes the Bernoulli polynomial of degree $L+1$. In this paper, the most general trace that we will evaluate is

$$\mathrm{tr}\left[(Z^{\rm cl})^L \left(t_3^{k_1}\right)^{n_1} \otimes \left(t_3^{k_2}\right)^{n_2}\right] = \frac{(-1)^L}{x_3^L}\sum_{n=0}^{L}\binom{L}{n} i^{L-n}\,\mathrm{tr}\left[\left(t_3^{k_1}\right)^{n+n_1}\right]\mathrm{tr}\left[\left(t_3^{k_2}\right)^{L+n_2-n}\right]. \tag{D.2}$$

A particular term in this sum will not vanish if $n+n_1$ is even and $L+n_2-n$ is even. In order for the entire sum not to vanish we need that n_1 and $L+n_2$ have the same parity, or

JHEP01(2019)007

equivalently, we need that n_1 and $L+n_2$ are both even or both odd. In either case, only half of the terms in the sum will contribute to the result.

When n_1 is even and $L+n_2$ is even, only the terms with n even contribute. Thus, we must sum over a new variable m such that $n=2m$ and $m=0,\ldots,\lfloor\frac{L}{2}\rfloor$. If we expand for large k_1 and k_2, we obtain

$$\frac{(-1)^L}{2^{L+n_1+n_2}x_3^L}\sum_{m=0}^{\lfloor\frac{L}{2}\rfloor}\binom{L}{2m}i^{L-2m}\frac{k_1^{2m+n_1+1}}{(2m+n_1+1)}\frac{k_2^{L+n_2-2m+1}}{(L+n_2-2m+1)}+\mathcal{O}(k^{L+n_1+n_2+1}). \quad \text{(D.3)}$$

Here $\mathcal{O}(k^\ell)$ stands for terms where the combined powers of k_1 and k_2 are less than or equal to ℓ.

When n_1 is odd and $L+n_2$ is odd, only the terms with n odd contribute. Thus, we must sum over a new variable m such that $n=2m+1$ and $m=0,\ldots,\lfloor\frac{L-1}{2}\rfloor$. If we expand for large k_1 and k_2, we obtain

$$\frac{(-1)^L}{2^{L+n_1+n_2}x_3^L}\sum_{m=0}^{\lfloor\frac{L-1}{2}\rfloor}\binom{L}{2m+1}i^{L-2m-1}\frac{k_1^{2m+n_1+2}}{(2m+n_1+2)}\frac{k_2^{L+n_2-2m}}{(L+n_2-2m)}+\mathcal{O}(k^{L+n_1+n_2+2}). \quad \text{(D.4)}$$

The above sums can be carried out explicitly for particular values of n_1 and n_2. In all cases of interest for us, the traces will vanish for L odd, so we will assume that L is even in the rest of this section. It will also be convenient to express the results in terms of the angle

$$\psi_0\equiv\arctan\left(\frac{k_1}{k_2}\right). \quad \text{(D.5)}$$

In the following results, the symbol $\simeq$ means that the right-hand side only contains the leading-order term in k_1 and k_2. The trace for $n_1=0$ and $n_2=0$ is

$$\mathrm{tr}\left[\left(Z^{\mathrm{cl}}\right)^L\right]\simeq\frac{(-i)^L(k_1^2+k_2^2)^{\frac{L}{2}+1}\sin\left[(L+2)\psi_0\right]}{2^Lx_3^L(L+1)(L+2)}. \quad \text{(D.6)}$$

When $(n_1,n_2)=(1,0)$ or $(n_1,n_2)=(0,1)$, we find

$$\begin{aligned}\mathrm{tr}\left[\left(Z^{\mathrm{cl}}\right)^{L-1}t_3^{k_1}\otimes\mathbb{1}_{k_2}\right]&\simeq\frac{(-i)^L(k_1^2+k_2^2)^{\frac{L}{2}}}{2^Lx_3^{L-1}L(L+1)(L+2)}\Big[-k_1k_2L\cos\left(L\psi_0\right)\\&\quad+\left[k_2^2+k_1^2(L+1)\right]\sin\left(L\psi_0\right)\Big],\\\mathrm{tr}\left[\left(Z^{\mathrm{cl}}\right)^{L-1}\mathbb{1}_{k_1}\otimes t_3^{k_2}\right]&\simeq\frac{(-i)^{L-1}(k_1^2+k_2^2)^{\frac{L}{2}}}{2^Lx_3^{L-1}L(L+1)(L+2)}\Big[+k_1k_2L\cos\left(L\psi_0\right)\\&\quad+\left[k_1^2+k_2^2(L+1)\right]\sin\left(L\psi_0\right)\Big].\end{aligned} \quad \text{(D.7)}$$

For the case $n_1=n_2=1$, the trace gives

$$\begin{aligned}\mathrm{tr}\left[\left(Z^{\mathrm{cl}}\right)^{L-2}t_3^{k_1}\otimes t_3^{k_2}\right]&\simeq\frac{(-i)^{L+1}(k_1^2+k_2^2)^{\frac{L}{2}}}{2^Lx_3^{L-2}L(L+2)(L-1)}\Big[+k_1k_2L\cos\left(L\psi_0\right)\\&\quad+(k_1-k_2)(k_1+k_2)\sin\left(L\psi_0\right)\Big].\end{aligned} \quad \text{(D.8)}$$

Finally, for the cases $(n_1, n_2) = (2, 0)$ and $(n_1, n_2) = (0, 2)$ the traces evaluate to

$$\begin{aligned}
\mathrm{tr}\Big[\Big(Z^{\mathrm{cl}}\Big)^{L-2}\Big(t_3^{k_1}\Big)^2 \otimes \mathbb{1}_{k_2}\Big] &\simeq -\frac{(-i)^L(k_1^2+k_2^2)^{\frac{L}{2}}}{2^L x_3^{L-2}(L-1)L(L+1)(L+2)}\Big[+2k_1k_2L\cos\left(L\psi_0\right) \\
&\quad + \left(-2k_2^2 + k_1^2L(L+1)\right)\sin\left(L\psi_0\right)\Big], \\
\mathrm{tr}\Big[\Big(Z^{\mathrm{cl}}\Big)^{L-2}\mathbb{1}_{k_1} \otimes \Big(t_3^{k_2}\Big)^2\Big] &\simeq \frac{(-i)^L(k_1^2+k_2^2)^{\frac{L}{2}}}{2^L x_3^{L-2}(L-1)L(L+1)(L+2)}\Big[+2k_1k_2L\cos\left(L\psi_0\right) \\
&\quad + \left(2k_1^2 - k_2^2L(L+1)\right)\sin\left(L\psi_0\right)\Big].
\end{aligned} \tag{D.9}$$

References

[1] N. Andrei et al., *Boundary and Defect CFT: Open Problems and Applications*, 2018, arXiv:1810.05697 [INSPIRE].

[2] N.R. Constable, R.C. Myers and O. Tafjord, *The Noncommutative bion core*, *Phys. Rev.* **D 61** (2000) 106009 [hep-th/9911136] [INSPIRE].

[3] A. Karch and L. Randall, *Open and closed string interpretation of SUSY CFT's on branes with boundaries*, *JHEP* **06** (2001) 063 [hep-th/0105132] [INSPIRE].

[4] M. de Leeuw, A.C. Ipsen, C. Kristjansen and M. Wilhelm, *Introduction to Integrability and One-point Functions in $\mathcal{N} = 4$ SYM and its Defect Cousin*, in *Les Houches Summer School: Integrability: From Statistical Systems to Gauge Theory*, Les Houches France (2016) [arXiv:1708.02525] [INSPIRE].

[5] O. DeWolfe, D.Z. Freedman and H. Ooguri, *Holography and defect conformal field theories*, *Phys. Rev.* **D 66** (2002) 025009 [hep-th/0111135] [INSPIRE].

[6] J. Erdmenger, Z. Guralnik and I. Kirsch, *Four-dimensional superconformal theories with interacting boundaries or defects*, *Phys. Rev.* **D 66** (2002) 025020 [hep-th/0203020] [INSPIRE].

[7] J.L. Cardy, *Conformal Invariance and Surface Critical Behavior*, *Nucl. Phys.* **B 240** (1984) 514 [INSPIRE].

[8] M. de Leeuw, C. Kristjansen and K. Zarembo, *One-point Functions in Defect CFT and Integrability*, *JHEP* **08** (2015) 098 [arXiv:1506.06958] [INSPIRE].

[9] I. Buhl-Mortensen, M. de Leeuw, C. Kristjansen and K. Zarembo, *One-point Functions in AdS/dCFT from Matrix Product States*, *JHEP* **02** (2016) 052 [arXiv:1512.02532] [INSPIRE].

[10] M. de Leeuw, C. Kristjansen and S. Mori, *AdS/dCFT one-point functions of the* SU(3) *sector*, *Phys. Lett.* **B 763** (2016) 197 [arXiv:1607.03123] [INSPIRE].

[11] M. De Leeuw, C. Kristjansen and G. Linardopoulos, *Scalar one-point functions and matrix product states of AdS/dCFT*, *Phys. Lett.* **B 781** (2018) 238 [arXiv:1802.01598] [INSPIRE].

JHEP01(2019)007

[12] I. Buhl-Mortensen, M. de Leeuw, A.C. Ipsen, C. Kristjansen and M. Wilhelm, *One-loop one-point functions in gauge-gravity dualities with defects*, *Phys. Rev. Lett.* **117** (2016) 231603 [arXiv:1606.01886] [INSPIRE].

[13] I. Buhl-Mortensen, M. de Leeuw, A.C. Ipsen, C. Kristjansen and M. Wilhelm, *A Quantum Check of AdS/dCFT*, *JHEP* **01** (2017) 098 [arXiv:1611.04603] [INSPIRE].

[14] I. Buhl-Mortensen, M. de Leeuw, A.C. Ipsen, C. Kristjansen and M. Wilhelm, *Asymptotic One-Point Functions in Gauge-String Duality with Defects*, *Phys. Rev. Lett.* **119** (2017) 261604 [arXiv:1704.07386] [INSPIRE].

[15] K. Nagasaki and S. Yamaguchi, *Expectation values of chiral primary operators in holographic interface CFT*, *Phys. Rev.* **D 86** (2012) 086004 [arXiv:1205.1674] [INSPIRE].

[16] K. Nagasaki, H. Tanida and S. Yamaguchi, *Holographic Interface-Particle Potential*, *JHEP* **01** (2012) 139 [arXiv:1109.1927] [INSPIRE].

[17] D.E. Berenstein, J.M. Maldacena and H.S. Nastase, *Strings in flat space and pp waves from $\mathcal{N} = 4$ superYang-Mills*, *JHEP* **04** (2002) 013 [hep-th/0202021] [INSPIRE].

[18] Z. Bern, M. Czakon, L.J. Dixon, D.A. Kosower and V.A. Smirnov, *The Four-Loop Planar Amplitude and Cusp Anomalous Dimension in Maximally Supersymmetric Yang-Mills Theory*, *Phys. Rev.* **D 75** (2007) 085010 [hep-th/0610248] [INSPIRE].

[19] N. Beisert, B. Eden and M. Staudacher, *Transcendentality and Crossing*, *J. Stat. Mech.* **0701** (2007) P01021 [hep-th/0610251] [INSPIRE].

[20] F. Cachazo, M. Spradlin and A. Volovich, *Four-loop cusp anomalous dimension from obstructions*, *Phys. Rev.* **D 75** (2007) 105011 [hep-th/0612309] [INSPIRE].

[21] C. Kristjansen, G.W. Semenoff and D. Young, *Chiral primary one-point functions in the D3-D7 defect conformal field theory*, *JHEP* **01** (2013) 117 [arXiv:1210.7015] [INSPIRE].

[22] O. Bergman, N. Jokela, G. Lifschytz and M. Lippert, *Quantum Hall Effect in a Holographic Model*, *JHEP* **10** (2010) 063 [arXiv:1003.4965] [INSPIRE].

[23] R.C. Myers and M.C. Wapler, *Transport Properties of Holographic Defects*, *JHEP* **12** (2008) 115 [arXiv:0811.0480] [INSPIRE].

[24] G. Grignani, N. Kim and G.W. Semenoff, *D3-D5 holography with flux*, *Phys. Lett.* **B 715** (2012) 225 [arXiv:1203.6162] [INSPIRE].

[25] C. Kristjansen and G.W. Semenoff, *Giant D5 Brane Holographic Hall State*, *JHEP* **06** (2013) 048 [arXiv:1212.5609] [INSPIRE].

[26] C. Kristjansen, R. Pourhasan and G.W. Semenoff, *A Holographic Quantum Hall Ferromagnet*, *JHEP* **02** (2014) 097 [arXiv:1311.6999] [INSPIRE].

[27] J. Hutchinson, C. Kristjansen and G.W. Semenoff, *Conductivity Tensor in a Holographic Quantum Hall Ferromagnet*, *Phys. Lett.* **B 738** (2014) 373 [arXiv:1408.3320] [INSPIRE].

[28] N. Jokela, G. Lifschytz and M. Lippert, *Holographic anyonic superfluidity*, *JHEP* **10** (2013) 014 [arXiv:1307.6336] [INSPIRE].

[29] N. Jokela, G. Lifschytz and M. Lippert, *Flowing holographic anyonic superfluid*, *JHEP* **10** (2014) 21 [arXiv:1407.3794] [INSPIRE].

[30] A. Gimenez Grau, C. Kristjansen, M. Volk and M. Wilhelm, work in progress.

JHEP01(2019)007

[31] A. Chatzistavrakidis, H. Steinacker and G. Zoupanos, *On the fermion spectrum of spontaneously generated fuzzy extra dimensions with fluxes*, *Fortsch. Phys.* **58** (2010) 537 [arXiv:0909.5559] [INSPIRE].

[32] L.F. Alday, J.M. Henn, J. Plefka and T. Schuster, *Scattering into the fifth dimension of $\mathcal{N} = 4$ super Yang-Mills*, *JHEP* **01** (2010) 077 [arXiv:0908.0684] [INSPIRE].

[33] C.P. Burgess and G.D. Moore, *The standard model: A primer*, Cambridge University Press, Cambridge U.K. (2006).

[34] M. Ammon and J. Erdmenger, *Gauge/gravity duality*, Cambridge University Press, Cambridge U.K. (2015).

[35] T. Kawano and K. Okuyama, *Spinor exchange in $AdS(d+1)$*, *Nucl. Phys.* **B 565** (2000) 427 [hep-th/9905130] [INSPIRE].

[36] D. Gaiotto and E. Witten, *Supersymmetric Boundary Conditions in $\mathcal{N} = 4$ Super Yang-Mills Theory*, *J. Statist. Phys.* **135** (2009) 789 [arXiv:0804.2902] [INSPIRE].

[37] M. de Leeuw, A.C. Ipsen, C. Kristjansen, K.E. Vardinghus and M. Wilhelm, *Two-point functions in AdS/dCFT and the boundary conformal bootstrap equations*, *JHEP* **08** (2017) 020 [arXiv:1705.03898] [INSPIRE].

[38] W. Siegel, *Supersymmetric Dimensional Regularization via Dimensional Reduction*, *Phys. Lett.* **84B** (1979) 193 [INSPIRE].

[39] D.M. Capper, D.R.T. Jones and P. van Nieuwenhuizen, *Regularization by Dimensional Reduction of Supersymmetric and Nonsupersymmetric Gauge Theories*, *Nucl. Phys.* **B 167** (1980) 479 [INSPIRE].

[40] J.K. Erickson, G.W. Semenoff and K. Zarembo, *Wilson loops in $\mathcal{N} = 4$ supersymmetric Yang-Mills theory*, *Nucl. Phys.* **B 582** (2000) 155 [hep-th/0003055] [INSPIRE].

[41] D. Nandan, C. Sieg, M. Wilhelm and G. Yang, *Cutting through form factors and cross sections of non-protected operators in $\mathcal{N} = 4$ SYM*, *JHEP* **06** (2015) 156 [arXiv:1410.8485] [INSPIRE].

[42] W. Siegel, *Inconsistency of Supersymmetric Dimensional Regularization*, *Phys. Lett.* **B 94** (1980) 37 [INSPIRE].

[43] L.V. Avdeev, G.A. Chochia and A.A. Vladimirov, *On the Scope of Supersymmetric Dimensional Regularization*, *Phys. Lett.* **B 105** (1981) 272 [INSPIRE].

[44] L.V. Avdeev, *Noninvariance of Regularization by Dimensional Reduction: An Explicit Example of Supersymmetry Breaking*, *Phys. Lett.* **B 117** (1982) 317 [INSPIRE].

[45] L.V. Avdeev and A.A. Vladimirov, *Dimensional Regularization and Supersymmetry*, *Nucl. Phys.* **B 219** (1983) 262 [INSPIRE].

[46] J.A. Minahan and K. Zarembo, *The Bethe ansatz for $\mathcal{N} = 4$ superYang-Mills*, *JHEP* **03** (2003) 013 [hep-th/0212208] [INSPIRE].

[47] B. Guo, *Lollipop diagrams in defect $\mathcal{N} = 4$ super Yang-Mills theory*, MSc Thesis, University of British Columbia, Vancouver Canada (2017).

[48] M. de Leeuw, A.C. Ipsen, C. Kristjansen and M. Wilhelm, *One-loop Wilson loops and the particle-interface potential in AdS/dCFT*, *Phys. Lett.* **B 768** (2017) 192 [arXiv:1608.04754] [INSPIRE].

[49] J. Aguilera-Damia, D.H. Correa and V.I. Giraldo-Rivera, *Circular Wilson loops in defect Conformal Field Theory*, *JHEP* **03** (2017) 023 [arXiv:1612.07991] [INSPIRE].

JHEP01(2019)007

[50] M. Preti, D. Trancanelli and E. Vescovi, *Quark-antiquark potential in defect conformal field theory*, *JHEP* **10** (2017) 079 [arXiv:1708.04884] [INSPIRE].

[51] E. Widen, *Two-point functions of* SU(2)*-subsector and length-two operators in dCFT*, *Phys. Lett.* **B 773** (2017) 435 [arXiv:1705.08679] [INSPIRE].

[52] L. Piroli, B. Pozsgay and E. Vernier, *What is an integrable quench?*, *Nucl. Phys.* **B 925** (2017) 362 [arXiv:1709.04796] [INSPIRE].

[53] M. de Leeuw, C. Kristjansen and K.E. Vardinghus, work in progress.

[54] M. de Leeuw, C. Kristjansen and G. Linardopoulos, *One-point functions of non-protected operators in the* SO(5) *symmetric D3–D7 dCFT*, *J. Phys.* **A 50** (2017) 254001 [arXiv:1612.06236] [INSPIRE].

[55] B. de Wit, J. Hoppe and H. Nicolai, *On the Quantum Mechanics of Supermembranes*, *Nucl. Phys.* **B 305** (1988) 545 [INSPIRE].

[56] J. Hoppe, *Quantum theory of a massless relativistic surface and a two-dimensional bound state problem*, Ph.D. Thesis, Massachusetts Institute of Technology, Cambridge U.S.A. (1982), http://hdl.handle.net/1721.1/15717.

JHEP01(2019)007

Published for SISSA by Springer

Received: October 10, 2019
Accepted: December 22, 2019
Published: January 14, 2020

Embedding Feynman integral (Calabi-Yau) geometries in weighted projective space

Jacob L. Bourjaily,[a,b] **Andrew J. McLeod,**[a] **Cristian Vergu,**[a] **Matthias Volk,**[a] **Matt von Hippel**[a] **and Matthias Wilhelm**[a]

[a] *Niels Bohr International Academy and Discovery Center, Niels Bohr Institute, University of Copenhagen, Blegdamsvej 17, DK-2100, Copenhagen Ø, Denmark*

[b] *Center for the Fundamental Laws of Nature, Department of Physics, Jefferson Physical Laboratory, Harvard University, 17 Oxford street, Cambridge, MA 02138, U.S.A.*

E-mail: bourjaily@nbi.ku.dk, amcleod@nbi.ku.dk, c.vergu@nbi.ku.dk, mvolk@nbi.ku.dk, mvonhippel@nbi.ku.dk, matthias.wilhelm@nbi.ku.dk

Abstract: It has recently been demonstrated that Feynman integrals relevant to a wide range of perturbative quantum field theories involve periods of Calabi-Yau manifolds of arbitrarily large dimension. While the number of Calabi-Yau manifolds of dimension three or higher is considerable (if not infinite), those relevant to most known examples come from a very simple class: degree-$2k$ hypersurfaces in k-dimensional weighted projective space $\mathbb{WP}^{1,\ldots,1,k}$. In this work, we describe some of the basic properties of these spaces and identify additional examples of Feynman integrals that give rise to hypersurfaces of this type. Details of these examples at three loops and of illustrations of open questions at four loops are included as supplementary material to this work.

Keywords: Differential and Algebraic Geometry, Scattering Amplitudes

ArXiv ePrint: 1910.01534

https://doi.org/10.1007/JHEP01(2020)078

JHEP01(2020)078

Contents

1 Introduction and summary **1**

2 Calabi-Yau hypersurfaces in $\mathbb{WP}^{1,\ldots,1,k}$ **4**

3 Three-loop integrals involving Calabi-Yaus in $\mathbb{WP}^{1,\ldots,1,k}$ **9**
- 3.1 Identifying Calabi-Yau geometries via residues 10
- 3.2 Revisiting the three-loop traintrack integral 11
- 3.3 The three-loop wheel integral 12

4 Open problems at four loops and beyond **18**

A Desingularization by complex structure deformation **20**

B Hodge numbers and Euler characteristic **21**
- B.1 Euler characteristic 21
- B.2 Index theorems 23
- B.3 Lefschetz hyperplane theorem 23

C Feynman parametrization of the three-loop wheel **24**

D Feynman parametrization of the four-loop wheel **28**
- D.1 Interesting kinematic limits of the wheel integral $\mathfrak{W}^{(4)}$ 31

JHEP01(2020)078

1 Introduction and summary

Recent years have seen the development of a rich interplay between number theory, algebraic geometry, and the study of perturbative scattering amplitudes in quantum field theory. Even for what is arguably the simplest class of amplitudes — those that can be expressed in terms of multiple polylogarithms [1–6] — a great deal of conceptual and computational progress has been made [7–29] by harnessing the geometric (or motivic) structures with which these functions are endowed when viewed as iterated integrals on the moduli space of the Riemann sphere with marked points [2, 3, 30–38].

Slightly more complicated amplitudes can be described in terms of elliptic multiple polylogarithms, which can be understood as iterated integrals over the (moduli space of the) torus. This class of functions has been the focus of a great deal of recent work and is now also under reasonably good theoretical control (in part based on an understanding of modular forms) [39–61].

In general, one expects increasingly complicated classes of integrals to appear in scattering amplitudes at higher perturbative orders, corresponding to integrals over manifolds

with higher dimension and/or genus. Even for amplitudes known or expected to be polylogarithmic, this feature may be impossible to realize while preserving locality (see for example ref. [62] and the examples discussed in ref. [63]). A general understanding of the types of integrals that can show up is currently lacking. However, in a surprisingly large number of cases, it has been observed that these manifolds are Calabi-Yau [61, 64–70].

Even at dimensions as low as three or four, large numbers of Calabi-Yau manifolds are known to exist — having been constructed and studied, in part, because of their role in string compactifications (see e.g. refs. [71–74]). One may wonder if a similarly vast number of geometries are relevant to Feynman integrals in perturbative quantum field theories. The answer seems to be *no*. Indeed, all the examples identified in ref. [64] and the entire class of 'maximally rigid, marginal' integrals described in ref. [66] are members of a special family: they are given as codimension-one (degree-$2k$) hypersurfaces in the k-dimensional weighted projective space $\mathbb{WP}^{1,\ldots,1,k}$. This motivates us to better understand this family of Calabi-Yau manifolds and explore the consequences of their geometry for physics.

The coefficients of the polynomials that define these hypersurfaces are functions of kinematic data. Virtually all known examples involve (highly) *singular* Calabi-Yau hypersurfaces, and there is little doubt that these singularities will play a significant role in our understanding of these Feynman integrals. But in this work we mostly set these bigger questions aside and discuss the geometry of the smooth case — obtainable, in general, by sufficiently 'regularizing' complex structure deformations. This regularization makes it possible for us to compute various topological quantities, such as Hodge numbers. The reader may wonder what is the significance of these quantities. While a complete answer is not available at this point, we believe it is likely that the Hodge numbers will account for part of the contribution to the dimension of integral bases in terms of which integrals sharing a given topology decompose.

This work is organized as follows. In section 2, we review some basic algebraic and differential-geometric aspects of these particular Calabi-Yau geometries. In particular, we discuss their Dolbeault cohomology groups $H^{p,q}$ and how to compute the associated Hodge numbers $h^{p,q}$, and discuss the Euler characteristics of (smooth) Calabi-Yau hypersurfaces of $\mathbb{WP}^{1,\ldots,1,k}$. We also review the construction of canonical holomorphic forms (unique up to an overall scaling), and discuss how the integral of this form over various cycles defines the independent periods of the hypersurface (which in some sense characterize its geometry).

We study these aspects of Calabi-Yau hypersurfaces in $\mathbb{WP}^{1,\ldots,1,k}$ with the general expectation that the integral geometries appearing in Feynman diagrams can be found to encode some of the physics of these diagrams. Characterizing these geometries is a first and necessary step for identifying such connections. We also expect these geometries to be relevant to the development of technology for representing these Feynman integrals in terms of iterated integrals. For instance, periods play an important role in the definition of elliptic multiple polylogarithms [51, 52, 54, 56] and are required to bring differential equations into ϵ-canonical form [53]. However, for general Calabi-Yau $(k-1)$-folds beyond the elliptic case ($k = 2$), the calculation of these periods still poses a challenging problem. (But see ref. [75] for an example where it has been done for the quintic Calabi-Yau hypersurface in $\mathbb{P}^4$.) Additionally, a connection between the dimension of certain cohomology groups and numbers of master integrals has recently been established using intersection theory [76–78].

JHEP01(2020)078

(a) (b)

Figure 1. The three-loop traintrack (a) and wheel (b) integrals.

After this geometric primer, we go on in section 3 to describe in detail two examples of Calabi-Yau geometries relevant to massless, four-dimensional planar theories at three loops. Unlike the analysis in refs. [64, 66], which identified these geometries using direct integration, we here identify such hypersurfaces by taking sequences of residues (as done in ref. [67]). We do this by first deriving manifestly dual-conformal-invariant six-fold representations of these integrals using loop-by-loop Feynman parametrization [67, 79–81]. As both integrals contribute to planar maximally supersymmetric Yang-Mills theory, we expect all six remaining integrations to be transcendental; therefore, each residue mimics a polylogarithmic integration.[1] In both integrals, Calabi-Yau hypersurfaces appear in the denominator when no more residues can be taken.

The first integral we study in this way is the three-loop traintrack (or triple-box) integral shown in figure 1a, which has already been identified as a K3 surface by several of the authors [67]. We show here how to realize it as a hypersurface in $\mathbb{WP}^{1,1,1,3}$. The second integral is the three-loop wheel shown in figure 1b, which involves a hypersurface in $\mathbb{WP}^{1,1,1,1,4}$. While the general three-loop wheel depends on nine kinematic variables, we also study several of its interesting kinematic limits, some of which we evaluate in terms of polylogarithms. Moreover, we show that the three-loop wheel permits a toy model similar to that of the elliptic double-box [80], which has only three parameters while still involving a Calabi-Yau threefold.

The three-loop traintrack and wheel integrals are the minimal representatives (in terms of loop order and particle multiplicity) of massless planar topologies that contain these Calabi-Yau geometries. They occur in massless φ^4 theory (in the case of the wheel, as a dual graph), the planar limit of maximally supersymmetric Yang-Mills theory, and integrable conformal fishnet models [82–84], as well as in more general four-dimensional massless theories via generalized unitarity [85–91]. For this reason, they merit focused investigation. While the present work inaugurates this study, it offers only a coarse analysis of the involved Calabi-Yau geometries. A more refined analysis, including e.g. Picard ranks, has been possible for some integrals containing K3 surfaces [65, 68–70, 92, 93], for instance, using differential equations. It would be important to analyze the Calabi-Yau surfaces identified here and in refs. [64, 66, 67] in a similar way, although these cases will be more difficult due to the larger number of kinematic variables.

[1] This follows from the expectation that three-loop integrals will evaluate to functions with uniform transcendental weight six. Even though the notion of transcendental weight is not established beyond the case of polylogarithms, both integrals degenerate to weight-six polylogarithms in known limits.

JHEP01(2020)078

We conclude in section 4 by highlighting open problems at four loops and beyond. In addition to discussing some of the broader questions that remain to be answered regarding the appearance of higher-dimensional varieties in Feynman integrals (and the technology required to cope with them), we consider the four-loop traintrack and wheel integrals. Intriguingly, we are not able to identify either of these example as a Calabi-Yau hypersurface in $\mathbb{WP}^{1,\ldots,1,k}$.

In appendices A and B, we provide more background on the desingularization of hypersurfaces in weighted projective space and the computation of Hodge numbers and Euler characteristics. In appendix C we review loop-by-loop Feynman parametrization [67, 79–81] and derive a manifestly dual-conformal six-fold representation of the three-loop wheel integral, and in appendix D we derive a dual-conformal nine-fold representation of the four-loop wheel. In the latter case, we also describe several interesting kinematic limits and toy models. In the supplementary material, we include the details of these examples, as well as the equations defining the hypersurfaces obtained.

2 Calabi-Yau hypersurfaces in $\mathbb{WP}^{1,\ldots,1,k}$

In this section, we characterize the k-dimensional weighted projective space $\mathbb{WP}^{1,\ldots,1,k}$, which involves k coordinates of weight 1 and a single coordinate of weight k. This space can be defined as the quotient of $\mathbb{C}^{k+1} \setminus \{0\}$ by the equivalence relation

$$(x_1, \ldots, x_k, y) \sim (\lambda x_1, \ldots, \lambda x_k, \lambda^k y)\,. \tag{2.1}$$

Here, $\lambda \in \mathbb{C}^\star$ denotes a non-zero complex number and $(x_1, \ldots, x_k, y)$ are referred to as homogeneous coordinates on $\mathbb{WP}^{1,\ldots,1,k}$.

We will be interested in defining an algebraic hypersurface embedded into $\mathbb{WP}^{1,\ldots,1,k}$ as the zero-locus of a polynomial Q in the homogeneous coordinates. Of course, such a polynomial relation has to be consistent with the equivalence relation (2.1). In unweighted projective space, this would correspond to the requirement that the polynomial be homogeneous. Analogously, in weighted projective space, the total weight of each monomial must be the same; this number is called the (overall) degree of the polynomial.

One can show (see for example ref. [94]) that the zero-locus of any single polynomial in the coordinates of a weighted projective space defines a codimension-one Calabi-Yau hypersurface if the overall degree of the polynomial equals the sum of the weights of the weighted projective space. In the case of $\mathbb{WP}^{1,\ldots,1,k}$, a Calabi-Yau hypersurface can thus be defined by a polynomial Q of degree $(\sum_{i=1}^{k} 1) + k = 2k$, which has the most general form

$$Q(x_1, \ldots, x_k, y) = \sum_{\substack{(\vec{\alpha},\beta)\in\mathbb{N}_0^{k+1} \\ |\vec{\alpha}|+k\beta=2k}} c_{\vec{\alpha},\beta} \prod_{i=1}^{k} x_i^{\alpha_i} y^{\beta}\,, \tag{2.2}$$

where α_i denotes the i^{th} component of $\vec{\alpha}$ and $|\vec{\alpha}| \coloneqq \sum_i \alpha_i$. The coefficients $c_{\vec{\alpha},\beta} \in \mathbb{C}$ are complex numbers, and can in general depend on additional parameters (which for us will be kinematics). However, these coefficients are only defined up to $\mathbb{WP}^{1,\ldots,1,k}$ coordinate

JHEP01(2020)078

transformations. In particular, we can rescale all coordinates using the equivalence relation (2.1) to set $c_{\vec{0},2} \to 1$, and additionally shift y by a degree-k polynomial in the x_i to eliminate the terms linear in y (thereby setting $c_{\vec{\alpha},1} \to 0$). This brings Q into the form

$$Q(x_1, \ldots, x_k, y) = y^2 - P(x_1, \ldots, x_k). \tag{2.3}$$

Finally, we can act with a GL(k) transformation on the x_i. This can be used to eliminate k^2 of the $\binom{3k-1}{k-1}$ possible monomials in P. The remaining $\binom{3k-1}{k-1} - k^2$ coefficients yield distinct hypersurfaces, which are usually parametrized by $\binom{3k-1}{k-1} - k^2$ complex structure moduli. We should emphasize that hypersurfaces taking the form (2.2) may be singular for some values of the coefficients. For generic coefficients, they are however smooth (see the discussion in appendix A).

We now consider a Calabi-Yau manifold X embedded as a codimension-one hypersurface in $\mathbb{WP}^{1,\ldots,1,k}$ and study the forms on X. Since X is a complex manifold, any m-form on X can be decomposed into a sum of forms with p holomorphic and q antiholomorphic pieces such that $p+q=m$. Moreover, the exterior derivative decomposes as $\mathrm{d} = \partial + \overline{\partial}$. In analogy with de Rham cohomology, one can then define the Dolbeault cohomology groups $H^{p,q}(X)$ as the cohomology groups of $\overline{\partial}$. The dimensions of the Dolbeault cohomology groups are known as Hodge numbers, $h^{p,q}(X) \coloneqq \dim(H^{p,q}(X))$. Moreover, the dimensions of the de Rham cohomology groups h^m are given by $h^m = \sum_{p+q=m} h^{p,q}$. Recall that via Poincaré duality and de Rham's theorem, h^m are exactly the Betti numbers, which count the numbers of independent m-cycles on X.

In an n-dimensional complex manifold in which p and q run from 0 to n, one might naïvely expect $(n+1)^2$ different Hodge numbers. However, due to various symmetries many of these numbers are not independent. For example, in the case of a Calabi-Yau threefold ($k=4$), $h^{1,1}$ and $h^{2,1}$ fix the values of all other Hodge numbers.

In general, the computation of the Hodge numbers of a complex manifold poses a difficult problem.[2] In the case of Calabi-Yau hypersurfaces embedded in toric varieties — of which weighted projective space is an example — the mirror-symmetry construction due to Batyrev [95] provides a framework to compute (some of the) Hodge numbers from purely combinatorial data. (For more pedagogical introductions on this topic see, for instance, refs. [96, 97].) In short, one associates to a defining polynomial (such as Q in eq. (2.2)) a pair of dual polytopes $(\Delta, \Delta^\star)$. The polytope Δ is called the Newton polytope and its vertices are given by the (shifted) vectors of exponents of the polynomial. (Note that the vertices of Δ therefore lie in an integer lattice.) One can show that in terms of $(\Delta, \Delta^\star)$ the Calabi-Yau condition becomes the statement that the dual polytope $\Delta^\star$ only has integer vertices and that both polytopes contain only the origin as an interior lattice point. Some

[2]For smooth varieties, this can be achieved in general by Gröbner bases computations. We thank the referee for pointing this out to us.

JHEP01(2020)078

of the Hodge numbers can then be computed from the polytopes as

$$h^{1,n} = \delta_{1,n}\left[\ell(\Delta^\star) - (d+1) - \sum_{\operatorname{codim}\theta^\star = 1} \ell_{\text{int}}(\theta^\star)\right] + \delta_{d-2,n}\left[\ell(\Delta) - (d+1) - \sum_{\operatorname{codim}\theta = 1} \ell_{\text{int}}(\theta)\right] + \sum_{\operatorname{codim}\theta^\star = n+1} \ell_{\text{int}}(\theta^\star)\ell_{\text{int}}(\theta). \tag{2.4}$$

Here ℓ and ℓ_{int} count the total and interior lattice points of a polytope, respectively, and the sums run over faces of Δ and $\Delta^\star$, denoted by θ and $\theta^\star$, with the given codimension. Note that Batyrev's framework explicitly excludes the case of K3 surfaces ($k = 3$).

This construction can be generalized to so-called complete intersection Calabi-Yaus (CICYs) embedded into a toric variety and one can obtain more Hodge numbers as the expansion coefficients of a two-variable generating function known as stringy E-function [98, 99],

$$E(u,v) = \sum_{p,q} (-1)^{p+q} h^{p,q} u^p v^q. \tag{2.5}$$

The construction of the function E relies on a generalization of the reflexive polytope criterion outlined above by so-called nef-partitions. The function has been implemented in `PALP` [100], which is available from `SageMath` [101].

For the case of a Calabi-Yau hypersurface in $\mathbb{WP}^{1,\ldots,1,k}$, the Newton polytope and its dual take a relatively simple form and allow us to compute $h^{1,j}$ from eq. (2.4): for any $k \geq 4$, we find

$$h^{1,j} = \begin{cases} \binom{3k-1}{k-1} - k^2 & j = k-2, \\ 1 & j = 1, \\ 0 & \text{otherwise.} \end{cases} \tag{2.6}$$

The non-trivial Hodge number $h^{1,k-2}$ counts the complex structure moduli discussed above, while $h^{1,1}$ counts the single Kähler structure modulus. We have moreover verified this formula by comparing to the stringy E-function implemented in `PALP` [100], which also computes the remaining Hodge numbers.

For the elliptic curve ($k = 2$), the Hodge numbers are well-known to be

$$\begin{array}{ccc} & h^{0,0} & \\ h^{1,0} & & h^{0,1} \\ & h^{1,1} & \end{array} = \begin{array}{ccc} & 1 & \\ 1 & & 1 \\ & 1 & \end{array} . \tag{2.7}$$

As already mentioned, the case of the K3 surface, $k = 3$, is excluded in the general framework above. Here, in addition to the $\binom{6+2}{2} - 9 = 19$ complex structure moduli, the Kähler structure modulus contributes to $h^{1,1}$, allowing us to obtain the well-known result

$$\begin{array}{ccccc} & & h^{0,0} & & \\ & h^{1,0} & & h^{0,1} & \\ h^{2,0} & & h^{1,1} & & h^{0,2} \\ & h^{2,1} & & h^{1,2} & \\ & & h^{2,2} & & \end{array} = \begin{array}{ccccc} & & 1 & & \\ & 0 & & 0 & \\ 1 & & 20 & & 1 \\ & 0 & & 0 & \\ & & 1 & & \end{array} . \tag{2.8}$$

JHEP01(2020)078

For higher k, we find the following patterns of Hodge numbers:

- Calabi-Yau threefold, $k = 4$:

$$\begin{array}{ccccccc} & & & h^{0,0} & & & \\ & & h^{1,0} & & h^{0,1} & & \\ & h^{2,0} & & h^{1,1} & & h^{0,2} & \\ h^{3,0} & & h^{2,1} & & h^{1,2} & & h^{0,3} \\ & h^{3,1} & & h^{2,2} & & h^{2,3} & \\ & & h^{3,2} & & h^{2,3} & & \\ & & & h^{3,3} & & & \end{array} = \begin{array}{ccccccc} & & & 1 & & & \\ & & 0 & & 0 & & \\ & 0 & & 1 & & 0 & \\ 1 & & 149 & & 149 & & 1 \\ & 0 & & 1 & & 0 & \\ & & 0 & & 0 & & \\ & & & 1 & & & \end{array} . \tag{2.9}$$

- Calabi-Yau fourfold, $k = 5$:

$$\begin{array}{ccccccccc} & & & & h^{0,0} & & & & \\ & & & h^{1,0} & & h^{0,1} & & & \\ & & h^{2,0} & & h^{1,1} & & h^{0,2} & & \\ & h^{3,0} & & h^{2,1} & & h^{1,2} & & h^{0,3} & \\ h^{4,0} & & h^{3,1} & & h^{2,2} & & h^{1,3} & & h^{0,4} \\ & h^{4,1} & & h^{3,2} & & h^{1,3} & & h^{1,4} & \\ & & h^{4,2} & & h^{3,3} & & h^{2,4} & & \\ & & & h^{4,3} & & h^{3,4} & & & \\ & & & & h^{4,4} & & & & \end{array} = \begin{array}{ccccccccc} & & & & 1 & & & & \\ & & & 0 & & 0 & & & \\ & & 0 & & 1 & & 0 & & \\ & 0 & & 0 & & 0 & & 0 & \\ 1 & & 976 & & 3952 & & 976 & & 1 \\ & 0 & & 0 & & 0 & & 0 & \\ & & 0 & & 1 & & 0 & & \\ & & & 0 & & 0 & & & \\ & & & & 1 & & & & \end{array} . \tag{2.10}$$

- Calabi-Yau fivefold, $k = 6$:

$$\begin{array}{ccccccccccc} & & & & & 1 & & & & & \\ & & & & 0 & & 0 & & & & \\ & & & 0 & & 1 & & 0 & & & \\ & & 0 & & 0 & & 0 & & 0 & & \\ & 0 & & 0 & & 1 & & 0 & & 0 & \\ 1 & & 6152 & & 67662 & & 67662 & & 6152 & & 1 \\ & 0 & & 0 & & 1 & & 0 & & 0 & \\ & & 0 & & 0 & & 0 & & 0 & & \\ & & & 0 & & 1 & & 0 & & & \\ & & & & 0 & & 0 & & & & \\ & & & & & 1 & & & & & \end{array} . \tag{2.11}$$

k	2	3	4	5	6	7	8	9
$\chi(X)$	0	24	-296	5910	-147624	4482044	-160180656	6588215370

Table 1. Euler characteristic $\chi(X)$ of $(k-1)$-dimensional Calabi-Yau hypersurfaces X in $\mathbb{WP}^{1,\ldots,1,k}$ for low values of k.

- Calabi-Yau sixfold, $k = 7$:

$$\begin{array}{ccccccccccccccccccccc}
 & & & & & & & & 1 & & & & & & & & & & \\
 & & & & & & & 0 & & 0 & & & & & & & & & \\
 & & & & & & 0 & & 1 & & 0 & & & & & & & & \\
 & & & & & 0 & & 0 & & 0 & & 0 & & & & & & & \\
 & & & & 0 & & 0 & & 1 & & 0 & & 0 & & & & & & \\
 & & & 0 & & 0 & & 0 & & 0 & & 0 & & 0 & & & & & \\
1 & & 38711 & & 965644 & & 2473326 & & 965644 & & 38711 & & 1 & & . \\
 & & 0 & & 0 & & 0 & & 0 & & 0 & & 0 & & & & & & \\
 & & & 0 & & 0 & & 1 & & 0 & & 0 & & & & & & & \\
 & & & & 0 & & 0 & & 0 & & 0 & & & & & & & & \\
 & & & & & & 0 & & 1 & & 0 & & & & & & & & \\
 & & & & & & & 0 & & 0 & & & & & & & & & \\
 & & & & & & & & 1 & & & & & & & & & &
\end{array} \tag{2.12}$$

The structure of these Hodge diamonds is very simple; a nontrivial cohomology only exists for degrees (p, p) and $(p, k-p-1)$, corresponding to their middle column and row. Interestingly, the form of these Hodge diamonds is compatible with hypersurfaces embedded in ordinary (unweighted) projective space (see appendix B.3 for a short discussion). It would be interesting to understand why this occurs, as we currently do not know how to embed our hypersurfaces in unweighted projective space.

To further characterize the Calabi-Yau manifold X in $\mathbb{WP}^{1,\ldots,1,k}$, we compute its Euler characteristic $\chi(X)$. The Euler characteristic is equal to the alternating sum of the dimensions of the de Rham cohomology groups, $\chi(X) = \sum_m (-1)^m \sum_{p+q=m} h^{p,q}$. Following ref. [94], we can obtain a closed expression for it using an index theorem, see appendix B.1 for details. We find

$$\chi(X) = \frac{1-(1-2k)^k+2k^2}{2k}\,. \tag{2.13}$$

The Euler characteristic of X for low values of k is given in table 1.

We have seen above that a codimension-one Calabi-Yau hypersurface X in $\mathbb{WP}^{1,\ldots,1,k}$ is defined by a polynomial $Q(x_1,\ldots,x_k,y)$ of the form given in eq. (2.2). In the examples considered in the following sections, we will find polynomials of precisely this form with different coefficients $c_{\vec{\alpha},\beta}$, i.e. with different complex structure moduli. The complex structure moduli of X are in principle determined by integrating the holomorphic form of maximal degree along a basis of cycles on the manifold. While in practice this is a difficult problem, we still give an account of how this form is constructed.

JHEP01(2020)078

On $\mathbb{WP}^{1,\ldots,1,k}$, the canonical k-form Ω_k is given by

$$\Omega_k = k\, y \left(\bigwedge_{n=1}^{k} dx_n \right) + \sum_{n=1}^{k} (-1)^n x_n \, dy \wedge \left(\bigwedge_{m \neq n} dx_m \right) . \tag{2.14}$$

The Calabi-Yau hypersurface X is defined as the zero-locus of the polynomial $Q(x_1, \ldots, x_k, y)$ in eq. (2.2). The holomorphic form ω_{k-1} of (maximal) degree $k-1$ on X is then given by

$$\omega_{k-1} = \operatorname{Res} \frac{\Omega_k}{Q} . \tag{2.15}$$

The residue above is determined[3] by the property that

$$\frac{\Omega_k}{Q} = \left(\operatorname{Res} \frac{\Omega_k}{Q} \right) \wedge \frac{dQ}{Q} + \cdots , \tag{2.16}$$

where the omitted terms are regular on the surface $Q = 0$.

The hypersurfaces we encounter in the following sections turn out not to be smooth — i.e. there are non-trivial solutions to the system of polynomial equations $Q(x_1, \ldots, x_k, y) = \mathrm{d}\, Q(x_1, \ldots, x_k, y) = 0$. Heuristically, the reason for this is that some of the monomials that would in principle be allowed for homogeneous polynomials in the coordinates of $\mathbb{WP}^{1,\ldots,1,k}$ are missing in Q. Moreover, the coefficients depend on a limited number of kinematic variables, which is usually much smaller than the number of complex structure moduli. In order to regularize the polynomials arising during integration, we can however consider a deformation of the complex structure, i.e. of the coefficients of the $c_{\vec{\alpha},\beta}$ in eq. (2.2). Equivalently, we may say that we are considering the polynomials that we encounter in the following examples as special cases of a generic (smooth) polynomial Q as defined in eq. (2.2). We provide more details on desingularization by complex structure deformation in appendix A.

3 Three-loop integrals involving Calabi-Yaus in $\mathbb{WP}^{1,\ldots,1,k}$

Among the growing list of examples of Feynman integrals involving Calabi-Yau geometries are those with surprisingly few propagators — such as the so-called 'banana' integrals or 'tardigrades',

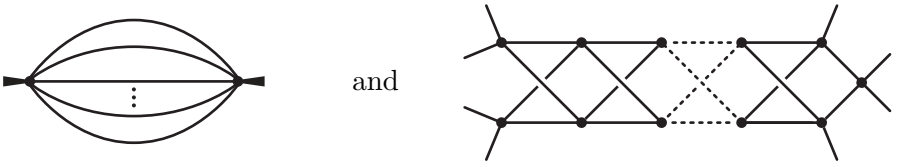

(3.1)

These integrals are sub-topologies[4] of almost all Feynman integrands at sufficiently high multiplicity, and it seems that any integral with a sub-topology involving a Calabi-Yau itself

[3] Outside of the hypersurface X, this residue is not uniquely defined since we could add to Res $\frac{\Omega_k}{Q}$ terms proportional to Q. However, when pulled back to X, these terms vanish.

[4] We consider one Feynman integrand a sub-topology of another if the graph of the former's propagators is a quotient of the latter's by an (internal) edge contraction.

JHEP01(2020)078

involves a Calabi-Yau. Thus, even for the special classes of scattering amplitudes that are expected to be polylogarithmic to all orders (see e.g. ref. [102]), it seems impossible that any local, Feynman-integrand-level representation can have this property term-by-term. Thus, it is essential that we learn to better understand these examples.

This sense of the ubiquity of Calabi-Yau geometries can be made more precise in the context of generalized unitarity, where it is possible to describe *bases* of Feynman integrands subject to certain constraints. A basis large enough to represent all-multiplicity amplitudes in planar, maximally ($\mathcal{N} = 4$) supersymmetric Yang-Mills (SYM) theory through three loops was described in ref. [90]. Although $\mathcal{N} = 4$ SYM theory in the planar limit is an unquestionably simple theory, this basis represents a necessary part of any larger basis needed to represent amplitudes in theories with ultraviolet behavior worse than $\mathcal{N} = 4$ SYM theory (including the Standard Model). Thus, it is a natural place to start our understanding of the Calabi-Yau geometries relevant to general amplitudes.

At three loops, the basis of integrands needed for planar $\mathcal{N} = 4$ SYM theory consists of the traintrack and wheel integrands shown in figure 1, and all irreducible integrands that contain one (or both) as sub-topologies and scale like either integrand (or better) in the ultraviolet. Thus, these two examples arise nearly ubiquitously (at large enough multiplicity) in three-loop amplitudes, motivating us in this section to study the Calabi-Yau geometry that arises in each. But first, let us describe the methods by which we may uncover these geometries.

3.1 Identifying Calabi-Yau geometries via residues

Several infinite classes of Feynman diagrams have been shown to involve Calabi-Yau hypersurfaces in $\mathbb{WP}^{1,\ldots,1,k}$ using direct integration [64, 66]. For instance, the two-dimensional banana graphs and four-dimensional tardigrades shown in eq. (3.1) both fall into this category. In fact, these integral families both achieve the maximum possible degree of non-polylogarithmicity for marginal integrals. More precisely, the L-loop representative of each family saturates a bound on the possible 'rigidity' of marginal integrals, where the rigidity of an integral is defined to be the dimension of the algebraic variety one must integrate over after a maximal number of polylogarithmic integrations have been carried out [66]. The banana graphs have rigidity $L-1$, while the tardigrades have rigidity $2(L-1)$.[5] The two-dimensional massive banana graphs are required, for example, in the calculation of the electron self-energy in QED [103], while the massless two-loop tardigrades enter the integrand basis for massless two-loop amplitudes using prescriptive unitarity [63, 90, 91, 104, 105].

In this work, we instead use sequences of residues to identify Calabi-Yau hypersurfaces in Feynman integrals, as done in ref. [67]. In particular, we begin with representations of (here non-marginal) Feynman integrals at L loops in terms of rational integrands involving only $2L$ integration variables (motivated by the conjectured bound of transcendental weight

[5] In the case of equal masses, the three-loop banana integral was recently expressed in terms of elliptic multiple polylogarithms [61]. While it involves a K3 surface, this K3 surface is related to the elliptic curve describing the two-loop sunrise graph in a way that drastically simplifies the problem [92]. For general Calabi-Yau hypersurfaces, we would not expect this procedure to work, but it would be interesting to see to what extent it is possible. (See ref. [69] for some work in this direction.)

JHEP01(2020)078

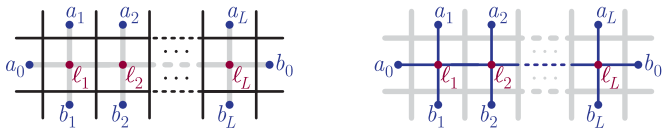

Figure 2. The L-loop traintrack integral and its dual graph.

$2L$ at L loops in four dimensions). We then examine the singular locus of these integrands by taking as many residues as we can.[6] This leads us to an expression of the form

$$\frac{d\vec{x}}{\sqrt{P(\vec{x})}}, \tag{3.2}$$

where $P(\vec{x})$ is a polynomial which is cubic or higher degree in the remaining variables without repeated roots. After projectivization, this polynomial defines a codimension-one hypersurface in $\mathbb{WP}^{1,\ldots,1,k}$ via eq. (2.3).

It is important to note that the above procedure mimics *but is not equivalent to* the procedure of direct hyperlogarithmic integration. They are superficially similar in that direct integration partial-fractions rational integrands to isolate poles in the integration variable, while taking sequential residues also isolates poles. However, the partial-fractioning step of direct integration generates a term for each pole of the integrand, and preserves information about that pole in the form of the polylogarithmic function it constructs. If *any* of these poles introduce a square root in the remaining variables, then this dependence will appear in the polylogarithmic integrand and direct integration may be obstructed. In contrast, by taking residues we may avoid this type of obstruction. As a result, the hypersurfaces we discuss in this section will not necessarily correspond to the degree of rigidity of the integrals involved; the integrals may be more 'rigid' than the geometry we describe would suggest.

While our residue procedure does not necessarily uncover the maximally rigid geometry, it does uncover a geometry that is important and necessary to the understanding of these Feynman integrals. In particular, it is a geometry that should characterize the periods obtained by analytic continuation in the kinematics. To motivate this, recall that we can isolate any particular residue of the integrand with an integration contour tailored to that purpose. These closed integration contours represent potential ambiguities in the original Feynman integration contour, corresponding to the possibility to encircle additional branch cuts. Much as analytically continuing polylogarithmic functions around branch cuts results in factors of $2\pi i$, analytically continuing one of the integrals discussed in this work should give rise to integrals over the maximal residues we can perform — that is, integrals over the holomorphic forms of the Calabi-Yau manifolds we describe.

3.2 Revisiting the three-loop traintrack integral

In ref. [67], some of the authors provided evidence that the L-loop traintrack integral, depicted in figure 2, involves an integral over a Calabi-Yau $(L-1)$-fold. There, a manifestly

[6] If necessary, we perform changes of variables to rationalize square roots of quadratic polynomials along the lines of ref. [106].

JHEP01(2020)078

dual-conformally invariant $2L$-fold representation was given for this integral:

$$\mathfrak{T}^{(L)} = \int_0^\infty \left[d^L\vec{\alpha}\right] d^L\vec{\beta} \frac{1}{(f_1 \cdots f_L) g_L}\,, \tag{3.3}$$

where[7]

$$\begin{aligned} f_k &:= (a_0 a_{k-1}; a_k b_{k-1})(a_{k-1} b_k; b_{k-1} a_0)(a_k b_k; b_{k-1} a_{k-1}) f_{k-1} + \alpha_0(\alpha_k + \beta_k) + \alpha_k \beta_k \\ &\quad + \sum_{j=1}^{k-1} \Big[\alpha_j \alpha_k (b_j a_0; a_j a_k) + \alpha_j \beta_k (b_j a_0; a_j b_k) + \alpha_k \beta_j (a_0 a_j; a_k b_j) + \beta_j \beta_k (a_0 a_j; b_k b_j)\Big], \\ g_L &:= \alpha_0 + \sum_{j=1}^{L} \Big[\alpha_j (b_j a_0; a_j b_0) + \beta_j (a_0 a_j; b_0 b_j)\Big], \end{aligned} \tag{3.4}$$

and $(xy;zw)$ denotes the cross-ratio

$$(xy;zw) := \frac{(x|y)(z|w)}{(x|z)(y|w)}\,. \tag{3.5}$$

The notation $(a|b) := (x_a - x_b)^2$ is intended to be suggestive of the embedding (or momentum-twistor) formalism.

We now specialize to three loops. Since each f_k is linear in every integration variable, we can take residues in β_1, β_2, and β_3 on the locus of $f_1 = f_2 = f_3 = 0$. This leaves a single factor in the denominator, which is a rational function of $\alpha_0, \alpha_1, \alpha_2$, and α_3. Performing one final residue in α_3, we obtain a square root of a polynomial with no repeated roots, $P_{\mathfrak{T}}(\alpha_0, \alpha_1, \alpha_2)$. This polynomial is degree six in α_0 and α_1 and degree four in α_2 (the latter fact motivated the authors of ref. [67] to put this polynomial into Weierstrass form with respect to α_2, which will here prove unnecessary). Importantly, it can be checked that $P_{\mathfrak{T}}$ is a *homogeneous* polynomial in α_0, α_1, and α_2 of (overall) degree six. Therefore, writing this hypersurface as

$$Q(x_1, x_2, x_3, y) = y^2 - P_{\mathfrak{T}}(x_1, x_2, x_3) = 0, \tag{3.6}$$

we identify it as a degree-six hypersurface in $\mathbb{WP}^{1,1,1,3}$. Generic surfaces of this type are well known to be K3 manifolds, which have Hodge diamond (2.8) and Euler characteristic 24. We include the original three-loop integrand (from eq. (3.3)) in MATHEMATICA format in the supplementary material `integrands_and_varieties.m`.

3.3 The three-loop wheel integral

The three-loop scalar wheel integral is drawn in momentum space and dual-momentum space in figure 3. Using the notation presented in the previous subsection, it is given by

$$\mathfrak{W}^{(3)} := \int \frac{d^4x_A d^4x_B d^4x_C \;\; (a_1|a_2)(b_1|b_2)(c_1|c_2)}{(A|C)(A|a_1)(A|a_2)(A|B)(B|b_1)(B|b_2)(B|C)(C|c_1)(C|c_2)}\,, \tag{3.7}$$

[7] Note that we have fixed a typo in f_k from the published version of ref. [67].

JHEP01(2020)078

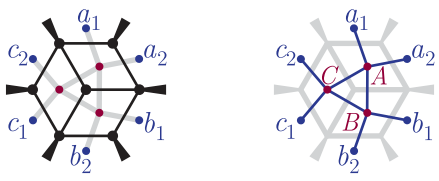

Figure 3. The three-loop wheel integral and its dual graph.

where we have included a numerator that renders it dual-conformally invariant. In appendix C, we derive an equivalent six-fold integral representation of this integral, following the strategy of refs. [67, 79, 81]. We quote the result here for convenience:

$$\mathfrak{W}^{(3)} = \int_0^\infty d^2\vec{\alpha}\, d^2\vec{\beta}\, d^2\vec{\gamma}\, \frac{n_0}{f_1\, f_2\, f_3}, \tag{3.8}$$

where

$$\begin{aligned}
n_0 &:= v_1(u_1u_2u_3v_1v_2v_3)\,,\\
f_1 &:= \alpha_1+\alpha_2+\alpha_1\alpha_2\,,\\
f_2 &:= \alpha_1(1+\alpha_2+\beta_1+\beta_2+\gamma_2)+\alpha_2(1+u_1w_2(w_3\beta_1+\beta_2)+\gamma_2)\\
&\quad +\beta_1v_1(1+u_1u_3v_2w_2\beta_2+\gamma_2)+u_2v_1(u_1v_3\gamma_1+\beta_2(1+\gamma_2))\,,\\
f_3 &:= (1+\alpha_2+\beta_1+\beta_2+\gamma_2)\Big[\alpha_1\Big(\gamma_1+\beta_2(1+\alpha_2+u_3v_1v_2\beta_1+\gamma_2)+w_3\beta_1(1+\alpha_2+\gamma_2)\Big)\\
&\quad +(1+\gamma_2)\big(w_3\alpha_2\beta_1+(\alpha_2+u_3v_1v_2\beta_1)\beta_2\big)\Big]+\gamma_1\Big[\alpha_2(1+u_1(w_3\beta_1+\beta_2)+\gamma_2)\\
&\quad +u_3v_1(u_2w_1\beta_2(1+\gamma_2)+\beta_1(1+u_1v_2\beta_2+\gamma_2))\Big]\,,
\end{aligned} \tag{3.9}$$

and where we have used the following basis of dual-conformal invariant cross-ratios:

$$\begin{aligned}
u_1 &:= (c_1a_1;a_2b_2)\,, \quad u_2 := (a_1b_1;b_2c_2)\,, \quad u_3 := (b_1c_1;c_2a_2)\,,\\
v_1 &:= (a_1a_2;b_1c_2)\,, \quad v_2 := (b_1b_2;c_1a_2)\,, \quad v_3 := (c_1c_2;a_1b_2)\,,\\
w_1 &:= (b_2c_1;c_2b_1)\,, \quad w_2 := (c_2a_1;a_2c_1)\,, \quad w_3 := (a_2b_1;b_2a_1)\,.
\end{aligned} \tag{3.10}$$

Note that the dihedral symmetry of $\mathfrak{W}^{(3)}$ acts quite naturally on these variables. Specifically, under the dihedral group that leaves the graph in figure 3 invariant, the u_i's, v_i's and w_i's each form a three-orbit. We include this integrand in MATHEMATICA format in the supplementary material `integrands_and_varieties.m`.

To analyze the geometry of $\mathfrak{W}^{(3)}$ (3.8), we first take three residues on the locus $f_i = 0$ by eliminating the variables α_1, β_2, and γ_1. We thereby obtain a three-form

$$\frac{d\alpha_2 d\beta_1 d\gamma_2}{\sqrt{P_{\mathfrak{W}}(\alpha_2,\beta_1,\gamma_2)}}, \tag{3.11}$$

where $P_{\mathfrak{W}}$ is a *non-homogeneous* polynomial. However, assigning α_2, β_1, and γ_2 all weight one, we can homogenize $P_{\mathfrak{W}}(\alpha_2,\beta_1,\gamma_2)$ by adding a fourth (auxiliary) weight-one coordinate

JHEP01(2020)078

x_4. The resulting homogeneous polynomial can be chosen to have overall degree eight, and we denote it $P^8_{\mathfrak{W}}(\alpha_2, \beta_1, \gamma_2, x_4)$. As it is rather long, we do not present this polynomial in the text, but we provide it in the supplementary material `integrands_and_varieties.m`. Finally, introducing a weight-four variable y with $y^2 = P^8_{\mathfrak{W}}(x_1, x_2, x_3, x_4)$, we obtain a three-form which can be expressed as

$$\omega_3 = \frac{x_4 dx_1 dx_2 dx_3}{y} \tag{3.12}$$

in the patch where x_4 is a non-vanishing constant.

Up to a numerical factor, the three-form ω_3 can be obtained from eq. (2.15) by taking the residue of

$$\frac{\Omega_4}{y^2 - P^8_{\mathfrak{W}}(x_1, x_2, x_3, x_4)} \tag{3.13}$$

at the locus defined by the vanishing of the denominator, where Ω_4 is the canonical four-form on $\mathbb{WP}^{1,1,1,1,4}$ given in eq. (2.14),

$$\begin{aligned}\Omega_4 = 4y dx_1 dx_2 dx_3 dx_4 + dy\Big(&- x_1 dx_2 dx_3 dx_4 + x_2 dx_1 dx_3 dx_4 \\ &- x_3 dx_1 dx_2 dx_4 + x_4 dx_1 dx_2 dx_3\Big).\end{aligned} \tag{3.14}$$

It follows that $Q(x_1, x_2, x_3, x_4, y) = y^2 - P^8_{\mathfrak{W}}(x_1, x_2, x_3, x_4) = 0$ defines a Calabi-Yau threefold in $\mathbb{WP}^{1,1,1,1,4}$. The polynomial $P^8_{\mathfrak{W}}$ has $\binom{8+3}{3} = 165$ coefficients, which can be parametrized by $\binom{8+3}{3} - 16 = 149$ complex structure moduli, but in our case they depend only on the nine cross-ratios in eq. (3.10). Hence, by varying these cross-ratios, we only explore a small part of the complex structure moduli space of our Calabi-Yau threefold.

Interesting kinematic limits. We start by considering the limit in which the legs at the rungs of the wheel become massless. This corresponds to the condition that the dual coordinates on either side of these legs become light-like separated, namely $(a_2|b_1) \to 0$, $(b_2|c_1) \to 0$, and $(c_2|a_1) \to 0$. In the variables (3.10), this sets all three parameters $w_i = 0$:

$$\big\{(a_2|b_1) \to 0,\ (b_2|c_1) \to 0,\ (c_2|a_1) \to 0\big\} \quad \Leftrightarrow \quad \big\{w_1 \to 0,\ w_2 \to 0,\ w_3 \to 0\big\} \tag{3.15}$$

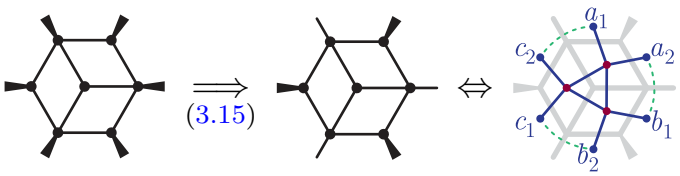

(3.16)

(Notice that we denote light-like separated points in the dual graph by dashed green lines.) It can be checked that the resulting integral is still a Calabi-Yau hypersurface in $\mathbb{WP}^{1,1,1,1,4}$.

To see this Calabi-Yau threefold factorize into simpler geometries, we now consider the limit in which one of these massless legs becomes soft. It can easily be checked that

JHEP01(2020)078

identifying $a_2 = b_1$ sets $u_3 = v_1 = v_2 = 1$:

$$\{u_3 \to 1,\ v_1 \to 1,\ v_2 \to 1,\ w_i \to 0\} \tag{3.17}$$

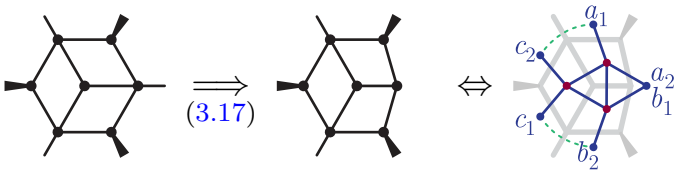

(3.18)

In this limit, $P(\alpha_2, \beta_1, \gamma_2)$ factorizes, and one of its factors is a perfect square. This allows us to take an additional residue. Continuing on in this fashion, we find we can take residues in all six integration variables; so from the residue analysis, there is no irreducible geometry. However, direct integration is obstructed after just a single integration; as we emphasized in section 3.1, these functions may appear to be more rigid under direct integration than their residue analysis would suggest.

It turns out this obstruction can be avoided by additionally setting $v_3 = 1$ (in this case our choice is purely pragmatic, and not particularly motivated by physics). On this kinematic slice, the integral evaluates to

$$\begin{aligned}
\frac{u_1 u_2}{u_1 - u_2}\Big\{ & G^{u_1}_{0,1,1,0,1,0} + G^{u_1}_{0,1,0,1,0,0} + G^{u_1}_{0,0,1,0,0,0} + G^{u_1}_{0,0,0,1,1,0} - G^{u_1}_{0,1,1,0,0,0} - G^{u_1}_{0,1,0,1,1,0} \\
& - G^{u_1}_{0,0,1,0,1,0} - G^{u_1}_{0,0,0,1,0,0} + G^{u_2}_{0}\Big(G^{u_1}_{1,1,0,0,0} + G^{u_1}_{1,0,1,1,0} + G^{u_1}_{0,1,0,1,0} + G^{u_1}_{0,0,1,0,0} \\
& - G^{u_1}_{1,1,0,1,0} - G^{u_1}_{1,0,1,0,0} - G^{u_1}_{0,1,0,0,0} - G^{u_1}_{0,0,1,1,0}\Big) + \Big(G^{u_2}_{1,0} - G^{u_2}_{0,0}\Big)\Big(G^{u_1}_{1,0,1,0} \\
& - G^{u_1}_{1,0,0,0} - G^{u_1}_{0,1,1,0} + G^{u_1}_{0,1,0,0}\Big) - \Big(G^{u_2}_{1,1,0} - G^{u_2}_{1,0,0}\Big)\Big(G^{u_1}_{0,1,0} - G^{u_1}_{0,0,0}\Big) \\
& + \zeta_2\Big[G^{u_1}_{1,0,0,0} + G^{u_1}_{0,1,0,1} + G^{u_1}_{0,0,1,0} - G^{u_1}_{1,0,1,0} - G^{u_1}_{0,1,0,0} - G^{u_1}_{0,0,0,1} \\
& \quad + G^{u_2}_{1}\Big(G^{u_1}_{0,1,0} - G^{u_1}_{0,0,0}\Big) - G^{u_2}_{0}\Big(G^{u_1}_{1,0,1} - G^{u_1}_{1,0,0} + G^{u_1}_{0,1,0} - G^{u_1}_{0,0,1}\Big) \\
& \quad + G^{u_2}_{1,0}\Big(G^{u_1}_{0,1} - G^{u_1}_{0,0}\Big) - G^{u_2}_{0,0}G^{u_1}_{0,1}\Big] + 2\zeta_3\Big[G^{u_1}_{1,0,0} - G^{u_1}_{1,1,0} - G^{u_1}_{0,1,1} + G^{u_1}_{0,0,1} \\
& + G^{u_2}_{1}\Big(G^{u_1}_{1,0} - G^{u_1}_{0,0}\Big) + G^{u_2}_{0}\Big(G^{u_1}_{1,1} - G^{u_1}_{0,1}\Big)\Big] - \frac{7}{5}\zeta_2^2\Big(G^{u_1}_{1,0} - G^{u_1}_{0,1} + G^{u_2}_{0}G^{u_1}_{1}\Big) \\
& + 4\,\zeta_2\,\zeta_3 G^{u_1}_{1}\Big\} + (u_1 \leftrightarrow u_2),
\end{aligned} \tag{3.19}$$

using the shorthand $G^{z}_{\vec{w}} \coloneqq G(\{\vec{w}\}, z)$. We also include this expression in the supplementary material `integrands_and_varieties.m`.

Further simplifications may be achieved by taking a second of the massless legs to be soft. Identifying $a_1 = c_2$ after taking the limit (3.17) additionally sets $u_2 = v_3 = 1$, making this integral the $u_2 \to 1$ limit of expression (3.19):

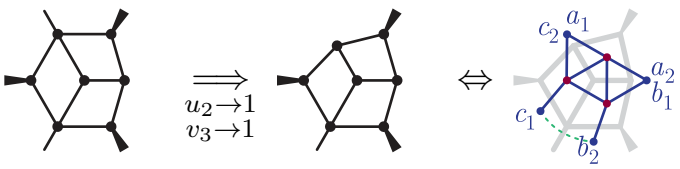

(3.20)

JHEP01(2020)078

where

$$
\begin{aligned}
= \frac{u_1}{1-u_1}\Big[\;& G^{u_1}_{0,1,1,0,0,0} + G^{u_1}_{0,1,0,1,1,0} + G^{u_1}_{0,0,1,0,1,0} + G^{u_1}_{0,0,0,1,0,0} \\
& - G^{u_1}_{0,1,1,0,1,0} - G^{u_1}_{0,1,0,1,0,0} - G^{u_1}_{0,0,1,0,0,0} - G^{u_1}_{0,0,0,1,1,0} \\
& + \zeta_2 \Big(G^{u_1}_{0,1,1,0} - G^{u_1}_{0,1,0,1} - G^{u_1}_{0,0,1,0} + G^{u_1}_{0,0,0,1} \Big) \\
& + 2\zeta_3 \Big(G^{u_1}_{0,1,1} + G^{u_1}_{0,1,0} - G^{u_1}_{0,0,1} - G^{u_1}_{0,0,0} \Big) - 6\zeta_4 \Big(G^{u_1}_{0,1} - G^{u_1}_{0,0} \Big) \\
& - 2(5\zeta_5 + \zeta_2\zeta_3) G^{u_1}_{0} + 4(\zeta_2^3 - \zeta_3^2) + 3\zeta_6 \Big] \,.
\end{aligned}
\tag{3.21}
$$

We also include this expression in the supplementary material `integrands_and_varieties.m`.

The last massless leg is removed by setting the final cross-ratio $u_1 = 1$:

(3.22)

In this limit, the integral evaluates to

$$= 20\zeta_5 . \tag{3.23}$$

This might naïvely be surprising, as one expects the three-loop wheel to have transcendental weight six. However, one can observe that the rational prefactor diverges in the $u_1 \to 1$ limit of expression (3.20); in order to take this limit one should therefore expand the polylogarithmic part of this function in a power series, which leads to a drop in weight [15, 107–114].

A three-parameter toy model. The three-loop wheel integral allows for a three-parameter toy model similar to that of the elliptic double-box [80]. This toy model is defined by taking all six dual-momentum points defining the three-loop wheel integral to be light-like separated in sequence. That is, we take

$$(a_1|b_2) = (b_2|c_1) = (c_1|a_2) = (a_2|b_1) = (b_1|c_2) = (c_2|a_1) = 0 \,. \tag{3.24}$$

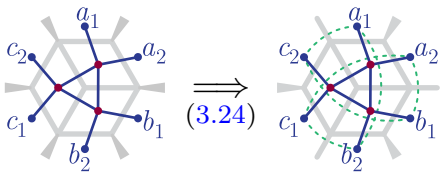

(3.25)

JHEP01(2020)078

In this limit, some of the rescalings of the Feynman parameters in our derivation become singular.[8] The cross-ratios chosen in eq. (3.10) also become problematic; individually we have $v_i, w_i \to 0$, $u_i \to \infty$, while the ratios

$$t_1 \coloneqq \frac{1}{u_1 v_2 v_3} = (b_1 c_1; b_2 c_2), \quad t_2 \coloneqq \frac{1}{u_2 v_3 v_1} = (a_1 c_1; a_2 c_2), \quad t_3 \coloneqq \frac{1}{u_3 v_1 v_2} = (a_1 b_1; a_2 b_2) \tag{3.27}$$

remain finite. Accounting for both of these issues, we find the six-fold integral representation becomes

$$\mathfrak{W}^{(3)} \underset{\substack{(3.26)\\(3.24)}}{\longmapsto} \mathfrak{W}^{\text{toy}} \coloneqq \int_0^\infty d^2\vec{\alpha}\; d^2\vec{\beta}\; d^2\vec{\gamma}\; \frac{1}{g_1\, g_2\, g_3}\,, \tag{3.28}$$

where

$$\begin{aligned} g_1 \coloneqq\;& \alpha_1{+}\alpha_2{+}\alpha_1\alpha_2\,, \\ g_2 \coloneqq\;& \alpha_1(1{+}\alpha_2{+}\beta_1{+}\gamma_2){+}(\alpha_2{+}\beta_2)(1{+}\gamma_2){+}\gamma_1\,, \\ g_3 \coloneqq\;& \alpha_1\beta_2(1{+}\alpha_2{+}\beta_1{+}\gamma_2)(\beta_1{+}t_3(1{+}\alpha_2{+}\gamma_2)){+}\gamma_1\big[t_1\beta_1(1{+}\gamma_2){+}t_2(t_3\alpha_2{+}\beta_1)\beta_2\big] \\ &{+}\beta_2(1{+}\alpha_2{+}\beta_1{+}\gamma_2)(t_3\alpha_2{+}\beta_1)(1{+}\gamma_2)\,, \end{aligned} \tag{3.29}$$

in terms of the cross-ratios (3.27).

As before, we can take residues in α_1, β_2, and γ_1, obtaining a non-homogeneous curve $P^{\text{toy}}_{\mathfrak{W}}(\alpha_2, \beta_1, \gamma_2) = P^{\text{toy}}_{\mathfrak{W}}(x_1, x_2, x_3)$ that we can then homogenize with an auxiliary variable x_4. The resulting degree-eight polynomial is

$$\begin{aligned} P^{8,\text{toy}}_{\mathfrak{W}} = \Big[&x_2(x_1^2 x_3 - x_1 x_2 x_4)t_2 + x_1^2\big(x_1 x_3(t_2-1) - (x_2+x_3)x_3 - (x_2 t_2 + x_3)x_4\big)t_3 \\ &- x_2(x_1+x_2+x_3+x_4)(x_1 x_3 + (x_3+x_4)x_4)\Big]^2 - 2t_1 x_2 (x_1+x_4)(x_3+x_4)^2 \\ &\times \Big[(x_1+x_2+x_3+x_4)\big(x_1^2\, x_3\, t_3 + x_1 x_2 x_3 + x_2 x_4(x_3+x_4)\big) \\ &+ t_2 x_1(x_1 t_3 + x_2)(x_1 x_3 - x_2 x_4)\Big] + t_1^2 x_2^2 (x_1+x_4)^2 (x_3+x_4)^4\,. \end{aligned} \tag{3.30}$$

We include both the toy model integrand and the above hypersurface in MATHEMATICA format in the supplementary material `integrands_and_varieties.m`.

We pause here to highlight that it is possible to see this polynomial factorize into simpler polynomials in simple kinematic limits. Despite its presentation, the toy model's *geometry* must be invariant under permutations of t_1, t_2, and t_3; thus, we may consider taking limits in any variable. However, these limits can naïvely look different; for instance,

[8] Concretely, the rescalings of the Feynman parameters β_2 taken in eq. (C.19) and those for γ_i in eq. (C.24) are singular in the limit (3.24). However, this observation clearly signals how these problems can be remedied: to access this limit smoothly from our previous expression (C.25), we merely need to rescale

$$\begin{aligned} &\beta_2 \mapsto \beta_2 \frac{(a_1|b_2)(a_2|c_2)}{(a_1|a_2)(b_2|c_2)}, \quad \gamma_1 \mapsto \gamma_1 \frac{(a_2|c_1)(b_2|c_2)}{(a_2|b_2)(c_1|c_2)}, \\ &\gamma_2 \mapsto \gamma_2 \frac{(a_1|a_2)(b_2|c_2)}{(a_1|b_2)(a_2|c_2)}, \quad \gamma_3 \mapsto 1 \times \frac{(a_1|a_2)(b_2|c_2)}{(a_1|b_2)(a_2|c_2)}\,, \end{aligned} \tag{3.26}$$

take into account the relevant Jacobians, and collect terms. After this has been done, the limit (3.24) can be taken smoothly.

JHEP01(2020)078

if we set $t_1 \to 0$ or $t_2 \to 0$, the polynomial becomes a perfect square of a polynomial with overall degree four, while in the limit $t_3 \to 0$ it factorizes into x_2^2 times a polynomial of overall degree six. By symmetry, the irreducible geometry in each of these limits must be the same. In the first case (taking the limit in either t_1 or t_2), the resulting (squared) polynomial has degree three in x_1 and x_4, and degree two in x_2 and x_3. This lets us perform an additional residue in either x_2 or x_3, by which we obtain a square root of a polynomial of overall degree six. In the second case (taking the limit in t_3) we instead take a residue at $x_2 = 0$, after which the remaining polynomial has overall degree six. Both of the resulting polynomials define a K3, although it is not easy to see that they describe the same geometry (i.e. that they correspond to different parametrizations of the same hypersurface).

If we take an additional cross-ratio to zero, the curve degenerates again. It becomes a square of a polynomial that is cubic in one variable and quadratic in the remaining two. This allows an additional residue in one of the quadratic variables, giving rise to a square root of a quadratic polynomial in the remaining two variables. Such square roots are rationalizable under a change of variables, so the integral should be polylogarithmic in this limit.

4 Open problems at four loops and beyond

Having shown that the three-loop traintrack and wheel both involve Calabi-Yau hypersurfaces that can be embedded in $\mathbb{WP}^{1,\ldots,1,k}$, it is natural to ask whether their four-loop counterparts also involve such hypersurfaces.

The four-loop traintrack. Equations (3.3) and (3.4) provide an eight-fold integral representation of the four-loop traintrack integral (which we again provide in MATHEMATICA format in the supplementary material `integrands_and_varieties.m`). We can analyze the residues of this integral in the same way as was done for the three-loop integrals in the last section, to see if it contains a Calabi-Yau hypersurface in $\mathbb{WP}^{1,\ldots,1,k}$. Here we can take four residues, in $\beta_1, \beta_2, \beta_3$, and β_4, on the locus $f_1 = f_2 = f_3 = f_4 = 0$, then one final residue in α_4 on $g_4 = 0$ to obtain a square root of a polynomial $P^{(4)}_{\mathfrak{T}}(\alpha_0, \alpha_1, \alpha_2, \alpha_3)$ with no repeated roots. This polynomial is homogeneous, but has overall degree *ten*. It is degree ten in α_0 and α_1, degree six in α_2, and degree four in α_3. Taking other sequences of residues also result in degree ten, twelve, or sixteen polynomials.

As $P^{(4)}_{\mathfrak{T}}(\alpha_0, \alpha_1, \alpha_2, \alpha_3)$ has degree ten, $y^2 - P^{(4)}_{\mathfrak{T}}(\alpha_0, \alpha_1, \alpha_2, \alpha_3) = 0$ cannot be embedded in $\mathbb{WP}^{1,1,1,1,4}$. It can be embedded in weighted projective space $\mathbb{WP}^{1,1,1,1,5}$, but this does not satisfy the Calabi-Yau condition. We currently know of no way to embed this variety in a weighted projective space so that it satisfies the Calabi-Yau condition.

JHEP01(2020)078

The four-loop wheel. The four-loop scalar wheel (or 'window') integral, $\mathfrak{W}^{(4)}$, may be drawn in momentum space and dual-momentum space as

$$\mathfrak{W}^{(4)} \coloneqq$$ 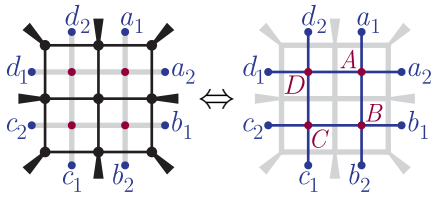 (4.1)

$$= \int \frac{d^4x_A d^4x_B d^4x_C d^4x_D \quad (a_1|a_2)(b_1|b_2)(c_1|c_2)(d_1|d_2)}{(D|A)(A|a_1)(A|a_2)(A|B)(B|b_1)(B|b_2)(B|C)(C|c_1)(C|c_2)(C|D)(D|d_1)(D|d_2)}\,, \tag{4.2}$$

where in the last line we have written the integral explicitly in dual-momentum space. We derive a manifestly dual-conformally invariant integral representation of the four-loop wheel integral in general kinematics in appendix D, finding

$$\mathfrak{W}^{(4)} = \int_0^\infty d^2\vec{\alpha}\; d^2\vec{\beta}\; d^2\vec{\gamma}\; d^3\vec{\delta} \frac{n_0}{f_1\, f_2\, f_3} \left(\frac{n_1}{f_2} + \frac{n_2}{f_3}\right). \tag{4.3}$$

The expressions for n_0, n_1, n_2, f_1, f_2, and f_3 are lengthy, but are given in MATHEMATICA format in the supplementary material `integrands_and_varieties.m`.

Unfortunately, this expression is a *nine*-fold integral, while considerations of transcendental weight suggest that it should be possible to write down an eight-fold representation. This has direct consequences for the validity of our residue analysis. In particular, it means that we cannot directly associate the number of remaining integration parameters after taking a maximum number of residues with the dimension of an irreducible geometry. With this proviso in mind, we can take residues in $\alpha_1, \delta_1, \beta_1$, and α_2, leaving a quartic with no repeated roots in five (non-projective) variables. This means that the geometry is at most a fivefold hypersurface, but could be of lower dimension. Without an eight-fold integral representation, we cannot distinguish these possibilities.

This integral has several limits with applications to integrable theories, which would make it particularly interesting to compute. We discuss these limits (some of which are polylogarithmic), as well as a nine-parameter toy model similar to the three-loop toy model (3.24), in appendix D.1.

Further directions. There are many open questions regarding the types of varieties that appear in Feynman integrals. While an increasingly large number of examples have now been identified to be Calabi-Yau, it remains unclear whether all such varieties have this property (and what this tells us about Feynman integrals in general).[9] In this paper, we have identified two further examples of Calabi-Yaus that can be realized as hypersurfaces in the weighted projective space $\mathbb{WP}^{1,\ldots,1,k}$ and have characterized hypersurfaces of this type in a number of ways. However, it again remains unclear how universal this property

[9]The Calabi-Yau condition in the embedding we are considering restricts the degree of the defining polynomial; since we can deprojectivize and reprojectivize to increase the degree, it is effectively an upper bound. Thus, Calabi-Yaus are the first class one naturally encounters.

JHEP01(2020)078

might be, and what it encodes about these specific Feynman graphs. To better connect the properties of these varieties to the physics encoded in Feynman diagrams, it may prove necessary to move to a differential equation approach [53, 70, 92, 93, 115].

There remains a great deal of technology to be developed before the integrals that we consider might be 'computed'. It should be possible, for instance, to develop special functions analogous to the elliptic multiple polylogarithms [41, 48, 51, 52, 54, 56], in terms of which these integrals could be evaluated. In particular, a coaction of the type that has proven useful in the polylogarithmic [9, 31, 33, 34] and elliptic cases [54] should also exist for such functions [116]. It should also be possible to develop iterated integral representations involving the relevant Calabi-Yau geometries, akin to what has been done for instance in refs. [41, 59]. Developing a better understanding of these spaces of functions is sure to lead to new surprises and simplifications, as has happened in the case of polylogarithmic and elliptic Feynman integrals over the last few years.

Acknowledgments

We are grateful to Chuck Doran and Pierre Vanhove for useful discussions, and to Philip Candelas and Yinan Wang for involvement in earlier stages of this work. We are also indebted to insightful comments from Gregory Korchemsky about the relevance of $\mathfrak{W}^{(4)}$ to the conformal fishnet theory, and to Miguel Paulos for discussions about Feynman parametrization and for encouraging us in particular to find a conformal parametric representation of $\mathfrak{W}^{(4)}$. This work was supported in part by the Danish Independent Research Fund under grant number DFF-4002-00037 (MV, MW), the Danish National Research Foundation (DNRF91), the research grant 00015369 from Villum Fonden, a Starting Grant (No. 757978) from the European Research Council (JLB,AJM,MV,MvH,MW), the European Union's Horizon 2020 research and innovation program under grant agreement No. 793151 (MvH), a Carlsberg Postdoctoral Fellowship (CF18-0641) (AJM), and the research grant 00025445 from Villum Fonden (MW). Finally, JLB, AJM and MvH are grateful for the hospitality of the Aspen Center for Physics, which is supported by National Science Foundation grant PHY-1607611.

A Desingularization by complex structure deformation

The varieties we encounter when doing Feynman integrals are typically singular; they may have singularities at fixed points in the Feynman parameters or at points which vary with the external kinematics. To define a smooth variety, we deform the polynomial(s) that define the variety. In practice, this amounts to adding new monomials and changing the values of the coefficients already present. Such deformations turn out to be *complex structure* deformations.

One may worry that, even after performing such deformations, we do not obtain a smooth variety. At this point, we may invoke the Bertini theorem (see for example ref. [94] for a textbook presentation).

JHEP01(2020)078

Theorem 1 (Bertini) *Given a compact complex manifold X and a holomorphic line bundle L over X such that at every point $x \in X$ the line bundle L has at least one non-zero section, then the points where a generic section f of L vanishes define a smooth hypersurface $M = f^{-1}(0)$.*

One way we can apply this theorem is to take the embedding space to be $\mathbb{P}^n$, and L to be a holomorphic line bundle whose sections are homogeneous polynomials of degree d. Then the Bertini theorem assures us that for a generic section f of L i.e. for almost every choice of values for the coefficients of a homogeneous degree d polynomial, the variety defined by $\{x \in \mathbb{P}^n \mid f(x) = 0\}$ is smooth.

In the following, we will apply reasoning analogous to the Bertini theorem to embeddings in a weighted projective space of type $\mathbb{WP}^{1,\ldots,1,k}$. Strictly speaking, the conditions of the Bertini theorem are not satisfied since the embedding space itself has a singularity. If the singularity were to have dimension one or larger, then it would generically intersect any hypersurface, and the hypersurface would inherit the singularity.

However, in the case of $\mathbb{WP}^{1,\ldots,1,k}$, the singularity arises at just the point with homogeneous coordinates $(0,\ldots,0,1)$. As a result, in the neighborhood of this point we need to make the identifications

$$(x_1,\ldots,x_k,1) \simeq (\xi x_1,\ldots,\xi x_k,1), \tag{A.1}$$

where ξ is a k-th root of unity. Since the singularity arises at only a single point, a codimension-one hypersurface will not generically contain it. (Moreover, we can explicitly check to see if this happens). In fact, even if our variety contains this singularity, we may define a resolution and compute its Euler characteristic using for example eq. (5.1.14) of ref. [94].

B Hodge numbers and Euler characteristic

B.1 Euler characteristic

One way to compute the Euler characteristic is to integrate the top Chern class over the manifold. We may obtain the Chern classes of an embedded hypersurface from the Chern classes of the embedding manifold and some data about the embedding. There are several good presentations of this material in the literature (see for example refs. [94, 117]), so we will be brief.

Given a bundle E, the total Chern class $c(E)$ is the sum of all Chern classes of all degrees. Given an exact sequence of bundles $0 \to A \to B \to C \to 0$, we have $c(B) = c(A) \wedge c(C)$. Using this fact, we conclude that the Chern class of a weighted projective space with weights $(w_0,\ldots,w_n)$ is

$$c(\mathbb{WP}^{w_0,\ldots,w_n}) = \prod_{i=0}^{n}(1 + w_i J), \tag{B.1}$$

where $J = c_1(\mathcal{O}(1))$ is the first Chern class of the bundle $\mathcal{O}(1)$ whose sections are polynomials of homogeneity one. Depending on the weights w_i, this bundle may not exist as

JHEP01(2020)078

a holomorphic bundle on $\mathbb{WP}^{w_0,\ldots,w_n}$, but can nevertheless be used as a building block for other bundles.

We can define a codimension-m variety Y as the vanishing locus of m homogeneous polynomials of degrees d_i, for $i = 1, \ldots, m$. Then, the Chern class of Y is

$$c(Y) = \frac{\prod_{i=0}^{n}(1 + w_i J)}{\prod_{r=1}^{m}(1 + d_r J)}. \tag{B.2}$$

In this case, the Calabi-Yau condition reads

$$\sum_{i=0}^{n} w_i = \sum_{r=1}^{m} d_r. \tag{B.3}$$

Then the Euler characteristic is

$$\chi(Y_{n-m}) = \int_Y c_{n-m} = \prod_{r=1}^{m} d_r \int_{\mathbb{WP}^{w_0,\ldots,w_n}} c_{n-m} J^m, \tag{B.4}$$

where we have extended the integral from Y to the full $\mathbb{WP}^{w_0,\ldots,w_n}$ by wedging with a form that encodes the contribution of the normal.

For our explicit examples of a codimension-one variety X in $\mathbb{WP}^{1,\ldots,1,k}$, we have the Chern class

$$c(X) = \frac{(1 + J)^k (1 + kJ)}{1 + 2kJ}, \tag{B.5}$$

while the Euler characteristic is

$$\chi(X_{k-1}) = \int_X c_{k-1}(X_{k-1}) = \int_{\mathbb{WP}^{1,\ldots,1,k}} 2kJ \wedge c_{k-1}(X_{k-1}). \tag{B.6}$$

The final piece of information we need is $\int_{\mathbb{WP}^{1,\ldots,1,k}} J^k = \frac{1}{k}$ because it corresponds to the intersection of k hyperplanes at the singular point $(0, \ldots, 0, 1)$, which has a cyclic singularity of order k.

Using this normalization, and the expression for c_{k-1} obtained by expanding the ratio of polynomials in J,

$$c_{k-1}(X_{k-1}) = \frac{1}{4k}\left(1 - (1 - 2k)^k + 2k^2\right) J^{k-1}, \tag{B.7}$$

we eventually find

$$\chi(X_{k-1}) = \frac{1 - (1 - 2k)^k + 2k^2}{2k}. \tag{B.8}$$

We have tabulated the Euler characteristic for the first few values of k in table 1.

JHEP01(2020)078

B.2 Index theorems

We can also compute further combinations of Hodge numbers as a cross-check using various index theorems. In particular, we have

$$\chi(X_{k-1}) = \sum_r (-1)^r \dim H^r_{dR}(X) = \int_X c_{k-1}(X_{k-1}), \tag{B.9}$$

$$\chi_h(X_{k-1}) = \sum_q (-1)^q \dim H^{0,q}_{\bar\partial}(X_{k-1}) = \int_X td_{k-1}(X_{k-1}), \tag{B.10}$$

$$\tau_H(X_{k-1}) = \sum_{p,q} (-1)^q \dim H^{p,q}_{\bar\partial}(X_{k-1}) = \int_X L_{k-1}(X_{k-1}), \tag{B.11}$$

where χ_h is the arithmetic genus and τ_H is the Hirzebruch signature. Also, td is the Todd class and L is the Hirzebruch polynomial. We present just the final answers for these computations:

$$k = 3: \qquad \chi_h = 2, \qquad \tau_H = -16, \tag{B.12}$$

$$k = 4: \qquad \chi_h = 0, \qquad \tau_H = 0, \tag{B.13}$$

$$k = 5: \qquad \chi_h = 2, \qquad \tau_H = 2002. \tag{B.14}$$

The reader can easily check that these values are consistent with the Hodge diamonds presented in section 2.

B.3 Lefschetz hyperplane theorem

The cohomology of a hypersurface is strongly constrained by the cohomology of the embedding space. The Lefschetz-Bott theorem characterizes the connections between these cohomology groups. We follow the presentations in ref. [94] (see theorem 1.4 on page 44).

In the Lefschetz-Bott theorem, we are given a complex compact manifold X of dimension $n+1$ and a positive line bundle $\mathcal{L}$ over X. Then, given a holomorphic section λ, we denote by $\lambda^{-1}(0)$ the points of X where λ vanishes. We then have[10]

$$H_q(\lambda^{-1}(0), \mathbb{Z}) \simeq H_q(X, \mathbb{Z}), \qquad q \neq n, \tag{B.15}$$

$$H_n(\lambda^{-1}(0), \mathbb{Z}) \to H_n(X, \mathbb{Z}), \tag{B.16}$$

where the last map is surjective. Dualizing to cohomology and using the Hodge decomposition (and the fact that (p,q)-forms pull back to (p,q)-forms), we obtain the result for cohomology. We can also use the Lefschetz-Bott theorem to constrain the cohomology of complete intersections in projective spaces, by repeated application of the theorem.

Stated concretely, equations (B.15) and (B.16) tell us that the upper and lower rows of the Hodge diamonds that describe our Calabi-Yau hypersurfaces are inherited directly from $\mathbb{WP}^{1,\ldots,1,k}$, while its middle row can involve numbers greater than or equal to those describing $\mathbb{WP}^{1,\ldots,1,k}$. Interestingly, this means the Hodge numbers of these hypersurfaces

[10] In fact, the result is more general and holds for homotopy groups. The version for homology is listed as a corollary, presumably by an application of the Hurewicz theorem.

JHEP01(2020)078

could also arise from a codimension-one embedding in unweighted projective space, which has Hodge numbers $h^{p,q}(\mathbb{P}^k) = \delta_{p,q}$. (We do not, however, know how to realize our Calabi-Yau hypersurfaces as embeddings in unweighted projective space.)

C Feynman parametrization of the three-loop wheel

In this appendix, we describe the concrete steps by which the three-loop wheel

$\mathfrak{W}^{(3)}$ $\Leftrightarrow$ 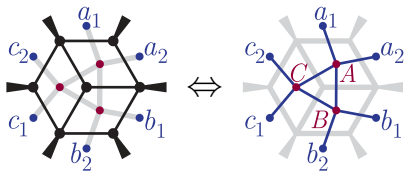 $\Leftrightarrow$, (C.1)

defined in eq. (3.7) and discussed at length in section 3.3, can be expressed as a *rational* and *manifestly conformal* integral. This form was quoted in eq. (3.8).

Provided only a mild degree of cleverness, it is not hard to Feynman-parametrize and integrate each of the loop variables. This is especially true for (any choice of) the first two integrations, which are easily seen to be conformal box integrals. Let us briefly review the mechanics of how those integrals may be performed before applying these techniques to the integral in question.

***Review*: conformal box integrals in the embedding formalism.** For the sake of reference and for those readers less familiar with the embedding formalism, let us recall that the box integral

$$\int d^4x_\ell \, \frac{1}{(\ell|x_1)(\ell|x_2)(\ell|x_3)(\ell|x_4)} \tag{C.2}$$

can be Feynman-parametrized by introducing

$$|\mathcal{Y}) \coloneqq \alpha_1|x_1) + \alpha_2|x_2) + \alpha_3|x_3) + \alpha_4|x_4) \tag{C.3}$$

so that the second Symanzik polynomial $\mathscr{F}$ may be written as

$$\mathscr{F} = \sum_{i\leq j}^{4} \alpha_i\alpha_j(x_i|x_j) = \frac{1}{2}(\mathcal{Y}|\mathcal{Y}) =: (\mathcal{Y}\mathcal{Y}), \tag{C.4}$$

upon which the Feynman integral (C.2) becomes

$$\int d^4x_\ell \, \frac{1}{(\ell|x_1)(\ell|x_2)(\ell|x_3)(\ell|x_4)} \propto \int_0^\infty \big[d^3\vec{\alpha}\big] \, \frac{1}{(\mathcal{Y}\mathcal{Y})^2} \, . \tag{C.5}$$

Above, we have used the notation $\big[d^k\vec{\alpha}\big]$ to denote the volume form on $\mathbb{P}^k$ as expressed in terms of homogeneous coordinates $(\alpha_1, \alpha_2, \ldots, \alpha_{k+1})$. Specifically,

$$\big[d^k\vec{\alpha}\big] \coloneqq d\alpha_1 \cdots d\alpha_{k+1} \, \delta\big(\alpha_i - 1\big) \tag{C.6}$$

JHEP01(2020)078

for any α_i. The attentive reader will notice that Feynman's own de-projectivization prescription, $d\alpha_1 \cdots d\alpha_{k+1}\, \delta\big(\sum_i \alpha_i - 1\big)$, is related to that in eq. (C.6) by a change of variables with unit Jacobian and which preserves the domain of integration, $\alpha_i \in [0, \infty]$.

Provided that there is at least one point $|a_i)$ such that $(a_i|a_i) = 0$, then $(\mathcal{Y}\!\upharpoonright\!\mathcal{Y})$ will be linear in its Feynman parameter α_i. When this happens, this Feynman parameter can be trivially integrated rationally. If the reader will forgive us for being somewhat pedantic, suppose that $|\mathcal{Y})$ may be written of the form

$$|\mathcal{Y}) =: |\mathcal{Q}) + \eta|q) \tag{C.7}$$

for any $|q)$ such that $(q|q) = 0$ and for any $\eta \in \{\alpha_1, \ldots\}$; then

$$(\mathcal{Y}\!\upharpoonright\!\mathcal{Y}) = (\mathcal{Q}\!\upharpoonright\!\mathcal{Q}) + \eta(\mathcal{Q}|q)\,, \tag{C.8}$$

and

$$\int_0^\infty [d^3\vec{\alpha}]\, \frac{1}{(\mathcal{Y}\!\upharpoonright\!\mathcal{Y})^2} = \int_0^\infty [d^2\vec{\alpha}] \int_0^\infty d\eta\, \frac{1}{\big[(\mathcal{Q}\!\upharpoonright\!\mathcal{Q}) + \eta(\mathcal{Q}|q)\big]^2} = \int_0^\infty [d^2\vec{\alpha}]\, \frac{1}{(\mathcal{Q}\!\upharpoonright\!\mathcal{Q})(\mathcal{Q}|q)}\,. \tag{C.9}$$

The Feynman parametrization of the three-loop wheel integral follows directly from iteration of the above steps (with only mild cleverness at the end).

The Feynman parametrization of the wheel integral $\mathfrak{W}^{(3)}$. Let us begin with the (dual-momentum-)space-time definition of the wheel:

$$\mathfrak{W}^{(3)} \coloneqq \int \frac{d^4x_A d^4x_B d^4x_C \;\; (a_1|a_2)(b_1|b_2)(c_1|c_2)}{(A|C)(A|a_1)(A|a_2)(A|B)(B|b_1)(B|b_2)(B|C)(C|c_1)(C|c_2)}\,. \tag{C.10}$$

We have used embedding-formalism-motivated notation to denote the squared-differences of points in dual-momentum space — i.e., $(a_1|a_2) \coloneqq (\vec{a}_1 - \vec{a}_2)^2$. Notice that all the points in dual-momentum space appearing in eq. (C.10) — both those being integrated and those defining the external kinematics — satisfy $(x|x) = 0$.

Let us begin with the integration over the loop momentum x_A. It is not hard to see that this part of the integral is trivially identical to the box integral just discussed. Thus, we may introduce

$$|\mathcal{Y}_A) \coloneqq \alpha_1|a_1) + \alpha_2|a_2) + \alpha_3|C) + \eta_A|B) =: |\mathcal{Q}_A) + \eta_A|B) \tag{C.11}$$

and perform the integral over x_A and η_A to arrive at

$$\mathfrak{W}^{(3)} = \int_0^\infty [d^2\vec{\alpha}] \int \frac{d^4x_B d^4x_C \;\; (a_1|a_2)(b_1|b_2)(c_1|c_2)}{(\mathcal{Q}_A\!\upharpoonright\!\mathcal{Q}_A)(B|\mathcal{Q}_A)(B|b_1)(B|b_2)(B|C)(C|c_1)(C|c_2)}\,. \tag{C.12}$$

Now, as with x_A, the integral over x_B in eq. (C.12) is just an ordinary conformal box integral. The only minor novelty is that one of the 'propagators' of this integral, $(B|\mathcal{Q}_A)$, involves a 'non-simple' point in embedding space — one for which $(\mathcal{Q}_A|\mathcal{Q}_A) \neq 0$. This does not actually cause any trouble, however, because the Symanzik formalism defining

JHEP01(2020)078

the inner product $(\cdot|\cdot)$ in eq. (C.4) did not require the points to be simple. (The simplicity of the external points only played a role in making it trivial to integrate out one Feynman parameter rationally.) Thus, we may introduce

$$|\mathcal{Y}_B) \coloneqq \beta_1|b_1) + \beta_2|b_2) + \beta_3|\mathcal{Q}_A) + \eta_B|C) =: |\mathcal{Q}_B) + \eta_B|C) \tag{C.13}$$

and integrate over x_B and η_B to arrive at

$$\mathfrak{W}^{(3)} = \int_0^\infty \left[d^2\vec{\alpha}\right]\left[d^2\vec{\beta}\right] \int \frac{d^4x_C \;\; (a_1|a_2)(b_1|b_2)(c_1|c_2)}{(\mathcal{Q}_A\overset{\backprime}{|}\mathcal{Q}_A)(\mathcal{Q}_B\overset{\backprime}{|}\mathcal{Q}_B)(C|\mathcal{Q}_B)(C|c_1)(C|c_2)} \,. \tag{C.14}$$

The careful reader should now be mildly worried as the integral over x_C in eq. (C.14) is not at all a recognizable (box) integral. Even worse: it is not even manifestly conformal in x_C! To appreciate the magnitude of this problem, notice that the factor $(\mathcal{Q}_A|\mathcal{Q}_A)$ in the denominator of eq. (C.14) involves a *sum* of terms with *different* conformal weights:

$$(\mathcal{Q}_A\overset{\backprime}{|}\mathcal{Q}_A) = \alpha_1\alpha_2(a_1|a_2) + \alpha_1\alpha_3(C|a_1) + \alpha_2\alpha_3(C|a_2) \,. \tag{C.15}$$

Restoring conformality of this term turns out to be relatively easy. Consider rescaling the Feynman parameters α_i according to[11]

$$\alpha_1 \mapsto \alpha_1(C|a_2) \,, \quad \alpha_2 \mapsto \alpha_2(C|a_1) \,, \quad \alpha_3 \mapsto (a_1|a_2) \,. \tag{C.16}$$

Notice that we are actually eliminating the projective redundancy of $\left[d^2\vec{\alpha}\right]$ by fixing $\alpha_3 \mapsto (a_1|a_2)$. (This is just done for notational compactness going forward.)

Under this rescaling,

$$(\mathcal{Q}_A\overset{\backprime}{|}\mathcal{Q}_A) \underset{\text{(C.16)}}{\longmapsto} (a_1|a_2)(C|a_1)(C|a_2)\big(\alpha_1 + \alpha_2 + \alpha_1\alpha_2\big) \,. \tag{C.17}$$

The prefactor of eq. (C.17) cancels precisely against the Jacobian from eq. (C.16), resulting in

$$\mathfrak{W}^{(3)} \underset{\text{(C.16)}}{\longmapsto} \int_0^\infty d^2\vec{\alpha}\left[d^2\vec{\beta}\right] \int \frac{d^4x_C \;\; (a_1|a_2)(b_1|b_2)(c_1|c_2)}{(\alpha_1 + \alpha_2 + \alpha_1\alpha_2)(\mathcal{Q}_B\overset{\backprime}{|}\mathcal{Q}_B)(C|\mathcal{Q}_B)(C|c_1)(C|c_2)} \,. \tag{C.18}$$

We have certainly improved the situation with respect to the x_C integration, but not entirely. Notice, for example, that under the rescaling (C.16), $(\mathcal{Q}_B|\mathcal{Q}_B)$ becomes an irreducible (and inhomogeneous!) degree-two polynomial in $|C)$. (This is trivial to see, considering eq. (C.17), and $(\mathcal{Q}_B|\mathcal{Q}_B) = (\mathcal{Q}_A|\mathcal{Q}_A) + \ldots$.)

In fact, this problem can be remedied without too much hassle. Upon rescaling the β_i's according to

$$\beta_1 \mapsto \beta_1\frac{(C|a_1)(a_1|a_2)}{(a_1|b_1)} \,, \quad \beta_2 \mapsto \beta_2\frac{(C|a_1)(a_1|a_2)}{(a_1|b_2)} \,, \quad \beta_3 \mapsto 1 \,, \tag{C.19}$$

[11] We hope the reader can forgive the abuse of notation in using the same variables α_i to label the integration parameters before and after the rescaling.

JHEP01(2020)078

and taking into account the corresponding Jacobian, the reader may verify that eq. (C.18) takes the form

$$\mathfrak{W}^{(3)} \underset{\text{(C.19)}}{\longmapsto} \int_0^\infty d^2\vec{\alpha}\; d^2\vec{\beta} \int \frac{d^4x_C \;\; (a_1|a_2)^2(b_1|b_2)(c_1|c_2)/(a_1|b_1)}{(\alpha_1+\alpha_2+\alpha_1\alpha_2)(C|\mathcal{R})(C|\mathcal{S})(C|c_1)(C|c_2)}\,, \tag{C.20}$$

where we have defined the 'propagators' $(C|\mathcal{R}), (C|\mathcal{S})$ according to

$$\begin{aligned}
|\mathcal{R}) &:= \; |a_2)(\alpha_1+\alpha_2) + |b_1)\beta_1\frac{(a_1|a_2)}{(a_1|b_1)} + |b_2)\beta_2\frac{(a_1|a_2)}{(a_1|b_2)}\,,\\
|\mathcal{S}) &:= \; |\mathcal{R})(a_1|b_2) + |a_1)\left[\alpha_2\beta_1\frac{(a_1|b_2)(a_2|b_1)}{(a_1|b_1)} + \alpha_2\beta_2(a_2|b_2) + \beta_1\beta_2\frac{(a_1|a_2)(b_1|b_2)}{(a_1|b_1)}\right]\\
&\quad + |a_2)\Big[\alpha_1(\alpha_2+\beta_1+\beta_2)(a_1|b_2)\Big]\,.
\end{aligned} \tag{C.21}$$

Although these new propagators are not especially simple, we may now observe that eq. (C.20) is a standard conformal box integral with respect to x_C(!). As such, our discussion above can be immediately applied. We merely introduce

$$|\mathcal{Y}_C) := \gamma_1|c_1) + \gamma_2|\mathcal{R}) + \gamma_3|\mathcal{S}) + \eta_C|c_2) =: |\mathcal{Q}_C) + \eta_C|c_2)\,, \tag{C.22}$$

and integrate over x_C and η_C to find

$$\mathfrak{W}^{(3)} \;= \int_0^\infty d^2\vec{\alpha}\; d^2\vec{\beta}\big[d^2\vec{\gamma}\big] \;\; \frac{(a_1|a_2)^2(b_1|b_2)(c_1|c_2)/(a_1|b_1)}{(\alpha_1+\alpha_2+\alpha_1\alpha_2)(\mathcal{Q}_C|c_2)(\mathcal{Q}_C\,\overleftarrow{\partial}\,\mathcal{Q}_C)}\,. \tag{C.23}$$

We are essentially done. However, the representation (C.23) is still not manifestly conformal in the external points. This can be quickly remedied. All we need to do is rescale the γ_i Feynman parameters so that $|\mathcal{Q}_C)$ in eq. (C.22) becomes uniform in weight. This can be achieved by rescaling them according to

$$\gamma_1 \mapsto \gamma_1\frac{(a_1|a_2)(a_2|b_2)}{(a_2|c_1)}\,, \quad \gamma_2 \mapsto \gamma_2(a_1|b_2)\,, \quad \gamma_3 \mapsto 1\,. \tag{C.24}$$

Upon including the Jacobian, gathering terms, and some minor simplifications, we obtain the formula quoted in eq. (3.8) — namely, eq. (C.23) becomes

$$\mathfrak{W}^{(3)} \underset{\text{(C.24)}}{\longmapsto} \int_0^\infty d^2\vec{\alpha}\; d^2\vec{\beta}\; d^2\vec{\gamma}\;\; \frac{n_0}{f_1\, f_2\, f_3}\,, \tag{C.25}$$

where

$$\begin{aligned}
n_0 &:= \; v_1(u_1u_2u_3v_1v_2v_3)\,,\\
f_1 &:= \; \alpha_1+\alpha_2+\alpha_1\alpha_2\,,\\
f_2 &:= \; \alpha_1(1+\alpha_2+\beta_1+\beta_2+\gamma_2) + \alpha_2(1+u_1w_2(w_3\beta_1+\beta_2)+\gamma_2)\\
&\quad + \beta_1v_1(1+u_1u_3v_2w_2\beta_2+\gamma_2) + u_2v_1(u_1v_3\gamma_1+\beta_2(1+\gamma_2))\,,\\
f_3 &:= (1+\alpha_2+\beta_1+\beta_2+\gamma_2)\Big[\alpha_1\Big(\gamma_1+\beta_2(1+\alpha_2+u_3v_1v_2\beta_1+\gamma_2)+w_3\beta_1(1+\alpha_2+\gamma_2)\Big)\\
&\quad + (1+\gamma_2)\big(w_3\alpha_2\beta_1+(\alpha_2+u_3v_1v_2\beta_1)\beta_2\big)\Big] + \gamma_1\Big[\alpha_2(1+u_1(w_3\beta_1+\beta_2)+\gamma_2)\\
&\quad + u_3v_1(u_2w_1\beta_2(1+\gamma_2)+\beta_1(1+u_1v_2\beta_2+\gamma_2))\Big]\,,
\end{aligned} \tag{C.26}$$

JHEP01(2020)078

expressed in terms of the basis of dual-conformal invariant cross-ratios

$$\begin{aligned} u_1 &:= (c_1a_1;a_2b_2)\,, \quad u_2 := (a_1b_1;b_2c_2)\,, \quad u_3 := (b_1c_1;c_2a_2)\,, \\ v_1 &:= (a_1a_2;b_1c_2)\,, \quad v_2 := (b_1b_2;c_1a_2)\,, \quad v_3 := (c_1c_2;a_1b_2)\,, \\ w_1 &:= (b_2c_1;c_2b_1)\,, \quad w_2 := (c_2a_1;a_2c_1)\,, \quad w_3 := (a_2b_1;b_2a_1)\,. \end{aligned} \tag{C.27}$$

Recall that these are defined according to

$$(xy;zw) := \frac{(x|y)(z|w)}{(x|z)(y|w)}\,. \tag{C.28}$$

Although there appeared to be some magic in the Feynman-parametric rescaling in eq. (C.19) — which restored not only conformality in the x_C integration, but also its manifest linearity in each factor of the denominator of eq. (C.20) — this magic in some sense 'had to work'. Indeed, Miguel Paulos has shown [118] that all dual-conformal Feynman integrals whose dual-graphs involve internal loop momenta connected via trees are always possible to compute conformally by integrating one loop at a time (as described in ref. [79]) and rescaling Feynman parameters accordingly. His proof extends also to integrals whose dual graphs are free of four-cycles — and hence, his argument also applies to $\mathfrak{W}^{(3)}$. Nevertheless, the existence of four-cycles in the dual graph (as will be the case for $\mathfrak{W}^{(4)}$ discussed below) prevent this line of reasoning from being applied. As such, it is natural to wonder if there is any obstruction to the magic found in the rescaling (C.19) when considered in the context of a four (or higher-)loop wheel.

D Feynman parametrization of the four-loop wheel

Similarly to three loops, the four-loop wheel (also known as the 'window' integral) can be defined in dual-momentum space as

$$\mathfrak{W}^{(4)} := \int \frac{d^4x_A d^4x_B d^4x_C d^4x_D \quad (a_1|a_2)(b_1|b_2)(c_1|c_2)(d_1|d_2)}{(D|A)(A|a_1)(A|a_2)(A|B)(B|b_1)(B|b_2)(B|C)(C|c_1)(C|c_2)(C|D)(D|d_1)(D|d_2)}\,. \tag{D.1}$$

As before, sequentially introducing Feynman parameters will proceed semi-trivially until the last step as each integral is a standard, conformal box integral. Thus, we may save ourselves some of the pedantry of the previous discussion and cut to the chase — to the non-trivial steps at the end.

To integrate over the first three loop momenta, x_A, x_B, x_C in eq. (D.1), we introduce Feynman parameters according to

$$\begin{aligned} |\mathcal{Y}_A) &:= \alpha_1|a_1) + \alpha_2|a_2) + \ \alpha_3|D) \ + \eta_A|B) =: |\mathcal{Q}_A) + \eta_A|B)\,, \\ |\mathcal{Y}_B) &:= \beta_1|b_1) \ + \beta_2|b_2) + \beta_3|\mathcal{Q}_A) + \eta_B|C) =: |\mathcal{Q}_B) + \eta_B|C)\,, \\ |\mathcal{Y}_C) &:= \gamma_1|c_1) \ + \gamma_2|c_2) + \gamma_3|\mathcal{Q}_B) + \eta_C|D) =: |\mathcal{Q}_C) + \eta_C|D)\,, \end{aligned} \tag{D.2}$$

and integrate over the Feynman parameters η_A, η_B, η_C to arrive at

$$\mathfrak{W}^{(4)} = \int_0^\infty \left[d^2\vec{\alpha}\right]\left[d^2\vec{\beta}\right]\left[d^2\vec{\gamma}\right] \int \frac{d^4x_D \quad (a_1|a_2)(b_1|b_2)(c_1|c_2)(d_1|d_2)}{(\mathcal{Q}_A\,\overleftarrow{\partial}\,\mathcal{Q}_A)(\mathcal{Q}_B\,\overleftarrow{\partial}\,\mathcal{Q}_B)(\mathcal{Q}_C\,\overleftarrow{\partial}\,\mathcal{Q}_C)(D|\mathcal{Q}_C)(D|d_1)(D|d_2)}\,. \tag{D.3}$$

JHEP01(2020)078

As was the case with three loops, we now find an obstruction in the last loop integration of eq. (D.3), as it is far from manifestly conformal.

(To reiterate a point made above, we should be clear that *mere* conformality is not sufficient for us to Feynman parametrize and do the loop integrations. For example, consider an integral of the form

$$\int d^4x_\ell \, \frac{1}{(\ell|a)(\ell|b)\big[(\ell|c)(\ell|d)+(\ell|e)(\ell|f)\big]} \,. \tag{D.4}$$

We know of no method by which such integrals can be systematically integrated.[12] In this work, we take a much more conservative approach, and demand that integrands be brought to the form such that their (loop-dependent) denominators are built directly as products of propagators.)

Somewhat surprisingly, it turns out to be fairly straightforward to bring eq. (D.3) into a recognizable form by a sequence of rescalings as done for three loops. In particular, if we rescale (and eliminate the projective redundancy of) the Feynman parameters according to[13]

$$\begin{aligned}
&\alpha_1 \mapsto \alpha_1 (D|a_2), && \alpha_2 \mapsto \alpha_2 (D|a_1), && \alpha_3 \mapsto 1\times(a_1|a_2),\\
&\beta_1 \mapsto \beta_1 \frac{(D|a_1)(a_1|a_2)}{(a_1|b_1)}, && \beta_2 \mapsto \beta_2 \frac{(D|a_1)(a_1|a_2)}{(a_1|b_2)}, && \beta_3 \mapsto 1,\\
&\gamma_1 \mapsto \gamma_1 \frac{(D|a_1)(a_1|a_2)(b_1|b_2)}{(a_1|b_2)(b_1|c_1)}, && \gamma_2 \mapsto \gamma_2 \frac{(D|a_1)(a_1|a_2)(b_1|b_2)}{(a_1|b_1)(b_2|c_2)}, && \gamma_3 \mapsto 1,
\end{aligned} \tag{D.5}$$

then the integral (D.3) becomes

$$\mathfrak{W}^{(4)} \underset{\text{(D.5)}}{\longmapsto} \int_0^\infty d^2\vec{\alpha}\; d^2\vec{\beta}\; d^2\vec{\gamma} \int \frac{d^4x_D \qquad \kappa\,(D|a_1)}{(\alpha_1+\alpha_2+\alpha_1\alpha_2)(D|\mathcal{R})(D|\mathcal{S})(D|\mathcal{T})(D|d_1)(D|d_2)} \,, \tag{D.6}$$

where the prefactor in the numerator is

$$\kappa := \frac{(a_1|a_2)^3(b_1|b_2)^3(c_1|c_2)(d_1|d_2)}{(a_1|b_1)^2(a_1|b_2)^2(b_1|c_1)(b_2|c_2)}, \tag{D.7}$$

which arises from the various Jacobians. Moreover, the new 'propagators' are

$$\begin{aligned}
|\mathcal{R}) :=\;& |a_1)\left[\alpha_2\beta_1\frac{(a_2|b_1)}{(a_1|b_1)}+\alpha_2\beta_2\frac{(a_2|b_2)}{(a_1|b_2)}+\beta_1\beta_2\frac{(a_1|a_2)(b_1|b_2)}{(a_1|b_1)(a_1|b_2)}\right]\\
&+|a_2)\big[\alpha_1(1+\alpha_2+\beta_1+\beta_2)+\alpha_2\big]+|\mathcal{U})\,,\\
|\mathcal{S}) :=\;& |a_2)(\alpha_1+\alpha_2)+|\mathcal{U})+|\mathcal{V})\,,\\
|\mathcal{T}) :=\;& |\mathcal{S})+|a_1)f_{\mathcal{T}}+|a_2)\alpha_1\left[\alpha_2+\beta_1+\beta_2+\gamma_1\frac{(a_1|c_1)(b_1|b_2)}{(a_1|b_2)(b_1|c_1)}+\gamma_2\frac{(a_1|c_2)(b_1|b_2)}{(a_1|b_1)(b_2|c_2)}\right],
\end{aligned} \tag{D.8}$$

[12] Integrands such as (D.4) arise in the context of all-loop recursion relations [119], and it would be incredibly interesting to develop methods for these integrations.

[13] A more symmetrical choice of rescalings — one which treats the γ_i's more similarly to the β_i's — would have worked. We have chosen the somewhat unbalanced set of rescalings in order to maximize the number of smoothly accessible toy-model-like limits.

JHEP01(2020)078

in terms of

$$\begin{aligned} |\mathcal{U}) &:= |b_1)\beta_1 \frac{(a_1|a_2)}{(a_1|b_1)} + |b_2)\beta_2 \frac{(a_1|a_2)}{(a_1|b_2)}\,, \\ |\mathcal{V}) &:= |c_1)\gamma_1 \frac{(a_1|a_2)(b_1|b_2)}{(a_1|b_2)(b_1|c_1)} + |c_2)\gamma_2 \frac{(a_1|a_2)(b_1|b_2)}{(a_1|b_1)(b_2|c_2)}\,, \end{aligned} \tag{D.9}$$

and where we have defined the scalar function

$$\begin{aligned} f_{\mathcal{T}} := \frac{(a_1|a_2)(b_1|b_2)}{(a_1|b_1)(a_1|b_2)} \Bigg[&\beta_1\beta_2 + \beta_1\gamma_1 + \beta_2\gamma_2 + \alpha_2 \left(\beta_1 \frac{(a_1|b_2)(a_2|b_1)}{(a_1|a_2)(b_1|b_2)} \right. \\ &\left. + \beta_2 \frac{(a_1|b_1)(a_2|b_2)}{(a_1|a_2)(b_1|b_2)} + \gamma_1 \frac{(a_1|b_1)(a_2|c_1)}{(a_1|a_2)(b_1|c_1)} + \gamma_2 \frac{(a_1|b_2)(a_2|c_2)}{(a_1|a_2)(b_2|c_2)} \right) \\ &+ \beta_1\gamma_2 \frac{(a_1|b_2)(b_1|c_2)}{(a_1|b_1)(b_2|c_2)} + \beta_2\gamma_1 \frac{(a_1|b_1)(b_2|c_1)}{(a_1|b_2)(b_1|c_1)} + \gamma_1\gamma_2 \frac{(b_1|b_2)(c_1|c_2)}{(b_1|c_1)(b_2|c_2)} \Bigg]\,. \end{aligned} \tag{D.10}$$

The integral (D.6) is a conformal integral (with respect to x_D) which can be done almost as trivially as the box integral. In particular, its Feynman parametrization follows more-or-less trivially from differentiation (with respect to ℓ) of the (Feynman parametrized) box integral. (The interested reader should consult, e.g., ref. [79].)

Feynman parametrization of the integral (D.6) may be done by introducing

$$|\mathcal{Y}_D) := \delta_1|d_1) + \delta_2|\mathcal{R}) + \delta_3|\mathcal{S}) + \delta_4|\mathcal{T}) + \eta_D|d_2) =: |\mathcal{Q}_D) + \eta_D|d_2)\,, \tag{D.11}$$

and integrating over x_D in the ordinary way. This results in a representation of $\mathfrak{W}^{(4)}$ of the form

$$\begin{aligned} \mathfrak{W}^{(4)} &= \int_0^\infty d^2\vec{\alpha}\; d^2\vec{\beta}\; d^2\vec{\gamma} \left[d^3\vec{\delta}\right] \int_0^\infty d\eta_D \frac{\kappa\,(\mathcal{Y}_D|a_1)}{(\alpha_1+\alpha_2+\alpha_1\alpha_2)(\mathcal{Y}_D|\mathcal{Y}_D)^3} \\ &= \int_0^\infty d^2\vec{\alpha}\; d^2\vec{\beta}\; d^2\vec{\gamma} \left[d^3\vec{\delta}\right] \int_0^\infty d\eta_D \frac{\kappa\,\big((\mathcal{Q}_D|a_1) + \eta_D(d_2|a_1)\big)}{(\alpha_1+\alpha_2+\alpha_1\alpha_2)\big[(\mathcal{Q}_D|\mathcal{Q}_D) + \eta_D(\mathcal{Q}_D|d_2)\big]^3} \\ &= \int_0^\infty d^2\vec{\alpha}\; d^2\vec{\beta}\; d^2\vec{\gamma} \left[d^3\vec{\delta}\right] \frac{\kappa}{2(\alpha_1+\alpha_2+\alpha_1\alpha_2)} \left[\frac{(d_2|a_2)}{(\mathcal{Q}_D|d_2)^2(\mathcal{Q}_D|\mathcal{Q}_D)} + \frac{(\mathcal{Q}_D|a_1)}{(\mathcal{Q}_D|d_2)(\mathcal{Q}_D|\mathcal{Q}_D)^2} \right]. \end{aligned} \tag{D.12}$$

As before, the only thing we must do to render the expression (D.12) manifestly conformal with respect to the external momenta is to rescale the δ_i's such that $|\mathcal{Q}_D)$ becomes uniform in weight. This is in fact easy, as the reader can easily observe that all of the factors defined in eq. (D.8) scale like $|a_2)$; as such, the only term in eq. (D.11) which has the wrong scaling weights is the first one. Rescaling as required and eliminating the projective redundancy (now just for consistency with the previous analysis) according to

$$\delta_1 \mapsto \delta_1 (a_1|a_2)(a_1|d_1)\,, \qquad \delta_4 \mapsto 1\,, \tag{D.13}$$

the four-loop wheel takes the form

$$\mathfrak{W}^{(4)} \underset{\text{(D.13)}}{\longmapsto} \int_0^\infty d^2\vec{\alpha}\; d^2\vec{\beta}\; d^2\vec{\gamma}\; d^3\vec{\delta} \frac{n_0}{f_1\, f_2\, f_3} \left(\frac{n_1}{f_2} + \frac{n_2}{f_3} \right), \tag{D.14}$$

JHEP01(2020)078

where n_i's and the f_i's are all *directly* expressible in terms of dual-conformally invariant cross-ratios.

We might ask if we could have done better, and found a representation as an eight-fold integral. The difficulty here is in dealing with the final pentagon integral, which we here represent as a three-fold. These integrals can be expanded into boxes, and this would indeed give rise to a two-fold representation. However, writing out this box expansion shows that it contains dilogs which have square-root arguments — and these square roots would involve the other Feynman parameters. As such, while one can indeed write down some two-fold representation, it would not help us to understand its transcendental properties. At present, we know of no way to write the four-loop wheel as a rational eight-fold integral.

D.1 Interesting kinematic limits of the wheel integral $\mathfrak{W}^{(4)}$

The four-loop wheel integral has several interesting kinematic limits. We discuss them below, and provide expressions for the integral in each of these limits in MATHEMATICA format in the supplementary material `integrands_and_varieties.m`.

The 'fishnet' limit of the wheel integral $\mathfrak{W}^{(4)}$. The first limit we consider is the one in which all middle legs are light-like:

$$(a_2|b_1) = (b_2|c_1) = (c_2|d_1) = (d_2|a_1) = 0\,. \tag{D.15}$$

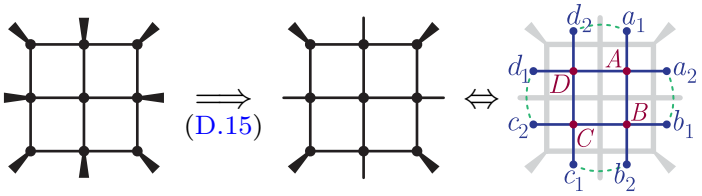

(D.16)

Notice that a particular case of this limit — where the 'massive' momenta flowing into the corners of the wheel are pairs of massless particles — is itself a particular planar amplitude in the integrable conformal fishnet theory [82–84],

$$\mathcal{A}(\varphi_{12},\varphi_{12},\varphi_{12},\varphi_{13},\varphi_{13},\varphi_{13},\varphi_{34},\varphi_{34},\varphi_{34},\varphi_{24},\varphi_{24},\varphi_{24}) =$$

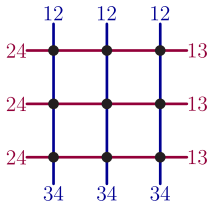

, (D.17)

which is also a particular *component amplitude* of the 12-point N^{4}MHV scattering amplitude in planar $\mathcal{N}=4$ supersymmetric Yang-Mills theory, $\mathcal{A}^{(4)}_{12}$. This component of the supersymmetric amplitude corresponds to

$$\int\left(d\tilde{\eta}^1_1 d\tilde{\eta}^1_2\cdots d\tilde{\eta}^1_6\right)\left(d\tilde{\eta}^2_{10} d\tilde{\eta}^2_{11}\cdots d\tilde{\eta}^2_3\right)\left(d\tilde{\eta}^3_4 d\tilde{\eta}^3_5\cdots d\tilde{\eta}^3_9\right)\left(d\tilde{\eta}^4_7 d\tilde{\eta}^4_8\cdots d\tilde{\eta}^4_{12}\right)\mathcal{A}^{(4)}_{12}\,. \tag{D.18}$$

We also note that in this limit (and hence all those below it), n_1 of eq. (D.14) vanishes.

JHEP01(2020)078

A nine-dimensional toy model of the wheel integral $\mathfrak{W}^{(4)}$. This limit is analogous to the toy models discussed in section 3.3 and ref. [80]. In this case, there are several ways to 'route' 8 light-like points among the external points. The only one which will be dihedrally invariant is the one defined by the conditions (D.15) and

$$(a_1|c_2) = (a_2|c_1) = (b_1|d_2) = (b_2|d_1)\,. \tag{D.19}$$

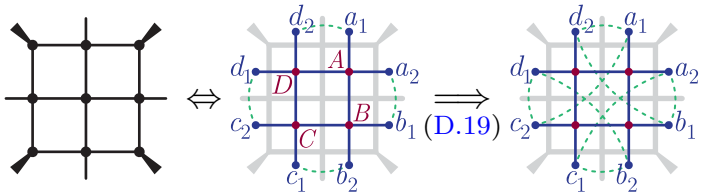

(D.20)

In this limit, the integral will depend on the space of kinematics associated with 8 pairwise light-like separated points — a nine-dimensional parameter space. We do not expect this limit to lead to any drop in rigidity.

The Basso-Dixon fishnet integral $I_{2,2}$ as a limit of $\mathfrak{W}^{(4)}$. Another special case of interest is the Basso-Dixon fishnet integral $I_{2,2}$, which contributes to the four-point correlation function in planar φ^4 theory. This corresponds to taking the limit where the eight dual points defining the wheel integral $\mathfrak{W}^{(4)}$ are pairwise identified according to

$$d_2 = a_1, \quad a_2 = b_1, \quad b_2 = c_1, \quad c_2 = d_1\,. \tag{D.21}$$

Graphically, this corresponds to

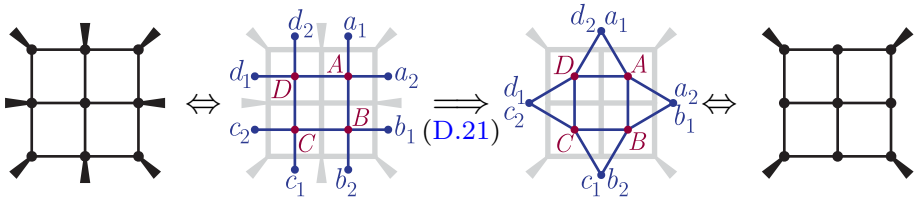

(D.22)

This limit is known explicitly [120], and in particular is polylogarithmic.

A two-dimensional toy model of the wheel integral $\mathfrak{W}^{(4)}$. One final limit of interest is one that appeared in ref. [121] — also in the context of the conformal fishnet theory. This limit corresponds to a different pairwise identification of the eight dual points which define the integral, namely,

$$a_1 = c_2, \quad a_2 = c_1, \quad b_1 = d_2, \quad b_2 = d_1\,. \tag{D.23}$$

This limit can perhaps be best understood as a 'non-planar' gluing of the original dual integral — obtained via the sequence

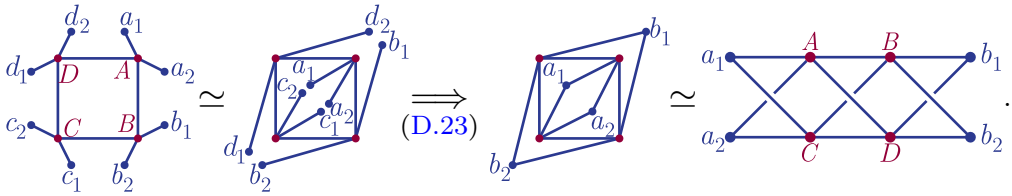

(D.24)

JHEP01(2020)078

In this limit, the integral can be seen to contribute to the '2-magnon' 4-point function as drawn on the right-hand part of figure 1 of ref. [121]. At leading order, this four-point function is given by a single Feynman integral: that drawn in eq. (D.24). This function is known to be non-polylogarithmic. Fourier-transformed, it corresponds to the five-loop amoeba integral of ref. [66], which is maximally rigid.

References

[1] K.-T. Chen, *Iterated path integrals*, *Bull. Amer. Math. Soc.* **83** (1977) 831.

[2] A. Goncharov, *Geometry of configurations, polylogarithms and motivic cohomology*, *Adv. Math.* **114** (1995) 197.

[3] A.B. Goncharov, *Multiple polylogarithms, cyclotomy and modular complexes*, *Math. Res. Lett.* **5** (1998) 497 [arXiv:1105.2076] [INSPIRE].

[4] E. Remiddi and J.A.M. Vermaseren, *Harmonic polylogarithms*, *Int. J. Mod. Phys.* **A 15** (2000) 725 [hep-ph/9905237] [INSPIRE].

[5] J.M. Borwein, D.M. Bradley, D.J. Broadhurst and P. Lisoněk, *Special values of multiple polylogarithms*, *Trans. Amer. Math. Soc.* **353** (2001) 907 [math.CA/9910045].

[6] S. Moch, P. Uwer and S. Weinzierl, *Nested sums, expansion of transcendental functions and multiscale multiloop integrals*, *J. Math. Phys.* **43** (2002) 3363 [hep-ph/0110083] [INSPIRE].

[7] A.B. Goncharov, M. Spradlin, C. Vergu and A. Volovich, *Classical polylogarithms for amplitudes and Wilson loops*, *Phys. Rev. Lett.* **105** (2010) 151605 [arXiv:1006.5703] [INSPIRE].

[8] S. Caron-Huot, *Superconformal symmetry and two-loop amplitudes in planar $N = 4$ super Yang-Mills*, *JHEP* **12** (2011) 066 [arXiv:1105.5606] [INSPIRE].

[9] C. Duhr, *Hopf algebras, coproducts and symbols: an application to Higgs boson amplitudes*, *JHEP* **08** (2012) 043 [arXiv:1203.0454] [INSPIRE].

[10] L.J. Dixon, J.M. Drummond, M. von Hippel and J. Pennington, *Hexagon functions and the three-loop remainder function*, *JHEP* **12** (2013) 049 [arXiv:1308.2276] [INSPIRE].

[11] L.J. Dixon, J.M. Drummond, C. Duhr and J. Pennington, *The four-loop remainder function and multi-Regge behavior at NNLLA in planar $\mathcal{N} = 4$ super-Yang-Mills theory*, *JHEP* **06** (2014) 116 [arXiv:1402.3300] [INSPIRE].

[12] L.J. Dixon and M. von Hippel, *Bootstrapping an NMHV amplitude through three loops*, *JHEP* **10** (2014) 065 [arXiv:1408.1505] [INSPIRE].

[13] J.M. Drummond, G. Papathanasiou and M. Spradlin, *A symbol of uniqueness: the cluster bootstrap for the 3-loop MHV heptagon*, *JHEP* **03** (2015) 072 [arXiv:1412.3763] [INSPIRE].

[14] L.J. Dixon, M. von Hippel and A.J. McLeod, *The four-loop six-gluon NMHV ratio function*, *JHEP* **01** (2016) 053 [arXiv:1509.08127] [INSPIRE].

[15] E. Panzer and O. Schnetz, *The Galois coaction on φ^4 periods*, *Commun. Num. Theor. Phys.* **11** (2017) 657 [arXiv:1603.04289] [INSPIRE].

JHEP01(2020)078

[16] S. Caron-Huot, L.J. Dixon, A. McLeod and M. von Hippel, *Bootstrapping a five-loop amplitude using Steinmann relations*, *Phys. Rev. Lett.* **117** (2016) 241601 [arXiv:1609.00669] [INSPIRE].

[17] L.J. Dixon, M. von Hippel, A.J. McLeod and J. Trnka, *Multi-loop positivity of the planar $\mathcal{N} = 4$ SYM six-point amplitude*, *JHEP* **02** (2017) 112 [arXiv:1611.08325] [INSPIRE].

[18] L.J. Dixon, J. Drummond, T. Harrington, A.J. McLeod, G. Papathanasiou and M. Spradlin, *Heptagons from the Steinmann cluster bootstrap*, *JHEP* **02** (2017) 137 [arXiv:1612.08976] [INSPIRE].

[19] Ø. Almelid, C. Duhr, E. Gardi, A. McLeod and C.D. White, *Bootstrapping the QCD soft anomalous dimension*, *JHEP* **09** (2017) 073 [arXiv:1706.10162] [INSPIRE].

[20] O. Schnetz, *The Galois coaction on the electron anomalous magnetic moment*, *Commun. Num. Theor. Phys.* **12** (2018) 335 [arXiv:1711.05118] [INSPIRE].

[21] S. Caron-Huot, L.J. Dixon, M. von Hippel, A.J. McLeod and G. Papathanasiou, *The double pentaladder integral to all orders*, *JHEP* **07** (2018) 170 [arXiv:1806.01361] [INSPIRE].

[22] J. Drummond, J. Foster, Ö. Gürdoğan and G. Papathanasiou, *Cluster adjacency and the four-loop NMHV heptagon*, *JHEP* **03** (2019) 087 [arXiv:1812.04640] [INSPIRE].

[23] V. Del Duca, C. Duhr, F. Dulat and B. Penante, *All two-loop MHV remainder functions in multi-Regge kinematics*, *JHEP* **01** (2019) 162 [arXiv:1811.10398] [INSPIRE].

[24] S. Abreu, L.J. Dixon, E. Herrmann, B. Page and M. Zeng, *The two-loop five-point amplitude in $\mathcal{N} = 4$ super-Yang-Mills theory*, *Phys. Rev. Lett.* **122** (2019) 121603 [arXiv:1812.08941] [INSPIRE].

[25] D. Chicherin, T. Gehrmann, J.M. Henn, P. Wasser, Y. Zhang and S. Zoia, *Analytic result for a two-loop five-particle amplitude*, *Phys. Rev. Lett.* **122** (2019) 121602 [arXiv:1812.11057] [INSPIRE].

[26] D. Chicherin, T. Gehrmann, J.M. Henn, P. Wasser, Y. Zhang and S. Zoia, *The two-loop five-particle amplitude in $\mathcal{N} = 8$ supergravity*, *JHEP* **03** (2019) 115 [arXiv:1901.05932] [INSPIRE].

[27] S. Abreu, L.J. Dixon, E. Herrmann, B. Page and M. Zeng, *The two-loop five-point amplitude in $\mathcal{N} = 8$ supergravity*, *JHEP* **03** (2019) 123 [arXiv:1901.08563] [INSPIRE].

[28] S. Caron-Huot, L.J. Dixon, F. Dulat, M. von Hippel, A.J. McLeod and G. Papathanasiou, *Six-gluon amplitudes in planar $\mathcal{N} = 4$ super-Yang-Mills theory at six and seven loops*, *JHEP* **08** (2019) 016 [arXiv:1903.10890] [INSPIRE].

[29] S. Caron-Huot, L.J. Dixon, F. Dulat, M. Von Hippel, A.J. McLeod and G. Papathanasiou, *The cosmic Galois group and extended Steinmann relations for planar $\mathcal{N} = 4$ SYM amplitudes*, *JHEP* **09** (2019) 061 [arXiv:1906.07116] [INSPIRE].

[30] A.B. Goncharov, *Multiple polylogarithms and mixed Tate motives*, math.AG/0103059 [INSPIRE].

[31] A.B. Goncharov, *Galois symmetries of fundamental groupoids and noncommutative geometry*, *Duke Math. J.* **128** (2005) 209 [math.AG/0208144] [INSPIRE].

[32] F.C.S. Brown, *Multiple zeta values and periods of moduli spaces $\mathfrak{M}_{0,n}(\mathbb{R})$*, *Annales Sci. École Norm. Sup.* **42** (2009) 371 [math.AG/0606419] [INSPIRE].

JHEP01(2020)078

[33] F. Brown, *On the decomposition of motivic multiple zeta values*, in *Galois-Teichmüller theory and arithmetic geometry*, Mathematical Society of Japan, Tokyo, Japan (2012), pg. 31 [arXiv:1102.1310] [INSPIRE].

[34] F. Brown, *Mixed Tate motives over Z*, *Annals Math.* **175** (2012) 949 [arXiv:1102.1312].

[35] M. Deneufchâtel, G.H.E. Duchamp, V.H.N. Minh and A.I. Solomon, *Independence of hyperlogarithms over function fields via algebraic combinatorics*, arXiv:1101.4497.

[36] C. Duhr, H. Gangl and J.R. Rhodes, *From polygons and symbols to polylogarithmic functions*, *JHEP* **10** (2012) 075 [arXiv:1110.0458] [INSPIRE].

[37] O. Schnetz, *Graphical functions and single-valued multiple polylogarithms*, *Commun. Num. Theor. Phys.* **08** (2014) 589 [arXiv:1302.6445] [INSPIRE].

[38] F. Brown, *Feynman amplitudes, coaction principle and cosmic Galois group*, *Commun. Num. Theor. Phys.* **11** (2017) 453 [arXiv:1512.06409] [INSPIRE].

[39] S. Laporta and E. Remiddi, *Analytic treatment of the two loop equal mass sunrise graph*, *Nucl. Phys.* **B 704** (2005) 349 [hep-ph/0406160] [INSPIRE].

[40] S. Muller-Stach, S. Weinzierl and R. Zayadeh, *From motives to differential equations for loop integrals*, PoS(LL2012)005 (2012) [arXiv:1209.3714] [INSPIRE].

[41] F. Brown and A. Levin, *Multiple elliptic polylogarithms*, arXiv:1110.6917.

[42] S. Bloch and P. Vanhove, *The elliptic dilogarithm for the sunset graph*, *J. Number Theor.* **148** (2015) 328 [arXiv:1309.5865] [INSPIRE].

[43] L. Adams, C. Bogner and S. Weinzierl, *The two-loop sunrise graph with arbitrary masses*, *J. Math. Phys.* **54** (2013) 052303 [arXiv:1302.7004] [INSPIRE].

[44] L. Adams, C. Bogner and S. Weinzierl, *The two-loop sunrise graph in two space-time dimensions with arbitrary masses in terms of elliptic dilogarithms*, *J. Math. Phys.* **55** (2014) 102301 [arXiv:1405.5640] [INSPIRE].

[45] L. Adams, C. Bogner and S. Weinzierl, *The two-loop sunrise integral around four space-time dimensions and generalisations of the Clausen and Glaisher functions towards the elliptic case*, *J. Math. Phys.* **56** (2015) 072303 [arXiv:1504.03255] [INSPIRE].

[46] L. Adams, C. Bogner and S. Weinzierl, *The iterated structure of the all-order result for the two-loop sunrise integral*, *J. Math. Phys.* **57** (2016) 032304 [arXiv:1512.05630] [INSPIRE].

[47] L. Adams, C. Bogner, A. Schweitzer and S. Weinzierl, *The kite integral to all orders in terms of elliptic polylogarithms*, *J. Math. Phys.* **57** (2016) 122302 [arXiv:1607.01571] [INSPIRE].

[48] L. Adams and S. Weinzierl, *Feynman integrals and iterated integrals of modular forms*, *Commun. Num. Theor. Phys.* **12** (2018) 193 [arXiv:1704.08895] [INSPIRE].

[49] L. Adams, E. Chaubey and S. Weinzierl, *Simplifying differential equations for multiscale Feynman integrals beyond multiple polylogarithms*, *Phys. Rev. Lett.* **118** (2017) 141602 [arXiv:1702.04279] [INSPIRE].

[50] C. Bogner, A. Schweitzer and S. Weinzierl, *Analytic continuation and numerical evaluation of the kite integral and the equal mass sunrise integral*, *Nucl. Phys.* **B 922** (2017) 528 [arXiv:1705.08952] [INSPIRE].

JHEP01(2020)078

[51] J. Brödel, C. Duhr, F. Dulat and L. Tancredi, *Elliptic polylogarithms and iterated integrals on elliptic curves. Part I: general formalism*, *JHEP* **05** (2018) 093 [arXiv:1712.07089] [INSPIRE].

[52] J. Brödel, C. Duhr, F. Dulat and L. Tancredi, *Elliptic polylogarithms and iterated integrals on elliptic curves. Part II: an application to the sunrise integral*, *Phys. Rev.* **D 97** (2018) 116009 [arXiv:1712.07095] [INSPIRE].

[53] L. Adams and S. Weinzierl, *The ε-form of the differential equations for Feynman integrals in the elliptic case*, *Phys. Lett.* **B 781** (2018) 270 [arXiv:1802.05020] [INSPIRE].

[54] J. Brödel, C. Duhr, F. Dulat, B. Penante and L. Tancredi, *Elliptic symbol calculus: from elliptic polylogarithms to iterated integrals of Eisenstein series*, *JHEP* **08** (2018) 014 [arXiv:1803.10256] [INSPIRE].

[55] L. Adams, E. Chaubey and S. Weinzierl, *Planar double box integral for top pair production with a closed top loop to all orders in the dimensional regularization parameter*, *Phys. Rev. Lett.* **121** (2018) 142001 [arXiv:1804.11144] [INSPIRE].

[56] J. Brödel, C. Duhr, F. Dulat, B. Penante and L. Tancredi, *Elliptic Feynman integrals and pure functions*, *JHEP* **01** (2019) 023 [arXiv:1809.10698] [INSPIRE].

[57] L. Adams, E. Chaubey and S. Weinzierl, *Analytic results for the planar double box integral relevant to top-pair production with a closed top loop*, *JHEP* **10** (2018) 206 [arXiv:1806.04981] [INSPIRE].

[58] I. Hönemann, K. Tempest and S. Weinzierl, *Electron self-energy in QED at two loops revisited*, *Phys. Rev.* **D 98** (2018) 113008 [arXiv:1811.09308] [INSPIRE].

[59] C. Bogner, S. Müller-Stach and S. Weinzierl, *The unequal mass sunrise integral expressed through iterated integrals on $\overline{\mathcal{M}}_{1,3}$*, arXiv:1907.01251 [INSPIRE].

[60] J. Brödel, C. Duhr, F. Dulat, B. Penante and L. Tancredi, *Elliptic polylogarithms and Feynman parameter integrals*, *JHEP* **05** (2019) 120 [arXiv:1902.09971] [INSPIRE].

[61] J. Brödel, C. Duhr, F. Dulat, R. Marzucca, B. Penante and L. Tancredi, *An analytic solution for the equal-mass banana graph*, *JHEP* **09** (2019) 112 [arXiv:1907.03787] [INSPIRE].

[62] J.L. Bourjaily, P. Heslop and V.-V. Tran, *Perturbation theory at eight loops: novel structures and the breakdown of manifest conformality in $\mathcal{N} = 4$ supersymmetric Yang-Mills theory*, *Phys. Rev. Lett.* **116** (2016) 191602 [arXiv:1512.07912] [INSPIRE].

[63] J.L. Bourjaily, E. Herrmann, C. Langer, A.J. McLeod and J. Trnka, *Prescriptive unitarity for non-planar six-particle amplitudes at two loops*, *JHEP* **12** (2019) 073 [arXiv:1909.09131] [INSPIRE].

[64] F.C.S. Brown, *On the periods of some Feynman integrals*, arXiv:0910.0114 [INSPIRE].

[65] F. Brown and O. Schnetz, *A K3 in φ^4*, *Duke Math. J.* **161** (2012) 1817 [arXiv:1006.4064] [INSPIRE].

[66] J.L. Bourjaily, A.J. McLeod, M. von Hippel and M. Wilhelm, *Bounded collection of Feynman integral Calabi-Yau geometries*, *Phys. Rev. Lett.* **122** (2019) 031601 [arXiv:1810.07689] [INSPIRE].

JHEP01(2020)078

[67] J.L. Bourjaily, Y.-H. He, A.J. Mcleod, M. Von Hippel and M. Wilhelm, *Traintracks through Calabi-Yau manifolds: scattering amplitudes beyond elliptic polylogarithms*, *Phys. Rev. Lett.* **121** (2018) 071603 [arXiv:1805.09326] [INSPIRE].

[68] D. Festi and D. van Straten, *Bhabha scattering and a special pencil of K3 surfaces*, *Commun. Num. Theor. Phys.* **13** (2019) 463 [arXiv:1809.04970] [INSPIRE].

[69] M. Besier, D. Festi, M. Harrison and B. Naskrecki, *Arithmetic and geometry of a K3 surface emerging from virtual corrections to Drell-Yan scattering*, arXiv:1908.01079 [INSPIRE].

[70] C.F. Doran, A.Y. Novoseltsev and P. Vanhove, *Mirroring towers: Calabi-Yau geometry of the multiloop Feynman sunset integrals*, to appear.

[71] V. Braun, *On free quotients of complete intersection Calabi-Yau manifolds*, *JHEP* **04** (2011) 005 [arXiv:1003.3235] [INSPIRE].

[72] L.B. Anderson, J. Gray, A. Lukas and E. Palti, *Two hundred heterotic Standard Models on smooth Calabi-Yau threefolds*, *Phys. Rev.* **D 84** (2011) 106005 [arXiv:1106.4804] [INSPIRE].

[73] L.B. Anderson, J. Gray, A. Lukas and E. Palti, *Heterotic line bundle standard models*, *JHEP* **06** (2012) 113 [arXiv:1202.1757] [INSPIRE].

[74] J. Gray, A.S. Haupt and A. Lukas, *All complete intersection Calabi-Yau four-folds*, *JHEP* **07** (2013) 070 [arXiv:1303.1832] [INSPIRE].

[75] P. Candelas, X.C. De La Ossa, P.S. Green and L. Parkes, *A pair of Calabi-Yau manifolds as an exactly soluble superconformal theory*, *Nucl. Phys.* **B 359** (1991) 21 [INSPIRE].

[76] S. Mizera, *Scattering amplitudes from intersection theory*, *Phys. Rev. Lett.* **120** (2018) 141602 [arXiv:1711.00469] [INSPIRE].

[77] P. Mastrolia and S. Mizera, *Feynman integrals and intersection theory*, *JHEP* **02** (2019) 139 [arXiv:1810.03818] [INSPIRE].

[78] H. Frellesvig, F. Gasparotto, M.K. Mandal, P. Mastrolia, L. Mattiazzi and S. Mizera, *Vector space of Feynman integrals and multivariate intersection numbers*, *Phys. Rev. Lett.* **123** (2019) 201602 [arXiv:1907.02000] [INSPIRE].

[79] J.L. Bourjaily, F. Dulat and E. Panzer, *Manifestly dual-conformal loop integration*, *Nucl. Phys.* **B 942** (2019) 251 [arXiv:1901.02887] [INSPIRE].

[80] J.L. Bourjaily, A.J. McLeod, M. Spradlin, M. von Hippel and M. Wilhelm, *Elliptic double-box integrals: massless scattering amplitudes beyond polylogarithms*, *Phys. Rev. Lett.* **120** (2018) 121603 [arXiv:1712.02785] [INSPIRE].

[81] J.L. Bourjaily, A.J. McLeod, M. von Hippel and M. Wilhelm, *Rationalizing loop integration*, *JHEP* **08** (2018) 184 [arXiv:1805.10281] [INSPIRE].

[82] Ö. Gürdoğan and V. Kazakov, *New integrable 4D quantum field theories from strongly deformed planar $\mathcal{N} = 4$ supersymmetric Yang-Mills theory*, *Phys. Rev. Lett.* **117** (2016) 201602 [*Addendum ibid.* **117** (2016) 259903] [arXiv:1512.06704] [INSPIRE].

[83] C. Sieg and M. Wilhelm, *On a CFT limit of planar γ_i-deformed $\mathcal{N} = 4$ SYM theory*, *Phys. Lett.* **B 756** (2016) 118 [arXiv:1602.05817] [INSPIRE].

[84] D. Grabner, N. Gromov, V. Kazakov and G. Korchemsky, *Strongly γ-deformed $\mathcal{N} = 4$ supersymmetric Yang-Mills theory as an integrable conformal field theory*, *Phys. Rev. Lett.* **120** (2018) 111601 [arXiv:1711.04786] [INSPIRE].

JHEP01(2020)078

[85] Z. Bern, L.J. Dixon, D.C. Dunbar and D.A. Kosower, *One loop n-point gauge theory amplitudes, unitarity and collinear limits*, *Nucl. Phys.* **B 425** (1994) 217 [hep-ph/9403226] [INSPIRE].

[86] Z. Bern, L.J. Dixon, D.C. Dunbar and D.A. Kosower, *Fusing gauge theory tree amplitudes into loop amplitudes*, *Nucl. Phys.* **B 435** (1995) 59 [hep-ph/9409265] [INSPIRE].

[87] Z. Bern, L.J. Dixon and D.A. Kosower, *One loop amplitudes for e^+e^- to four partons*, *Nucl. Phys.* **B 513** (1998) 3 [hep-ph/9708239] [INSPIRE].

[88] R. Britto, F. Cachazo and B. Feng, *Generalized unitarity and one-loop amplitudes in $\mathcal{N} = 4$ super-Yang-Mills*, *Nucl. Phys.* **B 725** (2005) 275 [hep-th/0412103] [INSPIRE].

[89] Z. Bern, J.J.M. Carrasco, H. Johansson and D.A. Kosower, *Maximally supersymmetric planar Yang-Mills amplitudes at five loops*, *Phys. Rev.* **D 76** (2007) 125020 [arXiv:0705.1864] [INSPIRE].

[90] J.L. Bourjaily, E. Herrmann and J. Trnka, *Prescriptive unitarity*, *JHEP* **06** (2017) 059 [arXiv:1704.05460] [INSPIRE].

[91] J.L. Bourjaily, E. Herrmann and J. Trnka, *Building bases of loop integrands*, to appear.

[92] S. Bloch, M. Kerr and P. Vanhove, *A Feynman integral via higher normal functions*, *Compos. Math.* **151** (2015) 2329 [arXiv:1406.2664] [INSPIRE].

[93] S. Bloch, M. Kerr and P. Vanhove, *Local mirror symmetry and the sunset Feynman integral*, *Adv. Theor. Math. Phys.* **21** (2017) 1373 [arXiv:1601.08181] [INSPIRE].

[94] T. Hübsch, *Calabi-Yau manifolds: a bestiary for physicists*, World Scientific, Singapore (1992) [INSPIRE].

[95] V.V. Batyrev, *Dual polyhedra and mirror symmetry for Calabi-Yau hypersurfaces in toric varieties*, *J. Alg. Geom.* **3** (1994) 493 [alg-geom/9310003] [INSPIRE].

[96] V.I. Danilov, *The geometry of toric varieties*, *Russ. Math. Surv.* **33** (1978) 97.

[97] K. Hori et al., *Mirror symmetry*, volume 1 of *Clay mathematics monographs*, American Mathematical Society, Providence, RI, U.S.A. (2003) [INSPIRE].

[98] V.V. Batyrev and L.A. Borisov, *Mirror duality and string theoretic Hodge numbers*, *Invent. Math.* **126** (1996) 183 [alg-geom/9509009] [INSPIRE].

[99] M. Kreuzer, E. Riegler and D.A. Sahakyan, *Toric complete intersections and weighted projective space*, *J. Geom. Phys.* **46** (2003) 159 [math.AG/0103214] [INSPIRE].

[100] M. Kreuzer and H. Skarke, *PALP: a package for analyzing lattice polytopes with applications to toric geometry*, *Comput. Phys. Commun.* **157** (2004) 87 [math.NA/0204356] [INSPIRE].

[101] The Sage developers, `SageMath`, *the Sage mathematics software system (version* 8.8*)*, https://www.sagemath.org, (2019).

[102] N. Arkani-Hamed, J.L. Bourjaily, F. Cachazo and J. Trnka, *Singularity structure of maximally supersymmetric scattering amplitudes*, *Phys. Rev. Lett.* **113** (2014) 261603 [arXiv:1410.0354] [INSPIRE].

[103] S. Laporta, *Analytical expressions of* 3 *and* 4*-loop sunrise Feynman integrals and* 4*-dimensional lattice integrals*, *Int. J. Mod. Phys.* **A 23** (2008) 5007 [arXiv:0803.1007] [INSPIRE].

JHEP01(2020)078

[104] J.L. Bourjaily, S. Caron-Huot and J. Trnka, *Dual-conformal regularization of infrared loop divergences and the chiral box expansion*, *JHEP* **01** (2015) 001 [arXiv:1303.4734] [INSPIRE].

[105] J.L. Bourjaily and J. Trnka, *Local integrand representations of all two-loop amplitudes in planar SYM*, *JHEP* **08** (2015) 119 [arXiv:1505.05886] [INSPIRE].

[106] M. Besier, D. Van Straten and S. Weinzierl, *Rationalizing roots: an algorithmic approach*, *Commun. Num. Theor. Phys.* **13** (2019) 253 [arXiv:1809.10983] [INSPIRE].

[107] D.J. Broadhurst and D. Kreimer, *Knots and numbers in φ^4 theory to 7 loops and beyond*, *Int. J. Mod. Phys.* **C 6** (1995) 519 [hep-ph/9504352] [INSPIRE].

[108] O. Schnetz, *Quantum periods: a census of φ^4-transcendentals*, *Commun. Num. Theor. Phys.* **4** (2010) 1 [arXiv:0801.2856] [INSPIRE].

[109] J.M. Drummond, *Generalised ladders and single-valued polylogarithms*, *JHEP* **02** (2013) 092 [arXiv:1207.3824] [INSPIRE].

[110] F. Brown and O. Schnetz, *Proof of the zig-zag conjecture*, arXiv:1208.1890 [INSPIRE].

[111] C. Bogner and F. Brown, *Feynman integrals and iterated integrals on moduli spaces of curves of genus zero*, *Commun. Num. Theor. Phys.* **09** (2015) 189 [arXiv:1408.1862] [INSPIRE].

[112] E. Panzer, *Feynman integrals and hyperlogarithms*, Ph.D. thesis, Humboldt U., Berlin, Germany (2015) [arXiv:1506.07243] [INSPIRE].

[113] M. Golz, E. Panzer and O. Schnetz, *Graphical functions in parametric space*, *Lett. Math. Phys.* **107** (2017) 1177 [arXiv:1509.07296] [INSPIRE].

[114] D.J. Broadhurst, *Massless scalar Feynman diagrams: five loops and beyond*, arXiv:1604.08027 [INSPIRE].

[115] S. Müller-Stach, S. Weinzierl and R. Zayadeh, *Picard-Fuchs equations for Feynman integrals*, *Commun. Math. Phys.* **326** (2014) 237 [arXiv:1212.4389] [INSPIRE].

[116] F. Brown, *Notes on motivic periods*, arXiv:1512.06410.

[117] V. Bouchard, *Lectures on complex geometry, Calabi-Yau manifolds and toric geometry*, hep-th/0702063 [INSPIRE].

[118] M.F. Paulos, private communication.

[119] N. Arkani-Hamed, J.L. Bourjaily, F. Cachazo, S. Caron-Huot and J. Trnka, *The all-loop integrand for scattering amplitudes in planar $\mathcal{N} = 4$ SYM*, *JHEP* **01** (2011) 041 [arXiv:1008.2958] [INSPIRE].

[120] B. Basso and L.J. Dixon, *Gluing ladder Feynman diagrams into fishnets*, *Phys. Rev. Lett.* **119** (2017) 071601 [arXiv:1705.03545] [INSPIRE].

[121] N. Gromov, V. Kazakov and G. Korchemsky, *Exact correlation functions in conformal Fishnet theory*, *JHEP* **08** (2019) 123 [arXiv:1808.02688] [INSPIRE].

JHEP01(2020)078

JHEP

Published for SISSA by Springer

Received: November 26, 2019
Accepted: January 3, 2020
Published: February 4, 2020

Rooting out letters: octagonal symbol alphabets and algebraic number theory

Jacob L. Bourjaily,[a,b,c] **Andrew J. McLeod,**[a] **Cristian Vergu,**[a] **Matthias Volk,**[a] **Matt von Hippel**[a] **and Matthias Wilhelm**[a]

[a] *Niels Bohr International Academy and Discovery Center, Niels Bohr Institute, University of Copenhagen, Blegdamsvej 17, Copenhagen Ø, DK-2100 Denmark*

[b] *Center for the Fundamental Laws of Nature, Department of Physics, Harvard University, 17 Oxford Street, Cambridge, MA 02138, U.S.A.*

[c] *Institute for Gravitation and the Cosmos, Department of Physics, Pennsylvania State University, 104 Davey Lab, University Park, PA 16892, U.S.A.*

E-mail: bourjaily@psu.edu, amcleod@nbi.ku.dk, c.vergu@nbi.ku.dk, mvolk@nbi.ku.dk, mvonhippel@nbi.ku.dk, matthias.wilhelm@nbi.ku.dk

Abstract: It is widely expected that NMHV amplitudes in planar, maximally supersymmetric Yang-Mills theory require symbol letters that are not rationally expressible in terms of momentum-twistor (or cluster) variables starting at two loops for eight particles. Recent advances in loop integration technology have made this an 'experimentally testable' hypothesis: compute the amplitude at some kinematic point, and see if algebraic symbol letters arise. We demonstrate the feasibility of such a test by directly integrating the most difficult of the two-loop topologies required. This integral, together with its rotated image, suffices to determine the simplest NMHV component amplitude: the unique component finite at this order. Although each of these integrals involve algebraic symbol alphabets, the combination contributing to this amplitude is — surprisingly — rational. We describe the steps involved in this analysis, which requires several novel tricks of loop integration and also a considerable degree of algebraic number theory. We find dramatic and unusual simplifications, in which the two symbols initially expressed as almost ten million terms in over two thousand letters combine in a form that can be written in five thousand terms and twenty-five letters.

Keywords: Scattering Amplitudes, Supersymmetric Gauge Theory

ArXiv ePrint: 1910.14224

https://doi.org/10.1007/JHEP02(2020)025

JHEP02(2020)025

Contents

1 Introduction **1**

2 The simplest NMHV octagon component amplitude **3**
- 2.1 Direct, (Feynman-)parametric integration of $\Omega[1,3,5,7]$ 5
- 2.2 Eliminating identities among 'spurious' algebraic letters 7
- 2.3 Cancellations in the component amplitude 10

3 Conclusions and outlook **11**

A A proposal for representing NMHV octagon amplitudes **12**
- A.1 Notational preliminaries: NMHV Yangian invariants 12
- A.2 An optimal basis for octagonal NMHV amplitudes 13

B Some notions of algebraic number theory **16**

JHEP02(2020)025

1 Introduction

The analytic structure and functional form of scattering amplitudes computed in (perturbative) quantum field theory continues to hold interesting surprises. Beyond leading order, amplitudes are typically transcendental functions — the simplest of which are known as generalized 'polylogarithms': iterated integrals over differential forms with exclusively simple (logarithmic) poles in each integration variable. Although wider classes of functions are known to be needed for most amplitudes (see e.g. [1–12]), polylogarithms are often sufficient at low loop order and particle multiplicity, and are by far the best understood. Much of this understanding has emerged in the context of 'symbology' [13, 14], which exploits the coproduct and Hopf algebra structure of these functions [15–19]. (See e.g. [20] for an introduction to these ideas.)

One of the key aspects of symbols is that they encode complete information about the (iterated) branch cut structure of polylogarithms in terms of an *alphabet* of primitive logarithmic branch-points called *letters*. Knowledge about the alphabets relevant for certain polylogarithmic amplitudes has allowed incredible reaches into perturbation theory, well beyond what would be possible through any known (e.g. Feynman) diagrammatic expansion. Examples of such triumphs include the recent determination of certain six-particle amplitudes in planar maximally supersymmetric ($\mathcal{N}=4$) Yang-Mills theory (sYM) through seven loops [21–29], and through four loops for seven particles [30–32].

A microcosm of progress in scattering amplitudes more broadly, these calculations have fueled and been fueled by concrete examples. One still mysterious aspect of most known examples in this theory is that their symbol alphabets are found to be generated by

cluster mutations [33] — rational transformations that define cluster algebras [34]. Such algebras naturally appear in the context of the positive Grassmannian geometry of on-shell scattering amplitudes [35], and seem to encode physical aspects of amplitudes such as the Steinmann relations [36–39]; they also encode further types of structure whose physical interpretation remains less clear [40–42].

Despite the intriguing role played by cluster algebras, it has long been known that even in planar sYM this story cannot be complete. Not only are non-polylogarithmic functions needed for most scattering amplitudes (at sufficiently high multiplicity or loop order), but even most polylogarithmic ($\mathrm{N}^{k\geq 2}$MHV) amplitudes at one loop require symbol letters that are not rationally related to any known cluster algebra. These algebraic roots arise, for example, as Gram determinants in the analysis of Landau singularities (see e.g. [43–46]).

It is therefore natural to wonder what kinds of letters arise in this theory's MHV and NMHV amplitudes, which have been argued to be polylogarithmic to all orders [47]. The symbol of all two-loop MHV amplitudes — computed in [48] — involve only letters drawn from the coordinates of Grassmannian cluster algebras (which are related to canonical coordinates on the space of positive momentum-twistor variables) [33, 40]. Similarly, the symbol of the two-loop seven-point NMHV amplitude (computed in [49]) is entirely composed of cluster coordinates. Whether or not this continues to hold beyond seven particles constitutes an important open question. In particular, in [45] it was suggested that square roots could appear in NMHV amplitudes at two loops (and in MHV amplitudes at three loops) starting for eight particles.

In this work, we probe the existence of these algebraic roots by directly computing a particular component of the eight-point two-loop NMHV amplitude. While we are not currently able to compute this component in full kinematics, it is sufficient to compute it analytically at a single (sufficiently generic) kinematic point. Note that it is, however, necessary to consider an entire amplitude, as it is well known that local integral representations can involve 'spurious' symbol letters (or even 'spurious' non-polylogarithmic parts — see e.g. [50, 51]) that cancel between terms. Surprisingly, in the component under study, this is precisely what happens: the local integrals that contribute to the amplitude individually involve quadratic roots, but these roots cancel. This of course has no implications for whether square roots will appear in other NMHV component amplitudes.

We begin in section 2 by defining the particular component we will examine. In section 2.1, we describe a direct integration strategy that can be used to compute it at a kinematic point; while it is not linearly reducible in the conventional sense, we find the integral can be divided up into parts that can be integrated after respective rationalizing changes of the integration variables. The resulting functional form involves many spurious algebraic letters in addition to the expected ones, so algebraic identities are required to eliminate them at symbol level, as we describe in section 2.2. While the individual integrals contributing to this component contain quadratic roots, we show in section 2.3 that the component as a whole does not. We then conclude, discussing further questions and potential applications.

We also present two appendices. Appendix A discusses a nice basis of R-invariants for this amplitude, while appendix B reviews pertinent notions in algebraic number theory.

JHEP02(2020)025

We additionally include several pieces of supplementary material: the integrand of the integral we compute as `Omega1357Integrand.m`, expressions in multiple polylogarithms in `Omega1357MPLs.m` and `Omega3571MPLs.m`, and the simplified symbols we obtain as `Omega1357Symbol.m` and `Omega3571Symbol.m`. We also include a table of prime factorizations of the symbol letters conjectured in [45] for comparison with our results as `PrimeFactorLetters.pdf`.

2 The simplest NMHV octagon component amplitude

Explicit, prescriptive formulae for all two-loop n-point N^{k}MHV amplitude integrands for planar sYM, which we denote by $\mathcal{A}_n^{(k),2}$, were given in [52] (see also [53]); these amplitudes are expressed in terms of a basis of dual-conformal Feynman integrands involving only local propagators. Each integral in this basis can be Feynman parameterized and conformally regulated as described in [54, 55]. These integrals are not all yet known analytically.

Consider for example the local integrand representation of MHV amplitudes at two loops [56, 57]:

$$\mathcal{A}_n^{(0),2} = \sum_{\substack{1\leq a<b<c\\ c<d<n+a}} \quad =: \sum_{\substack{1\leq a<b<c\\ c<d<n+a}} \Omega[a,b,c,d]\,. \tag{2.1}$$

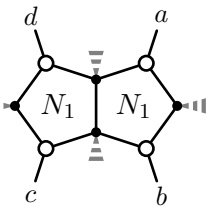

Here, the 'N_1's indicate specific choices of loop-dependent numerators for these sets of (otherwise ordinary) Feynman propagators as defined in [52]. Among these terms is the integral

$$\Omega\big[1,3,5,7\big] = \tag{2.2}$$

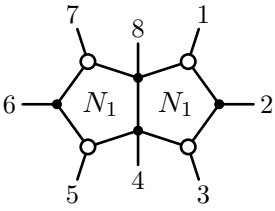

which was referred to as 'octagon K' in [46], where the particular challenges to its direct integration were described at some length (see also [58]). This integral is in fact the most difficult integral topology required for any eight-point amplitude at two loops for the simple reason that it is the only topology that depends on eight dual-momentum points. (Equivalently, it is the only topology which depends on 9 conformal degrees of freedom.) In general, the ratio function will involve all of the terms in (2.1) — including $\Omega[1,3,5,7]$ — because the 2-loop MHV amplitude is required to compute the ratio function. No analytic expression for $\Omega[1,3,5,7]$ is currently known, making the analysis of any octagon amplitude a considerable challenge.

Luckily, the question regarding whether or not algebraic letters appear in an amplitude can be answered for individual components. (We give a less component-oriented motivation for this amplitude in appendix A.) Moreover, provided the kinematics are parameterized

JHEP02(2020)025

appropriately, this question can be answered at a *single kinematic point*. For the eight-point NMHV amplitude, there is in fact a *simplest* component amplitude to consider:[1]

$$\begin{aligned}\mathcal{A}_8\Big(\psi_1^{+\frac{1}{2}},\phi_{12}^0,\psi_2^{+\frac{1}{2}},\phi_{23}^0,\psi_3^{+\frac{1}{2}},\phi_{34}^0,\psi_4^{+\frac{1}{2}},\phi_{41}^0\Big) \qquad (2.3)\\ = \int \big(d\widetilde{\eta}_8^1 d\widetilde{\eta}_1^1 d\widetilde{\eta}_2^1\big)\big(d\widetilde{\eta}_2^2 d\widetilde{\eta}_3^2 d\widetilde{\eta}_4^2\big)\big(d\widetilde{\eta}_4^3 d\widetilde{\eta}_5^3 d\widetilde{\eta}_6^3\big)\big(d\widetilde{\eta}_6^4 d\widetilde{\eta}_7^4 d\widetilde{\eta}_8^4\big)\ \mathcal{A}_8\big(\lambda,\widetilde{\lambda},\widetilde{\eta}\big)\\ = \langle 82\rangle\langle 24\rangle\langle 46\rangle\langle 68\rangle \int \big(d\eta_1^1\big)\big(d\eta_3^2\big)\big(d\eta_5^3\big)\big(d\eta_7^4\big)\ \ \mathcal{A}_8\big(\mathcal{Z}_1,\ldots,\mathcal{Z}_8\big)\,,\end{aligned}$$

where $\langle ab\rangle := \det\big(\lambda_a,\lambda_b\big)$ in terms of spinor variables with $p_a =: \lambda_a\widetilde{\lambda}_a$, and where η_a is the fermionic component of the super momentum-twistor $\mathcal{Z}_a := (z_a,\eta_a)$ [59–61]. This component amplitude is singled out by the fact that it happens to vanish exactly at tree level and one loop (see e.g. [54, 62, 63]), rendering this two-loop amplitude *infrared finite* and equal to the ratio function.

Using the results of [52], it is easy to confirm that the two-loop component (2.3) in momentum-twistor variables is simply:

$$\int d\eta_1^1 d\eta_3^2 d\eta_5^3 d\eta_7^4\ \mathcal{A}_8^{L=2} = \frac{1}{\langle 1357\rangle}\Bigg[$$

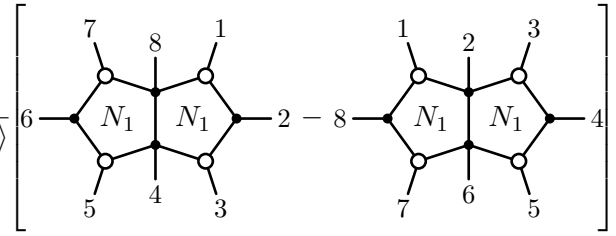

$$\Bigg], \qquad (2.4)$$

where $\langle abcd\rangle := \det\big(z_a,z_b,z_c,z_d\big)$. Notice that the *sum* of these integrals contributes to the MHV amplitude (2.1), while their *difference* is relevant to us here. The good news is that this component amplitude only requires one integral; the bad news is that it requires what is arguably the hardest eight-point integral at two loops.

Following [55], it is reasonably straightforward to Feynman parameterize (2.4) without breaking conformal invariance. We give this Feynman-parametric representation in the supplementary material, in `Omega1357Integrand.m`, expressed in terms of a particular momentum-twistor (cluster) coordinate chart (see [35, 46] for context):

$$Z := \begin{pmatrix} \overline{s}_{23} & 1 & s_2 s_3 & 0 & -s_2 s_3 & 0 & \overline{s}_2 s_3 & 0 \\ -\overline{s}_3 s_4 & 0 & \overline{s}_{34} u & 1 & s_3 s_4 & 0 & -s_3 s_4 & 0 \\ s_1 s_4 & 0 & -s_1\overline{s}_4 u & 0 & \overline{s}_{41} u & 1 & s_1 s_4 & 0 \\ -s_1 s_2 & 0 & s_1 s_2 u & 0 & -\overline{s}_1 s_2 u & 0 & \overline{s}_{12} u & 1 \end{pmatrix} \Leftrightarrow \qquad (2.5)$$

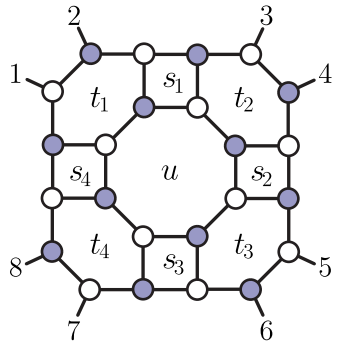

[1] Component fields of external supermultiplets are specified by their helicity and $\mathrm{SU}(4)_R$-charges, written in superscript and subscript, respectively.

JHEP02(2020)025

where $\overline{s}_{jk}\coloneqq(1+s_j+s_k+s_j s_k+t_k)$ and $\overline{s}_i\coloneqq(1+s_i)$, introduced entirely for the sake of notational compression. Here, these coordinates correspond to the charts

$$s_1\coloneqq\frac{\langle 2346\rangle\langle 4568\rangle}{\langle 2468\rangle\langle 3456\rangle}\,,\quad t_1\coloneqq\frac{\langle 1246\rangle\langle 2345\rangle\langle 3468\rangle}{\langle 1234\rangle\langle 2468\rangle\langle 3456\rangle}\,,\quad u\coloneqq\frac{\langle 1248\rangle\langle 2346\rangle\langle 2678\rangle\langle 4568\rangle}{\langle 1246\rangle\langle 2478\rangle\langle 2568\rangle\langle 3468\rangle}\,,\tag{2.6}$$

with $s_2\coloneqq r^2(s_1)$, $t_2\coloneqq r^2(t_1)$, etc. defined by sequential two-fold rotations $r^2{:}z_i\mapsto z_{i+2}$.

As described in [46], any rational parameterization of momentum twistors will be free of square roots associated with six-dimensional Gramians, and any rational point in momentum-twistor space can be accessed rationally in any cluster coordinate chart. And so the question of whether or not algebraic letters arise can be answered at *any* rational point in momentum-twistor space. For the analysis described below, we chose to consider the (nearly symmetrical) point in kinematic space specified by the momentum-twistor matrix

$$Z\longrightarrow Z^*\coloneqq\big(z_1,\ldots,z_n\big)\coloneqq\begin{pmatrix}5&1&1&0&-1&0&2&0\\-2&0&5&1&1&0&-1&0\\1&0&-2&0&5&1&1&0\\-1&0&1&0&-2&0&6&1\end{pmatrix}\tag{2.7}$$

obtained from (2.5) by setting $t_2=2$ and all other coordinates (s_i,t_i,u) to 1. Landau analysis (see [45]) suggests that (2.2) may involve the roots associated with the four-dimensional Gramians:

$$\Delta\big[abcd\big]\coloneqq\sqrt{(1-u-v)^2-4uv}\quad\text{with}\quad u\coloneqq(ab;cd)\,,\quad v\coloneqq(bc;da)\,,\tag{2.8}$$

where

$$(ab;cd)\coloneqq\frac{\langle a-1a\,b-1b\rangle\langle c-1c\,d-1d\rangle}{\langle a-1a\,c-1c\rangle\langle b-1b\,d-1d\rangle}\,.\tag{2.9}$$

For the kinematic point defined by (2.7), these are

$$\Delta\big[1357\big]=\frac{1}{806}\sqrt{644801}\,,\quad\Delta\big[2468\big]=\frac{1}{5}\sqrt{21}\,.\tag{2.10}$$

Our question, therefore, is whether or not the roots (2.10) — or any others — arise as part of the symbol alphabet for the component (2.4). Answering this question turned out to require more cleverness and subtlety than expected. We shall now describe the concrete steps involved.

2.1 Direct, (Feynman-)parametric integration of $\Omega[1,3,5,7]$

The loop-momentum integral over $\Omega[1,3,5,7]$ corresponds to a five-fold parametric integral of Feynman (or Schwinger) parameters:

$$\Omega\big[1,3,5,7\big]=:\int_0^\infty\big[d^3\vec{\alpha}\big]\,d^2\vec{\beta}\;\mathcal{I}(\alpha_1,\ldots,\alpha_4,\beta_1,\beta_2)\,.\tag{2.11}$$

Here, the integrals over $\{\alpha_1,\ldots,\alpha_4\}$ are projective, and those over β_1,β_2 are not. (This distinction is irrelevant from the viewpoint of the Cheng-Wu theorem, but reflects how the parameterization was derived.)

JHEP02(2020)025

The principle obstruction to parametric integration is that $\mathcal{I}(\vec{\alpha},\vec{\beta})$ is not linearly reducible in the sense of [64]. In particular, using compatibility-graph reduction [65] (as implemented for example in the package `HyperInt` [66][2]), one can readily find that at most two integrations can be carried out without introducing algebraic roots. For instance, upon integrating out β_1 and β_2 (in that order), further integration seems to be obstructed along every path. For example, the pathway in which α_1 is integrated next is obstructed by the existence of a quadratic polynomial $Q_1(\alpha_1)$ in the denominator, as this leads to a result that involves the square root of the discriminant of Q_1; this square root involves the remaining integration parameters, naïvely taking us out of the space of multiple polylogarithms. There is a similar obstruction with respect to α_4, due to a quadratic denominator factor $Q_4(\alpha_4)$. (The obstructions in α_2 and α_3 are given by three quadratic polynomials each.)

Luckily, after integrating over β_1 and β_2, there are no terms that *simultaneously* depend on both quadratic factors $Q_1(\alpha_1)$ and $Q_4(\alpha_4)$. Thus, we may divide them according to whether or not $Q_1(\alpha_1)$ appears. Specifically, we define

$$\int_0^\infty d^2\vec{\beta}\ \mathcal{I}(\alpha_1,\ldots,\alpha_4,\beta_1,\beta_2) =: \mathcal{I}(\vec{\alpha}) =: \mathcal{I}_A + \mathcal{I}_B\,, \tag{2.12}$$

with $\mathcal{I}_B$ consisting of all terms that involve $Q_1(\alpha_1)$, and $\mathcal{I}_A$ being all terms that do not depend on $Q_1(\alpha_1)$. To be clear, $\mathcal{I}_A$ consists of both those terms involving $Q_4(\alpha_4)$, and also those depending on neither quadratic factor. Note that $\mathcal{I}_A$ and $\mathcal{I}_B$ are separately finite.

Before we describe further integrations, it is worth mentioning one potential subtlety. We will ultimately be interested in fixing the projective redundancy of different parts of the original integral in different ways. To do so, we must first reprojectivize these integrals by making the replacement $\alpha_i \mapsto \alpha_i/(\sum \alpha_i)$.[3] This is done before we set any parameter to unity.

Let us first consider the integration of $\mathcal{I}_A$. Free of the quadratic obstruction $Q_1(\alpha_1)$, we can integrate over α_1 and subsequently α_2, leaving us with a one-fold projective integral. The α_2 integration, however, result in terms that involve square roots of two more irreducible quadratics $q_1(\alpha_3,\alpha_4)$ and $q_2(\alpha_3,\alpha_4)$. While the appearance of such factors would generally obstruct further integration, it turns out that no single term contains both roots. Thus, we can further divide $\mathcal{I}_A$ into three parts: $\mathcal{I}_{A_0}$, which is free of any square roots, $\mathcal{I}_{A_1}$, which involves only $\sqrt{q_1(\alpha_3,\alpha_4)}$, and $\mathcal{I}_{A_2}$, which involves only $\sqrt{q_2(\alpha_3,\alpha_4)}$. After setting the projective variable $a_4 = 1$, we can then use a standard change of variables known as Euler substitution (see also [67]) to rationalize $\sqrt{q_1(\alpha_3,1)}$ and $\sqrt{q_2(\alpha_3,1)}$, respectively, in the latter two groups.

We can integrate each of the terms in $\mathcal{I}_B$ following a very similar strategy. Specifically, we first integrate out α_4 and then α_3, which results in terms that individually involve one (or neither) of a pair of square roots of different quadratic polynomials, $\widetilde{q}_1(\alpha_1,\alpha_2)$ and

[2] `HyperInt` is obtainable at https://bitbucket.org/PanzerErik/hyperint/wiki/Home.

[3] This is due to the arguments of the logarithms (and polylogarithms) introduced by previous integrations, which are not homogeneous.

JHEP02(2020)025

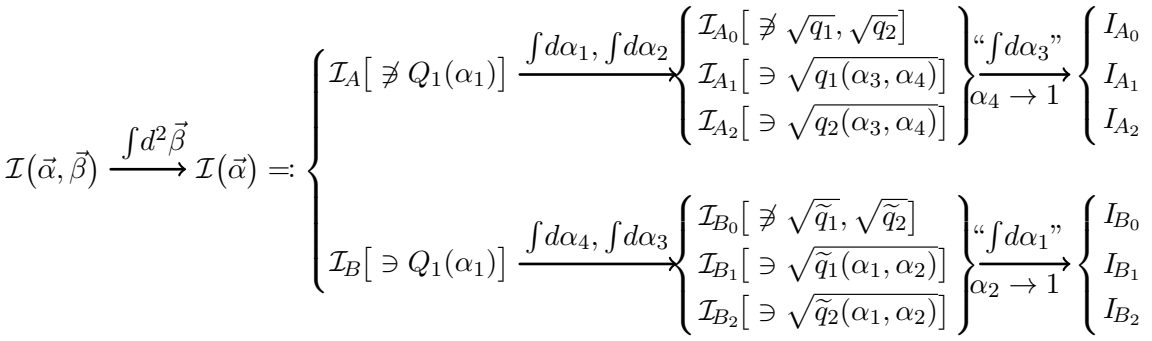

Figure 1. Integration strategy for $\Omega[1,3,5,7]$. Here, the final integrations are written in quotes to clarify that this step should be understood as integration *after* the changes of variables made to rationalize the quadratic roots; these changes depend on which roots exist, and so are different for different groups $\mathcal{I}_{A_i}$ and $\mathcal{I}_{B_i}$.

$\widetilde{q}_2(\alpha_1,\alpha_2)$. Splitting these pieces in the same way as for $\mathcal{I}_A$, fixing $\alpha_2 = 1$ and changing variables to rationalize each root, we can do the final integration.

The steps involved in this divide-and-conquer strategy are summarized in figure 1. The result is a sum of terms, each expressed in terms of multiple polylogarithms depending on algebraic arguments of high degree (up to 16 in some cases). These expressions can be evaluated to arbitrarily high precision — for example, using `GiNaC` [68, 69] — and have been checked to agree with the numerical (Monte Carlo) integration of the Feynman parametric integral (in MATHEMATICA). We attach these results as `Omega1357MPLs.m` and `Omega3571MPLs.m`.

Unfortunately, as mentioned, the multiple polylogarithms that arise in this process depend on *many* algebraic roots. In addition to the expected roots from the Landau analysis at this kinematic point, $\sqrt{21}$ and $\sqrt{644801}$, we find that $\Omega[1,3,5,7]$ and $\Omega[3,5,7,1]$ each involve 85 distinct square roots, with only 12 in common between the two integrals. Each also involves irreducible roots of four distinct fourth-order polynomials, only one of which appears in both integrals. The vast majority of these algebraic roots are certain to be 'spurious': arising entirely through the change of variables introduced in the final stages of the integration strategy (required to rationalize the final integrations). To assess whether or not these roots (or any others) are truly spurious, we analyze the symbol of each integral.

2.2 Eliminating identities among 'spurious' algebraic letters

As described above, we are able to evaluate $\Omega[1,3,5,7]$ and $\Omega[3,5,7,1]$ as complicated expressions in terms of multiple polylogarithms, which we expect to satisfy many nontrivial relations. To investigate these relations, we take the symbol of each function.[4] Doing so,

[4]It is sometimes colloquially stated that the symbol of a constant is zero; while this is true for the constants we most familiarly encounter (namely, the multiple zeta values), it is not true in general. One letter that is dropped in the symbol is 1 (which correspond to $\log(1) = 0$). We have also dropped all the roots of unity; if $\zeta^n = 1$, then $\log(\zeta) \to \frac{1}{n}\log(1) = 0$. Allowing this type of transformation is called "working modulo n-torsion" in the mathematics literature.

JHEP02(2020)025

we obtain a pair of extremely complicated expressions, each involving a large number of spurious letters. Factoring each letter naïvely (including factoring any integer primes), $\Omega\big[1,3,5,7\big]$ has a symbol composed of 8,367,616 terms that involve 2,024 letters, while the symbol of $\Omega\big[3,5,7,1\big]$ contains 9,941,483 terms and 2,156 letters.

Clearly, these symbols must be simplified. To do so, we want to find a set of multiplicatively independent letters $\mathcal{S}$ in terms of which both of these symbols can be expressed. Landau analysis suggests that the final alphabet $\mathcal{S}$ should be drawn from the union of the two algebraic number fields $\mathbb{Q}(\sqrt{21})\cup\mathbb{Q}(\sqrt{644801})$. However, our integration procedure yields a symbol with a *much* larger initial alphabet, involving for instance algebraic numbers up to degree 16. Finding algebraic relations between these complicated letters in order to reduce them to elements of $\mathcal{S}$ can be extremely difficult. To give the reader a sense of this complexity, we consider some examples.

Let $P_i \in K[X]$ be some degree-four polynomials (indexed by i) with coefficients[5] in $K = \mathbb{Q}(\sqrt{21}, \sqrt{644801})$. Our initial alphabet includes various roots of P_i, denoted $\sigma^*_{i,r}$ for $r = 1, \ldots, 4$. An example of the kind of roots that arise for us are those of the fourth-degree polynomial:

$$\begin{aligned} P_1 = \quad & (515426609 + 641880\sqrt{644801}) + (2105546840 + 2622160\sqrt{644801})X \\ & + (3225674840 + 4015200\sqrt{644801})X^2 + (2240256000 + 2676800\sqrt{644801})X^3 \\ & + 1120128000X^4 \,. \end{aligned} \tag{2.13}$$

Clearly, we expect the four roots of P_1 that arise in our symbol alphabet to be spurious. Therefore, we must find some way to demonstrate that they cancel.

Actually, an alphabet merely involving $\sigma^*_{i,r}$ would not be so difficult. It turns out in our case that the most complicated letters we see are of the type $\rho - \sigma^*_{i,r}$, where ρ can be an integer or a linear combination of up to two square roots. When there are two roots, one always belongs to K. Furthermore, when $\rho = m + n\sqrt{c}$ with $m, n \in K$ and $c \in \mathbb{Z}$ appears, then its conjugate $\overline{\rho} = m - n\sqrt{c}$ also appears.

There are two types of relations involving the roots $\sigma^*_{i,r}$ that turn out to be useful for us. The first type involves products $\prod_{r=1}^{4}(\rho - \sigma^*_{i,r})$. These products are completely symmetric in the roots of P_i, so they belong to an extension of the field K by ρ — in particular, they can be written as linear combinations of square roots and integers. Actually, it turns out that products of certain pairs of roots of P_i also yield simple answers. We believe it should be possible to explain the existence of these latter mysterious identities using Galois theory, but we have not performed this analysis.

The second type of identities involve products of type $(\rho - \sigma^*_{i,r})(\overline{\rho} - \sigma^*_{i,r})$, where $\overline{\rho}$ is one of the conjugates of ρ. Expanding out this product we obtain a degree-two polynomial in $\sigma^*_{i,r}$ with coefficients in K. Next, we search for exponents e_ρ corresponding to values of ρ such that, in the product of these letters raised to power e_ρ, the $\sigma^*_{i,r}$ cancels and the answer is of degree two. It turns out to be sufficient to bound the search so that $|e_\rho| \leq 2$. The

[5] To be more precise, two of these minimal polynomials are with coefficients in $\mathbb{Z}$, one is with coefficients in $\mathbb{Z}[\sqrt{21}]$ while another has coefficients in $\mathbb{Z}[\sqrt{644801}]$.

JHEP02(2020)025

calculation of these products can be conveniently performed using `SageMath` [70], which uses `Pari` [71].

Let us be more concrete with an example of this second type of identity. For the polynomial P_1 given in (2.13), we find the letters

$$\begin{aligned}
a_1(\sigma^*_{1,r}) &\coloneqq (1668888 + 2080\sqrt{644801}) + (25600\sigma^*_{1,r} + 4160\sqrt{644801})\sigma^*_{1,r},\\
a_2(\sigma^*_{1,r}) &\coloneqq (1412136 + 1760\sqrt{644801}) + (3097600\sigma^*_{1,r} + 3520\sqrt{644801})\sigma^*_{1,r},\\
a_3(\sigma^*_{1,r}) &\coloneqq (10013328 + 12480\sqrt{644801}) + (17305600\sigma^*_{1,r} + 24960\sqrt{644801})\sigma^*_{1,r},\\
a_4(\sigma^*_{1,r}) &\coloneqq (11938968 + 14880\sqrt{644801}) + (24601600\sigma^*_{1,r} + 29760\sqrt{644801})\sigma^*_{1,r},\\
a_5(\sigma^*_{1,r}) &\coloneqq (2456474760 + 3061600\sqrt{644801}) + (5069440000\sigma^*_{1,r} + 6123200\sqrt{644801})\sigma^*_{1,r}
\end{aligned} \tag{2.14}$$

(among many others involving $\sigma^*_{1,r}$), where $\sigma^*_{1,r}$ is any root of P_1. It is not hard to verify that

$$\frac{a_1 a_2^2}{a_3 a_4 a_5} = -\frac{121}{358670} \in K \tag{2.15}$$

using `SageMath` (or even MATHEMATICA).

Fortunately, the method described above turns out to be sufficient to find all required relations between the most complicated letters that appear in our initial symbols, allowing us to get rid of all higher-degree roots. However, many other potentially-spurious letters remain — in particular, there still exist linear combinations of up to two square roots, and square roots beyond the two physical ones in (2.10).

For the letters containing square roots, we group them according to the algebraic number fields to which they belong and compute the factorization of the principal ideal they generate (see appendix B for more details). For this step we use again `SageMath` and `Pari`. Using this factorization, we can find multiplicative relations between these letters. Note that the integer prime factors we generated in the first step belong to each of these number fields, so their decomposition in prime ideals has to be computed as well.

This factorization also contains a unit part, which is a term belonging to the group of units of the various rings we consider. In some of the cases we encounter, the unit part is ± 1, but in others it is non-trivial. We keep a list of all the units arising during the calculations in a given ring, and if two of them are identical we obtain a new identity by taking the ratio. In principle a more sophisticated approach is possible.

Using these methods, we decompose our letters into a multiplicatively independent set $\mathcal{S}$. Doing so, many of the spurious letters in our symbols combine cleanly into integer letters. Others cancel entirely, removing terms and causing other spurious letters to drop out. In the end, we find the symbol of each function simplifies dramatically. Expressing $\Omega\big[1,3,5,7\big]$ and $\Omega\big[3,5,7,1\big]$ in terms of a shared, multiplicatively independent symbol alphabet, we find only 35 letters are needed. These letters only involve the expected square roots: five involve $\sqrt{644801}$, two involve $\sqrt{21}$, and the rest are integer primes. Expressed in these letters, $\Omega\big[1,3,5,7\big]$ is 5316 terms long, while $\Omega\big[3,5,7,1\big]$ contains 5245 terms. We attach the symbol of each in supplementary material `Omega1357Symbol.m` and `Omega3571Symbol.m`, respectively.

JHEP02(2020)025

Interestingly, some of the symbol letters that contain $\sqrt{21}$ and $\sqrt{644801}$ can be constructed simply in dual twistor space. Namely, out of eight points $z_1, \ldots, z_8$, we can form four skew lines (z_1, z_2), (z_3, z_4), (z_5, z_6), (z_7, z_8). These four skew lines have two transversals (lines that intersect all four of them). From the points of intersection on each of these transversals we can form a cross ratio. A similar construction can be carried out starting from the (z_2, z_3), $\ldots$, (z_8, z_1). Some of the cross ratios that can be formed in this way appear directly in our symbol expression for $\Omega\big[1,3,5,7\big]$ and $\Omega\big[3,5,7,1\big]$.

2.3 Cancellations in the component amplitude

Individually, $\Omega\big[1,3,5,7\big]$ and $\Omega\big[3,5,7,1\big]$ both contain square-root letters. Now that we have expressed them in the same alphabet, we can examine their difference $\Omega\big[1,3,5,7\big] - \Omega\big[3,5,7,1\big]$, the combination that appears in this component of the NMHV amplitude. Remarkably, this difference is free of square-root letters! Recall that we are using a multiplicatively independent alphabet: as such, the vanishing of square roots in $\Omega\big[1,3,5,7\big] - \Omega\big[3,5,7,1\big]$ requires that terms involving each of the six independent square-root-containing letters cancel separately. We find that the difference $\Omega\big[1,3,5,7\big] - \Omega\big[3,5,7,1\big]$ contains just 25 letters, all integer primes.

The sum $\Omega\big[1,3,5,7\big] + \Omega\big[3,5,7,1\big]$ contributes to the eight-point MHV amplitude. This sum is not free of square roots, and depends on all of the letters present in the two integrals. This observation is still consistent with the observed absence of square roots in the alphabet of the two-loop eight-point MHV amplitude because several other root-containing integrals contribute to this amplitude — including two other permutations of the integral we computed here. Other cancellations, much like those we observed, must be present in this combination.

We find that square-root letters are present in the second and third entry of $\Omega\big[1,3,5,7\big]$ and $\Omega\big[3,5,7,1\big]$, but not the first or fourth entry. This is as expected, as first entries should correspond to Mandelstam invariants while last entries are constrained by the $\overline{Q}$ equation [49]. More specifically, first entries should be composed of four-brackets of the form $\langle i, i+1, j, j+1\rangle$. Examining our symbol, we find first entries of $2, 3, 5, 11, 13$, and 31. Computing the expected first entries at our kinematic point, we find

$$\begin{aligned}
&\langle 1,2,3,4\rangle = 1\,, && \langle 1,2,4,5\rangle = 3\,, && \langle 1,2,5,6\rangle = 5\,, && \langle 1,2,6,7\rangle = 13\,,\\
&\langle 1,2,7,8\rangle = 1\,, && \langle 2,3,4,5\rangle = 1\,, && \langle 2,3,5,6\rangle = 11\,, && \langle 2,3,6,7\rangle = 31\,,\\
&\langle 2,3,7,8\rangle = 3\,, && \langle 1,2,3,8\rangle = 1\,, && \langle 3,4,5,6\rangle = 1\,, && \langle 3,4,6,7\rangle = 4\,,\\
&\langle 3,4,7,8\rangle = 5\,, && \langle 1,3,4,8\rangle = 11\,, && \langle 4,5,6,7\rangle = 2\,, && \langle 4,5,7,8\rangle = 11\,,\\
&\langle 1,4,5,8\rangle = 26\,, && \langle 5,6,7,8\rangle = 1\,, && \langle 1,5,6,8\rangle = 3\,, && \langle 1,6,7,8\rangle = 1\,,
\end{aligned} \tag{2.16}$$

which indeed cover all observed first entries.

We can also investigate whether the prime-number symbol entries we observe elsewhere in the symbol can originate from the entries predicted in [45]. We have attached this analysis as supplementary material, as `PrimeFactorLetters.pdf`, where we tabulate the prime factors of each of the predicted letters at this kinematic point. We find these factors

JHEP02(2020)025

span all of the letters that we observe. There are additional prime factors occurring in predicted letters in [45] that we do not observe; these are marked by an asterisk in our table.

In addition to these observations, we find that the two square roots $\sqrt{644801}$ and $\sqrt{21}$ do not appear together in the same term of the symbol: the symbol can be separated into terms depending on one root, terms depending on the other, and terms depending on neither.

3 Conclusions and outlook

In this work, we have computed a component of the two-loop eight-point NMHV amplitude in planar sYM at a specific kinematic point. We find that, while the individual integrals contributing to this amplitude do have letters depending on square roots of four-dimensional Gramians, these square roots cancel in the combination present in this component. In order to do this, we have employed an unusual direct integration strategy of breaking the integral into multiple integration pathways, and simplified our result from millions to thousands of terms using algebraic number theory.

This work shows that this particular component is free of square-root letters, but it does not establish that other components of the NMHV amplitude will not depend on such roots. In order to establish this, we would need to compute many more integrals, potentially of similar complexity. Alternatively, other methods may be able to compute these amplitudes much more efficiently, yielding a conclusive answer.

The use of symbol methods with square-root letters is still largely unexplored territory. While previous forays have involved heuristic or numerical elements (e.g. [72, 73]), our use of factorization in prime ideals should yield a more canonical and complete analysis of the relations between algebraic letters, and we believe similar methods should be applicable elsewhere.

It is interesting to ask if the cancellation of square roots we observed could have been detected at a later stage. For the individual integrals, better integration methods may exist that would make these cancellations manifest earlier, or even avoid the introduction of spurious roots altogether. For the full component amplitude, one might hope that some analog of Landau analysis might be possible.

Acknowledgments

We are grateful to Herbert Gangl and Francesco Moriello for discussion of alternate methods, to Mark Spradlin for motivation, and to Erik Panzer for help developing our integration strategy. We are also grateful to Song He for discussing soon to be published results [77] with relevance to this work. This work was supported in part by the Danish Independent Research Fund under grant number DFF-4002-00037 (MV, MW), the Danish National Research Foundation (DNRF91), two grants from the Villum Fonden, a Starting Grant (No. 757978) from the European Research Council (JLB, AJM, MV, MvH, MW),

JHEP02(2020)025

the European Union's Horizon 2020 research and innovation program under grant agreement No. 793151 (MvH), and a Carlsberg Postdoctoral Fellowship (CF18-0641) (AJM). AJM, MV and MW thank the Center for the Fundamental Laws of Nature and JLB, AJM, MV and MW thank the Center Of Mathematical Sciences And Applications for kind hospitality during final stages of this work. Finally, JLB, AJM and MvH are grateful for the hospitality of the Aspen Center for Physics, which is supported by National Science Foundation grant PHY-1607611.

A A proposal for representing NMHV octagon amplitudes

In this appendix we describe a particular representation of eight-point NMHV amplitudes, analogous to the decomposition of hexagon and heptagon functions into specific bases. This is a bit outside the line of the main result in this work, but it does provide an independent logic behind why the particular component amplitude (2.4) plays a special role. In order to do this, we must first introduce and motivate a small amount of new notation that we promise will be worthwhile.

A.1 Notational preliminaries: NMHV Yangian invariants

The reader should be aware that NMHV amplitudes can be expressed in terms of so-called R-invariants that, when expressed in momentum-twistor space, are superfunctions defined by

$$R[a,b,c,d,e] \coloneqq \frac{\delta^{1\times 4}\big(\langle bcde\rangle\eta_a+\langle cdea\rangle\eta_b+\langle deab\rangle\eta_c+\langle eabc\rangle\eta_d+\langle abcd\rangle\eta_e\big)}{\langle abcd\rangle\langle bcde\rangle\langle cdea\rangle\langle deab\rangle\langle eabc\rangle} \tag{A.1}$$

for any five (super-)momentum twistors labelled by $\{a,b,c,d,e\}$. An equivalent definition of the R-invariant is that it is simply the five-particle NMHV tree-level amplitude involving the momentum twistors $\{a,b,c,d,e\}$. It will turn out to be useful to consider NMHV tree-level amplitudes involving other sets of external particles including sets of more than five. In particular, let us use the symbol

$$\mathfrak{A}_n \coloneqq \mathfrak{A}(1\cdots n) \coloneqq \mathcal{A}_n^{(k=1),L=0}(z_1,\ldots,z_n) \tag{A.2}$$

to denote the n-point NMHV tree-level amplitude involving momentum twistors $\{z_1,\ldots,z_n\}$. (Recall that '$\mathfrak{A}$' is the Fraktur-script form of the letter 'A'.) Thus, we may define the R-invariant simply as

$$R[1,2,3,4,5] \coloneqq \mathfrak{A}(1,2,3,4,5) = \mathfrak{A}_5\,. \tag{A.3}$$

Especially at low multiplicity, we find it useful to denote tree amplitudes by which among the ambient n twistors *they do not depend*. Because such notation, however convenient, is liable to cause confusion when several multiplicities are discussed, we propose to keep this information manifest in the way we write them. We denote these complements by

$$(a\cdots b)_n^c \coloneqq \mathfrak{A}([n]\backslash\{a,\ldots,b\})\,. \tag{A.4}$$

JHEP02(2020)025

Notice that this would allow us to write

$$\mathfrak{A}_n = \mathfrak{A}(1\cdots n) =: ()^c_n \tag{A.5}$$

— a notation that we cannot imagine ever actually using. More realistically, however, we should notice that in this notation the symbol for a single R-invariant would be multiplicity dependent. For example,

$$R[1,2,3,4,5] = \mathfrak{A}(12345) = (6)^c_6 = (67)^c_7 = (678)^c_8 = \cdots = (6\cdots n)^c_n\,. \tag{A.6}$$

One (BCFW) representation (among many) of the NMHV tree amplitude (A.2) would be,

$$\mathfrak{A}_n = \mathfrak{A}_{n-1} + \sum_{a=3}^{n-2} \mathfrak{A}(1\ a\ {-1}a\ n\ {-1}\,n) = \sum_{a=3}^{n-2}\sum_{b=a+2}^{n} \mathfrak{A}(1\ a\ {-1}a\ b\ {-1}\,b)\,; \tag{A.7}$$

but as already mentioned, we will have little recourse to decompose tree amplitudes into smaller objects. This is in part because, while $\mathfrak{A}(1\cdots n)$ is in fact dihedrally-invariant in its indices, no *formula* of the form (A.7) will make this manifest.

Equivalence between various dihedrally-related BCFW formulae (A.7) generates all the functional relations among R-invariants. In general, there are $\binom{n-1}{4}$ linearly independent n-point NMHV Yangian invariants.

At seven particles, for example, there are 15 linearly independent superfunctions into which any amplitude may be decomposed. Although 7 does not divide 15, most authors (see e.g. [31, 32, 74]) have chosen to write heptagon functions in terms of the cyclic seeds $\{(12)^c_7, (14)^c_7, \mathfrak{A}_7\}$ which generate 2 cyclic classes of length 7 and one cyclic singlet, $\mathfrak{A}_7$. That is, these authors have chosen to decompose all *other* 7-point superfunctions according to the 'elimination rules' generated cyclically by

$$\begin{aligned}(13)^c_7 &= -(34)^c_7 - (56)^c_7 - (71)^c_7 - (36)^c_7 - (51)^c_7 + \mathfrak{A}_7\,,\\ (1)^c_7 &= -(34)^c_7 - (56)^c_7 - (36)^c_7 + \mathfrak{A}_7\,.\end{aligned} \tag{A.8}$$

Having used such eliminations, the heptagon ratio function can be written as

$$R^L_7 =: \left[\left((12)^c_7 V^{7,(L)}_{(12)^c_7} + (14)^c_7 V^{7,(L)}_{(14)^c_7} + \mathfrak{A}_7 V^{7,(L)}_0\right) + \text{cyclic}_7\right]. \tag{A.9}$$

(We believe that a *better basis* for heptagon amplitudes would have been generated by $\{(1)^c_7, (12)^c_7, \mathfrak{A}_7\}$, but this is not presently our concern.) Let us now describe a similar basis for eight-point NMHV Yangian invariants that is in a precise sense 'optimal'.

A.2 An optimal basis for octagonal NMHV amplitudes

Unlike for seven particles (which is somewhat anomalously nice), there is no easy way to choose among the 56 different R-invariants — 7 cyclic classes — into non-redundant classes spanning $35 = \binom{7}{4}$ independent superfunctions. The situation is not obviously much improved if we include the cyclic singlet $\mathfrak{A}_8$, or other lower-point tree-level amplitudes.

JHEP02(2020)025

Including also superfunctions corresponding to tree-level amplitudes involving intermediate subsets of the 8 legs, we have 13 cyclic classes of superfunctions, generated by

$$\big\{(123)_8^c,(124)_8^c,(125)_8^c,(126)_8^c,(134)_8^c,(135)_8^c,(136)_8^c,(12)_8^c,(13)_8^c,(14)_8^c,(15)_8^c,(1)_8^c,\mathfrak{A}_8\big\}\,. \tag{A.10}$$

From this list, how are we to choose a basis of length 35? Of the cyclic classes generated by those in (A.10), all but two represent classes of length 8. The exceptions are $\mathfrak{A}_8$ and $(15)_8^c=\mathfrak{A}(234678)$, which forms a class of length 4. We are virtually forced to consider the inclusion of this length-4 class into our basis, as any other choice would lead to even greater redundancy.

Including $\mathfrak{A}_8$, the four cyclic images of $(15)_8^c=\mathfrak{A}(234678)$, and some other choice of four length-8 cyclic classes from among those generated by (A.10), we would have 37 superfunctions in all. In the best case, the two redundancies could be captured entirely by the length-four class (as 2 divides 4 nicely), with the rest independent. It turns out that there are 172 such choices available. The basis choice we describe presently is the one in which the 'elimination rules' of all other superfunctions (in the sense of (A.8)) involve the shortest expressions.

The basis we propose can be defined first in terms of the 37 functions generated by the seeds

$$\begin{aligned}
&\mathfrak{a}_1\coloneqq\mathfrak{A}(12345)=(678)_8^c\,,\quad \mathfrak{b}_1\coloneqq\mathfrak{A}(12346)=(578)_8^c\,,\quad \mathfrak{c}_1\coloneqq\mathfrak{A}(123456)=(78)_8^c\,,\\
&\mathfrak{d}_1^0\coloneqq\mathfrak{A}(123567)=(48)_8^c\,,\quad \mathfrak{e}_1\coloneqq\mathfrak{A}(1234567)=(8)_8^c\,,\quad \mathfrak{f}\coloneqq\mathfrak{A}(12345678)=\mathfrak{A}_8\,,
\end{aligned} \tag{A.11}$$

with other basis elements generated by cyclic rotations. Before we discuss the final, non-redundant basis, it is worthwhile to enumerate the (cyclic generators of all) elimination rules — by which non-basis superfunctions may be expanded:

$$\begin{aligned}
(124)_8^c&=-(467)_8^c+(12)_8^c+(67)_8^c+(4)_8^c-\mathfrak{A}_8 &&=-\mathfrak{b}_8+\mathfrak{c}_3+\mathfrak{c}_8+\mathfrak{e}_5-\mathfrak{f}\,;\\
(125)_8^c&=-(123)_8^c-(127)_8^c+(12)_8^c &&=-\mathfrak{a}_4-\mathfrak{b}_3+\mathfrak{c}_3\,;\\
(126)_8^c&=-(128)_8^c+(467)_8^c-(67)_8^c-(4)_8^c+\mathfrak{A}_8 &&=-\mathfrak{a}_3+\mathfrak{b}_8-\mathfrak{c}_8-\mathfrak{e}_5+\mathfrak{f}\,;\\
*(135)_8^c&=\ (178)_8^c+(567)_8^c+(15)_8^c-(3)_8^c-\mathfrak{A}_8 &&=\ \mathfrak{a}_2+\mathfrak{a}_8+\mathfrak{d}_2^0+\mathfrak{e}_4-\mathfrak{f}\,;\\
(136)_8^c&=\ (567)_8^c-(134)_8^c+(356)_8^c-(18)_8^c-(56)_8^c+(1)_8^c &&=\ \mathfrak{a}_8-\mathfrak{b}_5+\mathfrak{b}_7-\mathfrak{c}_2-\mathfrak{c}_7+\mathfrak{e}_2\,;\\
(13)_8^c&=\ (567)_8^c+(1)_8^c+(3)_8^c-\mathfrak{A}_8 &&=\ \mathfrak{a}_8+\mathfrak{e}_2+\mathfrak{e}_4-\mathfrak{f}\,;\\
(14)_8^c&=\ (134)_8^c-(467)_8^c-(34)_8^c+(4)_8^c &&=\ \mathfrak{b}_5-\mathfrak{b}_8-\mathfrak{c}_5+\mathfrak{e}_5\,;\\
\mathfrak{d}_3^0=(26)_8^c&=-(678)_8^c-(128)_8^c-(234)_8^c-(456)_8^c-(48)_8^c+\mathfrak{A}_8 &&=-\mathfrak{a}_1-\mathfrak{a}_3-\mathfrak{a}_5-\mathfrak{a}_7-\mathfrak{d}_1^0+\mathfrak{f}\,;\\
\mathfrak{d}_4^0=(37)_8^c&=-(178)_8^c-(123)_8^c-(345)_8^c-(567)_8^c-(15)_8^c+\mathfrak{A}_8 &&=-\mathfrak{a}_2-\mathfrak{a}_4-\mathfrak{a}_6-\mathfrak{a}_8-\mathfrak{d}_2^0+\mathfrak{f}\,.
\end{aligned} \tag{A.12}$$

There are a few things to note about these decompositions. As always, other superfunctions are eliminated according to rotations of (A.12). In addition, there are two aspects of (A.12) regarding $\mathfrak{d}_i^0$ that deserve comment. First, note that the only superfunction from (A.11) whose decomposition involves $\mathfrak{d}_i^0$ (except those of the $\mathfrak{d}_i^0$'s) is $(135)_8^c$ — indicated with a '$*$' in (A.12).[6]

The second aspect to notice about the elimination rules (A.12) is that the last two are for $\mathfrak{d}_3^0$ and $\mathfrak{d}_4^0$, which are generated by our initial seeds upon rotation. As evidenced by the

[6]It is worth mentioning that this particular superfunction, $(135)_8^c$, does not appear as any leading singularity (hence integral coefficient) until at three loops — where it certainly appears.

JHEP02(2020)025

simple fact that they have elimination rules (and also that $35 = 37 - 2$), these two will not be basis elements. Moreover, it is easy to see that

$$\mathfrak{d}_1^0 + \mathfrak{d}_3^0 = \mathfrak{f} - \mathfrak{a}_1 - \mathfrak{a}_3 - \mathfrak{a}_5 - \mathfrak{a}_7 \quad \text{and similarly,} \quad \mathfrak{d}_2^0 + \mathfrak{d}_4^0 = \mathfrak{f} - \mathfrak{a}_2 - \mathfrak{a}_4 - \mathfrak{a}_6 - \mathfrak{a}_8 \,. \tag{A.13}$$

However, the differences between them are good basis elements. And up to the alternating sign, they form a length-2 cyclic class of superfunctions. Let us define

$$\mathfrak{d}_1 := \mathfrak{d}_1^0 - \mathfrak{d}_3^0 \quad \text{and} \quad \mathfrak{d}_2 := \mathfrak{d}_2^0 - \mathfrak{d}_4^0 \,. \tag{A.14}$$

These, combined with the other basis elements in (A.11), non-redundantly span the space of 35 independent superfunctions in terms of four cyclic classes of length 8, one of length 2, and one of length 1. This is our proposed basis for eight-point NMHV amplitudes.

In this basis, the eight-point NMHV ratio function may be represented as

$$R_8^{(L)} := \left[\left(\mathfrak{a}_1 V_{\mathfrak{a}}^{(L)} + \mathfrak{b}_1 V_{\mathfrak{b}}^{(L)} + \mathfrak{c}_1 V_{\mathfrak{c}}^{(L)} + \mathfrak{d}_1 V_{\mathfrak{d}}^{(L)} + \mathfrak{e}_1 V_{\mathfrak{e}}^{(L)} + \mathfrak{f} V_{\mathfrak{f}}^{(L)} \right) + \text{cyclic}_8 \right] . \tag{A.15}$$

(As with seven points, please notice that we are adding all of these terms (8-fold-) cyclically. This has the admittedly unfortunate effect of causing $V_{\mathfrak{f}}^{(0)}$ to be 1/8; it will also require us to account for the over-counting in $V_{\mathfrak{d}}^{(L)}$.)

For reference, at one loop, these are easy to write explicitly [54, 75]. They are

$$\begin{aligned}
V_{\mathfrak{a}}^{(1)} &= -\operatorname{Li}_2(1-v_2) - \operatorname{Li}_2(1-u_1u_4v_4) - \log(u_2)\log(u_3) - \log(u_1u_4v_4)\log(v_2) + \zeta_2 \,, \\
V_{\mathfrak{b}}^{(1)} &= \operatorname{Li}_2(1-u_5v_1) - \operatorname{Li}_2(1-u_2u_5v_1) - \operatorname{Li}_2(1-u_4v_3) + \operatorname{Li}_2(1-u_4u_7v_3) \\
&\quad - \log(u_2)\log(u_4v_3) + \log(u_5v_1)\log(u_7) \,, \\
V_{\mathfrak{c}}^{(1)} &= -\operatorname{Li}_2(1-u_7) - \operatorname{Li}_2(1-u_5v_1) + \operatorname{Li}_2(1-u_2u_5v_1) - \operatorname{Li}_2(1-u_2v_2) + \operatorname{Li}_2(1-u_2u_7v_2) \\
&\quad - \log(u_4v_3)\log(v_2) - \log(u_5v_1)\log(u_7) \,, \\
V_{\mathfrak{d}}^{(1)} &= 0 \,, \\
V_{\mathfrak{e}}^{(1)} &= -\operatorname{Li}_2(1-u_2u_7v_2) - \operatorname{Li}_2(1-u_8v_4) - \log(u_2u_7v_2)\log(u_8v_4) + \zeta_2 \,, \\
V_{\mathfrak{f}}^{(1)} &= \operatorname{Li}_2(1-u_1) + \frac{1}{2}\operatorname{Li}_2(1-v_1) + \operatorname{Li}_2(1-u_1v_1) - \frac{1}{2}\log(v_1)\log(v_2) + \frac{3}{4}\log(v_1)\log(v_3) \\
&\quad + \log(u_1v_4)\log(u_2u_3v_3) - \zeta_2 \,.
\end{aligned} \tag{A.16}$$

We have written these function in terms of the 12 multiplicatively independent dual-conformally invariant cross-ratios,

$$u_1 := (13;48), \quad v_1 := (14;58) \quad \text{with} \quad u_i := r^{(i-1)}(u_1), \quad v_i := r^{(i-1)}(v_1) \,. \tag{A.17}$$

Notice that $V_{\mathfrak{d}}$ is zero at one loop. At two loops, it is not hard to confirm that

$$V_{\mathfrak{d}}^{(2)} = -\frac{1}{4} \left[\quad \right. \tag{A.18}$$

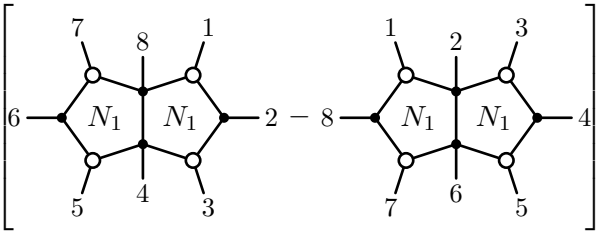

B Some notions of algebraic number theory

When working with symbols, it is valuable to be able to put them into a canonical form, for instance to decide whether two symbols are equal. As an example, many of the amplitudes that have been computed in planar sYM to date can be uniquely expressed in terms of a known set of Plücker coordinates. In more complicated amplitudes, a basis of symbol letters is not generally known. In such cases, we can simply factorize each symbol letter, as long as this factorization is unique.

It is easy to see that factorization will give rise to a unique expression when all symbol letters are integers. However, this is not automatic once algebraic roots are introduced. Consider, for instance, the situation where $\sqrt{-5}$ appears in some letters. The number 9 then has two 'factorizations':

$$9 = 3 \times 3 = (2 + \sqrt{-5})(2 - \sqrt{-5})\,, \tag{B.1}$$

where the second factorization of 9 is possible when viewed as an element of $\mathbb{Z}[\sqrt{-5}]$. By $\mathbb{Z}[\sqrt{-5}]$, we denote the set of numbers of type $a + b\sqrt{-5}$ for $a, b \in \mathbb{Z}$, with the obvious addition and multiplication properties.[7] This set of numbers, with these operations, defines a *ring*.

From the example above it looks like 9 can be factorized in two different ways, but perhaps unique factorization can still be salvaged if some of the factors can be further factored. It turns out that this is not what is happening here.

Before clarifying what is happening, we need to make a distinction between irreducible and prime elements of a ring R. First, we introduce the notion of *unit*. The elements of R which have multiplicative inverses are the units of R (denoted by $U(R)$). For the integers, the units are ± 1. An element $x \in R$ is *irreducible* if it can not be written as a product of two elements of R neither of which is a unit. Finally, an element $x \in R$ is *prime* if for any $a, b \in R$ such that x divides ab, then it divides a or b. For the integers there is no distinction between primes and irreducibles, but in general rings there is.

We now return to the above example: is 3 a prime in $\mathbb{Z}[\sqrt{-5}]$? We can show that it is not. If it were prime, it would follow from the fact that 3 divides $(2 + \sqrt{-5})(2 - \sqrt{-5})$ that it also divides either $2 + \sqrt{-5}$ or $2 - \sqrt{-5}$. But 3 divides $a + b\sqrt{-5}$ only if it divides both a and b, which is not the case here.

Is 3 irreducible instead? One can show that the units of $\mathbb{Z}[\sqrt{-5}]$ are ± 1. It is then a simple exercise to show that 3 is indeed irreducible (just use the definition and show that there are no suitable solutions). So the hope that perhaps each of the terms in the factorization can be factorized further to a prime decomposition which is the same in the l.h.s. and r.h.s. is not fulfilled. We conclude that $\mathbb{Z}[\sqrt{-5}]$ is not a UFD (unique factorization domain).

For this reason, it may look like there is no way to achieve unique factorization. But if we enlarge our perspective a little, we can recover this desired property. We will now

[7] We should not think of $\sqrt{-5}$ as being a complex number, but rather as an abstract symbol whose property is that it squares to -5. In fact, $\mathbb{Z}[\sqrt{-5}]$ can be embedded in the complex numbers in two ways, by sending $\sqrt{-5}$ to each of the two roots of -5 in $\mathbb{C}$.

JHEP02(2020)025

explain how to do this. The construction we will describe is possible for rings which are *Dedekind domains*.

Let us start with the familiar case of integers. In this case, to a prime p we associate the set of all its multiples. This set has two important properties. First, it is closed under addition; second, multiplying it by any integer lands us back in the same set. This is just the definition of an *ideal* of the ring of integers $\mathbb{Z}$. For the case of a prime we obtain a *prime ideal*, but the construction works in general. The set of multiples of p is denoted by (p). This is also called the ideal generated by p.

The notion of divisibility can be translated to the language of ideals: we say that a divides b if $(b) \subseteq (a)$. It is easy to check that this corresponds to the usual notion of divisibility for the integers. Now that we have expressed divisibility in terms of ideals, we may consider ideals generated by more than one element. The ideals generated by one element, such as (p), are called *principal ideals*. An ideal generated by two elements a and b is denoted by (a, b); as a set, it contains the linear combinations $ma + nb$ where m, n belong to the ring and a, b belong to the ideal. This satisfies all the properties of an ideal.

Ideals can be multiplied; we have $(p)(q) = (pq)$ and $(a, b)(c, d) = (ac, ad, bc, bd)$ and the pattern continues in the obvious way, for ideals generated by more generators. These ideals have some pretty obvious properties:

$$(a, b) = (a \pm b, b)\,, \qquad (a, b, a \pm b) = (a, b)\,, \qquad (1, a) = (1)\,. \tag{B.2}$$

Using these rules we can compute the following products, which will be useful momentarily:

$$\begin{aligned}(3, 1 + \sqrt{-5})(3, 1 - \sqrt{-5}) &= (9, 3 + 3\sqrt{-5}, 3 - 3\sqrt{-5}, 6) = (9, 3 + 3\sqrt{-5}, 6) \\ &= (3)(3, 1 + \sqrt{-5}, 2) = (3)(1, 1 + \sqrt{-5}, 2) = (3)(1) = (3).\end{aligned} \tag{B.3}$$

Similarly, we find

$$\begin{aligned}(3, 1+\sqrt{-5})^2 &= (9, 3+3\sqrt{-5}, -4+2\sqrt{-5}) = (9, -6+3\sqrt{-5}, -4+2\sqrt{-5}) \\ &= ((2+\sqrt{-5})(2-\sqrt{-5}), -3(2-\sqrt{-5}), -4(2-\sqrt{-5})) \\ &= (2-\sqrt{-5})(2+\sqrt{-5}, -3, -4) = (2-\sqrt{-5})(2+\sqrt{-5}, 1, -4) = (2-\sqrt{-5}).\end{aligned} \tag{B.4}$$

We also have $(3, 1 + \sqrt{-5})^2 = (2 + \sqrt{-5})$.

Now that we have made the transition from elements of a ring to the principal ideal they generate, we can explain the change of perspective mentioned above. Instead of considering principal ideals, we consider ideals generated by any number of generators. Indeed, now we can refine the factorization as follows:

$$(9) = (3)(3) = (2 + \sqrt{-5})(2 - \sqrt{-5}) = (3, 1 + \sqrt{-5})^2(3, 1 - \sqrt{-5})^2. \tag{B.5}$$

To finish, we should show that the ideals appearing in this factorization are prime. We will not do this explicitly here.

This works in general. The factorization is unique in the following sense: any ideal can be decomposed as a product of prime ideals, up to ordering. Finally, we have achieved

JHEP02(2020)025

unique factorization, but at the cost that the factors are some abstract, less familiar quantities.

An *algebraic number field* is a finite extension of $\mathbb{Q}$ constructed as follows. Consider a root ρ of a degree n polynomial with rational coefficients. Then, $\mathbb{Q}[\rho]$ is the ring generated by rational linear combinations of powers 0 through $n-1$ of ρ (higher powers can be reduced). We also define $K = \mathbb{Q}(\rho)$ as the field generated by ρ (whose elements are ratios of elements of $\mathbb{Q}[\rho]$). Inside K we find the *algebraic integers* $\mathcal{O}_K$ which are the elements of K whose minimal polynomial is monic[8] and with integer coefficients. It is a theorem that the ring of algebraic integers $\mathcal{O}_K$ of an algebraic number field K is a Dedekind domain, so it has a unique factorization.

Some of the letters we would like to factorize are not actually algebraic integers, so we cannot construct an ideal they generate inside $\mathcal{O}_K$. Nevertheless, we can construct a *fractional ideal* instead, which is a slight generalization of the notion of ideal. We will not give a full definition here, but the reader who wants to have an intuition for what a fractional ideal is can think of $\frac{p}{q} \cdot \mathbb{Z}$ as a fractional ideal of $\mathbb{Z}$. In other words, we also allow denominators.

Now the strategy for computing relations between several elements of a number field K should be clear. For each of these elements we compute the prime ideal decomposition of the principal fractional ideal they generate. The exponents form a matrix with integer coefficients whose rows are labeled by the elements of K and whose columns are labeled by the prime ideals. Every element of the left kernel of this matrix yields a multiplicative relation between the given elements of K.

Historically, it was Kummer who started developing these ideas in connection with Fermat's conjecture. His ideas were refined and generalized by Dedekind, Hilbert, Noether and many others. A good reference and resource for the material described in this appendix is [76].

References

[1] D.J. Broadhurst, J. Fleischer and O.V. Tarasov, *Two loop two point functions with masses: Asymptotic expansions and Taylor series, in any dimension*, *Z. Phys.* **C 60** (1993) 287 [hep-ph/9304303] [INSPIRE].

[2] S. Laporta and E. Remiddi, *Analytic treatment of the two loop equal mass sunrise graph*, *Nucl. Phys.* **B 704** (2005) 349 [hep-ph/0406160] [INSPIRE].

[3] S. Bloch and P. Vanhove, *The elliptic dilogarithm for the sunset graph*, *J. Number Theor.* **148** (2015) 328 [arXiv:1309.5865] [INSPIRE].

[4] L. Adams, C. Bogner and S. Weinzierl, *The two-loop sunrise graph with arbitrary masses*, *J. Math. Phys.* **54** (2013) 052303 [arXiv:1302.7004] [INSPIRE].

[8] A *monic* polynomial has its leading coefficient equal to one.

JHEP02(2020)025

[5] S. Bloch, M. Kerr and P. Vanhove, *A Feynman integral via higher normal functions*, *Compos. Math.* **151** (2015) 2329 [arXiv:1406.2664] [INSPIRE].

[6] L. Adams, C. Bogner, A. Schweitzer and S. Weinzierl, *The kite integral to all orders in terms of elliptic polylogarithms*, *J. Math. Phys.* **57** (2016) 122302 [arXiv:1607.01571] [INSPIRE].

[7] S. Bloch, M. Kerr and P. Vanhove, *Local mirror symmetry and the sunset Feynman integral*, *Adv. Theor. Math. Phys.* **21** (2017) 1373 [arXiv:1601.08181] [INSPIRE].

[8] J.L. Bourjaily, A.J. McLeod, C. Vergu, M. Volk, M. Von Hippel and M. Wilhelm, *Embedding Feynman Integral (Calabi-Yau) Geometries in Weighted Projective Space*, arXiv:1910.01534 [INSPIRE].

[9] J.L. Bourjaily, A.J. McLeod, M. von Hippel and M. Wilhelm, *Bounded Collection of Feynman Integral Calabi-Yau Geometries*, *Phys. Rev. Lett.* **122** (2019) 031601 [arXiv:1810.07689] [INSPIRE].

[10] J.L. Bourjaily, Y.-H. He, A.J. Mcleod, M. Von Hippel and M. Wilhelm, *Traintracks through Calabi-Yau Manifolds: Scattering Amplitudes beyond Elliptic Polylogarithms*, *Phys. Rev. Lett.* **121** (2018) 071603 [arXiv:1805.09326] [INSPIRE].

[11] J.L. Bourjaily, A.J. McLeod, M. Spradlin, M. von Hippel and M. Wilhelm, *Elliptic Double-Box Integrals: Massless Scattering Amplitudes beyond Polylogarithms*, *Phys. Rev. Lett.* **120** (2018) 121603 [arXiv:1712.02785] [INSPIRE].

[12] L. Adams, E. Chaubey and S. Weinzierl, *Planar Double Box Integral for Top Pair Production with a Closed Top Loop to all orders in the Dimensional Regularization Parameter*, *Phys. Rev. Lett.* **121** (2018) 142001 [arXiv:1804.11144] [INSPIRE].

[13] A.B. Goncharov, M. Spradlin, C. Vergu and A. Volovich, *Classical Polylogarithms for Amplitudes and Wilson Loops*, *Phys. Rev. Lett.* **105** (2010) 151605 [arXiv:1006.5703] [INSPIRE].

[14] C. Duhr, H. Gangl and J.R. Rhodes, *From polygons and symbols to polylogarithmic functions*, *JHEP* **10** (2012) 075 [arXiv:1110.0458] [INSPIRE].

[15] A.B. Goncharov, *Galois symmetries of fundamental groupoids and noncommutative geometry*, *Duke Math. J.* **128** (2005) 209 [math/0208144] [INSPIRE].

[16] F. Brown, *On the Decomposition of Motivic Multiple Zeta Values*, arXiv:1102.1310 [INSPIRE].

[17] F. Brown, *Mixed Tate Motives over* $\mathbb{Z}$, *Ann. Math.* **175** (2012) 949 [arXiv:1102.1312].

[18] C. Duhr, *Hopf algebras, coproducts and symbols: an application to Higgs boson amplitudes*, *JHEP* **08** (2012) 043 [arXiv:1203.0454] [INSPIRE].

[19] F. Chavez and C. Duhr, *Three-mass triangle integrals and single-valued polylogarithms*, *JHEP* **11** (2012) 114 [arXiv:1209.2722] [INSPIRE].

[20] C. Duhr, *Mathematical aspects of scattering amplitudes*, in proceedings of the *Theoretical Advanced Study Institute in Elementary Particle Physics: Journeys Through the Precision Frontier: Amplitudes for Colliders (TASI 2014)*, Boulder, Colorado, U.S.A., 2–27 June 2014, pp. 419–476 [arXiv:1411.7538] [INSPIRE].

[21] L.J. Dixon, J.M. Drummond and J.M. Henn, *Analytic result for the two-loop six-point NMHV amplitude in* $\mathcal{N} = 4$ *super Yang-Mills theory*, *JHEP* **01** (2012) 024 [arXiv:1111.1704] [INSPIRE].

JHEP02(2020)025

[22] L.J. Dixon, J.M. Drummond, M. von Hippel and J. Pennington, *Hexagon functions and the three-loop remainder function*, *JHEP* **12** (2013) 049 [arXiv:1308.2276] [INSPIRE].

[23] L.J. Dixon, J.M. Drummond, C. Duhr and J. Pennington, *The four-loop remainder function and multi-Regge behavior at NNLLA in planar $\mathcal{N} = 4$ super-Yang-Mills theory*, *JHEP* **06** (2014) 116 [arXiv:1402.3300] [INSPIRE].

[24] L.J. Dixon and M. von Hippel, *Bootstrapping an NMHV amplitude through three loops*, *JHEP* **10** (2014) 065 [arXiv:1408.1505] [INSPIRE].

[25] L.J. Dixon, M. von Hippel and A.J. McLeod, *The four-loop six-gluon NMHV ratio function*, *JHEP* **01** (2016) 053 [arXiv:1509.08127] [INSPIRE].

[26] L.J. Dixon, M. von Hippel, A.J. McLeod and J. Trnka, *Multi-loop positivity of the planar $\mathcal{N} = 4$ SYM six-point amplitude*, *JHEP* **02** (2017) 112 [arXiv:1611.08325] [INSPIRE].

[27] S. Caron-Huot, L.J. Dixon, A. McLeod and M. von Hippel, *Bootstrapping a Five-Loop Amplitude Using Steinmann Relations*, *Phys. Rev. Lett.* **117** (2016) 241601 [arXiv:1609.00669] [INSPIRE].

[28] S. Caron-Huot, L.J. Dixon, F. Dulat, M. von Hippel, A.J. McLeod and G. Papathanasiou, *Six-Gluon amplitudes in planar $\mathcal{N} = 4$ super-Yang-Mills theory at six and seven loops*, *JHEP* **08** (2019) 016 [arXiv:1903.10890] [INSPIRE].

[29] S. Caron-Huot, L.J. Dixon, F. Dulat, M. Von Hippel, A.J. McLeod and G. Papathanasiou, *The Cosmic Galois Group and Extended Steinmann Relations for Planar $\mathcal{N} = 4$ SYM Amplitudes*, *JHEP* **09** (2019) 061 [arXiv:1906.07116] [INSPIRE].

[30] J.M. Drummond, G. Papathanasiou and M. Spradlin, *A Symbol of Uniqueness: The Cluster Bootstrap for the 3-Loop MHV Heptagon*, *JHEP* **03** (2015) 072 [arXiv:1412.3763] [INSPIRE].

[31] L.J. Dixon, J.M. Drummond, T. Harrington, A.J. McLeod, G. Papathanasiou and M. Spradlin, *Heptagons from the Steinmann Cluster Bootstrap*, *JHEP* **02** (2017) 137 [arXiv:1612.08976] [INSPIRE].

[32] J.M. Drummond, J. Foster, Ö. Gürdoğan and G. Papathanasiou, *Cluster adjacency and the four-loop NMHV heptagon*, *JHEP* **03** (2019) 087 [arXiv:1812.04640] [INSPIRE].

[33] J. Golden, A.B. Goncharov, M. Spradlin, C. Vergu and A. Volovich, *Motivic Amplitudes and Cluster Coordinates*, *JHEP* **01** (2014) 091 [arXiv:1305.1617] [INSPIRE].

[34] S. Fomin and A. Zelevinsky, *Cluster algebras I: Foundations*, *J. Am. Math. Soc.* **15** (2002) 497 [math.RT/0104151].

[35] N. Arkani-Hamed, J.L. Bourjaily, F. Cachazo, A.B. Goncharov, A. Postnikov and J. Trnka, *Scattering Amplitudes and the Positive Grassmannian*, arXiv:1212.5605 [INSPIRE].

[36] J.M. Drummond, J. Foster and Ö. Gürdoğan, *Cluster Adjacency Properties of Scattering Amplitudes in $\mathcal{N} = 4$ Supersymmetric Yang-Mills Theory*, *Phys. Rev. Lett.* **120** (2018) 161601 [arXiv:1710.10953] [INSPIRE].

[37] J.M. Drummond, J. Foster and Ö. Gürdoğan, *Cluster adjacency beyond MHV*, *JHEP* **03** (2019) 086 [arXiv:1810.08149] [INSPIRE].

[38] J. Golden, A.J. McLeod, M. Spradlin and A. Volovich, *The Sklyanin Bracket and Cluster Adjacency at All Multiplicity*, *JHEP* **03** (2019) 195 [arXiv:1902.11286] [INSPIRE].

[39] J. Mago, A. Schreiber, M. Spradlin and A. Volovich, *Yangian invariants and cluster adjacency in $\mathcal{N} = 4$ Yang-Mills*, *JHEP* **10** (2019) 099 [arXiv:1906.10682] [INSPIRE].

JHEP02(2020)025

[40] J. Golden and M. Spradlin, *A Cluster Bootstrap for Two-Loop MHV Amplitudes*, *JHEP* **02** (2015) 002 [arXiv:1411.3289] [INSPIRE].

[41] J. Golden, M.F. Paulos, M. Spradlin and A. Volovich, *Cluster Polylogarithms for Scattering Amplitudes*, *J. Phys.* **A 47** (2014) 474005 [arXiv:1401.6446] [INSPIRE].

[42] J. Golden and A.J. Mcleod, *Cluster Algebras and the Subalgebra Constructibility of the Seven-Particle Remainder Function*, *JHEP* **01** (2019) 017 [arXiv:1810.12181] [INSPIRE].

[43] T. Dennen, M. Spradlin and A. Volovich, *Landau Singularities and Symbology: One- and Two-loop MHV Amplitudes in SYM Theory*, *JHEP* **03** (2016) 069 [arXiv:1512.07909] [INSPIRE].

[44] T. Dennen, I. Prlina, M. Spradlin, S. Stanojevic and A. Volovich, *Landau Singularities from the Amplituhedron*, *JHEP* **06** (2017) 152 [arXiv:1612.02708] [INSPIRE].

[45] I. Prlina, M. Spradlin, J. Stankowicz, S. Stanojevic and A. Volovich, *All-Helicity Symbol Alphabets from Unwound Amplituhedra*, *JHEP* **05** (2018) 159 [arXiv:1711.11507] [INSPIRE].

[46] J.L. Bourjaily, A.J. McLeod, M. von Hippel and M. Wilhelm, *Rationalizing Loop Integration*, *JHEP* **08** (2018) 184 [arXiv:1805.10281] [INSPIRE].

[47] N. Arkani-Hamed, J.L. Bourjaily, F. Cachazo and J. Trnka, *Singularity Structure of Maximally Supersymmetric Scattering Amplitudes*, *Phys. Rev. Lett.* **113** (2014) 261603 [arXiv:1410.0354] [INSPIRE].

[48] S. Caron-Huot, *Superconformal symmetry and two-loop amplitudes in planar $\mathcal{N} = 4$ super Yang-Mills*, *JHEP* **12** (2011) 066 [arXiv:1105.5606] [INSPIRE].

[49] S. Caron-Huot and S. He, *Jumpstarting the All-Loop S-matrix of Planar $\mathcal{N} = 4$ Super Yang-Mills*, *JHEP* **07** (2012) 174 [arXiv:1112.1060] [INSPIRE].

[50] J.L. Bourjaily, P. Heslop and V.-V. Tran, *Perturbation Theory at Eight Loops: Novel Structures and the Breakdown of Manifest Conformality in $\mathcal{N} = 4$ Supersymmetric Yang-Mills Theory*, *Phys. Rev. Lett.* **116** (2016) 191602 [arXiv:1512.07912] [INSPIRE].

[51] J.L. Bourjaily, E. Herrmann, C. Langer, A.J. McLeod and J. Trnka, *Prescriptive Unitarity for Non-Planar Six-Particle Amplitudes at Two Loops*, *JHEP* **12** (2019) 073 [arXiv:1909.09131] [INSPIRE].

[52] J.L. Bourjaily and J. Trnka, *Local Integrand Representations of All Two-Loop Amplitudes in Planar SYM*, *JHEP* **08** (2015) 119 [arXiv:1505.05886] [INSPIRE].

[53] J.L. Bourjaily, E. Herrmann and J. Trnka, *Prescriptive Unitarity*, *JHEP* **06** (2017) 059 [arXiv:1704.05460] [INSPIRE].

[54] J.L. Bourjaily, S. Caron-Huot and J. Trnka, *Dual-Conformal Regularization of Infrared Loop Divergences and the Chiral Box Expansion*, *JHEP* **01** (2015) 001 [arXiv:1303.4734] [INSPIRE].

[55] J.L. Bourjaily, F. Dulat and E. Panzer, *Manifestly Dual-Conformal Loop Integration*, *Nucl. Phys.* **B 942** (2019) 251 [arXiv:1901.02887] [INSPIRE].

[56] N. Arkani-Hamed, J.L. Bourjaily, F. Cachazo and J. Trnka, *Local Integrals for Planar Scattering Amplitudes*, *JHEP* **06** (2012) 125 [arXiv:1012.6032] [INSPIRE].

[57] N. Arkani-Hamed, J.L. Bourjaily, F. Cachazo, S. Caron-Huot and J. Trnka, *The All-Loop Integrand For Scattering Amplitudes in Planar $\mathcal{N} = 4$ SYM*, *JHEP* **01** (2011) 041 [arXiv:1008.2958] [INSPIRE].

JHEP02(2020)025

[58] J. Henn, E. Herrmann and J. Parra-Martinez, *Bootstrapping two-loop Feynman integrals for planar $\mathcal{N} = 4$ SYM*, *JHEP* **10** (2018) 059 [arXiv:1806.06072] [INSPIRE].

[59] A. Hodges, *Eliminating spurious poles from gauge-theoretic amplitudes*, *JHEP* **05** (2013) 135 [arXiv:0905.1473] [INSPIRE].

[60] L.J. Mason and D. Skinner, *Dual Superconformal Invariance, Momentum Twistors and Grassmannians*, *JHEP* **11** (2009) 045 [arXiv:0909.0250] [INSPIRE].

[61] N. Arkani-Hamed, F. Cachazo and C. Cheung, *The Grassmannian Origin Of Dual Superconformal Invariance*, *JHEP* **03** (2010) 036 [arXiv:0909.0483] [INSPIRE].

[62] J.L. Bourjaily, *Efficient Tree-Amplitudes in $\mathcal{N} = 4$: Automatic BCFW Recursion in Mathematica*, arXiv:1011.2447 [INSPIRE].

[63] J.L. Bourjaily, *Positroids, Plabic Graphs and Scattering Amplitudes in Mathematica*, arXiv:1212.6974 [INSPIRE].

[64] F. Brown, *The Massless higher-loop two-point function*, *Commun. Math. Phys.* **287** (2009) 925 [arXiv:0804.1660] [INSPIRE].

[65] F. Brown, *On the periods of some Feynman integrals*, arXiv:0910.0114 [INSPIRE].

[66] E. Panzer, *Algorithms for the symbolic integration of hyperlogarithms with applications to Feynman integrals*, *Comput. Phys. Commun.* **188** (2015) 148 [arXiv:1403.3385] [INSPIRE].

[67] M. Besier, D. van Straten and S. Weinzierl, *Rationalizing roots: an algorithmic approach*, *Commun. Num. Theor. Phys.* **13** (2019) 253 [arXiv:1809.10983] [INSPIRE].

[68] C.W. Bauer, A. Frink and R. Kreckel, *Introduction to the GiNaC framework for symbolic computation within the C++ programming language*, *J. Symb. Comput.* **33** (2000) 1 [cs/0004015] [INSPIRE].

[69] J. Vollinga and S. Weinzierl, *Numerical evaluation of multiple polylogarithms*, *Comput. Phys. Commun.* **167** (2005) 177 [hep-ph/0410259] [INSPIRE].

[70] The Sage Developers, *SageMath, the Sage Mathematics Software System (Version 8.8)*, (2019) http://www.sagemath.org/.

[71] The PARI Group, *PARI/GP version 2.11.0*, (2018) http://pari.math.u-bordeaux.fr/.

[72] M. Heller, A. von Manteuffel and R.M. Schabinger, *Multiple polylogarithms with algebraic arguments and the two-loop EW-QCD Drell-Yan master integrals*, arXiv:1907.00491 [INSPIRE].

[73] R. Bonciani et al., *Evaluating two-loop non-planar master integrals for Higgs + jet production with full heavy-quark mass dependence*, arXiv:1907.13156 [INSPIRE].

[74] J.M. Drummond, J. Henn, G.P. Korchemsky and E. Sokatchev, *Generalized unitarity for $\mathcal{N} = 4$ super-amplitudes*, *Nucl. Phys.* **B 869** (2013) 452 [arXiv:0808.0491] [INSPIRE].

[75] H. Elvang, D.Z. Freedman and M. Kiermaier, *Dual conformal symmetry of 1-loop NMHV amplitudes in $\mathcal{N} = 4$ SYM theory*, *JHEP* **03** (2010) 075 [arXiv:0905.4379] [INSPIRE].

[76] W. Stein, *Algebraic Number Theory, a Computational Approach*, (2012) and online pdf version at https://wstein.org/books/ant/ant.pdf.

[77] C. Zhang, Z. Li and S. He, *Two-loop Octagons, Algebraic Letters and $\overline{Q}$ Equations*, arXiv:1911.01290 [INSPIRE].

JHEP02(2020)025

JHEP

Published for SISSA by Springer

Received: December 18, 2019
Accepted: March 25, 2020
Published: April 21, 2020

A quantum framework for AdS/dCFT through fuzzy spherical harmonics on S^4

Aleix Gimenez-Grau,[a] **Charlotte Kristjansen,**[b] **Matthias Volk**[b] **and Matthias Wilhelm**[b]

[a] *DESY Hamburg, Theory Group,*
Notkestraße 85, 22607 Hamburg, Germany
[b] *Niels Bohr Institute, Copenhagen University,*
Blegdamsvej 17, 2100 Copenhagen Ø, Denmark

E-mail: aleix.gimenez@desy.de, kristjan@nbi.ku.dk, mvolk@nbi.ku.dk, matthias.wilhelm@nbi.ku.dk

Abstract: We consider a non-supersymmetric domain-wall version of $\mathcal{N} = 4$ SYM theory where five out of the six scalar fields have non-zero classical values on one side of a wall of codimension one. The classical fields have commutators which constitute an irreducible representation of the Lie algebra $\mathfrak{so}(5)$ leading to a highly non-trivial mixing between color and flavor components of the quantum fields. Making use of fuzzy spherical harmonics on S^4, we explicitly solve the mixing problem and derive not only the spectrum of excitations at the quantum level but also the propagators of the original fields needed for perturbative quantum computations. As an application, we derive the one-loop one-point function of a chiral primary and find complete agreement with a supergravity prediction of the same quantity in a double-scaling limit which involves a limit of large instanton number in the dual D3-D7 probe-brane setup.

Keywords: 1/N Expansion, AdS-CFT Correspondence, Supersymmetric Gauge Theory

ArXiv ePrint: 1912.02468

https://doi.org/10.1007/JHEP04(2020)132

JHEP04(2020)132

Contents

1 Introduction and summary **1**

2 Diagonalization of the mass matrix **3**
- 2.1 Expansion of the action 3
- 2.2 Decomposition of the color matrices and easy bosons 5
- 2.3 Complicated bosons 7
- 2.4 Fermions 9

3 Propagators **10**
- 3.1 Off-diagonal block 11
- 3.2 Adjoint block 13

4 One-loop corrections to the classical solution and one-point functions **15**
- 4.1 One-loop correction to the classical solution 15
- 4.2 One-loop correction to $\langle \mathrm{tr}(Z^L) \rangle$ 17

5 Conclusion and outlook **18**

A Conventions **20**
- A.1 $\mathcal{N} = 4$ SYM action 20
- A.2 $\mathfrak{so}(5)$ and $\mathfrak{so}(6)$ 20
- A.3 G matrices 21

B Details on the diagonalization **22**
- B.1 Complicated bosons 22
- B.2 Fermions 25

C Details on the propagators **26**

D Effective vertex **29**

E Matrix elements and Clebsch-Gordan coefficients **30**

1 Introduction and summary

There exists a number of domain-wall versions of $\mathcal{N} = 4$ SYM theory characterized by some or possibly all of the scalar fields acquiring non-vanishing and spacetime-dependent vacuum expectation values (vevs) on one side of a codimension-one wall. These theories constitute defect conformal field theories and have well-defined holographic duals in the form of probe-brane models with non-vanishing background gauge-field flux or instanton number [1–7]. They have been studied both from the perspective of supersymmetric boundary conditions [8] and from the perspective of condensed matter physics, the probe-brane models being capable of describing strongly coupled Dirac fermions in 2+1 dimensions [9–14].

JHEP04(2020)132

More recently, these models have been analyzed from the point of view of integrability, where the domain wall or defect is viewed as a boundary state of the integrable bulk $\mathcal{N}=4$ SYM theory [15–21]; see also [22, 23]. Furthermore, the models have been studied with the aim of testing AdS/dCFT in situations where supersymmetry is partially or completely broken [24–26], the comparison between gauge theory and string theory being made possible by the introduction of a certain double-scaling limit [6, 7]. Table 1 below summarizes the status of these investigations.

In the present paper, we fill the last gap in the table. We will study the most complicated of the above mentioned domain-wall versions of $\mathcal{N}=4$ SYM theory where five out of the six scalar fields have vevs whose commutators constitute an irreducible representation of the Lie algebra $\mathfrak{so}(5)$. The string-theory dual of this dCFT is a D3-D7 probe-brane system where the geometry of the probe brane is $AdS_4\times S^4$, and where a non-Abelian background gauge field forms an instanton bundle with instanton number d_G on the S^4 [2, 9]. The instanton number on the string-theory side translates into the dimension, d_G, of the $\mathfrak{so}(5)$ representation on the gauge-theory side, where

$$d_G=\frac{1}{6}(n+1)(n+2)(n+3),\qquad n\in\mathbb{N}. \tag{1.1}$$

Combining the large-N limit with the following double scaling [7],

$$\lambda\to\infty,\quad n\to\infty,\quad \frac{\lambda}{\pi^2n^2}\quad\text{fixed}, \tag{1.2}$$

one can by means of a supergravity approximation derive results for simple observables such as one-point functions or Wilson loops. Certain results allow an expansion in positive powers of the double-scaling parameter $\frac{\lambda}{\pi^2n^2}$ and open for the possibility of comparing to a perturbative gauge-theory calculation. We notice that the perturbative regime in the gauge theory lies within the parameter region where the probe-brane system is stable, which is given by [9]

$$\frac{\lambda}{\pi^2(n+1)(n+3)}<\frac{2}{7}. \tag{1.3}$$

One simple observable that can be studied using both supergravity and gauge theory is the one-point function of the unique $\mathfrak{so}(5)$-symmetric chiral primary of even length L, $\mathcal{O}_L$. In [7], this one-point function was calculated in supergravity to the leading order in the double-scaling parameter. The computation can straightforwardly be extended to subleading order and results in the following prediction for the ratio between the full one-point function and its tree-level value:

$$\frac{\langle\mathcal{O}_L\rangle}{\langle\mathcal{O}_L\rangle_{\text{tree}}}=1+\frac{\lambda}{\pi^2n^2}\frac{L(L+3)}{4(L-1)}+\mathcal{O}\left(\left(\frac{\lambda}{\pi^2n^2}\right)^2\right). \tag{1.4}$$

This prediction trivially carries over to the simple chiral primary $\operatorname{tr} Z^L$ with $Z=\phi_5+i\phi_6$, which has a non-vanishing projection on the $\mathfrak{so}(5)$-symmetric one.

In the present paper, we will confirm this supergravity prediction by a rather intricate gauge-theory computation. The non-vanishing $\mathfrak{so}(5)$-symmetric vevs of the scalars

JHEP04(2020)132

	D3-D5	D3-D7	D3-D7
Supersymmetry	1/2-BPS	None	None
Brane geometry	$AdS_4\times S^2$	$AdS_4\times S^2\times S^2$	$AdS_4\times S^4$
Flux/Instanton number	k	k_1, k_2	$\frac{(n+1)(n+2)(n+3)}{6}$
Double-scaling parameter	$\frac{\lambda}{\pi^2 k^2}$	$\frac{\lambda}{\pi^2(k_1^2+k_2^2)}$	$\frac{\lambda}{\pi^2 n^2}$
Boundary state	Integrable	Non-integrable	Integrable
AdS/dCFT match	Yes	Yes	Yes (this work)

Table 1. The string theory configurations dual to the dCFT versions of $\mathcal{N}=4$ SYM theory with non-vanishing vevs. The discussion of the integrability properties of the corresponding boundary states can be found in [19, 20] and the test of the match between gauge theory and string theory referred to in the first two columns can be found in [24–26].

introduce a complicated (spacetime-dependent) mass matrix mixing color and flavor components of the standard fields of $\mathcal{N}=4$ SYM theory. Needless to say, the diagonalization of this mass matrix requires the machinery of representation theory of orthogonal groups, the key element being the introduction of fuzzy spherical harmonics on S^4.

Our motivation for setting up the perturbative program for this dCFT is not only a wish to reproduce the formula (1.4) and thus provide a positive test of AdS/dCFT in a situation where supersymmetry is completely broken. Having a perturbative program will also make it possible to generate a wealth of new data which could provide input to the boundary conformal bootstrap program as well as to the search for higher-loop integrability in the one-point function problem in AdS/dCFT.

Our paper is organized as follows. We start by describing the diagonalization of the mass matrix in section 2 and explicitly give the complete spectrum of quantum excitations including their multiplicities. The propagators of the fields which diagonalize the mass matrix are found following the procedure of [25], and due to the spacetime-dependence of the vevs, become propagators in an auxiliary AdS_4 space. For concrete perturbative calculations, it is convenient to have the contraction rules and propagators formulated in terms of the original fields of $\mathcal{N}=4$ SYM theory and the complete set of these are presented in section 3. In section 4, we calculate the one-loop correction to the classical solution as well as to the one-point function of $\mathrm{tr}\, Z^L$ and confirm the prediction (1.4) in the double-scaling limit; explicit expression for both quantities at finite n are also attached as *Supplementary material* to this paper. Finally, section 5 contains our conclusion and outlook. A number of technical details are relegated to appendices.

2 Diagonalization of the mass matrix

2.1 Expansion of the action

We will be considering a domain-wall version of $\mathcal{N}=4$ SYM theory where five of the six real scalar fields ϕ_i have non-vanishing vevs on one side of a codimension-one wall, say for $x_3>0$, and we will be interested in calculating observables in this region of spacetime.

JHEP04(2020)132

With $A_\mu^{\rm cl} = \psi^{\rm cl} = 0$, the classical equations of motion for the six scalars read[1]

$$\nabla^2 \phi_i^{\rm cl} = \left[\phi_j^{\rm cl}, \left[\phi_j^{\rm cl}, \phi_i^{\rm cl}\right]\right], \quad i = 1, \ldots, 6. \tag{2.1}$$

A classical solution with $\mathfrak{so}(5)$ symmetry was found in [2, 29];

$$\phi_i^{\rm cl}(x) = \frac{1}{\sqrt{2}x_3} \begin{pmatrix} G_{i6} & 0 \\ 0 & 0 \end{pmatrix}, \quad \phi_6^{\rm cl}(x) = 0, \quad x_3 > 0. \tag{2.2}$$

Here the matrices G_{i6} together with $G_{ij} \equiv -i[G_{i6}, G_{j6}]$ for $i, j = 1, \ldots, 5$ are generators of the representation $(\frac{n}{2}, \frac{n}{2}, \frac{n}{2})$ of the Lie algebra $\mathfrak{so}(6)$.[2] From the commutation relations of $\mathfrak{so}(6)$, one can check that (2.2) indeed solves the equations of motion. The matrices G_{i6} can be constructed as an n-fold symmetrized tensor product of γ matrices and their dimension is given in (1.1); see appendix A.3 for details.

To take into account quantum effects, we expand the scalar fields around the classical solution (2.2) as

$$\phi_i(x) = \phi_i^{\rm cl}(x) + \tilde{\phi}_i(x). \tag{2.3}$$

Inserting the expansion into the action of $\mathcal{N} = 4$ SYM theory generates (spacetime-dependent) mass terms for some of the fields, as well as novel cubic and quartic interaction terms. This has been worked out in detail in [24–26].

Upon insertion of the expansion (2.3), the kinetic terms of the action remain canonical, while the mass terms acquire a non-trivial mixing between different fields. We can rewrite the mass matrices in a compact form in terms of the operators

$$L_{ij} \equiv \mathrm{ad}\left(G_{ij} \oplus 0_{N-d_G}\right) \quad i, j = 1, \ldots, 6. \tag{2.4}$$

The mass terms split into three different pieces:

$$S_{\rm mass} = S_{\rm m,b,e} + S_{\rm m,b,c} + S_{\rm m,f}. \tag{2.5}$$

The first one involves only bosonic terms, and following [25] we call it *easy* because the mixing only involves color degrees of freedom,

$$S_{\rm m,b,e} = \frac{2}{g_{\rm YM}^2} \int \mathrm{d}^4x \left(\frac{-1}{2x_3^2}\right) \mathrm{tr}\left[\frac{1}{2} E^\dagger \sum_{i=1}^{5} \left(L_{i6}\right)^2 E\right], \quad E = \begin{pmatrix} A_0 \\ A_1 \\ A_2 \\ \tilde{\phi}_6 \end{pmatrix}. \tag{2.6}$$

[1] See appendix A for a full set of our conventions. We refer to the reviews [27, 28] for an introduction to the study of domain-wall versions of $\mathcal{N} = 4$ SYM theory and their one-point functions.

[2] We are using the eigenvalues of the three generators of the Cartan subalgebra to label the $\mathfrak{so}(6)$ representation, see appendix A.2.

JHEP04(2020)132

We call the second term *complicated*, because it mixes color and flavor degrees of freedom,

$$S_{\mathrm{m,b,c}} = \frac{2}{g_{\mathrm{YM}}^2}\int \mathrm{d}^4x \left(\frac{-1}{2x_3^2}\right) \mathrm{tr}\left[C^\dagger \begin{pmatrix} \frac{1}{2}\sum_{i=1}^5 (L_{i6})^2 - \frac{1}{2}\sum_{i,j=1}^5 S_{ij}L_{ij} & \sqrt{2}\sum_{i=1}^5 R_i L_{i6} \\ \sqrt{2}\sum_{i=1}^5 R_i^\dagger L_{i6} & \frac{1}{2}\sum_{i=1}^5 (L_{i6})^2 \end{pmatrix} C\right], \tag{2.7}$$

with the vector of complicated fields

$$C = \begin{pmatrix} \tilde{\phi}_1 \\ \vdots \\ \tilde{\phi}_5 \\ A_3 \end{pmatrix}. \tag{2.8}$$

In the above expression, S_{ij} are 5×5 matrices that form the fundamental representation of $\mathfrak{so}(5)$, whereas R_i are five-dimensional column vectors with components $(R_j)_k = i\delta_{jk}$. Finally, we have a mass term for the fermions. In this case, not only is there mixing between color and flavor, but also the different chiralities are mixed. It is therefore useful to separate the fermions into their chiral components using the projectors $P_L = \frac{1}{2}(1+\gamma_5)$ and $P_R = \frac{1}{2}(1-\gamma_5)$. We obtain

$$S_{\mathrm{m,f}} = \frac{2}{g_{\mathrm{YM}}^2}\int \mathrm{d}^4x \left(\frac{-1}{2x_3}\right) \mathrm{tr}\left(\bar{\psi}_\alpha \mathcal{C}_{\alpha\beta}(P_L\psi_\beta) + \bar{\psi}_\alpha \mathcal{C}^\dagger_{\alpha\beta}(P_R\psi_\beta)\right). \tag{2.9}$$

The components of $\mathcal{C}_{\alpha\beta}$ involve the operators L_{i6} and thus act non-trivially on the color part of the fields. They are explicitly given in appendix B.2.

To set up the perturbative program, we first need to gauge fix introducing ghosts[3] as in [25, 26] and subsequently to diagonalize the mass matrix, i.e. to expand the fields in a basis on which all the operators and matrices in the quadratic part of the action act diagonally. We postpone the somewhat technical construction of this basis to appendix B and proceed to summarize the spectrum which can largely be understood from the representation theory of $\mathfrak{so}(5)$ and $\mathfrak{so}(6)$.

2.2 Decomposition of the color matrices and easy bosons

From the color structure of the classical solution (2.2), it is natural to decompose the $\mathrm{U}(N)$ adjoint fields into blocks as[4]

$$\Phi = [\Phi]_{m,m'}F^m{}_{m'} + [\Phi]_{m,a}F^m{}_a + [\Phi]_{a,m}F^a{}_m + [\Phi]_{a,a'}F^a{}_{a'} = \begin{pmatrix} [\Phi]_{m,m'} & [\Phi]_{m,a} \\ [\Phi]_{a,m} & [\Phi]_{a,a'} \end{pmatrix}, \tag{2.10}$$

where $m, m' = 1, \ldots, d_G$ and $a, a' = d_G+1, \ldots, N$. Since we rewrote the mass terms using L_{ij}, it is natural to ask how it acts on the different blocks. Anticipating their transformation

[3] For the purpose of diagonalizing the mass matrix, the ghosts behave as easy bosons.

[4] The $N\times N$ basis matrices $F^m{}_{m'}$ are zero everywhere except at position (m, m'), where they are one.

JHEP04(2020)132

behavior, we will often refer to $[\Phi]_{m,m'}$ as the fields in the adjoint block, whereas $[\Phi]_{m,a}$ and $[\Phi]_{a,m}$ will simply be called fields in the off-diagonal block.

First, we note that $L_{ij}F^{a}{}_{a'} = 0$, so all the fields in the $(N - d_G) \times (N - d_G)$ block are massless. We will see in later sections that the fields in this block do not contribute to the one-point functions we will calculate, and we will mostly ignore them. The fields in the off-diagonal block transform as

$$L_{ij}F^{m}{}_{a} = F^{m'}{}_{a}[G_{ij}]_{m',m}, \quad L_{ij}F^{a}{}_{m} = F^{a}{}_{m'}[-(G_{ij})^{T}]_{m',m}. \tag{2.11}$$

This means that an upper index m transforms in the $(\frac{n}{2}, \frac{n}{2}, \frac{n}{2})$ of $\mathfrak{so}(6)$, while a lower index m transforms in the dual representation $\overline{(\frac{n}{2}, \frac{n}{2}, \frac{n}{2})}$. Finally, the fields in the $d_G \times d_G$ dimensional adjoint block carry one index and its dual, so they transform as the product of the two representations. This product can be decomposed into a direct sum of irreducible representations

$$\left(\frac{n}{2}, \frac{n}{2}, \frac{n}{2}\right) \otimes \overline{\left(\frac{n}{2}, \frac{n}{2}, \frac{n}{2}\right)} = \bigoplus_{m=0}^{n} (m, m, 0). \tag{2.12}$$

The key observation (see also [30, 31]) to obtain the spectrum and diagonalize the easy mass term is that it is given by the difference of Casimir operators for $\mathfrak{so}(5)$ and $\mathfrak{so}(6)$,

$$\frac{1}{2}\sum_{i=1}^{5}(L_{i6})^2 = \frac{1}{2}\sum_{1\le i<j\le 6}(L_{ij})^2 - \frac{1}{2}\sum_{1\le i<j\le 5}(L_{ij})^2 = \frac{1}{2}\left(C_6 - C_5\right). \tag{2.13}$$

Any representation of $\mathfrak{so}(6)$ can be decomposed into a direct sum of irreducible representations of $\mathfrak{so}(5)$. Equation (2.13) implies that fields belonging to different $\mathfrak{so}(5)$ representations will have different masses.

For example, we have seen that the fields in the off-diagonal block transform as the $(\frac{n}{2}, \frac{n}{2}, \frac{n}{2})$ of $\mathfrak{so}(6)$ and its dual. It turns out that they are irreducible representations of $\mathfrak{so}(5)$:

$$[\Phi]_{m,a} : \left(\frac{n}{2}, \frac{n}{2}, \frac{n}{2}\right) \to \left(\frac{n}{2}, 0\right), \qquad [\Phi]_{a,m} : \overline{\left(\frac{n}{2}, \frac{n}{2}, \frac{n}{2}\right)} \to \left(\frac{n}{2}, 0\right), \tag{2.14}$$

where our notation and conventions are explained in appendix A.2. Thus, all fields in the off-diagonal block have the same mass, which we can easily obtain from (2.13) and the formulas for the eigenvalues of the Casimirs in (A.11).

For the adjoint block, we saw in (2.12) that the fields decompose into a sum of irreducible representations of $\mathfrak{so}(6)$. Each of these representations of the form $(m, m, 0)$ can in turn be decomposed into $\mathfrak{so}(5)$ components using the branching rule (A.12)

$$[\Phi]_{m,m'} : \left(\frac{n}{2}, \frac{n}{2}, \frac{n}{2}\right) \otimes \overline{\left(\frac{n}{2}, \frac{n}{2}, \frac{n}{2}\right)} \to \bigoplus (L_1, L_2), \tag{2.15}$$

where the sum runs over all half-integers (L_1, L_2) such that

$$0 \le L_2 \le L_1, \qquad L_1 + L_2 \le n. \tag{2.16}$$

JHEP04(2020)132

Eigenstate	Mass	Multiplicity
$[E]_{a,a'}$	0	$(N-d_G)(N-d_G)$
$[E]_{m,a}$	$m^2_{\text{easy}} = \frac{1}{8}n(n+4)$	$2d_G(N-d_G)$
$[E]_{\mathbf{L}}$	$\hat{m}^2_{\text{easy}} = 2L_1L_2 + L_1 + 2L_2$	$d_5(L_1,L_2)$

Table 2. Masses of the easy bosons $E = A_0, A_1, A_2, \tilde{\phi}_6$. The allowed ranges of L_1 and L_2 are $0 \leq L_2 \leq L_1$, $L_1+L_2 \leq n$. The definitions of d_5 and d_G can be found in (1.1) and (A.8), respectively.

Therefore, fields with several different masses occur in the adjoint block, one for each $\mathfrak{so}(5)$ representation in the above sum. Once again, from the expression of the Casimir operators (A.11) we obtain the easy masses summarized in table 2. It is important to note that the $\mathfrak{so}(6)$ Casimir needs to be evaluated for $(L_1+L_2, L_1+L_2, 0)$, which can be seen from working out the decomposition (2.15) explicitly.

So far we have only focused on the spectrum, but we have not discussed how the diagonalization can explicitly be carried out. We can find an explicit orthonormal basis that diagonalizes the easy mass term, namely

$$[\Phi]_{m,m'}F^{m}{}_{m'} = \sum_{\mathbf{L}} [\Phi]_{\mathbf{L}} \hat{Y}_{\mathbf{L}}, \qquad \text{tr}\left(\hat{Y}^{\dagger}_{\mathbf{L}'}\hat{Y}_{\mathbf{L}}\right) = \delta_{\mathbf{L}',\mathbf{L}}. \tag{2.17}$$

The matrices $\hat{Y}_{\mathbf{L}}$ are $\mathfrak{so}(5)$-symmetric fuzzy spherical harmonics — the $\mathfrak{so}(5)$ analogue of the basis used in [24, 25]. For our purposes, only the existence of this basis will be important. An explicit construction of the matrices can be found in [32]. In general, we use the notation $\mathbf{L}$ to collectively refer to the quantum numbers that uniquely specify an $\mathfrak{so}(5)$ state within a representation. This is described in more detail in appendix A.2. For example, the sum over $\mathbf{L}$ includes a sum over all possible highest weights (L_1, L_2) in (2.15), and for each of them also the $d_5(L_1, L_2)$ states that form the representation.

2.3 Complicated bosons

We now turn towards the complicated mass terms, for which color and flavor degrees of freedom mix. The key observation of [26] is that if one can find an eigenvector of the 5×5 block of the mass matrix in (2.7) which is annihilated by the 1×5 block $R_i^{\dagger}L_i$, then we obtain an eigenvector of the full matrix.

In particular, to diagonalize the 5×5 block we define the total $\mathfrak{so}(5)$ 'angular momentum' operator J_{ij}, such that

$$J_{ij} \equiv L_{ij} + S_{ij} \quad \Rightarrow \quad \frac{1}{2}\sum_{i,j=1}^{5} S_{ij}L_{ij} = \frac{1}{2}\sum_{1\leq i<j\leq 5}\Big[(J_{ij})^2 - (L_{ij})^2 - (S_{ij})^2\Big]. \tag{2.18}$$

On the right hand side, we have a combination of $\mathfrak{so}(5)$ Casimir operators, which act trivially on irreducible representations. As mentioned above, the matrices S_{ij} form the fundamental of $\mathfrak{so}(5)$ which is labeled by $(\frac{1}{2}, \frac{1}{2})$. After decomposing the fields in $\mathfrak{so}(5)$ fuzzy spherical harmonics, they therefore transform in the product representation $(L_1, L_2) \otimes (\frac{1}{2}, \frac{1}{2})$.

JHEP04(2020)132

This product decomposes into irreducible representations with well-defined total angular momentum (J_1, J_2) as

$$(L_1, L_2) \otimes \left(\frac{1}{2}, \frac{1}{2}\right) = \left(L_1 + \frac{1}{2}, L_2 + \frac{1}{2}\right) \oplus \left(L_1 - \frac{1}{2}, L_2 - \frac{1}{2}\right) \oplus (L_1, L_2) \\ \oplus \left(L_1 + \frac{1}{2}, L_2 - \frac{1}{2}\right) \oplus \left(L_1 - \frac{1}{2}, L_2 + \frac{1}{2}\right), \quad \text{for } 0 < L_2 < L_1, \tag{2.19a}$$

$$(L_1, L_1) \otimes \left(\frac{1}{2}, \frac{1}{2}\right) = \left(L_1 + \frac{1}{2}, L_1 + \frac{1}{2}\right) \oplus \left(L_1 - \frac{1}{2}, L_1 - \frac{1}{2}\right) \oplus \left(L_1 + \frac{1}{2}, L_1 - \frac{1}{2}\right), \tag{2.19b}$$

$$(L_1, 0) \otimes \left(\frac{1}{2}, \frac{1}{2}\right) = \left(L_1 + \frac{1}{2}, \frac{1}{2}\right) \oplus (L_1, 0) \oplus \left(L_1 - \frac{1}{2}, \frac{1}{2}\right). \tag{2.19c}$$

The masses of the fields that diagonalize the 5×5 block of the complicated action can now again be obtained from the Casimir operators,

$$\frac{1}{2}\left(\sum_{i=1}^{5} (L_{i6})^2 - \sum_{i,j=1}^{5} S_{ij} L_{ij}\right) = \frac{1}{2}\left[C_6(L_1 + L_2, L_1 + L_2, 0) - C_5(J_1, J_2) + C_5\left(\frac{1}{2}, \frac{1}{2}\right)\right]. \tag{2.20}$$

Generically, we obtain the five fields $B_{\pm,\pm}$, $B_{\pm,\mp}$ and B_{00} from the decomposition (2.19a) that diagonalize the 5×5 block. It turns out that $B_{\pm,\pm}$ and B_{00} are indeed mass eigenstates of the full complicated mass term, as the corresponding basis states are annihilated by $\sum_{i=1}^{5} R_i^\dagger L_{i6}$. As we describe in appendix B.1, the remaining complicated fields $B_{\pm,\mp}$ and A_3 still mix through a 3×3 matrix. Diagonalizing this matrix we find the six mass eigenstates $B_{\pm,\pm}$, B_{00}, $D_\pm$ and D_0, where the last three are simple linear combinations of $B_{\pm,\mp}$ and A_3. We list their masses in table 3. There are two edge cases in the decomposition of $(L_1, L_2) \otimes (\frac{1}{2}, \frac{1}{2})$ corresponding to (2.19b) and (2.19c). We find that for (L_1, L_1) the B_{00} and D_0 fields are missing, and for $(L_1, 0)$ the B_{--} and D_0 fields are missing. This concludes the derivation of the spectrum for the complicated bosons in the adjoint block.

The diagonalization for the complicated bosons in the off-diagonal block proceeds in a similar manner. In this case, the relevant decomposition is

$$\left(\frac{n}{2}, 0\right) \otimes \left(\frac{1}{2}, \frac{1}{2}\right) = \left(\frac{n+1}{2}, \frac{1}{2}\right) \oplus \left(\frac{n}{2}, 0\right) \oplus \left(\frac{n-1}{2}, \frac{1}{2}\right). \tag{2.21}$$

In this case, B_{00} and A_3 mix in a 2×2 matrix which is diagonalized by $D_\pm$. We list the spectrum of the fields in the off-diagonal blocks in table 4. By abuse of notation, we reuse some of the previous names for the diagonal fields.

JHEP04(2020)132

Eigenstate	Mass	Multiplicity
B_{++}	$\hat{m}^2_{++} = (2L_1+1)L_2$	$d_5(L_1+\frac{1}{2}, L_2+\frac{1}{2})$
B_{--}	$\hat{m}^2_{--} = (2L_1+3)(L_2+1)$	$d_5(L_1-\frac{1}{2}, L_2-\frac{1}{2})$
B_{00}	$\hat{m}^2_{00} = L_1+2L_2(L_1+1)+2$	$d_5(L_1, L_2)$
D_0	$\hat{m}^2_{0} = L_1+2L_2(L_1+1)+2$	$d_5(L_1, L_2)$
D_+	$\hat{m}^2_{+} = 1+(L_1+2L_2(L_1+1))+\sqrt{1+4(L_1+2L_2(L_1+1))}$	$d_5(L_1, L_2)$
D_-	$\hat{m}^2_{-} = 1+(L_1+2L_2(L_1+1))-\sqrt{1+4(L_1+2L_2(L_1+1))}$	$d_5(L_1, L_2)$

Table 3. Masses and eigenstates of the complicated bosons in the adjoint block. The allowed ranges of L_1 and L_2 are $0 \leq L_2 \leq L_1$, $L_1+L_2 \leq n$. Note that in the case $L_2 = L_1$ the B_{00} and D_0 fields are missing, and in the case $L_2 = 0$ the B_{--} and D_0 fields are missing. The definition of d_5 can be found in (A.8).

Eigenstate	Mass	Multiplicity
B_{++}	$m^2_{++} = \frac{1}{8}n^2$	$2d_5(\frac{n+1}{2}, \frac{1}{2})(N-d_G)$
B_{-+}	$m^2_{-+} = \frac{1}{8}(n+4)^2$	$2d_5(\frac{n-1}{2}, \frac{1}{2})(N-d_G)$
D_+	$m^2_{+} = \frac{1}{8}\left(n^2+4n+8+4\sqrt{2(n^2+4n+2)}\right)$	$2d_5(\frac{n}{2}, 0)(N-d_G)$
D_-	$m^2_{-} = \frac{1}{8}\left(n^2+4n+8-4\sqrt{2(n^2+4n+2)}\right)$	$2d_5(\frac{n}{2}, 0)(N-d_G)$

Table 4. Masses and eigenstates of the complicated bosons in the off-diagonal block. The definition of d_5 can be found in (A.8).

2.4 Fermions

The diagonalization of the fermionic mass matrix $\mathcal{C}_{\alpha\beta}$ is non-trivial, so we will consider first a simplified version of the problem. The observation we make is that the eigenvalues of $\mathcal{C}^\dagger\mathcal{C}$ are actually the fermionic masses squared. Moreover, we will use the eigenvectors of $\mathcal{C}^\dagger\mathcal{C}$ to construct the eigenvectors of $\mathcal{C}$. From the explicit form of $\mathcal{C}_{\alpha\beta}$ given in appendix B.2, we obtain

$$\mathcal{C}^\dagger\mathcal{C} = \frac{1}{2}\left(\sum_{i=1}^{5}(L_{i6})^2 - \sum_{i,j=1}^{5}\tilde{S}_{ij}L_{ij}\right). \tag{2.22}$$

The 4×4 matrices $(\tilde{S}_{ij})_{\alpha\beta}$ constitute the four-dimensional representation of $\mathfrak{so}(5)$ which is labelled by $(\frac{1}{2}, 0)$.

Notice the similarity of this problem with that of the 5×5 block of the complicated bosonic mass term. In particular, a variant of (2.20) still holds, with the difference that now the total angular momentum (J_1, J_2) takes values in the decomposition[5]

$$(L_1, L_2)\otimes\left(\frac{1}{2}, 0\right) = \left(L_1+\frac{1}{2}, L_2\right)\oplus\left(L_1-\frac{1}{2}, L_2\right)\oplus\left(L_1, L_2+\frac{1}{2}\right)\oplus\left(L_1, L_2-\frac{1}{2}\right), \tag{2.23a}$$

$$\text{for } 0 < L_2 < L_2,$$

[5]We also have to change the last term in (2.20) to $C_5(\frac{1}{2}, 0)$.

JHEP04(2020)132

Eigenstate	Mass	Multiplicity
$\tilde{D}_{+0}$	$\hat{m}_{+0} = \sqrt{2(L_1+1)L_2}$	$d_5(L_1+\frac{1}{2}, L_2)$
$\tilde{D}_{-0}$	$\hat{m}_{-0} = \sqrt{2(L_1+1)(L_2+1)}$	$d_5(L_1-\frac{1}{2}, L_2)$
$\tilde{D}_{0+}$	$\hat{m}_{0+} = \sqrt{\frac{1}{2}(2L_1+1)(2L_2+1)}$	$d_5(L_1, L_2+\frac{1}{2})$
$\tilde{D}_{0-}$	$\hat{m}_{0-} = \sqrt{\frac{1}{2}(2L_1+3)(2L_2+1)}$	$d_5(L_1, L_2-\frac{1}{2})$

Table 5. Mass eigenvalues of the fermions in the adjoint block. The allowed ranges of L_1 and L_2 are $0 \leq L_2 \leq L_1$, $L_1 + L_2 \leq n$. Note that in the case $L_2 = L_1$ the fields $\tilde{D}_{-0}$ and $\tilde{D}_{0+}$ are missing, and in the case $L_2 = 0$ the $\tilde{D}_{0-}$ fields are missing. The definition of d_5 can be found in (A.8).

Eigenstate	Mass	Multiplicity
$\tilde{D}_{+0}$	$m_{+0} = \frac{1}{\sqrt{8}}n$	$2d_5(\frac{n+1}{2}, 0)(N - d_G)$
$\tilde{D}_{-0}$	$m_{-0} = \frac{1}{\sqrt{8}}(n+4)$	$2d_5(\frac{n-1}{2}, 0)(N - d_G)$
$\tilde{D}_{0+}$	$m_{0+} = \frac{1}{\sqrt{8}}(n+2)$	$2d_5(\frac{n}{2}, \frac{1}{2})(N - d_G)$

Table 6. Mass eigenvalues of the fermions in the off-diagonal block. The definition of d_G can be found in (1.1).

$$(L_1, L_1) \otimes \left(\frac{1}{2}, 0\right) = \left(L_1 + \frac{1}{2}, L_1\right) \oplus \left(L_1, L_1 - \frac{1}{2}\right), \tag{2.23b}$$

$$(L_1, 0) \otimes \left(\frac{1}{2}, 0\right) = \left(L_1 + \frac{1}{2}, 0\right) \oplus \left(L_1 - \frac{1}{2}, 0\right) \oplus \left(L_1, \frac{1}{2}\right). \tag{2.23c}$$

It is now an easy exercise to extract the masses of the fermionic diagonal fields. Note that compared to the complicated bosons there is no further mixing of fields after coupling the $\mathfrak{so}(5)$ representations (L_1, L_2) and $(\frac{1}{2}, 0)$ appropriately. In analogy to the previous section, we will denote the diagonal fields by $\tilde{D}_{\alpha,\beta}$. The fermionic masses are listed in table 5 for the adjoint block and in table 6 for the off-diagonal block.

3 Propagators

In the previous section, we have presented the spectrum of 'masses' of all the fields in the theory. In the action, these masses combine with a spacetime-dependent factor into $\frac{m^2}{x_3^2}$ for the bosons, and $\frac{m}{x_3}$ for the fermions. The propagators of fields in $(d+1)$-dimensional Minkowski space with such spacetime-dependent mass terms are related to the propagators of fields in AdS_{d+1}, as observed in [24, 25, 33].

For the purpose of our computation in section 4, only the propagators of fields evaluated at the same point in spacetime will be relevant. Since they are divergent, we need to introduce a regulator to keep them finite, and we will accomplish this working in dimensional reduction with $d = 3 - 2\epsilon$, such that the codimension of the defect remains one. For

JHEP04(2020)132

the bosonic fields, the regulated propagator is [25]

$$K^{m^2}(x,x) = \frac{g_{\rm YM}^2}{2}\frac{1}{16\pi^2 x_3^2}\left[m^2\left(-\frac{1}{\epsilon}-\log(4\pi)+\gamma_{\rm E}-2\log(x_3)+2\Psi\left(\nu+\frac{1}{2}\right)-1\right)-1\right], \quad (3.1)$$

where $\nu = \sqrt{m^2+\frac{1}{4}}$. Similarly, the (spinor trace of the) regularized propagator for the fermions is

$$\begin{aligned}\operatorname{tr} K_F^m(x,x) = \frac{g_{\rm YM}^2}{8\pi^2 x_3^3}\Bigg[&m^3+m^2-3m-1 \\ &+m(m^2-1)\left(-\frac{1}{\epsilon}-\log(4\pi)+\gamma_{\rm E}-2\log(x_3)+2\Psi(m)-2\right)\Bigg].\end{aligned} \quad (3.2)$$

In the above expressions, $\Psi(x)$ is the digamma function and γ_E is the Euler-Mascheroni constant.

As discussed in section 2, one can change basis from the fields $\tilde{\phi}_i$, A_μ and ψ_α in the action to the diagonal fields $B_{\pm,\pm}$, B_{00}, $D_\pm$ and D_0, such that the mass terms become diagonal. The propagators between these diagonal fields are then of the form (3.1) and (3.2) we just presented. However, it is easier to perform field-theory computations if we know the propagators between the original fields in the action. This can be achieved by inverting the steps in the diagonalization procedure, as explained in more detail in [25, 26]. In the resulting propagators there is mixing between color and flavor degrees of freedom, which is introduced by the presence of matrix elements of $\mathfrak{so}(6)$ generators.

Throughout this section, we denote by $K^{m_i^2}$ the scalar propagator with the mass m_i^2 being one of the masses listed in tables 3–6, and similarly for the fermions. We will merely present the final results in the main text and refer the reader to appendix C for more details.

3.1 Off-diagonal block

We begin with the propagators between fields from the off-diagonal block, because they are the most important ones for the purposes of later calculations in the large-N limit. We remind the reader that these fields are of the form $[\Phi]_{m,a}$, where $m = 1,\ldots,d_G$ and $a = d_G+1,\ldots,N$. The propagators will be expressed in terms of the matrix elements $[G_{ij}]_{m,m'}$ of the matrices G_{ij} that appear in the classical solution; see appendix A.3 for more details.

The simplest propagator is the one between two easy fields $E = A_0, A_1, A_2, \tilde{\phi}_6$, because in this case there is no mixing between the flavor and the color structure,

$$\langle [E]_{m,a}[E]^\dagger_{m',a'}\rangle = \delta_{m,m'}\delta_{a,a'}K^{m^2_{\rm easy}}. \quad (3.3)$$

Note that the propagator between two different easy fields vanishes.

JHEP04(2020)132

The remaining scalars $\tilde{\phi}_i$ with $i = 1, \ldots, 5$ mix with each other in the following way:

$$\langle [\tilde{\phi}_i]_{m,a} [\tilde{\phi}_j]^\dagger_{m',a'} \rangle = \delta_{a,a'} \left[\delta_{ij} \delta_{m,m'} f^{\text{sing}} + [G_{ij}]_{m,m'} f^{\text{lin}} + 4 [G_{i6} G_{j6}]_{m,m'} f^{\text{prod}} \right]. \tag{3.4}$$

The functions f above are linear combinations of bosonic propagators, with coefficients which only depend on n:

$$\begin{aligned} f^{\text{sing}} &= \frac{n}{2(n+2)} K^{m^2_{-+}} + \frac{n+4}{2(n+2)} K^{m^2_{++}}, \\ f^{\text{lin}} &= \frac{i}{n+2} \left(K^{m^2_{-+}} - K^{m^2_{++}} \right), \\ f^{\text{prod}} &= -\frac{K^{m^2_{-+}}}{2n(n+2)} - \frac{K^{m^2_{++}}}{2(n+2)(n+4)} + \frac{K^{m^2_{-}}}{4N_+} + \frac{K^{m^2_{+}}}{4N_-}, \end{aligned} \tag{3.5}$$

where the (normalization) factor $N_\pm$ is given by

$$N_\pm = 4m^2_{\text{easy}} + 1 \pm \sqrt{4m^2_{\text{easy}} + 1}\,. \tag{3.6}$$

As discussed in the diagonalization, the five scalars $\tilde{\phi}_i$ and the third component of the gauge field also couple in a non-trivial way,

$$\langle [\tilde{\phi}_i]_{m,a} [A_3]^\dagger_{m',a'} \rangle = -i \delta_{a,a'} \frac{1}{\sqrt{n(n+4)+2}} [G_{i6}]_{m,m'} \left(K^{m^2_{-}} - K^{m^2_{+}} \right), \tag{3.7}$$

while the third component of the gauge field with itself gives

$$\langle [A_3]_{m,a} [A_3]^\dagger_{m',a'} \rangle = \frac{\delta_{a,a'} \delta_{m,m'}}{2} \left[\left(1 + \frac{1}{\sqrt{4m^2_{\text{easy}}+1}} \right) K^{m^2_{-}} + \left(1 - \frac{1}{\sqrt{4m^2_{\text{easy}}+1}} \right) K^{m^2_{+}} \right]. \tag{3.8}$$

Note the similarity between these propagators, and the ones obtained for the defect theory dual to a D3-D7 setup with $\mathfrak{so}(3) \times \mathfrak{so}(3)$ symmetry [26]. In that case, the propagators had precisely the same structure if one makes the schematic replacement $G_{i6} \to t_i$, where t_i are generators of $\mathfrak{so}(3) \times \mathfrak{so}(3)$ (see (3.25)-(3.29) of [26] for further details).

Finally, in the diagonalization of the fermions ψ_α with $\alpha = 1, \ldots, 4$, different chiralities are mixed with the color and flavor degrees of freedom. As a result, the propagators will contain γ_5. Moreover, matrix elements $(C_i)_{\alpha\beta}$ will appear, where C_i are the matrices that couple scalars and fermions in the action of $\mathcal{N} = 4$ SYM theory, see (A.2). The propagators

JHEP04(2020)132

have the following structure:[6]

$$
\begin{aligned}
\langle [\psi_\alpha]_{m,a}[\overline{\psi_\beta}]_{a',m'}\rangle = \delta_{a,a'}\Bigg[&\delta_{m,m'}\left[\delta_{\alpha,\beta}\left(f_F^{0,+}-\gamma_5 f_F^{0,+}\gamma_5\right)+i(C_6)_{\alpha,\beta}\left(f_F^{0,-}+\gamma_5 f_F^{0,-}\gamma_5\right)\right]\\
&-\delta_{\alpha\beta}[G_{45}]_{m,m'}\left(f_F^{1,+}+\gamma_5 f_F^{1,+}\gamma_5\right)+i\sum_{i=1}^{3}\sum_{j=4}^{5}(C_iC_j)_{\alpha,\beta}[G_{ij}]_{m,m'}\left(\gamma_5 f_F^{1,-}-f_F^{1,-}\gamma_5\right)\\
&+\left(\frac{1}{2}\sum_{i,j,k=1}^{3}\epsilon_{ijk}(C_i)_{\alpha,\beta}[G_{jk}]_{m,m'}+i(C_6)_{\alpha,\beta}[G_{45}]_{m,m'}\right)\left(f_F^{1,-}-\gamma_5 f_F^{1,-}\gamma_5\right)\\
&+\sum_{i=1}^{3}(C_i)_{\alpha,\beta}[G_{i6}]_{m,m'}\left(f_F^{2,+}+\gamma_5 f_F^{2,+}\gamma_5\right)-\sum_{i=4}^{5}(C_i)_{\alpha,\beta}[G_{i6}]_{m,m'}\left(\gamma_5 f_F^{2,+}+f_F^{2,+}\gamma_5\right)\\
&+i\sum_{i=1}^{3}(C_iC_6)_{\alpha,\beta}[G_{i6}]_{m,m'}\left(f_F^{2,-}-\gamma_5 f_F^{2,-}\gamma_5\right)\\
&-i\sum_{i=4}^{5}(C_iC_6)_{\alpha,\beta}[G_{i6}]_{m,m'}\left(\gamma_5 f_F^{2,-}-f_F^{2,-}\gamma_5\right)\\
&+\frac{i}{2}\sum_{i,j,k=1}^{3}\sum_{l=4}^{5}\epsilon_{ijk}(C_iC_l)_{\alpha,\beta}[G_{[j6}G_{k6}G_{l6]}]_{m,m'}\left(\gamma_5 f_F^{3}+f_F^{3}\gamma_5\right)\\
&+\frac{1}{2}\sum_{i,j,k=4}^{6}\sum_{l=1}^{3}\epsilon_{ijk}(C_iC_l)_{\alpha,\beta}[G_{[j6}G_{k6}G_{l6]}]_{m,m'}\left(f_F^{3}+\gamma_5 f_F^{3}\gamma_5\right)\Bigg].
\end{aligned}
\tag{3.9}
$$

As for the complicated bosons, the f_F are functions that depend on n and the fermionic propagators (3.2)

$$
\begin{aligned}
f_F^{0,\pm} &= \frac{(n+4)}{8(n+1)}K_F^{m_{+0}} \pm \frac{n(n+4)}{4(n+1)(n+3)}K_F^{m_{0+}} + \frac{n}{8(n+3)}K_F^{m_{-0}},\\
f_F^{1,\pm} &= \pm\frac{1}{4(n+1)}K_F^{m_{+0}} + \frac{1}{2(n+1)(n+3)}K_F^{m_{0+}} \mp \frac{1}{4(n+3)}K_F^{m_{-0}},\\
f_F^{2,\pm} &= \frac{1}{4(n+1)}K_F^{m_{+0}} \pm \frac{(n+2)}{2(n+1)(n+3)}K_F^{m_{0+}} + \frac{1}{4(n+3)}K_F^{m_{-0}},\\
f_F^{3} &= -\frac{3}{(n+1)(n+2)}K_F^{m_{+0}} - \frac{6}{(n+1)(n+2)(n+3)}K_F^{m_{0+}} + \frac{3}{(n+2)(n+3)}K_F^{m_{-0}}.
\end{aligned}
\tag{3.10}
$$

The fermionic masses $m_{\alpha\beta}$ can be found in table 6.

3.2 Adjoint block

Now we present the propagators in the adjoint block. In this case, the fields are $[\Phi]_{m,m'}$ with $m = 1,\ldots,d_G$, but it is convenient to express them in terms of irreducible $\mathfrak{so}(5)$ representations. As explained in section 2, this is achieved by changing basis: $[\Phi]_{m,m'}F^{m}{}_{m'} = [\Phi]_{\mathbf{L}}\hat{Y}_{\mathbf{L}}$. In particular, the matrix elements of generators $L_{ij} = \mathrm{ad}\, G_{ij}$ will appear, and they can be

[6] The notation $[jkl]$ denotes antisymmetrization of the three indices, normalized by $\frac{1}{3!}$.

JHEP04(2020)132

computed as

$$\langle \mathbf{L}|L_{ij}|\mathbf{L}'\rangle = \mathrm{tr}\left(\hat{Y}^\dagger_{\mathbf{L}} L_{ij} \hat{Y}_{\mathbf{L}'}\right) = \mathrm{tr}\left(\hat{Y}^\dagger_{\mathbf{L}}\left[G_{ij}, \hat{Y}_{\mathbf{L}'}\right]\right). \tag{3.11}$$

However, using this expression is hard in general, because we do not have explicit formulas for $\hat{Y}_{\mathbf{L}}$. What one can do instead is to compute the matrix elements thinking of L_{ij} as an operator acting on an abstract vector $|\mathbf{L}\rangle$ in a certain $\mathfrak{so}(5)$ representation. We give a prescription on how to do this in appendix E.

The propagator between two easy fields $E = A_0, A_1, A_3, \tilde{\phi}_6$ is simple because there is no mixing of color and flavor

$$\langle [E]_{\mathbf{L}} [E]^\dagger_{\mathbf{L}'}\rangle = \delta_{\mathbf{L},\mathbf{L}'} K^{\hat{m}^2_{\text{easy}}}. \tag{3.12}$$

For the propagators between the five scalars $\tilde{\phi}_i$ with $i = 1, \ldots, 5$, the resulting structure is more complicated than in the off-diagonal block:

$$\begin{aligned}\langle [\tilde{\phi}_i]_{\mathbf{L}} [\tilde{\phi}_j]^\dagger_{\mathbf{L}'}\rangle = {} & \delta_{ij}\delta_{\mathbf{L},\mathbf{L}'}\, \hat{f}^{\,\text{sing}} + \langle \mathbf{L}|L_{ij}|\mathbf{L}'\rangle\, \hat{f}^{\,\text{lin}} + \langle \mathbf{L}|\{L_{ik}, L_{jl}\}L_{kl}|\mathbf{L}'\rangle\, \hat{f}^{\,\text{cubic}} \\ & + \langle \mathbf{L}|\{L_{ik}, L_{kj}\}|\mathbf{L}'\rangle\, \hat{f}^{\text{sym}}_5 \\ & + \langle \mathbf{L}|\{L_{i6}, L_{6j}\}|\mathbf{L}'\rangle \left[\delta_{L_1,L'_1}\delta_{L_2,L'_2}\, \hat{f}^{\text{sym}}_6 + \delta_{L'_1,L_1\pm 1}\delta_{L'_2,L_2\mp 1}\, \hat{f}^{\,\text{opp}}\right],\end{aligned} \tag{3.13}$$

and

$$\langle [\tilde{\phi}_i]_{\mathbf{L}} [A_3]^\dagger_{\mathbf{L}'}\rangle = i\langle \mathbf{L}|L_{i6}|\mathbf{L}'\rangle (\delta_{L_1,L'_1+\frac{1}{2}}\delta_{L_2,L'_2-\frac{1}{2}} + \delta_{L_1,L'_1-\frac{1}{2}}\delta_{L_2,L'_2+\frac{1}{2}})\hat{f}^{\,\phi A}(L'_1, L'_2). \tag{3.14}$$

The third component of the gauge field has the following propagator:

$$\langle [A_3]_{\mathbf{L}} [A_3]^\dagger_{\mathbf{L}'}\rangle = \delta_{\mathbf{L},\mathbf{L}'} \left(\frac{\left(-1 + \sqrt{4\hat{m}^2_{\text{easy}} + 1}\right)^2}{2N_-} K^{\hat{m}^2_+} + \frac{\left(1 + \sqrt{4\hat{m}^2_{\text{easy}} + 1}\right)^2}{2N_+} K^{\hat{m}^2_-} \right), \tag{3.15}$$

where $N_\pm$ were introduced in (3.6).[7]

Finally, one can obtain the propagators between the fermions in the adjoint block in a similar manner. Rewriting the propagators in terms of matrix elements is a complex task, and in most applications only certain traces of them will appear. In particular, one has that

$$\begin{aligned}\mathrm{tr}\,\langle [\psi_\alpha]_{\mathbf{L}} [\overline{\psi_\beta}]_{\mathbf{L}'}\rangle = {} & \sum_{i=1}^{3} (C_i)_{\alpha,\beta} \langle \mathbf{L}|L_{i6}|\mathbf{L}'\rangle\, \mathrm{tr}\, \hat{f}^{\text{lin}}_F(L_1, L_2; L'_1, L'_2) \\ & + \left(\sum_{i,j,k=4}^{6} \sum_{l=1}^{3} \epsilon_{ijk} (C_i C_l)_{\alpha,\beta}\, \langle \mathbf{L}|L_{[j6}L_{k6}L_{l6]}|\mathbf{L}'\rangle \right. \\ & \left. - \frac{i}{3} \sum_{i,j,k,l=1}^{3} \epsilon_{ijk} (C_i C_l)_{\alpha,\beta}\, \langle \mathbf{L}|L_{[j6}L_{k6}L_{l6]}|\mathbf{L}'\rangle \right) \mathrm{tr}\, \hat{f}^{\text{cub}}_F(L_1, L_2; L'_1, L'_2),\end{aligned} \tag{3.16}$$

[7] Note that $N_\pm$ needs to be evaluated using $\hat{m}^2_{\text{easy}}$ instead of m^2_{easy}.

JHEP04(2020)132

and

$$\mathrm{tr}\left(\gamma_5\langle[\psi_\alpha]_{\mathbf{L}}[\overline{\psi_\beta}]_{\mathbf{L}'}\rangle\right) = -\sum_{i=4}^{5}(C_i)_{\alpha,\beta}\langle\mathbf{L}|L_{i6}|\mathbf{L}'\rangle\,\mathrm{tr}\,\hat{f}_F^{\mathrm{lin}}(L_1,L_2;L_1',L_2') \tag{3.17}$$
$$+\,i\sum_{i,j,k=1}^{3}\sum_{l=4}^{6}\epsilon_{ijk}(C_iC_l)_{\alpha,\beta}\,\langle\mathbf{L}|L_{[j6}L_{k6}L_{l6]}|\mathbf{L}'\rangle\,\mathrm{tr}\,\hat{f}_F^{\mathrm{cub}}(L_1,L_2;L_1',L_2').$$

The full propagators $\langle[\psi_\alpha]_{\mathbf{L}}[\overline{\psi_\beta}]_{\mathbf{L}'}\rangle$ would have a structure similar to that of (3.9), but containing many more terms and matrix elements of products of generators L_{ij} up to cubic order.

As for the off-diagonal case, the functions $\hat{f}_F$ are linear combinations of the propagators between mass eigenstates (3.1) and (3.2). Again, these functions only depend on the labels (L_1, L_2) of the external fields. However, since their expressions are more involved than in the off-diagonal case, we postpone their explicit formulas until appendix C.

4 One-loop corrections to the classical solution and one-point functions

Following previous work [25, 26], we will now use the propagators to compute the first quantum correction to the vacuum expectation value of the five scalars ϕ_i for $i = 1, \ldots 5$, as well as the one-loop one-point function of the 1/2-BPS operator $\mathrm{tr}(Z^L)$, where $Z = \phi_5 + i\phi_6$. Throughout this section we will work in the large-N limit, and we will specify which results are applicable for finite n or in the large-n regime.[8] One-loop corrections to one-point functions of more general, non-protected operators can similarly be obtained in analogy with [25, 26].

4.1 One-loop correction to the classical solution

The first quantum correction to the classical solution is given by the contraction of an external scalar with an effective three-vertex,

$$\langle\phi_i\rangle_{1\text{-loop}}(x) = \tilde{\phi}_i(x)\int \mathrm{d}^4y \sum_{\Phi_1,\Phi_2,\Phi_3} V_3(\Phi_1(y),\overbrace{\Phi_2(y),\Phi_3(y)}). \tag{4.1}$$

The sum on the right-hand side runs over all fields in the theory. We show in appendix D that

$$\sum_{\Phi_1,\Phi_2,\Phi_3} V_3(\Phi_1(y),\overbrace{\Phi_2(y),\Phi_3(y)}) = -\frac{4\sqrt{2}N}{\pi^2(y_3)^3}W(n)\,\mathrm{tr}\left(\tilde{\phi}_iG_{i6}\right). \tag{4.2}$$

[8] It should also be possible to extend this to finite N following [25, 34].

JHEP04(2020)132

The function $W(n)$ is positive for $n \geq 0$, and is given explicitly

$$\begin{aligned} W(n) = -\frac{1}{64}\Bigg(& \frac{2(n-4)(n+8)}{n(n+4)} + \frac{2\sqrt{2}(n+2)(n(n+4)-4)}{(n+1)(n+3)} + \frac{n\left(n^2-8\right)\Psi(m_{+0})}{2(n+1)} \\ & + \frac{(n+2)^2(n(n+4)-4)\Psi(m_{0+})}{(n+1)(n+3)} + \frac{(n+4)(n(n+8)+8)\Psi(m_{-0})}{2(n+3)} \\ & - \frac{\left(n^4+8n^3-32n+8n^2+64\right)\Psi\left(\nu_{\text{easy}}+\frac{1}{2}\right)}{n(n+4)} \\ & - \frac{n^3(n+5)\Psi\left(\nu_{++}+\frac{1}{2}\right)}{2(n+2)(n+4)} - \frac{(n-1)(n+4)^3\Psi\left(\nu_{-+}+\frac{1}{2}\right)}{2n(n+2)}\Bigg), \end{aligned} \tag{4.3}$$

in terms of the masses of bosons and fermions in the off-diagonal blocks (see tables 4 and 6) and $\nu_i = \sqrt{m_i^2 + \frac{1}{4}}$. We also attach a completely explicit expression for $W(n)$ as *Supplementary material* to this paper. In section 4.2 we will be interested in this function in the double-scaling limit (1.2). Expanding for $n \to \infty$, this function simplifies dramatically:

$$W(n) = \frac{1}{4n^2} + \mathcal{O}(n^{-3})\,. \tag{4.4}$$

From the individual terms in (4.3), one would expect terms growing as fast as $n^2\log(n)$ in the large-n limit. However, from the supergravity calculation we know that all terms growing faster than $1/n^2$ should not be present. This "miraculous" cancellation provides a very non-trivial check for our results.

Moreover, using the relation between the matrices G_{i6} and the $\mathfrak{so}(5)$ fuzzy spherical harmonics given in appendix A.3, we can compute the contraction

$$\overbrace{\tilde{\phi}_i\,\mathrm{tr}\left(\tilde{\phi}_j G_{j6}\right)} = K^{m^2=6}(x,y)\,G_{i6}. \tag{4.5}$$

The remaining spacetime integral was already computed in [26]:

$$\int \mathrm{d}^4 y \frac{1}{y_3^3} K^{m^2=6}(x,y) = \frac{g_{\text{YM}}^2}{2}\frac{1}{4x_3}. \tag{4.6}$$

Assembling the pieces, we see that the one-loop correction to the classical solution is proportional to the classical solution such that we can write

$$\langle\phi_i(x)\rangle = \left(1 - \frac{\lambda}{\pi^2}W(n) + \mathcal{O}\left(\lambda^2\right)\right)\langle\phi_i(x)\rangle_{\text{tree}}. \tag{4.7}$$

We note that this correction is non-vanishing, fitting the picture observed so far that for a domain-wall setup which conserves part of the supersymmetry there is no correction to the classical field [25] whereas for setups which break the supersymmetry there can be a correction [26]. The one-loop corrections to vanishing classical vevs are all vanishing.

JHEP04(2020)132

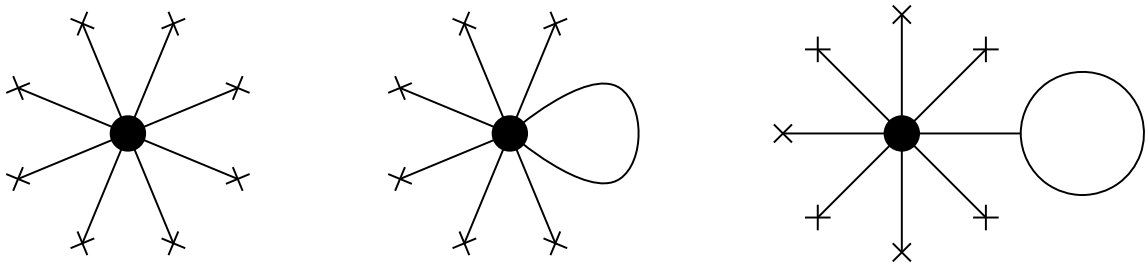

(a) Tree level (b) Tadpole (c) Lollipop

Figure 1. Diagrams (identical to the ones of [25]) that contribute at tree level (a) and one-loop order (b)-(c) to a single-trace operator such as $\langle \mathrm{tr}\, Z^L \rangle_{L=8}$ (in the planar limit). The black dot denotes the operator and the crosses signify the insertion of the classical solution.

4.2 One-loop correction to $\langle \mathrm{tr}(Z^L) \rangle$

Next, we consider the scalar single-trace operator $\mathrm{tr}(Z^L)$ with $Z = \phi_5 + i\phi_6$ and aim to compute the first quantum correction to its one-point function.

At tree level, the one-point function $\langle \mathrm{tr}(Z^L) \rangle$ was first computed in [35]; it is simply obtained by inserting the classical solution $Z^{\mathrm{cl}} = \phi_5^{\mathrm{cl}}$ into the trace:

$$\langle \mathrm{tr}\, Z^L \rangle_{\mathrm{tree}} = \frac{1}{(\sqrt{2}x_3)^L}\, \mathrm{tr}\, G_{56}^L = \begin{cases} 0, & L \quad \text{odd}, \\ \frac{1}{(\sqrt{2}x_3)^L}\left[\frac{2}{L+3} B_{L+3}(-\frac{n}{2}) - \frac{(n+2)^2}{2(L+1)} B_{L+1}(-\frac{n}{2})\right], & L \quad \text{even}, \end{cases} \tag{4.8}$$

where B_l denotes the l-th Bernoulli polynomial.

The general procedure for computing the one-loop one-point function of scalar single-trace operators can be found in [24–26]. As was derived there, there are only two contributions for the operator $\mathrm{tr}(Z^L)$, which were called tadpole and lollipop, see figure 1:

$$\langle \mathrm{tr}\, Z^L \rangle_{1-\mathrm{loop}} = \langle \mathrm{tr}\, Z^L \rangle_{\mathrm{tad}} + \langle \mathrm{tr}\, Z^L \rangle_{\mathrm{lol}}. \tag{4.9}$$

In particular, since the operator is 1/2-BPS, there is no correction to its wave function as well as no renormalization.

The tadpole diagram corresponds to inserting the classical solution for $L-2$ scalars and contracting the remaining two fields. This can be done in L inequivalent ways, so we obtain

$$\langle \mathrm{tr}\, Z^L \rangle_{\mathrm{tad}} = L\, \mathrm{tr}\left[(Z^{\mathrm{cl}})^{L-2} \overbrace{Z\, Z}\right]. \tag{4.10}$$

The contraction of Z with itself is simply

$$\overbrace{Z\, Z} = \overbrace{\tilde{\phi}_5\, \tilde{\phi}_5} - \overbrace{\tilde{\phi}_6\, \tilde{\phi}_6}\,, \tag{4.11}$$

JHEP04(2020)132

since ϕ_5 and ϕ_6 are an easy and a complicated field respectively and there is no propagator that mixes them. Using the propagators presented in the previous section and taking into account that only the fields in the off-diagonal block contribute in the large-N limit, we find

$$\langle \operatorname{tr} Z^L \rangle_{\text{tad}} = LN \left[\operatorname{tr} \left((Z^{\text{cl}})^{L-2} \right) \left(f^{\text{sing}} - K^{m^2_{\text{easy}}} \right) + 4 \operatorname{tr} \left((Z^{\text{cl}})^{L-2} G_{56} G_{56} \right) f^{\text{prod}} \right], \quad (4.12)$$

using the combinations of propagators f given in (3.5). Note that this gives us the contribution of the tadpole for any finite value of n, because the color trace is known in terms of Bernoulli polynomials, see (4.8). As for the effective vertex $W(n)$, we have a cancellation of the regulator-dependent terms coming from the spacetime propagator for any finite n.

In order to compare our result to the supergravity prediction, we need to evaluate the expression in the large-n limit. Inserting the expression for the traces (4.8) into (4.12) and expanding for $n \to \infty$, we find that the leading order term is

$$\langle \operatorname{tr} Z^L \rangle_{\text{tad}} \xrightarrow{n\to\infty} \frac{\lambda}{\pi^2 n^2} \frac{L(L+1)}{2(L-1)} \langle \operatorname{tr} Z^L \rangle_{\text{tree}}. \quad (4.13)$$

Notice how once again, only terms which are at most of order n^{-2} contribute in the large-n limit, even though from (4.12) one could expect a growth-rate faster than this.

The second type of diagram is the lollipop diagram, which is nothing but the one-loop correction to the classical solution for one of the scalars in the operator. We find, using our result (4.7),

$$\langle \operatorname{tr} Z^L \rangle_{\text{lol}} = L \operatorname{tr} \left[(Z^{\text{cl}})^{L-1} \langle Z \rangle_{\text{1-loop}} \right] = -\frac{\lambda L}{\pi^2} W(n) \langle \operatorname{tr} Z^L \rangle_{\text{tree}} \xrightarrow{n\to\infty} -\frac{\lambda L}{4\pi^2 n^2} \langle \operatorname{tr} Z^L \rangle_{\text{tree}}. \quad (4.14)$$

In the last step, we have used the expansion (4.4) of $W(n)$ for $n \to \infty$.

Combining the tree-level result (4.8) with the values of the tadpole and lollipop diagrams (4.13) and (4.14) respectively, we find

$$\frac{\langle \operatorname{tr} Z^L \rangle}{\langle \operatorname{tr} Z^L \rangle_{\text{tree}}} = 1 + \frac{\lambda}{\pi^2 n^2} \frac{L(L+3)}{4(L-1)} + \mathcal{O}\left(\left(\frac{\lambda}{\pi^2 n^2} \right)^2 \right). \quad (4.15)$$

Up to first order in the double-scaling parameter, this matches precisely the result from the supergravity computation (1.4). Note that as in [25, 26] we are actually forced to consider the above ratio in order to compare the supergravity to the field-theory result: the supergravity result computes the one-point function of the unique $\mathfrak{so}(5)$-symmetric chiral primary on which the operator $\operatorname{tr}(Z^L)$ has a non-vanishing projection.

A completely explicit expression for $\langle \operatorname{tr} Z^L \rangle_{1-\text{loop}}$ at finite n is attached as *Supplementary material* to this paper.

5 Conclusion and outlook

Making use of fuzzy spherical harmonics on S^4, we have set up the framework required to carry out perturbative calculations of observables in the domain-wall version of $\mathcal{N} = 4$

JHEP04(2020)132

SYM theory where five scalar fields have $\mathfrak{so}(5)$-symmetric vevs in a half-space. As an application, we have computed the one-loop correction to the one-point function of a specific chiral primary and found that it agrees in a double-scaling limit with the prediction from a supergravity computation in the dual string-theory setup. We notice that a match between gauge and string theory is obtained for all defect setups of the given type regardless of whether supersymmetry is fully or only partially broken and regardless of whether the relevant boundary state is characterized as integrable or non-integrable, cf. table 1.

With the perturbative framework fully developed, one can of course compute other types of observables of the dCFT, such as more general correlation functions or Wilson loops. The study of Wilson loops in the closely related dCFT dual to the D3-D5 probe-brane system listed in table 1 has revealed interesting novel examples of Gross-Ooguri like phase transitions [33, 36–39]. Furthermore, the investigation of two-point functions in the same setup has led to new insights concerning conformal data of dCFTs [40, 41] and in general such data might prove useful as input for the boundary conformal bootstrap program [42–44].

The one-loop contribution to the one-point function of general non-protected operators in the present $\mathfrak{so}(5)$-symmetric setup could potentially provide important information for the integrability program. The corresponding boundary state has been argued to be integrable [19] and the derivation of a closed formula for all tree-level one-point functions is in progress [45]. Explicit results at one-loop order might make it possible to package the results for the two leading orders into one formula, put forward a proposal for an asymptotic formula for higher loop orders as was done for the D3-D5 case [18] and eventually bootstrap an exact all-loop order formula for both cases.

From the string-theory perspective, the most burning open problem is to understand the reason for the integrability or non-integrability of the boundary states associated with the different probe-brane models considered here, cf. table 1.

Acknowledgments

C.K., M.V. and M.W. were supported in part by DFF-FNU through the grant DFF-FNU 4002-00037. M.V. and M.W. were moreover supported by the ERC starting grant 757978 and the research grant 00015369 from Villum Fonden. M.W. was also supported by the research grant 00025445 from Villum Fonden. A.G. was partially supported by the DFG through project number 400570283. A.G would like to thank the NBI for hospitality during the completion of this work.

JHEP04(2020)132

A Conventions

A.1 $\mathcal{N}=4$ SYM action

Throughout our work, we consider a mostly-positive metric $\eta^{\mu\nu} = \text{diag}(-1,+1,+1,+1)$. The action of $\mathcal{N}=4$ SYM theory is given by

$$S_{\mathcal{N}=4} = \frac{2}{g_{\text{YM}}^2}\int \mathrm{d}^4x\ \text{tr}\Bigg(-\frac{1}{4}F_{\mu\nu}F^{\mu\nu} - \frac{1}{2}D_\mu\phi_i D^\mu\phi_i + \frac{i}{2}\bar{\psi}\gamma^\mu D_\mu\psi \\ + \frac{1}{4}[\phi_i,\phi_j][\phi_i,\phi_j] + \frac{1}{2}\sum_{i=1}^{3}\bar{\psi}C_i[\phi_i,\psi] + \frac{1}{2}\sum_{i=4}^{6}\bar{\psi}C_i[\phi_i,\gamma_5\psi]\Bigg), \tag{A.1}$$

where $(C_i)_{\alpha\beta}$ are 4×4 matrices of Clebsch-Gordan coefficients that couple the two spinors with the scalars. We will use the same conventions as [25]:

$$\begin{aligned} &C_1 \equiv C_1^{(1)} = i\begin{pmatrix} 0 & -\sigma_3 \\ \sigma_3 & 0\end{pmatrix}, \quad C_2 \equiv C_2^{(1)} = i\begin{pmatrix} 0 & \sigma_1 \\ -\sigma_1 & 0\end{pmatrix}, \quad C_3 \equiv C_3^{(1)} = \begin{pmatrix} \sigma_2 & 0 \\ 0 & \sigma_2\end{pmatrix}, \\ &C_4 \equiv C_1^{(2)} = i\begin{pmatrix} 0 & -\sigma_2 \\ -\sigma_2 & 0\end{pmatrix}, \quad C_5 \equiv C_2^{(2)} = \begin{pmatrix} 0 & -\mathbb{1}_2 \\ \mathbb{1}_2 & 0\end{pmatrix}, \quad C_6 \equiv C_3^{(2)} = i\begin{pmatrix} \sigma_2 & 0 \\ 0 & -\sigma_2\end{pmatrix}. \end{aligned} \tag{A.2}$$

The matrices in the first line are Hermitian, $(C_i^{(1)})^\dagger = C_i^{(1)}$, while those in the second are anti-Hermitian, $(C_i^{(2)})^\dagger = -C_i^{(2)}$. Furthermore, we note some useful properties:

$$\left\{C_i^{(1)}, C_j^{(1)}\right\} = +2\delta_{ij}, \qquad \left\{C_i^{(2)}, C_j^{(2)}\right\} = -2\delta_{ij}, \tag{A.3}$$

$$\left[C_i^{(1)}, C_j^{(1)}\right] = -2i\epsilon_{ijk}C_k^{(1)}, \quad \left[C_i^{(2)}, C_j^{(2)}\right] = -2\epsilon_{ijk}C_k^{(2)}, \tag{A.4}$$

and the two sets commute $\left[C_i^{(1)}, C_j^{(2)}\right] = 0$.

A.2 $\mathfrak{so}(5)$ and $\mathfrak{so}(6)$

Given an $\mathfrak{so}(n)$ Lie Algebra, we normalize the generators $L_{ij} = -L_{ji}$ such that

$$[L_{ij}, L_{kl}] = i\left(\delta_{ik}L_{jl} + \delta_{jl}L_{ik} - \delta_{jk}L_{il} - \delta_{il}L_{jk}\right) \quad \text{for} \quad i,j,k,l = 1,\ldots,n. \tag{A.5}$$

We will label our representations in terms of the quantum numbers of the highest weight. Our conventions follow [46] since we will make use of some of the Clebsch-Gordan coefficients for coupling different $\mathfrak{so}(5)$ representations published there. For $\mathfrak{so}(5)$, we need two quantum numbers (L_1, L_2) to specify a representation, which correspond to the eigenvalues of $\frac{1}{2}(L_{12} \pm L_{34})$ acting on the highest weight state. The most relevant examples for our work will be

$$\mathfrak{so}(5)\ :\quad \mathbf{4} = \left(\frac{1}{2}, 0\right), \quad \mathbf{5} = \left(\frac{1}{2}, \frac{1}{2}\right), \quad \mathbf{10} = (1,0). \tag{A.6}$$

Our notation is related to the $\mathfrak{so}(5)$ Dynkin labels (e.g. used in [47]) by $(L_1, L_2) = [2L_2, 2(L_1 - L_2)]$.

JHEP04(2020)132

Similarly, for $\mathfrak{so}(6)$ we need three quantum numbers (P_1, P_2, P_3), which correspond to the eigenvalues of L_{12}, L_{34} and L_{56} acting on the highest weight state. Some simple examples are

$$\mathfrak{so}(6) \;:\quad \mathbf{4} = \left(\frac{1}{2}, \frac{1}{2}, \frac{1}{2}\right), \quad \bar{\mathbf{4}} = \left(\frac{1}{2}, \frac{1}{2}, -\frac{1}{2}\right). \tag{A.7}$$

Our notation is related to the $\mathfrak{so}(6)$ Dynkin labels by $(P_1, P_2, P_3) = [P_1 - P_2, P_2 + P_3, P_2 - P_3]$. With our conventions, the dimensions of the irreducible $\mathfrak{so}(5)$ and $\mathfrak{so}(6)$ representations are

$$d_5\,(L_1, L_2) = \frac{1}{6}(2L_1 + 2L_2 + 3)(2L_1 - 2L_2 + 1)(2L_2 + 1)(2L_1 + 2), \tag{A.8}$$

$$\begin{aligned} d_6(P_1, P_2, P_3) = \frac{1}{12}&(1 + P_1 - P_2)(3 + P_1 + P_2)(2 + P_1 - P_3) \\ &\times (1 + P_2 - P_3)(2 + P_1 + P_3)(1 + P_2 + P_3). \end{aligned} \tag{A.9}$$

The Casimir operator is defined as the sum over all independent generators squared:

$$C_n = \sum_{i<j} (L_{ij})^2. \tag{A.10}$$

With our normalizations, it has eigenvalues

$$C_5(L_1, L_2) = 2\Big[L_1(L_1 + 2) + L_2(L_2 + 1)\Big], \tag{A.11a}$$

$$C_6(P_1, P_2, P_3) = P_1(P_1 + 4) + P_2(P_2 + 2) + P_3^2. \tag{A.11b}$$

Let us also write the branching rule of $\mathfrak{so}(6)$ representations into $\mathfrak{so}(5)$,

$$(P_1, P_2, P_3) \to \bigoplus (L_1, L_2)\,, \quad \text{where} \quad P_3 \le L_1 - L_2 \le P_2 \le L_1 + L_2 \le P_1. \tag{A.12}$$

The most relevant cases for us are $(P_1, P_2, P_3) = (\frac{n}{2}, \frac{n}{2}, \frac{n}{2})$ which implies $(L_1, L_2) = (\frac{n}{2}, 0)$ for the fields in the off-diagonal block, and $(P_1, P_2, P_3) = (L_1 + L_2, L_1 + L_2, 0)$ for the fields in the adjoint block.

To label the states in a given $\mathfrak{so}(5)$ representation, we use the collective label $\mathbf{L} = (L_1, L_2)\,\ell_1 \ell_2\, m_1 m_2$. Here m_1 and m_2 are the eigenvalues of the two Cartan generators $\frac{1}{2}(L_{12} + L_{34})$ and $\frac{1}{2}(L_{12} - L_{34})$ covering the ranges $m_i = -\ell_i, \ldots, +\ell_i$. The spins ℓ_i are subject to the constraints

$$-L_1 + L_2 \le \ell_1 - \ell_2 \le L_1 - L_2 \le \ell_1 + \ell_2 \le L_1 + L_2, \tag{A.13}$$

and $\ell_1 + \ell_2 \in \mathbb{Z}$ [46].

A.3 G matrices

Consider a four-dimensional representation of the $\mathfrak{so}(5)$ Clifford algebra

$$\{\gamma_i, \gamma_j\} = 2\delta_{ij} \mathbb{1}_{4\times 4}. \tag{A.14}$$

JHEP04(2020)132

This can be used as a building block for some particular types of $\mathfrak{so}(5)$ and $\mathfrak{so}(6)$ representations as follows. Take the n-fold tensor product and project to $\mathrm{Sym}(\otimes^n \mathbb{C}^4)$ as

$$G_{i6} = \frac{1}{2}\big(\underbrace{\gamma_i \otimes 1 \otimes \cdots \otimes 1}_{n \text{ factors}} + \cdots + 1 \otimes \cdots \otimes 1 \otimes \gamma_i\big)_{\text{sym}}, \tag{A.15}$$

and define

$$G_{ij} \equiv -i\,[G_{i6}, G_{j6}]\,, \quad i,j = 1,\ldots,5. \tag{A.16}$$

From the anticommutation relations (A.14), one can verify that G_{ij} for $i,j = 1,\ldots,5$ satisfy the commutation relations of $\mathfrak{so}(5)$ and G_{ij} for $i,j = 1,\ldots,6$ satisfy the commutation relations of $\mathfrak{so}(6)$. We also refer to the appendix of [29], where some useful identities for the matrices G_{ij} can be found. The matrices G_{i6} are related to the $\mathfrak{so}(5)$ fuzzy spherical harmonics $\hat{Y}_{\mathbf{J}}$ by

$$\begin{aligned}
G_{16} &= \frac{1}{\sqrt{2}} a_n \left(\hat{Y}_{++} + \hat{Y}_{--}\right), & G_{26} &= -\frac{i}{\sqrt{2}} a_n \left(\hat{Y}_{++} - \hat{Y}_{--}\right), \\
G_{36} &= -\frac{1}{\sqrt{2}} a_n \left(\hat{Y}_{-+} - \hat{Y}_{+-}\right), & G_{46} &= -\frac{i}{\sqrt{2}} a_n \left(\hat{Y}_{-+} + \hat{Y}_{+-}\right), \\
G_{56} &= -a_n \hat{Y}_{00},
\end{aligned} \tag{A.17}$$

where

$$a_n = \frac{1}{2}\sqrt{\frac{1}{5}\, n(n+4)\, d_5\left(\frac{n}{2}, 0\right)}, \quad \text{and} \quad \hat{Y}_{\alpha\beta} \equiv \hat{Y}_{(\frac{1}{2},\frac{1}{2})\frac{1}{2}\frac{1}{2}\alpha\beta},\ \hat{Y}_{00} \equiv \hat{Y}_{(\frac{1}{2},\frac{1}{2})0000}. \tag{A.18}$$

B Details on the diagonalization

In this appendix, we provide details of the diagonalization procedure outlined in section 2.

B.1 Complicated bosons

In (2.7) we have written the mass terms for the complicated bosons, i.e. those for which color and flavor degrees of freedom mix. As stated in section 2.3, the key observation is that we can diagonalize this mass term by starting with the 5×5 block for which we can rewrite the mixing term as

$$\frac{1}{2} S_{ij} L_{ij} = \frac{1}{2} \sum_{1 \le i < j \le 5} \left[(J_{ij})^2 - (L_{ij})^2 - (S_{ij})^2\right]. \tag{B.1}$$

We thus have to find the eigenstates of the total angular momentum operator $J_{ij} = L_{ij} + S_{ij}$. Concretely, this works as follows.

JHEP04(2020)132

The matrices S_{ij} form the fundamental representation of $\mathfrak{so}(5)$,[9] and we bring them into canonical form by transforming the five complicated scalars as

$$\begin{pmatrix}\phi_1\\ \phi_2\\ \phi_3\\ \phi_4\\ \phi_5\end{pmatrix} \to \frac{1}{\sqrt{2}}\begin{pmatrix}-i & 0 & 0 & -i & 0\\ 1 & 0 & 0 & -1 & 0\\ 0 & -i & i & 0 & 0\\ 0 & 1 & 1 & 0 & 0\\ 0 & 0 & 0 & 0 & i\sqrt{2}\end{pmatrix}^{\dagger}\begin{pmatrix}\phi_1\\ \phi_2\\ \phi_3\\ \phi_4\\ \phi_5\end{pmatrix} \equiv \begin{pmatrix}C_{++}\\ C_{+-}\\ C_{-+}\\ C_{--}\\ C_{00}\end{pmatrix} = \sum_{\alpha_1,\alpha_2} C_{\alpha_1,\alpha_2}\hat{e}_{\alpha_1,\alpha_2}. \tag{B.2}$$

The fields C_{α_1,α_2} are the five components of the $(\frac{1}{2},\frac{1}{2})$ representation of $\mathfrak{so}(5)$. In particular, we use the notation $C_{\alpha_1,\alpha_2} \equiv C_{\mathbf{S}}$, where $\mathbf{S} = (\frac{1}{2},\frac{1}{2})\,|\alpha_1||\alpha_2|\,\alpha_1\alpha_2$, to make manifest that C_{α_1,α_2} has magnetic quantum numbers α_1 and α_2 with respect to the $\mathfrak{su}(2)\times\mathfrak{su}(2)$ subalgebra of $\mathfrak{so}(5)$.[10] These fields are now expanded in terms of $\mathfrak{so}(5)$ fuzzy spherical harmonics and we denote the components by $(C_{\mathbf{S}})_{\mathbf{L}}$. Finally, the $\hat{e}_{\alpha_1,\alpha_2}$ in (B.2) are five-dimensional unit vectors, for example $\hat{e}_{++} = (1,0,0,0,0)$, and so on.

It is clear that the $(C_{\mathbf{S}})_{\mathbf{L}}$ transform as the product representation $(L_1,L_2)\otimes(\frac{1}{2},\frac{1}{2})$. However, we are interested in fields that are diagonal with respect to the total angular momentum J_{ij}, and so will belong to the representations (2.19). In particular, we will denote by B_{α_1,α_2} the diagonal fields in the $(J_1,J_2) = (L_1+\alpha_1, L_2+\alpha_2)$ representation. All the states in this total angular momentum representation are labelled by distinct values of $\mathbf{J} = (J_1,J_2)\,j_1 j_2\, m_1 m_2$. As familiar from quantum mechanics, the explicit change of basis is

$$(B_{\alpha_1,\alpha_2})_{\mathbf{J}} = \sum_{\mathbf{L},\mathbf{S}} \langle \mathbf{L};\mathbf{S}|\mathbf{J}\rangle (C_{\mathbf{S}})_{\mathbf{L}}, \tag{B.3}$$

where $\langle \mathbf{L};\mathbf{S}|\mathbf{J}\rangle$ are the Clebsch-Gordan coefficients for coupling the $\mathfrak{so}(5)$ states labeled by $\mathbf{L}$ and $\mathbf{S}$ to $\mathbf{J}$. For the present case, i.e. the coupling of the fundamental of $\mathfrak{so}(5)$ with an arbitrary state in the irrep (L_1,L_2), the coefficients can be found in [46]; see also appendix E for more details.

The fields $(B_{\alpha_1,\alpha_2})_{\mathbf{J}}$ will have some corresponding basis elements $\hat{Y}_{\mathbf{J}}^{\alpha_1,\alpha_2}$, which are defined implicitly from

$$\sum_{\mathbf{L},\mathbf{S}} (C_{\mathbf{S}})_{\mathbf{L}}\, \hat{Y}_{\mathbf{L}} \otimes \hat{e}_{\mathbf{S}} = \sum_{\alpha_1,\alpha_2}\sum_{\mathbf{J}} (B_{\alpha_1,\alpha_2})_{\mathbf{J}}\, \hat{Y}_{\mathbf{J}}^{\alpha_1,\alpha_2}. \tag{B.4}$$

Having obtained eigenstates of the 5×5 block, it remains to see how they transform under the action of $\sum_{i=1}^{5} R_i^{\dagger} L_{i6}$, the 1×5 block in (2.7). One can compute that

$$\left(\sum_{i=1}^{5} R_i^{\dagger} L_{i6}\right) \hat{Y}_{\mathbf{J}}^{\alpha_1,\alpha_2} = T^{P_1,P_2,P_3}_{J_1-\alpha_1,J_2-\alpha_2;J_1,J_2}\, \hat{Y}_{\mathbf{J}}. \tag{B.5}$$

The right-hand side of this equation is proportional to the $\mathfrak{so}(5)$ state $\hat{Y}_{\mathbf{J}}$ with a constant of proportionality T that only depends on the irrep (J_1,J_2) and (α_1,α_2), *not* on all quantum

[9] In our conventions, S_{jk} contains a $-i$ at position (jk) and an i at position (kj).

[10] Note that the subscripts $+$, $-$ and 0 on the fields C denote half-integers, e.g. C_{+-} has $\alpha_1 = \frac{1}{2}$ and $\alpha_2 = -\frac{1}{2}$.

JHEP04(2020)132

numbers contained in $\mathbf{J}$. In fact, the T's are certain reduced matrix elements of $\mathfrak{so}(6)$ generators; for more details, see appendix E. Their value also depends on which $\mathfrak{so}(6)$ representation the fields transform as and we will have to distinguish between the adjoint block with $\mathfrak{so}(6)$ irrep $(L_1+L_2, L_1+L_2, 0)$ and the off-diagonal block with $(\frac{n}{2}, \frac{n}{2}, \frac{n}{2})$.

Let us start with the adjoint block, in which case it turns out that the reduced matrix elements T vanish if $(J_1, J_2) \in \{(L_1+\frac{1}{2}, L_2+\frac{1}{2}), (L_1, L_2), (L_1-\frac{1}{2}, L_2-\frac{1}{2})\}$. More explicitly, we get

$$\begin{aligned}
&\left(\sum_{i=1}^{5} R_i^\dagger L_{i6}\right) \hat{Y}_{\mathbf{J}}^{++} = \left(\sum_{i=1}^{5} R_i^\dagger L_{i6}\right) \hat{Y}_{\mathbf{J}}^{--} = \left(\sum_{i=1}^{5} R_i^\dagger L_{i6}\right) \hat{Y}_{\mathbf{J}}^{00} = 0, \\
&\left(\sum_{i=1}^{5} R_i^\dagger L_{i6}\right) \hat{Y}_{\mathbf{J}}^{\pm\mp} \equiv T^{\pm\mp} \hat{Y}_{\mathbf{J}},
\end{aligned} \tag{B.6}$$

where the coefficients $T^{\pm\mp}$ take the following values:

$$T^{+-} = \sqrt{2}\sqrt{\frac{(2J_1+1)\,(J_1-J_2)\,(J_2+1)}{2J_1-2J_2+1}}, \quad T^{-+} = -\sqrt{2}\sqrt{\frac{(2J_1+3)\,(J_1-J_2+1)\,J_2}{2J_1-2J_2+1}}. \tag{B.7}$$

We now write the vector of complicated fields as

$$C = \begin{pmatrix} \sum_{\alpha_1,\alpha_2,\mathbf{J}} (B_{\alpha_1,\alpha_2})_{\mathbf{J}} \hat{Y}_{\mathbf{J}}^{\alpha_1,\alpha_2} \\ \sum_{\mathbf{L}} (A_3)_{\mathbf{L}} \hat{Y}_{\mathbf{L}} \end{pmatrix}, \tag{B.8}$$

and insert into the mass term (2.7). The mass term then becomes

$$\begin{aligned}
&\hat{m}_{++}^2 (B_{++})_{\mathbf{J}}^\dagger (B_{++})_{\mathbf{J}} + \hat{m}_{--}^2 (B_{--})_{\mathbf{J}}^\dagger (B_{--})_{\mathbf{J}} + \hat{m}_{00}^2 (B_{00})_{\mathbf{J}}^\dagger (B_{00})_{\mathbf{J}} \\
&+ \begin{pmatrix} (B_{+-})_{\mathbf{J}}^\dagger & (B_{-+})_{\mathbf{J}}^\dagger & (A_3)_{\mathbf{J}}^\dagger \end{pmatrix} \begin{pmatrix} \hat{m}_{\text{easy}}^2 + 2 & 0 & -\sqrt{2}T^{+-} \\ 0 & \hat{m}_{\text{easy}}^2 + 2 & -\sqrt{2}T^{-+} \\ -\sqrt{2}T^{+-} & -\sqrt{2}T^{-+} & \hat{m}_{\text{easy}}^2 \end{pmatrix} \begin{pmatrix} (B_{+-})_{\mathbf{J}} \\ (B_{-+})_{\mathbf{J}} \\ (A_3)_{\mathbf{J}} \end{pmatrix}.
\end{aligned} \tag{B.9}$$

As pointed out above, the reduced Clebsch-Gordan coefficients only depend on the $\mathfrak{so}(5)$ and $\mathfrak{so}(6)$ irreps, not any other quantum numbers. We can therefore simply diagonalize the remaining 3×3 matrix; the fields that achieve this diagonalization are given by

$$D_0 = \frac{-1}{\sqrt{2\hat{m}_{\text{easy}}^2}} \left(T^{-+} B_{+-} - T^{+-} B_{-+}\right), \tag{B.10}$$

$$D_\mp = \frac{\pm 1 + \sqrt{4\hat{m}_{\text{easy}}^2 + 1}}{\sqrt{2N_\pm}} A_3 \pm \frac{1}{\sqrt{N_\pm}} \left(T^{+-} B_{+-} + T^{-+} B_{-+}\right). \tag{B.11}$$

The eigenvalues are listed in table 3.

The diagonalization for the off-diagonal block proceeds similarly. In this case the reduced matrix elements are non-zero only if $(J_1, J_2) = (L_1, L_2)$, resulting in a 2×2 matrix

JHEP04(2020)132

that has to be diagonalized in the final step. The mass term becomes diagonal in terms of the fields B_{++}, B_{-+} and

$$D_\pm = \pm\sqrt{\frac{1}{2} \pm \frac{1}{2\sqrt{4m^2_{\text{easy}}+1}}}B_{00} + \sqrt{\frac{1}{2} \mp \frac{1}{2\sqrt{4m^2_{\text{easy}}+1}}}A_3. \tag{B.12}$$

The eigenvalues are listed in table 4.

B.2 Fermions

The mass term for the fermions as written in (2.9) is

$$\text{tr}(\bar{\psi}_\alpha \mathcal{C}_{\alpha\beta}(P_L\psi_\beta) + \bar{\psi}_\alpha \mathcal{C}^\dagger_{\alpha\beta}(P_R\psi_\beta)), \tag{B.13}$$

where P_L and P_R are the chiral projectors. The components of the matrix $\mathcal{C}_{\alpha\beta}$ are

$$\mathcal{C}_{\alpha\beta} = -\frac{1}{\sqrt{2}}\sum_{i=1}^{5}(C_i)_{\alpha\beta}L_{i6}, \tag{B.14}$$

where the $(C_i)_{\alpha\beta}$ were defined in (A.2). One can show that $\mathcal{C}^\dagger\mathcal{C} \neq \mathcal{C}\mathcal{C}^\dagger$; thus, we cannot diagonalize $\mathcal{C}$ with a unitary transformation. We will now follow a standard procedure to diagonalize a fermionic mass matrix used e.g. also in the standard model; see for example [48].

We begin by finding the eigenvectors of $\mathcal{C}^\dagger\mathcal{C} = \frac{1}{2}(\sum_{i=1}^5 (L_{i6})^2 - \sum_{i,j=1}^5 \tilde{S}_{ij}L_{ij})$. The 4×4 matrices $\tilde{S}_{ij}$ form the four-dimensional representation of $\mathfrak{so}(5)$; thus, $\mathcal{C}^\dagger\mathcal{C}$ is diagonalized by coupling a general $\mathfrak{so}(5)$ representation (L_1, L_2) with $(\frac{1}{2}, 0)$. As it was the case for the complicated bosons, we start by bringing the matrices $\tilde{S}_{ij}$ into canonical form with the transformation

$$\begin{pmatrix}\psi_1\\ \psi_2\\ \psi_3\\ \psi_4\end{pmatrix} \to \frac{1}{2}\begin{pmatrix}1 & -i & -1 & i\\ -i & 1 & i & -1\\ -1 & -i & -1 & -i\\ i & 1 & i & 1\end{pmatrix}^\dagger \begin{pmatrix}\psi_1\\ \psi_2\\ \psi_3\\ \psi_4\end{pmatrix} \equiv \begin{pmatrix}\tilde{C}_{+0}\\ \tilde{C}_{-0}\\ \tilde{C}_{0+}\\ \tilde{C}_{0-}\end{pmatrix}. \tag{B.15}$$

Here the fields $\tilde{C}_{\alpha_1\alpha_2} \equiv (\tilde{C}_{\mathbf{S}})_{\mathbf{J}}$ have well defined orbital and angular momentum. Now the eigenvectors are found in terms of Clebsch-Gordan coefficients:

$$\hat{Y}^{(L_1,L_2)}_{\mathbf{J}} = \sum_{\mathbf{L},\mathbf{S}} \langle \mathbf{L};\mathbf{S}|\mathbf{J}\rangle\, \hat{Y}_{\mathbf{L}} \otimes \hat{e}_{\mathbf{S}}. \tag{B.16}$$

This concludes the diagonalization of $\mathcal{C}^\dagger\mathcal{C}$.

Now we will use the basis of eigenvectors of $\mathcal{C}^\dagger\mathcal{C}$ to build a basis of eigenvectors of $\mathcal{C}$. For the fields in the adjoint block, after a long calculation one can find how $\mathcal{C}$ acts on the four eigenvectors:

$$\mathcal{C}\,\hat{Y}^{(J_1\pm\frac{1}{2},J_2)}_{\mathbf{J}} = \chi_1(\mathbf{J})\, m_{\pm0}(J_1,J_2)\left(\hat{Y}^{(J_1,J_2\pm\frac{1}{2})}_{\mathbf{J}_\text{r}}\right)^\star, \tag{B.17}$$

$$\mathcal{C}\,\hat{Y}^{(J_1,J_2\pm\frac{1}{2})}_{\mathbf{J}} = \chi_2(\mathbf{J})\, m_{0\pm}(J_1,J_2)\left(\hat{Y}^{(J_1\pm\frac{1}{2},J_2)}_{\mathbf{J}_\text{r}}\right)^\star, \tag{B.18}$$

JHEP04(2020)132

with the 'reversed' total angular momentum $\mathbf{J}_\mathrm{r} \equiv (J_1, J_2)\, j_2 j_1\, m_2 m_1$ and some phase factors $\chi_1(\mathbf{J})$ and $\chi_2(\mathbf{J})$. It turns out that $m_{\pm 0}$ and $m_{0\pm}$ are the same when written in terms of J_1 and J_2 so that we can obtain eigenvectors of $\mathcal{C}$ by essentially adding the two previous equations and taking care of the phase factors. After the dust has settled, the eigenvectors of $\mathcal{C}$ turn out to be

$$\hat{Y}^{\alpha\beta}_{\mathbf{J}} = \frac{\chi(\mathbf{J};\alpha,\beta)}{\sqrt{2}} \left[\hat{Y}^{(J_1+\frac{\alpha}{2},J_2)}_{\mathbf{J}} + \beta \hat{Y}^{(J_1,J_2+\frac{\alpha}{2})}_{\mathbf{J}_\mathrm{r}} \right], \tag{B.19}$$

for the four combinations of $\alpha, \beta \in \{-1, +1\}$ and the phase

$$\chi(\mathbf{J};\alpha,\beta) = (-1)^{-\frac{1}{2}(2J_1+m_1+m_2+\alpha+\frac{1}{2})} i^{\frac{1-\beta}{2}}. \tag{B.20}$$

The fermions in the action can now be expanded in this basis and the mass term becomes diagonal in terms of component fields which we call $(\tilde{D}_{\alpha\beta})_{\mathbf{J}}$, and which are related to $(\tilde{C}_{\mathbf{S}})_{\mathbf{J}}$ by

$$\sum_{\alpha,\beta} \sum_{\mathbf{J}} (\tilde{D}_{\alpha\beta})_{\mathbf{J}}\, \hat{Y}^{\alpha\beta}_{\mathbf{J}} = \sum_{\mathbf{S},\mathbf{L}} (\tilde{C}_{\mathbf{S}})_{\mathbf{L}}\, \hat{Y}_{\mathbf{L}} \otimes \hat{e}_{\mathbf{S}}. \tag{B.21}$$

One can diagonalize the fields in the off-diagonal block in a similar fashion, the only difference being that different orbital angular momentum representations are not mixed with each other. There is still mixing between $\mathbf{J}$ and $\mathbf{J}_r$, which can be diagonalized easily with an extra step similar to (B.19).

C Details on the propagators

In this appendix, we provide further details on the derivation of the propagators presented in section 3. In particular, we give the explicit formulas for the coefficients $\hat{f}$ that do not appear in the main text.

The fields in which the mass matrix for the bosons becomes diagonal are $B_{\pm,\pm}$, $B_{0,0}$, $D_\pm$ and D_0. The propagators between them are simply

$$\langle [B_{++}]_{\mathbf{L}} [B_{++}]^\dagger_{\mathbf{L}'} \rangle = \delta_{\mathbf{L},\mathbf{L}'} K^{\hat{m}^2_{++}}, \tag{C.1}$$

and similarly for B_{--}, B_{00}, $D_\pm$ and D_0. In order to invert the Clebsch-Gordan procedure, we have to express the non-diagonal fields $B_{\pm,\mp}$ and A_3 in terms of the diagonal fields. This is achieved by

$$B_{\pm,\mp} = \mp \frac{T^{\mp,\pm}}{\sqrt{2\hat{m}^2_{\mathrm{easy}}}} D_0 - T^{\pm,\mp} \left(\frac{D_+}{\sqrt{N_-}} - \frac{D_-}{\sqrt{N_+}} \right), \tag{C.2}$$

$$A_3 = \frac{-1 + \sqrt{4\hat{m}^2_{\mathrm{easy}} + 1}}{\sqrt{2N_-}} D_+ + \frac{1 + \sqrt{4\hat{m}^2_{\mathrm{easy}} + 1}}{\sqrt{2N_+}} D_-. \tag{C.3}$$

From (C.3) it is immediate to obtain the propagator $\langle A_3\, A_3^\dagger \rangle$, see (3.15) in the main text. Similarly, for the propagator $\langle \phi_i\, A_3^\dagger \rangle$ the two fields couple through propagators $\langle B_{\pm,\mp}\, A_3^\dagger \rangle$.

JHEP04(2020)132

It is therefore natural to introduce the following function

$$\hat{f}^{\,\phi A}(L_1,L_2)=\frac{-1+\sqrt{4\hat{m}^2_{\text{easy}}+1}}{\sqrt{2}N_-}K^{\hat{m}^2_+}-\frac{1+\sqrt{4\hat{m}^2_{\text{easy}}+1}}{\sqrt{2}N_+}K^{\hat{m}^2_-}, \tag{C.4}$$

which captures such contributions.[11]

The situations is more complicated for the propagators $\langle\phi_i\,\phi_j^\dagger\rangle$, because there are several possible contributions. The first one comes from the propagator $\langle B_{+,-}\,B^\dagger_{-,+}\rangle$, and it is captured by the function

$$\hat{f}^{\,\text{opp}}(L_1,L_2)=\frac{1}{2}\left(-\frac{K^{\hat{m}^2_0}}{2\hat{m}^2_{\text{easy}}}+\frac{K^{\hat{m}^2_+}}{N_-}+\frac{K^{\hat{m}^2_-}}{N_+}\right). \tag{C.5}$$

The other contributions come from propagators between identical B fields $\langle B_{\alpha,\beta}\,B^\dagger_{\alpha,\beta}\rangle$, and we will encode them in the functions $h_{\alpha,\beta}$. These functions are particularly simple for the B fields that are diagonal after the Clebsch-Gordan decomposition

$$h_{\pm,\pm}(L_1,L_2)=K^{\hat{m}^2_{\pm\pm}},\qquad h_{0,0}(L_1,L_2)=K^{\hat{m}^2_{00}}. \tag{C.6}$$

For the fields $B_{\pm,\mp}$, we can read off the corresponding contribution from (C.2), namely

$$h_{\pm,\mp}(L_1,L_2)=\frac{(T^{\mp\pm})^2}{2\hat{m}^2_{\text{easy}}}K^{\hat{m}^2_0}+(T^{\pm\mp})^2\left(\frac{K^{\hat{m}^2_+}}{N_-}+\frac{K^{\hat{m}^2_-}}{N_+}\right). \tag{C.7}$$

Note that here the $T^{\pm,\mp}$ given in (B.7) are to be evaluated at (L_1,L_2), i.e. one has to replace $(J_1,J_2)\to(L_1,L_2)$.

The functions $\hat{f}$ and $h_{\alpha\beta}$ we just defined are the building blocks of the final propagators. In order to obtain the full expressions, we start with a certain propagator, and expand it using (B.3) and (B.2), and then evaluate the propagators of B fields and A_3 in the way we just described. The result will be a complicated combination of products of Clebsch-Gordan coefficients and the functions $\hat{f}$ and $h_{\alpha\beta}$. These expressions can always be rewritten in terms of matrix elements of $\mathfrak{so}(6)$ generators[12] to obtain the form presented in section 3.2.

In (3.13) we have written the propagators between the scalars in terms of the functions $\hat{f}^{\,\text{sing}}$, $\hat{f}^{\,\text{cub}}$, $\hat{f}^{\,\text{lin}}$, $\hat{f}_5^{\,\text{sym}}$, $\hat{f}_6^{\,\text{sym}}$ and $\hat{f}^{\,\text{opp}}$ that are linear combinations of propagators between mass eigenstates. To write them in a more compact way, we define

$$Z_{\alpha,\beta}(L_1,L_2)\equiv\frac{1}{2}\left(C_5\left(L_1+\frac{\alpha}{2},L_2+\frac{\beta}{2}\right)-C_5(L_1,L_2)\right), \tag{C.8}$$

and

$$D_{\alpha,\beta}(L_1,L_2)\equiv\begin{cases}i^{\alpha-\beta}2(L_1+1)(2L_2+1)Z_{\alpha,\beta}(2Z_{\alpha,\beta}-1) & (\alpha,\beta)\neq(0,0)\,,\\ \prod_{(\gamma,\delta)\neq(0,0)}Z_{\gamma,\delta} & (\alpha,\beta)=(0,0)\,.\end{cases} \tag{C.9}$$

[11] The prefactor $T^{\pm\mp}$ that would naively appear gets absorbed in the matrix element of L_{i6}, as one can see by doing the calculation of the propagators carefully. A similar prefactor will also get absorbed by the matrix elements of the generators in (C.5).

[12] In practice, it is easiest to make an ansatz for the propagators and if the coefficients can be fixed for all possible combination, then the ansatz is correct.

JHEP04(2020)132

The indices (α,β) run over the five values $(\pm1,\pm1)$ and $(0,0)$. After a complicated calculation, on can see that $\hat{f}$ are given by[13]

$$\begin{aligned}\hat{f}^{\,\mathrm{sing}}(L_1,L_2) = \sum_{(\alpha,\beta)} \frac{1}{2D_{\alpha,\beta}} \Big[&-2Z_{\alpha,\beta}^2\left(1+C_5-Z_{\alpha,\beta}^2\right) - C_5 - 2(Z_{+,-}Z_{-,+})^2 \\ &- 2(1+C_5)Z_{+,-}Z_{-,+}\Big] h_{\alpha,\beta}\left(L_1+\frac{\alpha}{2},L_2+\frac{\beta}{2}\right),\end{aligned} \tag{C.10}$$

and

$$\hat{f}^{\,\mathrm{lin}}(L_1,L_2) = \sum_{(\alpha,\beta)} \frac{i}{4D_{\alpha,\beta}} \left(2Z_{\alpha,\beta}+1\right)\left(2C_5-2Z_{\alpha,\beta}^2-3\right) h_{\alpha,\beta}\left(L_1+\frac{\alpha}{2},L_2+\frac{\beta}{2}\right), \tag{C.11}$$

$$\hat{f}^{\,\mathrm{cub}}(L_1,L_2) = \sum_{(\alpha,\beta)} \frac{-i}{4D_{\alpha,\beta}} \left(2Z_{\alpha,\beta}+1\right) h_{\alpha,\beta}\left(L_1+\frac{\alpha}{2},L_2+\frac{\beta}{2}\right), \tag{C.12}$$

$$\hat{f}_5^{\,\mathrm{sym}}(L_1,L_2) = \sum_{(\alpha,\beta)} \frac{-1}{2D_{\alpha,\beta}} \left(\frac{1}{2}+Z_{+,-}Z_{-,+}+Z_{\alpha,\beta}^2\right) h_{\alpha,\beta}\left(L_1+\frac{\alpha}{2},L_2+\frac{\beta}{2}\right), \tag{C.13}$$

$$\hat{f}_6^{\,\mathrm{sym}}(L_1,L_2) = \sum_{(\alpha,\beta)} \frac{-1}{4D_{\alpha,\beta}} \left(2Z_{+,-}+1\right)\left(2Z_{-,+}+1\right) h_{\alpha,\beta}\left(L_1+\frac{\alpha}{2},L_2+\frac{\beta}{2}\right). \tag{C.14}$$

As the reader can observe, the functions $D_{\alpha\beta}$ and $Z_{\alpha\beta}$ allowed to compactly write the $\hat{f}$, but we do not think they have any physical meaning beyond this.

In order to obtain the fermionic propagators, we follow an identical procedure as described above. We start with a given propagator, expand it following the steps described in the diagonalization, and then identify the result in terms of propagators of diagonal fields and matrix elements of $\mathfrak{so}(6)$ generators. The result is given by (3.16) and (3.17), where the explicit expressions for $\hat{f}_F$ are

$$\begin{aligned}\hat{f}_F^{\,\mathrm{lin}}\left(L_1,L_2;L_1+\frac{1}{2},L_2-\frac{1}{2}\right) &= \frac{(L_1+L_2+1)\,K_F^{m=\sqrt{2(L_1+1)(L_2+1)}}}{\sqrt{(2L_1+3)\,(2L_2+1)}\,(2L_1+2L_2+3)} \\ &\quad + \frac{(L_1+L_2+2)\,K_F^{m=\sqrt{2L_2(L_1+1)}}}{2\sqrt{(L_1+1)\,L_2}\,(2L_1+2L_2+3)}, \\ \hat{f}_F^{\,\mathrm{lin}}\left(L_1,L_2;L_1-\frac{1}{2},L_2+\frac{1}{2}\right) &= \frac{(L_1+L_2+1)\,K_F^{m=\sqrt{2(L_1+1)(L_2+1)}}}{2\sqrt{(L_1+1)\,(L_2+1)}\,(2L_1+2L_2+3)} \\ &\quad + \frac{(L_1+L_2+2)\,K_F^{m=\sqrt{2L_2(L_1+1)}}}{\sqrt{(2L_1+1)\,(2L_2+1)}\,(2L_1+2L_2+3)},\end{aligned} \tag{C.15}$$

[13] In the following equations $Z_{\alpha,\beta}$, $D_{\alpha,\beta}$ and C_5 are always evaluated at (L_1,L_2) unless noted otherwise.

JHEP04(2020)132

and

$$\hat{f}_F^{\text{cub}}\left(L_1,L_2;L_1+\frac{1}{2},L_2-\frac{1}{2}\right)=\frac{3K_F^{m=\sqrt{2(L_1+1)(L_2+1)}}}{\sqrt{(2L_1+3)(2L_2+1)}(2L_1+2L_2+3)}-\frac{3K_F^{m=\sqrt{2L_2(L_1+1)}}}{2\sqrt{(L_1+1)L_2}(2L_1+2L_2+3)},$$
$$\hat{f}_F^{\text{cub}}\left(L_1,L_2;L_1-\frac{1}{2},L_2+\frac{1}{2}\right)=\frac{3K_F^{m=\sqrt{2(L_1+1)(L_2+1)}}}{2\sqrt{(L_1+1)(L_2+1)}(2L_1+2L_2+3)}-\frac{3K_F^{m=\sqrt{2L_2(L_1+1)}}}{\sqrt{(2L_1+1)(2L_2+1)}(2L_1+2L_2+3)}. \tag{C.16}$$

D Effective vertex

In this appendix, we will give some extra details on how to compute the effective vertex. We remind the reader that we started with the $\mathcal{N}=4$ SYM action, and we expanded around a classical solution $\phi_i=\phi_i^{\text{cl}}+\tilde{\phi}_i$. This gives rise to a number of cubic interaction vertices:

$$S_3=\frac{2}{g_{\text{YM}}^2}\int \mathrm{d}^4x\ \mathrm{tr}\left(i[A^\mu,A^\nu]\partial_\mu A_\nu+\tilde{\phi}_i[\tilde{\phi}_j,[\phi_i^{\text{cl}},\tilde{\phi}_j]]+i[A^\mu,\tilde{\phi}_i]\partial_\mu\tilde{\phi}_i+\tilde{\phi}_i[A^\mu,[\phi_i^{\text{cl}},A_\mu]]\right.$$
$$\left.+\frac{1}{2}\bar{\psi}\gamma^\mu[A_\mu,\psi]+\frac{1}{2}\sum_{i=1}^{3}\bar{\psi}C_i[\tilde{\phi}_i,\psi]+\frac{1}{2}\sum_{i=4}^{6}\bar{\psi}C_i[\tilde{\phi}_i,\gamma_5\psi]+i(\partial_\mu\bar{c})[A_\mu,c]-\bar{c}[\phi_i^{\text{cl}}[\tilde{\phi}_i,c]]\right). \tag{D.1}$$

These are the only vertices that can contribute to the computation of the effective vertex. The following calculation proceeds in exactly the same manner as that of [25, 26]. We will only write the contractions that contribute, all other possible Wick contractions being zero.

There is one contribution from the ghost fields, which behave simply as easy scalars

$$-\mathrm{tr}\left(\overbrace{\bar{c}[\phi_i^{\text{cl}},[\tilde{\phi}_i,c]]}\right)=\frac{\sqrt{2}N}{y_3}K^{m^2_{\text{easy}}}\mathrm{tr}\left(\tilde{\phi}_i G_{i6}\right). \tag{D.2}$$

Only two contractions survive in the vertex that couples two scalars with the gauge field[14]

$$\mathrm{tr}\left(i[\overbrace{A^\mu,\tilde{\phi}_i}]\partial_\mu\tilde{\phi}_i\right)+\mathrm{tr}\left(i[\overbrace{A^\mu,\tilde{\phi}_i}]\partial_\mu\tilde{\phi}_i\right)=+6iN\partial_3 f^{A\phi}\,\mathrm{tr}\left(\tilde{\phi}_i\,G_{i6}\right), \tag{D.3}$$

[14] In the second contraction, we can use (D.21) from [25], since we have

$$\nu_-=\sqrt{m_-^2+\frac{1}{4}}=\nu_{\text{easy}}-1,\quad \nu_+=\sqrt{m_+^2+\frac{1}{4}}=\nu_{\text{easy}}+1,$$

for both the fields in the diagonal and in the off-diagonal blocks, and the propagator $\hat{K}^{A\phi}$ has the desired form $K^{\nu-1}-K^{\nu+1}$.

JHEP04(2020)132

where

$$f^{A\phi} = \frac{-i}{2\sqrt{n(n+4)+2}} \left(K^{m_-^2} - K^{m_+^2} \right). \tag{D.4}$$

For the vertex that couples three scalars, all possible Wick contractions contribute

$$\mathrm{tr}\left(\tilde{\phi}_i[\overbrace{\tilde{\phi}_j}, [\phi_i^{\mathrm{cl}}, \tilde{\phi}_j]]\right) = -\frac{\sqrt{2}N}{y_3}\left[5f^{\mathrm{sing}} + n(n+4)f^{\mathrm{prod}} + K^{m^2_{\mathrm{easy}}}\right] \mathrm{tr}\left(\tilde{\phi}_i G_{i6}\right), \tag{D.5a}$$

$$\mathrm{tr}\left(\tilde{\phi}_i[\overbrace{\tilde{\phi}_j}, [\phi_i^{\mathrm{cl}}, \tilde{\phi}_j]]\right) = \frac{\sqrt{2}N}{y_3}\left[f^{\mathrm{sing}} + 2if^{\mathrm{lin}} + \left[n(n+4)-8\right]f^{\mathrm{prod}}\right] \mathrm{tr}\left(\tilde{\phi}_i G_{i6}\right), \tag{D.5b}$$

$$\mathrm{tr}\left(\tilde{\phi}_i[\overbrace{\tilde{\phi}_j}, [\phi_i^{\mathrm{cl}}, \tilde{\phi}_j]]\right) = \frac{4\sqrt{2}N}{y_3}\left[if^{\mathrm{lin}} - 2f^{\mathrm{prod}}\right] \mathrm{tr}\left(\tilde{\phi}_i G_{i6}\right). \tag{D.5c}$$

The regularization procedure becomes important when we consider the vertex that couples two gauge fields and a scalar. We work in dimensional reduction [49, 50] with $d = 3 - 2\epsilon$ space dimensions, hence $n_{\mathrm{A,easy}} = 3 - 2\epsilon$ and we should add 2ϵ scalars to the action that behave exactly as the easy components of the gauge field. The choice of this regularization procedure is motivated by the fact that it is supersymmetry preserving and hence compatible with the symmetries of the bulk $\mathcal{N} = 4$ SYM theory which we must recover far from the domain wall, cf. the discussion in [25, 26]. In total, we get

$$\begin{aligned}\mathrm{tr}\left(\tilde{\phi}_i[\overbrace{A^{\mu}}, [\phi_i^{\mathrm{cl}}, A_{\mu}]]\right) + \mathrm{tr}\left(\tilde{\phi}_i[\overbrace{A^{2\epsilon}}, [\phi_i^{\mathrm{cl}}, A_{2\epsilon}]]\right) \\ = -\frac{\sqrt{2}N}{y_3}\left((n_{A,\mathrm{easy}} + 2\epsilon)K^{m^2_{\mathrm{easy}}} + f^{AA}\right) \mathrm{tr}\left(\tilde{\phi}_i G_{i6}\right),\end{aligned} \tag{D.6}$$

where

$$f^{AA} = \frac{1}{2}\left[\left(1 + \frac{1}{\sqrt{4m^2_{\mathrm{easy}}+1}}\right) K^{m_-^2} + \left(1 - \frac{1}{\sqrt{4m^2_{\mathrm{easy}}+1}}\right) K^{m_+^2}\right]. \tag{D.7}$$

Finally, we can also have fermions running in the loop, which contribute as

$$\frac{1}{2}\sum_{i=1}^{3}(C_i)_{\alpha\beta}\,\mathrm{tr}\left(\overbrace{\bar{\psi}_\alpha[\tilde{\phi}_i, \psi_\beta]}\right) + \frac{1}{2}\sum_{i=4}^{5}(C_i)_{\alpha\beta}\,\mathrm{tr}\left(\overbrace{\bar{\psi}_\alpha[\tilde{\phi}_i, \gamma_5\psi_\beta]}\right) = 8N\,\mathrm{tr}\, f_F^{2,+}\ \mathrm{tr}(\tilde{\phi}_i G_{i6}). \tag{D.8}$$

One can sum all the contributions above, and simplify the resulting expression using identities such as $\Psi(z+1) = \Psi(z) + 1/z$. The result that one obtains is (4.3), where one notices that the dependence on the regulator ϵ drops completely.

E Matrix elements and Clebsch-Gordan coefficients

In this appendix, we describe how to compute matrix elements of $\mathfrak{so}(6)$ generators acting on general representations and where to obtain the Clebsch-Gordan coefficients relevant for the calculations in this work.

JHEP04(2020)132

Labels $\mathbf{S}$	Tensor operator $T_{\mathbf{S}}$
$((1,0),1,0,0,0)$	$\frac{1}{2}(L_{12}+L_{34})$
$((1,0),1,0,\pm1,0)$	$\frac{1}{2\sqrt{2}}(\mp(L_{14}+L_{23})+i(L_{13}-L_{24}))$
$((1,0),0,1,0,0)$	$\frac{1}{2}(L_{12}-L_{34})$
$((1,0),1,0,\pm1,0)$	$\frac{1}{2\sqrt{2}}(\mp(L_{14}-L_{23})-i(L_{13}+L_{24}))$
$((1,0),\frac{1}{2},\frac{1}{2},\pm\frac{1}{2},\pm\frac{1}{2})$	$\frac{1}{2}(\pm L_{25}-iL_{15})$
$((1,0),\frac{1}{2},\frac{1}{2},\pm\frac{1}{2},\mp\frac{1}{2})$	$\frac{1}{2}(L_{45}\mp iL_{35})$
$((\frac{1}{2},\frac{1}{2}),0,0,0,0)$	$-L_{56}$
$((\frac{1}{2},\frac{1}{2}),\frac{1}{2},\frac{1}{2},\pm\frac{1}{2},\pm\frac{1}{2})$	$\frac{1}{\sqrt{2}}(L_{16}\pm iL_{26})$
$((\frac{1}{2},\frac{1}{2}),\frac{1}{2},\frac{1}{2},\pm\frac{1}{2},\mp\frac{1}{2})$	$\frac{1}{\sqrt{2}}(\pm L_{36}+iL_{46})$

Table 7. Relation between the tensor operators of $\mathfrak{so}(6)$ and the corresponding generators L_{ij}.

In table 7 we map the generators L_{ij} to the tensor operators $T_{\mathbf{S}}$, as the latter have much simpler matrix elements. Notice how these tensor operators are labeled by a set of $\mathfrak{so}(5)$ quantum numbers $\mathbf{S}=(S_1,S_2),s_1,s_2,m_1,m_2$. The tensor operators which transform in the ten-dimensional representation $(1,0)$ of $\mathfrak{so}(5)$ only act on the $\mathfrak{so}(5)$ labels $\mathbf{L}$. The matrix elements are

$$\langle \mathbf{L}'|T_{\mathbf{S}}|\mathbf{L}\rangle = \delta_{L_1,L_1'}\delta_{L_2,L_2'}\sqrt{L_1(L_1+2)+L_2(L_2+1)}\langle \mathbf{L};\mathbf{S}|\mathbf{L}'\rangle. \tag{E.1}$$

The square root is sometimes called a reduced matrix element or isoscalar factor, and the second term is an $\mathfrak{so}(5)$ Clebsch-Gordan coefficient from coupling $\mathbf{L}$ and $\mathbf{S}$.

On the other hand, the tensor operators which transform in the five-dimensional representation $(\frac{1}{2},\frac{1}{2})$ of $\mathfrak{so}(5)$ will affect both the $\mathfrak{so}(5)$ and $\mathfrak{so}(6)$ quantum numbers. Therefore, we compute matrix elements of these operators with $\mathfrak{so}(6)$ states with labels $\mathbf{P}=(P_1,P_2,P_3)\mathbf{L}$, where $\mathbf{L}$ are the labels of the $\mathfrak{so}(5)$ subgroup. Then, the matrix elements are

$$\langle \mathbf{P}'|T_{\mathbf{S}}|\mathbf{P}\rangle = \delta_{P_1,P_1'}\delta_{P_2,P_2'}\delta_{P_3,P_3'}\,T^{P_1,P_2,P_3}_{L_1,L_2;L_1',L_2'}\,\langle \mathbf{L};\mathbf{S}|\mathbf{L}'\rangle. \tag{E.2}$$

As before, the matrix element is a product of a reduced matrix element $T^{P_1,P_2,P_3}_{L_1,L_2;L_1',L_2'}$ and an $\mathfrak{so}(5)$ Clebsch-Gordan coefficient.

The reduced matrix elements $T^{P_1,P_2,P_3}_{L_1,L_2;L_1',L_2'}$ that appear in (E.2) are more complicated than those in (E.1) and we have derived them using the strategy described in [46]. The main idea is the following. On the one hand, a construction by Gel'fand and Tsetlin [51] gives the matrix elements of $\mathfrak{so}(n)$ generators for any n. On the other hand, these matrix elements factorize into $\mathfrak{so}(n-1)$ Clebsch-Gordan coefficients and the reduced matrix elements that we are after. This factorization is the content of the Wigner-Eckart theorem. Since the relevant $\mathfrak{so}(5)$ Clebsch-Gordan coefficients are known, e.g. from [46], one can construct the

JHEP04(2020)132

matrix elements for $\mathfrak{so}(6)$ and essentially compare the two expressions. The missing factors are then the reduced matrix elements, which we present in table 8.

We have shown that with knowledge of certain $\mathfrak{so}(5)$ Clebsch-Gordan coefficients one can construct the matrix elements for any $\mathfrak{so}(6)$ generator. The $\mathfrak{so}(5)$ Clebsch-Gordan coefficients factorize as

$$\begin{aligned}\langle (L_1,L_2),\ell_1,\ell_2,m_{\ell 1},m_{\ell 2};(S_1,S_2),s_1,s_2,m_{s1},m_{s2}|(J_1,J_2),j_1,j_2,m_{j1},m_{j2}\rangle \\ = \langle (L_1,L_2),\ell_1,\ell_2;(S_1,S_2),s_1,s_2||(J_1,J_2),j_1,j_2\rangle \\ \times \langle \ell_1,m_{\ell 1};s_1,m_{s1}|j_1,m_{j1}\rangle\langle \ell_2,m_{\ell 2};s_2,m_{s2}|j_2,m_{j2}\rangle .\end{aligned} \tag{E.3}$$

The double-barred coefficients are reduced $\mathfrak{so}(5)$ Clebsch-Gordan coefficients, while the other two terms are usual $\mathfrak{su}(2)$ Clebsch-Gordan coefficients. The reduced coefficients were computed in [46] for the cases $(S_1,S_2)=(\frac{1}{2},0),(\frac{1}{2},\frac{1}{2}),(1,0)$.[15] In order to make it easy for the interested reader to reproduce our results, we attach a `Mathematica` file with all the relevant $\mathfrak{so}(5)$ Clebsch-Gordan coefficients and the reduced matrix elements from table 8. We are also happy to provide more details on request.

[15] In the notation from [46] one has $J_m = L_1$, $\Lambda_m = L_2$, $\ell_1 = J$, and so on. Except for these minor notation differences, our conventions are identical to theirs, and one can directly extract the double-barred coefficients from the tables at the end of that paper.

JHEP04(2020)132

(L_1', L_2')	$T^{P_1,P_2,P_3}_{L_1,L_2;L_1',L_2'}$
$(L_1-\frac{1}{2}, L_2-\frac{1}{2})$	$\left(\frac{(L_1+L_2-P_1-1)(L_1+L_2+P_1+3)(L_1+L_2-P_2)(L_1+L_2+P_2+2)(L_1+L_2-P_3+1)(L_1+L_2+P_3+1)}{2(2L_1+1)L_2(L_1+L_2+1)(2L_1+2L_2+1)}\right)^{1/2}$
$(L_1-\frac{1}{2}, L_2+\frac{1}{2})$	$-\left(\frac{(L_1-L_2-P_1-2)(L_1-L_2+P_1+2)(L_1-L_2-P_2-1)(L_1-L_2+P_2+1)(L_1-L_2-P_3)(L_1-L_2+P_3)}{2(2L_1+1)(L_2+1)(L_1-L_2)(2L_1-2L_2-1)}\right)^{1/2}$
(L_1, L_2)	$-\left(\frac{(P_1+2)^2(P_2+1)^2{P_3}^2}{(L_1-L_2)(L_1-L_2+1)(L_1+L_2+1)(L_1+L_2+2)}\right)^{1/2}$
$(L_1+\frac{1}{2}, L_2-\frac{1}{2})$	$\left(\frac{(L_1-L_2-P_1-1)(L_1-L_2+P_1+3)(L_1-L_2-P_2)(L_1-L_2+P_2+2)(L_1-L_2-P_3+1)(L_1-L_2+P_3+1)}{2(2L_1+3)L_2(L_1-L_2+1)(2L_1-2L_2+3)}\right)^{1/2}$
$(L_1+\frac{1}{2}, L_2+\frac{1}{2})$	$-\left(\frac{(L_1+L_2-P_1)(L_1+L_2+P_1+4)(L_1+L_2-P_2+1)(L_1+L_2+P_2+3)(L_1+L_2-P_3+2)(L_1+L_2+P_3+2)}{2(2L_1+3)(L_2+1)(L_1+L_2+2)(2L_1+2L_2+5)}\right)^{1/2}$

Table 8. Reduced matrix elements appearing in (E.2).

References

[1] A. Karch and L. Randall, *Open and closed string interpretation of SUSY CFT's on branes with boundaries*, *JHEP* **06** (2001) 063 [hep-th/0105132] [INSPIRE].

[2] N.R. Constable, R.C. Myers and O. Tafjord, *NonAbelian brane intersections*, *JHEP* **06** (2001) 023 [hep-th/0102080] [INSPIRE].

[3] N.R. Constable, R.C. Myers and O. Tafjord, *The Noncommutative bion core*, *Phys. Rev.* **D 61** (2000) 106009 [hep-th/9911136] [INSPIRE].

[4] O. DeWolfe, D.Z. Freedman and H. Ooguri, *Holography and defect conformal field theories*, *Phys. Rev.* **D 66** (2002) 025009 [hep-th/0111135] [INSPIRE].

[5] J. Erdmenger, Z. Guralnik and I. Kirsch, *Four-dimensional superconformal theories with interacting boundaries or defects*, *Phys. Rev.* **D 66** (2002) 025020 [hep-th/0203020] [INSPIRE].

[6] K. Nagasaki and S. Yamaguchi, *Expectation values of chiral primary operators in holographic interface CFT*, *Phys. Rev.* **D 86** (2012) 086004 [arXiv:1205.1674] [INSPIRE].

[7] C. Kristjansen, G.W. Semenoff and D. Young, *Chiral primary one-point functions in the D3-D7 defect conformal field theory*, *JHEP* **01** (2013) 117 [arXiv:1210.7015] [INSPIRE].

[8] D. Gaiotto and E. Witten, *Supersymmetric Boundary Conditions in $\mathcal{N} = 4$ Super Yang-Mills Theory*, *J. Statist. Phys.* **135** (2009) 789 [arXiv:0804.2902] [INSPIRE].

[9] R.C. Myers and M.C. Wapler, *Transport Properties of Holographic Defects*, *JHEP* **12** (2008) 115 [arXiv:0811.0480] [INSPIRE].

[10] O. Bergman, N. Jokela, G. Lifschytz and M. Lippert, *Quantum Hall Effect in a Holographic Model*, *JHEP* **10** (2010) 063 [arXiv:1003.4965] [INSPIRE].

[11] G. Grignani, N. Kim and G.W. Semenoff, *D3-D5 holography with flux*, *Phys. Lett.* **B 715** (2012) 225 [arXiv:1203.6162] [INSPIRE].

[12] C. Kristjansen and G.W. Semenoff, *Giant D5 Brane Holographic Hall State*, *JHEP* **06** (2013) 048 [arXiv:1212.5609] [INSPIRE].

[13] C. Kristjansen, R. Pourhasan and G.W. Semenoff, *A Holographic Quantum Hall Ferromagnet*, *JHEP* **02** (2014) 097 [arXiv:1311.6999] [INSPIRE].

[14] J. Hutchinson, C. Kristjansen and G.W. Semenoff, *Conductivity Tensor in a Holographic Quantum Hall Ferromagnet*, *Phys. Lett.* **B 738** (2014) 373 [arXiv:1408.3320] [INSPIRE].

[15] M. de Leeuw, C. Kristjansen and K. Zarembo, *One-point Functions in Defect CFT and Integrability*, *JHEP* **08** (2015) 098 [arXiv:1506.06958] [INSPIRE].

[16] I. Buhl-Mortensen, M. de Leeuw, C. Kristjansen and K. Zarembo, *One-point Functions in AdS/dCFT from Matrix Product States*, *JHEP* **02** (2016) 052 [arXiv:1512.02532] [INSPIRE].

[17] M. de Leeuw, C. Kristjansen and S. Mori, *AdS/dCFT one-point functions of the* SU(3) *sector*, *Phys. Lett.* **B 763** (2016) 197 [arXiv:1607.03123] [INSPIRE].

JHEP04(2020)132

[18] I. Buhl-Mortensen, M. de Leeuw, A.C. Ipsen, C. Kristjansen and M. Wilhelm, *Asymptotic One-Point Functions in Gauge-String Duality with Defects*, *Phys. Rev. Lett.* **119** (2017) 261604 [arXiv:1704.07386] [INSPIRE].

[19] M. De Leeuw, C. Kristjansen and G. Linardopoulos, *Scalar one-point functions and matrix product states of AdS/dCFT*, *Phys. Lett.* **B 781** (2018) 238 [arXiv:1802.01598] [INSPIRE].

[20] M. de Leeuw, C. Kristjansen and K.E. Vardinghus, *A non-integrable quench from AdS/dCFT*, *Phys. Lett.* **B 798** (2019) 134940 [arXiv:1906.10714] [INSPIRE].

[21] A.C. Ipsen and K.E. Vardinghus, *The dilatation operator for defect conformal $\mathcal{N} = 4$ SYM*, arXiv:1909.12181 [INSPIRE].

[22] L. Piroli, B. Pozsgay and E. Vernier, *What is an integrable quench?*, *Nucl. Phys.* **B 925** (2017) 362 [arXiv:1709.04796] [INSPIRE].

[23] B. Pozsgay, L. Piroli and E. Vernier, *Integrable Matrix Product States from boundary integrability*, *SciPost Phys.* **6** (2019) 062 [arXiv:1812.11094] [INSPIRE].

[24] I. Buhl-Mortensen, M. de Leeuw, A.C. Ipsen, C. Kristjansen and M. Wilhelm, *One-loop one-point functions in gauge-gravity dualities with defects*, *Phys. Rev. Lett.* **117** (2016) 231603 [arXiv:1606.01886] [INSPIRE].

[25] I. Buhl-Mortensen, M. de Leeuw, A.C. Ipsen, C. Kristjansen and M. Wilhelm, *A Quantum Check of AdS/dCFT*, *JHEP* **01** (2017) 098 [arXiv:1611.04603] [INSPIRE].

[26] A. Gimenez Grau, C. Kristjansen, M. Volk and M. Wilhelm, *A Quantum Check of Non-Supersymmetric AdS/dCFT*, *JHEP* **01** (2019) 007 [arXiv:1810.11463] [INSPIRE].

[27] M. de Leeuw, A.C. Ipsen, C. Kristjansen and M. Wilhelm, *Introduction to integrability and one-point functions in $\mathcal{N} = 4$ supersymmetric Yang-Mills theory and its defect cousin*, in *Proceedings, Les Houches Summer School: Integrability: From Statistical Systems to Gauge Theory: Les Houches, France, June, 2016*, vol. 106, arXiv:1708.02525 [INSPIRE].

[28] M. de Leeuw, *One-point functions in AdS/dCFT*, 2019, arXiv:1908.03444 [INSPIRE].

[29] J. Castelino, S. Lee and W. Taylor, *Longitudinal five-branes as four spheres in matrix theory*, *Nucl. Phys.* **B 526** (1998) 334 [hep-th/9712105] [INSPIRE].

[30] J. Medina and D. O'Connor, *Scalar field theory on fuzzy S^4*, *JHEP* **11** (2003) 051 [hep-th/0212170] [INSPIRE].

[31] H.C. Steinacker, *One-loop stabilization of the fuzzy four-sphere via softly broken SUSY*, *JHEP* **12** (2015) 115 [arXiv:1510.05779] [INSPIRE].

[32] S. Ramgoolam, *On spherical harmonics for fuzzy spheres in diverse dimensions*, *Nucl. Phys.* **B 610** (2001) 461 [hep-th/0105006] [INSPIRE].

[33] K. Nagasaki, H. Tanida and S. Yamaguchi, *Holographic Interface-Particle Potential*, *JHEP* **01** (2012) 139 [arXiv:1109.1927] [INSPIRE].

[34] B. Guo, *Lollipop diagrams in defect $\mathcal{N} = 4$ super Yang-Mills theory*, MSc Thesis, University of British Columbia, (2017), DOI.

[35] M. de Leeuw, C. Kristjansen and G. Linardopoulos, *One-point functions of non-protected operators in the* SO(5) *symmetric D3-D7 dCFT*, *J. Phys.* **A 50** (2017) 254001 [arXiv:1612.06236] [INSPIRE].

JHEP04(2020)132

[36] M. de Leeuw, A.C. Ipsen, C. Kristjansen and M. Wilhelm, *One-loop Wilson loops and the particle-interface potential in AdS/dCFT*, *Phys. Lett.* **B 768** (2017) 192 [arXiv:1608.04754] [INSPIRE].

[37] J. Aguilera-Damia, D.H. Correa and V.I. Giraldo-Rivera, *Circular Wilson loops in defect Conformal Field Theory*, *JHEP* **03** (2017) 023 [arXiv:1612.07991] [INSPIRE].

[38] M. Preti, D. Trancanelli and E. Vescovi, *Quark-antiquark potential in defect conformal field theory*, *JHEP* **10** (2017) 079 [arXiv:1708.04884] [INSPIRE].

[39] S. Bonansea, S. Davoli, L. Griguolo and D. Seminara, *Circular Wilson loops in defect $\mathcal{N} = 4$ SYM: phase transitions, double-scaling limits and OPE expansions*, *JHEP* **03** (2020) 084 [arXiv:1911.07792] [INSPIRE].

[40] M. de Leeuw, A.C. Ipsen, C. Kristjansen, K.E. Vardinghus and M. Wilhelm, *Two-point functions in AdS/dCFT and the boundary conformal bootstrap equations*, *JHEP* **08** (2017) 020 [arXiv:1705.03898] [INSPIRE].

[41] E. Widen, *Two-point functions of* SU(2)*-subsector and length-two operators in dCFT*, *Phys. Lett.* **B 773** (2017) 435 [arXiv:1705.08679] [INSPIRE].

[42] M. Billò, V. Gonçalves, E. Lauria and M. Meineri, *Defects in conformal field theory*, *JHEP* **04** (2016) 091 [arXiv:1601.02883] [INSPIRE].

[43] P. Liendo and C. Meneghelli, *Bootstrap equations for $\mathcal{N} = 4$ SYM with defects*, *JHEP* **01** (2017) 122 [arXiv:1608.05126] [INSPIRE].

[44] D. Mazáč, L. Rastelli and X. Zhou, *An analytic approach to $BCFT_d$*, *JHEP* **12** (2019) 004 [arXiv:1812.09314] [INSPIRE].

[45] M. de Leeuw, T. Gombor, C. Kristjansen, G. Linardopoulos and B. Pozsgay, work in progress.

[46] K. Hecht, *Some simple R5 Wigner Coefficients and their application*, *Nucl. Phys.* **63** (1965) 177.

[47] R. Feger and T.W. Kephart, *LieART — A Mathematica application for Lie algebras and representation theory*, *Comput. Phys. Commun.* **192** (2015) 166 [arXiv:1206.6379] [INSPIRE].

[48] C.P. Burgess and G.D. Moore, *The standard model: A primer*, Cambridge University Press, (2006).

[49] W. Siegel, *Supersymmetric Dimensional Regularization via Dimensional Reduction*, *Phys. Lett.* **84B** (1979) 193 [INSPIRE].

[50] D.M. Capper, D.R.T. Jones and P. van Nieuwenhuizen, *Regularization by Dimensional Reduction of Supersymmetric and Nonsupersymmetric Gauge Theories*, *Nucl. Phys.* **B 167** (1980) 479 [INSPIRE].

[51] I. Gelfand and M.L. Tsetlin, *Finite-dimensional representations of groups of orthogonal matrices*, *Dokl. Akad. Nauk SSSR* **71** (1950) 1017.

JHEP04(2020)132

JHEP

Published for SISSA by Springer

Received: December 23, 2019
Accepted: February 3, 2020
Published: February 17, 2020

Conformally-regulated direct integration of the two-loop heptagon remainder

Jacob L. Bourjaily,[a,b,c] **Matthias Volk**[a] **and Matt von Hippel**[a]

[a] *Niels Bohr International Academy and Discovery Center, Niels Bohr Institute, University of Copenhagen, Blegdamsvej 17, DK-2100, Copenhagen Ø, Denmark*

[b] *Center for the Fundamental Laws of Nature, Department of Physics, Jefferson Physical Laboratory, Harvard University, Cambridge, MA 02138, U.S.A.*

[c] *Institute for Gravitation and the Cosmos, Department of Physics, Pennsylvania State University, University Park, PA 16892, U.S.A.*

E-mail: bourjaily@psu.edu, mvolk@nbi.ku.dk, mvonhippel@nbi.ku.dk

Abstract: We reproduce the two-loop seven-point remainder function in planar, maximally supersymmetric Yang-Mills theory by direct integration of conformally-regulated chiral integrands. The remainder function is obtained as part of the two-loop logarithm of the MHV amplitude, the regularized form of which we compute directly in this scheme. We compare the scheme-dependent anomalous dimensions and related quantities in the conformal regulator with those found for the Higgs regulator.

Keywords: Scattering Amplitudes, Supersymmetric Gauge Theory

ArXiv ePrint: 1912.05690

https://doi.org/10.1007/JHEP02(2020)095

JHEP02(2020)095

Contents

1 Introduction and overview **1**

2 Local integrands for (logarithms of) MHV amplitudes **3**
2.1 Specific contributions to the seven-point logarithm 6

3 Feynman parameterization and direct integration **6**
3.1 (Cluster) coordinate charts for heptagon integrals 7
3.2 Divide and conquer: parametric integration via various pathways 7
3.3 Refining the results of integration (removing spurious letters) 8

4 The two-loop heptagon remainder function **10**
4.1 Exempli gratia: Higgs-regulated (logarithms of) MHV amplitudes 10
4.2 Conformally-regulated (logarithms of) MHV amplitudes 11
4.3 Symbology and the alphabets of individual integral contributions 12

5 Discussion **13**

JHEP02(2020)095

1 Introduction and overview

The study of scattering amplitudes in recent decades has led to tremendous advances in both our understanding of quantum field theory and also our technical progress in computing the predictions made for experiment. Much of this progress can be attributed to the remarkable (and still surprising) simplicity of massless quantum field theories in four dimensions. Any such theory turns out to possess a connection to Grassmannian geometry [1–4] which has led to novel applications and greater understanding of perturbative amplitudes for an expanding class of quantum theories. This is true despite the subtlety involved in even defining the S-matrix for massless field theories! (But see [5, 6] for recent progress on this problem.)

Many of the difficulties of working with massless quantum field theories can be postponed by focusing on loop *integrands* ('the sum of Feynman diagrams'). At the integrand level, there are several new and extremely powerful frameworks for expressing perturbative scattering amplitudes of an increasingly general class of theories. These tools include all-loop recursion relations [7, 8], bootstrap methods [9–11], Q-cuts [12], and the broad reach of generalized [13–22] and prescriptive [23–29] unitarity. It remains to be seen, however, how much of the simplicity of integrands can survive loop integration. Considering the extent to which the simplicity at the integrand-level arises specifically for theories of *massless* particles in exactly *four* dimensions, and that it is precisely these features that are responsible for infrared divergences whose regularization necessarily spoils them, it

would not be surprising if much of this extra structure was lost to the infrared. Indeed, it would be reasonable to be skeptical that anything remarkable would be found for the actual infrared-safe quantities in which we are ultimately interested.

To test whether or not any of the niceness of amplitudes at the integrand-level survives the wrath and fury (the infrared regularization) of loop integration, it would be reasonable to simply 'shut up and calculate' — by any means necessary — and see what emerges in the '[theoretical] data', so to speak. Of course, this will always be easier to accomplish for especially simple quantum field theories such as maximally supersymmetric ($\mathcal{N}=4$) Yang-Mills ('sYM') in the planar limit, for which the greatest computational leverage exists (largely due to this theory's special properties [30–35]).

There is a now-quite-famous example which illustrates what can be discovered through such a 'compute first, understand later' strategy. It involves one of the simplest non-constant and non-trivial infrared-safe quantities in planar sYM: the (BDS) *remainder function* for six particles at two-loop order. This quantity was determined through truly heroic efforts, first numerically [20] and then analytically [36] — in both cases, starting from an integrand-level expression obtained using unitarity-based methods; then regulating; then integrating. Within months of the publication of the analytic result, however, breathtaking simplicity was indeed found: the 18-page sum of hyperlogarithms in [36] could be written in a single line [37]!

The ideas that led to the discovery of this simplicity would lead to a watershed of new and powerful techniques developed hand-in-hand with even greater evidence of simplicity surviving regularization and loop integration. Today, this particular quantity — the six-particle remainder function in planar sYM — is known to *seven*(!) loops; and the seven-particle remainder is known (at least at 'symbol-level') to four loops [38–49]. Interestingly, after the two-loop result was found 'the old fashioned way' in [36] — namely, by integrating Feynman integrands — all subsequent results were obtained using methods that *made no reference to loop integrands or loop integration whatsoever*! While these ideas have more recently been applied to non-planar amplitudes in supersymmetric theories [50, 51] and more broadly [51–60], they suffer from several fundamental limitations in applicability — in multiplicity, in the understanding (and simplicity) of the kinds of transcendental functions that arise in perturbation theory (including those described in e.g. [61]) — that prevent these ideas from rewriting the methods taught in textbooks, say.

One of the key motivations for our present work is the question of how much simplicity of loop integrands can be preserved through loop integration and regularization. Specifically, how can this bridge be crossed by *direct* and general methods — without reference to any ansatz about the kinds of functions that may arise in particular cases. A key source of hope that a more direct (and therefore general) connection between the remarkable integrands for amplitudes in planar sYM [24–26] and the simple expressions that we now expect to find for infrared-safe quantities is the is the existence of the regulator introduced in [24], which allows infrared divergences to be regulated *without breaking (dual-)conformal invariance*. Another critical source of optimism is the recent renaissance in direct-integration technology for Feynman-parametric integrands [62–64] (see also [65, 66]).

JHEP02(2020)095

In this work, we test the robustness of this emerging bridge from integrands to integrals in the highly non-trivial case of the seven-point remainder function at two loops. This quantity was first determined at symbol-level in [67] (see also [68, 69]), and later upgraded to a function-level result in [70]. Here, we start from the chiral integrand representation for the logarithm of the amplitude given in [23], use the conformal regulator of [24], Feynman-parameterize these terms according to [71], and integrate each piece using the technology of [62–64]. The result is a novel (if not superior) representation of the two-loop remainder function, and a proof of concept that such a strategy can work. As a bonus, by combining this result with that of [71] for six particles, we are able to determine all of the scheme-dependent parts of the two-loop MHV-amplitude logarithm in the conformal regularization scheme.

This work is organized as follows. We start in section 2 with a review of the local integrands necessary for MHV amplitudes and their logarithms in planar sYM at two-loops and how these integrands can be regulated while preserving dual-conformal invariance. In section 3 we discuss how we can *directly* integrate each of the integrands needed for the seven-particle logarithm, resulting in a representation in terms of explicit hyperlogarithmic functions. Our main results regarding the heptagon remainder function are described in section 4, where we determine the scheme-dependent parts of the logarithm of MHV amplitudes in the conformal regularization scheme and compare these with what is found for the Higgs regulator.

Available as supplementary material attached to this paper, we have prepared the supplementary file `heptagon_logarithm_seed_data.m`. This file contains: Feynman-parametric integrands for the five (cyclic) seeds which generate the seven-point logarithm at two loops; analytic expressions for each seed integral — given in terms of Goncharov hyperlogarithms — obtained via direct integration; details regarding the novel alphabets that arise for these integrals; and reference details regarding how our coordinates related to those used by [70] in their representation of the two-loop heptagon remainder function.

2 Local integrands for (logarithms of) MHV amplitudes

In this section, we give a rapid review of the representation (in terms of local Feynman integrals) of MHV amplitudes and their logarithms at two loops in the planar limit of sYM. In [7] (see also the earlier work [20, 72, 73]), it was guessed (and checked) that the n-particle MHV amplitude integrand could be represented as[1]

$$\mathcal{A}_n^{(L=2)} := \frac{1}{2} \sum_{\substack{1\leq a\leq n \\ a<b<c< \\ d<n+a}}$$

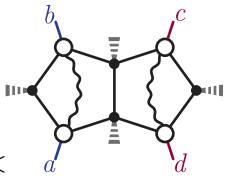

, (2.1)

[1] Notice that we have dropped the typical notation indicating N$^{(\mathbf{k}=0)}$MHV degree in '$\mathcal{A}_n^{(L)}$', as no other helicity sectors will be considered in this work.

JHEP02(2020)095

where the double-pentagons, herein '$\Omega\big[(a,b),(c,d)\big]$', have precise loop-dependent numerators (indicated by the wavy-lines in the figure) expressed in terms of momentum twistors [74]:

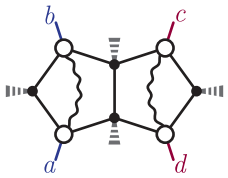

$$\coloneqq \Omega\big[(a,b),(c,d)\big] \tag{2.2}$$
$$\coloneqq \frac{\langle(\ell_1)(a-1\,a\,a+1)\cap(b-1\,b\,b+1)\rangle\langle ba\,dc\rangle\langle(\ell_2)(c-1\,c\,c+1)\cap(d-1\,d\,d+1)\rangle}{(\ell_1|a)(\ell_1|a+1)(\ell_1|b)(\ell_1|b+1)(\ell_1|\ell_2)(\ell_2|c)(\ell_2|c+1)(\ell_2|d)(\ell_2|d+1)}.$$

As usual, we are using the notations $(a|b)\coloneqq(x_a-x_b)^2$ where x_a are the dual coordinates related to the momenta through $p_a=:x_{a+1}-x_a$, and $\langle abcd\rangle\coloneqq\det(z_a,z_b,z_c,z_d)$ for the ordinary four-brackets of momentum twistors.

We should clarify that the factor of '1/2' appearing in (2.1) is really a *symmetry factor*: it accounts for the fact that the summand includes each contribution exactly twice — provided we view the integrand in (2.2) as being (implicitly) symmetrized with respect to $\ell_1\leftrightarrow\ell_2$; in particular, this factor of 1/2 could be dispensed by an instruction to 'delete duplicates' from the r.h.s. (something often left implicit in the relevant literature). As $\Omega\big[(a,b),(c,d)\big]$ and $\Omega\big[(c,d),(a,b)\big]$ are identical upon integration, *we consider them equivalent* (a.k.a. 'duplicates') — a potential source of confusion below, for which we apologize.

Notice that the definition of $\Omega\big[(a,b),(c,d)\big]$ depends on up to twelve momentum twistors

$$\{z_{a-1},z_a,z_{a+1}\}\cup\{z_{b-1},z_b,z_{b+1}\}\cup\{z_{c-1},z_c,z_{c+1}\}\cup\{z_{d-1},z_d,z_{d+1}\}\,, \tag{2.3}$$

with cyclic labeling understood. Especially for low multiplicity, these indices can overlap considerably. When it is necessary to disambiguate the multiplicity n, implicit in the definition (2.2) above, we will signify this by writing '$\Omega^{(n)}\big[(a,b),(c,d)\big]$'.

Shortly after the formula (2.1) appeared in [7], a similar expression was derived in [23] for the four-dimensional integrand of the two-loop *logarithm* of the MHV amplitude,

$$\log\big(\mathcal{A}_n\big)^{(L=2)}=\mathcal{A}_n^{(L=2)}-\frac{1}{2}\Big(\mathcal{A}_n^{(L=1)}\Big)^2=-\frac{1}{4}\sum_{\substack{1\leq a<n\\ a<c<b<\\ d<n+a}}\Omega\big[(a,b),(c,d)\big]\,. \tag{2.4}$$

(As before, the factor of '1/4' above is merely a symmetry factor: the appropriate prefactor would be 1 times each term in the summand *without duplication*.) Notice that the summand in (2.4) now excludes the possibility that $a+1=b$ and — more importantly — the summand requires that $c\in\{a+1,\ldots,b-1\}$.

It is instructive to see a few instances of equation (2.4). Without symmetry factors, but being explicit about the fact that cyclic seeds should be summed only *without duplication*, and being very careful about which cyclic seeds necessitate clarification about when multiplicity matters, the two-loop logarithms of MHV amplitudes for 4-8 particles are as

JHEP02(2020)095

follows:

$$\log\left(\mathcal{A}_4\right)^{(2)} = -\left[\Omega^{(4)}\left[(2,4),(3,1)\right] + \underset{\text{(no dupl.)}}{\text{cyclic}_4}\right] = -\Omega^{(4)}\left[(2,4),(3,1)\right], \tag{2.5}$$

$$\log\left(\mathcal{A}_5\right)^{(2)} = -\left[\Omega^{(5)}\left[(2,4),(3,5)\right] + \underset{\text{(no dupl.)}}{\text{cyclic}_5}\right] = -\left[\Omega^{(5)}\left[(2,4),(3,5)\right] + \text{cyclic}_5\right], \tag{2.6}$$

$$\log\left(\mathcal{A}_6\right)^{(2)} = -\left[\Omega\left[(2,4),(3,5)\right] + \Omega^{(6)}\left[(2,4),(3,6)\right] + \Omega^{(6)}\left[(2,5),(3,6)\right] + \underset{\text{(no dupl.)}}{\text{cyclic}_6}\right], \tag{2.7}$$

$$\begin{aligned}\log\left(\mathcal{A}_7\right)^{(2)} = -\Big[&\Omega\left[(2,4),(3,5)\right] + \Omega\left[(2,4),(3,6)\right] + \Omega\left[(2,5),(3,6)\right] \\ &+ \Omega^{(7)}\left[(2,4),(3,7)\right] + \Omega^{(7)}\left[(2,5),(3,7)\right] + \underset{\text{(no dupl.)}}{\text{cyclic}_7}\Big],\end{aligned} \tag{2.8}$$

$$\begin{aligned}\log\left(\mathcal{A}_8\right)^{(2)} = -\Big[&\Omega\left[(2,4),(3,5)\right] + \Omega\left[(2,4),(3,6)\right] + \Omega\left[(2,5),(3,6)\right] \\ &+ \Omega\left[(2,4),(3,7)\right] + \Omega\left[(2,5),(3,7)\right] + \Omega\left[(2,6),(3,7)\right] + \Omega^{(8)}\left[(2,4),(3,8)\right] \\ &+ \Omega^{(8)}\left[(2,5),(3,8)\right] + \Omega^{(8)}\left[(2,5),(4,8)\right] + \Omega^{(8)}\left[(2,6),(4,8)\right] + \underset{\text{(no dupl.)}}{\text{cyclic}_8}\Big].\end{aligned} \tag{2.9}$$

There are a couple of things to notice about these representations. First, observe that for more than six particles the majority of cyclic seeds can be chosen to be independent of n; therefore, these contributions remain unchanged beyond some threshold multiplicity. The second thing to notice is that it is fairly easy to organize contributions according to their degrees of infrared divergence:[2]

$$\begin{aligned}&\log^2\text{-divergent: } \Omega\left[(2,4),(3,5)\right] \;\; \textit{only}, \\ &\log^1\text{-divergent: } \Omega\left[(2,4),(3,b)\right] \;\; \text{for } b > 5,\end{aligned} \tag{2.10}$$

with all other integrals finite. In particular, notice that the *only* cyclic seed with a $\log^2$-divergence is $\Omega\left[(2,4),(3,5)\right]$ and that this integral is n-independent once it is evaluated for any $n \geq 6$. We will return to the consequences of this fact momentarily.

To regulate these divergences, we employ the so-called 'dual-conformal' regularization scheme introduced in [24], wherein each (massless) external particle is taken off the lightcone by an amount proportional to the conformally-invariant parameter denoted 'δ' according to

$$p_a^2 \mapsto p_a^2 + \delta\frac{(p_{a-1}+p_a)^2(p_a+p_{a+1})^2}{(p_{a-1}+p_a+p_{a+1})^2} = (a|a+1) + \delta\frac{(a-1|a+1)(a|a+2)}{(a-1|a+2)}. \tag{2.11}$$

(There is an alternative definition of this regulator expressed in terms of dual-momentum coordinates — where each dual coordinate x_a is shifted by a small amount in the direction of its cyclic neighbor, x_{a+1}; these two definitions are not identical for finite δ, but they result in regulated integrals equivalent to $\mathcal{O}(\delta)$.)

[2] In dimensional regularization, '$\log^k$-divergent' should be understood as '$1/\epsilon^k$-divergent'.

JHEP02(2020)095

2.1 Specific contributions to the seven-point logarithm

As seven particles is the primary example of interest to us here, it is worthwhile to give the five cyclic generators in (2.8) individual names. Let us therefore define

$$\begin{aligned} &\mathcal{I}_1 \coloneqq \Omega\big[(2,4),(3,5)\big]\,, \qquad \mathcal{I}_2 \coloneqq \Omega\big[(2,4),(3,6)\big]\,, \qquad \mathcal{I}_3 \coloneqq \Omega\big[(2,5),(3,6)\big]\,, \\ &\mathcal{I}_4 \coloneqq \Omega^{(7)}\big[(2,4),(3,7)\big]\,, \quad \mathcal{I}_5 \coloneqq \Omega^{(7)}\big[(2,5),(3,7)\big]\,. \end{aligned} \tag{2.12}$$

Notice that from our discussion above, only $\mathcal{I}_1$ will be $\log^2$-divergent in the infrared upon integration, while $\{\mathcal{I}_2, \mathcal{I}_4\}$ will be $\log^1$-divergent; the two seeds $\{\mathcal{I}_3, \mathcal{I}_5\}$ are infrared finite, and therefore do not require any regularization.

We will discuss how each of the contributions (2.12) can be evaluated in the following section. But already now we can observe an important consequence of the fact that $\mathcal{I}_1$ depends exclusively on momentum twistors $\{z_1, \ldots, z_6\}$: its evaluation will be the same for seven particles as it was for six. More specifically, $\mathcal{I}_1$ is essentially identical to what was computed (as part of what was called '$\mathcal{I}_{15}$') in [71]

$$\begin{aligned} I_1 &\coloneqq \int d^4\ell_1 d^4\ell_2\, \mathcal{I}_1 \\ &= \frac{1}{4}\Big[2\zeta_2 \log^2(\delta) + 6\zeta_3\Big[\log(\delta)+1\Big] - \zeta_2^2 - 2\zeta_2 G_{0,1}(1-w) + G_{0,0,0,1}(1-w) - G_{0,1,0,1}(1-w)\Big]\,, \end{aligned} \tag{2.13}$$

where

$$w \coloneqq \frac{(3|5)(6|2)}{(3|6)(5|2)} = \frac{\langle 23\,45\rangle\langle 56\,12\rangle}{\langle 23\,56\rangle\langle 45\,12\rangle}. \tag{2.14}$$

Notice that we are reserving calligraphic symbols to denote *integrands* and *italic* symbols to indicate *integrals*.

As $\mathcal{I}_1$ is the only cyclic seed with a $\log^2$-divergence for arbitrary n, it is wholly responsible for the leading divergence of the logarithm of MHV amplitudes at two loops. The coefficient of this divergence is related to the (scheme independent) *cusp anomalous dimension*, and the attentive reader can already see that (2.13) captures the right behavior. We will see this in detail in section 4 below; but before we do, it is worthwhile to describe how the other seven-point seeds have been evaluated analytically.

3 Feynman parameterization and direct integration

Following the strategy described in [71], it is straightforward to Feynman-parameterize and regulate each of the contributions (2.12). For each of the double-pentagon integrals, this will result in a rational, five-dimensional parametric integral representation of the form[3]

$$I_i \coloneqq \int_0^\infty \big[d^3\vec{\alpha}\big]\, d^2\vec{\beta}\;\; \mathcal{I}_i\big(\vec{\alpha}, \vec{\beta}; \{z_1, \ldots, z_7\}, \delta\big) \tag{3.1}$$

[3]We hope the reader will forgive our abuse of notation in using '$\mathcal{I}_i$' to denote both the loop-momentum-space and Feynman-parametric integrands.

JHEP02(2020)095

In the integral above, $\big[d^3\vec{\alpha}\big]\coloneqq d^4\vec{\alpha}\,\delta\big(\alpha_j-1\big)$ (for any j) represents a projective, 3-dimensional volume-form; while the β integrations are not taken to be projective. This distinction is largely irrelevant due to the Cheng-Wu theorem [75]; but it reflects the way in which the parametric representations were derived via [71], and we find it useful to keep this information. In the supplementary material, we provide a parametric representation of each of the seven-point integrals in (2.12).

3.1 (Cluster) coordinate charts for heptagon integrals

In (2.2) we have given the formula for $\Omega\big[(a,b),(c,d)\big]$ in terms of momentum twistors $z_a \in \mathbb{P}^3$ for $a = 1,\ldots,n$ that parameterize the kinematic space of n massless particles. As described in detail in [65] a momentum-twistor parameterization is preferred over one expressed in terms of dual-momentum x-coordinates, as twistor space immediately provides us with an integrand that is rational in terms of an independent set of conformal variables.

It turns out that the default cluster coordinates on $G_+(4,n)$ of the MATHEMATICA package `positroids` [76] provide a very convenient chart for our present purposes. For a more detailed discussion of these coordinates we again refer the reader to [65]. For seven points, we can think of these coordinates as parameterizing seven momentum twistors $Z =: (z_1 \cdots z_7)$ according to

$$Z(\{e_a^i\}) \coloneqq \begin{pmatrix} 1 & 1+e_6^3+e_7^3 & e_6^3+(1+e_6^2)e_7^3 & e_6^2 e_7^3 & 0 & 0 & 0 \\ 0 & 1 & 1+e_6^2+e_7^2 & e_6^2+(1+e_6^1)e_7^2 & e_6^1 e_7^2 & 0 & 0 \\ 0 & 0 & 1 & 1+e_6^1+e_7^1 & e_6^1+e_7^1 & e_7^1 & 0 \\ 0 & 0 & 0 & 1 & 1 & 1 & 1 \end{pmatrix}; \tag{3.2}$$

or, if viewed as coordinates (maps from $G_+(4,7) \mapsto \mathbb{R}^6$), the parameters $\{e_a^i\}$ correspond to the conformal cross-ratios

$$\begin{aligned} e_6^1 &\coloneqq \frac{\langle 1234\rangle\langle 1256\rangle}{\langle 1236\rangle\langle 1245\rangle}, & e_6^2 &\coloneqq \frac{\langle 1235\rangle\langle 1456\rangle}{\langle 1256\rangle\langle 1345\rangle}, & e_6^3 &\coloneqq \frac{\langle 1245\rangle\langle 3456\rangle}{\langle 1456\rangle\langle 2345\rangle}, \\ e_7^1 &\coloneqq \frac{\langle 1234\rangle\langle 1235\rangle\langle 1267\rangle}{\langle 1236\rangle\langle 1237\rangle\langle 1245\rangle}, & e_7^2 &\coloneqq \frac{\langle 1236\rangle\langle 1245\rangle\langle 1567\rangle}{\langle 1256\rangle\langle 1267\rangle\langle 1345\rangle}, & e_7^3 &\coloneqq \frac{\langle 1256\rangle\langle 1345\rangle\langle 4567\rangle}{\langle 1456\rangle\langle 1567\rangle\langle 2345\rangle}. \end{aligned} \tag{3.3}$$

3.2 Divide and conquer: parametric integration via various pathways

The seed integrands expressed in this way can be integrated in terms of hyperlogarithms [77–79] (e.g. using `HyperInt` [63, 64]) if there exists an order of the integration variables in which the integrand is linearly reducible. Naïvely, however, this turns out not to be the case for any of the integrals at hand: all require some minor 'tricks' of integration analogous to those discussed in, for example, [65, 66, 71, 78, 80].

Among the integration techniques required are those that allow us to extract the leading terms in the limit of $\delta \to 0^+$ (for the integrals which require regularization). We were able to effectively use the methods discussed in [71]; we refer the reader to appendix B.1 and the ancillary files of that work for a more thorough explanation and illustrative examples.

Of the two infrared finite integral seeds, only $\mathcal{I}_5$ required mild cleverness to integrate directly. For this integral, a strategy which started along similar lines to that described in [66] worked quite well. Specifically, starting from the Feynman-parametric integrand

JHEP02(2020)095

representation of the form (3.1) (provided in the supplementary material), we found that the integrals over α_2, β_1, and β_2 could each be performed rationally — i.e. without introducing any algebraic dependence on the remaining integration variables in the arguments of the hyperlogarithms or their prefactors.

The (projective) two-fold parametric representation of $\mathcal{I}_5$ obtained in this way suffers from a mild problem all-too familiar in these examples: integration in any one of the remaining variables would result in some terms with a square root depending (quadratically) on the final integration variable. Such an obstruction is easy to overcome by changing variables (Euler substitution) as described in e.g. [78, 80]. But a better pathway to integration turns out to exist: the individual terms of the two-fold parametric representation of $\mathcal{I}_5$ can be divided into groups which separately avoid this issue with respect to integration in α_4 or α_1. This results in a final expression with fewer 'spurious' algebraic symbol letters — to be discussed in the next section.

3.3 Refining the results of integration (removing spurious letters)

Following the strategies discussed above, it was fairly easy to obtain hyperlogarithmic (regulated, if necessary) expressions for integrals $\{I_1, \ldots, I_4\}$; but integration of $\mathcal{I}_5$ required some cleverness, resulting in a representation of I_5 that is considerably more complicated in two key aspects: first, the representation we obtained for I_5 was not manifestly *pure* in the sense of [23, 81] — namely, it was expressed as a sum of hyperlogarithms with non-constant (algebraic) coefficients; and second, it was expressed in terms of hyperlogarithms with many (suspected to be 'spurious') algebraic branch points. Let us discuss each of these complications in turn.

The first complication, regarding the non-manifest 'purity' of I_5 turns out to be straightforward to deal with. First, we should clarify why we expected I_5 to be pure despite its representation. Although the conformal regulator is known to spoil an integrand's purity (see the discussion in [71]), we strongly expect the logarithm of the amplitude (the cyclic sum of all seeds) to be pure; as $\{I_1, \ldots, I_4\}$ were individually pure, it would require considerable magic for impurities of I_5 to cancel amongst themselves in the cyclic sum.

Setting aside our expectations about I_5's purity, it turns out to be fairly easy to test whether or not any non-manifestly pure sum of hyperlogarithms is in fact pure. Suppose that some non-manifestly pure sum of hyperlogarithms $I(\{e_a^i\})$ depending on parameters $\{e_a^i\}$ is in fact pure; then we should be able to re-express it in terms of some *basis* of hyperlogarithms $\{G_\beta\}$:

$$I(\{e_a^i\}) \coloneqq \sum_\alpha R_\alpha(\{e_a^i\}) G_\alpha(\{e_a^i\}) \Rightarrow \sum_\beta c_\beta G_\beta\big(\{e_a^i\}\big) \ , \tag{3.4}$$

where R_α are rational(/algebraic)-function prefactors, c_β are constants, and G_α, G_β multiple polylogarithms. In order for (3.4) to be true, there would need to be some relations among the functions G_α. Crucially, any such relations would necessarily be linear and have *constant* coefficients — as all relations between multiple polylogarithms are expected to preserve transcendental weight and not involve any rational functions of their arguments.

JHEP02(2020)095

Now suppose we were to Taylor-expand each coefficient R_α in (3.4) around some point $\widehat{e}_a^i$ where all the R_α's are non-singular. Then we would have

$$\sum_\alpha \left[\sum_{j=0}^{\infty} R_\alpha^{(j)} \left(e_a^i - \widehat{e}_a^i\right)^j\right] G_\alpha(\{e_a^i\}) = \sum_\beta c_\beta G_\beta\big(\{e_a^i\}\big) \ . \tag{3.5}$$

Since all purported relations among the $\{G_\alpha\}$ are linear, this requires that the identity (3.5) holds for each term in the Taylor series separately. In particular, it must hold at leading order. Moreover, as each $R_\alpha^{(0)}$ is just some constant, this term in the left-hand side of (3.5) is itself pure.

The above discussion shows that *when an integral is in fact pure*, any representation like that on the l.h.s. of (3.4) can be replaced by series-expanding each coefficient to leading order around any non-singular point, resulting in a manifestly pure representation. To test whether or not an integral is in fact pure, we can simply evaluate both ends of this algorithm numerically and check that they agree. For I_5 we have checked in this way that it is in fact pure, and have provided a manifestly pure representation (obtained in this way) in the supplementary material.

The second complication about the representation of I_5 obtained in the manner described above (namely, divide and conquer) is that this method has a tendency to introduce 'spurious' branch points among terms (which cancel between the divided pieces). When these spurious branch points are not rational in the variables $\{e_a^i\}$, we know of no general strategy to canonically eliminate them (as we would by choosing a fibration basis, for example, had they been rational). Removing a dependence on spurious square roots from polylogarithmic expressions is in general a difficult problem, and one we will not attempt to solve here.

Although we have not found a representation for I_5 free of spurious square-root branch points, we are able to confirm that all non-rational branch points are indeed spurious. To do this, we first compute the symbol [37, 82] of I_5, resulting in an alphabet of 85 letters, 22 of which involve square roots. These algebraic letters appear in pairs of the form $\rho \pm \sqrt{\sigma}$, which can be multiplied to generate root-free letters, leaving us with only 11 algebraic letters to analyze.

These 11 spurious letters are not all independent. Unlike for symbols involving only rational letters, merely factoring square-root letters is not enough to trivialize all identities due to the absence of a unique factorization domain (for further discussion, see [66]). Here we do not need to make use of the more mathematically sophisticated methods [66]. Instead, we simply observe that products of pairs of our remaining eleven letters can yield letters that appear elsewhere in the symbol. By taking into account all such pairings, we find six relations between the 11 letters, and imposing these results in a manifestly rational symbol. This rationalized symbol for I_5 can now be viewed as canonical, and consists of 47 letters (functions of momentum twistor cross-ratios).

From the symbol of I_5, it would be possible to *reconstruct* a rational, hyperlogarithmic representation — using essentially the same techniques by which the two-loop heptagon remainder function was first obtained in [70] from its symbol, which in turn was first

JHEP02(2020)095

computed in [67] (see also [68, 69]). We choose not to pursue this for I_5 because functional *reconstruction* is not our goal here. Rather, we are interested in how far we may push *direct* integration of local integrals. One can easily check that the representation we give for I_5 — despite its spurious letters — perfectly matches Monte Carlo integration.

4 The two-loop heptagon remainder function

We are now ready to describe the results of our analysis — to discover the form of the (all-orders) relationship between the logarithm of the MHV amplitude and the so-called 'BDS' remainder function [20] in the conformal regularization scheme. Both for the sake of comparison and in order to introduce some useful notation, let us first pause to review the form of this relationship in the so-called 'Higgs' regularization scheme described in [83, 84].

4.1 Exempli gratia: Higgs-regulated (logarithms of) MHV amplitudes

At leading order in the coupling $a \coloneqq g^2 N_c/(8\pi^2)$, the MHV amplitude (divided by the tree) and its logarithm are identical (in any regularization scheme 'reg.'):

$$\log\big(A_{n,\text{reg.}}\big) \coloneqq \sum_{\ell=1}^{\infty} a^\ell \log\big(A_{n,\text{reg.}}\big)^{(\ell)} = a A^{(1)}_{n,\text{reg.}} + a^2 \left[A^{(2)}_{n,\text{reg.}} - \frac{1}{2}\big(A^{(1)}_{n,\text{reg.}}\big)^2\right] + \mathcal{O}(a^3)\,. \tag{4.1}$$

(Recall our convention that calligraphic symbols such as $\mathcal{A}$ denote *integrands* while italic symbols such as A denote *integrals*.) As such, it is useful to first review the form of the one-loop amplitude in the relevant regularization scheme.

For the Higgs regulator described in [83, 84], one loop MHV amplitudes take the form

$$A^{(1)}_{n,\text{Higgs}} =: -\frac{1}{4}\left[\sum_{a=1}^{n} \log^2\left(\frac{m_a^2}{(a|a+2)}\right)\right] + F^{(1)}_{n,\text{Higgs}} + \mathcal{O}(m_a^2)\,, \tag{4.2}$$

where $F^{(1)}_{n,\text{Higgs}}$ is the so-called[4] 'finite part' of the one-loop amplitude in this scheme, and where we have added an index 'a'$\in[n]$ to distinguish between the various internal masses m_a^2 (which are typically taken to be the same). Notice that we are using dual-momentum notation where $(a|b) \coloneqq (x_a - x_b)^2 \coloneqq (p_a + \ldots + p_{b-1})^2$. It is worthwhile to consider the direction along the Higgs branch where these masses scale according to

$$m_a^2 \mapsto \delta \frac{(a-1|a+1)(a|a+2)}{(a-1|a+2)} \tag{4.3}$$

under which

$$A^{(1)}_{n,\text{Higgs}} \underset{(4.3)}{\longmapsto} -\frac{1}{4}\left[n\log^2(\delta) + \log(\delta)\log(w_1\cdots w_n) + \sum_{a=1}^{n}\log^2\left(\frac{(a|a+2)}{(a|a+3)}\right)\right] + F^{(1)}_{n,\text{Higgs}} + \mathcal{O}(\delta)\,, \tag{4.4}$$

where the cross-ratio w_a is given by

$$w_a \coloneqq \frac{(a|a+2)(a+3|a+5)}{(a|a+3)(a+2|a+5)}\,. \tag{4.5}$$

[4] It is so-called despite the fact that the leading term of (4.2) includes parts finite as $m_a^2 \to 0$.

JHEP02(2020)095

This is extremely similar to the form of the one loop amplitude in the conformal regularization scheme. Before we get to that, however, let us first recall a few more facts about the Higgs regulator and the form that the logarithm (4.1) takes in this scheme.

In [84], the all-order form of the logarithm (4.1) was represented according to the BDS ansatz [85] as

$$\begin{aligned}\log(A_{n,\text{Higgs}}) &\rightleftharpoons -\frac{\gamma_c(a)}{16}A^{(1)}_{n,\text{Higgs}}+\frac{\widetilde{\mathcal{G}}_0(a)}{2}\sum_{a=1}^{n}\log\left(\frac{m_a^2}{(a|a+2)}\right)+n\widetilde{f}(a)+\widetilde{C}(a)+R_n(a)\\ &\xrightarrow[(4.3)]{}-\frac{\gamma_c(a)}{16}A^{(1)}_{n,\text{Higgs}}+\frac{\widetilde{\mathcal{G}}_0(a)}{2}\left[n\log(\delta)+\frac{1}{2}\log(w_1\cdots w_n)\right]\\ &\quad+n\widetilde{f}(a)+\widetilde{C}(a)+R_n(a)\end{aligned} \tag{4.6}$$

where $\gamma_c(a)$ is the (scheme-independent) *cusp anomalous dimension* [86, 87]

$$\gamma_c(a) \rightleftharpoons \sum_{\ell=1}^{\infty} a^\ell \gamma_c^{(\ell)} = 4a-4\zeta_2 a^2+22\zeta_4 a^3-\left(24\zeta_2^3+4\zeta_3^2+2\zeta_2\zeta_4+\zeta_6\right)a^4+\mathcal{O}(a^5)\,, \tag{4.7}$$

$\widetilde{\mathcal{G}}_0(a), \widetilde{f}(a), \widetilde{C}(a)$ are scheme-dependent functions of the coupling and $R_n(a)$ is the *remainder function* [20]. In the Higgs regularization scheme these functions were determined by [83, 84] to be

$$\widetilde{\mathcal{G}}_0(a) = -\zeta_3 a^2+\mathcal{O}(a^3), \quad \widetilde{f}(a) = \frac{1}{2}\zeta_4 a^2+\mathcal{O}(a^3), \quad \widetilde{C}(a) = -\frac{5}{4}\zeta_4 a^2+\mathcal{O}(a^3)\,, \tag{4.8}$$

at two-loop order. (See e.g. [88, 89] for more recent, higher-order results.)

With this comparison in mind, let us now return to the main purpose of this work and describe the form the logarithm takes for the conformal regularization scheme.

4.2 Conformally-regulated (logarithms of) MHV amplitudes

Using the conformal regulator described in [24] the divergences of one-loop amplitudes take a form strikingly similar to that of (4.4). In this scheme, the n-point MHV amplitude is given by[5]

$$A^{(1)}_{n,\text{DCI}} \coloneqq -\frac{1}{2}\left[n\log^2(\delta)+\log(\delta)\log(w_1\cdots w_n)+n\zeta_2+F^{(1)}_{n,\text{DCI}}\right]+\mathcal{O}(\delta)\,, \tag{4.9}$$

where the cross-ratios w_a are the same as those defined in (4.5) and

$$F^{(1)}_{n,\text{DCI}} = \left[\sum_{b=4}^{\lfloor n/2\rfloor+1}\text{Li}_2(1-u_{1,b})+\frac{1}{2}\log(u_{1,b})\log(v_{1,b})\right]+\underset{\text{(delete duplicates)}}{\text{cyclic}_n} \tag{4.10}$$

where the cross-ratios $u_{a,b}$ and $v_{a,b}$ are given by

$$u_{a,b} \coloneqq \frac{(a+1|b)(b+1|a)}{(a+1|b+1)(b|a)}\,, \quad v_{a,b} \coloneqq \frac{(a-1|a+1)(a|a+2)(b-1|b+1)(b|b+2)}{(a-1|a+2)(a|b)(b-1|b+2)(b+1|a+1)}\,. \tag{4.11}$$

[5] We have added a factor of 1/2 relative to [24] to match conventions for the coupling a.

JHEP02(2020)095

In terms of the regulated amplitude at one loop (4.9), it was suggested in [71] that the conformally regulated logarithm (4.1) would take the form

$$\begin{aligned}\log(A_{n,\text{DCI}}) =: &-\frac{\gamma_c(a)}{8}A^{(1)}_{n,\text{DCI}}+\frac{B_\delta(a)}{2}\left[n\log(\delta)+n+\frac{1}{2}\log(w_1\cdots w_n)\right]\\ &+n\widehat{f}(a)+\widehat{C}(a)+R_n(a)\end{aligned} \tag{4.12}$$

where $B_\delta(a) \coloneqq 3\zeta_3 a^2+\mathcal{O}(a^3)$ is the so-called *virtual* anomalous dimension [90, 91], and the functions $\widehat{f}(a)$ and $\widehat{C}(a)$ are analogous to $\widetilde{f}(a)$ and $\widetilde{C}(a)$ — which could not be disentangled from each other knowing the logarithm for six particles alone.

In [71], the six-point logarithm was shown to take the form[6]

$$\log(A_{6,\text{DCI}})^{(2)} = -\zeta_2 A^{(1)}_{6,\text{DCI}}+\frac{3}{2}\zeta_3\left[6\log(\delta)+6+\frac{1}{2}\log(w_1\cdots w_6)\right]-\frac{49\,\pi^4}{720}+R^{(2)}_6\,; \tag{4.13}$$

and for five particles, starting from representation given in (2.6), it is not hard to show that[7]

$$\log(A_{5,\text{DCI}})^{(2)} = -\zeta_2 A^{(1)}_{5,\text{DCI}}+\frac{3}{2}\zeta_3\Big[5\log(\delta)+5+\log(w_1\cdots w_5)\Big]-\frac{17\,\pi^4}{288}+R^{(2)}_5\,. \tag{4.14}$$

Combining this with our new result for seven particles,

$$\log(A_{7,\text{DCI}})^{(2)} = -\zeta_2 A^{(1)}_{7,\text{DCI}}+\frac{3}{2}\zeta_3\left[7\log(\delta)+7+\frac{1}{2}\log(w_1\cdots w_7)\right]-\frac{37\,\pi^4}{480}+R^{(2)}_7\,, \tag{4.15}$$

allows us to conclude that, in the conformal regularization scheme,

$$\widehat{f}(a) = -\frac{1}{2}\Big(\zeta_4+\frac{1}{4}\zeta_2^2\Big)a^2+\mathcal{O}(a^3)\,,\quad \widehat{C}(a) = -\frac{1}{2}\zeta_2^2 a^2+\mathcal{O}(a^3)\,. \tag{4.16}$$

Although already mentioned in the introduction, it is worth pausing to note that, in the representation of the logarithm (4.15), the remainder function $R^{(2)}_7$ numerically matches the analytic expression derived in [70] from the symbol (from [67]).

4.3 Symbology and the alphabets of individual integral contributions

Interestingly, almost all of the seed integrals we compute contain symbol letters that are not present in the full remainder function. The integral I_1 is the only exception: it in fact requires only the ordinary hexagon-function symbol alphabet. However, each of the other integrals involve spurious (but rational) symbol letters. Specifically, each of $\{I_2, I_3, I_4\}$ involve two 'new' letters relative to the remainder function, and I_5 involves nine additional letters (after all the simplifications described in subsection 3.3). In cyclic sum, however, all these additional letters cancel — and quite nontrivially. For example, among these contributions only the *entire* cyclic sum of $\big(I_2+I_3+I_4+I_5\big)$ is free of 'spurious' letters relative to the 42 letter alphabet expected for heptagon functions [70] (see also [47–49, 92–96]). For the sake of those readers interested in more details, we have provided the additional symbol letters that arise for the cyclic seed integrals in the supplementary material attached to this work.

[6] Nota bene: for six particles, $(w_1\cdots w_6) = (w_1 w_2 w_3)^2$, with w_i more familiarly denoted $\{u, v, w\}$.

[7] Nota bene: for five particles, $w_a = 1$ for all a and $R^{(\ell)}_5 = 0$ for all ℓ.

JHEP02(2020)095

5 Discussion

In this paper, we have computed the logarithm of the two-loop MHV amplitude at seven points in planar, maximally supersymmetric ($\mathcal{N}=4$) super Yang-Mills theory directly from a local integrand representation. In doing so, we have shown that carefully preserving the symmetries of the theory makes computations dramatically easier, even when using otherwise traditional methods. However, these methods are still not optimal: as we have seen, issues of linear reducibility make some of the integrals we find unsuitable for expansion into a fibration basis (by known methods), resulting in a sometimes unnecessarily-spurious symbol alphabet. It would be interesting to see whether other common methods (for example, differential equations, or integration-by-parts reduction) can simplify this calculation further.

In using the dual conformal regularization of [71], we have checked the conjectures for the scheme dependence of the logarithm of the amplitude put forward in that paper. It would be interesting to check these conjectures at higher loop orders, and more generally, to understand in detail the relationship between the conformal regulator and the Higgs regulator.

Acknowledgments

This work was supported in part by the Danish National Research Foundation (DNRF91), an ERC Starting Grant (No. 757978), a grant from the Villum Fonden (No. 15369), and the European Union's Horizon 2020 research and innovation program under grant agreement No. 793151 (MvH). We are grateful for the hospitality of the Harvard Center for Mathematical Sciences and Applications, and JLB and MvH would like to thank the Aspen Center for Physics, which is supported by National Science Foundation grant PHY-1607611.

References

[1] N. Arkani-Hamed, F. Cachazo, C. Cheung and J. Kaplan, *A Duality For The S Matrix*, *JHEP* **03** (2010) 020 [arXiv:0907.5418] [INSPIRE].

[2] N. Arkani-Hamed, J. Bourjaily, F. Cachazo and J. Trnka, *Unification of Residues and Grassmannian Dualities*, *JHEP* **01** (2011) 049 [arXiv:0912.4912] [INSPIRE].

[3] N. Arkani-Hamed, J.L. Bourjaily, F. Cachazo, A.B. Goncharov, A. Postnikov and J. Trnka, *Grassmannian Geometry of Scattering Amplitudes*, Cambridge University Press (2016) [arXiv:1212.5605] [INSPIRE].

[4] N. Arkani-Hamed and J. Trnka, *The Amplituhedron*, *JHEP* **10** (2014) 030 [arXiv:1312.2007] [INSPIRE].

[5] C. Frye, H. Hannesdottir, N. Paul, M.D. Schwartz and K. Yan, *Infrared Finiteness and Forward Scattering*, *Phys. Rev.* **D 99** (2019) 056015 [arXiv:1810.10022] [INSPIRE].

[6] H. Hannesdottir and M.D. Schwartz, *A Finite S-matrix*, arXiv:1906.03271 [INSPIRE].

JHEP02(2020)095

[7] N. Arkani-Hamed, J.L. Bourjaily, F. Cachazo, S. Caron-Huot and J. Trnka, *The All-Loop Integrand For Scattering Amplitudes in Planar $\mathcal{N} = 4$ SYM*, *JHEP* **01** (2011) 041 [arXiv:1008.2958] [INSPIRE].

[8] P. Benincasa, *On-shell diagrammatics and the perturbative structure of planar gauge theories*, arXiv:1510.03642 [INSPIRE].

[9] J.L. Bourjaily, A. DiRe, A. Shaikh, M. Spradlin and A. Volovich, *The Soft-Collinear Bootstrap: $\mathcal{N} = 4$ Yang-Mills Amplitudes at Six and Seven Loops*, *JHEP* **03** (2012) 032 [arXiv:1112.6432] [INSPIRE].

[10] J.L. Bourjaily, P. Heslop and V.-V. Tran, *Perturbation Theory at Eight Loops: Novel Structures and the Breakdown of Manifest Conformality in $\mathcal{N} = 4$ Supersymmetric Yang-Mills Theory*, *Phys. Rev. Lett.* **116** (2016) 191602 [arXiv:1512.07912] [INSPIRE].

[11] J.L. Bourjaily, P. Heslop and V.-V. Tran, *Amplitudes and Correlators to Ten Loops Using Simple, Graphical Bootstraps*, *JHEP* **11** (2016) 125 [arXiv:1609.00007] [INSPIRE].

[12] C. Baadsgaard, N.E.J. Bjerrum-Bohr, J.L. Bourjaily, S. Caron-Huot, P.H. Damgaard and B. Feng, *New Representations of the Perturbative S-matrix*, *Phys. Rev. Lett.* **116** (2016) 061601 [arXiv:1509.02169] [INSPIRE].

[13] Z. Bern, L.J. Dixon, D.C. Dunbar and D.A. Kosower, *One loop n-point gauge theory amplitudes, unitarity and collinear limits*, *Nucl. Phys.* **B 425** (1994) 217 [hep-ph/9403226] [INSPIRE].

[14] Z. Bern, L.J. Dixon, D.C. Dunbar and D.A. Kosower, *Fusing gauge theory tree amplitudes into loop amplitudes*, *Nucl. Phys.* **B 435** (1995) 59 [hep-ph/9409265] [INSPIRE].

[15] R. Britto, F. Cachazo and B. Feng, *Generalized unitarity and one-loop amplitudes in $\mathcal{N} = 4$ super-Yang-Mills*, *Nucl. Phys.* **B 725** (2005) 275 [hep-th/0412103] [INSPIRE].

[16] Z. Bern, M. Czakon, L.J. Dixon, D.A. Kosower and V.A. Smirnov, *The Four-Loop Planar Amplitude and Cusp Anomalous Dimension in Maximally Supersymmetric Yang-Mills Theory*, *Phys. Rev.* **D 75** (2007) 085010 [hep-th/0610248] [INSPIRE].

[17] C. Anastasiou, R. Britto, B. Feng, Z. Kunszt and P. Mastrolia, *D-dimensional unitarity cut method*, *Phys. Lett.* **B 645** (2007) 213 [hep-ph/0609191] [INSPIRE].

[18] Z. Bern, J.J.M. Carrasco, H. Johansson and D.A. Kosower, *Maximally supersymmetric planar Yang-Mills amplitudes at five loops*, *Phys. Rev.* **D 76** (2007) 125020 [arXiv:0705.1864] [INSPIRE].

[19] F. Cachazo, *Sharpening The Leading Singularity*, arXiv:0803.1988 [INSPIRE].

[20] Z. Bern et al., *The Two-Loop Six-Gluon MHV Amplitude in Maximally Supersymmetric Yang-Mills Theory*, *Phys. Rev.* **D 78** (2008) 045007 [arXiv:0803.1465] [INSPIRE].

[21] C.F. Berger et al., *An Automated Implementation of On-Shell Methods for One-Loop Amplitudes*, *Phys. Rev.* **D 78** (2008) 036003 [arXiv:0803.4180] [INSPIRE].

[22] S. Abreu, F. Febres Cordero, H. Ita, M. Jaquier, B. Page and M. Zeng, *Two-Loop Four-Gluon Amplitudes from Numerical Unitarity*, *Phys. Rev. Lett.* **119** (2017) 142001 [arXiv:1703.05273] [INSPIRE].

[23] N. Arkani-Hamed, J.L. Bourjaily, F. Cachazo and J. Trnka, *Local Integrals for Planar Scattering Amplitudes*, *JHEP* **06** (2012) 125 [arXiv:1012.6032] [INSPIRE].

JHEP02(2020)095

[24] J.L. Bourjaily, S. Caron-Huot and J. Trnka, *Dual-Conformal Regularization of Infrared Loop Divergences and the Chiral Box Expansion*, *JHEP* **01** (2015) 001 [arXiv:1303.4734] [INSPIRE].

[25] J.L. Bourjaily and J. Trnka, *Local Integrand Representations of All Two-Loop Amplitudes in Planar SYM*, *JHEP* **08** (2015) 119 [arXiv:1505.05886] [INSPIRE].

[26] J.L. Bourjaily, E. Herrmann and J. Trnka, *Prescriptive Unitarity*, *JHEP* **06** (2017) 059 [arXiv:1704.05460] [INSPIRE].

[27] J.L. Bourjaily, E. Herrmann and J. Trnka, *Maximally supersymmetric amplitudes at infinite loop momentum*, *Phys. Rev.* **D 99** (2019) 066006 [arXiv:1812.11185] [INSPIRE].

[28] J.L. Bourjaily, E. Herrmann, C. Langer, A.J. McLeod and J. Trnka, *Prescriptive Unitarity for Non-Planar Six-Particle Amplitudes at Two Loops*, *JHEP* **12** (2019) 073 [arXiv:1909.09131] [INSPIRE].

[29] J.L. Bourjaily, E. Herrmann, C. Langer, A.J. McLeod and J. Trnka, *All-Multiplicity Non-Planar MHV Amplitudes in SYM at Two Loops*, arXiv:1911.09106 [INSPIRE].

[30] S. Mandelstam, *Light Cone Superspace and the Ultraviolet Finiteness of the $\mathcal{N} = 4$ Model*, *Nucl. Phys.* **B 213** (1983) 149 [INSPIRE].

[31] L. Brink, O. Lindgren and B.E.W. Nilsson, *The Ultraviolet Finiteness of the $\mathcal{N} = 4$ Yang-Mills Theory*, *Phys. Lett.* **123B** (1983) 323 [INSPIRE].

[32] P.S. Howe, K.S. Stelle and P.K. Townsend, *Miraculous Ultraviolet Cancellations in Supersymmetry Made Manifest*, *Nucl. Phys.* **B 236** (1984) 125 [INSPIRE].

[33] J.M. Drummond, J. Henn, V.A. Smirnov and E. Sokatchev, *Magic identities for conformal four-point integrals*, *JHEP* **01** (2007) 064 [hep-th/0607160] [INSPIRE].

[34] L.F. Alday and J.M. Maldacena, *Gluon scattering amplitudes at strong coupling*, *JHEP* **06** (2007) 064 [arXiv:0705.0303] [INSPIRE].

[35] J.M. Drummond, J. Henn, G.P. Korchemsky and E. Sokatchev, *Dual superconformal symmetry of scattering amplitudes in $N = 4$ super-Yang-Mills theory*, *Nucl. Phys.* **B 828** (2010) 317 [arXiv:0807.1095] [INSPIRE].

[36] V. Del Duca, C. Duhr and V.A. Smirnov, *The Two-Loop Hexagon Wilson Loop in $\mathcal{N} = 4$ SYM*, *JHEP* **05** (2010) 084 [arXiv:1003.1702] [INSPIRE].

[37] A.B. Goncharov, M. Spradlin, C. Vergu and A. Volovich, *Classical Polylogarithms for Amplitudes and Wilson Loops*, *Phys. Rev. Lett.* **105** (2010) 151605 [arXiv:1006.5703] [INSPIRE].

[38] L.J. Dixon, J.M. Drummond and J.M. Henn, *Analytic result for the two-loop six-point NMHV amplitude in $N = 4$ super Yang-Mills theory*, *JHEP* **01** (2012) 024 [arXiv:1111.1704] [INSPIRE].

[39] L.J. Dixon, J.M. Drummond, M. von Hippel and J. Pennington, *Hexagon functions and the three-loop remainder function*, *JHEP* **12** (2013) 049 [arXiv:1308.2276] [INSPIRE].

[40] L.J. Dixon, J.M. Drummond, C. Duhr and J. Pennington, *The four-loop remainder function and multi-Regge behavior at NNLLA in planar $\mathcal{N} = 4$ super-Yang-Mills theory*, *JHEP* **06** (2014) 116 [arXiv:1402.3300] [INSPIRE].

[41] L.J. Dixon and M. von Hippel, *Bootstrapping an NMHV amplitude through three loops*, *JHEP* **10** (2014) 065 [arXiv:1408.1505] [INSPIRE].

JHEP02(2020)095

[42] L.J. Dixon, M. von Hippel and A.J. McLeod, *The four-loop six-gluon NMHV ratio function*, *JHEP* **01** (2016) 053 [arXiv:1509.08127] [INSPIRE].

[43] L.J. Dixon, M. von Hippel, A.J. McLeod and J. Trnka, *Multi-loop positivity of the planar $\mathcal{N} = 4$ SYM six-point amplitude*, *JHEP* **02** (2017) 112 [arXiv:1611.08325] [INSPIRE].

[44] S. Caron-Huot, L.J. Dixon, A. McLeod and M. von Hippel, *Bootstrapping a Five-Loop Amplitude Using Steinmann Relations*, *Phys. Rev. Lett.* **117** (2016) 241601 [arXiv:1609.00669] [INSPIRE].

[45] S. Caron-Huot, L.J. Dixon, F. Dulat, M. von Hippel, A.J. McLeod and G. Papathanasiou, *Six-Gluon amplitudes in planar $\mathcal{N} = 4$ super-Yang-Mills theory at six and seven loops*, *JHEP* **08** (2019) 016 [arXiv:1903.10890] [INSPIRE].

[46] S. Caron-Huot, L.J. Dixon, F. Dulat, M. Von Hippel, A.J. McLeod and G. Papathanasiou, *The Cosmic Galois Group and Extended Steinmann Relations for Planar $\mathcal{N} = 4$ SYM Amplitudes*, *JHEP* **09** (2019) 061 [arXiv:1906.07116] [INSPIRE].

[47] J.M. Drummond, G. Papathanasiou and M. Spradlin, *A Symbol of Uniqueness: The Cluster Bootstrap for the 3-Loop MHV Heptagon*, *JHEP* **03** (2015) 072 [arXiv:1412.3763] [INSPIRE].

[48] L.J. Dixon, J. Drummond, T. Harrington, A.J. McLeod, G. Papathanasiou and M. Spradlin, *Heptagons from the Steinmann Cluster Bootstrap*, *JHEP* **02** (2017) 137 [arXiv:1612.08976] [INSPIRE].

[49] J. Drummond, J. Foster, Ö. Gürdoğan and G. Papathanasiou, *Cluster adjacency and the four-loop NMHV heptagon*, *JHEP* **03** (2019) 087 [arXiv:1812.04640] [INSPIRE].

[50] S. Abreu, L.J. Dixon, E. Herrmann, B. Page and M. Zeng, *The two-loop five-point amplitude in $\mathcal{N} = 4$ super-Yang-Mills theory*, *Phys. Rev. Lett.* **122** (2019) 121603 [arXiv:1812.08941] [INSPIRE].

[51] D. Chicherin, T. Gehrmann, J.M. Henn, P. Wasser, Y. Zhang and S. Zoia, *Analytic result for a two-loop five-particle amplitude*, *Phys. Rev. Lett.* **122** (2019) 121602 [arXiv:1812.11057] [INSPIRE].

[52] T. Gehrmann, J.M. Henn and N.A. Lo Presti, *Analytic form of the two-loop planar five-gluon all-plus-helicity amplitude in QCD*, *Phys. Rev. Lett.* **116** (2016) 062001 [*Erratum ibid.* **116** (2016) 189903] [arXiv:1511.05409] [INSPIRE].

[53] S. Badger, C. Brønnum-Hansen, H.B. Hartanto and T. Peraro, *First look at two-loop five-gluon scattering in QCD*, *Phys. Rev. Lett.* **120** (2018) 092001 [arXiv:1712.02229] [INSPIRE].

[54] S. Abreu, F. Febres Cordero, H. Ita, B. Page and M. Zeng, *Planar Two-Loop Five-Gluon Amplitudes from Numerical Unitarity*, *Phys. Rev.* **D 97** (2018) 116014 [arXiv:1712.03946] [INSPIRE].

[55] S. Abreu, F. Febres Cordero, H. Ita, B. Page and V. Sotnikov, *Planar Two-Loop Five-Parton Amplitudes from Numerical Unitarity*, *JHEP* **11** (2018) 116 [arXiv:1809.09067] [INSPIRE].

[56] S. Badger, C. Brønnum-Hansen, H.B. Hartanto and T. Peraro, *Analytic helicity amplitudes for two-loop five-gluon scattering: the single-minus case*, *JHEP* **01** (2019) 186 [arXiv:1811.11699] [INSPIRE].

[57] S. Abreu, J. Dormans, F. Febres Cordero, H. Ita and B. Page, *Analytic Form of Planar Two-Loop Five-Gluon Scattering Amplitudes in QCD*, *Phys. Rev. Lett.* **122** (2019) 082002 [arXiv:1812.04586] [INSPIRE].

JHEP02(2020)095

[58] D. Chicherin, T. Gehrmann, J.M. Henn, P. Wasser, Y. Zhang and S. Zoia, *All Master Integrals for Three-Jet Production at Next-to-Next-to-Leading Order*, *Phys. Rev. Lett.* **123** (2019) 041603 [arXiv:1812.11160] [INSPIRE].

[59] D. Chicherin, T. Gehrmann, J.M. Henn, P. Wasser, Y. Zhang and S. Zoia, *The two-loop five-particle amplitude in $\mathcal{N} = 8$ supergravity*, *JHEP* **03** (2019) 115 [arXiv:1901.05932] [INSPIRE].

[60] S. Abreu, L.J. Dixon, E. Herrmann, B. Page and M. Zeng, *The two-loop five-point amplitude in $\mathcal{N} = 8$ supergravity*, *JHEP* **03** (2019) 123 [arXiv:1901.08563] [INSPIRE].

[61] J.L. Bourjaily, A.J. McLeod, M. von Hippel and M. Wilhelm, *Bounded Collection of Feynman Integral Calabi-Yau Geometries*, *Phys. Rev. Lett.* **122** (2019) 031601 [arXiv:1810.07689] [INSPIRE].

[62] F.C.S. Brown, *On the periods of some Feynman integrals*, arXiv:0910.0114 [INSPIRE].

[63] E. Panzer, *Algorithms for the symbolic integration of hyperlogarithms with applications to Feynman integrals*, *Comput. Phys. Commun.* **188** (2015) 148 [arXiv:1403.3385] [INSPIRE].

[64] `HyperInt`, https://bitbucket.org/PanzerErik/hyperint/wiki/Home.

[65] J.L. Bourjaily, A.J. McLeod, M. von Hippel and M. Wilhelm, *Rationalizing Loop Integration*, *JHEP* **08** (2018) 184 [arXiv:1805.10281] [INSPIRE].

[66] J.L. Bourjaily, A.J. McLeod, C. Vergu, M. Volk, M. Von Hippel and M. Wilhelm, *Rooting Out Letters: Octagonal Symbol Alphabets and Algebraic Number Theory*, *JHEP* **02** (2020) 025 [arXiv:1910.14224] [INSPIRE].

[67] S. Caron-Huot, *Superconformal symmetry and two-loop amplitudes in planar $\mathcal{N} = 4$ super Yang-Mills*, *JHEP* **12** (2011) 066 [arXiv:1105.5606] [INSPIRE].

[68] S. Caron-Huot, *Notes on the scattering amplitude/Wilson loop duality*, *JHEP* **07** (2011) 058 [arXiv:1010.1167] [INSPIRE].

[69] S. Caron-Huot and S. He, *Jumpstarting the All-Loop S-matrix of Planar $\mathcal{N} = 4$ Super Yang-Mills*, *JHEP* **07** (2012) 174 [arXiv:1112.1060] [INSPIRE].

[70] J. Golden and M. Spradlin, *An analytic result for the two-loop seven-point MHV amplitude in $\mathcal{N} = 4$ SYM*, *JHEP* **08** (2014) 154 [arXiv:1406.2055] [INSPIRE].

[71] J.L. Bourjaily, F. Dulat and E. Panzer, *Manifestly Dual-Conformal Loop Integration*, *Nucl. Phys.* **B 942** (2019) 251 [arXiv:1901.02887] [INSPIRE].

[72] C. Vergu, *Higher point MHV amplitudes in $\mathcal{N} = 4$ Supersymmetric Yang-Mills Theory*, *Phys. Rev.* **D 79** (2009) 125005 [arXiv:0903.3526] [INSPIRE].

[73] C. Vergu, *The Two-loop MHV amplitudes in $\mathcal{N} = 4$ supersymmetric Yang-Mills theory*, *Phys. Rev.* **D 80** (2009) 125025 [arXiv:0908.2394] [INSPIRE].

[74] A. Hodges, *Eliminating spurious poles from gauge-theoretic amplitudes*, *JHEP* **05** (2013) 135 [arXiv:0905.1473] [INSPIRE].

[75] H. Cheng and T.T. Wu, *Expanding Protons: Scattering at High Energies*, Cambridge, U.S.A., MIT-PR. (1987) [INSPIRE].

[76] J.L. Bourjaily, *Positroids, Plabic Graphs and Scattering Amplitudes in Mathematica*, arXiv:1212.6974 [INSPIRE].

[77] C. Anastasiou, C. Duhr, F. Dulat and B. Mistlberger, *Soft triple-real radiation for Higgs production at N_3LO*, *JHEP* **07** (2013) 003 [arXiv:1302.4379] [INSPIRE].

JHEP02(2020)095

[78] E. Panzer, *On hyperlogarithms and Feynman integrals with divergences and many scales*, *JHEP* **03** (2014) 071 [arXiv:1401.4361] [INSPIRE].

[79] F. Brown, *The Massless higher-loop two-point function*, *Commun. Math. Phys.* **287** (2009) 925 [arXiv:0804.1660] [INSPIRE].

[80] M. Besier, D. Van Straten and S. Weinzierl, *Rationalizing roots: an algorithmic approach*, *Commun. Num. Theor. Phys.* **13** (2019) 253 [arXiv:1809.10983] [INSPIRE].

[81] N. Arkani-Hamed, J.L. Bourjaily, F. Cachazo and J. Trnka, *Singularity Structure of Maximally Supersymmetric Scattering Amplitudes*, *Phys. Rev. Lett.* **113** (2014) 261603 [arXiv:1410.0354] [INSPIRE].

[82] C. Duhr, H. Gangl and J.R. Rhodes, *From polygons and symbols to polylogarithmic functions*, *JHEP* **10** (2012) 075 [arXiv:1110.0458] [INSPIRE].

[83] L.F. Alday, J.M. Henn, J. Plefka and T. Schuster, *Scattering into the fifth dimension of $\mathcal{N} = 4$ super Yang-Mills*, *JHEP* **01** (2010) 077 [arXiv:0908.0684] [INSPIRE].

[84] J.M. Henn, S.G. Naculich, H.J. Schnitzer and M. Spradlin, *More loops and legs in Higgs-regulated $\mathcal{N} = 4$ SYM amplitudes*, *JHEP* **08** (2010) 002 [arXiv:1004.5381] [INSPIRE].

[85] Z. Bern, L.J. Dixon and V.A. Smirnov, *Iteration of planar amplitudes in maximally supersymmetric Yang-Mills theory at three loops and beyond*, *Phys. Rev.* **D 72** (2005) 085001 [hep-th/0505205] [INSPIRE].

[86] G.F. Sterman and M.E. Tejeda-Yeomans, *Multiloop amplitudes and resummation*, *Phys. Lett.* **B 552** (2003) 48 [hep-ph/0210130] [INSPIRE].

[87] N. Beisert, B. Eden and M. Staudacher, *Transcendentality and Crossing*, *J. Stat. Mech.* **0701** (2007) P01021 [hep-th/0610251] [INSPIRE].

[88] D. Correa, J. Henn, J. Maldacena and A. Sever, *The cusp anomalous dimension at three loops and beyond*, *JHEP* **05** (2012) 098 [arXiv:1203.1019] [INSPIRE].

[89] J.M. Henn and T. Huber, *The four-loop cusp anomalous dimension in $\mathcal{N} = 4$ super Yang-Mills and analytic integration techniques for Wilson line integrals*, *JHEP* **09** (2013) 147 [arXiv:1304.6418] [INSPIRE].

[90] A.V. Kotikov, L.N. Lipatov, A.I. Onishchenko and V.N. Velizhanin, *Three loop universal anomalous dimension of the Wilson operators in $\mathcal{N} = 4$ SUSY Yang-Mills model*, *Phys. Lett.* **B 595** (2004) 521 [*Erratum ibid.* **B 632** (2006) 754] [hep-th/0404092] [INSPIRE].

[91] L. Freyhult, A. Rej and M. Staudacher, *A Generalized Scaling Function for AdS/CFT*, *J. Stat. Mech.* **0807** (2008) P07015 [arXiv:0712.2743] [INSPIRE].

[92] J. Golden and M. Spradlin, *The differential of all two-loop MHV amplitudes in $\mathcal{N} = 4$ Yang-Mills theory*, *JHEP* **09** (2013) 111 [arXiv:1306.1833] [INSPIRE].

[93] J. Golden, A.B. Goncharov, M. Spradlin, C. Vergu and A. Volovich, *Motivic Amplitudes and Cluster Coordinates*, *JHEP* **01** (2014) 091 [arXiv:1305.1617] [INSPIRE].

[94] J. Golden and M. Spradlin, *A Cluster Bootstrap for Two-Loop MHV Amplitudes*, *JHEP* **02** (2015) 002 [arXiv:1411.3289] [INSPIRE].

[95] J. Golden, M.F. Paulos, M. Spradlin and A. Volovich, *Cluster Polylogarithms for Scattering Amplitudes*, *J. Phys.* **A 47** (2014) 474005 [arXiv:1401.6446] [INSPIRE].

[96] J. Drummond, J. Foster and Ö. Gürdoğan, *Cluster Adjacency Properties of Scattering Amplitudes in $\mathcal{N} = 4$ Supersymmetric Yang-Mills Theory*, *Phys. Rev. Lett.* **120** (2018) 161601 [arXiv:1710.10953] [INSPIRE].

JHEP02(2020)095

Physics Letters B 806 (2020) 135520

Contents lists available at ScienceDirect

Physics Letters B

www.elsevier.com/locate/physletb

Wilson lines in AdS/dCFT

Sara Bonansea, Khalil Idiab, Charlotte Kristjansen *, Matthias Volk

Niels Bohr Institute, Copenhagen University, Blegdamsvej 17, 2100 Copenhagen Ø, Denmark

ARTICLE INFO

Article history:
Received 22 April 2020
Received in revised form 20 May 2020
Accepted 21 May 2020
Available online 26 May 2020
Editor: N. Lambert

Keywords:
AdS/CFT correspondence
Defect CFT
D7 probe branes
Wilson lines

ABSTRACT

We consider the expectation value of Wilson lines in two defect versions of $\mathcal{N}=4$ SYM, both with supersymmetry completely broken, where one is described in terms of an integrable boundary state, the other one not. For both cases, imposing a certain double scaling limit, we find agreement to two leading orders between the expectation values calculated from respectively the field theory- and the string theory side of the AdS/dCFT correspondence.

1. Introduction

Understanding the interplay between supersymmetry and integrability in the AdS/CFT correspondence might hold the key to understanding the deeper reason for the integrability of the systems involved. Motivated by such considerations we will be pursuing a line of investigation which involves breaking the supersymmetry of $\mathcal{N}=4$ SYM in a simple way by introducing a domain wall, a co-dimension one defect, separating two regions of space-time with different vacuum expectation values (vevs) for the scalar fields. To be more precise, we will assign vevs in a particular way to either five or to all six of the scalar fields on one side of the defect while keeping the vevs zero on the other side. In the language of integrability the defect can be described as a matrix product state or a boundary state [1] and for one of the set-ups the boundary state has been found to be integrable [2], for the other one not [3], where the notion of integrability of a matrix product state was introduced in [4]. The string theory duals of these defect CFTs are two D3-D7 probe brane systems, named I and II, with non-vanishing background gauge field flux and instanton number respectively, cf. Table 1.

Our aim will be to calculate a non-local observable, the expectation value of a Wilson line, running parallel to the defect, both from the gauge theory- and the string theory perspective. A double scaling limit, invented for a related supersymmetric D3-D5 probe brane set-up in [5] and generalized to the two relevant D3-D7 probe brane set-ups in [6] will allow us to compare the results of the two calculations. We remark that the gauge theory calculations are rather involved due to the non-vanishing vevs which mix color as well as flavor components of the $\mathcal{N}=4$ SYM fields but the perturbative framework necessary for the calculations has been set up in [7] and [8].

Earlier studies of Wilson loops in domain wall versions of $\mathcal{N}=4$ SYM have been limited to the supersymmetric and integrable case of the D3-D5 probe brane system. For the D3-D5 case using the perturbative set-up developed in [9,10], agreement between gauge and string theory calculations in the double scaling limit was found for a single Wilson line in [11,12], a pair of Wilson lines in [13] and a circular Wilson loop in [14], see also [15].

With the present work we are able to address AdS/dCFT while eliminating both supersymmetry and (boundary) integrability. Interestingly, we find agreement between the gauge- and string theory result to two leading orders in the double scaling parameter for both of the non-supersymmetric set-ups and in particular both for the integrable and the non-integrable case.

Our paper is organized in the following simple way. In section 2 we compute the expectation value of the Wilson line for our two defect set-ups from the gauge theory perspective whereafter in section 3 we perform the computations from the string theory perspective. Finally, section 4 contains our conclusion and outlook.

* Corresponding author.
E-mail addresses: sara.bonansea@nbi.ku.dk (S. Bonansea), khalil903@gmail.com (K. Idiab), kristjan@nbi.dk (C. Kristjansen), mvolk@nbi.ku.dk (M. Volk).

https://doi.org/10.1016/j.physletb.2020.135520

Table 1
The probe brane configurations dual to the dCFT versions of $\mathcal{N}=4$ SYM theory considered in this paper and their corresponding double scaling (d.s.) parameters. The discussion of the integrability properties of the associated boundary states can be found in [2,3].

D3-D7 set-up	I	II
Supersymmetry	None	None
Brane geometry	$AdS_4\times S^2\times S^2$	$AdS_4\times S^4$
Flux/Instanton no.	k_1, k_2	$\frac{(n+1)(n+2)(n+3)}{6}$
D.s. parameter	$\frac{\lambda}{\pi^2(k_1^2+k_2^2)}$	$\frac{\lambda}{\pi^2 n^2}$
Boundary state	Non-integrable	Integrable

2. The gauge theory computation

2.1. The defect theories

The gauge theory duals of the two probe-brane setups of Table 1 are obtained as defect versions of $\mathcal{N}=4$ SYM in which (some of) the scalar fields are assigned a non-vanishing vacuum expectation value for $x_3>0$. The vevs are solutions to the classical equations of motion,

$$\nabla^2\phi_i^{\rm cl}(x)=\Big[\phi_j^{\rm cl}(x),\Big[\phi_j^{\rm cl}(x),\phi_i^{\rm cl}(x)\Big]\Big]. \tag{1}$$

For system I (cf. Table 1), the relevant solution to (1) with $SO(3)\times SO(3)$ symmetry is [6]

$$\begin{aligned}\varphi_i^{\rm cl}(x)&=-\frac{1}{x_3}\begin{pmatrix} t_i^{(k_1)}\otimes\mathbb{1}^{(k_2)} & 0\\ 0 & 0^{(N-k_1k_2)}\end{pmatrix},\ i=1,2,3,\\ \varphi_i^{\rm cl}(x)&=-\frac{1}{x_3}\begin{pmatrix} \mathbb{1}^{(k_1)}\otimes t_{i-3}^{(k_2)} & 0\\ 0 & 0^{(N-k_1k_2)}\end{pmatrix},\ i=4,5,6.\end{aligned} \tag{2}$$

Here the matrices $t_i^{(k)}$ constitute the k-dimensional irreducible representation of the Lie algebra $\mathfrak{su}(2)$ and we denote by $0^{(N-k_1k_2)}$ the zero matrix of dimension $(N-k_1k_2)\times(N-k_1k_2)$. We will only need the explicit form of the diagonal matrix $t_3^{(k)}$; its eigenvalues are

$$d_{j,k}=\frac{1}{2}(k-2j+1),\qquad j=1,\dots,k. \tag{3}$$

For system II (cf. Table 1), the solution to (1) with SO(5) symmetry is given by [16,17]

$$\phi_i^{\rm cl}(x)=\frac{1}{\sqrt{2}x_3}\begin{pmatrix} G_{i6} & 0\\ 0 & 0^{(N-d_G)}\end{pmatrix},\ i=1,\dots 5;\quad \phi_6^{\rm cl}(x)=0. \tag{4}$$

The matrices G_{i6} together with $G_{ij}=-i\big[G_{i6},G_{j6}\big]$ form the $d_G=\frac{1}{6}(n+1)(n+2)(n+3)$ dimensional irreducible representation of the Lie algebra of SO(6). For the purpose of this paper, we only need an explicit representation of G_{56}. This matrix can be taken to be diagonal [18]; its eigenvalues $\eta_{j,n}$ and the corresponding multiplicity $\mu_{j,n}$ are

$$\eta_{j,n}=-\frac{n}{2}+j-1,\quad \mu_{j,n}=j(n-j+2),\quad j=1,\dots,n+1. \tag{5}$$

Note that for both systems, the classical solutions (2) and (4) pertain to $x_3>0$. The vevs for all other fields in $\mathcal{N}=4$ SYM are zero in this region. For $x_3<0$, the vevs for all fields vanish.

We shall calculate the expectation value of the Wilson line perturbatively in λ at tree level and at one-loop, and in both cases consider only the leading order in respectively n and k_1,k_2 as $n,k_1,k_2\to\infty$. This is motivated by a string theory analysis [5,6], which introduced the following double scaling limits (d.s.l.)

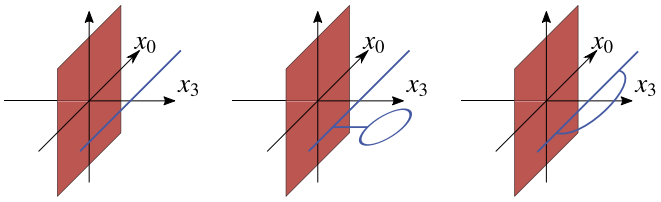

Fig. 1. Diagrams at tree level and one-loop order. (Figure adapted from [12].)

$$\text{I}:\quad \lambda\to\infty,\quad k_1,\,k_2\to\infty,\quad \frac{\lambda}{\pi^2\left(k_1^2+k_2^2\right)}\ \text{finite}, \tag{6}$$

$$\text{II}:\quad \lambda\to\infty,\quad n\to\infty,\quad \frac{\lambda}{\pi^2 n^2}\ \text{finite}, \tag{7}$$

where in case I also the ratio k_2/k_1 has to be taken finite. Imposing the d.s.l. on the string theory side allows one to expand string theory observables, such the expectation value of the Wilson line, as a power series in the double scaling parameter and formally compare the result to a perturbative gauge theory computation.

2.2. Wilson line setup

As in [11,12], we consider a straight Wilson line parallel to the defect parametrized by $\gamma(t)=(t,0,0,z)$, i.e. a straight line at a fixed distance z from the defect. For this case, the Wilson line is given by

$$\operatorname{tr}U(\alpha,\beta)=\operatorname{tr}\left[\operatorname{Pexp}\int_\alpha^\beta dt\,\mathcal{A}(t)\right], \tag{8}$$

with

$$\mathcal{A}^{(\rm I)}(t)=iA_0(t)-\varphi_3(t)\sin(\chi)-\varphi_6(t)\cos(\chi), \tag{9}$$

$$\mathcal{A}^{(\rm II)}(t)=iA_0(t)-\phi_5(t)\sin(\chi)-\phi_6(t)\cos(\chi), \tag{10}$$

for the two set-ups respectively. We will be interested in the gauge invariant infinite line given by

$$W=\lim_{T\to\infty}\operatorname{tr}U\left(-\frac{T}{2},\frac{T}{2}\right), \tag{11}$$

which is related to the physical particle-interface potential. In order to compute the expectation value of the Wilson line, we expand the fields around the classical solution as

$$\mathcal{A}(t)=\mathcal{A}^{\rm cl}(t)+\tilde{\mathcal{A}}(t). \tag{12}$$

To one-loop order, the path-ordered exponential becomes

$$\begin{aligned}U(\alpha,\beta)&=U^{\rm cl}(\alpha,\beta)+\int_\alpha^\beta dt\,U^{\rm cl}(\alpha,t)\tilde{\mathcal{A}}(t)U^{\rm cl}(t,\beta)\\ &+\int_\alpha^\beta dt\int_t^\beta dt'\,U^{\rm cl}(\alpha,t)\tilde{\mathcal{A}}(t)U^{\rm cl}(t,t')\tilde{\mathcal{A}}(t')U^{\rm cl}(t',\beta)+\mathcal{O}\left(\tilde{\mathcal{A}}^3\right),\end{aligned} \tag{13}$$

where $U^{\rm cl}(\alpha,\beta)$ is the path-ordered exponential for the classical solution. The corresponding diagrams are illustrated in Fig. 1 and the following subsections will be devoted to dealing with each of the terms.

2.3. Tree-level

The tree level contribution is given by the first term of (13) and is now evaluated in the large T limit,

$$\langle W\rangle_{\text{tree}} = \lim_{T\to\infty} \text{tr}\, \text{Pexp} \int_{-T/2}^{T/2} dt\, \mathcal{A}^{\text{cl}}(t) \tag{14}$$

$$= \lim_{T\to\infty} \left[\exp\left(T\mathcal{A}^{\text{cl}}\right)\right]_{i,i}, \tag{15}$$

since the classical solutions are time-independent. In the large T limit, only the largest eigenvalue of $\mathcal{A}^{\text{cl}}$ contributes, which gives

$$\langle W\rangle_{\text{tree}} = \mu \exp\left(T\frac{\eta}{z}\right), \tag{16}$$

where η/z is the largest eigenvalue of $\mathcal{A}^{\text{cl}}$ and μ its multiplicity. For the first setup, we have $2\eta^{(\text{I})} = (k_1-1)\sin(\chi)+(k_2-1)\cos(\chi)$ and $\mu^{(\text{I})}=1$. For the second setup, we have $\eta^{(\text{II})} = \frac{n}{\sqrt{8}}\sin(\chi)$ and $\mu^{(\text{II})} = (n+1)$. We may thus write the tree level results as

$$\langle W\rangle^{(\text{I})}_{\text{tree}} = \mu^{(\text{I})} \exp\left(T\frac{(k_1-1)\sin(\chi)+(k_2-1)\cos(\chi)}{2z}\right), \tag{17}$$

$$\langle W\rangle^{(\text{II})}_{\text{tree}} = \mu^{(\text{II})} \exp\left(T\frac{n\sin(\chi)}{\sqrt{8}z}\right). \tag{18}$$

They lead to the following particle-interface potentials

$$V^{(\text{I})}_{\text{tree}} = -\lim_{T\to\infty}\frac{1}{T}\log\langle W\rangle^{(\text{I})}_{\text{tree}} = -\frac{k_1\sin(\chi)+k_2\cos(\chi)}{2z}, \tag{19}$$

$$V^{(\text{II})}_{\text{tree}} = -\lim_{T\to\infty}\frac{1}{T}\log\langle W\rangle^{(\text{II})}_{\text{tree}} = -\frac{n\sin(\chi)}{\sqrt{8}z}, \tag{20}$$

having taken the limit $k_1, k_2 \to \infty$ in (19) as implied by the double scaling limit.

2.4. Lollipop

The focus of this subsection is the second term of (13), which involves the one-loop expectation value of $\tilde{\mathcal{A}}$ and which we call the lollipop contribution.

$$\langle W\rangle_{\text{lol}} = \lim_{T\to\infty}\left\langle \text{tr}\int_{-T/2}^{T/2} dt\, U^{\text{cl}}\left(-\tfrac{T}{2},t\right)\tilde{\mathcal{A}}(t)U^{\text{cl}}\left(t,\tfrac{T}{2}\right)\right\rangle \tag{21}$$

$$= \lim_{T\to\infty} T\left[e^{T\mathcal{A}^{\text{cl}}}\right]_{ij}\left\langle\left[\tilde{\mathcal{A}}\right]_{ji}\right\rangle_{1-\text{loop}}, \tag{22}$$

where we have used the fact that the expectation values are time independent. The one-loop corrections to the vevs for the two set-ups are given in [7,8]. Notice that as opposed to what was the case for the supersymmetric D3-D5 probe brane set-up [9,10], these corrections are non-vanishing. In the large T limit, only the components multiplying the fastest growing exponential will contribute, which in both conventions is also the first component

$$\langle W\rangle_{\text{lol}} = T\mu e^{T\eta/x_3}\left\langle\left[\tilde{\mathcal{A}}\right]_{11}\right\rangle_{1-\text{loop}}. \tag{23}$$

Given the one-loop correction to the vevs, we find

$$\langle W\rangle^{(\text{I})}_{\text{lol}} = -\mu^{(\text{I})}\frac{\lambda T e^{T\eta^{(\text{I})}/z}}{4\pi^2 z\left(k_1^2+k_2^2\right)^3}\left(k_1k_2^4\sin(\chi)+k_2k_1^4\cos(\chi)\right), \tag{24}$$

$$\langle W\rangle^{(\text{II})}_{\text{lol}} = -\mu^{(\text{II})}\frac{\lambda T e^{T\eta^{(\text{II})}/z}}{4\sqrt{8}\pi^2 zn}\sin(\chi), \tag{25}$$

having again taken the double scaling limit in (24).

2.5. Tadpole

As in [12], the third term of (13) is the least straight forward term to compute. However, the same techniques can be employed with just minor complications. The tadpole term is

$$U_{\text{tad}}(\alpha,\beta) = \int_\alpha^\beta dt\int_t^\beta dt' U^{\text{cl}}(\alpha,t)\tilde{\mathcal{A}}(t)U^{\text{cl}}(t,t')\tilde{\mathcal{A}}(t')U^{\text{cl}}(t',\beta). \tag{26}$$

The fields are all $N\times N$ matrices; decomposing them into the block structure given by the classical solutions (2) and (4) and writing out the matrix indices explicitly, we find

$$\langle \text{tr}\, U_{\text{tad}}(\alpha,\beta)\rangle = \int_\alpha^\beta dt\int_t^\beta dt'\langle[\tilde{\mathcal{A}}(t)]_{\mu\rho}[\tilde{\mathcal{A}}(t')]_{\rho\mu}\rangle \tag{27}$$

$$+\int_\alpha^\beta dt\int_t^\beta dt'\left[e^{(t'-t)\mathcal{A}^{\text{cl}}}\right]_{cd}\langle[\tilde{\mathcal{A}}(t')]_{d\mu}[\tilde{\mathcal{A}}(t)]_{\mu c}\rangle$$

$$+\int_\alpha^\beta dt\int_t^\beta dt'\left[e^{(\beta-\alpha+t-t')\mathcal{A}^{\text{cl}}}\right]_{eb}\langle[\tilde{\mathcal{A}}(t)]_{b\rho}[\tilde{\mathcal{A}}(t')]_{\rho e}\rangle$$

$$+\int_\alpha^\beta dt\int_t^\beta dt'\left[e^{(\beta-\alpha+t-t')\mathcal{A}^{\text{cl}}}\right]_{eb}\left[e^{(t'-t)\mathcal{A}^{\text{cl}}}\right]_{cd}\langle[\tilde{\mathcal{A}}(t)]_{bc}[\tilde{\mathcal{A}}(t')]_{de}\rangle.$$

For the first setup the latin indices run from 1 to k_1k_2 and the greek indices run from k_1k_2+1 to N, while for the second setup the latin indices run from 1 to d_G and the greek indices run from d_G+1 to N. In the large N limit only the second and third term contribute, given the propagators found in [7,8]. We thus have

$$\langle W\rangle_{\text{tad}} = \lim_{T\to\infty}\int_{-T/2}^{T/2} d\alpha\int_\alpha^{T/2} d\beta \left[e^{-(\alpha-\beta)\mathcal{A}^{\text{cl}}}+e^{(\alpha-\beta+T)\mathcal{A}^{\text{cl}}}\right]_{cd}\langle[\tilde{\mathcal{A}}]_{d\mu}(\alpha)[\tilde{\mathcal{A}}]_{\mu c}(\beta)\rangle. \tag{28}$$

For both setups the propagator has the form

$$\langle[\tilde{\mathcal{A}}]_{d\mu}(\alpha)[\tilde{\mathcal{A}}]_{\mu c}(\beta)\rangle = \sum_n D^n_{dc}\sum_i \lambda_{i,n}K^{m^2_{i,n}}(\alpha,\beta), \tag{29}$$

where D is a diagonal prefactor and $K^{m^2_{i,n}}$ is the spacetime part of the propagator given in (31) below. This means we have to perform integrals of the form

$$\langle W\rangle_{\text{tad}} = \lim_{T\to\infty}\int_{-T/2}^{T/2} d\alpha\int_\alpha^{T/2} d\beta \left[e^{-(\alpha-\beta)\mathcal{A}^{\text{cl}}}+e^{(\alpha-\beta+T)\mathcal{A}^{\text{cl}}}\right]_{cd}\sum_n D^n_{dc}\sum_i \lambda_{i,n}K^{m^2_{i,n}}(\alpha,\beta). \tag{30}$$

Following [12], we proceed by using the following representation of the propagator

$$K^{m_i^2}(\alpha,\beta)=\frac{g_{YM}^2 z}{4\pi^2}\int_0^\infty dr\, r\frac{\sin(\delta r)}{\delta}I_{\nu_i}(rz)K_{\nu_i}(rz), \tag{31}$$

$$\nu_i=\sqrt{m_i^2+\frac{1}{4}}, \tag{32}$$

having defined $\delta=\beta-\alpha$. We may now plug this back into (30), change variables $\alpha=\delta-T/2$, rescale $r\to r/z$ and do the β integration,

$$\langle W\rangle_{\text{tad}}=\frac{g_{YM}^2}{4\pi^2 z}\lim_{T\to\infty}\int_0^T d\delta\,(T-\delta)\int_0^\infty dr\, r\frac{\sin(\delta r/z)}{\delta}$$
$$\left[e^{\delta\mathcal{A}^{\text{cl}}}+e^{(T-\delta)\mathcal{A}^{\text{cl}}}\right]_{cd}\sum_n D_{dc}^n\sum_i\lambda_{i,n}I_{\nu_{i,n}}(r)K_{\nu_{i,n}}(r). \tag{33}$$

Integration by parts is performed on the r integration in order to cancel the $\frac{1}{\delta}$ such that the integration over δ can be carried out,

$$\langle W\rangle_{\text{tad}}=\frac{g_{YM}^2}{4\pi^2 z^2}\lim_{T\to\infty}\int_0^T d\delta\,(T-\delta)\left[e^{\delta\mathcal{A}^{\text{cl}}}+e^{(T-\delta)\mathcal{A}^{\text{cl}}}\right]_{cd} \tag{34}$$
$$\sum_n D_{dc}^n\int_0^\infty dr\cos(\delta r/z)\int_r^\infty dr' r'\sum_i\lambda_{i,n}I_{\nu_{i,n}}(r')K_{\nu_{i,n}}(r').$$

Using this antiderivative makes the boundary term vanish at infinity, whilst the $\sin(\delta r/z)$ part makes the boundary term vanish at $r=0$. We can now perform the δ integration. In the large T limit we have

$$\int_0^T d\delta\,(T-\delta)\left[e^{\delta\mathcal{A}^{\text{cl}}}+e^{(T-\delta)\mathcal{A}^{\text{cl}}}\right]_{cd}\sum_n D_{dc}^n\cos(\delta r/z)$$
$$=\mu e^{\eta T/z}Tz\frac{\eta}{\eta^2+r^2}\sum_n D_{1,1}^n, \tag{35}$$

since for our two setups the largest eigenvalue of D coincides with the largest eigenvalue of $\mathcal{A}^{\text{cl}}$. We use this result in (34),

$$\langle W\rangle_{\text{tad}}=\mu\frac{g_{YM}^2 T e^{\eta T/z}}{4\pi^2 z}\int_0^\infty dr\,\frac{\eta}{\eta^2+r^2}$$
$$\sum_n D_{1,1}^n\int_r^\infty dr'\,r'\sum_i\lambda_{i,n}I_{\nu_{i,n}}(r')K_{\nu_{i,n}}(r'). \tag{36}$$

It is here and in the following implicit that T is large. We will now perform the r' integration in the double scaling limit and for convenience we define the functions A and F

$$A(r)=\int_r^\infty dr'\,r'\sum_i\lambda_{i,n}I_{\nu_{i,n}}(r')K_{\nu_{i,n}}(r') \tag{37}$$
$$=-\sum_i\lambda_{i,n}F_{\nu_{i,n}}(r)+\lim_{r'\to\infty}\sum_i\lambda_{i,n}F_{\nu_{i,n}}(r'), \tag{38}$$

$$F_{\nu_{i,n}}(r)=\int_0^r dr'\,r'I_{\nu_{i,n}}(r')K_{\nu_{i,n}}(r'). \tag{39}$$

By doing the integral from (39), we find $F_{\nu_{i,n}}(r)$ to be

$$F_{\nu_{i,n}}(r)=-\frac{\nu_{i,n}}{2}+\frac{1}{2}\left(r^2+\nu_{i,n}^2\right)I_{\nu_{i,n}}(r)K_{\nu_{i,n}}(r)$$
$$-\frac{1}{2}r^2 I'_{\nu_{i,n}}(r)K'_{\nu_{i,n}}(r). \tag{40}$$

In the double scaling limit, we can use the behavior of the Bessel functions at large order and finite argument [19] and find

$$F_{\nu_{i,n}}(r)=-\frac{\nu_{i,n}}{2}+\frac{1}{2}\left(\nu_{i,n}^2+r^2\right)^{1/2}+\mathcal{O}\left(\nu_{i,n}^{-1}\right). \tag{41}$$

We note that $A(r)$ is divergent unless $\sum_i\lambda_{i,n}=0$, but by properly bunching our terms we can show that this condition is satisfied. Then, we find

$$A(r)=-\frac{1}{2}\sum_i\lambda_{i,n}\left(\nu_{i,n}^2+r^2\right)^{1/2}+\mathcal{O}\left(\nu_{i,n}^{-1}\right). \tag{42}$$

This result is now plugged into (36) and the final integral is performed

$$\langle W\rangle_{\text{tad}}=-\mu\frac{g_{YM}^2 T e^{\eta T/z}}{8\pi^2 z}\sum_n D_{1,1}^n \tag{43}$$
$$\int_0^\infty dr\,\frac{\eta}{\eta^2+r^2}\sum_i\lambda_{i,n}\left(\nu_{i,n}^2+r^2\right)^{1/2}$$
$$=-\mu\frac{g_{YM}^2 T e^{\eta T/z}}{16\pi^2 z}\sum_n D_{1,1}^n \tag{44}$$
$$\sum_i\lambda_{i,n}\left[2\sqrt{\nu_{i,n}^2-\eta^2}\,\text{arccot}\left(\frac{\eta}{\sqrt{\nu_{i,n}^2-\eta^2}}\right)-\eta\log\left(\nu_{i,n}^2\right)\right],$$

where we again used $\sum_i\lambda_{i,n}=0$ in the second line. We finally plug in the coefficients for the first setup, let $k_2=k_1\tan(\psi_0)$ and take the large k_1 limit

$$\langle W\rangle_{\text{tad}}^{(\text{I})}=-\mu^{(\text{I})}\frac{\lambda T e^{T\eta^{(\text{I})}/z}\cos(\psi_0)}{4\pi^2 z k_1}\frac{\sin^2(\psi_0+\chi)}{4\cos^3(\psi_0+\chi)}$$
$$(2\psi_0+2\chi-\pi+\sin(2\psi_0+2\chi)), \tag{45}$$

notice that $\cos(\psi_0)/k_1=\left(k_1^2+k_2^2\right)^{-1/2}$ gives the combination appearing in the double scaling parameter. For the second setup in the large n limit we find

$$\langle W\rangle_{\text{tad}}^{(\text{II})}=-\mu^{(\text{II})}\frac{\lambda T e^{T\eta^{(\text{II})}/z}}{4\sqrt{8}\pi^2 z n}\frac{\sin^2(\chi)}{\cos^3(\chi)}(2\chi-\pi+\sin(2\chi)). \tag{46}$$

2.6. Full one-loop result

The full one-loop result is now obtained by adding the lollipop and the tadpole contribution

$$\langle W\rangle_{1-\text{loop}}^{(\text{I})}$$
$$=-\mu^{(\text{I})}\frac{\lambda T e^{T\eta^{(\text{I})}/z}\cos(\psi_0)}{4\pi^2 z k_1}\Big[\cos(\chi)\sin(\psi_0)\cos^4(\psi_0)$$
$$+\sin(\chi)\cos(\psi_0)\sin^4(\psi_0)$$
$$+\frac{\sin^2(\psi_0+\chi)}{4\cos^3(\psi_0+\chi)}(2\psi_0+2\chi-\pi+\sin(2\psi_0+2\chi))\Big], \tag{47}$$

having also expressed the lollipop contribution in terms of $\psi_0=\arctan(k_2/k_1)$. For the second setup we have

$$\langle W\rangle^{(\mathrm{II})}_{1-\mathrm{loop}} = -\mu^{(\mathrm{II})}\frac{\lambda T}{4\pi^2 n}\frac{e^{T\eta^{(\mathrm{II})}/z}}{\sqrt{8}z}\left[\sin(\chi)-\frac{\sin^2(\chi)}{\cos^3(\chi)}\left(\pi-2\chi-\sin(2\chi)\right)\right]. \quad (48)$$

The corresponding correction to the particle-interface potential is given by

$$V_{1-\mathrm{loop}} = -\lim_{T\to\infty}\frac{1}{T}\frac{\langle W\rangle_{1-\mathrm{loop}}}{\langle W\rangle_{\mathrm{tree}}}, \quad (49)$$

which concludes the gauge theory computation with the following results:

$$V^{(\mathrm{I})}_{1-\mathrm{loop}} = V^{(\mathrm{I})}_{\mathrm{tree}}\left(\frac{\lambda}{\pi^2\left(k_1^2+k_2^2\right)}\right)\frac{1}{2\sin(\psi_0+\chi)}\left[\frac{\sin^2(\psi_0+\chi)}{4\cos^3(\psi_0+\chi)}\left(\pi-2\psi_0-2\chi-\sin(2\psi_0+2\chi)\right)\right.$$
$$\left.-\cos(\chi)\sin(\psi_0)\cos^4(\psi_0)-\sin(\chi)\cos(\psi_0)\sin^4(\psi_0)\right], \quad (50)$$

$$V^{(\mathrm{II})}_{1-\mathrm{loop}} = V^{(\mathrm{II})}_{\mathrm{tree}}\left(\frac{\lambda}{\pi^2 n^2}\right)\left[\frac{\sin(\chi)}{4\cos^3(\chi)}\left(\pi-2\chi-\sin(2\chi)\right)-\frac{1}{4}\right]. \quad (51)$$

3. The string theory computation

As summarized in Table 1, we will be considering two different D3-D7 probe brane systems. In the set-up I, the probe D7-brane has geometry $AdS_4\times S^2\times S^2$, and a background gauge field has k_1 and k_2 units of magnetic flux through the two S^2 spheres, respectively. In the second configuration, II, the D3-branes are intersected by a (small) number of D7-branes with $AdS_4\times S^4$ geometry and a background gauge field supports a non-vanishing instanton number on S^4. In both cases, the system is stabilized for sufficiently large values of the flux or instanton number.[1]

It is convenient to write the $AdS_5\times S^5$ metric in two different ways, depending on the D7 geometry that we are considering

$$\mathrm{d}s^2_{\mathrm{I}} = \frac{1}{y^2}\left(\mathrm{d}y^2+\mathrm{d}x_\mu\mathrm{d}x_\nu\eta^{\mu\nu}\right)+\mathrm{d}\psi^2+\cos^2\psi\,\mathrm{d}\Omega^2_{S^2}+\sin^2\psi\,\mathrm{d}\tilde{\Omega}^2_{S^2}, \quad (52)$$

$$\mathrm{d}s^2_{\mathrm{II}} = \frac{1}{y^2}\left(\mathrm{d}y^2+\mathrm{d}x_\mu\mathrm{d}x_\nu\eta^{\mu\nu}\right)+\mathrm{d}\psi^2+\cos^2\psi\,\mathrm{d}\Omega^2_{S^4}, \quad (53)$$

where $\mathrm{d}\Omega^2_{S^2}$ and $\mathrm{d}\tilde{\Omega}^2_{S^2}$ are the metrics of the two S^2 spheres and $d\Omega^2_{S^4}$ denotes the metric of the S^4 inside the S^5. In both cases $x_\mu=(x_0,x_1,x_2,x_3)$ and the boundary of AdS_5 is located at $y=0$. In the set-up I, the D7-brane has world volume coordinates $(x_0,x_1,x_2,y,\Omega_{S^2},\tilde{\Omega}_{S^2})$, while in the configuration II the D7-branes wrap the four-sphere and extend in the $(x_0,\,x_1,\,x_2,\,y)$ directions. The embedding of the D7 in the target space is given by [16,20,6]

$$\mathrm{I}:\quad y=\frac{x_3}{\Lambda_{\mathrm{I}}},\qquad \Lambda_{\mathrm{I}}=\frac{f_1 f_2}{\sqrt{(f_1^2+4\cos^4\psi)(f_2^2+4\sin^4\psi)-f_1^2 f_2^2}}, \quad (54)$$

where $f_{1,2}=\frac{2\pi k_{1,2}}{\sqrt{\lambda}}$ and the angle ψ has to satisfy

[1] We notice that the perturbative regime for the double scaling parameter, considered in the gauge theory computations, lies within the region of stability of the probe brane systems [7,8].

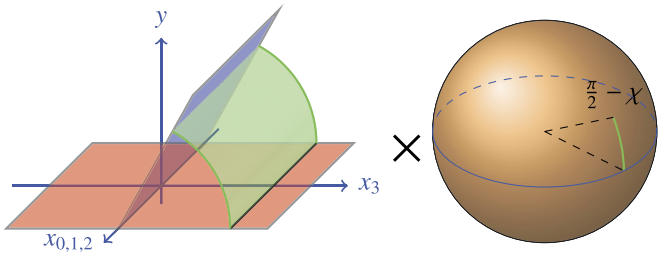

Fig. 2. The minimal surface corresponding to the Wilson line for the set-up II. In the AdS_5 factor, the minimal surface (green) stretches from the Wilson line (black) on the boundary (red) to the D7 brane (blue). In the S^5 factor, it stretches from the S^4 wrapped by the D7-brane (blue) along the perpendicular direction for an angular extent of $\frac{\pi}{2}-\chi$. For the set-up II, the minimal surface in the AdS part of the geometry looks similar whereas in the spherical part it is somewhat different, cf. eqns. (52), (53). (Figure adapted from [12].)

$$(f_1^2+4\cos^4\psi)\tan^2\psi=(f_2^2+4\sin^4\psi), \quad (55)$$

$$\mathrm{II}:\quad y=\frac{x_3}{\Lambda_{\mathrm{II}}},\qquad \psi=0, \quad (56)$$

$$\text{when}\quad n\to\infty:\quad \Lambda_{\mathrm{II}}\sim\frac{\pi n}{\sqrt{2}\sqrt{\lambda}}-\frac{\sqrt{\lambda}}{4\sqrt{2}\pi n}+\mathcal{O}\left(\frac{\lambda^{3/2}}{\pi^3 n^3}\right).$$

In both cases, the D7-brane intersects AdS_5 along an AdS_4 hyperplane, tilted with respect to the boundary $y=0$ at an angle that depends on Λ_{I} or Λ_{II}. In the supergravity limit $\lambda\to\infty$, following the idea of [21–23], the Wilson line expectation value is described by the area of a minimal surface stretching from the boundary of AdS_5 to the D7-brane in the interior. Notice that the minimal surface attaches to the D7-brane along a straight line in its AdS part as well as along an arc in its spherical part, cf. Fig. 2.

We parametrize the worldsheet using coordinates (τ,σ) with $\tau\in[-\frac{T}{2},\frac{T}{2}]$ and $\sigma\in[0,\tilde{\sigma}]$. For the straight Wilson line (parallel to the defect) we make the following ansatz for the embedding of the string [11,13]

$$t=\tau,\qquad y=y(\sigma),\qquad x_3=x_3(\sigma)\quad\text{and}\quad \psi=\psi(\sigma). \quad (57)$$

A new feature in the defect set-up is that the extremal surface has to satisfy two different sets of boundary conditions. At the boundary of AdS_5, which is approached when $\sigma\to 0$, the usual Dirichlet boundary conditions must be imposed

$$y(0)=0,\qquad x_3(0)=z\quad\text{and}\quad \psi(0)=\frac{\pi}{2}-\chi\,. \quad (58)$$

The second set of boundary conditions ensures that the extremal surface intersects the boundary brane at $\tilde{\sigma}$ orthogonally

$$\mathrm{I}:\quad y(\tilde{\sigma})=\frac{x_3(\tilde{\sigma})}{\Lambda_{\mathrm{I}}},\ y'(\tilde{\sigma})+\Lambda_{\mathrm{I}}x_3'(\tilde{\sigma})=0,\ \psi(\tilde{\sigma})=\psi_1, \quad (59)$$

$$\mathrm{II}:\quad y(\tilde{\sigma})=\frac{x_3(\tilde{\sigma})}{\Lambda_{\mathrm{II}}},\ y'(\tilde{\sigma})+\Lambda_{\mathrm{II}}x_3'(\tilde{\sigma})=0,\ \psi(\tilde{\sigma})=0\,, \quad (60)$$

where $\tilde{\sigma}$ is the maximum value of the worldsheet coordinate σ and ψ_1 has to satisfy eq. (55) and $\psi_1\in[0,\pi/2]$. The construction of the solution follows the idea of [11]. The Euclidean Polyakov action in conformal gauge reduces to

$$S=\frac{1}{4\pi\alpha'}\int d\tau d\sigma\,\frac{1}{y^2}\left(1+y'^2+x_3'^2+y^2\psi'^2\right). \quad (61)$$

The Euler-Lagrange equations of motion for the action (61) must be combined with the Virasoro constraint

$$y'^2+x_3'^2+y^2\psi'^2=1. \quad (62)$$

Since the coordinates x_3 and ψ are cyclic variables, cf. (61), their equations of motion immediately translate into two conservation laws

$$x_3'(\sigma) = -cy^2(\sigma) \qquad \text{and} \qquad \psi'(\sigma) = j, \tag{63}$$

where j and c are two integration constants to be determined. The equation of motion for $y(\sigma)$ is given by

$$yy'' - y'^2 + 1 + c^2 y^4 = 0\,. \tag{64}$$

Using the Virasoro constraint we get the following first order differential equation for $y'(\sigma)$

$$y' = \sqrt{1 - j^2 y^2 - c^2 y^4}\,. \tag{65}$$

The solutions to eqs. (63) and (65) are[2]

$$y(\sigma) = \sqrt{\frac{m+1}{j^2}}\,\mathrm{sn}\left(\sqrt{\frac{j^2}{m+1}}\sigma \,\middle|\, m\right), \tag{66}$$

$$x_3(\sigma) = z - \sqrt{-\frac{m+1}{m\,j^2}}\left[\mathbb{E}\left(\mathrm{am}\left(\sqrt{\frac{j^2}{m+1}}\sigma, m\right), m\right) - \sqrt{\frac{j^2}{m+1}}\sigma\right], \tag{67}$$

$$\psi(\sigma) = j\sigma + \frac{\pi}{2} - \chi\,, \tag{68}$$

where to determine the form of the solutions we have used the boundary conditions at $\sigma = 0$. The parameter m is the elliptic modulus and it ranges from 0 to -1. The boundary conditions on $\tilde{\sigma}$ fix the remaining parameters $(\tilde{\sigma},\ j,\ m)$ in terms of the geometrical data $(z,\ \Lambda_{\mathrm{I}}$ or $\Lambda_{\mathrm{II}},\ \chi)$

$$\mathrm{I}: \quad \tilde{\sigma} = \frac{1}{j}\left(\psi_1 + \chi - \frac{\pi}{2}\right), \qquad 0 \le \psi_1 + \chi \le \frac{\pi}{2}, \tag{69}$$

$$\mathrm{II}: \quad \tilde{\sigma} = \frac{1}{j}\left(\chi - \frac{\pi}{2}\right), \qquad 0 \le \chi \le \frac{\pi}{2}, \tag{70}$$

$$j^2 = \left(\frac{\Lambda}{z}\sqrt{m+1}\,\mathrm{sn}\left(\sqrt{\frac{j^2}{m+1}}\tilde{\sigma}\,\middle|\, m\right) + \frac{\sqrt{m+1}}{z\sqrt{-m}}\left[\mathbb{E}\left(\mathrm{am}\left(\sqrt{\frac{j^2}{m+1}}\tilde{\sigma}, m\right), m\right) - \sqrt{\frac{j^2}{m+1}}\tilde{\sigma}\right]\right)^2, \tag{71}$$

$$\Lambda_{\mathrm{I,\,(II)}} = \frac{\mathrm{cn}\left(\sqrt{\frac{j^2}{m+1}}\tilde{\sigma}_{\mathrm{I,\,(II)}}\,\middle|\, m\right)\mathrm{dn}\left(\sqrt{\frac{j^2}{m+1}}\tilde{\sigma}_{\mathrm{I,\,(II)}}\,\middle|\, m\right)}{\sqrt{-m}\,\mathrm{sn}\left(\sqrt{\frac{j^2}{m+1}}\tilde{\sigma}_{\mathrm{I,\,(II)}}\,\middle|\, m\right)^2}. \tag{72}$$

Choosing the convention in which $\tilde{\sigma}$ is positive, for the value of the angles considered in (69) and (70), j has to be negative.

The area of the minimal surface is obtained by evaluating the Polyakov action on the classical solution. As usual, one has to introduce a cut-off ϵ in the y coordinate such that the regularized area is given by an integral in the region $y \ge \epsilon$ and then remove the divergent piece before comparing to the field-theory computation. The expression for the regularized action is

$$\mathcal{S}_{\mathrm{I,\,(II)}} = \frac{\sqrt{\lambda}T}{2\pi}\sqrt{\frac{j^2}{m+1}}\left[\sqrt{\frac{j^2}{m+1}}\tilde{\sigma}_{\mathrm{I,\,(II)}} - \mathbb{E}\left(\mathrm{am}\left(\sqrt{\frac{j^2}{m+1}}\tilde{\sigma}_{\mathrm{I,\,(II)}}\,\middle|\, m\right)\middle|\, m\right) - \frac{\mathrm{cn}\left(\sqrt{\frac{j^2}{m+1}}\tilde{\sigma}_{\mathrm{I,\,(II)}}\,\middle|\, m\right)\mathrm{dn}\left(\sqrt{\frac{j^2}{m+1}}\tilde{\sigma}_{\mathrm{I,\,(II)}}\,\middle|\, m\right)}{\mathrm{sn}\left(\sqrt{\frac{j^2}{m+1}}\tilde{\sigma}_{\mathrm{I,\,(II)}}\,\middle|\, m\right)}\right]. \tag{73}$$

We can rewrite $\mathcal{S}_{\mathrm{I,\,(II)}}$ in a more compact form using eq. (71) to replace the incomplete elliptic integral of the second kind and noticing that

$$y'(\tilde{\sigma}) = \mathrm{cn}\left(\sqrt{\frac{j^2}{m+1}}\tilde{\sigma}_{\mathrm{I,\,(II)}}\,\middle|\, m\right)\mathrm{dn}\left(\sqrt{\frac{j^2}{m+1}}\tilde{\sigma}_{\mathrm{I,\,(II)}}\,\middle|\, m\right), \tag{74}$$

we get

$$\mathcal{S}_{\mathrm{I,\,(II)}} = -\frac{\sqrt{\lambda}T}{2\pi}z\,c\,, \tag{75}$$

where $c = \frac{j^2\sqrt{-m}}{m+1}$. To compare the supergravity and the gauge theory results, we have to expand our results in the double scaling parameter given in eqns. (6) and (7). One can get the expansion for Λ_{I} in powers of $\frac{\lambda}{\pi^2(k_1^2+k_2^2)}$ looking at its definition in eq. (54). Notice that eq. (55) is satisfied in the large flux limit if

$$\psi_1 = \psi_0 + \frac{\cos\psi_0(\sin\psi_0 - \sin 3\psi_0)}{4\pi^2}\frac{\lambda}{k_1^2+k_2^2} + \mathcal{O}\left(\frac{\lambda^2}{\pi^4\left(k_1^2+k_2^2\right)^2}\right), \tag{76}$$

where $\tan\psi_0 = \frac{k_2}{k_1}$. Thus, the expansion for Λ_{I} is

$$\Lambda_{\mathrm{I}} = \sqrt{\frac{k_1^2+k_2^2}{\lambda}}\pi - \frac{\sin^2 2\psi_0}{8\pi}\sqrt{\frac{\lambda}{k_1^2+k_2^2}} + \mathcal{O}\left(\frac{\lambda}{\pi^2(k_1^2+k_2^2)}\right). \tag{77}$$

The double-scaling expansion for Λ_{II} can be read off from eq. (56). Notice that in this limit also $\Lambda_{\mathrm{I,II}}$ have to be large. Namely, we require that the denominator in eq. (72) vanishes. This occurs when m goes to zero. Moreover, we can assume the following expansion for m

$$m = \sum_{l=1}^{\infty}\frac{a_{2l}}{\Lambda_{\mathrm{I,II}}^{2l}}, \tag{78}$$

in such a way that eq. (72) is satisfied. The coefficient in the above expansion can be determined by solving iteratively equation (72). In the end, we get the following expansions for the particle-defect potential in the two different cases I and II

$$V^{(\mathrm{I})} = -\frac{k_1\sin(\chi) + k_2\cos(\chi)}{2z}\left\{1 + \frac{\lambda}{\pi^2\left(k_1^2+k_2^2\right)}\frac{1}{2\sin(\psi_0+\chi)}\left[\frac{\sin^2(\psi_0+\chi)}{4\cos^3(\psi_0+\chi)}\left(\pi - 2\psi_0 - 2\chi - \sin(2\psi_0+2\chi)\right)\right.\right.$$

[2] Our notation for elliptic functions and integrals follows that of the Wolfram Language of Mathematica.

$$- \cos(\chi)\sin(\psi_0)\cos^4(\psi_0) - \sin(\chi)\cos(\psi_0)\sin^4(\psi_0)\Big] + \mathcal{O}\left(\frac{\lambda^2}{\pi^4(k_1^2+k_2^2)^2}\right)\Bigg\}, \tag{79}$$

$$V^{(\mathrm{II})} = -\frac{n\sin(\chi)}{2\sqrt{2}z}\left\{1+\frac{\lambda}{\pi^2 n^2}\left[\frac{\sin(\chi)}{4\cos^3(\chi)}(\pi - 2\chi - \sin(2\chi)) - \frac{1}{4}\right] + \mathcal{O}\left(\frac{\lambda^2}{\pi^4 n^4}\right)\right\}. \tag{80}$$

We thus find perfect agreement with the field theory results to two leading orders in the double scaling limit. Notice also that when $\psi_0 \to 0$ (namely $k_2/k_1 \to 0$), the expansion for the action in (79) reduces to the result for the Wilson line in the D3-D5 case [11,12]. For the set-up II the correction to the potential looks similar to the one of the D3-D5 brane case up to a replacement of n by $\sqrt{2}k$. This is a peculiarity of the one-loop approximation where only the first term in the expansion in eqn. (56) contributes, and it will not remain true at higher loop orders. Finally, we mention that for the set-up I there is no particular point of symmetry where the potential vanishes. This is due to the fact that for set-up I all scalar fields get vevs, and it is not possible to choose a direction on the sphere which is unaffected by these.

4. Conclusion and outlook

Our investigation of Wilson lines provides an example that the AdS/dCFT dictionary for non-local observables remains valid upon breaking of both supersymmetry and (boundary) integrability. In addition, it serves as an important consistency check of the perturbative framework that was set up in references [7,8] for the dCFTs involved. We stress that having a perturbative framework for these defect CFTs is indispensable as these theories, due to the lack of supersymmetry, are not amenable to methods such as localization. For other defect versions of $\mathcal{N}=4$ SYM, conserving part of the supersymmetries, such as the D3-D5 probe brane model, important progress on the use of localization has recently been made in [26].

With the perturbative framework and the AdS/dCFT dictionary in place, possibilities for further scrutiny of the present defect CFTs open up. F.inst. one can scan the parameter spaces of the models for the presence of Gross-Ooguri like phase transitions [24] as it was done for the supersymmetric D3-D5 probe brane set-up in [15,14,25]. It would likewise be interesting to study the transport properties of the various defect CFTs, supersymmetric or not, by calculating correlation functions of the stress energy tensor across the defect or other related quantities.

Declaration of competing interest

The authors declare that they have no known competing financial interests or personal relationships that could have appeared to influence the work reported in this paper.

Acknowledgements

S.B. was supported by “Fondazione Angelo Della Riccia” and the University of Florence. C.K. and M.V. were supported by DFF-FNU through grant number DFF-4002-00037.

References

[1] M. de Leeuw, C. Kristjansen, K. Zarembo, One-point functions in defect CFT and integrability, J. High Energy Phys. 08 (2015) 098, https://doi.org/10.1007/JHEP08(2015)098, arXiv:1506.06958.
[2] M. De Leeuw, C. Kristjansen, G. Linardopoulos, Scalar one-point functions and matrix product states of AdS/dCFT, Phys. Lett. B 781 (2018) 238–243, https://doi.org/10.1016/j.physletb.2018.03.083, arXiv:1802.01598.
[3] M. de Leeuw, C. Kristjansen, K.E. Vardinghus, A non-integrable quench from AdS/dCFT, Phys. Lett. B 798 (2019) 134940, https://doi.org/10.1016/j.physletb.2019.134940, arXiv:1906.10714.
[4] L. Piroli, B. Pozsgay, E. Vernier, What is an integrable quench?, Nucl. Phys. B 925 (2017) 362–402, https://doi.org/10.1016/j.nuclphysb.2017.10.012, arXiv:1709.04796.
[5] K. Nagasaki, S. Yamaguchi, Expectation values of chiral primary operators in holographic interface CFT, Phys. Rev. D 86 (2012) 086004, https://doi.org/10.1103/PhysRevD.86.086004, arXiv:1205.1674.
[6] C. Kristjansen, G.W. Semenoff, D. Young, Chiral primary one-point functions in the D3-D7 defect conformal field theory, J. High Energy Phys. 01 (2013) 117, https://doi.org/10.1007/JHEP01(2013)117, arXiv:1210.7015.
[7] A. Gimenez Grau, C. Kristjansen, M. Volk, M. Wilhelm, A quantum check of non-supersymmetric AdS/dCFT, J. High Energy Phys. 01 (2019) 007, https://doi.org/10.1007/JHEP01(2019)007, arXiv:1810.11463.
[8] A. Gimenez-Grau, C. Kristjansen, M. Volk, M. Wilhelm, A quantum framework for AdS/dCFT through fuzzy spherical harmonics on S^4, J. High Energy Phys. 04 (2020) 132, https://doi.org/10.1007/JHEP04(2020)132, arXiv:1912.02468.
[9] I. Buhl-Mortensen, M. de Leeuw, A.C. Ipsen, C. Kristjansen, M. Wilhelm, One-loop one-point functions in gauge-gravity dualities with defects, Phys. Rev. Lett. 117 (23) (2016) 231603, https://doi.org/10.1103/PhysRevLett.117.231603, arXiv:1606.01886.
[10] I. Buhl-Mortensen, M. de Leeuw, A.C. Ipsen, C. Kristjansen, M. Wilhelm, A quantum check of AdS/dCFT, J. High Energy Phys. 01 (2017) 098, https://doi.org/10.1007/JHEP01(2017)098, arXiv:1611.04603.
[11] K. Nagasaki, H. Tanida, S. Yamaguchi, Holographic interface-particle potential, J. High Energy Phys. 01 (2012) 139, https://doi.org/10.1007/JHEP01(2012)139, arXiv:1109.1927.
[12] M. de Leeuw, A.C. Ipsen, C. Kristjansen, M. Wilhelm, One-loop Wilson loops and the particle-interface potential in AdS/dCFT, Phys. Lett. B 768 (2017) 192–197, https://doi.org/10.1016/j.physletb.2017.02.047, arXiv:1608.04754.
[13] M. Preti, D. Trancanelli, E. Vescovi, Quark-antiquark potential in defect conformal field theory, J. High Energy Phys. 10 (2017) 079, https://doi.org/10.1007/JHEP10(2017)079, arXiv:1708.04884.
[14] S. Bonansea, S. Davoli, L. Griguolo, D. Seminara, Circular Wilson loops in defect $\mathcal{N}=4$ SYM: phase transitions, double-scaling limits and OPE expansion, J. High Energy Phys. 03 (2020) 084, https://doi.org/10.1007/JHEP03(2020)084, arXiv:1911.07792.
[15] J. Aguilera-Damia, D.H. Correa, V.I. Giraldo-Rivera, Circular Wilson loops in defect conformal field theory, J. High Energy Phys. 03 (2017) 023, https://doi.org/10.1007/JHEP03(2017)023, arXiv:1612.07991.
[16] N.R. Constable, R.C. Myers, O. Tafjord, Non-abelian brane intersections, J. High Energy Phys. 06 (2001) 023, https://doi.org/10.1088/1126-6708/2001/06/023, arXiv:hep-th/0102080.
[17] J. Castelino, S. Lee, W. Taylor, Longitudinal five-branes as four spheres in matrix theory, Nucl. Phys. B 526 (1998) 334–350, https://doi.org/10.1016/S0550-3213(98)00291-0, arXiv:hep-th/9712105.
[18] M. de Leeuw, C. Kristjansen, G. Linardopoulos, One-point functions of non-protected operators in the SO(5) symmetric D3–D7 dCFT, J. Phys. A 50 (25) (2017) 254001, https://doi.org/10.1088/1751-8121/aa714b, arXiv:1612.06236.
[19] F.W. Olver, D.W. Lozier, R.F. Boisvert, C.W. Clark, NIST Handbook of Mathematical Functions, Hardback and CD-ROM, Cambridge University Press, 2010.
[20] R.C. Myers, M.C. Wapler, Transport properties of holographic defects, J. High Energy Phys. 12 (2008) 115, https://doi.org/10.1088/1126-6708/2008/12/115, arXiv:0811.0480.
[21] S.-J. Rey, J.-T. Yee, Macroscopic strings as heavy quarks in large N gauge theory and anti-de Sitter supergravity, Eur. Phys. J. C 22 (2001) 379–394, https://doi.org/10.1007/s100520100799, arXiv:hep-th/9803001.
[22] J.M. Maldacena, Wilson loops in large N field theories, Phys. Rev. Lett. 80 (1998) 4859–4862, https://doi.org/10.1103/PhysRevLett.80.4859, arXiv:hep-th/9803002.
[23] N. Drukker, D.J. Gross, H. Ooguri, Wilson loops and minimal surfaces, Phys. Rev. D 60 (1999) 125006, https://doi.org/10.1103/PhysRevD.60.125006, arXiv:hep-th/9904191.
[24] D.J. Gross, H. Ooguri, Aspects of large N gauge theory dynamics as seen by string theory, Phys. Rev. D 58 (1998) 106002, https://doi.org/10.1103/PhysRevD.58.106002, arXiv:hep-th/9805129.
[25] S. Bonansea, R. Sanchéz, Work in progress.
[26] Y. Wang, Taming defects in $\mathcal{N}=4$ super-Yang-Mills, arXiv:2003.11016, March 2020.

Published for SISSA by Springer

Received: June 8, 2020
Accepted: June 15, 2020
Published: July 22, 2020

JHEP07(2020)160

Traintrack Calabi-Yaus from twistor geometry

Cristian Vergu and Matthias Volk

Niels Bohr International Academy and Discovery Center, Niels Bohr Institute, University of Copenhagen, Blegdamsvej 17, Copenhagen Ø, DK-2100 Denmark

E-mail: c.vergu@nbi.ku.dk, mvolk@nbi.ku.dk

Abstract: We describe the geometry of the leading singularity locus of the traintrack integral family directly in momentum twistor space. For the two-loop case, known as the elliptic double box, the leading singularity locus is a genus one curve, which we obtain as an intersection of two quadrics in $\mathbb{P}^3$. At three loops, we obtain a K3 surface which arises as a branched surface over two genus-one curves in $\mathbb{P}^1 \times \mathbb{P}^1$. We present an analysis of its properties. We also discuss the geometry at higher loops and the supersymmetrization of the construction.

Keywords: Scattering Amplitudes, Supersymmetric Gauge Theory

ArXiv ePrint: 2005.08771

https://doi.org/10.1007/JHEP07(2020)160

Contents

1 Introduction **1**

2 Two loops: the elliptic double box **3**
2.1 Construction 3
2.2 Analysis of the two-loop leading singularity locus 5

3 Three and more loops **7**
3.1 K3 surface 7
3.1.1 Construction 7
3.1.2 Analysis 9
3.2 Three-fold and beyond 12
3.2.1 Three-fold 12
3.2.2 General case 13

4 Supersymmetrization **14**

5 Summary and outlook **15**

A Automorphisms of K3 surfaces **16**

JHEP07(2020)160

1 Introduction

While it was initially hoped that the integrals which appear in computations in planar $\mathcal{N} = 4$ SYM are expressible in terms of generalized polylogarithms, it has by now become clear that this is not the case.[1] Not only are the generalized polylogarithms insufficient but, by any reasonable measure, most of the integrals in $\mathcal{N} = 4$ SYM seem to require more complicated classes of functions, which are as of yet very poorly understood.

One class of integrals which is relatively well-understood is the class of pure integrals. These integrals have leading singularities (see ref. [3]) which are pure numbers such as 0 or ± 1. In all known examples they are computable in terms of generalized polylogarithms.

Recall that to obtain leading singularities one takes residues in the propagators of the integral. Doing so, Jacobian factors are generated in which one can often take further residues. If we start with an integral with fewer propagators than integration variables, two things can happen. Either one can generate enough Jacobian factors to take residues in, so that the integral localizes, or not. If the integral does not localize, then the process

[1] Work on the Kontsevich conjecture by Belkale and Brosnan [1] had given good reasons to be pessimistic. More recently, Brown and Schnetz [2] have given explicit examples in ϕ^4 theory, which contain K3 geometries.

of taking residues ends with a holomorphic form. This form may however develop poles for special kinematics.

The leading singularity locus, when it is not a set of points, turns out to be an interesting variety of Calabi-Yau type. The discussion above makes it plausible that one is more likely to find integrals which do not localize if we consider examples with as few propagators as possible. Since triangles are not possible in a dual-conformal expansion in planar $\mathcal{N} = 4$ SYM, the examples we consider are box integrals. As it turns out, ladder integrals are computable in terms of classical polylogarithms (see ref. [4]). The simplest integral which can not be localized by taking residues is the elliptic double box integral, studied in refs. [5, 6]. It is part of a family of integrals, called traintrack integrals (see figure 1). There are many other examples in the literature, where Calabi-Yau geometries have been identified in loop integrals, see e.g. [2, 7–14].

The traintrack integrals were studied in ref. [15]. This reference studied three- and four-loop integrals using Feynman parametrization. The leading singularity loci were defined as hypersurfaces in various weighted projective spaces, whose coordinates were related to the Feynman parameters of the original integral. The constructions in ref. [15] were pretty involved, in that they required complicated changes of variables which did not seem to fit a pattern that could be generalized to all loops.

In this paper we study the leading singularity locus by using the momentum twistor description of the traintrack integrals. Momentum twistors were introduced by Hodges [16] in order to make the dual conformal symmetry [17–19] more manifest. The translation from momentum space to twistor space proceeds as follows. Given a planar Feynman integral such as the one in figure 1, we introduce dual coordinates x_{ℓ_i} for each loop and x_i for each external region. Under the twistor correspondence, each of these dual points corresponds to a projective line $\mathbb{P}^1$ inside a $\mathbb{P}^3$ space. This $\mathbb{P}^3$ is called momentum twistor space. Under this dictionary, the action of the conformal group on the dual space with coordinates x becomes the familiar PSL(4) action on $\mathbb{P}^3$.

Two dual points are light-like separated if their corresponding lines in momentum twistor space intersect. This simple geometric fact, which is manifestly invariant under PSL(4) transformations, will be central to our discussions below. Indeed, the leading singularity locus is obtained by imposing a number of light-like conditions between the dual points. Using the momentum twistor constructions these constraints yield a configuration of intersecting lines, which is much easier to describe than the set of quadratic equations which one has to solve in momentum space or dual space.

Another advantage of the momentum twistor description is that it automatically picks for us a compactification and complexification of the dual space which is compatible with the dual conformal symmetry. The complexification is essential as well since all the varieties we will describe below are complex varieties.

Our analysis is similar in spirit to the analysis done by Hodges [20] for the one-loop box integral. The one-loop box example is however much simpler, since its leading singularity locus is a set of two points.

In this paper we obtain the following results. We describe the leading singularity locus of the elliptic double box as an intersection of two quadrics in $\mathbb{P}^3$. We compute the j-

JHEP07(2020)160

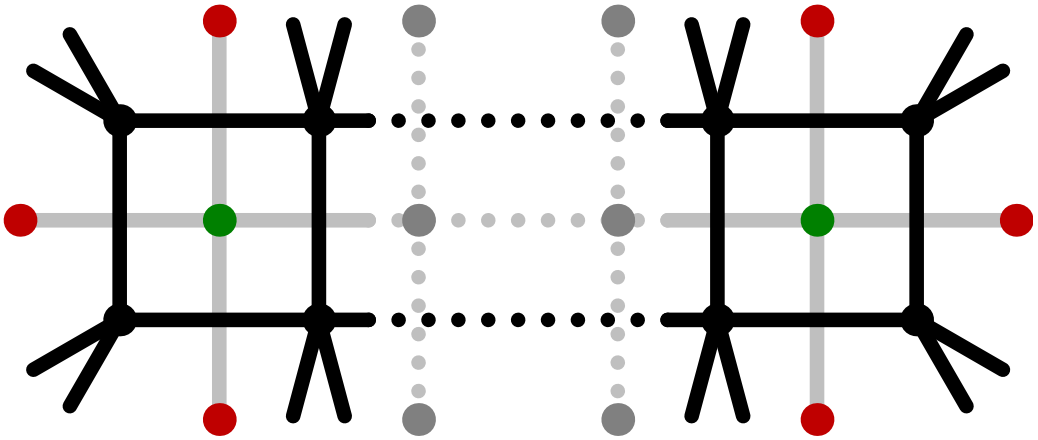

Figure 1. The traintrack integrals.

invariant of this intersection and compare with the answer obtained in ref. [6]. Next, we analyze the three-loop case and we identify the leading singularity locus with a K3 surface. The K3 surface is described as a branched surface over the union of two genus-one curves in $\mathbb{P}^1 \times \mathbb{P}^1$. We compute its Euler characteristic and the number of moduli. Then, we analyze the leading singularity locus in the four-loop case. We obtain a Calabi-Yau three-fold which can be realized as a complete intersection. We analyze its topology using the methods of Batyrev and Borisov. Finally we end with short discussions of the higher-loop cases and of the supersymmetrization.

2 Two loops: the elliptic double box

2.1 Construction

We consider the two-loop traintrack diagram, i.e. the two-loop version of the class of diagrams depicted in figure 1. Its leading singularity is determined as follows. There are three dual points x_1, x_2, x_3 corresponding to the left loop and three dual points x_4, x_5, x_6 corresponding to the right loop. The left loop internal dual point x_{ℓ_1} has to be light-like separated from the three dual points x_1, x_2, x_3. The right loop internal dual point x_{ℓ_2} has to be light-like separated from the three dual points x_4, x_5, x_6. Finally, the points x_{ℓ_1} and x_{ℓ_2} have to be light-like separated.

In momentum twistor space this can be described as follows. To each dual point x_i we associate a line $A_i \wedge B_i$ in momentum twistor space $\mathbb{P}^3$. Two dual points are light-like separated if their corresponding lines in $\mathbb{P}^3$ intersect. At first, we assume that all the lines corresponding to external dual points are skew (do not meet in $\mathbb{P}^3$). When some of these lines intersect, the geometry simplifies.

Given three skew lines, there is a one-dimensional family of lines which intersect all of them. This can be seen by using several fundamental results about quadrics in $\mathbb{P}^3$. The first fact is that three skew lines uniquely determine a non-singular quadric Q. The second fact is that a non-singular quadric Q in $\mathbb{P}^3$ contains two families of lines where the lines in a given family are skew while two lines in different families always intersect. Finally,

JHEP07(2020)160

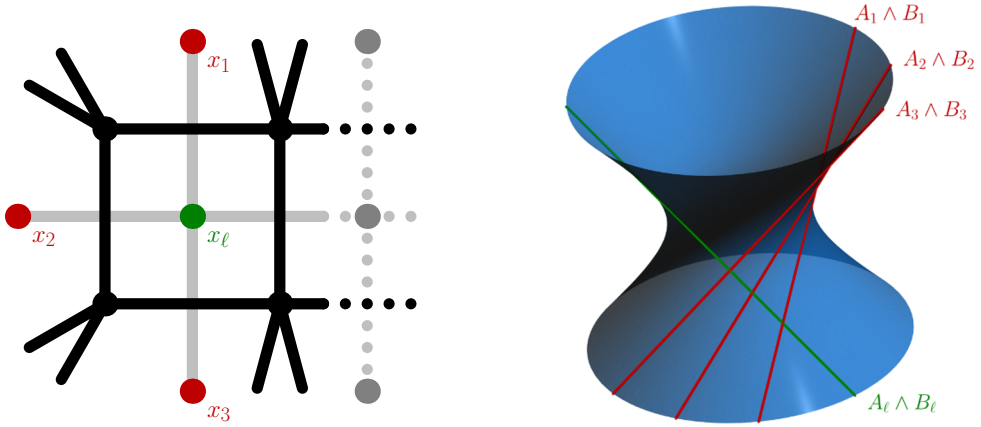

Figure 2. Relationship between the endcap of the traintrack and the quadric.

through a given point passes a unique line from each family of lines. Such families of lines on a quadric are called *rulings*.

More concretely, given three skew lines $A_i \wedge B_i$ for $i = 1, 2, 3$, the quadric they determine can be written as

$$Q(Z) = \langle Z A_1 B_1 A_3 \rangle \langle Z A_2 B_2 B_3 \rangle - \langle Z A_1 B_1 B_3 \rangle \langle Z A_2 B_2 A_3 \rangle. \tag{2.1}$$

Here Z, A_i and B_i are points in $\mathbb{P}^3$ and $\langle ABCD \rangle = \det(A, B, C, D)$ is the usual four-bracket of momentum twistors. The three lines appear symmetrically, but this is not manifest in the formula above. Using Plücker relations one can show that the symmetry holds.

Then, to the dual points x_1, x_2, x_3 neighboring the left loop we can associate a quadric Q_L and to the points x_4, x_5, x_6 neighboring the right loop we can associate a quadric Q_R; cf. figure 2. Next, consider the intersection $C \coloneqq Q_L \cap Q_R \subset \mathbb{P}^3$ of these two quadrics, which is a curve. To each point on C we can associate a line in Q_L which intersects all the three lines determining Q_L. This line corresponds to the interior dual point x_{ℓ_1} of the left loop. Similarly, through the same point of C we can construct a line which intersects all the lines in Q_R corresponding to the interior dual point x_{ℓ_2}. The line in Q_L and the one in Q_R intersect in a point in C so their corresponding dual points are also light-like separated as required for the leading singularity.

The intersection of two quadrics in $\mathbb{P}^3$ is a genus-one algebraic curve, see figure 3.

We can connect this construction to the more familiar picture of a cubic curve in $\mathbb{P}^2$ as follows: without loss of generality, we can take the point $[X_0 : X_1 : X_2 : X_3] = [0 : 0 : 0 : 1]$ to belong to both quadrics. Then the equations for the two quadrics can be written as

$$Q_L = X_3 L_L + M_L, \qquad Q_R = X_3 L_R + M_R, \tag{2.2}$$

where L_L and L_R are of homogeneous of degree one and M_L and M_R are homogeneous of degree two in X_0, X_1 and X_2. When eliminating X_3, we obtain $L_L M_R - L_R M_L = 0$, which is a cubic in $\mathbb{P}^2$.

JHEP07(2020)160

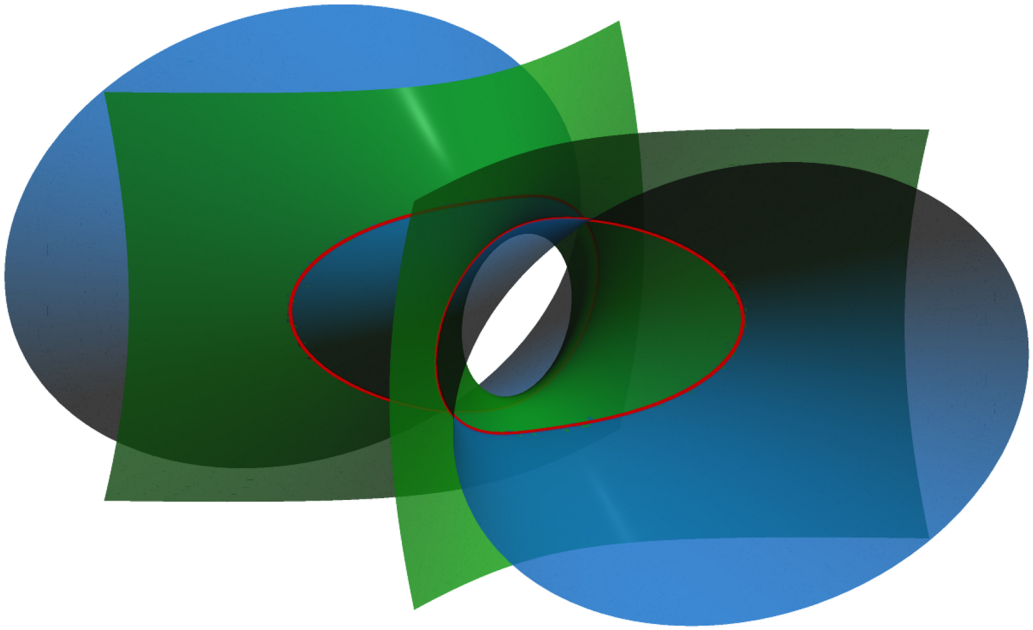

Figure 3. Two intersecting quadrics. Their intersection is the genus-one curve C in the elliptic double box.

2.2 Analysis of the two-loop leading singularity locus

Having constructed a genus-one curve C as the intersection of two quadrics in $\mathbb{P}^3$, we now proceed to analyze its properties.

The holomorphic differential one-form on the curve can be found by taking Poincaré residues,

$$\omega_C = \mathrm{Res}_{Q_L} \mathrm{Res}_{Q_R} \frac{\omega_{\mathbb{P}^3}}{Q_L Q_R}. \tag{2.3}$$

Here $\omega_{\mathbb{P}^3}$ is the PSL(4)-invariant, weight-four holomorphic three-form on $\mathbb{P}^3$. The quadrics Q_L and Q_R both have weight two so that the ratio $\frac{\omega_{\mathbb{P}^3}}{Q_L Q_R}$ is invariant under rescaling of the homogeneous coordinates of $\mathbb{P}^3$. Then, we take two Poincaré residues which yields a one-form localized on C. This is in fact the unique holomorphic one-form on C so the curve C is indeed a genus-one curve. A genus-one curve is characterized by only one modulus, which can be taken to be its j-invariant.

We can also see that there is only one modulus by counting parameters as follows: there are six dual points, each with four coordinates. From this, we need to subtract the dimension of the four-dimensional conformal group, which is 15. In total we obtain $6 \times 4 - 15 = 9$, assuming the conformal group acts effectively. However, there are configurations of the three skew lines in the left quadric which generate the same quadric. Indeed, consider a line inside Q_L which intersects all the lines which determine Q_L. We can displace any of these three lines along the chosen line without changing Q_L. Hence, there is a three-dimensional space of three skew lines which parametrize the same quadric Q_L. The same holds for Q_R. Moreover, the same curve C can be obtained by considering any two members

JHEP07(2020)160

of the so-called *pencil of quadrics* generated by Q_L and Q_R.[2] In other words, instead of using Q_L and Q_R we can use linear combinations of them, $\lambda_L Q_L + \lambda_R Q_R$ and $\mu_L Q_L + \mu_R Q_R$, where $[\lambda_L : \lambda_R]$ and $[\mu_L : \mu_R]$ are homogeneous coordinates on a projective line. This amounts to two extra parameters which do not appear in the moduli of C. In the end, C has $9 - 3 - 3 - 2 = 1$ moduli.

The pencil of quadrics $\lambda_L Q_L + \lambda_R Q_R$ also allows us to compute the j-invariant of the curve C. As mentioned above, C is obtained as the intersection of any two members of the pencil. We now think of each of the quadrics as a 4×4 symmetric matrix of the coefficients in the defining equation (2.1) and consider the determinant

$$\det(\lambda_L Q_L + \lambda_R Q_R). \tag{2.4}$$

This is a polynomial of degree four in the homogeneous coordinates $[\lambda_L : \lambda_R]$ of $\mathbb{P}^1$. Hence, it vanishes at four points in $\mathbb{P}^1$ and we conclude that there are four singular members of the pencils.[3] The cross-ratio of these four points is an invariant of the pencil. More concretely, let us denote the four points where (2.4) vanishes by $\lambda^i := [\lambda_L^i : \lambda_R^i]$. Then, we can form the cross-ratio $z = \frac{\langle 12\rangle\langle 34\rangle}{\langle 13\rangle\langle 24\rangle}$, where $\langle ij\rangle = \det(\lambda^i, \lambda^j)$, and the j-invariant

$$j = 256\frac{(z^2 - z + 1)^3}{z^2(z-1)^2}. \tag{2.5}$$

As pointed out above, the curve C is obtained as the intersection of *any* two members of the pencil of quadrics $\lambda_L Q_L + \lambda_R Q_R$. Thus we can characterize isomorphism classes of C by completely characterizing the pencil. The cross-ratio z formed above classifies the isomorphism classes of four ordered points on $\mathbb{P}^1$ up to projective equivalence. The j-invariant formed in (2.5) has the correct symmetries for the corresponding elliptic curve: in defining the cross-ratio z, we have the freedom of permuting three of the points λ^i on $\mathbb{P}^1$ while keeping one fixed without changing C. This permutation acts on z by sending $z \mapsto z' \in \left\{z, \frac{1}{z}, 1-z, 1-\frac{1}{z}, \frac{1}{1-z}, 1-\frac{1}{1-z}\right\}$. One can check that the j-invariant in (2.5) is invariant under this map.

In [6], the elliptic double box integral was analyzed using the method of direct integration. Starting from a dual-conformally invariant expression, Feynman parameters were introduced and as many integrations as possible were performed in terms of multiple polylogarithms. Eventually, the authors found a representation of the double box integral of the form

$$\int_0^\infty d\alpha \, \frac{H_3(\alpha)}{\sqrt{Q(\alpha)}}. \tag{2.6}$$

Here H_3 is a combination of weight-three multiple polylogarithms and $Q(\alpha)$ is a polynomial in α of degree four with coefficients depending on conformal cross-ratios. The equation $y^2 = Q(\alpha)$ thus defines an elliptic curve. We have checked that the j-invariant of this

[2] A pencil is a set of subvarieties, in this case quadrics, which are parametrized by a line [21].

[3] Note that we assume that the quadrics Q_L and Q_R are in general position such that the four roots of (2.4) are distinct. If they are not, then the intersection degenerates and the integral can be computed in terms of generalized polylogarithms.

JHEP07(2020)160

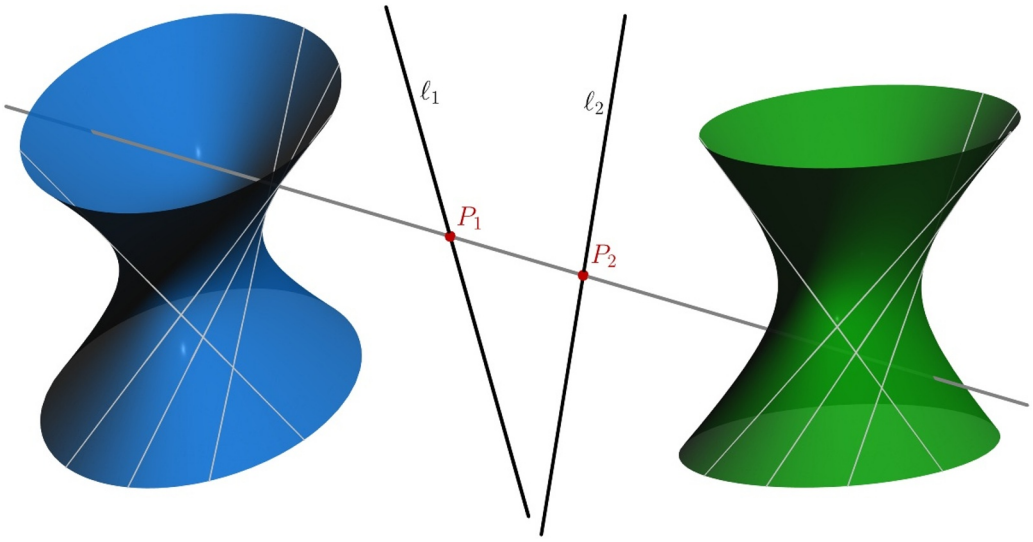

Figure 4. Quadrics and lines defining the K3 surface in the three-loop traintrack diagram.

curve matches the j-invariant of the curve constructed directly in momentum twistor space above. This is an encouraging result as it means that the geometry is not merely an artifact of the chosen parametrization but an intrinsic property of the leading singularity of the double box integral.

3 Three and more loops

3.1 K3 surface

3.1.1 Construction

The construction of a geometry for the three-loop traintrack integral is similar to the one for the two-loop case presented in section 2. This time, however, we have two extra lines in momentum twistor space corresponding to the two additional external dual points. The geometry in this case is given by two quadrics Q_L and Q_R, constructed in the same way as at two loops, together with two lines ℓ_1 and ℓ_2. Given points $P_1 \in \ell_1$ and $P_2 \in \ell_2$, we can construct a line $P_1 \wedge P_2$ whose corresponding dual point is light-like separated from both dual points corresponding to ℓ_1 and ℓ_2. The line $P_1 \wedge P_2$ corresponds to the middle loop in the three-loop traintrack integral. The moduli space of these lines is $\mathbb{P}^1 \times \mathbb{P}^1$ corresponding to the freedom in choosing P_1 and P_2. We illustrate the construction in figure 4.

The rest of the light-like constraints for the leading singularity can be imposed as follows. By Bezout's theorem, the line $P_1 \wedge P_2$ intersects the quadric Q_L in two points and the quadric Q_R in two points.[4] Choosing one of these intersections in Q_L and one in Q_R, we obtain a leading singularity configuration. In total, there are four choices. The total

[4]Bezout's theorem states that n hypersurfaces of degrees $d_1, \ldots, d_n$ in complex projective space $\mathbb{P}^n$ intersect in $d_1 \cdots d_n$ points, if the number of intersection points is finite [21]. In our case, the quadric has degree two, while a line can be seen as the intersection of two hyperplanes, each of degree one. Hence, the intersection consists of two points.

JHEP07(2020)160

space of leading singularities is therefore a four-fold cover of $\mathbb{P}^1 \times \mathbb{P}^1$, branched over the curves where the line $P_1 \wedge P_2$ is tangent to Q_L or Q_R.

To find out where this branching arises, consider the points $\alpha_1 P_1 + \alpha_2 P_2$ on the line $P_1 \wedge P_2$. The intersection with Q_L is given by the equation

$$\alpha_1^2\, Q_L(P_1, P_1) + 2\alpha_1\alpha_2\, Q_L(P_1, P_2) + \alpha_2^2\, Q_L(P_2, P_2) = 0. \tag{3.1}$$

The line $P_1 \wedge P_2$ is tangent to Q_L if this has a double root, i.e. when the discriminant with respect to α_1 or α_2 vanishes,

$$\Delta_L \coloneqq Q_L(P_1, P_2)^2 - Q_L(P_1, P_1) Q_L(P_2, P_2) = 0. \tag{3.2}$$

The polynomial Δ_L is homogeneous of bidegree $(2, 2)$ in the coordinates of $\mathbb{P}^1 \times \mathbb{P}^1$ that parametrize the points $P_1 \in \ell_1$ and $P_2 \in \ell_2$.

A similar analysis can be done for the right quadric and we obtain another polynomial Δ_R of bidegree $(2, 2)$. The curves determined by Δ_L and Δ_R intersect in eight points.[5] At these eight points, all the branches of the surface meet. Over the remaining points of the curves determined by Δ_L and Δ_R there are only two branches, while over the remaining points of $\mathbb{P}^1 \times \mathbb{P}^1$ there are four branches.

The curves in $\mathbb{P}^1 \times \mathbb{P}^1$ defined by the vanishing locus of Δ_L and Δ_R are themselves genus-one curves as can be seen as follows. If we choose coordinates $x = [x_0 : x_1]$ and $y = [y_0 : y_1]$ on $\mathbb{P}^1 \times \mathbb{P}^1$, then we can write the equation for a biquadratic as

$$\Delta(x, y) = \sum_{a,b,a',b'=0}^{1} A_{ab,a'b'}\, x_a x_b\, y_{a'} y_{b'}, \tag{3.3}$$

where A is symmetric in the first and second pair of indices independently and thus has 9 independent components. We now embed $\mathbb{P}^1 \times \mathbb{P}^1$ into $\mathbb{P}^3$ using the Segre map. Concretely, we identify the homogeneous coordinates $[z_0 : z_1 : z_2 : z_3]$ on $\mathbb{P}^3$ with the coordinates on $\mathbb{P}^1 \times \mathbb{P}^1$ as

$$z_0 = x_0 y_0, \qquad z_1 = x_0 y_1, \qquad z_2 = x_1 y_0, \qquad z_3 = x_1 y_1. \tag{3.4}$$

The image of $\mathbb{P}^1 \times \mathbb{P}^1$ is then a quadric in $\mathbb{P}^3$ given by $z_0 z_3 - z_1 z_2 = 0$. The biquadratic (3.3) becomes

$$\Delta(z) = \sum_{i,j=0}^{3} \tilde{A}_{ij}\, z_i z_j, \tag{3.5}$$

where $\tilde{A}$ is a 4×4 symmetric matrix that depends on the original coefficients $A_{ab,a'b'}$. This defines another quadric in $\mathbb{P}^3$. The intersection of these two quadrics is a genus-one curve with only one modulus, as we have discussed before.

[5] To see why, consider first the intersection of such a genus-one curve with a line in $\mathbb{P}^1 \times \mathbb{P}^1$ which sits at a point in the first or the second $\mathbb{P}^1$. It is easy to see that this intersection consists of two points. Now, consider a degeneration of the biquadratic into four lines. Two of the lines sit at a point in the first $\mathbb{P}^1$ while the other two sit at a point in the second $\mathbb{P}^1$. Each one of them intersects the biquadratic in two points. In total, there are eight intersection points. As we deform from a singular curve consisting of four lines to a non-singular one, the number of intersections is conserved. This type of argument is often used in Schubert problems (see ref. [22] for a detailed discussion).

JHEP07(2020)160

3.1.2 Analysis

The holomorphic two-form on the surface is

$$\omega_{K3} = \frac{\omega_{\mathbb{P}^1}\,\omega_{\mathbb{P}^1}}{\sqrt{\Delta_L}\sqrt{\Delta_R}}. \tag{3.6}$$

Notice that this ratio has the right homogeneity in $\mathbb{P}^1 \times \mathbb{P}^1$: the first $\omega_{\mathbb{P}^1}$ has bidegree $(2,0)$ while the second one has bidegree $(0,2)$. The polynomials Δ_L and Δ_R both have bidegree $(2,2)$ so that (3.6) has homogeneity zero as required.

An analogous construction can be done for the simpler case of a genus-one curve in $\mathbb{P}^2$ as a two-fold branched cover over four points in $\mathbb{P}^1$. In that case, we can define a polynomial P whose roots are the four points and the holomorphic form is $\frac{\omega_{\mathbb{P}^2}}{\sqrt{P}}$.

Euler characteristic. It is well-known that the Euler characteristic χ of a K3 surface is 24, but we can directly compute this from the construction in momentum twistor space. To do so, we will use the basic fact that χ is additive under surgery.

According to the branching described above, the K3 surface S has only one branch on the points $\mathbb{P}^1 \times \mathbb{P}^1$ where the two curves Δ_L and Δ_R meet, i.e. for the points in $\Delta_L \cap \Delta_R$. For the points that lie on either of the two curves, i.e. for $\Delta_L \cup \Delta_R \setminus \Delta_L \cap \Delta_R$, there are two branches. In the complement of the two curves, i.e. in $\mathbb{P}^1 \times \mathbb{P}^1 \setminus \Delta_L \cup \Delta_R$, there are four branches. It follows that

$$\begin{aligned}\chi(S) &= 4\left[\chi(\mathbb{P}^1 \times \mathbb{P}^1) - \chi(\Delta_L \cup \Delta_R)\right] + 2\left[\chi(\Delta_L \cup \Delta_R) - \chi(\Delta_L \cap \Delta_R)\right] \\ &\quad + \chi(\Delta_L \cap \Delta_R) \\ &= 4\chi(\mathbb{P}^1 \times \mathbb{P}^1) - 2\chi(\Delta_L \cup \Delta_R) - \chi(\Delta_L \cap \Delta_R).\end{aligned} \tag{3.7}$$

Next, we use the fact that $\chi(\mathbb{P}^1 \times \mathbb{P}^1) = \chi(\mathbb{P}^1)^2$, $\chi(\mathbb{P}^1) = 2$ and $\chi(\Delta_L \cup \Delta_R) = \chi(\Delta_L) + \chi(\Delta_R) - \chi(\Delta_L \cap \Delta_R)$. The Euler characteristic of a point is one and the intersection $\Delta_L \cap \Delta_R$ consists of eight points, thus we get $\chi(\Delta_L \cap \Delta_R) = 8$. Moreover, Δ_L and Δ_R are genus-one curves, thus $\chi(\Delta_L) = \chi(\Delta_R) = 0$. Finally, we get

$$\chi(S) = 4 \times 2 \times 2 - 2 \times (-8) - 8 = 24. \tag{3.8}$$

This is the expected number for a K3 surface which has Betti numbers $b_0 = 1$, $b_2 = 22$ and $b_4 = 1$ with the odd Betti numbers vanishing.

Counting the number of moduli. We would now like to count the number of moduli of these K3 surfaces. This amounts to a counting of degrees of freedom of two genus-one curves in $\mathbb{P}^1 \times \mathbb{P}^1$, intersecting in eight points. On top of that, there are moduli that roughly speaking describe the position of the quadrics corresponding to the endcaps of the traintrack integrals.

Before solving the first problem, recall the more familiar case of two cubic curves in the projective plane $\mathbb{P}^2$. A cubic curve in the projective plane is a non-zero linear combination of ten monomials. Hence, the set of cubic curves forms a $\mathbb{P}^9$. The condition that a point belongs to a cubic curve imposes a linear condition in $\mathbb{P}^9$. Given nine points in *general* position, there is a single cubic curve which contains all of them. The condition that the

JHEP07(2020)160

nine points be generic is essential here. In fact, consider two cubics in the projective plane. By Bezout's theorem, they intersect in nine points. In this case, these nine points can not be generic since they do not uniquely determine a cubic curve. In fact, they determine a pencil of cubics.

The theorem of Cayley-Bacharach states that if two plane cubics intersect in nine points, then any other cubic which passes through eight of them automatically passes through the ninth [21].[6]

Let us now return to genus-one curves in $\mathbb{P}^1 \times \mathbb{P}^1$. A biquadratic curve in $\mathbb{P}^1 \times \mathbb{P}^1$ is a linear combination of nine monomials of bidegree $(2,2)$. Hence, these curves form a $\mathbb{P}^8$. As before, the condition that a point belongs to such a curve is a linear condition in $\mathbb{P}^8$. Hence, eight points in *general* position uniquely determine a genus-one curve in $\mathbb{P}^1 \times \mathbb{P}^1$.

Next, consider two such biquadratic curves. They intersect in eight points. If the equations of the two biquadratics in homogeneous coordinates $x = [x_0 : x_1]$ and $y = [y_0 : y_1]$ of $\mathbb{P}^1 \times \mathbb{P}^1$ are

$$\Delta_{00}(y)x_0^2 + 2\Delta_{01}(y)x_0x_1 + \Delta_{11}(y)x_1^2 = 0, \tag{3.9}$$

$$\Delta'_{00}(y)x_0^2 + 2\Delta'_{01}(y)x_0x_1 + \Delta'_{11}(y)x_1^2 = 0, \tag{3.10}$$

then the intersection points have y coordinates satisfying

$$(\Delta'_{00}\Delta_{11} - \Delta_{00}\Delta'_{11})^2 + 4(\Delta'_{00}\Delta_{01} - \Delta_{00}\Delta'_{01})(\Delta'_{11}\Delta_{01} - \Delta'_{01}\Delta_{11}) = 0. \tag{3.11}$$

Here Δ_{ij} and Δ'_{ij} are quadratic in y such that this is a degree-eight polynomial and that generically there are eight such intersection points. For each of these values of y the corresponding value of $x \in \mathbb{P}^1$ is given by

$$2(\Delta'_{00}\Delta_{01} - \Delta_{00}\Delta'_{01})x_0 + (\Delta'_{00}\Delta_{11} - \Delta_{00}\Delta'_{11})x_1 = 0. \tag{3.12}$$

These eight points can not be in general position, otherwise there would be a unique biquadratic curve containing them. For this case, we have a variant of the Cayley-Bacharach theorem, stating that if two biquadratic curves meet in seven points then they meet in the eighth as well.

Returning to the problem of counting the moduli, we see that we have to specify seven points in $\mathbb{P}^1 \times \mathbb{P}^1$ which amounts to 14 parameters. From this we have to subtract 2×3 parameters due to PSL(2) transformations on each $\mathbb{P}^1$. Moreover, we need to pick two members of the pencil of quadrics $\lambda_L Q_L + \lambda_R Q_R$ which adds two additional moduli. It turns out that there is one more modulus corresponding to the relative position of the left and right quadric along the middle line through the points P_1 and P_2. In total, the number of moduli is

$$14 - 2 \times 3 + 2 + 1 = 11. \tag{3.13}$$

There is another, more direct way to establish 11 as an upper bound for the number of moduli: the K3 surface only depends on the left and right quadrics and the two lines ℓ_1

[6] The Cayley-Bacharach theorem is essential in proving the associativity of the group law on a genus-one curve.

JHEP07(2020)160

and ℓ_2. In dual space we have $8 \times 4 - 15 = 17$, where we subtracted 15 due to the action of the conformal group. As discussed in section 2.2, we can move each of the three lines defining a quadric up and down along a line from the opposite ruling without changing the quadric. Thus we can subtract $2 \times 3 = 6$ coordinates. In total we get $8 \times 4 - 15 - 6 = 11$ moduli.

For algebraic K3 surfaces, the sum of the dimension of the moduli space and the generic Picard rank has to equal 20 (see ref. [23]). Since we found a moduli space of dimension 11, then the generic Picard rank should be 9. Below, we find the same answer by looking at Nikulin involutions.

In [15], the authors analyzed the three-loop traintrack integral using Feynman parameters and identified a K3 surface as a hypersurface in a certain weighted projective space. For a generic hypersurface in this space they found an upper bound of 18 for the number of moduli which is compatible with the number that we found above. In the case of the elliptic curve we were able to compare the momentum twistor construction to the one found in Feynman-parametric integration using the j-invariant of the curve and found that they give the same geometry. For the K3 surfaces, a more thorough study of their characteristics is needed to conclude whether or not they are equal.

Automorphisms and Nikulin involutions. To further characterize the K3 surface S, we study its automorphisms, in particular those automorphisms that leave the holomorphic two-form on S invariant. Such automorphisms are called symplectic. If f is a symplectic automorphism of finite order n and $f \neq \mathrm{id}$, then one can show that the set of fixed points $\mathrm{Fix}(f) \subset S$ is non-empty and finite. Moreover, the number of fixed points satisfies $1 \leq |\mathrm{Fix}(f)| \leq 8$ and depends only on the order n of f, see for example ref. [24]. Nikulin [25] also showed that the order n can at most be eight, i.e. $n \leq 8$, which means that only the combinations of n and $|\mathrm{Fix}(f)|$ in table 1 are possible.

Symplectic automorphisms of order two are called *Nikulin involutions* and the corresponding number of fixed points is eight. Such involutions are realized in our K3 surface as follows.

Consider the left quadric Q_L and the line $P_1 \wedge P_2$ transversal to ℓ_1 and ℓ_2, see also figure 4. $P_1 \wedge P_2$ intersects Q_L in two points and exchanging these two points constitutes an involution of the left quadric. Recall that the points of intersection are given by the two roots of (3.1). Since this in a quadratic equation, the difference between the two roots is $\sqrt{\Delta_L}$. Thus, exchanging the two points of intersection, sends $\sqrt{\Delta_L}$ to $-\sqrt{\Delta_L}$. The fixed points of this involution of the left quadric are the points of Q_L at which $P_1 \wedge P_2$ becomes tangent, i.e. the points described by the genus-one curve $\Delta_L = 0$ in $\mathbb{P}^1 \times \mathbb{P}^1$. Since the map we described so far changes the sign of $\sqrt{\Delta_L}$, the holomorphic two-form (3.6) also changes sign and we only obtain a Nikulin involution of the K3 surface if we perform the same involution on the right quadric. The fixed points are then the eight intersection points of the curves Δ_L and Δ_R in $\mathbb{P}^1 \times \mathbb{P}^1$.

An involution which is not symplectic is the exchange of the two $\mathbb{P}^1$ corresponding to the lines ℓ_1 and ℓ_2. Indeed, under this transformation the holomorphic two-form in eq. (3.6) picks up a sign.

JHEP07(2020)160

The existence of automorphisms implies a lower bound for the Picard number $\rho(S)$ of the K3 surface [24]. For a Nikulin involution, i.e. a symplectic automorphism of order two, the bound is $\rho(S) \geq 9$ (see appendix A). Since the Picard number plus the dimension of the moduli space are equal to 20, this bound is consistent with the counting of the moduli above. In fact in our case the bound is satisfied, i.e. $\rho(S) = 9$; for this case a complete description of the Picard lattice of S can be found in ref. [26].

3.2 Three-fold and beyond

In this section, we demonstrate how we can build a Calabi-Yau manifold embedded in a toric variety for the four- and higher-loop traintrack integrals. It was shown by Batyrev that mirror families of Calabi-Yau manifolds can be constructed as anticanonical hypersurfaces in toric varieties and that their Hodge numbers can be computed combinatorially by counting points in an associated pair of reflexive polytopes [27]. This construction was generalized to complete intersection Calabi-Yau (CICY) manifolds by Batyrev and Borisov using the nef-partitions of a reflexive polytope pair [28, 29]. The Hodge numbers in this case can be computed by means of a recursive generating function; an implementation of this function is available in `PALP` [30].[7]

3.2.1 Three-fold

The leading singularity configuration for the four-loop traintrack integral is depicted in figure 5. Compared to the three-loop case discussed in section 3.1, we have two new lines, ℓ_3 and ℓ_4, corresponding to the two extra external dual points.

Let us introduce coordinates $([\alpha_1 : \alpha_2], [\beta_1 : \beta_2])$ for the $\mathbb{P}^1 \times \mathbb{P}^1$ corresponding to the lines ℓ_1 and ℓ_2 and similarly $([\gamma_1 : \gamma_2], [\delta_1 : \delta_2])$ for the lines ℓ_3 and ℓ_4. Then the embedding space is a toric variety defined by the relations

$$\begin{aligned}(\alpha_1, \alpha_2, \beta_1, \beta_2, y_L) &\sim (t_1\,\alpha_1, t_1\,\alpha_2, \beta_1, \beta_2, t_1\,y_L),\\ (\alpha_1, \alpha_2, \beta_1, \beta_2, y_L) &\sim (\alpha_1, \alpha_2, t_2\,\beta_1, t_2\,\beta_2, t_2\,y_L)\end{aligned} \tag{3.14}$$

for the left part of figure 5 and

$$\begin{aligned}(\gamma_1, \gamma_2, \delta_1, \delta_2, y_R) &\sim (t_3\,\gamma_1, t_3\,\gamma_2, \delta_1, \delta_2, t_3\,y_R),\\ (\gamma_1, \gamma_2, \delta_1, \delta_2, y_R) &\sim (\gamma_1, \gamma_2, t_4\,\delta_1, t_4\,\delta_2, t_4\,y_R)\end{aligned} \tag{3.15}$$

from the right part. Here $t_1, t_2, t_3, t_4 \in \mathbb{C} \setminus \{0\}$ and the role of y_L and y_R will be clarified momentarily. Since we have ten coordinates and four relations, we are left with a six-dimensional space.

Following the same construction as for the three-loop (K3) case, we obtain two polynomials Δ_L and Δ_R of bidegree $(2, 2)$ in $\mathbb{P}^1 \times \mathbb{P}^1$ from the left and right outermost loop of the traintrack. In the six-dimensional toric variety constructed above, the Calabi-Yau manifold is defined as a codimension-three subvariety by means of the constraints

$$y_L^2 = \Delta_L, \quad y_R^2 = \Delta_R, \quad \langle P_1 P_2 P_3 P_4 \rangle = 0. \tag{3.16}$$

[7] Note that technically the generating function computes the *stringy* Hodge numbers introduced in [31].

JHEP07(2020)160

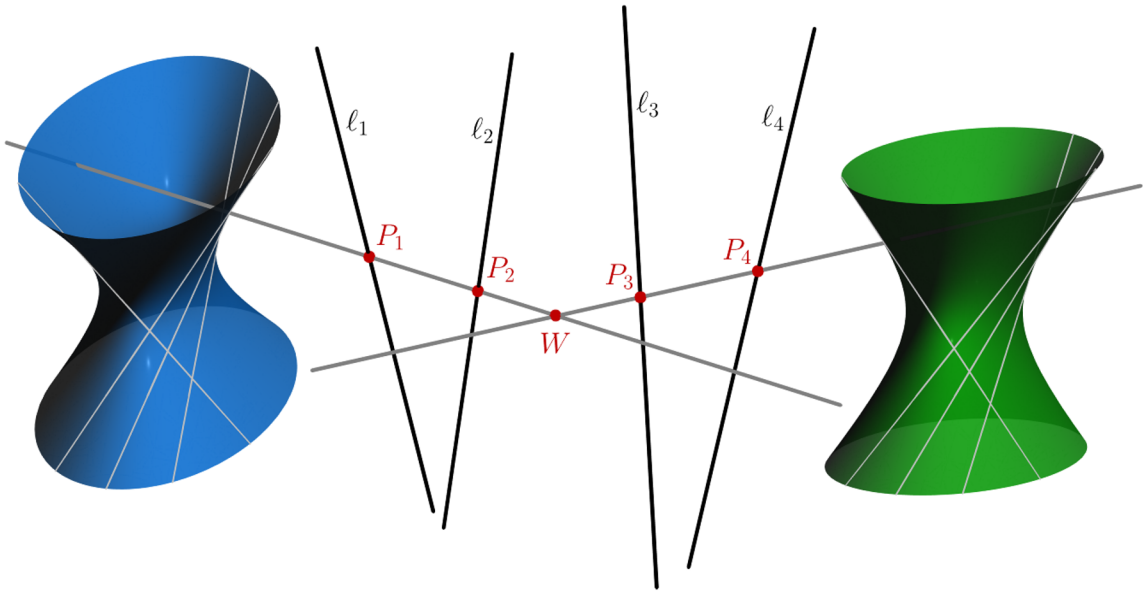

Figure 5. Quadrics and lines defining the CY three-fold in the four-loop traintrack diagram.

The last condition forces the two transversals $P_1 \wedge P_2$ and $P_3 \wedge P_4$ to intersect, see also figure 5.

The toric variety defined by the relations (3.14) and (3.15) can be described by a polytope with ten vertices in a six-dimensional integer lattice. Explicitly, the vertices are given by the columns of the matrix

$$\begin{pmatrix} 1 & 0 & 0 & 1 & -1 & 0 & 0 & 0 & 0 & 0 \\ 0 & 1 & 0 & 1 & -1 & 0 & 0 & 0 & 0 & 0 \\ 0 & 0 & 1 & -1 & 0 & 0 & 0 & 0 & 0 & 0 \\ 0 & 0 & 0 & 0 & 0 & 1 & 0 & 0 & 1 & -1 \\ 0 & 0 & 0 & 0 & 0 & 0 & 1 & 0 & 1 & -1 \\ 0 & 0 & 0 & 0 & 0 & 0 & 0 & 1 & -1 & 0 \end{pmatrix}. \tag{3.17}$$

The Hodge numbers of a generic codimension-three subvariety in this space can be obtained by computing the nef-partitions of the polytope defined by (3.17). Using `PALP` [30], in particular the component `nef.x`,[8] we find that there are 22 nef partitions. Out of these, we identify three that have defining equations with degrees compatible with the constraints (3.16). The Hodge numbers are $h^{11} = 12$ and $h^{12} = 28$ which gives a Euler characteristic of $\chi = -32$.

3.2.2 General case

The construction used for the three-fold, i.e. the four-loop case of the traintracks, generalizes to higher loops. For $L \geq 4$, we build a toric embedding space as follows: there are $2 + 4(L-2)$ coordinates, 2 from y_L and y_R and $2 \times 2(L-2)$ from the two external

[8] Note that we had to set `VERT_Nmax` to 96 in `Global.h` for the computation to succeed.

JHEP07(2020)160

dual points added with each loop. The number of relations between these coordinates is $2(L-2)$; thus the dimension of the embedding space is $2+4(L-2)-2(L-2)=2(L-1)$. In this space, we impose 2 quadratic constraints, namely $y_L^2=\Delta_L$ and $y_R^2=\Delta_R$, as well as $L-3$ multilinear constraints. Thus, the Calabi-Yau manifold is obtained as a subvariety of codimension $L-1$ in a toric variety of dimension $2(L-1)$. Note that the dimension of the manifold is also $L-1$.

As above, we can describe the embedding space by a polytope with vertices in an integer lattice. The dimension of this lattice equals the dimension of the embedding space, i.e. $2(L-1)$, while the number of vertices is equal to the number of coordinates, $2+4(L-2)$. The vertices are given in the general case by the columns of a block-diagonal matrix

$$\begin{pmatrix} \mathbf{A} & \mathbf{0} & \mathbf{0} & \cdots & \mathbf{0} \\ \mathbf{0} & \mathbf{A} & \mathbf{0} & & \\ \mathbf{0} & \mathbf{0} & \mathbf{B} & & \\ \vdots & & & \ddots & \vdots \\ \mathbf{0} & & & \cdots & \mathbf{B} \end{pmatrix}, \qquad \mathbf{A}=\begin{pmatrix} 1 & 0 & 0 & 1 & -1 \\ 0 & 1 & 0 & 1 & -1 \\ 0 & 0 & 1 & -1 & 0 \end{pmatrix}, \qquad \mathbf{B}=\begin{pmatrix} 1 & -1 \end{pmatrix}. \tag{3.18}$$

Note that in the case of the threefold (i.e. $L=4$) that was discussed above, $\mathbf{B}$ does not appear and the matrix reduces to (3.17).

We note that the codimension grows with the loop order and this makes the analysis of these varieties in terms of complete intersections more challenging. One may hope for a more "efficient" description of these varieties, but it remains to be seen if this is possible in way which is compatible with supersymmetry, as described in section 4.

4 Supersymmetrization

The constructions presented so far are manifestly dual-conformal invariant. Indeed, this is one reason why it makes sense to use momentum twistors to describe their geometry. However, we know that the scattering amplitudes in $\mathcal{N}=4$ are in fact dual *super*-conformal invariant. It is then natural to ask what becomes of the supersymmetry.

In order to describe the supersymmetrization, we will redo the previous analysis in such a way that the various incidence relations are described in terms of PSL(4)-invariant delta functions. The basic ingredient will be the delta function of two points on $\mathbb{P}^3$, which we denote by $\delta^3_{\mathbb{P}^3}(P_1;P_2)$, where $P_1,P_2\in\mathbb{P}^3$.

This quantity can be used to define $\delta^2_{\mathbb{P}^3}(L;P)$, which has support when the point P lies on the line L. If the line P contains two points P_0 and P_1, then we have

$$\delta^2_{\mathbb{P}^3}(L;P)=\int \omega_{\mathbb{P}^1}(\alpha)\delta_{\mathbb{P}^3}(\alpha_0P_0+\alpha_1P_1;P). \tag{4.1}$$

Similarly, we can define $\delta_{\mathbb{P}^3}(L_1;L_2)$, which has support when the two lines L_1 and L_2 intersect.

To define a delta function with support on a quadric, we use the fact that the quadric is determined by three skew lines L_1, L_2 and L_3. The quadric is ruled by a family of lines which intersect L_1, L_2 and L_3. Moreover, through any point on the quadric passes one line

JHEP07(2020)160

in this ruling. We can then describe the conditions that a point P belongs to the quadric Q determined by the skew lines L_1, L_2 and L_3 by the following integral

$$\delta_{\mathbb{P}^3}(Q;P) = \int \mu_{\mathbb{P}^3}(L)\delta_{\mathbb{P}^3}(L;L_1)\delta_{\mathbb{P}^3}(L;L_2)\delta_{\mathbb{P}^3}(L;L_3)\delta^2_{\mathbb{P}^3}(L;P), \tag{4.2}$$

where $\mu_{\mathbb{P}^3}(L)$ is the integral over the space of lines in $\mathbb{P}^3$. This integral is four-dimensional so, after performing the integrals, we are left with a single constraint. This is expected since a quadric is of codimension one in $\mathbb{P}^3$.

To obtain the genus-one curve we simply take the product of the two delta functions corresponding to Q_L and Q_R. This is a distribution which has support on the intersection of the two quadrics $Q_L \cap Q_R$. We can also obtain the holomorphic top form, but instead of taking Poincaré residues, we proceed as follows. We look for a one-form ω_C such that

$$\int_C \omega_C(Z)f(Z) = \int \omega_{\mathbb{P}^3}(Z)\delta_{\mathbb{P}^3}(Q_L;Z)\delta_{\mathbb{P}^3}(Q_R;Z)f(Z), \tag{4.3}$$

for any meromorphic function f on $\mathbb{P}^3$ whose poles lie outside $Q_L \cap Q_R$.

This construction is rather unnatural when done in $\mathbb{P}^3$, but its advantage lies in the fact that it can be pretty straightforwardly supersymmetrized to $\mathbb{P}^{3|4}$. Indeed, in $\mathbb{P}^{3|4}$ we have a delta function $\delta^{3|4}_{\mathbb{P}^{3|4}}(\mathcal{Z}_1;\mathcal{Z}_2)$, and so on. These supersymmetrizations were introduced in ref. [32]. For the superquadric we obtain $\delta^{1|8}_{\mathbb{P}^{3|4}}(\mathcal{Q},\mathcal{Z})$. Pursuing the same strategy as in the $\mathbb{P}^3$ case, we finally define $\omega_C^{1|12}$ using

$$\int_C \omega_C^{1|12}(Z)f(Z) = \int \omega_{\mathbb{P}^{3|4}}(\mathcal{Z})\delta_{\mathbb{P}^{3|4}}(\mathcal{Q}_l;\mathcal{Z})\delta_{\mathbb{P}^{3|4}}(\mathcal{Q}_r;\mathcal{Z})f(Z), \tag{4.4}$$

where $\mathcal{Z} = [Z_0 : Z_1 : Z_2 : Z_3 \,|\, \chi_1 : \chi_2 : \chi_3 : \chi_4]$ and $\omega_{\mathbb{P}^{3|4}}(\mathcal{Z}) = \omega_{\mathbb{P}^3}(Z)d\chi_1 d\chi_2 d\chi_3 d\chi_4$ is the PSL(4|4)-invariant form on $\mathbb{P}^{3|4}$.

This construction can be generalized to higher dimensions.

5 Summary and outlook

We have presented a few examples of Calabi-Yau varieties arising as the leading singularity loci of the class of traintrack integrals.

For the elliptic double box we have a pretty explicit understanding of the moduli space and how it relates to the external kinematics of the integral. We believe this should be a useful ingredient in the computation of these integrals.

The moduli space of algebraic K3 surfaces has a global description as a double coset of an orthogonal group (see ref. [23]). This moduli space should be somehow parametrized by the external kinematics, but this global description does not seem to arise naturally from the twistor representation of the kinematics. So, while we have described the topology of these varieties in some detail, our description of their moduli space has not been as detailed as we would like. One approach we have sketched is to use a parametrization where 10 moduli arise from an intersection of two genus-one curves in $\mathbb{P}^1 \times \mathbb{P}^1$ and an extra modulus arises from the intersections of transversals to these $\mathbb{P}^1$ with the two quadrics Q_L and Q_R.

JHEP07(2020)160

It remains to be seen if this parametrization will be useful for expressing the corresponding integral.

One slightly mysterious aspect remains in connection with Calabi-Yau varieties encountered in non-planar integrals. The twistor methods are well-adapted for studying planar integrals. How should non-planar integrals be described in this language? It is not clear yet if the momentum twistor approach is a useful description for the leading singularity locus of these integrals. We hope to report on this issue in future work.

We have also discussed supersymmetrization. The approach to supersymmetrization we have sketched generalizes to other cases as well. Clearly supersymmetry imposes some restriction on the geometry of these varieties and it would be interesting to understand this better.

Acknowledgments

We are grateful to Jacob Bourjaily, Andrew McLeod, Matt von Hippel and Matthias Wilhelm for discussions, collaboration on related topics and comments on the draft of this paper. This work was supported in part by the Danish Independent Research Fund under grant number DFF-4002-00037 (MV), the Danish National Research Foundation (DNRF91), the research grant 00015369 from Villum Fonden and a Starting Grant (No. 757978) from the European Research Council (CV, MV).

A Automorphisms of K3 surfaces

For an account of the automorphisms of K3 surfaces see for example ref. [24, chapter 15]. In the following we summarize some of the most important facts.

When studying the group of automorphisms $\mathrm{Aut}(S)$ of a K3 surface S, one distinguishes between symplectic and non-symplectic automorphisms. An automorphism $f : S \to S$ of a K3 surface S is symplectic if the induced action on $H^0(S, \Omega^2_S)$ is the identity, i.e. if it leaves the holomorphic two-form on S invariant. One can show that $\mathrm{Aut}(S)$ is discrete and that the subgroup $\mathrm{Aut}_s(S) \subset \mathrm{Aut}(S)$ of symplectic automorphisms is of finite index, at least for projective K3 surfaces.

One can moreover show the following result: let $f \in \mathrm{Aut}_s(S)$ be of finite order n and $f \neq \mathrm{id}$. Then the set of fixed points $\mathrm{Fix}(f)$ is non-empty and finite and

$$|\mathrm{Fix}(S)| = \frac{24}{n} \prod_{p|n} \left(1 + \frac{1}{p}\right)^{-1} . \tag{A.1}$$

Moreover the number of fixed point satisfies $1 \leq |\mathrm{Fix}(f)| \leq 8$ and only depends on the order n of f.

Nikulin also proved that for $f \in \mathrm{Aut}_s(S)$, the order n of f satisfies $n \leq 8$. This means that only the combinations of n and $|\mathrm{Fix}(S)|$ shown in table 1 can occur. For each n, one can also derive a lower bound for the Picard number $\rho(S)$ which is also shown in table 1. One can see that the Picard number of K3 surfaces with automorphisms tends to be quite high.

JHEP07(2020)160

Order n	2	3	4	5	6	7	8
$\lvert\mathrm{Fix}(S)\rvert$	8	6	4	4	2	3	2
$\rho(S) \geq$	9	13	15	17	17	19	19

Table 1. Symplectic automorphism orders and number of fixed points for a complex K3 surface S. Here $\rho(S)$ is the Picard number of S. Table from ref. [24].

Symplectic automorphisms of order two were studied by Nikulin [25] and are called *Nikulin involutions*. According to table 1, a Nikulin involution of a complex K3 surface has eight fixed points and Picard number $\rho(S) \geq 9$. A classification of all algebraic K3 surfaces with Picard number satisfying the lower bound, i.e. $\rho(S) = 9$ can be found in ref. [26].

References

[1] P. Belkale and P. Brosnan, *Matroids, motives, and a conjecture of Kontsevich*, *Duke Math. J.* **116** (2003) 147.

[2] F. Brown and O. Schnetz, *A K3 in ϕ^4*, *Duke Math. J.* **161** (2012) 1817 [arXiv:1006.4064] [INSPIRE].

[3] F. Cachazo, *Sharpening The Leading Singularity*, arXiv:0803.1988 [INSPIRE].

[4] N.I. Usyukina and A.I. Davydychev, *Exact results for three and four point ladder diagrams with an arbitrary number of rungs*, *Phys. Lett. B* **305** (1993) 136 [INSPIRE].

[5] S. Caron-Huot and K.J. Larsen, *Uniqueness of two-loop master contours*, *JHEP* **10** (2012) 026 [arXiv:1205.0801] [INSPIRE].

[6] J.L. Bourjaily, A.J. McLeod, M. Spradlin, M. von Hippel and M. Wilhelm, *Elliptic Double-Box Integrals: Massless Scattering Amplitudes beyond Polylogarithms*, *Phys. Rev. Lett.* **120** (2018) 121603 [arXiv:1712.02785] [INSPIRE].

[7] F.C.S. Brown, *On the periods of some Feynman integrals*, arXiv:0910.0114 [INSPIRE].

[8] J.L. Bourjaily, A.J. McLeod, M. von Hippel and M. Wilhelm, *Bounded Collection of Feynman Integral Calabi-Yau Geometries*, *Phys. Rev. Lett.* **122** (2019) 031601 [arXiv:1810.07689] [INSPIRE].

[9] M. Besier, D. Festi, M. Harrison and B. Naskrecki, *Arithmetic and geometry of a K3 surface emerging from virtual corrections to Drell-Yan scattering*, arXiv:1908.01079 [INSPIRE].

[10] D. Festi and D. van Straten, *Bhabha Scattering and a special pencil of K3 surfaces*, *Commun. Num. Theor. Phys.* **13** (2019) 463 [arXiv:1809.04970] [INSPIRE].

[11] J.L. Bourjaily, A.J. McLeod, C. Vergu, M. Volk, M. Von Hippel and M. Wilhelm, *Embedding Feynman Integral (Calabi-Yau) Geometries in Weighted Projective Space*, *JHEP* **01** (2020) 078 [arXiv:1910.01534] [INSPIRE].

[12] A. Klemm, C. Nega and R. Safari, *The l-loop Banana Amplitude from GKZ Systems and relative Calabi-Yau Periods*, *JHEP* **04** (2020) 088 [arXiv:1912.06201] [INSPIRE].

JHEP07(2020)160

[13] S. Bloch, M. Kerr and P. Vanhove, *A Feynman integral via higher normal functions*, *Compos. Math.* **151** (2015) 2329 [arXiv:1406.2664] [INSPIRE].

[14] S. Bloch, M. Kerr and P. Vanhove, *Local mirror symmetry and the sunset Feynman integral*, *Adv. Theor. Math. Phys.* **21** (2017) 1373 [arXiv:1601.08181] [INSPIRE].

[15] J.L. Bourjaily, Y.-H. He, A.J. Mcleod, M. Von Hippel and M. Wilhelm, *Traintracks through Calabi-Yau Manifolds: Scattering Amplitudes beyond Elliptic Polylogarithms*, *Phys. Rev. Lett.* **121** (2018) 071603 [arXiv:1805.09326] [INSPIRE].

[16] A. Hodges, *Eliminating spurious poles from gauge-theoretic amplitudes*, *JHEP* **05** (2013) 135 [arXiv:0905.1473] [INSPIRE].

[17] J.M. Drummond, J. Henn, V.A. Smirnov and E. Sokatchev, *Magic identities for conformal four-point integrals*, *JHEP* **01** (2007) 064 [hep-th/0607160] [INSPIRE].

[18] Z. Bern et al., *The Two-Loop Six-Gluon MHV Amplitude in Maximally Supersymmetric Yang-Mills Theory*, *Phys. Rev. D* **78** (2008) 045007 [arXiv:0803.1465] [INSPIRE].

[19] J.M. Drummond, J. Henn, G.P. Korchemsky and E. Sokatchev, *Hexagon Wilson loop = six-gluon MHV amplitude*, *Nucl. Phys. B* **815** (2009) 142 [arXiv:0803.1466] [INSPIRE].

[20] A. Hodges, *The Box Integrals in Momentum-Twistor Geometry*, *JHEP* **08** (2013) 051 [arXiv:1004.3323] [INSPIRE].

[21] P. Griffiths and J. Harris, *Principles of Algebraic Geometry*, John Wiley & Sons Inc., New York U.S.A. (1978).

[22] N. Arkani-Hamed, J.L. Bourjaily, F. Cachazo and J. Trnka, *Local Integrals for Planar Scattering Amplitudes*, *JHEP* **06** (2012) 125 [arXiv:1012.6032] [INSPIRE].

[23] P.S. Aspinwall, *K3 surfaces and string duality*, in proceedings of the *Theoretical Advanced Study Institute in Elementary Particle Physics (TASI 96): Fields, Strings, and Duality*, Boulder, CO, U.S.A., 2–28 June 1996, pp. 421–540 [hep-th/9611137] [INSPIRE].

[24] D. Huybrechts, *Lectures on K3 Surfaces*, Cambridge University Press, Cambridge U.K. (2016).

[25] V.V. Nikulin, *Finite automorphism groups of Kählerian surfaces of type K3*, *Tr. Mosk. Mat. O.-va* **38** (1979) 75.

[26] B. van Geemen and A. Sarti, *Nikulin involutions on K3 surfaces*, *Math. Z.* **255** (2007) 731.

[27] V.V. Batyrev, *Dual polyhedra and mirror symmetry for Calabi-Yau hypersurfaces in toric varieties*, *J. Alg. Geom.* **3** (1994) 493 [alg-geom/9310003] [INSPIRE].

[28] V.V. Batyrev and L.A. Borisov, *On Calabi-Yau complete intersections in toric varieties*, alg-geom/9412017 [INSPIRE].

[29] L. Borisov, *Towards the Mirror Symmetry for Calabi-Yau Complete intersections in Gorenstein Toric Fano Varieties*, alg-geom/9310001.

[30] M. Kreuzer and H. Skarke, *PALP: A Package for analyzing lattice polytopes with applications to toric geometry*, *Comput. Phys. Commun.* **157** (2004) 87 [math/0204356] [INSPIRE].

[31] V.V. Batyrev, *Stringy Hodge numbers of varieties with Gorenstein canonical singularities*, alg-geom/9711008.

[32] L.J. Mason and D. Skinner, *The Complete Planar S-matrix of $\mathcal{N} = 4$ SYM as a Wilson Loop in Twistor Space*, *JHEP* **12** (2010) 018 [arXiv:1009.2225] [INSPIRE].

JHEP07(2020)160

Published for SISSA by Springer

Received: *February 25, 2021*
Revised: *April 20, 2021*
Accepted: *April 20, 2021*
Published: *May 10, 2021*

JHEP05(2021)064

Cuts and isogenies

Hjalte Frellesvig, Cristian Vergu, Matthias Volk and Matt von Hippel

Niels Bohr International Academy, Niels Bohr Institute,
University of Copenhagen, Blegdamsvej 17, 2100 København, Denmark

E-mail: hjalte.frellesvig@nbi.ku.dk, c.vergu@nbi.ku.dk, mvolk@nbi.ku.dk, mvonhippel@nbi.ku.dk

Abstract: We consider the genus-one curves which arise in the cuts of the sunrise and in the elliptic double-box Feynman integrals. We compute and compare invariants of these curves in a number of ways, including Feynman parametrization, lightcone and Baikov (in full and loop-by-loop variants). We find that the same geometry for the genus-one curves arises in all cases, which lends support to the idea that there exists an invariant notion of genus-one geometry, independent on the way it is computed. We further indicate how to interpret some previous results which found that these curves are related by isogenies instead.

Keywords: Scattering Amplitudes, Differential and Algebraic Geometry

ArXiv ePrint: 2102.02769

https://doi.org/10.1007/JHEP05(2021)064

Contents

1 Introduction **1**

2 Lightning review: elliptic curves and isogenies **3**

3 The elliptic sunrise integral **3**
- 3.1 Feynman-parametric representation 4
- 3.2 Loop-by-loop Baikov representation 5
- 3.3 Full Baikov representation 7
- 3.4 Light-cone coordinates 8
- 3.5 Rationalizing the square roots in the Baikov representation 8
- 3.6 Derivation of the double cover relation 10
- 3.7 Singularities of the geometry and Landau analysis 12

4 The elliptic double-box integral **12**
- 4.1 Baikov representation 13
- 4.2 Four-dimensional derivation of the Baikov form 15

5 Conclusions **16**

A Baikov representations with derivations **18**
- A.1 The one-loop case 18
- A.2 Multi-loop, the loop-by-loop approach 20
- A.3 Multi-loop, the standard approach 21
- A.4 The elliptic double-box 21
- A.5 Derivation of a four-dimensional Baikov representation 22

JHEP05(2021)064

1 Introduction

There has recently been a flurry of interest in Feynman integrals associated with elliptic curves. Many different ways to represent these integrals have been developed [1–24], culminating in bases of functions that are believed to be powerful enough to represent all such integrals [25–27]. A common feature of most of these representations is the characterization of each integral in terms of a single, specific family of elliptic curves depending on the kinematic data of the Feynman integral. With the family specified, relations can be found between functions defined on the same family, allowing for the choice of a linearly independent basis.

What these representations typically do not consider are relations between Feynman integrals associated with distinct families of elliptic curves.[1] This deficit is thrown into sharp relief by a pair of papers, one by Adams and Weinzierl [15], and the other by Bogner, Müller-Stach, and Weinzierl [28], investigating the two-loop sunrise integral with all equal masses and with distinct internal masses respectively. These integrals have long been known to involve elliptic curves [1, 2, 4–6, 8, 13, 29–43]. What they found was that the sunrise integral can in fact be described by two distinct elliptic curves in different contexts, with the curves related by a quadratic transformation, characterized in the latter paper as an isogeny [28]. One curve appeared when analyzing the integral in terms of its Feynman-parametric representation, while another emerged from the maximal cut expressed in the Baikov representation [44] (see also [45–50]). They refer to these as the curve from the graph polynomial and the curve from the maximal cut, respectively.

In this work, we investigate the origin of the distinction between these two curves: whether they differ because one comes from the maximal cut, or due to their origin in different representations. We examine two diagrams, the sunrise with all distinct internal masses and the elliptic double-box [51, 52], in a variety of representations. In particular, we compare maximal cuts of these diagrams both in Baikov representations and in other representations (a light-cone representation in two dimensions, and a momentum twistor representation in four dimensions). We find that in general these representations can all give identical elliptic curves. Instead, we explain the observations of refs. [15, 28] as a consequence of a particular choice those references made when extracting an elliptic curve from the Baikov representation, involving combining two square roots. If we instead rationalize one of the roots, we find not an isogenous curve, but an *identical* curve to that found in Feynman parametrization.

The paper is organized as follows: after a quick review of the relevant mathematics in section 2, in section 3 we consider the sunrise integral with three distinct masses. We review the Feynman-parametric representation in subsection 3.1, and the loop-by-loop Baikov representation found in ref. [28] in subsection 3.2. We then derive two more representations, the traditional Baikov representation in subsection 3.3 and a representation in light-cone coordinates in subsection 3.4, and compare the resulting curves. In subsection 3.5 we explain the differing curves as a result of combining distinct square roots, and extract an alternate curve by rationalizing a quadratic root instead, finding consistency with other methods. We give another view on the relation between the curves that avoids introducing square roots in subsection 3.6. In subsection 3.7 we close with a brief discussion of how the elliptic j-invariants of these curves shed light on the singularities of the diagram. In section 4 we investigate the elliptic double-box, where we compute Baikov representations of the maximal cut to compare to curves extracted in prior work. Specifically, we compare a d-dimensional Baikov representation (subsection 4.1) and a Baikov representation derived in strictly four dimensions (subsection 4.2) finding agreement between the two. We then conclude and raise some topics for future investigation in section 5.

[1] From here on, we will in a slight abuse of language refer to distinct elliptic curves instead of distinct families of curves. This terminology is typical in the physics literature, and can be justified in cases where one compares representatives of both families at the same, fixed kinematic point.

JHEP05(2021)064

Our paper also includes an appendix, reviewing both the loop-by-loop and the standard approach to the Baikov representation in A.2 and A.3 respectively, as well as deriving our d-dimensional Baikov representation of the elliptic double-box in A.4 and presenting more details of our four-dimensional derivation in A.5. We also include two files as supplementary material: `doublebox_curve.txt`, presenting the elliptic curve for the double-box, and `doublebox_baikov_rep.txt`, presenting the Baikov representation for the double-box.

2 Lightning review: elliptic curves and isogenies

An elliptic curve is a smooth projective algebraic curve of genus one, together with a rational point which serves as the origin for its group structure.

There are many ways to represent such curves. One can write them as the vanishing loci of cubic polynomials in projective plane, or in terms of a quartic in a single variable with no repeated roots. One standard form is the so-called Weierstrass normal form, the equation

$$y^2 = 4x^3 - g_2 x - g_3\,, \tag{2.1}$$

for some coefficients g_2 and g_3.

Two elliptic curves are called isogenous when there is a non-constant map between them given by rational functions which sends the origin of the first to the origin of the second. To every isogeny corresponds a dual isogeny and their composition is a homomorphism from an elliptic curve to itself. If this homomorphism is the multiplication by two, we call the initial isogeny a two-isogeny. If an isogeny has an inverse (that is, when the inverse map is also rational), one further calls the two curves isomorphic [53]. Isomorphic curves have the same j-invariant, which can be specified in terms of the coefficients of the Weierstrass normal form as follows[2]

$$j = 1728\frac{g_2^3}{\Delta}, \tag{2.2}$$

where the elliptic discriminant $\Delta = g_2^3 - 27g_3^2$. The elliptic curve defined by the Weierstrass model (2.1) is smooth if and only if $\Delta \neq 0$.

3 The elliptic sunrise integral

The two-loop sunrise integral shown in figure 1 is given by

$$I(p^2, m_1^2, m_2^2, m_3^2) = \int \frac{\mathrm{d}^2k_1 \mathrm{d}^2k_2}{(k_2^2 - m_1^2)\left((k_1 - k_2)^2 - m_2^2\right)\left((p - k_1)^2 - m_3^2\right)}. \tag{3.1}$$

This integral is finite in two dimensions, so it is often studied in that context. In this section we will extract an elliptic curve from this integral in several ways, constructing the j-invariant for each such curve. We will find that the different methods we use provide only two distinct j-invariants, and are grouped as follows:

[2]The factor of $1728 = 2^6 \times 3^3$ is required for various number theoretic reasons which will not be relevant for us. We choose to keep it in order to minimize confusion, but also because some of the formulas we will find below actually look *nicer* when including this factor.

JHEP05(2021)064

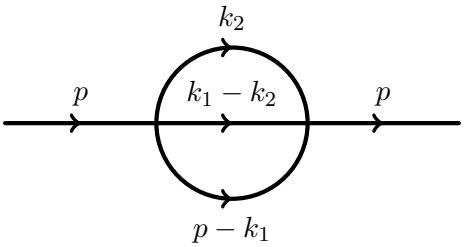

Figure 1. Sunrise integral. All internal propagators are massive and we consider the most general case where all masses can be unequal. The momentum labeling is chosen such as to make the loop-by-loop Baikov representation easier to derive.

- Feynman parametrization (subsection 3.1), solving the cut equations in light-cone coordinates (subsection 3.4)
- Loop-by-loop Baikov representation with 4 inverse propagators (subsection 3.2), full Baikov representation with 5 inverse propagators (subsection 3.3)

These two j-invariants correspond to two distinct elliptic curves, which are not isomorphic. However, as described in [28], the two curves are related by a two-isogeny.

In the rest of this section, we will describe how to extract an elliptic curve using each of these methods, and finish by reconciling the Baikov representations with the first set of methods, before briefly discussing this integral's Landau singularities.

3.1 Feynman-parametric representation

We begin by reviewing the two representations considered in ref. [28]. The first representation considered in that reference was for the full integral expressed in Feynman parameters. In Feynman parameters, the integral can be written as $\int \frac{\omega}{\mathfrak{F}}$ where $\mathfrak{F}$ is the second graph polynomial,

$$\mathfrak{F} = m_1^2 x_1^2 (x_2 + x_3) + m_2^2 x_2^2 (x_3 + x_1) + m_3^2 x_3^2 (x_1 + x_2) + (-p^2 + m_1^2 + m_2^2 + m_3^2) x_1 x_2 x_3 \tag{3.2}$$

and

$$\omega = x_1 \mathrm{d}x_2 \mathrm{d}x_3 - x_2 \mathrm{d}x_1 \mathrm{d}x_3 + x_3 \mathrm{d}x_1 \mathrm{d}x_2. \tag{3.3}$$

The variables x_1, x_2 and x_3 are homogeneous coordinates on $\mathbb{P}^2$ and the equation $\mathfrak{F} = 0$ defines an elliptic curve in $\mathbb{P}^2$.[3]

To compute the j-invariant of this curve we may first divide by p^2 to make the expression dimensionless, then transform to the Weierstrass normal form. For the purpose of writing the j-invariant for this curve, we define the following notation: writing $\mu_i^2 = \frac{m_i^2}{p^2}$, we then write,

$$\xi_0 = \mu_1 + \mu_2 + \mu_3, \quad \xi_1 = -\mu_1 + \mu_2 + \mu_3, \quad \xi_2 = \mu_1 - \mu_2 + \mu_3, \quad \xi_3 = \mu_1 + \mu_2 - \mu_3. \tag{3.4}$$

[3] In this paper we always write $\mathbb{P}^n$ for the complex projective space $\mathbb{P}^n(\mathbb{C})$.

JHEP05(2021)064

With this notation, we can specify the j-invariant:

$$j_F = \frac{\left[(\xi_0^2-1)(\xi_1^2-1)(\xi_2^2-1)(\xi_3^2-1)+16\mu_1^2\mu_2^2\mu_3^2\right]^3}{\mu_1^4\mu_2^4\mu_3^4\,(\xi_0^2-1)(\xi_1^2-1)(\xi_2^2-1)(\xi_3^2-1)} \tag{3.5}$$

where we have used a subscript F to indicate that this is computed from the Feynman parameter representation.

3.2 Loop-by-loop Baikov representation

Ref. [28] presented the maximal cut of the two-loop sunrise integral in a loop-by-loop Baikov representation (as distinct from the traditional, or "full" Baikov representation, see ref. [49], appendix A, or the next section to clarify the difference). We review below how to derive this representation in the case of this integral.

In the Baikov representation we want to change the integration variables in the integral $I(p^2, m_1^2, m_2^2, m_3^2)$ from the loop momenta k_1 and k_2 to the inverse propagators. For the integral in eq. (3.1) the inverse propagators are

$$D_1 = k_2^2 - m_1^2, \quad D_2 = (k_1-k_2)^2 - m_2^2, \quad D_3 = (p-k_1)^2 - m_3^2, \quad D_4 = k_1^2, \tag{3.6}$$

where we had to add D_4 to be able to express all scalar products between the momenta. In the following we consider the integral in the Euclidean region which corresponds to $p^2 < 0$ and $m_i^2 > 0$ for all masses.

The first step is to decompose the loop momenta into a part that is parallel and one that is orthogonal to the external momentum p:

$$k_1 = xp + k_{1,\perp}, \quad k_2 = yp + k_{2,\perp}. \tag{3.7}$$

The orthogonal parts satisfy $p \cdot k_{i,\perp} = 0$. As we are in two dimensions, $k_{1,\perp}$ and $k_{2,\perp}$ are proportional and we can write them as $k_{1,\perp} = up_\perp$ and $k_{2,\perp} = vp_\perp$. Here $p_\perp$ is chosen so that $p \cdot p_\perp = 0$ and $p_\perp^2 = p^2$. Expressing the inverse propagators in terms of the dimensionless quantities x, y, u and v we obtain

$$\begin{aligned} D_1 &= p^2(y^2+v^2) - m_1^2\,, & D_2 &= p^2(x-y)^2 + p^2(u-v)^2 - m_2^2\,, \\ D_3 &= p^2(x-1)^2 + p^2u^2 - m_3^2\,, & D_4 &= p^2(x^2+u^2)\,. \end{aligned} \tag{3.8}$$

Moreover, the integration measure becomes $\mathrm{d}^2k_1\mathrm{d}^2k_2 = p^4\,\mathrm{d}x\,\mathrm{d}y\,\mathrm{d}u\,\mathrm{d}v$.

We now want to change integration variables from (x, y, u, v) to (D_1, D_2, D_3, D_4) under which the measure transforms as $\mathrm{d}x\,\mathrm{d}y\,\mathrm{d}u\,\mathrm{d}v = J^{-1}\,\mathrm{d}D_1\,\mathrm{d}D_2\,\mathrm{d}D_3\,\mathrm{d}D_4$. For the Jacobian factor J we get

$$J \equiv \left|\frac{\partial(D_1, D_2, D_3, D_4)}{\partial(x, y, u, v)}\right| = -16p^8u(uy - vx). \tag{3.9}$$

This Jacobian now has to be expressed in terms of the new variables D_i. The equations (3.8) are quadratic in (x, y, u, v) and J can therefore not be expressed rationally in terms of the D_i. However, one can solve for the squares of u and $uy - vx$ in eq. (3.9) rationally. While

JHEP05(2021)064

this is possible for the full integral, here we only give the expression for the maximal cut corresponding to $D_1 = D_2 = D_3 = 0$:[4]

$$\begin{aligned} Q_1 &:= u^2 = -\frac{1}{4p^4}\left[D_4 - (m_3 - p)^2\right]\left[D_4 - (m_3 + p)^2\right], \\ Q_2 &:= (uy - vx)^2 = -\frac{1}{4p^4}\left[D_4 - (m_1 + m_2)^2\right]\left[D_4 - (m_1 - m_2)^2\right]. \end{aligned} \tag{3.10}$$

Note that in the Euclidean region p^2 is negative implying that the equation $D_1 = 0$ does not have a real solution. In order to impose the cut conditions we are thus forced to consider the analytic continuation of the integral.

Multiplying Q_1 and Q_2 from the previous two equations we obtain an expression for J^2 as a polynomial of degree four in D_4. This approach was followed in refs. [15, 28] and is equivalent to extracting the square root of each line in eq. (3.10) and combining the square roots under a common square root, i.e. to writing $J = -16p^8\sqrt{Q_1 Q_2}$. Another, inequivalent approach is to keep the square roots separate, i.e. to write $J = -16p^8\sqrt{Q_1}\sqrt{Q_2}$. As Q_1 and Q_2 are quadratic in D_4, one can again change variables to rationalize either $\sqrt{Q_1}$ or $\sqrt{Q_2}$. In subsection 3.5 we will show that this connects the elliptic curve arising from the first approach to the curve defined by the vanishing of the $\mathfrak{F}$-polynomial in subsection 3.1.

Following the approach taken in ref. [28], we define an elliptic curve by the equation $J^2 = (-16p^8)^2 Q_1 Q_2$. We can transform it to Weierstrass form and compute its j-invariant as in the previous section, obtaining:

$$j_B = \frac{\left[(\xi_0^2-1)(\xi_1^2-1)(\xi_2^2-1)(\xi_3^2-1) + 256\mu_1^2\mu_2^2\mu_3^2\right]^3}{\mu_1^2\mu_2^2\mu_3^2\,(\xi_0^2-1)^2(\xi_1^2-1)^2(\xi_2^2-1)^2(\xi_3^2-1)^2}, \tag{3.11}$$

where we have again made use of $\mu_i^2 = \frac{m_i^2}{p^2}$ and the variables ξ_i defined in eq. (3.4). This clearly differs from the j-invariant computed in the previous subsection, see eq. (3.5). However, as observed in ref. [28], the two curves are isogenous. This has been checked in ref. [28] by computing the complex structure parameter τ of the elliptic curve. Here we check it by using the relations between the j-invariants of the two elliptic curves. The j-invariants for a pair of two-isogenous elliptic curves are related by the modular polynomial $\Phi_2(X, Y)$ (see e.g. [54, Chapter 5])

$$\begin{aligned} \Phi_2(X,Y) = {} & X^3 + Y^3 - X^2Y^2 + 1488\left(X^2Y + XY^2\right) - 162000\left(X^2 + Y^2\right) \\ & + 40773375\,XY + 8748000000\,(X + Y) - 157464000000000. \end{aligned} \tag{3.12}$$

See ref. [55] for details about how these modular polynomials are computed. It can be checked that $\Phi_2(j_F, j_B) = 0$. This is an infinite precision test of two-isogeny. Ref. [28] used the approach of comparing the periods which are computed using elliptic integrals. This involves transcendental functions while the approach we followed here only requires algebraic operations with rational functions.

[4] By abuse of notation we are here writing p for the absolute value of the momentum p^μ.

JHEP05(2021)064

3.3 Full Baikov representation

For a "full" Baikov approach to an L-loop integral with $E+1$ external legs one needs $\frac{1}{2}L(L+1)+LE$ Baikov variables D_a. In the present case ($L=2$, $E=1$, $M=L+E=3$), the variables are $D_1,\ldots,D_5$ and the maximal cut corresponds to setting $D_1=D_2=D_3=0$ at the end of the computation.

We now follow [49] to derive the Baikov representation. The inverse propagators are

$$\begin{aligned} D_1 &= k_2^2 - m_1^2\,, & D_2 &= (k_1-k_2)^2 - m_2^2\,, & D_3 &= (p-k_1)^2 - m_3^2\,, \\ D_4 &= k_1^2\,, & D_5 &= (p-k_2)^2\,. \end{aligned} \tag{3.13}$$

Loosely following the notation of the paper above we set $q_1=k_1$, $q_2=k_2$ and $q_3=p$ and write $s_{ij}=q_i\cdot q_j$. The Gram determinant[5] is

$$\begin{aligned} G(k_1,k_2,p) &= \det\begin{pmatrix} s_{11} & s_{12} & s_{13} \\ s_{12} & s_{22} & s_{23} \\ s_{13} & s_{23} & p^2 \end{pmatrix} \\ &= s_{11}\left(p^2 s_{22} - s_{23}^2\right) - s_{12}\left(p^2 s_{12} - s_{13}s_{23}\right) + s_{13}\left(s_{12}s_{23} - s_{13}s_{22}\right). \end{aligned} \tag{3.14}$$

The Baikov polynomial is obtained by rewriting the Mandelstam variables s_{ij} in terms of the inverse propagators D_a in this Gram determinant,

$$P(D_1,\ldots,D_5) = G(k_1,k_2,p)\Big|_{s_{ij}(D_a)}. \tag{3.15}$$

The cut integral ($D_1=D_2=D_3=0$) is of the form

$$\int \frac{\mathrm{d}D_4\mathrm{d}D_5}{D_4^{\alpha_4}D_5^{\alpha_5}} P(0,0,0,D_4,D_5)^{(d-M-1)/2}. \tag{3.16}$$

Where α_4 and α_5 are the exponents of D_4 and D_5 in the original integral respectively. Since $M=3$, $d=2$ and $\alpha_4=\alpha_5=0$ we get

$$\int \frac{\mathrm{d}D_4\mathrm{d}D_5}{P(0,0,0,D_4,D_5)}, \tag{3.17}$$

where P is a polynomial of overall degree three in D_4 and D_5,

$$\begin{aligned} P = \frac{1}{4}\Big[&- D_4^2 D_5 + D_5(m_1^2-m_2^2)(m_3^2-p^2) - (m_1^2 m_3^2 - m_2^2 p^2)(m_1^2-m_2^2+m_3^2-p^2) \\ &- D_4(D_5^2 + (m_2^2-m_3^2)(m_1^2-p^2) - D_5(m_1^2+m_2^2+m_3^2+p^2))\Big]. \end{aligned} \tag{3.18}$$

The equation $P=0$ defines an elliptic curve. We may again transform this curve to Weierstrass form. As it turns out, this curve has the same j-invariant as that from the loop-by-loop Baikov computation in the previous section. Rather than repeating it here we thus refer back to eq. (3.11).

[5] The astute reader may notice that this Gram determinant vanishes when in strictly two dimensions. If one is uncomfortable with this one can instead derive a Baikov representation strictly in two dimensions. We will do something similar for the elliptic double-box in section 4.2. Details relevant for either case (in particular, how to handle cases when the internal momenta are spanned by the external momenta) are presented in appendix A.5.

JHEP05(2021)064

3.4 Light-cone coordinates

One convenient way to enforce on-shell conditions in two dimensions is via light-cone coordinates. We wish to enforce the conditions for the maximal cut:

$$k_2^2 - m_1^2 = 0, \quad (k_1 - k_2)^2 - m_2^2 = 0, \quad (p - k_1)^2 - m_3^2 = 0. \tag{3.19}$$

We define the auxiliary momentum $k_3 = k_1 - k_2$ and use that in light-cone coordinates the square of a momentum is given by $k_i^2 = k_i^+ k_i^-$. Then the first two conditions in eq. (3.19) are solved by

$$k_2^- = \frac{m_1^2}{k_2^+}, \quad k_3^- = \frac{m_2^2}{k_3^+}. \tag{3.20}$$

The last condition in eq. (3.19) becomes

$$(p^+ - k_2^+ - k_3^+)(p^- - k_2^- - k_3^-) - m_3^2 = (p^+ - k_2^+ - k_3^+)\left(p^- - \frac{m_1^2}{k_2^+} - \frac{m_2^2}{k_3^+}\right) - m_3^2 = 0. \tag{3.21}$$

Introducing dimensionless quantities as $k_2^+ = p^+ x$, $k_3^+ = p^+ y$ and again using $\mu_i^2 = \frac{m_i^2}{p^2}$, the previous equation becomes

$$(1 - x - y)\left(1 - \frac{\mu_1^2}{x} - \frac{\mu_2^2}{y}\right) - \mu_3^2 = 0. \tag{3.22}$$

In homogeneous coordinates $[x : y : z]$ and after multiplying by xyz we are left with a cubic curve in $\mathbb{P}^2$ given by the equation

$$P_L \equiv xyz\left(1 + \mu_1^2 + \mu_2^2 - \mu_3^2\right) + x^2\left(\mu_2^2 z - y\right) + y^2\left(\mu_1^2 z - x\right) - z^2\left(\mu_2^2 x + \mu_1^2 y\right) = 0. \tag{3.23}$$

This is an elliptic curve whose defining equation is closely related to the $\mathfrak{F}$-polynomial in (3.2). Specifically, their discriminants with respect to z are related by

$$\operatorname{disc}_z P_L(x, y, z) = \operatorname{disc}_z \mathfrak{F}(y, x, z). \tag{3.24}$$

Once again we can transform the curve to Weierstrass form, and evaluate its j-invariant. As suggested by the relationship in eq. (3.24), we find it has the same j-invariant as the Feynman parametric representation (given in eq. (3.5)), and a distinct (but isogenous) j-invariant to those in the two Baikov representations.

3.5 Rationalizing the square roots in the Baikov representation

In subsection 3.2 we derived a loop-by-loop Baikov representation of the sunrise integral and explained how the equation $J = -16p^8\sqrt{Q_1 Q_2}$ defines an elliptic curve isogenous to the one obtained by Feynman parameters and the light-cone computation as in ref. [28]. Combining $\sqrt{Q_1}$ and $\sqrt{Q_2}$ in this way is safe if both Q_1 and Q_2 are positive. However, for complex kinematics it may lead to an incorrect phase.

JHEP05(2021)064

Instead of combining the two roots, we can rationalize one of them. Recall that Q_1 and Q_2 were given in eq. (3.10) as

$$\begin{aligned} Q_1 &= -\frac{1}{4p^4}\left[D_4 - (m_3 - p)^2\right]\left[D_4 - (m_3 + p)^2\right], \\ Q_2 &= -\frac{1}{4p^4}\left[D_4 - (m_1 + m_2)^2\right]\left[D_4 - (m_1 - m_2)^2\right]. \end{aligned} \tag{3.25}$$

Choosing to rationalize $\sqrt{Q_2}$, the change of variables amounts to replacing

$$\begin{aligned} D_4 &\to 2t\left[\frac{m_1^2}{t-1} + \frac{m_2^2}{t+1}\right], \\ \sqrt{Q_2} &\to \frac{(t(m_1 - m_2) + (m_1 + m_2))(t(m_1 + m_2) + (m_1 - m_2))}{2p^2(t^2 - 1)}. \end{aligned} \tag{3.26}$$

It turns out that the Jacobian from the change of variables cancels against the transformed $\sqrt{Q_2}$ and a factor of $t^2 - 1$ coming from $\sqrt{Q_1}$. In the end we obtain

$$I(p^2, m_1^2, m_2^2, m_3^2)\Big|_{\text{cut}} = p^4 \int \frac{\mathrm{d}D_4}{J} = -\frac{1}{16p^4}\int \frac{\mathrm{d}D_4}{\sqrt{Q_1}\sqrt{Q_2}} = -\frac{1}{16p^2}\int \frac{\mathrm{d}t}{\sqrt{R}}, \tag{3.27}$$

where R is a polynomial of degree four in t,

$$\begin{aligned} R \equiv \frac{1}{64p^4}&\left[\left((m_3 - p)^2 - 2(m_1^2 + m_2^2)\right)t^2 - 2(m_1^2 - m_2^2)t - (m_3 - p)^2\right] \\ &\times\left[\left((m_3 + p)^2 - 2(m_1^2 + m_2^2)\right)t^2 - 2(m_1^2 - m_2^2)t - (m_3 + p)^2\right]. \end{aligned} \tag{3.28}$$

The equation $y^2 = R(t)$ defines an elliptic curve as a hypersurface in a weighted projective space $\mathbb{P}^{1:1:2}$. It turns out that this curve has the same j-invariant as that from the graph polynomial (given in eq. (3.5)). Note that this is *not* the same j-invariant as in the Baikov representations above, even though the loop-by-loop Baikov representation was our starting point: by rationalizing instead of combining roots we have achieved agreement with the graph polynomial and light-cone derivations of the elliptic curve.

Another way to think about how the two curves emerge is to track what happens to the branch points of the curves under the change of variables above. In ref. [28] and subsection 3.2 the elliptic curve arising from the Baikov representation is defined by $J^2 = (-16p^8)^2 Q_1 Q_2$. This is a double cover of $\mathbb{P}^1$ branched over four points. Since Q_1 and Q_2 are already factorized, the branch points are easy to read off:

$$D_{4,\pm}^{(1)} = (m_1 \pm m_2)^2, \quad D_{4,\pm}^{(2)} = (m_3 \pm p)^2. \tag{3.29}$$

These are four points on a projective line parametrized by the coordinate D_4. They have a cross-ratio λ with corresponding j-invariant $j = 256\frac{(\lambda^2-\lambda+1)^3}{\lambda^2(1-\lambda)^2}$. This approach gives the "Baikov" j-invariant shown in eq. (3.11).

On the other hand, when rationalizing the quadric Q_2 we write x as the image of a map from a different $\mathbb{P}^1$ with coordinate t,

$$t \mapsto x(t) = 2t\left[\frac{m_1^2}{t-1} + \frac{m_2^2}{t+1}\right]. \tag{3.30}$$

JHEP05(2021)064

Under this change of variables, Q_1 becomes a polynomial of degree four and we again define an elliptic curve as a double cover of $\mathbb{P}^1$, but this time the $\mathbb{P}^1$ has coordinate t. The branch points are the preimages of the two points $D^{(2)}_{4,+}$ and $D^{(2)}_{4,-}$. Since the change of variables is quadratic each point has two preimages and we indeed get four branch points as required. As we now again have four points on a projective line, we can form a cross-ratio and the corresponding j-invariant. This is the j-invariant that comes from the $\mathfrak{F}$-polynomial and the light-cone approach in eq. (3.5).

The analysis presented here applies to the loop-by-loop Baikov representation, and at first this may make the full Baikov result seem mysterious, as unlike the loop-by-loop representation it does not obviously involve combining square roots. However, if one derives the Baikov representation by dividing each loop momentum into perpendicular and parallel subspaces, as for example in ref. [46], then one naturally passes through a form closely related to the loop-by-loop representation in which there are indeed multiple square roots. In particular, the individual equations that need to be solved to land on the cut solution will be the same. If one understands the Baikov representation as a result of this kind of procedure, then the elliptic curve we found for it earlier can be explained in the same way as the loop-by-loop curve, and a similarly more careful treatment (especially one along the lines of the next section) will result in the same curve as was found from Feynman parameters and light-cone coordinates.

3.6 Derivation of the double cover relation

In this section we study the relation between the two genus-one curves from a different point of view. We describe the curves purely by polynomial equations and we avoid introducing square roots.

On the maximal cut we have $D_1 = D_2 = D_3 = 0$ and these equations together with $D_4 = p^2(x^2 + u^2)$ define a curve. We introduce a dimensionless variable $d_4 = \frac{D_4}{p^2}$. Then, the equations (3.8) can be simplified by solving

$$x = \frac{d_4 - \mu_3^2 + 1}{2}, \tag{3.31}$$

$$u^2 = -\frac{1}{4}(d_4 - (1+\mu_3)^2)(d_4 - (1-\mu_3)^2), \tag{3.32}$$

$$v^2 = \mu_1^2 - y^2, \tag{3.33}$$

$$uv = (1-y)\frac{d_4 - \mu_3^2 + 1}{2} + \frac{\mu_1^2 - \mu_2^2 + \mu_3^2 - 1}{2}. \tag{3.34}$$

We now obtain the equation for the curve in variables y and d_4, by substituting the expressions above in $(uv)^2 = u^2v^2$. This equation is

$$\begin{aligned} P(y,d_4) = &-4y^2d_4 + 2yd_4^2 + 2\left(\mu_1^2 - \mu_2^2 - \mu_3^2 + 1\right)yd_4 - \left(\mu_1^2 + 1\right)d_4^2 \\ &+ 2\left(-\mu_1^2\mu_3^2 + \mu_2^2\mu_3^2 + \mu_1^2 - \mu_2^2\right)y + 2\left(\mu_1^2\mu_3^2 + \mu_2^2\right)d_4 \\ &- \mu_1^2\mu_3^4 - \mu_1^4 + 2\mu_1^2\mu_2^2 - \mu_2^4 + 2\mu_1^2\mu_3^2 - \mu_1^2 = 0, \end{aligned} \tag{3.35}$$

JHEP05(2021)064

and is a cubic equation in y and d_4. It is not in Weierstrass form. The expression for the Jacobian can also be written in the variables y and d_4:

$$J = \frac{p^8}{4}(4yd_4 - (d_4 + \mu_1^2 - \mu_2^2)(d_4 - \mu_3^2 + 1)). \tag{3.36}$$

Note that this approach avoids introducing square roots, at the cost of working with two variables constrained by an algebraic relation.

Let us show that $\frac{\mathrm{d}d_4}{J}$ is the holomorphic one-form on this curve. Taking the differential of $P(y, d_4) = 0$ we obtain

$$\left(\frac{\partial P}{\partial y}\right)\mathrm{d}y + \left(\frac{\partial P}{\partial d_4}\right)\mathrm{d}d_4 = -2J(y, d_4)\,\mathrm{d}y + K(y, d_4)\,\mathrm{d}d_4 = 0, \tag{3.37}$$

where

$$K(y, d_4) = -4y^2 + 4yd_4 + 2(\mu_1^2 - \mu_2^2 - \mu_3^2 + 1)y - 2(\mu_1^2 + 1)d_4 + 2\mu_1^2\mu_3^2 + 2\mu_2^2. \tag{3.38}$$

Since we assume that the curve described by $P = 0$ is nonsingular, we have that $\frac{\partial P}{\partial y} = -2J$ and $\frac{\partial P}{\partial d_4} = K$ can not vanish simultaneously. Then, we have $\frac{\mathrm{d}d_4}{J} = 2\frac{\mathrm{d}y}{K}$. Hence, one can see that at the zeros of J this holomorphic form does not have poles, when written with the denominator K. It can be checked that this curve is the same as the one obtained by the more traditional Baikov approach.

However, one can see that the curve we started with, in the variables x, y, u, v and d_4 is a double cover of the curve $P(d_4, y) = 0$. Given a point (d_4, y), we can uniquely find x and u^2, v^2 and uv. This allows us to solve for u and v up to a sign. Hence, to a point on the curve $P(d_4, y) = 0$ correspond two points on the initial curve defined by $D_1 = D_2 = D_3 = 0$ and $d_4 = x^2 + u^2$.

To find a one-to-one projection of the curve which is easily recognizable as an elliptic curve, we proceed as follows. We can use a kind of Euclidean lightcone construction and transform the equations to

$$y + iv = \frac{\mu_1^2}{y - iv}, \tag{3.39}$$

$$(x - y) + i(u - v) = \frac{\mu_2^2}{(x - y) - i(u - v)}, \tag{3.40}$$

$$(x - 1) + iu = \frac{\mu_3^2}{(x - 1) - iu}. \tag{3.41}$$

Combining them, we find

$$\frac{\mu_1^2}{y - iv} + \frac{\mu_2^2}{(x - y) - i(u - v)} - \frac{\mu_3^2}{(x - 1) - iu} = 1. \tag{3.42}$$

If we introduce $\zeta = y - iv$ and $\xi = x - iu$, we have a curve

$$\frac{\mu_1^2}{\zeta} + \frac{\mu_2^2}{\xi - \zeta} - \frac{\mu_3^2}{\xi - 1} = 1, \tag{3.43}$$

JHEP05(2021)064

which is a cubic equation in (ζ, ξ). Once we have ζ and ξ we obtain

$$y = \frac{1}{2}\Big(\zeta + \frac{\mu_1^2}{\zeta}\Big), \qquad v = \frac{1}{2i}\Big(-\zeta + \frac{\mu_1^2}{\zeta}\Big), \tag{3.44}$$

and similarly for x and u. Finally, we obtain $d_4 = x^2 + u^2$. This time, given a point (ζ, ξ) we can find a unique point on the initial curve.

This second curve looks very similar to the lightcone solution of section 3.4 and indeed it has the same j-invariant.

3.7 Singularities of the geometry and Landau analysis

Recall that the j-invariant of an elliptic curve is

$$j = 1728\frac{g_2^3}{\Delta}, \tag{3.45}$$

where Δ is the elliptic discriminant. When Δ vanishes, j is singular, and the elliptic curve degenerates.

For the curve arising from Feynman parametrization and the light-cone computation we obtained

$$j_F = \frac{\left[(\xi_0^2-1)(\xi_1^2-1)(\xi_2^2-1)(\xi_3^2-1) + 16\mu_1^2\mu_2^2\mu_3^2\right]^3}{\mu_1^4\mu_2^4\mu_3^4\,(\xi_0^2-1)(\xi_1^2-1)(\xi_2^2-1)(\xi_3^2-1)} \tag{3.46}$$

while for the curve arising from the Baikov representation we obtained

$$j_B = \frac{\left[(\xi_0^2-1)(\xi_1^2-1)(\xi_2^2-1)(\xi_3^2-1) + 256\mu_1^2\mu_2^2\mu_3^2\right]^3}{\mu_1^2\mu_2^2\mu_3^2\,(\xi_0^2-1)^2(\xi_1^2-1)^2(\xi_2^2-1)^2(\xi_3^2-1)^2}. \tag{3.47}$$

The denominators of these expressions are distinct, but they clearly have the same zeros, just with different multiplicities. These zeros all correspond to physical singularities of the diagram, either to thresholds, pseudo-thresholds, or vanishing internal masses. Each corresponds to a consistent Landau diagram, for particular choices of the sign of the energies of each particle. The easiest to recognize are the thresholds, occurring when $(\xi_0)^2 = 1$ and thus $(m_1 + m_2 + m_3)^2 = p^2$, which is the condition for energy conservation when all of the intermediate particles are traveling in the same direction. The Landau analysis also reveals that there are other singularities, arising at pseudo-thresholds $p^2 = (-m_1 + m_2 + m_3)^2$, $p^2 = (m_1 - m_2 + m_3)^2$ and $p^2 = (m_1 + m_2 - m_3)^2$. In terms of variables ξ these are $(\xi_1)^2 = 1$, $(\xi_2)^2 = 1$ and $(\xi_3)^2 = 1$. Finally, the singularities arising when one of the masses vanishes are of a different type. They arise due to the fact that when one of the masses vanishes the integral becomes divergent.

4 The elliptic double-box integral

The elliptic double-box integral has previously been analyzed in ref. [52] from the point of view of direct integration in a Feynman parametric representation, and in ref. [56] from the point of view of the maximal cut in twistor space. In both papers the same elliptic curve was found using very different methods. In this section we derive a Baikov representation of the double-box, and show that it also defines the same curve.

JHEP05(2021)064

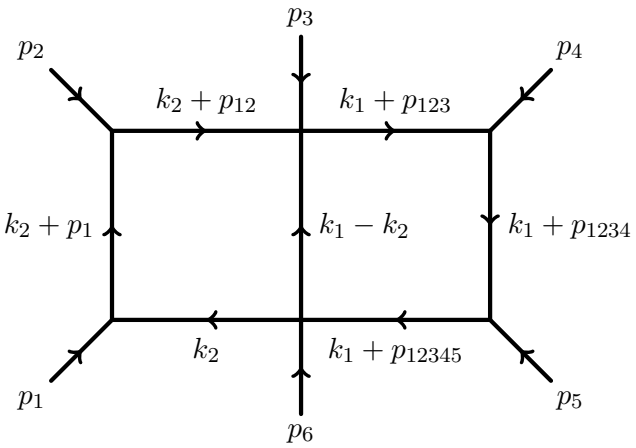

Figure 2. Double-box integral in momentum space. Incoming momenta are assumed to be off-shell, i.e. $p_i^2 \neq 0$, and $p_{i_1 \cdots i_n} \equiv p_{i_1} + \cdots + p_{i_n}$. The internal propagators are massless.

4.1 Baikov representation

The Baikov representation is a rewriting of Feynman integrals where the integration is over Lorentz-invariant quantities, such as dot products. In appendix A we derive such a representation for the elliptic double-box integral shown in figure 2 (see in particular appendix A.4).

The maximal cut of the elliptic double-box can be written in a loop-by-loop Baikov representation as an integral over two Baikov parameters. The cut integrand takes the following form:

$$\frac{\mathcal{J}\sqrt{\mathcal{G}_1}\,\mathrm{d}x_8\mathrm{d}x_9}{\mathcal{B}_1(x_8,x_9)\sqrt{\mathcal{B}_2(x_8,x_9)}}, \tag{4.1}$$

where x_8 and x_9 are the two remaining Baikov variables after all propagators have been cut. The polynomials $\mathcal{B}_1$ and $\mathcal{B}_2$ are of degree two in x_8 and also of degree two in x_9. The factors $\mathcal{J}$ and $\mathcal{G}_1$ only depend on the external kinematics. We include expressions for these polynomials in the supplementary material, `doublebox_baikov_rep.txt`.

To obtain an elliptic curve, we may begin by taking a residue around $\mathcal{B}_1(x_8, x_9) = 0$. Without loss of generality, let us take this residue in x_9. Solving $\mathcal{B}_1(x_8, x_9) = 0$ for x_9 introduces a square root that contains x_8, and this square root can be rationalized by Euler substitution as done in subsection 3.5 for the sunrise integral. Denoting by t the variable that replaces x_8 to rationalize the square root we find that $\mathcal{B}_2(t)$ becomes a quartic polynomial in t. We can therefore define an elliptic curve by $y^2 = \mathcal{B}_2(t)$ and compute its j-invariant through standard changes of variables.

The problem with this approach is that the change of variables from x_8 to t may itself introduce a square root in the kinematic parameters. Since the j-invariant of the elliptic curve is expected to be a rational function of the kinematics, this root is spurious and must cancel in j.

The spurious kinematic root can be avoided if we view x_8 and x_9 as a subset of the coordinates on a $\mathbb{P}^3$ with homogeneous coordinates $[x_8 : x_9 : y : z]$. From the denominator

JHEP05(2021)064

in the integrand in eq. (4.1) we define the two quadrics[6]

$$\begin{aligned} S_1 &:= \left\{ [x_8 : x_9 : y : z] \in \mathbb{P}^3 \mid \mathcal{B}_1(x_8, x_9, z) = 0 \right\}, \\ S_2 &:= \left\{ [x_8 : x_9 : y : z] \in \mathbb{P}^3 \mid y^2 - \mathcal{B}_2(x_8, x_9, z) = 0 \right\}. \end{aligned} \tag{4.2}$$

The integrand in eq. (4.1) corresponds to a differential form on the intersection of S_1 and S_2. For generic quadrics S_1 and S_2 this intersection is a smooth curve of genus one.

We now review briefly how this curve may be characterized and refer to [57, Chapter 22] for further details. The quadrics S_1 and S_2 generate a family of quadrics

$$\left\{ \lambda_0 s_1 + \lambda_1 s_2 \mid [\lambda_0 : \lambda_1] \in \mathbb{P}^1,\ s_1 \in S_1,\ s_2 \in S_2 \right\}. \tag{4.3}$$

This family is called the *pencil of quadrics* and the intersection $C = S_1 \cap S_2$ is called the *base locus* of the pencil. The members S_λ of the pencil are quadrics in $\mathbb{P}^3$ and for some choices of $\lambda \in \mathbb{P}^1$ they may be singular. If S_1 and S_2 intersect transversely, there are four such singular members S_{λ_i} with $i = 0, \ldots, 3$. Out of the four points λ_i we can form a cross-ratio κ and subsequently the invariant combination

$$j = 256 \frac{(\kappa^2 - \kappa + 1)^3}{\kappa^2 (\kappa - 1)^2}, \tag{4.4}$$

which characterizes the pencil of quadrics up to isomorphism. One can now moreover show that the base locus C of the pencil is isomorphic to a genus-one curve in the plane with the same j-invariant as the pencil.

An advantage of this description is that it allows us to compute the elliptic discriminant of the curve using only rational operations. Writing $\mathbf{S}_1$ and $\mathbf{S}_2$ for the 4×4 symmetric matrices associated to the quadrics S_1 and S_2 in eq. (4.2) respectively, the locations λ_i of the singular members of the pencil are given by the eigenvalues of the matrix $\mathbf{S}_2^{-1}\mathbf{S}_1$. The curve degenerates if two of those points in $\mathbb{P}^1$ are the same, i.e. if $\mathbf{S}_2^{-1}\mathbf{S}_1$ has a double eigenvalue. This leads to the expression

$$\Delta = \mathrm{disc}_\lambda \det(\lambda - \mathbf{S}_2^{-1}\mathbf{S}_1) \tag{4.5}$$

for the elliptic discriminant. Moreover, a defining equation for the curve is given by $y^2 = \det(x - \mathbf{S}_2^{-1}\mathbf{S}_1) = 0$. This depends rationally on the kinematic variables contained in $\mathbf{S}_1$ and $\mathbf{S}_2$ and a Weierstrass form and the j-invariant can subsequently be computed by rational transformations.

It turns out that the elliptic curve obtained in this way has the *same* j-invariant as those computed from twistor space in ref. [56] and from the parametric representation of ref. [52]. As we do not need to combine distinct square roots in this representation, this is consistent with our observations in the previous section.

In the supplementary material of this paper, we provide the file `doublebox_curve.txt` that contains an expression for the defining equation of the curve. With minor modifications the file should be readable with most computer programs.

[6] Note that here we are writing $\mathcal{B}_1(x_8, x_9, z)$ for the homogenization of the polynomial $\mathcal{B}_1$ in eq. (4.1) and similarly for $\mathcal{B}_2$.

JHEP05(2021)064

4.2 Four-dimensional derivation of the Baikov form

In this section we present a derivation of the Baikov form without using dimensional regularization. This avoids having to take the potentially somewhat tricky limit $d \to 4$. Equivalently, one can obtain the cut integrand as a one-form and it is not necessary to take one extra residue as in section 4.1.

Consider the loop parametrized by k_2 in the elliptic double-box. This loop has denominators

$$D_1 = k_2^2, \qquad D_2 = (p_1 + k_2)^2, \qquad D_3 = (p_{12} + k_2)^2, \qquad D_4 = (k_1 - k_2)^2. \tag{4.6}$$

It has "external" momenta p_1, p_2, $k_1 + p_{12}$ and k_1. The integral measure $\mathrm{d}^d k_2$ decomposes into an integral $\mathrm{d}^3 k_2^{\parallel}$ over the space spanned by the independent "external" momenta p_1, p_2 and k_1, and an orthogonal integral $\mathrm{d}^{d-3} k_2^{\perp}$. The dot products of k_2 with the "external" momenta are

$$k_2 \cdot p_1 = \frac{1}{2}(D_2 - p_1^2 - D_1), \tag{4.7}$$

$$k_2 \cdot p_2 = \frac{1}{2}(D_3 - D_2 - p_{12}^2 + p_1^2), \tag{4.8}$$

$$k_2 \cdot k_1 = -\frac{1}{2}(D_4 - D_1 - k_1^2). \tag{4.9}$$

Using identities from appendix A.5, it follows that

$$\mathrm{d}^3 k_2^{\parallel} = \frac{\mathrm{d}(k_2 \cdot p_1)\mathrm{d}(k_2 \cdot p_2)\mathrm{d}(k_2 \cdot k_1)}{\det G(p_1, p_2, k_1)^{\frac{1}{2}}} = -\frac{1}{8}\frac{\mathrm{d}D_2\mathrm{d}D_3\mathrm{d}D_4 + \mathrm{d}D_1(\cdots)}{\det G(p_1, p_2, k_1)^{\frac{1}{2}}}, \tag{4.10}$$

$$\mathrm{d}^{d-3} k_2^{\perp} = \frac{1}{2}\Omega_{d-3}\left(\frac{\det G(k_2, p_1, p_2, k_1)}{\det G(p_1, p_2, k_1)}\right)^{\frac{d-5}{2}} \mathrm{d}D_1. \tag{4.11}$$

Of course, we do not need to keep the dimension d arbitrary and we can set $d = 4$ here. In that case we have $\Omega_1 = 2$.

When computing the full $\mathrm{d}^4 k_2$ measure the extra terms in $\mathrm{d}^3 k_2^{\parallel}$ proportional to $\mathrm{d}D_1$ drop out:

$$\mathrm{d}^4 k_2 = -2\frac{1}{16}\mathrm{d}D_1\mathrm{d}D_2\mathrm{d}D_3\mathrm{d}D_4 (\det G(p_1, p_2, k_1))^{-\frac{1}{2}} \left(\frac{\det G(k_2, p_1, p_2, k_1)}{\det G(p_1, p_2, k_1)}\right)^{-\frac{1}{2}}. \tag{4.12}$$

Note that we have not canceled the factor $\det G(p_1, p_2, k_1)$ since we do not allow ourselves to combine square roots. Note also that we have some Gram determinants whose entries contain $k_1 \cdot p_1$, $k_1 \cdot p_2$ and k_1^2. We need to keep these dot products in mind when analyzing the k_1 integral, to which we turn next.

For the k_1 integral we have new denominators

$$D_5 = (k_1 + p_{123})^2, \qquad D_6 = (k_1 + p_{1234})^2, \qquad D_7 = (k_1 - p_6)^2, \tag{4.13}$$

while in the Jacobian of the $\mathrm{d}^d k_2$ integral we have k_1^2, $k_1 \cdot p_1$ and $k_1 \cdot p_2$. We introduce two new Lorentz-invariant quantities $D_8 = k_1^2$ and $D_9 = (k_1 + p_{12})^2$.

JHEP05(2021)064

However, not all quantities $D_5, \ldots, D_9$ can be independent; there are five such quantities and only four components for the vector k_1. The relation connecting these quantities can be obtained by computing the Gram determinant $\det G(k_1, p_{12}, p_{123}, p_{1234}, p_{12345}) = 0$. Equivalently, we can antisymmetrize in five different vectors to obtain

$$\begin{aligned} k_1^\mu \epsilon(p_{12}, p_{123}, p_{1234}, p_{12345}) - p_{12}^\mu \epsilon(k_1, p_{123}, p_{1234}, p_{12345}) + p_{123}^\mu \epsilon(k_1, p_{12}, p_{1234}, p_{12345}) \\ - p_{1234}^\mu \epsilon(k_1, p_{12}, p_{123}, p_{12345}) + p_{12345}^\mu \epsilon(k_1, p_{12}, p_{123}, p_{1234}) = 0. \end{aligned} \tag{4.14}$$

When decomposed over the basis p_{12}, p_{123}, p_{1234} and p_{12345}, k_1 has components $k_1 \cdot p_{12}$, etc., with a metric given by the inverse of the Gram matrix $G(p_{12}, p_{123}, p_{1234}, p_{12345})$. The scalar products k_1^2, $k_1 \cdot p_1$ and $k_1 \cdot p_2$ can be computed from this decomposition. In particular, this implies that we can compute $D_8 = k_1^2$ in terms of the other D_i (since here there are no transversal components there is no need to introduce D_8 at all). Let us compute the measure $\mathrm{d}^4 k_1$ in terms of D_9, D_5, D_6 and D_7. Using eq. (A.39), we find

$$\mathrm{d}^4 k_1 = \frac{1}{2^4} \frac{(\det M_0)^{-\frac{1}{2}} \det M_0}{(\det M_1 \det M_0)^{\frac{1}{2}}} \mathrm{d}D_9 \mathrm{d}D_5 \mathrm{d}D_6 \mathrm{d}D_7, \tag{4.15}$$

where

$$M_0 = G(p_{12}, p_{123}, p_{1234}, p_{12345}), \tag{4.16}$$

$$M_1 = \begin{pmatrix} D_9 & \frac{1}{2}(D_9 + D_5 - p_3^2) & \frac{1}{2}(D_9 + D_6 - p_{34}^2) & \frac{1}{2}(D_9 + D_7 - p_{345}^2) \\ & D_5 & \frac{1}{2}(D_5 + D_6 - p_4^2) & \frac{1}{2}(D_5 + D_7 - p_{45}^2) \\ & & D_6 & \frac{1}{2}(D_6 + D_7 - p_5^2) \\ & & & D_7 \end{pmatrix}. \tag{4.17}$$

Here we have written only some of the matrix entries, the others can be determined from these by symmetry.

When taking the cuts we need to set D_1 through D_7 to zero, and thus we only need the expression for $\det M_1$ when $D_1 = \cdots = D_7 = 0$. Then $\det M_1$ is a quadratic polynomial in D_9. Taking the squares of the Jacobians obtained in this section we obtain a genus-one curve as an intersection of two quadrics. This curve has the same j-invariant as the one obtained by considering the curve embedded in momentum twistor space as described in ref. [56].

5 Conclusions

We have shown that the maximal cut and the Feynman parametrization of the two-loop sunrise integral do not necessarily correspond to different elliptic curves. The observation of different curves for these two objects in the literature was an artifact due to combining two square roots, and a more careful treatment shows the same curve for both the Feynman-parametric and Baikov representation, reinforced by the observation of the same curve in a light-cone parametrization of the maximal cut. We have shown that similarly the Baikov and twistor representations of the elliptic double-box also describe the same elliptic curve.

JHEP05(2021)064

In some ways, the appearance of the same curve in different representations of these integrals should not be surprising. If one thinks of the maximal cut as a variety in loop momentum space, that variety should already define an elliptic curve. Whether we parametrize it with Baikov, light-cone, or twistor coordinates, we are performing changes of variables which should preserve invariant features of the geometry, such as the j-invariant. From this perspective, the surprise is actually that this curve is preserved in Feynman parameters. Feynman parameters do not correspond straightforwardly to a change of variables from the initial loop momenta, so the fact that they apparently preserve the geometry deserves further explanation.

One of the implications of our work is that analytic continuation of the Baikov representation away from the Baikov integration domain has to be done with some care. Inside this domain the Jacobians involved in changing coordinates are positive and one can pick the positive solution of any square roots that appear. However, while this is possible for Euclidean kinematics, there is no canonical choice of square roots outside this region.

In ref. [58], an extension of the notion of leading singularity was put forward which applies to integrals containing genus-one curves as well. The construction in that reference implicitly assumes a fixed geometry for the genus-one curve. If there were a genuine ambiguity in the underlying genus-one curve it is not clear how one should modify their construction. Fortunately, the results of this paper imply that such a modification may not be necessary.

In previous investigations of the elliptic double-box, conformal symmetry served as an important constraint that allowed for particularly clean representations. The Baikov representation is by its nature not conformal, as it uses momentum invariants as variables. It would be interesting to find a variant of Baikov that preserves conformal symmetry, to make better use of this kind of representation in the context of, e.g., $\mathcal{N} = 4$ super Yang-Mills.

Finally, there is a broader concern raised by the observations of refs. [15, 28] that we do not fully address. While we do find the same curve for both the cut and Feynman parametrization of the sunrise integral, this by no means shows that isogenies are never relevant to the elliptic integrals that occur in physics. In particular, while our work suggests that each elliptic Feynman integral has a preferred curve, it may be that there exist distinct diagrams whose corresponding curves are isogenous. If such an example were to be found, it would suggest the need for a formalism that relates not merely iterated integrals on the same elliptic curve, but iterated integrals on isogenous curves as well.

Acknowledgments

We thank Stefan Weinzierl for helpful discussions. This work was supported in part by the Danish Independent Research Fund under grant number DFF-4002-00037 (MV), the Danish National Research Foundation (DNRF91), the research grant 00015369 from Villum Fonden, a Starting Grant (No. 757978) from the European Research Council (MV, MvH, CV) and the European Union's Horizon 2020 research and innovation program under grant agreement No. 793151 (MvH). This project has received funding from the European

JHEP05(2021)064

Union's Horizon 2020 research and innovation program under the Marie Skłodowska-Curie grant agreement No. 847523 'INTERACTIONS' (HF). The work of HF has been partially supported by a Carlsberg Foundation Reintegration Fellowship.

A Baikov representations with derivations

In this appendix we carefully derive the Baikov representation in its loop-by-loop and its standard forms. This derivation mostly follows ref. [46] and the loop-by-loop part additionally ref. [49].

A.1 The one-loop case

As both the loop-by-loop and standard Baikov representations build off of the Baikov representation at one loop, we will start by reviewing the situation there. Writing a generic one-loop integral,

$$I = \int \frac{\mathrm{d}^d k}{i\pi^{d/2}} \frac{N(k)}{P_1(k)^{a_1} \cdots P_{\mathrm{P}}(k)^{a_{\mathrm{P}}}} \tag{A.1}$$

we then split the integral up in parts parallel and perpendicular to the space spanned by the E independent external momenta:

$$\mathrm{d}^d k = \mathrm{d}^E k_\parallel \mathrm{d}^{d-E} k_\perp \tag{A.2}$$

$$= \mathrm{d}^E k_\parallel \, |k_\perp|^{d-E-1} \, \mathrm{d}|k_\perp| \, \mathrm{d}^{d-E-1}\Omega. \tag{A.3}$$

Using

$$\int \mathrm{d}^{n-1}\Omega = \Omega_n = \frac{2\pi^{n/2}}{\Gamma(n/2)} \tag{A.4}$$

we get

$$I = \frac{2}{\Gamma((d-E)/2)\, i\pi^{E/2}} \int \frac{N(k) \, \mathrm{d}^E k_\parallel \, |k_\perp|^{d-E-1} \, \mathrm{d}|k_\perp|}{P_1(k)^{a_1} \cdots P_{\mathrm{P}}(k)^{a_{\mathrm{P}}}}. \tag{A.5}$$

We may write the parallel component as

$$k_\parallel = \sum_{i=1}^{E} z_i p_i, \tag{A.6}$$

which implies that

$$k_\parallel \cdot p_j = k \cdot p_j = \sum_{i=1}^{E} z_i p_i \cdot p_j. \tag{A.7}$$

We introduce the Gram matrix G with entries $G_{ij} = p_i \cdot p_j$. This allows us to write,

$$z_i = \sum_{j=1}^{E} G^{-1}_{ij} (k \cdot p_j). \tag{A.8}$$

JHEP05(2021)064

We further have that

$$k_{\parallel}^2 = \sum_{i,j=1}^{E} z_i z_j G_{ij} = \sum_{i,j=1}^{E} (k \cdot p_i)(G^{-1})_{ij}(k \cdot p_j). \tag{A.9}$$

We may pick a basis in which the quantities

$$\varsigma_i := k \cdot p_i \,. \tag{A.10}$$

are the components of the vector $k_{\parallel}$. In that case, the metric is nontrivial and is given by the inverse of the Gram matrix. The integration measure is then

$$\mathrm{d}^E k_{\parallel} = (\det G^{-1})^{\frac{1}{2}} \prod_{i=1}^{E} \mathrm{d}\varsigma_i. \tag{A.11}$$

The orthogonal part has norm $k_{\perp}^2 = k^2 - k_{\parallel}^2$. Including the expression for $k_{\parallel}^2$ we have

$$k_{\perp}^2 = k^2 - \sum_{i,j=1}^{E} (k \cdot p_i)(G^{-1})_{ij}(k \cdot p_j). \tag{A.12}$$

Let us form the $(E+1) \times (E+1)$ Gram matrix,

$$\hat{G} = \begin{pmatrix} k^2 & k \cdot p_i \\ k \cdot p_j & G_{ji} \end{pmatrix}. \tag{A.13}$$

Using the expression for the determinant of a matrix written in terms of blocks, we have that

$$\det \hat{G} = \left[k^2 - \sum_{i,j=1}^{E} (k \cdot p_i)(G^{-1})_{ij}(k \cdot p_j) \right] \det G. \tag{A.14}$$

Hence, $(k_{\perp})^2 = \frac{\det \hat{G}}{\det G}$.

Using the expression of $k_{\perp}^2$ from eq. (A.14), we find that $|k_{\perp}|\mathrm{d}|k_{\perp}| = |k|\mathrm{d}|k| + \ldots$, where the missing terms contain components $\mathrm{d}\varsigma_i$ which vanish when wedged into $\mathrm{d}^E k_{\parallel}$. This means that we get the relation

$$\mathrm{d}|k_{\perp}|\mathrm{d}^E k_{\parallel} = \tfrac{1}{2}|k_{\perp}|^{-1}\mathrm{d}\varsigma_0 \, \mathrm{d}^E k_{\parallel} \tag{A.15}$$

where we have used the notation $\varsigma_0 = k^2$.

Inserting eqs. (A.15), (A.12), (A.11) into eq. (A.5) we get

$$I = \frac{\mathcal{G}^{(E-d+1)/2}}{\Gamma((d-E)/2)\, i\pi^{E/2}} \int \frac{N(\varsigma)\, \mathcal{B}(\varsigma)^{(d-E-2)/2}\, \mathrm{d}^{E+1}\varsigma}{P_1(\varsigma)^{a_1} \cdots P_{\mathrm{P}}(\varsigma)^{a_{\mathrm{P}}}}, \tag{A.16}$$

where we have defined

$$\mathcal{B} := \det \hat{G} = \det G(k, p_1, \ldots, p_E) \,, \qquad \mathcal{G} := \det G = \det G(p_1, \ldots, p_E) \,, \tag{A.17}$$

with G denoting the Gram matrix.

JHEP05(2021)064

Now the only step left is to change to the Baikov variables x_i, which equal the propagators. If there are too few propagators ($\mathrm{P} < E+1$) one will need to introduce additional variables, but this is mostly relevant at higher loops. The Jacobian $\mathcal{J}$ for the change of variables will depend on the exact expressions used for the propagators, but for most conventions it equals,

$$\mathcal{J} = \pm\, 2^{-E}. \tag{A.18}$$

Thus the final result for a one-loop Baikov representation is

$$I = \frac{\mathcal{J}\,\mathcal{G}^{(E-d+1)/2}}{\Gamma((d-E)/2)\,i\pi^{E/2}} \int \frac{N(x)\;\mathcal{B}(x)^{(d-E-2)/2}\;\mathrm{d}^{E+1}x}{x_1^{a_1}\cdots x_{\mathrm{P}}^{a_{\mathrm{P}}}}. \tag{A.19}$$

A.2 Multi-loop, the loop-by-loop approach

With this representation in hand, we now want to apply it to multi-loop cases. A multi-loop Feynman integral is given by

$$I = \int \frac{\mathrm{d}^d k_1}{i\pi^{d/2}} \cdots \frac{\mathrm{d}^d k_L}{i\pi^{d/2}} \frac{N(\{k\})}{P_1(\{k\})^{a_1}\cdots P_{\mathrm{P}}(\{k\})^{a_{\mathrm{P}}}} \tag{A.20}$$

Our strategy will be to go through the steps from the previous section one loop at a time, starting with loop number L and then going down towards 1. We call E_l the number of momenta external to loop number l. This may include the loop momenta of lower-numbered loops. We will denote with $\mathcal{G}_l$ the Gram-matrix of the momenta external to loop l, while $\mathcal{B}_l$ is the same but with the loop-momentum k_l included. If we follow the steps of the previous section with this notation, we arrive at the correspondence

$$\frac{\mathrm{d}^d k_l}{i\pi^{d/2}} \;\to\; \frac{\mathcal{G}_l^{(E_l-d+1)/2}\,\mathcal{B}_l(\varsigma_l)^{(d-E_l-2)/2}}{\Gamma((d-E_l)/2)\,i\pi^{E_l/2}} \mathrm{d}^{E_l+1}\varsigma_l \tag{A.21}$$

where ς_l corresponds to the set of dot-products between k_l and itself along with the momenta external to the lth loop. Putting this together for each loop gives

$$I = \frac{(-i)^L\,\pi^{-(\sum_i E_i)/2}}{\prod_l^L \Gamma((d-E_l)/2)} \int \frac{N(\varsigma)\left(\prod_l^L \mathcal{G}_l^{(E_l-d+1)/2}\,\mathcal{B}_l^{(d-E_l-2)/2}\right)\mathrm{d}^{(\sum_i E_i)+L}\varsigma}{P_1(\varsigma)^{a_1}\cdots P_{\mathrm{P}}(\varsigma)^{a_{\mathrm{P}}}} \tag{A.22}$$

and changing to the Baikov variables gives the final expression for the loop-by-loop Baikov representation:

$$I = \frac{\mathcal{J}\;(-i)^L\,\pi^{-(\sum_i E_i)/2}}{\prod_l^L \Gamma((d-E_l)/2)} \int \frac{N(x)\left(\prod_l^L \mathcal{G}_l^{(E_l-d+1)/2}\,\mathcal{B}_l^{(d-E_l-2)/2}\right)\mathrm{d}^{(\sum_i E_i)+L}x}{x_1^{a_1}\cdots x_{\mathrm{P}}^{a_{\mathrm{P}}}} \tag{A.23}$$

where the Jacobian for the final variable change still depends on the specific expressions used for the propagators, but is usually given as

$$\mathcal{J} = \pm\, 2^{-(\sum_i E_i)}. \tag{A.24}$$

The expression of eq. (A.23) may also be found in ref. [59].

JHEP05(2021)064

A.3 Multi-loop, the standard approach

The standard approach to multi-loop Baikov parametrization can be thought of as a version of the loop-by-loop approach, but with the assumption that all loops depend on all lower loop-momenta and all external momenta. This means

$$E_l = E + l - 1 \tag{A.25}$$

If this is the case then $\mathcal{G}_l = \mathcal{B}_{l-1}$ since their definitions will be the same. We also have that the power of $\mathcal{G}_l$ which appears in the expression, $(E_l - d + 1)/2$, is equal to minus the power with which $\mathcal{B}_{l-1}$ appears, making the two contributions cancel. This will happen pairwise for each loop, leaving only $\mathcal{B}_L$ and $\mathcal{G}_1$. Renaming these to $\mathcal{B}$ and $\mathcal{G}$ means we have

$$\mathcal{B} = \det G(p_1, \ldots, p_E, k_1, \ldots, k_L) \qquad \text{and} \qquad \mathcal{G} = \det G(p_1, \ldots, p_E). \tag{A.26}$$

Then eq. (A.23) becomes

$$I = \frac{\mathcal{J}\ (-i)^L\, \pi^{L-n}\, \mathcal{G}^{(E-d+1)/2}}{\prod_{l=1}^{L} \Gamma((d+1-E-l)/2)} \int \frac{N(x)\ \mathcal{B}^{(d-E-L-1)/2}\, \mathrm{d}^n x}{x_1^{a_1} \cdots x_{\mathrm{P}}^{a_{\mathrm{P}}}} \tag{A.27}$$

where we have used and defined

$$n \equiv L + \sum_i E_i \ = \ EL + L(L+1)/2 \tag{A.28}$$

and where we (usually) have $\mathcal{J} = \pm 2^{L-n}$. We see that for $L = 1$ eq. (A.27) reduces nicely to eq. (A.19).

A.4 The elliptic double-box

Let us look at the example of the elliptic double-box shown in figure 2. We have the propagating momenta

$$\begin{aligned}
&q_1 = k_2, && q_2 = k_2 + p_1, && q_3 = k_2 + p_{12}, \\
&q_4 = k_1 + p_{123}, && q_5 = k_1 + p_{1234}, && q_6 = k_1 + p_{12345}, \\
&q_7 = k_1 - k_2, && q_8 = k_1, && q_9 = k_1 + p_{12}.
\end{aligned} \tag{A.29}$$

The last two q_8 and q_9 do not actually appear in the diagram, but they are needed to express all scalar products in terms of the Baikov variables.

We have $E_2 = 3$, counting the three momenta k_1, p_1, p_2 that are external to the k_2-loop, while $E_1 = 4$ since this is the maximum number of independent momenta in four space-time dimensions. The four Gram determinants appearing are

$$\begin{aligned}
&\mathcal{B}_2 = \det G(k_2, k_1, p_1, p_2), && \mathcal{G}_2 = \det G(k_1, p_1, p_2), \\
&\mathcal{B}_1 = \det G(k_1, p_3, p_4, p_5, p_6), && \mathcal{G}_1 = \det G(p_3, p_4, p_5, p_6).
\end{aligned} \tag{A.30}$$

We have $\mathcal{J} = \pm 2^{-7} \left(\frac{\det G(p_1,p_2,p_3,p_4)}{\det G(p_3,p_4,p_5,p_6)} \right)^{\frac{1}{2}}$. Putting this together in eq. (A.23) we obtain the expression

$$I = \frac{\mathcal{J}\, \pi^{-7/2}\, \mathcal{G}_1^{(5-d)/2}}{\Gamma((d-3)/2)\, \Gamma((d-4)/2)} \int \frac{N(x)\, \mathcal{G}_2^{(4-d)/2}\, \mathcal{B}_2^{(d-5)/2}\, \mathcal{B}_1^{(d-6)/2} \mathrm{d}^9 x}{x_1^{a_1} \cdots x_7^{a_7}}. \tag{A.31}$$

JHEP05(2021)064

A.5 Derivation of a four-dimensional Baikov representation

In this section we consider the case when there is no orthogonal component $k_\perp = 0$, which will be needed for our derivation of a Baikov representation in four dimensions. We also introduce the vectors v_i which are defined from the denominators $D_i = (k - v_i)^2$, corresponding to massless propagators. We take all of these vectors to be nonvanishing. In other words, we will use as new coordinates the quantities D_i, but k^2 will not be one of these coordinates.

Then, we have

$$\mathrm{d}^d k = (\det G^{-1})^{\frac{1}{2}} \prod_{i=1}^{d} \mathrm{d}(k \cdot v_i). \tag{A.32}$$

We want to express this in terms of $D_i = (k - v_i)^2$ instead of $k \cdot v_i$. We have

$$\begin{aligned}\prod_{i=1}^{d} \mathrm{d}D_i = \prod_{i=1}^{d} 2(k - v_i) \cdot \mathrm{d}v = 2^d \prod_{i=1}^{d} (k \cdot \mathrm{d}k - \mathrm{d}(k \cdot v_i)) \\ = (-2)^d \left[\prod_{i=1}^{d} \mathrm{d}(k \cdot v_i) - \sum_{j=1}^{d} (-1)^{j-1} (k \cdot \mathrm{d}k) \prod_{i \neq j} \mathrm{d}(k \cdot v_i) \right].\end{aligned} \tag{A.33}$$

Plugging in $k \cdot \mathrm{d}k = \sum_{k,l} (k \cdot v_k)(G^{-1})_{kl} \mathrm{d}(k \cdot v_l)$, we obtain

$$\prod_{i=1}^{d} \mathrm{d}D_i = (-2)^d \left[1 - \sum_{j,k=1}^{d} (k \cdot v_k)(G^{-1})_{kj} \right] \prod_{i=1}^{d} \mathrm{d}(k \cdot v_i). \tag{A.34}$$

Let us rewrite the Jacobian in a simpler way

$$\left[1 - \sum_{j,k=1}^{d} (k \cdot v_k)(G^{-1})_{kj} \right] \det G = \det \begin{pmatrix} 1 & k \cdot v_j \\ 1 & G_{ji} \end{pmatrix} = \det_{ij}((v_i - k) \cdot v_j). \tag{A.35}$$

To compute this last determinant, consider the decomposition of $k - v_i$ and $k - v_j$ on the basis of vectors v_k. Upon taking the dot product in this basis we obtain

$$(k - v_i) \cdot (k - v_j) = \sum_{k,l=1}^{d} ((k - v_i) \cdot v_k)(G^{-1})_{kl} ((k - v_j) \cdot v_l), \tag{A.36}$$

whence

$$\det_{ij}((k - v_i) \cdot (k - v_j)) = \left(\det_{ik}((k - v_i) \cdot v_k) \right)^2 (\det G)^{-1}. \tag{A.37}$$

Since

$$(k - v_i) \cdot (k - v_j) = \frac{1}{2} \left[(k - v_i)^2 + (k - v_j)^2 - (v_i - v_j)^2 \right] = \frac{1}{2} \left[D_i + D_j - (v_i - v_j)^2 \right], \tag{A.38}$$

the determinant $\det_{ij}((k - v_i) \cdot (k - v_j))$ can be written in terms of D variables and constants $(v_i - v_j)^2$. This determinant is the Cayley-Menger determinant which arises when computing the volume of a simplex in Euclidean space.

In the end, we find

$$\mathrm{d}^d k = \frac{(-1)^d}{2^d} \frac{(\det G)^{-\frac{1}{2}} \det G}{\left(\det_{ij}((k - v_i) \cdot (k - v_j)) \det G \right)^{\frac{1}{2}}} \prod_{i=1}^{d} \mathrm{d}D_i. \tag{A.39}$$

JHEP05(2021)064

References

[1] D.J. Broadhurst, J. Fleischer and O.V. Tarasov, *Two loop two point functions with masses: asymptotic expansions and Taylor series, in any dimension*, *Z. Phys. C* **60** (1993) 287 [hep-ph/9304303] [INSPIRE].

[2] S. Laporta and E. Remiddi, *Analytic treatment of the two loop equal mass sunrise graph*, *Nucl. Phys. B* **704** (2005) 349 [hep-ph/0406160] [INSPIRE].

[3] D.H. Bailey, J.M. Borwein, D. Broadhurst and M.L. Glasser, *Elliptic integral evaluations of Bessel moments*, *J. Phys. A* **41** (2008) 205203 [arXiv:0801.0891] [INSPIRE].

[4] S. Müller-Stach, S. Weinzierl and R. Zayadeh, *A second-order differential equation for the two-loop sunrise graph with arbitrary masses*, *Commun. Num. Theor. Phys.* **6** (2012) 203 [arXiv:1112.4360] [INSPIRE].

[5] L. Adams, C. Bogner and S. Weinzierl, *The two-loop sunrise graph with arbitrary masses*, *J. Math. Phys.* **54** (2013) 052303 [arXiv:1302.7004] [INSPIRE].

[6] S. Bloch and P. Vanhove, *The elliptic dilogarithm for the sunset graph*, *J. Number Theor.* **148** (2015) 328 [arXiv:1309.5865] [INSPIRE].

[7] J. Broedel, C.R. Mafra, N. Matthes and O. Schlotterer, *Elliptic multiple zeta values and one-loop superstring amplitudes*, *JHEP* **07** (2015) 112 [arXiv:1412.5535] [INSPIRE].

[8] L. Adams, C. Bogner and S. Weinzierl, *The two-loop sunrise integral around four space-time dimensions and generalisations of the Clausen and Glaisher functions towards the elliptic case*, *J. Math. Phys.* **56** (2015) 072303 [arXiv:1504.03255] [INSPIRE].

[9] J. Broedel, N. Matthes and O. Schlotterer, *Relations between elliptic multiple zeta values and a special derivation algebra*, *J. Phys. A* **49** (2016) 155203 [arXiv:1507.02254] [INSPIRE].

[10] L. Adams, C. Bogner and S. Weinzierl, *The iterated structure of the all-order result for the two-loop sunrise integral*, *J. Math. Phys.* **57** (2016) 032304 [arXiv:1512.05630] [INSPIRE].

[11] G. Passarino, *Elliptic polylogarithms and basic hypergeometric functions*, *Eur. Phys. J. C* **77** (2017) 77 [arXiv:1610.06207] [INSPIRE].

[12] A. Primo and L. Tancredi, *On the maximal cut of Feynman integrals and the solution of their differential equations*, *Nucl. Phys. B* **916** (2017) 94 [arXiv:1610.08397] [INSPIRE].

[13] E. Remiddi and L. Tancredi, *Differential equations and dispersion relations for Feynman amplitudes. The two-loop massive sunrise and the kite integral*, *Nucl. Phys. B* **907** (2016) 400 [arXiv:1602.01481] [INSPIRE].

[14] R. Bonciani, V. Del Duca, H. Frellesvig, J.M. Henn, F. Moriello and V.A. Smirnov, *Two-loop planar master integrals for Higgs→ 3 partons with full heavy-quark mass dependence*, *JHEP* **12** (2016) 096 [arXiv:1609.06685] [INSPIRE].

[15] L. Adams and S. Weinzierl, *Feynman integrals and iterated integrals of modular forms*, *Commun. Num. Theor. Phys.* **12** (2018) 193 [arXiv:1704.08895] [INSPIRE].

[16] A. von Manteuffel and L. Tancredi, *A non-planar two-loop three-point function beyond multiple polylogarithms*, *JHEP* **06** (2017) 127 [arXiv:1701.05905] [INSPIRE].

JHEP05(2021)064

[17] J. Ablinger et al., *Iterated elliptic and hypergeometric integrals for Feynman diagrams*, *J. Math. Phys.* **59** (2018) 062305 [arXiv:1706.01299] [INSPIRE].

[18] E. Remiddi and L. Tancredi, *An elliptic generalization of multiple polylogarithms*, *Nucl. Phys. B* **925** (2017) 212 [arXiv:1709.03622] [INSPIRE].

[19] M. Hidding and F. Moriello, *All orders structure and efficient computation of linearly reducible elliptic Feynman integrals*, *JHEP* **01** (2019) 169 [arXiv:1712.04441] [INSPIRE].

[20] J. Broedel, N. Matthes, G. Richter and O. Schlotterer, *Twisted elliptic multiple zeta values and non-planar one-loop open-string amplitudes*, *J. Phys. A* **51** (2018) 285401 [arXiv:1704.03449] [INSPIRE].

[21] R.N. Lee, A.V. Smirnov and V.A. Smirnov, *Solving differential equations for Feynman integrals by expansions near singular points*, *JHEP* **03** (2018) 008 [arXiv:1709.07525] [INSPIRE].

[22] L. Adams, E. Chaubey and S. Weinzierl, *Planar double box integral for top pair production with a closed top loop to all orders in the dimensional regularization parameter*, *Phys. Rev. Lett.* **121** (2018) 142001 [arXiv:1804.11144] [INSPIRE].

[23] L. Adams, E. Chaubey and S. Weinzierl, *Analytic results for the planar double box integral relevant to top-pair production with a closed top loop*, *JHEP* **10** (2018) 206 [arXiv:1806.04981] [INSPIRE].

[24] J. Ablinger, J. Blümlein, P. Marquard, N. Rana and C. Schneider, *Automated solution of first order factorizable systems of differential equations in one variable*, *Nucl. Phys. B* **939** (2019) 253 [arXiv:1810.12261] [INSPIRE].

[25] F. Brown and A. Levin, *Multiple elliptic polylogarithms*, arXiv:1110.6917.

[26] J. Broedel, C. Duhr, F. Dulat and L. Tancredi, *Elliptic polylogarithms and iterated integrals on elliptic curves. Part I. General formalism*, *JHEP* **05** (2018) 093 [arXiv:1712.07089] [INSPIRE].

[27] J. Broedel, C. Duhr, F. Dulat, B. Penante and L. Tancredi, *Elliptic Feynman integrals and pure functions*, *JHEP* **01** (2019) 023 [arXiv:1809.10698] [INSPIRE].

[28] C. Bogner, S. Müller-Stach and S. Weinzierl, *The unequal mass sunrise integral expressed through iterated integrals on $\overline{\mathcal{M}}_{1,3}$*, *Nucl. Phys. B* **954** (2020) 114991 [arXiv:1907.01251] [INSPIRE].

[29] F.A. Berends, M. Buza, M. Böhm and R. Scharf, *Closed expressions for specific massive multiloop selfenergy integrals*, *Z. Phys. C* **63** (1994) 227 [INSPIRE].

[30] S. Bauberger, M. Böhm, G. Weiglein, F.A. Berends and M. Buza, *Calculation of two-loop self-energies in the electroweak Standard Model*, *Nucl. Phys. B Proc. Suppl.* **37** (1994) 95 [hep-ph/9406404] [INSPIRE].

[31] S. Bauberger, F.A. Berends, M. Böhm and M. Buza, *Analytical and numerical methods for massive two loop selfenergy diagrams*, *Nucl. Phys. B* **434** (1995) 383 [hep-ph/9409388] [INSPIRE].

[32] S. Bauberger and M. Böhm, *Simple one-dimensional integral representations for two loop selfenergies: The Master diagram*, *Nucl. Phys. B* **445** (1995) 25 [hep-ph/9501201] [INSPIRE].

[33] M. Caffo, H. Czyz, S. Laporta and E. Remiddi, *The Master differential equations for the two loop sunrise selfmass amplitudes*, *Nuovo Cim. A* **111** (1998) 365 [hep-th/9805118] [INSPIRE].

JHEP05(2021)064

[34] S. Groote, J.G. Korner and A.A. Pivovarov, *On the evaluation of a certain class of Feynman diagrams in x-space: sunrise-type topologies at any loop order*, *Annals Phys.* **322** (2007) 2374 [hep-ph/0506286] [INSPIRE].

[35] S. Groote, J.G. Korner and A.A. Pivovarov, *A numerical test of differential equations for one- and two-loop sunrise diagrams using configuration space techniques*, *Eur. Phys. J. C* **72** (2012) 2085 [arXiv:1204.0694] [INSPIRE].

[36] E. Remiddi and L. Tancredi, *Schouten identities for Feynman graph amplitudes; The Master Integrals for the two-loop massive sunrise graph*, *Nucl. Phys. B* **880** (2014) 343 [arXiv:1311.3342] [INSPIRE].

[37] L. Adams, C. Bogner and S. Weinzierl, *The two-loop sunrise graph in two space-time dimensions with arbitrary masses in terms of elliptic dilogarithms*, *J. Math. Phys.* **55** (2014) 102301 [arXiv:1405.5640] [INSPIRE].

[38] S. Bloch, M. Kerr and P. Vanhove, *A Feynman integral via higher normal functions*, *Compos. Math.* **151** (2015) 2329 [arXiv:1406.2664] [INSPIRE].

[39] S. Bloch, M. Kerr and P. Vanhove, *Local mirror symmetry and the sunset Feynman integral*, *Adv. Theor. Math. Phys.* **21** (2017) 1373 [arXiv:1601.08181] [INSPIRE].

[40] D. Broadhurst, *Feynman integrals, L-series and Kloosterman moments*, *Commun. Num. Theor. Phys.* **10** (2016) 527 [arXiv:1604.03057] [INSPIRE].

[41] C. Bogner, A. Schweitzer and S. Weinzierl, *Analytic continuation and numerical evaluation of the kite integral and the equal mass sunrise integral*, *Nucl. Phys. B* **922** (2017) 528 [arXiv:1705.08952] [INSPIRE].

[42] J. Broedel, C. Duhr, F. Dulat and L. Tancredi, *Elliptic polylogarithms and iterated integrals on elliptic curves II: an application to the sunrise integral*, *Phys. Rev. D* **97** (2018) 116009 [arXiv:1712.07095] [INSPIRE].

[43] S. Groote and J.G. Körner, *Coordinate space calculation of two- and three-loop sunrise-type diagrams, elliptic functions and truncated Bessel integral identities*, *Nucl. Phys. B* **938** (2019) 416 [arXiv:1804.10570] [INSPIRE].

[44] P.A. Baikov, *Explicit solutions of the multiloop integral recurrence relations and its application*, *Nucl. Instrum. Meth. A* **389** (1997) 347 [hep-ph/9611449] [INSPIRE].

[45] R.N. Lee, *Calculating multiloop integrals using dimensional recurrence relation and D-analyticity*, *Nucl. Phys. B Proc. Suppl.* **205-206** (2010) 135 [arXiv:1007.2256] [INSPIRE].

[46] A.G. Grozin, *Integration by parts: an introduction*, *Int. J. Mod. Phys. A* **26** (2011) 2807 [arXiv:1104.3993] [INSPIRE].

[47] K.J. Larsen and Y. Zhang, *Integration-by-parts reductions from unitarity cuts and algebraic geometry*, *Phys. Rev. D* **93** (2016) 041701 [arXiv:1511.01071] [INSPIRE].

[48] J. Bosma, K.J. Larsen and Y. Zhang, *Differential equations for loop integrals in Baikov representation*, *Phys. Rev. D* **97** (2018) 105014 [arXiv:1712.03760] [INSPIRE].

[49] H. Frellesvig and C.G. Papadopoulos, *Cuts of Feynman integrals in Baikov representation*, *JHEP* **04** (2017) 083 [arXiv:1701.07356] [INSPIRE].

[50] M. Harley, F. Moriello and R.M. Schabinger, *Baikov-Lee representations of cut Feynman integrals*, *JHEP* **06** (2017) 049 [arXiv:1705.03478] [INSPIRE].

JHEP05(2021)064

[51] S. Caron-Huot and K.J. Larsen, *Uniqueness of two-loop master contours*, *JHEP* **10** (2012) 026 [arXiv:1205.0801] [INSPIRE].

[52] J.L. Bourjaily, A.J. McLeod, M. Spradlin, M. von Hippel and M. Wilhelm, *Elliptic Double-Box Integrals: Massless Scattering Amplitudes beyond Polylogarithms*, *Phys. Rev. Lett.* **120** (2018) 121603 [arXiv:1712.02785] [INSPIRE].

[53] T. LMFDB Collaboration, *The L-functions and modular forms database*, http://www.lmfdb.org, accessed on January 20 (2021).

[54] S. Lang, *Elliptic functions*, Graduate Texts in Mathematics volume 112, Springer, Germany (1987).

[55] R. Bröker, K. Lauter and A.V. Sutherland, *Modular polynomials via isogeny volcanoes*, *Math. Comp.* **81** (2012) 1201.

[56] C. Vergu and M. Volk, *Traintrack Calabi-Yaus from twistor geometry*, *JHEP* **07** (2020) 160 [arXiv:2005.08771] [INSPIRE].

[57] J. Harris, *Algebraic geometry: a first course*, Graduate Texts in Mathematics volume 133, Springer, Germany (1992).

[58] J.L. Bourjaily, N. Kalyanapuram, C. Langer, K. Patatoukos and M. Spradlin, *An elliptic Yangian-Invariant, 'leading singularity'*, arXiv:2012.14438 [INSPIRE].

[59] H. Frellesvig and L. Mattiazzi, *On the application of intersection theory to Feynman integrals: the univariate case*, in the proceedings of *MathemAmplitudes 2019: Intersection Theory and Feynman Integrals*, December 18–20, Padova, Italy (2021), arXiv:2102.01576 [INSPIRE].

JHEP05(2021)064